Department of Biomedical Engineering and Physics Medical University of Vienna

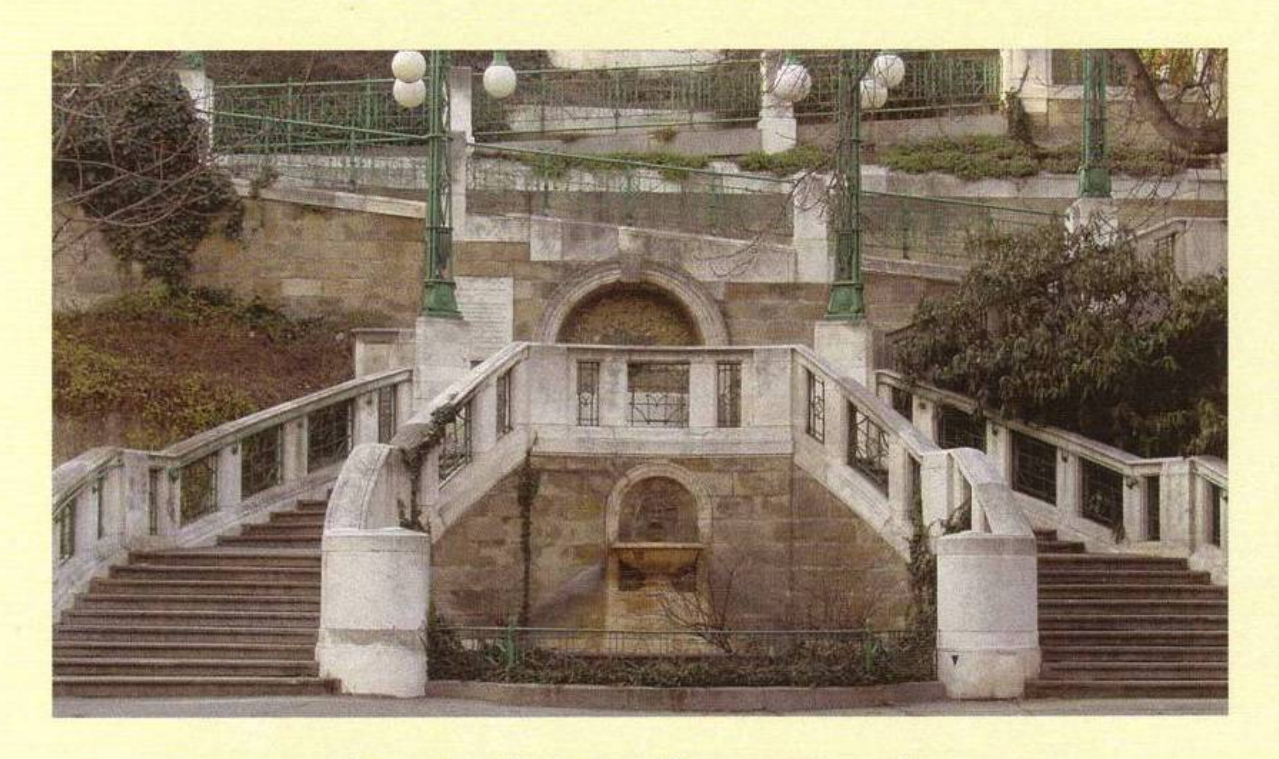
Austrian Society of Biomedical Engineering

International FES Society (IFESS)

8th VIENNA INTERNATIONAL WORKSHOP ON FUNCTIONAL ELECTRICAL STIMULATION

Basics, Technology, Application

Vienna, September 10th - 13th, 2004



Strudlhofstiege, Vienna, Austria

PROCEEDINGS

ISBN 3-900928-07-9

Proceedings

8th Vienna International Workshop on Functional Electrical Stimulation

Vienna, Austria, September 10-13, 2004

Edited by

Manfred Bijak Winfried Mayr Melitta Pichler

Published by

Department of Biomedical Engineering and Physics Medical University of Vienna, Vienna Medical School AKH 4L Währinger Gürtel 18-20 A-1090 Vienna Austria

Tel.: +43-1-40400-1984 Fax: +43-1-40400-3988

http://www.bmtp.akh-wien.ac.at

ISBN 3-900928-07-9

SESSION MOTOR CONTROL AND SPINAL CORD STIMULATION (SCS) 1	
M. Dimitrijevic , I. Persy, C. Forstner, H. Kern, M. Dimitrijevic (Houston, USA) MOTOR CONTROL IN THE HUMAN SPINAL CORD	2
F. Rattay , K. Minassian, B. Jilge, C. Hofer, H. Kern, M. Dimitrijevic (Vienna, Austria) NEUROMODELING AND THE HUMAN SPINAL CORD MOTOR CONTROL: NEURAL RESPONSES TO EPIDURAL STIMULATION	8
K. Minassian , F. Rattay, M. Vogelauer, H. Kern, M. Dimitrijevic (Vienna, Austria) INITIATION AND CONTROL OF LOCOMOTOR LIKE MOVEMENTS IN COMPLETE SCI PERSONS BY EPIDURAL SPINAL CORD STIMULATION	12
R. Herman , W. Willis, J. He, M. Carharts (Phoenix, US) METABOLIC AND PERFORMANCE EVENTS FOLLOWING EPIDURAL SPINAL CORD STIMULATION (ESCS) IN SUBJECTS WITH SPINAL CORD INJURY	16
SESSION 2 MOTOR CONTROL AND SPINAL CORD STIMULATION (SCS) 2	
O. Nikitin, Y. Gerasimenko, D. Okhocimski, A. Platonov, L. Ilieva-Mitutsova (St.Petersburg, Russia) COMBINED CENTRAL AND PERIPHERAL ACTIVATION OF CPG RESULTS IN EFFECTIVE RESTORATION OF LOCOMOTION IN SPINALIZED CATS	18
P. Musienko, I. Bogacheva, Y. Gerasimenko (Sankt-Petersburg, Russia) MECHANISMS OF CPG ACTIVATION IN DECEREBRATED AND SPINALIZED CATS UNDER EPIDURAL SPINAL CORD STIMULATION	19
I. Greshnova (Sankt-Petersburg, Russia) TRANSVERTEBRAL MICROPOLARIZATION IN THE COMPLEX TRIATING OF THE SPINAL DISORDERS: CLINIC EFFECTIVENESS	20
N. Scherbakova, I. Bogacheva, V. Kucher, P. Musienko, Y. Gerasimenko (St. Petersburg, Russia) EMG SIGNAL ANALYSIS OF THE LOCOMOTORY ACTIVITY EVOKED BY	21

MUSCLE WASTING: ROLE OF IGF-1

SESSION 3 FES OF DENERVATED MUSCULATURE 1	
W. Mayr, C. Hofer, D. Rafolt, M. Bijak, H. Lanmueller, M. Reichel, S. Sauermann, E. Unger (Vienna, Austria) THE EU-PROJECT RISE: GENERAL OVERVIEW AND ENGINEERING ASPECTS	24
H. Kern, M. Mödlin, C. Forstner (Vienna, Austria) THE RISE PATIENT STUDY: FES IN THE TREATMENT OF FLACCID PARAPLEGIA	27
SESSION 4 FES OF DENERVATED MUSCULATURE 2	
U. Carraro, M. Zanin, K. Rossini, M. Fabbian, S. Caccavale, W. Mayr, C. Hofer, H. Kern, C. Forstner, U. Hoellwarth, M. Vogelauer (Padova, Italy) SUSTAINED MYOFIBER REGENERATION IN HUMAN LONG-TERM DENERVATED MUSCLES DECREASES AFTER FES-INDUCED MUSCLE RECOVERY IN SCI SUBJECTS	32
S. Boncompagni , H. Kern, W. Mayr, U. Carraro, F. Protasi (Chieti, Italy) DEGENERATION OF CHRONICALLY DENERVATED HUMAN MUSCLE IS REVERSIBLE	36
W. Rossmanith, R. Bittner, K. Moser-Thier, H. Gruber (Vienna, Austria) METABOLIC CAPACITY OF HUMAN LONG-TERM DENERVATED MUSCLES	39
E. Gallasch , D. Rafolt, G. Kinz, M. Fend, H. Kern, W. Mayr (Graz, Austria) EVALUATION OF FES INDUCED ELASTIC AND VISCOUS JOINT MOMENTS IN PARAPLEGICS WITH DENERVATED MUSCLES	40
M. Reichel, J. Martinek, W. Mayr, F. Rattay (Vienna, Austria) FUNCTIONAL ELECTRICAL STIMULATION OF DENERVATED SKELETAL MUSCLE FIBERS IN 3D HUMAN THIGH - MODELING AND SIMULATION	44
A. Musaro , C. Giacinti, G. Dobrowolny, L. Pelosi, L. Barberi, M. Molinaro (Rome, Italy) INDUCING MUSCLE HYPERTROPHY AS A THERAPEUTIC STRATEGY FOR	48

_		
	SESSION 5 FES OF DENERVATED MUSCULATURE 3	
	S. Salmons , Z. Ashley, H. Sutherland, M. Russold, F. Li, J. Jarvis (Liverpool, United Kingdom)	52
	FES OF DENERVATED MUSCLES: BASIC ISSUES	
	Z. Ashley , H. Sutherland, H. Lanmueller, E. Unger, F. Li, W. Mayr, H. Kern, J. Jarvis, S. Salmons (Liverpool, United Kingdom) DETERMINATION OF THE CHRONAXIE AND RHEOBASE OF DENERVATED LIMB MUSCLES IN CONSCIOUS RABBITS	58
	W. Girsch, C. Hofer, D. Rafolt, W. Rossmanith, G. Weigel, E. Unger, W. Mayr (Vienna, Austria) FES OF DENERVATED TIBIALIS ANTERIOR IN THE PIG MODEL	62
	D. Dow , R. Dennis, J. Faulkner (Ann Arbor, USA) DISTRIBUTION OF REST PERIODS BETWEEN ELECTRICALLY GENERATED CONTRACTIONS IN DENERVATED MUSCLES OF RATS	63
	A. Jakubiec-Puka , K. Krawczyk, H. Chomontowska, D. Biral, U. Carraro (Warszawa, Poland) MORPHOLOGY OF THE 2-MONTH-DENERVATED RAT LEG MUSCLES	67
	D. Danieli , E. Germinario, D. Biral, M. Fabbian, M. Zanin, A. Megighian, H. Kern, U. Carraro, V. Vindigni, C. Hofer, M. Moedlin, W. Mayr (Padova, Italy) THE LONG-TERM DENERVATED RAT MYOFIBER: A NEW CONTRACTILE CELL TYPE	70
	U. Carraro, K. Rossini, M. Zanin, M. Fabbian, W. Mayr, C. Hofer, H. Kern	73
	(Padova, Italy) A NEW FAST AND RELIABLE SDS PAGE TO QUANTIFY TOTAL PROTEIN AND MYOSIN HEAVY CHAIN IN CRYO-SECTIONS OF NEEDLE BIOPSY SHOWS THAT LONG-TERM PERMANENT DENERVATED HUMAN MUSCLES RECOVER BY FES TRAINING	
	SESSION 6 LOWER EXTREMITIES: BASICS	
	A. Wernig , R. Schäfer, U. Knauf, M. Zweyer, O. Högemeier, R. Mundegar, G. Wernig, M. Wernig (Bonn, Deutschland)	76
	LITTLE EVIDENCE FOR CONTINUAL MUSCLE FIBER REPAIR BY PRESUMED CIRCULATING STEM CELLS.	
	A. Wernig , U. Knauf, R. Schäfer, M. Zweyer, R. Mundegar, T. Partridge (Bonn, Deutschland)	77
	FOLLOW UP OF HUMAN MYOGENIC CELLS FROM DONORS AGED 2- 82 YEARS	

TABLE OF CONTENTS

A. Thrasher , G. Graham, M.R. Popovic (Toronto, Canada) ATTEMPTS TO REDUCE MUSCLE FATIGUE BY RANDOMIZING FES PARAMETERS	80
E. Spaich, L. Arendt-Nielsen, O. Andersen (Aalborg, Denmark) REPETITIVE PAINFUL STIMULATION PRODUCES AN EXPANSION OF WITHDRAWAL REFLEX RECEPTIVE FIELDS IN HUMANS	84
E. Cacho , A. Cliquet Jr. (São Paulo, Brazil) THE EFFECT OF GAIT TRAINING WITH NEUROMUSCULAR ELECTRICAL STIMULATION ON THE ELECTROMYOGRAPHIC ACTIVITY IN PARAPLEGIC PATIENTS	88
H. Cerrel Bazo (Arcugnano, Italy) NEUROLOGICAL REHABILITATION, PLASTICITY AND ACTIVITY MEDIATED ASPECTS: A ROLE FOR LOCOMOTOR GENERATING ACTIVITY AND THE RESIDUAL POTENTIAL ON SCI INDIVIDUALS THROUGH FES WALKING?	92
SESSION 7 LOWER EXTREMITIES: GAIT	
M. Bijak, M. Rakos, C. Hofer, W. Mayr, M. Strohhofer, D. Raschka, H. Kern (Vienna, Austria) STIMULATION PARAMETER OPTIMISATION FOR FES SUPPORTED STANDING UP AND WALKING IN SCI PATIENTS	94
J. Van Vaerenbergh , S. de Ruijter, A. De Kegel, S. Vandenberghe, Y. D'Hont, L. Briers (Gent, Belgium) QUALITY AND SAFETY OF GAIT IN STROKE PATIENTS USING A DROPPED FOOT STIMULATOR	98
A. Olenšek, Z. Matjačić, T. Bajd (Ljubljana, Slovenia) STUDYING GAIT PATTERN WHEN EMULATING MUSCLE CONTRACTURE	102
J. Szecsi, S. Krafczyk, A. Straube, J. Quintern (München, Germany) FUNCTIONAL ELECTRICAL STIMULATION: PROPELLED CYCLING OF PARAPLEGICS - AN OCCUPATIONAL PHYSIOLOGICAL APPROACH	106
Z. Matjačić , S. Rusjan, I. Stanonik, N. Goljar, A. Olenšek (Ljubljana, Slovenia) METHODS FOR DYNAMIC BALANCE TRAINING DURING STANDING AND STEPPING	109
H. El Makssoud , S. Mohammed, P. Fraisse, P. Poignet, D. Guiraud (Montpellier, France) CONTROL OF THE KNEE JOINT UNDER FUNCTIONAL ELECTRICAL STIMULATION - SIMULATION RESULTS BASED ON A NEW PHYSIOLOGICAL MUSCLE MODEL	113

TABLE OF CONTENTS

C. Schmitt, P. Métrailler, J. Fournier, M. Bouri, R. Clavel, R. Brodard, A. Al-Khodairy (Lausanne, Switzerland) THE MOTIONMAKER TM : A REHABILITATION SYSTEM COMBINING AN ORTHOSIS WITH CLOSED-LOOP ELECTRICAL MUSCLE STIMULATION	117
SESSION 8 SENSORS AND CONTROL	
D. Rafolt , W. Mayr, E. Gallasch, K. Vetter, S. Sauermann, H. Lanmueller, E. Unger, M. Bijak, M. Reichel, C. Hofer (Vienna, Austria) SATURATION OF THE M-WAVE AMPLITUDE WITH INCREASING STIMULATION AMPLITUDE	122
G. Kurstjens , N. Rijkhoff, A. Borau, A. Rodríguez, J. Vidal, T. Sinkjær (Aalborg, Denmark) INTRAOPERATIVE RECORDING OF SACRAL ROOT NERVE SIGNALS IN HUMAN	125
I. Cikajlo, Z. Matjačić, T. Bajd, R. Futami, N. Hoshimiya (Ljubljana, Slovenia) SENSORY SUPPORTED FES CONTROL IN GAIT TRAINING OF INCOMPLETE SCI PERSONS	129
S. Sauermann, E. Unger, P. Protz, M. Bijak, D. Rafolt (Vienna, Austria) MICROPROCESSOR BASED INCLINOMETER SENSOR FOR USE IN FES	132
S. Mina, S. Hanke (Wr. Neustadt, Austria) MULTIMODAL, RF BASED BODY AREA NETWORK FOR DEVICE CONTROL	135
T. Watanabe , M. Otsuka, M. Yoshizawa, N. Hoshimiya (Sendai, JAPAN) COMPUTER SIMULATION FOR MULTICHANNEL CLOSED-LOOP FES CONTROL OF THE WRIST JOINT	138
M.B. Popovic, D.B. Popovic (Aalborg, Denmark) HIERARCHICAL HYBRID CONTROL FOR THERAPEUTIC ELECTRICAL STIMULATION OF UPPER EXTREMITIES	142
A. Vette, K. Masani, M.R. Popovic (Toronto, Canada) PHYSICAL IMPLEMENTATION OF A PD CONTROLLER FOR IMPROVING	146

HUMAN BALANCE DURING QUIET STANCE

SESSION)
---------	---

THERAPEUTIC EFFECTS

J. Huber , P. Lisiński, A. Kasiński, M. Kaczmarek, P. Kaczmarek, P. Mazurkiewicz, F. Ponulak, M. Wojtysiak (Poznań, Poland) THERAPEUTIC EFFECTS OF SPINAL CORD AND PERIPHERAL NERVE STIMULATION IN PATIENTS WITH THE MOVEMENT DISORDERS	152
D. Rosselli , M. Magliano, M. Vrola (Giaveno, Italy) THE EFFECTS OF THE ELECTRIC STIMULATION WITH MIDDLE FREQUENCY ON CENTRAL AND PERIPHERAL PALSY	153
T. Keller, M. Ellis, J. Dewald (Zürich, Switzerland) OVERCOMING ABNORMAL JOINT TORQUE PATTERNS IN PARETIC UPPER EXTREMITIES USING TRICEPS STIMULATION	154
W. Gruther, C. Zöch, R. Crevenna, T. Paternostro-Sluga, C. Spiss, P. Kraincuk, F. Kainberger, R. Peceny, M. Quittan (Vienna, Austria) ASSESSMENT OF MUSCLE LAYER THICKNESS OF QUADRICEPS MUSCLE IN INTENSIVE CARE UNIT PATIENTS DURING A PERIOD OF NMES TREATMENT USING ULTRASONOGRAPHY - PRELIMINARY DATA	158

session 10

VARIABILITY

TECHNOLOGY: IMPLANTS AND ELECTRODES

V. Simard, B. Gosselin, M. Sawan (Montreal, Canada) AN ANALOG WAVELET PROCESSOR FOR A FULLY IMPLANTABLE CORTICAL SIGNALS RECORDING SYSTEM	164
J. Sacristan , N. Lago, X. Navarro, M. Oses (Bellaterra, Spain) PROGRAMMABLE STIMULATION-RECORDING CIRCUITRY FOR CUFF AND SIEVE ELECTRODES	168
J. Coulombe , S. Carniguian, M. Sawan (Montreal, Canada) A POWER EFFICIENT ELECTRONIC IMPLANT FOR A VISUAL CORTICAL STIMULATOR	172
H. Lanmueller, E. Unger, M. Reichel, Z. Ashley, W. Mayr, A. Tschakert (Vienna, Austria) IMPLANTABLE STIMULATOR FOR THE CONDITIONING OF DENERVATED MUSCLES IN RABBIT	176
P. Meadows , C. Varga, J. Oakley, E. Krames, K. Bradley (Santa Clarita, USA) IMPEDANCE EFFECTS IN SPINAL CORD STIMULATION: CONTACT IMPEDANCE	179

TABLE OF CONTENTS

M. Russold, H. Sutherland, H. Lanmueller, M. Bijak, J. Jarvis, S. Salmons (Liverpool, United Kingdom) EXCITABILITY OF THE COMMON PERONEAL NERVE IN RABBITS, RATS AND MICE	183
A. Elsaify , J. Fothergill, W. Peasgood (Leicester, United Kingdom) A PORTABLE FES SYSTEM INCORPORATING AN ELECTRODE ARRAY AND FEEDBACK SENSORS	187
M. Lawrence, T. Kirstein, T. Keller (Zurich, Switzerland) ELECTRICAL STIMULATION OF THE FINGER FLEXORS USING 'VIRTUAL ELECTRODES'.	191
A. Popović-Bijelić , G. Bijelić, D. Bojanić, N. Jorgovanović, M.B. Popović, D.B. Popović (Aalborg, Denmark) MULTI-FIELD SURFACE ELECTRODE FOR SELECTIVE ELECTRICAL STIMULATION	195
SESSION 11 FES FROM HEAD TO TOE	
G. Novikov, T. Moshonkina (St.Petersburg, Russia) THREE TYPES OF EYE MOVEMENT PATTERNS ELICITED BY ELECTRICAL STIMULATION OF CATS SUPERIOR COLLICULUS AND OCCIPITAL CORTEX: PATTERN OF EYE MOVEMENTS AND RECEPTIVE FIELD PROPERTIES	200
I. Ramn Arine, M. Capoccia, Z. Ashley, H. Sutherland, M. Russold, F. Li, N. Summerfield, S. Salmons, J. Jarvis (Liverpool, United Kingdom) COMPARISON BETWEEN THE POWER OUTPUT OF A SKELETAL MUSCLE VENTRICLE AND OF THE LEFT VENTRICLE IN THE SAME CIRCULATION	201
H. Gollee, S. Coupaud, K. Hunt, D. Allan, M. Fraser, A. McLean (Glasgow, United Kingdom) A FEEDBACK SYSTEM FOR AUTOMATIC ELECTRICAL STIMULATION OF ABDOMINAL MUSCLES TO ASSIST RESPIRATORY FUNCTION IN TETRAPLEGIA	205
J. Rozman , M. Mihic, M. Bunc, T. Princi (Ljubljana, Republic of Slovenia) MODULATION OF PH IN THE STOMMACH OF A DOG BY SELECTIVE STIMULATION OF THE LEFT VAGUS NERVE	209
M. Spinelli, S. Malaguti, M. Lazzeri, G. Giardiello, L. Zanollo, J. Tarantola (Magenta (MI), Italy) DIFFERENT PARAMETERS FOR CHRONIC PUDENDAL NERVE STIMULATION WITH PUDENDAL PERCUTANEOUS IMPLANT (PPI) RELATED ON NEUROGENIC SITUATION	213

TABLE OF CONTENTS

J. Kutzenberger, B. Domurath, D. Sauerwein (Bad Wildungen, Germany)	215
SPASTIC BLADDER IN SPINAL CORD INJURY - 17 YEARS OF EXPERIENCE	
WITH SACRAL DEAFFERENTATION (SDAF) AND IMPLANTATION OF AN	
ANTERIOR ROOT STIMULATOR (SARS).	
C. Sevcencu, N. Rijkhoff, H. Gregersen, T. Sinkjær (Aalborg, Denmark)	218
ELECTRICAL STIMULATION TO INDUCE PROPULSIVE CONTRACTIONS IN THE	
DESCENDING COLON OF THE PIG	

POSTER PRESENTATIONS

M. Emadi , F. Bahrami, M. Yazdanpanah (Tehran, Iran) SIMULATION OF THE STS TRANSFER USING A MLP WITHOUT EMBEDDED INTERNAL FEEDBACK	224
C. Chouard (Paris, France) PRESENT STATUS OF HEARING ELECTRICAL ACTIVATION	226
R. Herman , W. Willis (Phoenix, US) MUSCLE FUEL SELECTION IN GOVERNING PREFERRED RATES OF MOVEMENT: A MOTOR CONTROL ISSUE	227
J. Martinek, M. Reichel, W. Mayr, F. Rattay (Vienna, Austria) ANALYSIS OF CALCULATED ELECTRICAL ACTIVATION OF DENERVATED MUSCLE FIBRES IN THE HUMAN THIGH	228
H. Eike, R. Koch, F. Feldhusen, H. Seifert (Hannover, Germany) CALCULATION OF CURRENT DENSITY DISTRIBUTION IN BIOLOGICAL MATTER WITH THE FINITE ELEMENT METHODE	232
T. Moshonkina , G. Novikov, E. Gilerovich, E. Fedorova, Y. Gerasimenko (St.Petersburg, Russia) STEPPING RESTORATION IN CHRONICALLY SPINALIZED RATS BY TREADMILL TRAINING	235
I. Persy, S. Harkema, J. Beres-Jones, M. Moedlin, H. Kern, K. Minassian, M. Dimitrijevic (Vienna, Austria) IMMEDIATE EFFECT OF MANUALLY ASSISTED TREADMILL STEPPING ON THE MOTOR UNITS ACTIVITY OF LEG MUSCLES IN COMPLETE SPINAL CORD INJURED PATIENTS	236
G. Cosendai , C. de Balthasar, A. Ignagni, R. Onders, K. Bradley, K. Purnell, A. Ripley, J. Mortimer, R. Davis, Y. Zilberman, J. Schulman (Santa Clarita, U.S.A.) PRELIMINARY RESULTS WITH TWO IMPLANTABLE DIAPHRAGM PACING SYSTEMS	240
T. Helgason, P. Gargiulo, F. Johannesdottir, P. Ingvarsson, S. Knutsdottir, V. Gudmundsdottir, S. Yngvason (Reykjavik, Iceland) APPLICATION OF STEREOLITHGRAPHIE IN MONITORING MUSCLE GROWTH INDUCED BY ELECTRICAL STIMULATION OF DENERVATED DEGENERATED MUSCLES	241
INDEX OF AUTHORS	244

Keynote lecture

M.R. Dimitrijevic (Houston, USA)

MOTOR CONTROL IN THE HUMAN SPINAL CORD

M.R. Dimitrijevic*, I. Persy**, C. Forstner**, H. Kern**, M.M. Dimitrijevic*

* Department of Physical Medicine and Rehabilitation, Baylor College of Medicine, Houston, Texas, USA.

** Ludwig Boltzmann Institute for Electrical Stimulation and Physical Rehabilitation, Vienna, Austria

Abstract

Features of the human spinal cord motor control are described using two spinal cord injury models: (i) the spinal cord completely separated from brain motor structures by accidental injury; (ii) the spinal cord receiving reduced and altered supraspinal input due to an incomplete lesion. Systematic studies using surface electrode polyelectromyography were carried out to assess skeletal muscle reflex responses to single and repetitve stimulation in a large number of subjects. In complete spinal cord injured subjects the functional integrity of three different neuronal circuits below the lesion level is demonstrated: First simple mono- and oligosynaptic reflex arcs and polysynaptic pathways. Second propriospinal interneuron system with their cell in the gray matter and the axons in the white matter of the spinal cord conducting activity between different spinal cord segments. And third, internuncial gray matter neurons with short axons and dense neuron contact within the spinal gray matter. All of these three systems participate continuously in the generation of spinal cord reflex output activitating muscles. The integration of these systems and their relative degree of excitation and set-up, produces characteristic functions of motor control. In incomplete spinal cord injured patients, the implementation of brain motor control depends on the profile of residual brain descending input and its integration with the functional neuronal circuits below the lesion. Locomotor patterns result from the establishment of a new structural relationship between brain and spinal cord. The functions of this new structural relationship are expressed as an alternative, but characteristic and consistent neurocontrol. The more we know about how the brain governs spinal cord networks, the better we can describe human motor control. On the other hand such knowledge is essential for the restoration of residual functions and for the reconstruction of new cord circuitry to expand the functions of the injured spinal cord.

Introduction

In this review clinical and neurophysiological features of motor control in spinal cord injured

(SCI) individuals are described using two models. First, motor control is considered in subjects with injury-induced complete division of the spinal cord from brain and brainstem structures, and second, in subjects with incomplete division (Fig.1).

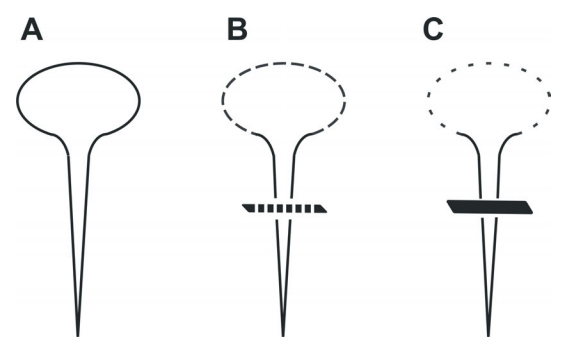


Fig. 1: Schematic drawing of three conditions: fully integrated spinal cord (A), spinal cord partially divided from brain (B) and completely divided (C).

In the complete SCI model motor control is considered as segmental and plurisegmental reflex activity that dominates the motor output to the muscles. In case of incomplete separation of the spinal cord from brain structures, motor control is defined as the manipulation of spinal reflexes and automatic activity by residual descending input. The profile of residual brain and brainstem originated input is modified by the reduction in descending long spinal tract fibers arriving at their targets in the spinal gray matter. This results in characteristic changes in motor output to the muscles that lead to the development of new neural strategies for control of segmental plurisegmental neural circuitry.

Spinal cord interneurons can maintain widespread connections with a variety of motoneurons across a large portion of the spinal cord. Through short- and long-axon spinal interneurons, the degree of excitation/inhibition exerted on motor nuclei of several flexor and extensor muscles can be adjusted so that they contract either alternatively or simultaneously. We argue, that isolated spinal cord neural circuitry is capable of organizing characteristic reflex events and coordinated motor

outputs that depend on the characteristics of the applied stimulus.

Material and Methods

In complete SCI subjects we systematically examined patellar and Achilles tendon jerks and recorded electromyographic (EMG) responses to single stimuli to study segmental organisation and after discharges of stretch reflexes [1].

Functional characteristics of the propriospinal interneuron system were studied by conditioning Achilles tendon jerks with noxious electrical stimuli applied to thoracic, lumbar, and sacral dermatomes [2].

Cutaneo-muscular reflexes and tendon reflexes elicited by repetitive and regular trains of stimulation were studied in complete spinal cord injured and able-bodied subjects [3,4,5].

We also studied a paradigm of spinal cord stimulation in complete spinal cord injured subjects with implanted electrode arrays. The electrodes were placed for spasticity control in the epidural space over the posterior structures of the lumbar cord [6]. Stimulus-induced muscle responses were recorded by surface electrodes placed over the major muscle groups of both lower limbs.

Results

Tendon tap can cause considerable activity in muscles other than the stretched one in complete SCI subjects. The muscles activated during the first 100 ms following the tendon tap are responding according to the normal patterns of reciprocal innervation. The spread of activity after the first 100 ms is due to after-discharge of the motor units of the stretched muscle and of other muscles. The distribution of this after-discharge follows no pattern of reciprocal innervation. However, when activity of the internuncial network is suppressed, features of the segmental reciprocal activity can be demonstrated, particularly by eliciting tendon jerks and simultaneous recording of the EMG responses in the agonist and antagonistic muscle groups.

Conditioning, noxious stimulation applied repetitively to thoracic, lumbar and sacral dermatomes caused descending, ascending and segmental effects in the form of modified ipsilateral and contralateral Achilles tendon responses. This finding of changes in reflex activity reflects excitability spread mediated by intraspinal pathways below the lesion level (Fig. 2).

By applying repetitive and regular stimulation to elicit cutaneous-muscular reflexes or tendon

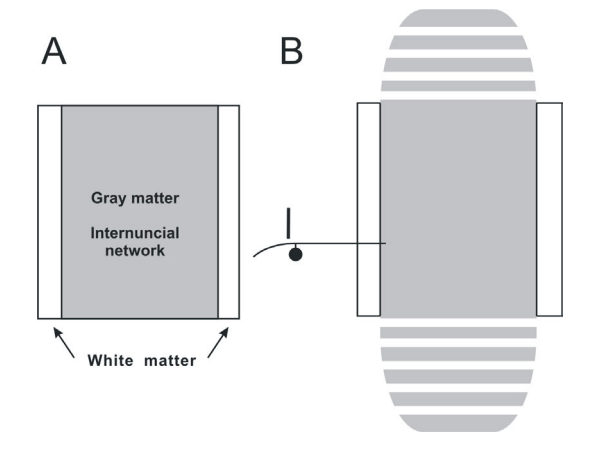


Fig. 2: Sketch of the effect of a single stimulus on cranial and caudal irradiation of the internuncial system in the chronic isolated spinal cord (B).

reflexes, the spinal cord responded with modification of these responses. The successively elicited responses demonstrated a characteristic pattern of: build up of response; fluctuation of response; diminution of activity; cessation of response. The duration of each of these phases depended on stimulus rate and intensity (Fig. 3).

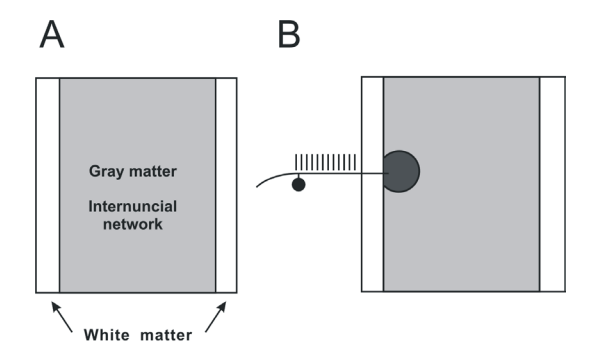


Fig. 3: Effect of repetitive regular nociceptive stimulation in the isolated spinal cord (B). Circular dark area represents the induced presynaptic inhibition with a characteristic local response.

Epidural stimulation of the posterior lumbar cord at 2.2 Hz elicited stimulus-coupled compound muscle action potentials in the lower limbs. The responses had short latencies, which were approximately half that of phasic stretch reflex latencies for the respective muscle groups. Stimulation at 5–15 Hz elicited sustained tonic and at 25–50 Hz rhythmic activity and could initiate lower limb extension or stepping-like movements, respectively (Fig. 4).

Discussion

Studies of SCI subjects with spasticity and clinically complete cord lesions showed that activity of internuncial network below the level of lesion is highly increased and can generate slow,

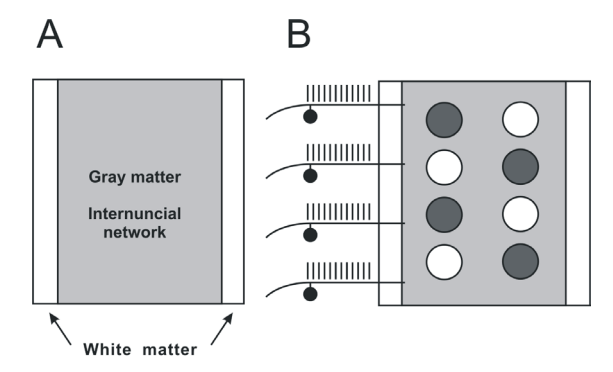


Fig. 4: Schematic drawing of the induced configuration of the locomotor pattern generator by continuous multisegmental input (B). Circular dark areas are representing presynaptic inhibition, white ones indicate excitation.

uncontrolled movements [1,7]. This increased activity of the internuncial gray matter network overrides mono- and oligosynaptic segmental reciprocal organization. The after-discharge is proportional to the amount of local input to the spinal cord. If reduced by any means, also the after-discharge is reduced. As most features of spasticity are due to the after-discharge, a reduction in the local input to the cord removes many features of spasticity. Furthermore, a singleimpulse input resulting in a plurisegmental motor unit activation hints on additional sources of excitatory inputs to the spinal cord interneuronal circuitry from other peripheral inputs cutaneous) or supraspinal sources the incomplete SCI model.

The observed increase of the Achilles tendon jerks by conditioning noxious stimulation applied repetitively to thoracic, lumbar and sacral dermatomes can be explained by excitation spread from distant ipsilateral and contralateral segments. It is likely that this effect is mediated by the fibers of the fasciculi proprii of the spinal cord since this propriospinal system below the lesion level survives complete transection of the spinal cord [8].

When nociceptive stimulus for eliciting flexor reflexes is delivered regularly and repetitively, the previous hyperactive responses can habituate. The cessation of the response is not due to a failure of transmitter substance. Moreover habituation to repeated cutaneous stimuli occurs within internuncial circuits at the same time in all responding muscles.

The question of whether a "lumbar locomotor pattern generator" similar to the Central Pattern Generator for locomotion found in animals exists in humans could not be answered conclusively until a short time ago [9,10]. In the complete SCI

model we have demonstrated, that stimulus induced tonic input with particular frequency (25–50 Hz) to the spinal cord can set up a functional configuration of internuncial interneurons that produces appropriate patterns for stepping movements. We suggest to consider this finding as direct evidence of the presence of pattern generating circuitry responsible for initiation and control of rhythmic activity within the lumbosacral cord [11,12,13].

In incomplete SCI patients, the organization of brain motor control depends on the profile of residual diffuse or restricted brain descending input and its integration within the spinal network below the lesion. The locomotor patterns in incomplete SCI patients are consistent and result from the establishment of a new structural relationship between brain and spinal cord caused by SCI. These are expressed as altered neurocontrol, but they are showing repeatable neurophysiological characteristics of motor unit activity.

References

- [1] Dimitrijevic M.R., Nathan P.W.: Studies of spasticity in man. 2. Analysis of stretch reflexes in spasticity. Brain, 90, Part II, 1967, 333-358
- [2] Faganel J., Dimitrijevic M.R.: Study of propriospinal interneurone system in Man. Cutaneous exteroceptive conditioning of stretch reflex. J. of the Neurological Sciences. 1982, 56, 155-172
- [3] Dimitrijevic M.R., Nathan, P.W.: Studies of spasticity in man. 4. Changes in flexion reflex with repetitive cutaneous stimulation in spinal man. Brain, 93, 1970, 743-768
- [4] Dimitrijevic M.R., Nathan P.W.: Studies of spasticity in man. 5. Dishabituation of the flexion reflex in spinal man. Brain, 90, Part I 1971, 77-90
- [5] Dimitrijevic M.R., Nathan P.W.: Studies of spasticity in man. 6. Habituation, dishabituation and sensitization of tendon reflexes in spinal man. Brain, 96, Part II, 1973, 337-354
- [6] Pinter M.M., Gerstenbrand F., Dimitrijevic M.R.: Epidural electrical stimulation of posterior structures of the human lumbosacral cord: Control of spasticity. Spinal Cord, 38, 2000, 524-531
- [7] Dimitrijevic M.R., Nathan P.W.: Studies of spasticity in man. Some features of spasticity. Brain, 90, Part I, 1967, 1-30

- [8] Nathan P.W., Smith M.C.: Fasciculus proprii of the spinal cord in man – Review of present knowledge. Brain, 82, 1959, 610-668
- [9] Illis L.S.: Is there central pattern generator in man. Paraplegia, 33, 1995, 239-240
- [10] Bussel B., Roby-Brami A., Neris O.R., Yakovleff A.: Evidence for a spinal stepping generator in man. Paraplegia, 34(2), 1996, 91-92.
- [11] Dimitrijevic M.R., Gerasimenko Y., Pinter M.M.: Evidence for a spinal central pattern generator in humans. Ann. NY Acad. Sci., 860, 1998, 360-376
- [12] Minassian K., Jilge B., Rattay F., Pinter M.M., Binder H., Gerstenbrand F., Dimitrijevic M.R.: Stepping-like movements in human with complete spinal cord injury induced by epidural stimulation of the lumbar cord: Electromyographic study of compound muscle action potentials. Spinal Cord 2004 (in press).
- [13] Jilge B., Minassian K., Rattay F., Pinter M.M., Gerstenbrand F., Binder H., Dimitrijevic M.R.: Initiating extension of the lower limbs in subjects with complete spinal cord injury by epidural lumbar cord stimulation. Exp Brain Res, 154, 2004, 308-326

Acknowledgements

We like to express our appreciation to Karen Minassian for his assistance in developing this manuscript.

Author's Address

Prof. Milan R. Dimitrijevic, M.D., D.Sc., Department of Physical Medicine and Rehabilitation, Baylor College of Medicine, 6550, Fannin Suite 1421, Houston, Texas 77030, USA

e-mail: naisus@cs.com

Session 1

Motor Control and Spinal Cord Stimulation (SCS) 1

Chairpersons:

M.R. Dimitrijevic (Houston, USA) F. Rattay (Vienna, Austria)

NEUROMODELING AND THE HUMAN SPINAL CORD MOTOR CONTROL: NEURAL RESPONSES TO EPIDURAL STIMULATION

F. Rattay*, K. Minassian**, B. Jilge*, C. Hofer**, H.Kern**, M.R. Dimitrijevic***

* TU-BioMed, Vienna University of Technology, Austria

** Ludwig Boltzmann Institute for Electrical Stimulation and Physical Rehabilitation, Vienna, Austria

*** Department of Physical Medicine and Rehabilitation, Baylor College of Medicine, Houston, Texas, USA

Abstract

Bipolar electrodes placed in the dorsomedial epidural space at lower (lumbosacral) spinal cord levels stimulate only sensory fibers of the spinal rootlets when amplitudes of 210 µs pulses are restricted to 10 Volt. For bypassing axons, spike initiation occurs close to the cathode. Sensory fibers located below the cathode level are stimulated at their entry point into the spinal cord. Dorsal column axons and other neural elements within the spinal cord are not directly stimulated even when they are closer to the electrodes than the excited afferent axons.

In subjects with chronic, complete spinal cord injury single pulses and low frequency stimulation cause synchronized short latency muscle twitches via monosynaptic pathways. Stimulation at, 5-50 Hz activates spinal interneurons that control the motoneuronal discharge, and the transmission through reflex pathways. Stimulation at 5-15 Hz can elicit sustained tonic activity and lower limb extension, and at 25-50 Hz stepping like lower limb movements.

Introduction

Computer simulation of the stimulating effect of electric fields on neural structures, and the analysis of latencies and shapes of electromyographic (EMG) responses are useful tools for understanding the evoked motor activities in the isolated spinal cord circuitry.

Figure 1 shows (A) the arrangement of the stimulating dipole and that of the electrodes for EMG recordings, (B) a scheme for a monosynaptic pathway that causes short latency muscle twitches and a polysynaptic pathway involved in patterned muscle responses and (C) recorded EMG activities demonstrating the differences of both neural pathways with respect to the envelope, latency and shape of the measured signal.

In order to explain the measured effects [1,2] we use a compartment model of a single neuron [3-6] and a simplified network model [7-9].

Material and Methods

Data were obtained from ten subjects with accidental, motor complete spinal cord injury at low cervical or at thoracic level. At vertebral levels ranging from T10 down to L1 they had an implanted epidural electrode array which was operated as a bipolar electrode with a contact separation of 27 mm. The stimulator (ITREL 3, Model 7425, MEDTRONIC) delivered continuous, non-patterned stimulation with 1–10 V at 2.2–100 Hz and asymmetric biphasic pulses with a 210 µs main pulse and a long second pulse for avoiding charge accumulation. Electromyographic activity was recorded with pairs of silver-silver chloride surface electrodes. For details see e.g. [1,2,5,6].

Electric potential distributions were calculated with finite element software ANSYS. The compartment models of the target neurons are based on the CRRSS (Chiu-Ritchie-Rogart-Stagg-Sweeney) model in the form described in [3]. The resulting differential equations were evaluated with software ACSL. Spike initiation points were also analyzed with the activating function concept [3-5,10].

The longer delays through polysynaptic pathways were simulated with a simple model consisting of a single interneuron that modulates the output by presynaptic inhibition and disynaptic (oligosynaptic) excitation of the motoneuron [7,8].

Results

In a first step we calculated the electrical field in the vicinity of the bipolar electrode in order to find the primarily stimulated neural elements (Fig. 2). In the second step the extracellular potential along a neural target pathway is used as input for a compartment model. Two hot spots in the afferent rootlet fibers are closely neighbored: the regions with sharp curvature before the entry point in the spinal cord and the entry point itself where a sudden change of the electric conductivity at the interface between two media support the initiation of action potentials. Both cases result in large values of the activating function, which is proportional to the second derivative of the

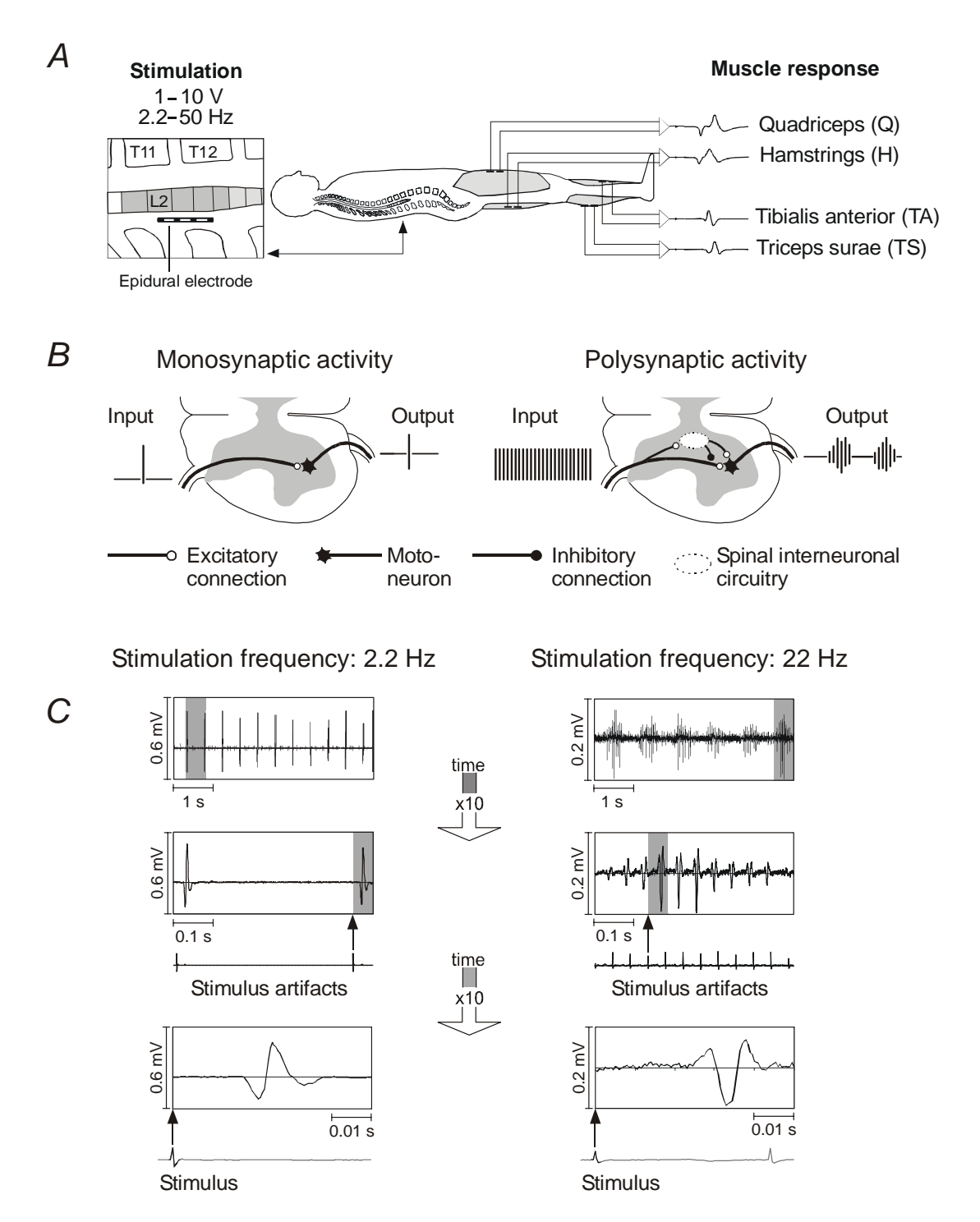


Fig. 1: Outline of the assessment design and analysis of stimulus-evoked EMG responses. (A) all recordings were conducted with the patients in a supine position. Pairs of surface EMG electrodes were placed over the lower limb muscles to assess the effects of epidural stimulation. (B) Neural path diagrams in cross-sections at lumbar segmental levels. Left: single pulse (2.2 Hz-) stimulation activates segmental primary sensory axons and affects monosynaptic excitatory action on motoneurons; right: same afferent structures repetitively stimulated at higher frequencies activate lumbar neuronal circuits that modulate the afferent flow through monosynaptic pathways by putatively presynaptic inhibitory mechanism and control motoneuronal discharge by excitatory oligosynaptic pathways. Sustained stimuli at 25–50 Hz organize the lumbar spinal interneurons by temporarily combining them into locomotor centers that project over several segments and coordinate the neural activity. (C) EMG responses of triceps surae to epidural stimulation at 2.2 Hz and 22 Hz. Potentials marked by gray backgrounds are shown in extended time scale (× 10) below the original EMG. Stimulus artifacts allow the identification of the onsets of applied voltage pulses.

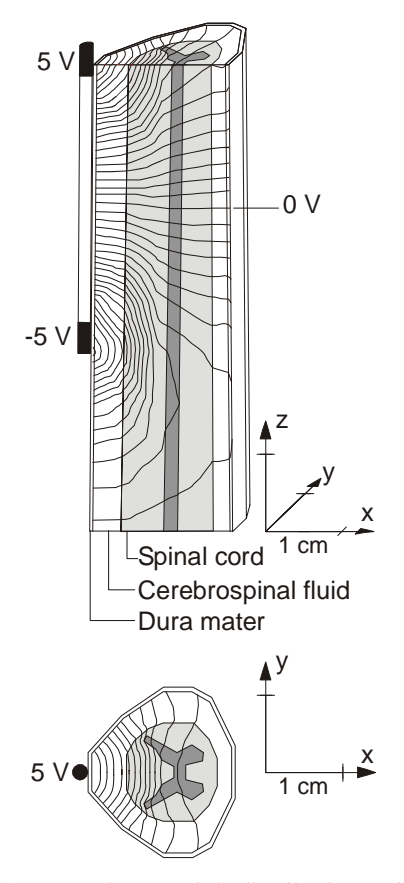


Fig. 2. Computed potential distribution within the dural sac in midsagittal and transversal plane generated by a bipolar electrode with 10 V potential difference between the two contacts.

extracellular potential along the neural pathway for axons with constant fiber parameters [3,5,10].

With the applied stimulus intensities spikes can typically be generated in rootlets which enter the spinal cord up to 2 cm below the level of the cathode (Fig. 3) but there is no spike initiation in the dorsal columns (indicated by vertical black arrow in Fig. 3A).

Already a rather simple three-neuron model (a stimulated afferent axon with a monosynaptic contact to a motoneuron that is influenced by an interneuron by presynaptic inhibition (Fig. 4) is able to mimic a stimulus frequency dependent network output as observed in the EMG recordings (Fig 1C, right pictures). For details see [7,8]. Comparison of the lowest pictures in Fig. 1C shows a longer delay for the polysynaptic response and also a change in the EMG shape. Similarly to the observed temporal characteristics (lowest pictures in Fig. 1C), the model network output switches to the polysynaptic response at higher frequencies as a result of input accumulation at the interneuron which responds with presynaptic inhibition at the sensory-motoneuron contact.

We could further show that the changes in the EMG shape occur gradually during stimulation with constant parameters, e.g., in the extension phase of the lower limb. Every single EMG potential f(t) within the train of patterns can be approximated by a weighted sum of two temporal

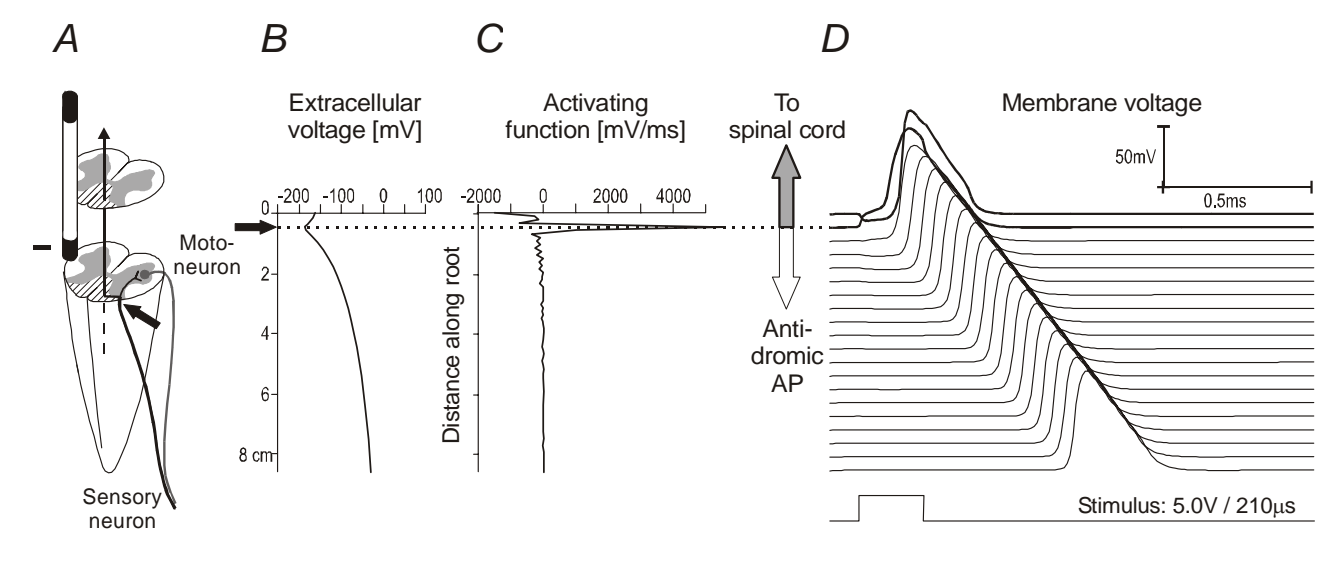


Fig. 3. (A) 3-dimensional view of the lower spinal cord with a sensory fiber (within the posterior root, curved trajectory) and its axonal branches in the back side of the spinal cord (hatched area, vertical arrow) with a single synaptic connection to a motoneuron. Black arrows and the dotted line indicate the "hot spot" for the spike-initiation at the site where the posterior root fiber enters the spinal cord. (B) Extracellular voltage generated by epidural stimulation, (C) activating function and, (D) membrane voltage for an S1-posterior root fiber stimulated 4% above the characteristic fiber threshold with a midsagittal electrode at L4-spinal cord level. Note that the positive part of the activating function is restricted to a single node (peak). In this hot spot an action potential is generated that propagates into the spinal cord and in antidromic direction.

components g(t) and h(t): f=a.g+b.h, where a and b are slowly changing variables [11].

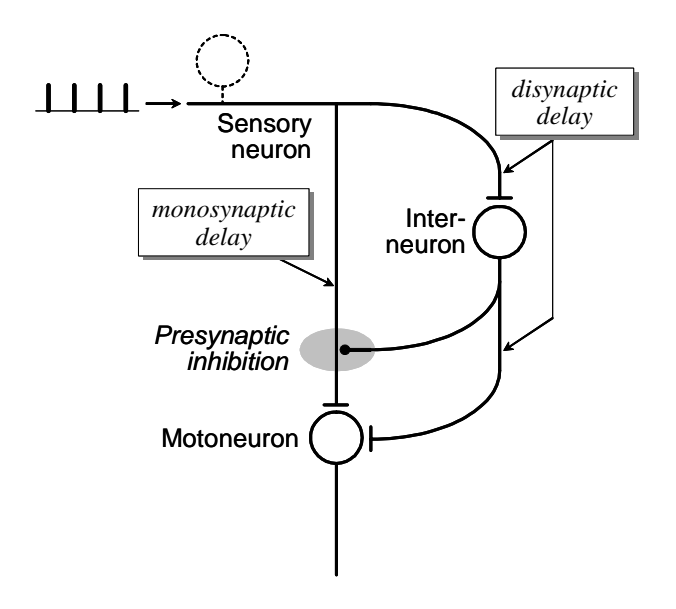


Fig. 4. Model network to simulate the neurophysiologically observed transition from short-(monosynaptic) to long-latency (disynaptic) responses to a sustained train of stimuli. An interneuron exerts inhibitory influence on afferent terminals on a motoneuron. Depending on specific parameters of the model neurons and the frequency of the sensory volley, the network output is either solely mono- or disynaptic or includes both components.

Discussion

In general, the complex interneural network of the spinal cord is not easy to simulate. However, in epidural stimulation of the human lumbar spinal cord we found rather simple relations between the network input, that is, spike initiation in the afferent axons are sharply synchronized to a train of cathodic pulses, and the output. This motoneuronal output, which is indirectly recorded as EMG activity, switches from monosynaptically generated muscle twitches at low frequencies to well defined complex patterns for the extension or for rhythmic stepping like movements of the lower limbs for 5-15 Hz and 25-50 Hz stimulation. respectively [1,2,11]. Also in these cases the motoneuronal firing is always synchronized with the stimuli.

Acknowledgements

We gratefully acknowledge the funding supports from the Austrian Science Fund (project P15469) and the Kent Waldrep National Paralysis Foundation in Addison, Texas, USA.

References

- [1] Dimitrijevic M.R., Gerasimenko Y., Pinter M.M.: Evidence for a spinal central pattern generator in humans. Ann. NY Acad. Sci., 860, 1998, 360-376
- [2] Minassian K., Jilge B., Rattay F., Pinter M.M., Binder H., Gerstenbrand F., Dimitrijevic M.R.: Stepping-like movements in humans with complete spinal cord injury induced by epidural stimulation of the lumbar cord: Electromyographic study of compound muscle action potentials. Spinal Cord, May 4, 2004 [Epub ahead of print]
- [3] Rattay F.: Electrical Nerve Stimulation: Theory, Experiments and Applications. Springer Wien 1990
- [4] Rattay F. The basic mechanism for the electrical stimulation of the nervous system. Neuroscience 89, 1999, 335-346
- [5] Rattay F., Minassian K., Dimitrijevic M. R.: Epidural electrical stimulation of posterior structures of the human lumbosacral cord: 2. quantitative analysis by computer modeling. Spinal cord 38, 2000, 473-489
- [6] Minassian K.: Modeling of a human spinal pattern generator for locomotion and its activation by electrical epidural stimulation. PhD Thesis, Vienna University of Technology, 2004
- [7] Jilge B.: Neurocontrol of standing and walking: Analysis of the electrically stimulated lumbar generator for extension in paraplegic human. PhD Thesis, Vienna University of Technology, 2003
- [8] Jilge B., Minassian K., Rattay F., Dimitrijevic M.R.: Frequency-dependent selection of alternative spinal pathways with common periodic sensory input. Biol. Cybern. (in press)
- [9] Graham B., Redman S.: A simulation of action potentials in synaptic boutons during presynaptic inhibition. J Neurophysiol 71, 1994, 538-549
- [10] Rattay F.: Analysis of models for external stimulation of axons. IEEE-Trans. Biomed. Eng. BME-33, 1986, 974-977
- [11] Jilge B., Minassian K., Rattay F., Pinter M.M., Gerstenbrand F., Binder H., Dimitrijevic M.R.: Initiating extension of the lower limbs in subjects with complete spinal cord injury by epidural lumbar cord stimulation. Exp. Brain Res. 154, 2004. 308-326

Author's Address

DDr. Frank Rattay TU-BioMed Vienna University of Technology Wiedner Hauptstraße 8–10/101 A-1040 Vienna, Austria

e-mail: frank.rattay@tuwien.ac.at

INITIATION AND CONTROL OF LOCOMOTOR-LIKE MOVEMENTS IN COMPLETE SPINAL CORD INJURED PERSONS BY EPIDURAL SPINAL CORD STIMULATION

K. Minassian*, F. Rattay**, M. Vogelauer*, H. Kern*, M.R. Dimitrijevic***

* Ludwig Boltzmann Institute for Electrical Stimulation and Physical Rehabilitation, Vienna, Austria

**TU-BioMed, Vienna University of Technology, Austria

*** Department of Physical Medicine and Rehabilitation, Baylor College of Medicine, Houston, Texas, USA

Abstract

It was previously demonstrated that tonic epidural stimulation of posterior lumbar cord structures can elicit stepping-like electromyographic (EMG) activity in supine individuals with chronic, complete spinal cord injury. In the present paper we emphasize that the patterns and amplitudes of the stimulus-evoked EMG activity is appropriate to induce involuntary stepping-like movements of the paralyzed lower limbs. Ten motor complete spinal cord injured subjects with electrodes placed in the posterior epidural space for spasticity control were included in this study. Surface-recorded EMG responses of the quadriceps, hamstrings, tibialis anterior, and triceps surae muscles to 1-10 V and 2.2–50 Hz stimulation were analyzed. Goniometers were applied to monitor stimulus-induced knee movements. The results were compared with the EMG activity induced in the paralyzed lower limb muscles by manually assisted, weight-bearing treadmill stepping. Non-patterned spinal cord stimulation with 6-10 V at 25-50 Hz induced alternating burst-style EMG activity in the lower limbs leading to involuntary stepping-like movements. Patterned peripheral feedback input associated with passive treadmill stepping generated EMG bursts characterized by low amplitudes and co-activations. This muscle activation was ineffective to induce independent lower limb movement. We suggest that a tonic component of the input delivered to lumbar neuronal circuits is essential to activate locomotor pattern generating networks and to induce stepping movements.

Introduction

Epidural spinal cord stimulation can effectively suppress the excitability within particular motor nuclei and thus reduce spinal spasticity of lower limbs, if the stimulating electrode is located at upper lumbar segmental levels, and the applied stimulus train has frequencies of 50–100 Hz [1]. Stimulation at frequencies below 50 Hz enhances the excitability of lumbosacral motor nuclei. We found that tonic stimulation of the posterior lumbar spinal cord at 25–50 Hz can induce rhythmic

stepping-like EMG activity in supine, complete spinal cord injured (SCI) subjects [2,3]. In the present paper we emphasize that this muscle activity evoked by non-patterned tonic stimulation is effective to *generate* involuntary stepping-like alternating flexion and extension *movements* of the paralyzed lower limbs. The movement is initiated under defined input conditions to the lumbar cord.

Material and Methods

Subjects

The analyses performed in this study are based on stimulus-evoked EMG activity of paralyzed lower limb muscles. These data were obtained from ten subjects with accidental, motor complete SCI at low cervical or at thoracic level (8 x ASIA A, 2 x ASIA B). At the time of data collection the subjects met the following criteria: closed, post-traumatic and chronic SCI; no antispastic medication; preserved stretch and cutaneomuscular reflexes; complete absence of volitional or other suprasegmental activation of motor units below the spinal cord lesion confirmed by brain motor control assessment [4]; and presence of surface recorded lumbosacral evoked potentials [5].

Recording set-up

EMG activity of quadriceps, hamstrings, tibialis anterior, and triceps surae was recorded with pairs of silver-silver chloride surface electrodes. A proximal electrode pair placed over the lumbar paraspinal trunk muscles was used to record stimulus artifacts during spinal cord stimulation. To monitor movements of the lower limbs, position sensors or goniometers were applied bilaterally to the knees.

Epidural Spinal Cord Stimulation

The subjects had an epidural electrode array implanted at some vertebral level ranging from T10 down to L1 (average level T11/T12). Each electrode lead had four cylindrical contacts 3 mm long and 1.27 mm in diameter (PISCES-QUAD electrode, Model 3487A, MEDTRONIC). The electrode array was operated as a bipolar electrode with a contact separation of 27 mm. The stimulator

(ITREL 3, Model 7425, MEDTRONIC) delivered continuous, non-patterned stimulation with 1–10 V at 2.2–100 Hz and a pulse width of 210 μs. During the recording sessions, the subjects were placed in a supine position on a comfortable examination table covered with soft sheepskin. This configuration allowed flexion/extension movements of the lower limbs to unfold smoothly and minimized friction between the heel and the supporting surface. During induced movements the lower limbs were weight-supported by physical therapists if necessary, providing a passive – but not activating – manual antigravity support.

Manually assisted treadmill stepping

Phasic peripheral feedback input to the spinal cord was induced by passive treadmill stepping in three of the studied subjects. The subjects were partially body weight supported, stepping movements were manually imposed by two physical therapists.

Results

Figure 1 displays continuous EMG recordings from lower limb muscles along with a position measuring flexion/extension trace movements of the knee (subject 1, ASIA A). The cathode was located at the T11-T12 intervertebral level. The functional cathode level identified by muscle twitch distribution patterns was at upper lumbar cord segments. Stimulation frequency was 25 Hz and constant, while the stimulation strength was increased in 0.5-Volt steps during continuous recording. At the threshold level of 3.5 V, low amplitude EMG activity was induced in quadriceps (Q). At 4 V the amplitudes of quadriceps activity increased and additionally hamstrings responses of smaller amplitudes were induced. A further increase in stimulation strength to 4.5 V elicited faint activity in the tibialis anterior (TA) and triceps surae (TS) muscles. The EMG activity of quadriceps decreased, while hamstrings showed reciprocal temporal changes in EMG amplitudes. This reciprocal influence is substantially different from muscle twitch responses to 2.2 Hz-stimulation. EMG amplitudes of twitch responses increase with increasing stimulus strength. The sustained stimulus train at 25 Hz and strengths of 3.5, 4 and 4.5 V induced a tonic EMG activity. The lower limb remained in extended position, the muscles were visibly contracting.

Another 0.5 V-increase in stimulation amplitude to 5 V abruptly replaced the tonic EMG activity with rhythmical activity of the lower limb muscles. Phases of burst-style activity alternated with phases of inactivity/low activity. The pattern and strength of the stimulus-evoked muscle activity was appropriate to induce stepping-like, alternating flexion and extension movements. This finding could be repeated in the same subject during different sessions, as well as in different subjects.

Optimal stimulation frequencies for inducing stepping-like lower limb movements were 25–50 Hz. The cathode position had to provide a dominant stimulation of the upper lumbar cord. Such position was characterized by lower activating thresholds of quadriceps than of triceps surae (see muscle recruitment order in Fig. 1). The average vertebral cathode level to obtain this recruitment order was the upper third of T12. The threshold for inducing stepping-like movements was above the level for eliciting responses in quadriceps as well as triceps surae for a given cathode position (Fig. 1). Stimulation generally induced unilateral stepping-like flexion/extension movements. This is a consequence of an asymmetric position of the epidural electrode array with respect to spinal cord structures. In these cases stepping-like movements of the side associated with the lower motor thresholds were induced. The contralateral lower limb responded either with tonic activity or with synchronous

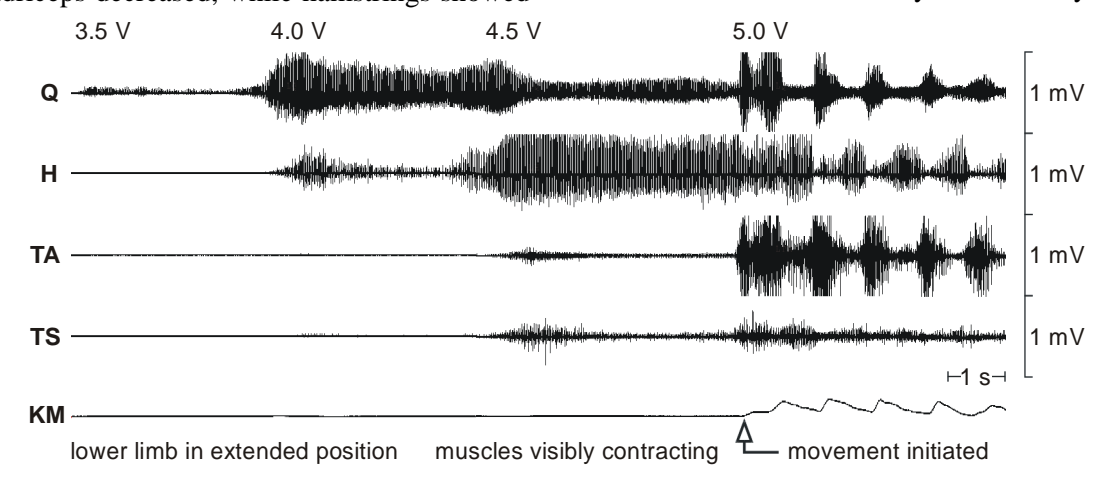


Fig. 1: EMG activity of quadriceps (Q), hamstrings (H), tibialis anterior (TA), and triceps surae (TS) induced by continuous spinal cord stimulation; knee movement sensor (KM). The cathode was at upper lumbar segmental level. Stimulation strength was increased from 3.5 V to 5 V at a constant frequency of 25 Hz (subject 1, ASIA A).

burst-style co-activations.

Figure 2A compares the motor output induced by (i) non-patterned epidural spinal cord stimulation (10 V, 31 Hz) applied in supine position and (ii) by patterned sensory input from the lower limbs related to manually assisted, weight-bearing treadmill stepping. In both cases data was derived from quadriceps (Q) and hamstrings (H) from the same, complete spinal cord injured subject (subject 2, ASIA A). Epidural stimulation elicited alternating burst-style **EMG** activity maximum amplitudes in the range of 200-300 µV and appropriate patterns resulting in rhythmical flexion/extension movements of the lower limbs. Peripheral feedback input related to passive stepping generated EMG bursts which were characterized by low amplitudes (< 50 µV) and coactivation of muscles. No activity was generated in while **EMG** bursts temporally quadriceps, synchronized to the step cycle were induced in hamstrings. Tibialis anterior and triceps surae demonstrated co-activation during the stance phases (not displayed). No independent lower limb movement resulted from this muscle activation. Figure 2B displays burst-style phases in extended time scale of quadriceps (#1) and of hamstrings (#2) induced by spinal cord stimulation. The onsets of applied stimulus pulses are indicated by black dots. During the burst-style phase, each pulse of the stimulus train elicited a single compound muscle action potential (CMAP). The CMAPs were subject well-defined amplitude to modulations resulting in a burst-like shape of the

EMG activity. Between two burst-style phases, the same continuous stimulation induced low-amplitude CMAPs or even failed to elicit any response. Figure 2C demonstrates that the hamstrings activity (#3) induced during the late swing and early stance phase of assisted treadmill stepping is composed of a rather continuous EMG "interference pattern" of low amplitude. Note the difference between the cycle duration of the movement induced by spinal cord stimulation (~1 s) and the step cycle duration during manually assisted treadmill stepping (~3 s, determined by treadmill belt velocity and manually imposed movements).

Discussion

Tonic stimulation of the posterior lumbar spinal cord can induce locomotor-like EMG activity and rhythmic limb movement in supine individuals with chronic, motor complete SCI. Stepping-like movements of the paralyzed lower limbs were initiated under following defined input conditions to the spinal cord: (i) no supraspinal input (ii) insignificant sensory feedback input (lower limbs initially in extended position, no conditioning by leg movement before the onset of stimulus-evoked movements) and (iii) externally-controlled tonic input generated by spinal cord stimulation. When stepping-like movements were induced and maintained by the spinal cord stimulation, conditions were set to minimize afferent feedbackinput from load receptors (see methods). It was shown that afferent feedback input associated with

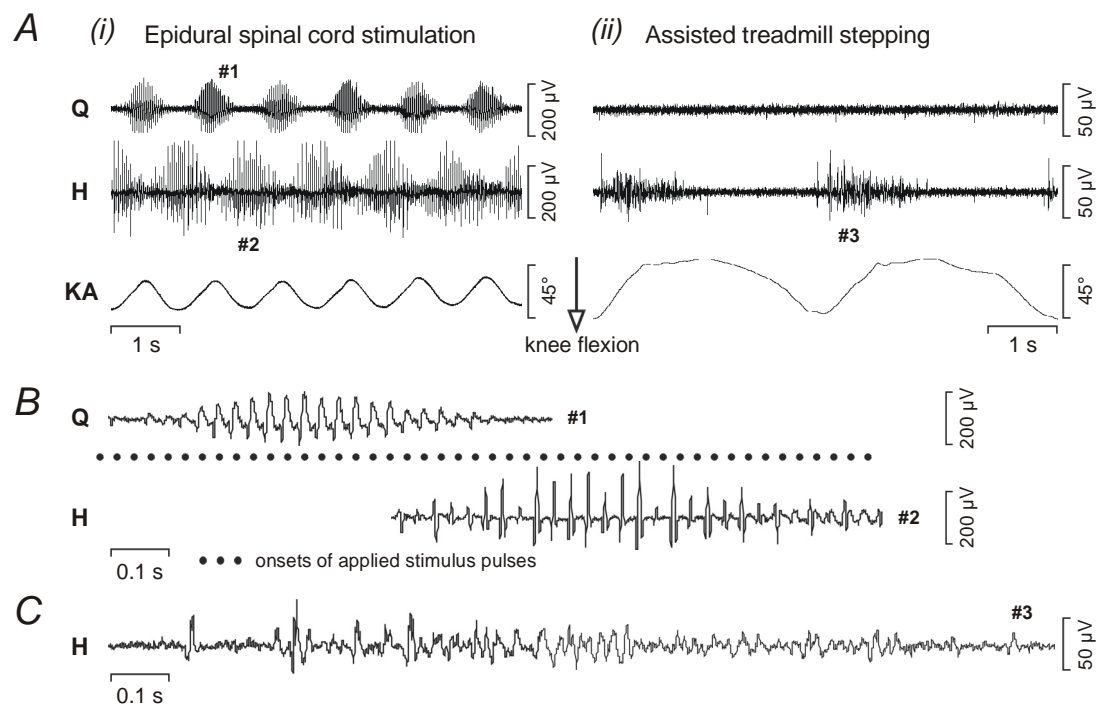


Fig. 2. A: EMG activity of quadriceps (Q) and hamstrings (H) induced by (i) tonic spinal cord stimulation (10 V, 31 Hz) and by (ii) patterned sensory input related to passive treadmill stepping (treadmill speed: 0.33 m/s; body weight support: 50%); knee joint angle (KA); subject 2 (ASIA 2). B, C: Burst-style phases displayed in extended time scale.

"air-stepping" alone is ineffective to induce rhythmic locomotor-like EMG activity in the paralyzed lower limbs [6,7]. Indeed, the analyzed EMG bursts consisted of separate CMAPs which could unequivocally be related to the stimulus-pulse which had triggered it (Fig. 2B). The EMG potentials did not interfere with each other like in the case of passive leg motion-related activity (Fig. 2C).

Epidural stimulation provided a repetitive, regular input to several lumbar and upper sacral cord segments via the posterior roots [3]. While coming from "periphery", the tonic input at a constant frequency is unlike physiological sensory feedback information. We speculate that this tonic input of particular frequencies can partially "mimic" the missing tonic components of brainstem-originated supraspinal driving input to the lumbar cord which had been abolished by accidental SCI. The input generated by spinal cord stimulation was capable of modifying the central state of lumbar networks and of establishing a pattern generating set-up of lumbar neuronal circuits.

Studies have also shown that rhythmic EMG patterns in individuals with clinically complete SCI could be induced when leg movements were assisted externally to provide stepping-related sensory signals to the spinal cord [8,9]. These patterns could not be solely attributed to rhythmic segmental reflexes, such as stretch reflexes [6]. A critical combination of (load- or hip joint-related) afferent signals was essential to generate a stepping-like **EMG** activity. However. independent leg movements resulted from this muscle activation in complete SCI individuals [9]. There was only passive leg motion imposed by the physical therapists. This was also seen in our study (Fig. 2).

Activating spinal pattern generating networks with phasic feedback input to generate functional stepping-like EMG activity in incomplete SCI subjects requires a regular locomotor training for an extended period of time. In complete SCI subjects, stepping-related sensory input to the spinal cord is ineffective to generate lower limb movements. This might be due to a not optimal code of the sensory feedback input used to activate the pattern generating networks, i.e. the lack of tonic components with particular frequencies. Therefore we suggest that sustained stimulation to elicit a multisegmental tonic afferent input with a "central code" to the lumbar spinal cord might be a valuable adjunct to treadmill training in spinal cord injured patients.

References

- [1] Pinter M.M., Gerstenbrand F., Dimitrijevic M.R.: Epidural electrical stimulation of posterior structures of the human lumbosacral cord: 3. Control of spasticity. Spinal Cord, 38(9), 2000, 524-531
- [2] Dimitrijevic M.R., Gerasimenko Y., Pinter M.M.: Evidence for a spinal central pattern generator in humans. Ann. NY Acad. Sci., 860, 1998, 360-376
- [3] Minassian K., Jilge B., Rattay F., Pinter M.M., Binder H., Gerstenbrand F., Dimitrijevic M.R.: Stepping-like movements in humans with complete spinal cord injury induced by epidural stimulation of the lumbar cord: Electromyographic study of compound muscle action potentials. Spinal Cord, May 4, 2004 [Epub ahead of print]
- [4] Sherwood A.M., McKay W.B., Dimitrijevic M.R.: Motor control after spinal cord injury: Assessment using surface EMG. Muscle Nerve, 19(8), 1996, 966-979
- [5] Beric A.: Stability of lumbosacral somatosensory evoked potentials in a long-term follow-up. Muscle Nerve, 11(6), 1988, 621-626
- [6] Harkema S.J., Hurley S.L., Patel U.K., Requejo P.S., Dobkin B.H., Edgerton V.R.: Human lumbosacral spinal cord interprets loading during stepping. J Neurophysiol., 77(2), 1997, 797-811
- [7] Dietz V., Muller R., Colombo G.: Locomotor activity in spinal man: significance of afferent input from joint and load receptors. Brain, 125(12): 2002, 2626-2634
- [8] Dobkin B.H., Harkema S., Requejo P., Edgerton V.R.: Modulation of locomotor-like EMG activity in subjects with complete and incomplete spinal cord injury. J Neurol. Rehabil., 9(4), 1995, 183-190
- [9] Dietz V., Colombo G., Jensen L., Baumgartner L.: Locomotor capacity of spinal cord in paraplegic patients. Ann. Neurol., 37(5), 1995, 574-582

Author's Address

Dr. Karen Minassian
Ludwig Boltzmann Institute for Electrical
Stimulation and Physical Rehabilitation,
Department of Physical Medicine,
Wilhelminenspital der Stadt Wien,
Montleartstraße 37, 1160 Vienna, Austria
e-mail: karen.minassian@wienkav.at

METABOLIC AND PERFORMANCE EVENTS FOLLOWING EPIDURAL SPINAL CORD STIMULATION (ESCS) IN SUBJECTS WITH SPINAL CORD INJURY

Herman R ^{1,2,3}, Willis W ³, He J ², Carharts M ²

Banner Good Samaritan Medical Center, Phoenix, AZ, USA (1) Harrington Dept. of Bioengineering and Arizona BioDesign Institute, Arizona State Univ., Tempe, USA (2)

Department of Kinesiology, Arizona State University, Tempe, USA (3)

We have observed that two incomplete, wheelchair-dependent, Spinal Cord Injury (SCI) subjects ("low ASIA C") trained to elicit rhythmic locomotor patterns following 4 months of Partial Weight Bearing Therapy did not exhibit corresponding changes in preferred rates of walking, endurance and perceived sense of effort (PE) during overground walking.

Hence, a trial of ESCS was conducted. Overground walking was examined: (1) under 2 conditions in one tetraplegic subject (C5,C6), i.e., with (suprasensory, submotor) and without ESCS; and (2) under 4 conditions in one paraplegic subject (T8), i.e. with no stimulation, with FES of the common peroneal nerve to elicit a phase-dependent reflex activity, with ESCS at suprasensory and motor threshold levels with/without FES.

When the ESCS system was implanted to excite upper lumbar neural segments, there was a strikingly rapid switch in locomotion behavior in that endurance and preferred rates of walking increased by 3-fold and sense of effort for a given distance decreased by roughly the same magnitude. ESCS more than FES improved locomotion performance with respect to preferred rates of walking (increasing in order of conditions in the second subject), endurance, PE, and reliance on a walker but improvement in ESCS-related movement kinematics was much less significant. Indirect calorimetry revealed that the enhanced physical performance and attenuation of PE was associated with only a modest reduction in O2 cost of transport; in contrast, ESCS promoted a profound switch in fuel selection by active muscle, increasing the apparent fat oxidation rate by ~ 8-fold.

We posit that the change in fuel selection accounts for the observations of "sense of lightness" of the limbs and reduced PE among MS patients treated with ESCS (Cook and Weinstein, 1973) and for the recovery of functional locomotion at home and community. Recruitment of an oxidative motor unit pool may be a mechanism.

Author's Address

Richard M Herman, Research Director Banner Good Samaritan Medical Center 1111 E. McDowell Rd 85006 Phoenix Arizona US

e-mail: richard.herman@bannerhealth.com

Session 2

Motor Control and Spinal Cord Stimulation (SCS) 2

Chairpersons:

M.M. Dimitrijevic (Houston, USA) R. Herman (Phoenix, USA)

COMBINED CENTRAL AND PERIPHERAL ACTIVATION OF CPG RESULTS IN EFFECTIVE RESTORATION OF LOCOMOTION IN SPINALIZED CATS.

Nikitin O¹, Gerasimenko Y¹, Okhocimski D², Platonov A², Ilieva-Mitutsova L³

I.P.Pavlov Institute of Physiology RAN, St-Petersburg, Russia (1) M.V.Keldysh Institute of Applied Mathematics, RAN, Russia (2) Institute of Mechanics BAN, Sofia, Bulgaria (3)

Recently we have shown, that the epidural stimulation of L4-L5 spinal cord segments evoke locomotorlike movements of hind limbs in decerebrated and spinalized cats. This phenomenon is connected with intraspinal CPG activation. It is known also, that the locomotor training by using forced walking movements can promote the process of restoration of locomotor of spinal cord abilities in spinalized animals. In the present study the comparative analysis of central and peripheral influences effectiveness to the restoration of the locomotor capacities of the spinal cord in chronic spinalized cats was carried out. Locomotor training was provided by special the robotic device. It was shown, that during the month period after spinalization the training of induced stepping by robotic device was not effective in restoration of the stepping. The epidural stimulation alone was not sufficient for generating of walking. Only their combination produce stepping movements. Such 2-month's combined training resulted in the possibility to initiate the stepping only by periphery input. Moreover, 3-4 month later the spinalized cat was capable to realize quadripedal waking on the treadmill belt and on the floor under body supporting. Crosscorrelation analisis of the spinal cord neurogramm and hindlimbs muscles EMG have shown, that the hindlimbs muscles reciprocness is not firmly fixed in spinalized cats spinal cord, but it is composed during waking movements, probably under the influence of afferent input. So, the combination of the central and peripheral (especially- hindlimbs pressure receptors) influences to the CPG is essential in restoration of the locomotor function.

The work is supported by RGNF grant № 03-06-00315.

Author's Address

Oleg Nikitin, I.P.Pavlov Institute of Physiology RAN, St-Petersburg, Russia Makarova, 6 199223 St-Petersburg Russia e-mail: nikitin@pavlov.infran.ru

MECHANISMS OF CPG ACTIVATION IN DECEREBRATED AND SPINALIZED CATS UNDER EPIDURAL SPINAL CORD STIMULATION

Musienko P¹, Bogacheva I¹, Gerasimenko Y¹

Pavlov Institute of Physiology RAN, St. Petersburg, Russia (1)

Micropolarization is the new treating method using direct current and high selectivity of influence.

The aim of the investigation was to study the ability of the spinal cord to produce of stepping pattern in response to the epidural spinal cord stimulation (SCS) in decerebrated and spinalized cats. It was determined that electric stimulation of dorsal surface of lumbar enlargement can evoke the rhythmical movements of hind limbs both in decerebrated, and spinalized animals. The rhythm of movements, interlimb coordination, reciprocity between proximal and distal muscles and between antagonist muscles correspond to stepping. The effective zone for inducing stepping is located in the fourth to fifth lumbar segments in cats. The optimal frequency of epidural stimulation for eliciting of the stepping pattern was 5-10 Hz. The data suggesting the impotance of the weight support and afferent input from foot pressure receptors in initiation locomotion. It was shown that afferent feedback is not a trigger but it acts as a correcting factor. The studies performed on acute spinalized model showed that the role of support and afferent input for generating locomotion significantly increases. One hour after spinal transection the delayed polysynaptic activity arises in the structure of EMG responses to epidural stimulation and becomes more pronounced with time. After 4-6 hours the delayed polysynaptic components combined forming bursts of EMG activity which occurred with certain rhythm. Visually this pattern of EMG activity corresponded to stepping of animals

Fundamental significance of this study is to prove that the spinal cord can produce and control the locomotor pattern. These findings suggest a method which may be applied clinically for the induction of limb alternations following epidural stimulation of the spinal cord. It can be used for the rehabilitation of the patients with vertebrospinal pathology.

Supported by RGNF grant № 03-06-00315.

Author's Address

Pavel Musienko, Pavlov Institute of Physiology RAN, St.Petersburg, Russia Makarova,6 199034 Sankt-Petersburg Russia e-mail: pol-spb@mail.ru

TRANSVERTEBRAL MICROPOLARIZATION IN THE COMPLEX TRIATING OF THE SPINAL DISORDERS: CLINIC EFFECTIVENESS

Greshnova I

Regional Hospital of Ulyanovsk, Ulyanovsk, Russia (1)

Micropolarization is the new treating method using direct current and high selectivity of influence.

The aim of this research is: the investigation of the transvertebal micropolarization (TVMP) effectiveness as treating method, its utilization in complex treating of chronic spinal pathology (spinal trauma, ishemic mielopathy, syringomielia). Similar processes are wide expanded, are badly subjected to traditional therapy and lower the level of patients life. Under the spinal pathology the disturbances of supraspinal control of nerve cells functional state below the injury level is observed and micropolarization permits to restore functional connections lost in the result of pathologic process.

Electromiographic characteristics: latency, duration and amplitude of H-response under the stimulation of n. tibialis served as criterion of TVMP effectiveness. Firstly these parameters were investigated in healthy peoples before and after TVMP under different electrodes localization (4 volunteers: anod in projection of C3 vertebrae, cathode-C5; 4 - opposite localization).

Under the rostral anode localization parameters of H-response changed: latency and duration increased, amplitude decreased, H-response was depressed by the less current strength. These changes evidence about decreasing of neurons excitability. Under the rostral cathode amplitude increased, H-response was depressed by the more current strength. This indicates the increasing of lumbar enlargement motoneurones excitability under TVMP of cervical part of the spinal cord.

Secondly we used TVMP in complex treating of patients. Before and after TVMP neurologic status and H-response parameters were studied. TVMP resulted in positive influence: vegetative disturbances and paresthesia became diminished, pathological muscle tonus decreased. After TVMP curse it was observed the appearance of H-response under the lower current amplitude, enlargement of its amplitude and decreasing of latency. It was proved the effectiveness of TVMP in the norm and pathology

EMG SIGNAL ANALYSIS OF THE LOCOMOTORY ACTIVITY EVOKED BY EPIDURAL SPINAL CORD STIMULATION.

Scherbakova N¹, Bogacheva I¹, Kucher V¹, Musienko P¹, Gerasimenko Y¹

Pavlov Institute Physiology of the Russian Academy of Science, St. Petersburg, Russia (1)

The recent experimental researches evidence that the spinal cord (SC) of mammals, including human, contains a network of interneurons acting as generator of stepping movements – central pattern generator (CPG). Such network produces coordinated rhythmical patterns activity, providing the locomotion. For this purposes we analysed the electromyographyc activity (EMG) of the leg muscles in response to electrical epidural stimulation of the spinal cord dorsal surface in the decerebrated cat. We used the frequencies of stimulation in range from 1 to 20 Hz with the current amplitude twice exceeded the threshold amplitude for reflectory responses of leg muscles. It was found that the optimal stimulus frequency for eliciting locomotor activity was 5Hz. Methods of EMG analysis with Hilbert transformation was performed for calculation of the EMG envelope so far as just the EMG envelope describes the muscles efforts. Then autocorrelation functions (ACF) were calculated for EMG envelopes for cases with stimulation of different frequencies. The shape of ACF for EMG of m. tibialis ant. (TA) and m. gastrocnemius (GM) to L4 stimulation with 5Hz are different from the shape of ACF calculated for activity of these muscles to stimulation of other frequencies. In particular the marked ACF peaks correspond exactly to the frequency of stimulation in cases of non-optimal frequencies, while in case of 5Hz stimulation these peaks are insignificant relatively whole ACF and new peaks appear at frequency about 1 Hz. Crosscorrelation analysis of the relation between EMG and stimulus signals reveals the marked weakening of the relation of the EMG activity patterns with stimulus impulse successions for 5Hz stimulation only. The results of our investigations allow us to speculate about the mechanisms of initiation the CPG and locomotion triggering. It is possible that the CPG works in regimen of taking the phase under non-optimal stimulus frequencies (with response on each stimulus impulse). But under certain optimal stimulus frequency the CPG turns into the regimen of its own fluctuations and produces the rhythmic locomotor pattern. The experimental data shows that the generation of locomotor activity continues after the cessation of the stimulation with the same properties of the bursting activity.

Supported by RGNF grant № 03-06-00315.

Session 3

FES of Denervated Musculature 1

Chairpersons:

S. Salmons (Liverpool, UK) W. Mayr (Vienna, Austria)

THE EUROPEAN PROJECT RISE: GENERAL OVERVIEW AND ENGINEERING ASPECTS

W. Mayr *, C. Hofer **, D. Rafolt *, M. Bijak *, H. Lanmueller *, M. Reichel *, S. Sauermann *, E. Unger *

*Dept. of Biomedical Engineering & Physics, Medical University of Vienna, Austria

**L. Boltzmann Inst. for Electrical Stimulation & Physical Rehabilitation, Wilhelminenspital Vienna

Abstract

It was and rather commonly still is general believe that restoration of denervated degenerated musculature (DDM) or even slowing down the muscular atrophy and the degeneration process after denervation is impossible. In contrast to this believe recent experimental and clinical work gives strong evidence that functional electrical stimulation (FES) is a powerful tool for regeneration, functional restoration and maintenance of denervated muscles.

Based on these promising preliminary findings the European project RISE was established within the 5th Framework Program to develop an efficient rehabilitation method and the associated technical equipment for the treatment of flaccid paraplegia. The project started with November 2001, has a lifetime of 4 years and includes 10 primary contractors, 3 additional contractors and 6 subcontractors from Austria, UK, Italy, Germany, Slovenia and Island.

The experimental and clinical results acquired so far have confirmed the sustained regenerative and myogenetic capacity of DDM even after denervation periods of more than 10 years. Restoration of heavily degenerated musculature requires years of daily training with biphasic long duration impulses, initially with durations of up to 300 ms, later gradually reduced to 30 - 40 ms. For post denervation time spans of less than about 2 years the dominant mechanism of muscle wasting is obviously atrophy and functional restoration of the musculature is significantly easier and less time consuming. The studies within RISE are ongoing and final results will be available with the end of 2005.

Introduction

Practically all established clinical FES applications are based on direct excitation of neural structures and in case of muscle functions indirect activation of the muscles. For the functional activation of denervated and especially denervated degenerated muscles (DDM) the technical requirements differ substantially from those for nerve stimulation. Due

to the absence of the neuromuscular junction and decomposition of motor units muscular contractions can only be elicited by depolarizing the cellular membrane of each single muscle fiber. The electrical membrane excitability strongly depends on the state of degeneration or restoration of the muscle cell, but in any case it is much lower than the excitability of a nerve cell.

As we know from preliminary experimental and clinical work, biphasic rectangular impulses with durations between 30 and 300 ms - the later in case of long term denervation and severe degeneration have to be applied in order to achieve contractions in DDM. Consequently also the required amplitude values are significantly higher than for comparable nerve stimulation. The recruitment of a sufficient fiber population is depending on a homogenously distributed electrical field more or less concentrated on the target muscle. The later condition is essential to minimize unwanted co-contractions of adjacent other muscles and intact neural structures in the adjacent tissue. Biphasic rectangular impulses are obviously the most efficient impulse shape for FES of DDM. In selected cases biphasic ramp-shaped impulses are advantageous. Those are less efficient in force development, but provide a significantly reduced excitation of neural structures lying within the stimulating electric field.

A severe problem that strongly inhibits the application of FES on denervated muscles lies in the current EU regulations for stimulators that limit the output energy to 300 mJ per impulse. This is by far not enough to elicit functionally usable contractions in denervated muscles, unless they are very small and not degenerated. To induce strong fused contractions is in addition to functional aspects not at least an important condition for an efficient muscle training.

The first real functional application on FES of denervated muscles was published by Valencic et. al. in 1986. He has demonstrated correction of dropped foot by stimulating the denervated tibialis anterior muscle in a patient study [1].

Based on the results from an extensive experimental study on sheep [2,3], where implanted

electrodes were used, and very promising preliminary clinical results with surface electrode based FES [4,5] we have successfully applied for the EU-project RISE: "Use of electrical stimulation to restore standing in paraplegics with long-term denervated degenerated muscles" that started with November 2001.

Material and Methods

The target patient group is the population of persons with flaccid paraplegia. This kind of paralysis is caused by a lesion in the region of the cauda equina, the lowest part of the spinal column. In this case the lowest part of the spinal cord respectively the originating spinal roots are concerned and the resulting damage of the lower motor neuron leads to a denervation of the more or less entire lower extremity musculature. Such an injury concerns about 20 persons per million EU citizens every year, about one third of all spinal cord injuries that result in paraplegia.

The objectives of RISE are

- 1) Development of a new efficient rehabilitation method for the target patient group, transferable to clinical practice
- 2) Development of the associated stimulation equipment for home based training, and test and measurement equipment for outpatient supervision, ready for transfer to industry
- 3) Establishing a firm scientific basis for adaptation of the EU regulation for stimulation equipment to the needs of FES of denervated musculature.

The project work is organized in 5 work packages:

Workpackages 1 is an experimental study on rabbits that aims in determination of save and efficient stimulation and training parameters first for restoring DDM and in a later phase for maintaining the restored muscle. The work is carried out by Stanley Salmons and his group in Liverpool, UK.

Workpackage 2 is a study on pigs under the responsibility of Werner Girsch in Vienna, Austria. It is dedicated to a transformation of the findings from the rabbit study to a bigger species with a musculature that is better comparable to the human one. In addition the pig provides the opportunity to test surface electrode based patient stimulation equipment under realistic conditions.

Workpackages 3 und 4 are dedicated to technical development of patient stimulation equipment for home based training respectively test and measurement equipment for patient supervision by an outpatient clinic. The development work is performed in Vienna, Austria by Winfried Mayr and colleagues.

Workpackage 5 is a patient study on application of FES in persons with a lesion in the cauda equina that results in a complete flaccid paraplegia. Helmut Kern is responsible for this study that involves 9 clinical centers in Austria, Germany, Italy and Island. Special main topics within this workpackage concern muscle physiology with research focused on muscle regeneration and myogenesis by Ugo Carraro, Padova, Italy and on metabolic capacity by Helmut Gruber, Vienna, Austria, and the development of a comprehensive neurological assessment protocol by Milan Dimitrijevic, Ljubljana Slovenia

The project RISE is coordinated by the first author of this paper.

Results

After passing the Mid-term Review we are now in the second half of the RISE project. We have obtained many preliminary but in most of the tasks of course not jet the final results. Especially all three studies are still under way. Initially we had some unexpected delay in obtaining the animal licenses due to new tightened regulations.

In the rabbit study we had a pilot study with 20 rabbits to obtain basic data for development of stimulation and measurement hardware and the experimental methodology. In addition to a bench stimulator and a dynamometer for the final assessments a battery powered single channel stimulator with a wireless control and programming link was developed. It is capable of delivering biphasic rectangular constant current impulses with up to +/- 10mA and impulse durations between 0,5 and 80ms per phase. The epifascial electrodes for the tibialis anterior muscle and cables are made of stainless steel and silicone. Meanwhile 50 stimulators were implanted. The time course of chronaxy after denervation for up to 36 weeks has been determined and several series applying different stimulation protocols have been started.

In the pig study we have denervation of the tibialis anterior in five animals and are in the phase of determining the time course of denervation with electrophysiological measurements and biopsy analysis for this model.

In the patient study 25 persons out of 93 meeting the inclusion criteria were selected for the study. Following the developed assessment protocol primary electrophysiological, biomechanical and biopsy data were obtained and therapy with a

standardized stimulation protocol was started. In a pilot phase data - including biopsy data - were obtained from pre-RISE patients with different state of muscle degeneration and FES induced restoration.

Within the technology workpackages the first generation of stimulation equipment for patients was developed: It is a dual channel version programmed by a Palm PDA via infrared link and powered by rechargeable batteries. It is capable of delivering biphasic impulses of various shapes with amplitudes of up to +/-80V and lengths of up to 150ms per phase (Fig. 1).

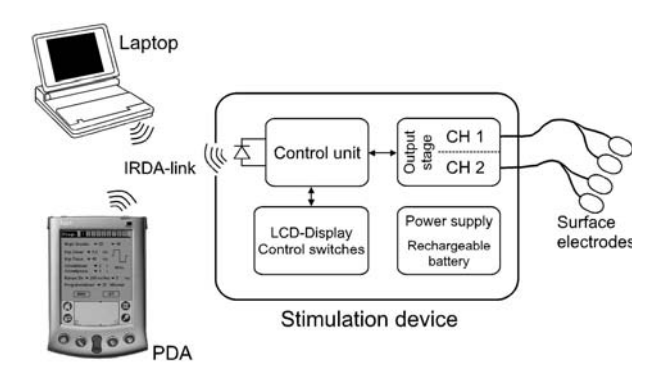


Fig. 1: Schematic diagram of the surface electrode based 2-channel stimulator for denervated musculature

For save and comfortable electrode application we work on electrode garments with integrated electrodes and cables that have to be made in such a way that the user is able to handle them when sitting in a wheel chair. To obtain valid data from even very far degenerated musculature new measurement techniques had to be developed. A pendulum test measures resistance data under different intensities of stimulation even if no muscle reaction is palpable. A twitch sensor applied at the patella tendon provides exact dynamic time constants of quadriceps twitches independently of unavoidable stimulus intensity dependant co-contractions of the antagonistic hamstring muscles.

Discussion

The experimental and clinical results acquired so far have confirmed the sustained regenerative and myogenetic capacity of DDM even after denervation periods of more than 10 years. Restoration of heavily degenerated musculature requires years of daily training with biphasic long duration impulses, initially with durations of up to 300 ms, later gradually reduced to 30 - 40 ms. For post denervation time spans of less than about 2 years

the dominant mechanism of muscle wasting is obviously atrophy and functional restoration of the musculature is significantly easier and less time consuming.

The studies within RISE are ongoing and final results will be available with the end of 2005.

References

- [1] Valencic V, Vodovnik L, Stefancic M, Jelnikar T. Improved motor response due to chronic electrical stimulation of denervated tibialis anterior muscle in humans. Muscle Nerve 9: 612-617, 1986.
- [2] Carraro U, Catani C, Saggin L, Zrunek M, Scabolcs M, Gruber H, Streinzer W, Mayr W, Thoma H: Isomyosin changes after functional electrostimulation of denervated sheep muscle. Muscle Nerve 11:1016-1028, 1988.
- [3] Zrunek M, Bigenzahn W, Mayr W, Unger E, Feldner-Busztin H. A laryngeal pacemaker for inspiration controlled direct electrical stimulation of denervated posterior cricoarytaenoid muscle in sheep. Eur Arch Otorhinolaryngol 248(8):445-448, 1991.
- [4] Kern H, Hofer C, Moedlin M, Forstner C, Raschka-Hoegler D, Mayr W, Stoehr H: Denervated muscles in humans limitations and problems of currently used functional electrical stimulation training protocols. Artif Organs 26(3): 216-218, 2002.
- [5] Mayr W, Hofer C, Bijak M, Rafolt D, Unger E, Sauermann S, Lanmueller H, Kern H. Functional Electrical Stimulation (FES) of denervated muscles: existing and prospective technological solutions. Basic Appl Myol 12(6): 287-290, 2002

Acknowledgements

Supported by EU Commission Shared Cost Project RISE, Contr. Nr. QLG5-CT-2001-02191 and Austrian Ministry of Education, Science and Culture.

Author's Address

Prof. Winfried Mayr Center of Biomedical Engineering and Physics Vienna Medical University Währinger Gürtel 18-20/4L A-1090 Vienna, Austria e-mail: winfried.mayr@meduniwien.ac.at home page: www.bmtp.akh-wien.ac.at

THE RISE PATIENT STUDY: FES IN THE TREATMENT OF FLACCID PARAPLEGIA

H. Kern, M. Mödlin, C. Forstner

* Ludwig Boltzmann Institute of Electrostimulation and Physical Rehabilitation, Department of Physical Medicine, Wilhelminenspital Wien, Vienna Austria

Introduction

The aim of the "RISE"-project is to develop a new rehabilitation method for patients with Long Term Denervated Degenerated Muscles (DDM) and to create a systematic body of basic scientific knowledge about the restorative effects of Functional Electrical Stimulation (FES).

With this scientific basis

- existing EU Regulations governing the use of electrical stimulation which currently exclude the possibility of therapeutic use in patients with DDM should be revised.
- equipment should be constructed and designed and brought to the point of commercial adoption.
- new diagnostic and measurement equipment for monitoring the progress of the therapy should be designed and constructed.

Material and Methods

Until now 28 patients (23 men, 5 women), 54 legs met the inclusion criteria of a flaccid paraplegia of the m. quadriceps femoris.

Paraplegia was caused by traumatic fracture mostly of Th 11 and 12 (Th 5 - L 1). At the beginning of the study the mean age of men was 36 yrs, of women 43 yrs. The mean denervation time in men was 4.9 yrs, in women 5.8 yrs. Mean weight of men was 77.8 kg, of women 64.8 kg, mean height of men 179 cm, of women 164 cm.

Patients who met the inclusion criteria were invited to Vienna. They were informed about the project and had to give their informed consent.

Afterwards all patients followed a clinical protocol and had to undergo the following assessments.

To achieve a more accurate description of the type of lesion and the remaining motor and sensory function and to be sure that m.

quadriceps fem. is completely denervated, we use apart from the conventional examinations a series of methods.

Electrical stimulation test of m. quadriceps:

Two rubber electrodes, each inside a wet sponge bag, are positioned above the thigh (m. quadriceps fem.). The muscle is stimulated with defined electrical stimuli (impulse duration 145ms, 42ms, 5ms, 2.6ms and 1.3ms). The contraction of the m. quadriceps fem. is tested manually on the muscle belly and the patella.

Needle EMG of m. rectus femoris:

The m. rectus femoris is examined by inserting the needle in different depths and four directions. When necessary additional needle EMG will be performed in m. vastus lateralis and medialis. Insertion activity, spontaneous activity during relaxation (fibrillation potentials, positive sharp waves) and volitional activity are assessed. Needle EMG examination is completed by stimulation of femoral nerve at the groin with a supramaximal single stimulus in order to elicit an M- wave.

BMCA – Brain Motor Control Assessment (Assessment of motor control in spinal cord injury):

Multichannel surface EMG recordings are used to document the absence of reflexes and motor unit action potentials during attempts of volitional movements. We use a standardised sequence of motor tasks with the subject in a supine position to characterise features of motor control. [1]

Transcranial and lumbosacral magnetic stimulation:

Recording conditions are the same as in BMCA. For transcranial stimulation a double coil is placed over Cz and the stimulus amplitude is increased from 30-100% (in steps of 10%). A symmetric response in biceps brachii and thenar must be reached. Lumbosacral stimulation is carried out at the level of Th12, L2, L4 by using a circular coil.

LSEP (Lumbosacral Evoked Potentials):

Surface recorded lumbosacral evoked potentials are used to assess the functions of the posterior structures and grey matter of the spinal cord and the dorsal and ventral spinal roots. To this end evoked potentials induced by stimulation of the tibial nerve (popliteal) are recorded with surface electrodes placed over the vertebral levels S1, L4, L2 and Th12 in reference to a Th6 positioned electrode. Corresponding cortical evoked potentials are additionally recorded with a pair of electrodes. 120 successively evoked potentials are averaged for each channel.

Evoked potentials are analysed for the presence of an R-wave (conducted by sensory axons within the posterior roots), A-wave (reflexively initiated efferent volley conducted by motor axons) and Swave (generated by spinal neurons) and any pathological differences of the waveforms and there latencies from common standard data of healthy subjects.

SSR (Sympathetic Skin Response):

SSR is used for examination of spinal cord injuries and represents an addition for the proof of disturbances of the vegetative nervous system. The response is recorded from the palm and dorsum of the hands and sole and dorsum of the feet. In order to release the sympathetic skin response, the N. medianus is electrical stimulated with a current of 25 mA and a duration of 0.1 ms.

To quantify the morphological status of the thigh the following investigations are done:

CT- Scan

to quantify the muscle cross-sectional area, muscle density and diameter of the cortical bone.

Skin biopsies

Muscle biopsies

for histological, electromicroscopical and biochemical analysis. [2]

Bone density measurements

Based on the experience from our pilot work an electrical stimulation protocol and a special electrical stimulation device especially adapted to the needs of denervated muscles was developed. [3, 4] The patients were carefully instructed how to put on the stimulation electrodes and operate the electrical stimulator. The training with electrical stimulation is carried out by the patient at home

and is adapted regularly throughout the study depending on the condition of the muscle and the findings of the accompanying animal experiments.

In the beginning the training protocol consists of two different stimulation patterns: in one program impulses last 120ms (1.6Hz), 5sec on, 2 sec off, in the other program impulse duration is 40ms (20Hz), 2 sec on, 2 sec off. The daily amount of stimulation per muscle is 15 to 30 minutes. [5]

The electrical stimulation and the force output are checked regularly.

The clinical study is designed as an uncontrolled cohort study. This means that parameters about effectiveness and reliability are collected throughout the therapy.

Results

We compare our data of biopsies of DDM with data of biopsies of 5 years functional electrical stimulated DDM.

The histological and electromicroscopical analysis showed regeneration of myofibers, of metabolism and function of the denervated muscles. [2, 6]

The minimum myofiber diameter of stimulated DDM was analogue to normal muscle or spastically paralysed muscle. In contrast unstimulated DDM showed a much smaller diameter [Fig. 1].

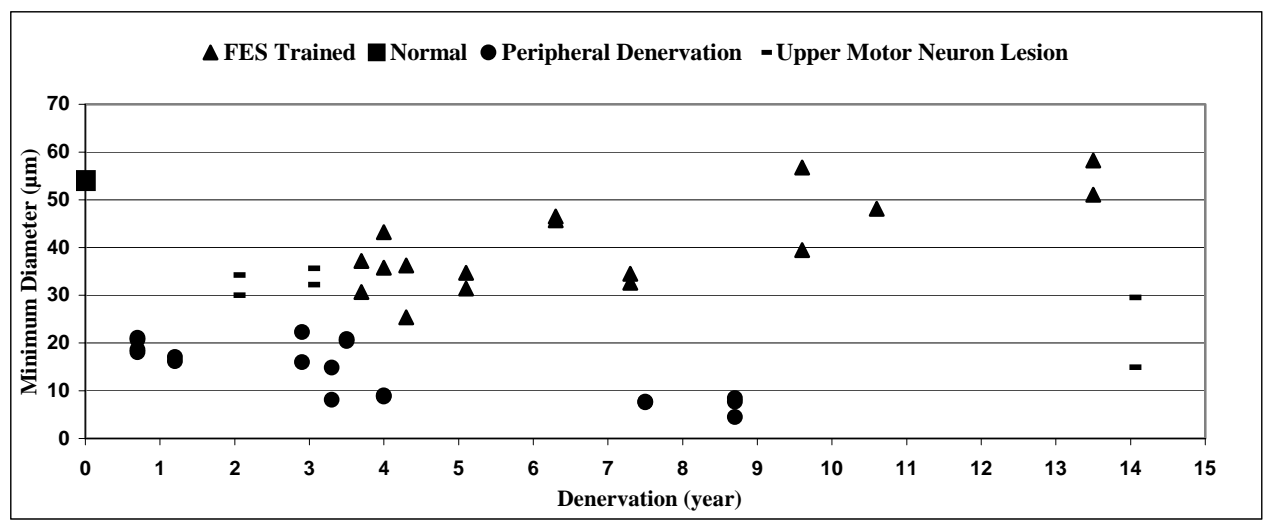


Fig.1 Differences in Minimum Myofiber Diameter between FES Trained DDM, DDM, Normal Muscle and Upper Motor Neuron Lesion - Ugo Carraro - Applied Myology Lab - Padova

References

- [1] Dimitrijevic et al. Neurophysiological assessment of spinal cord and head injury. J Neurotrauma 1992; 9 (Suppl 1): 293-300
- [2] Rossini et al. Stage and quantify regenerative myogenesis in FES-induced functional recovery of human long-term permanent denervated muscle. Basic Appl Myol 2002; 12: 277-286
- [3] Kern et al. Standing Up with Denervated Muscles in Humans Using Functional Electrical Stimulation. Artificial Organs 1999; 23(5): 447-452
- [4] Mayr et al. Functional Electrical Stimulation (FES) of denervated muscles: existing and prospectiv technological solutions. Basic Appl Myol 2002; 12 (6): 289-292
- [5] Kern et al. Denervated muscles in humans: limitations and problems of currently used functional electrical stimulation training protocols. Artif Organs 2002; 26: 216-218
- [6] Kern et al. Recovery of long-term denervated human muscles induced by electrical stimulation, Muscle Nerve (in press)

Acknowledgements

This work was supported by EU Commission Shared Cost Project RISE (Contract No. QLG5-CT-2001-02191).

Author's Address

Univ. Doz. Dr. Dr. Helmut Kern LBI of Electrostimulation and Physical Rehabilitation, Dept. of Physical Medicine Wilhelminenspital

A-1171 Vienna, AUSTRIA Tel.: +43 1 49150 3401

e-mail: Helmut.Kern@wienkav.at

Keynote lecture

U. Carraro (Padova, Italy)

SUSTAINED MYOFIBER REGENERATION IN HUMAN LONG-TERM DENERVATED MUSCLES DECREASES AFTER FES-INDUCED MUSCLE RECOVERY IN SCI SUBJECTS

U Carraro*, ME Zanin*, K Rossini*, M Fabbian*, S Caccavale*, W Mayr**, C Forstner***, U Hoellwarth***, M Vogelauer***, Ch Hofer***, H Kern***

* C.N.R. Institute of Neuroscience, Neuromuscular Section, Laboratory of Applied Myology, Department of Biomedical Science, University of Padova, Italy

** Department of Biomedical Engineering and Physics, University of Vienna, Austria.

***Ludwig Boltzmann Institute of Electrostimulation and Physical Rehabilitation, Vienna, Austria

Abstract

We assess the extent of myofiber regeneration in denervated and degenerated muscle (DDM) during long-term lower motor neuron denervation, and their contribution to FES-induced muscle recovery. Final diagnosis of conus cauda complete lesion was performed at the Department of Physical Medicine, Wilhelminenspital, Vienna, Austria. Muscle biopsies were harvested and sent to the University of Padova Laboratory of Applied Myology. where structural analyses and morphometry were performed. SCI subjects suffering complete conus cauda syndrome (CCCS) were biopsied from 0.7 to 37 years after lesion. After appropriate instruction, patients were able to carry out a functional electrical stimulation (FES) training program at home for 15 min/day, 5 days/week. CCCS subjects were submitted to FES at least after 0.7- to 10.6-year post-SCI, and biopsied after 1.3- to 9.4-year FES-training. Muscle biopsies were studied by H-E stain and immunohistochemistry with anti-MHCemb monoclonals. Muscle biopsies from CCCS subjects show the characteristics of long-term denervation, that is, they present a few atrophic or severely atrophic myofibers dispersed among adipocytes and loose or fibrous connective tissue. On the other hand, monoclonal antibody for embryonic myosin (anti-MHCemb) shows that many regenerative events continue to spontaneously occur in human long-term denervated muscle.

In the FES-trained muscle biopsies the cryosections consist mainly of large round myofibers and a few regenerated fibers. There is very little fat or fibrous connective tissue. The structural studies confirm that the protocol used is effective in reverting long-term atrophy/lipodystrophy of CCCS muscles and in maintaining the trophic state of regenerated myofibers in the FES-trained muscles of DDM subjects.

Introduction

Denervated skeletal muscle undergoes a rapid loss of both mass and contractile force in spinal-cord injury (SCI). The atrophy is especially severe when the injury involves lower motoneurons since several months after irreversible denervation atrophy is complicated by muscle fat substitution and fibrosis. While early denervation has been widely studied both in animal models and in humans, long-term effects of denervation has attracted much less attention since there is a general belief that all myofibers disappear within twelve months of denervation [1]. However, it has been also demonstrated by animal experiments that permanent lower motor neuron denervation is accompanied by a continuous production of new myofibers [1]. Activated satellite cells, myotubes, and regenerated myofibers are consistently present among atrophic myofibers of rats even after a yearlong permanent denervation in both hemidiaphragm and leg muscles [2]. Embryonic myosin is expressed in myotubes and young myofibers and represents the soundest molecular marker of early myogenic events in both developing and adult muscles. In rats a regenerated muscle tissue responds again to a repeated myotoxic injury with muscle regeneration [3].

By using immunohistochemistry we here show that regenerative myogenesis occurs in human denervated muscle up to 20-year after lower motoneuron denervation [4]. Furthermore we show that myofiber regeneration decreases after the DDM are subjected to a FES training regime, which effectively reverts long-term atrophy and maintains the trophic state of newly regenerated myofibers.

Material and Methods

Analyses of Human Muscle Biopsy

Subjects were either CCCS, or CCCS after FES training according to [4]. Needle biopsies of human muscles were taken from right and left leg.

Hematoxilin-eosin. Cryosections of frozen biopsies were stained with Hematoxilin-Eosin, using conventional techniques.

Immunohistochemistry. Serial cryo-sections were labeled with antibodies anti-MHC-emb (from

Novocastra, NCL-MHCd diluted 1:20) for 1 hour at room temperature. The slides were then washed twice with TBS (5 min each) and incubated with FITC-conjugated anti-mouse Ig (from Sigma, F-2266 diluted 1:200) for 1h at room temperature. This was followed by a second 5 minute washing of the slides with TBS and nuclei counter-staining by Hoechst 33258. In the negative controls, the primary antibody was omitted [5].

Morphometric analysis. Images were acquired using a Zeiss microscope connected to a Leica DC 300F camera at low magnitude under the same conditions that were used to acquire a reference ruler. Morphometric analysis was performed with Scion Image for Windows version Beta 4.0.2 (by 2000 Scion Corporation), free software downloaded from the web site: www.scioncorp.com. Figures were mounted and labeled using Adobe Photoshop® v6.0. The details of fiber typing and morphometry are reported in [5].

Results

Figure 1 shows representative examples of the stages, which undergo the long-term denervated human muscle. Up to one-year denervation muscle fibers decrease in size only (atrophy). Then (2-5 years), the severely atrophic myofibers lose all the contractile proteins. Finally, among myofibers which fully lost contractile proteins, adipocytes and loose connective tissue accumulate [4].

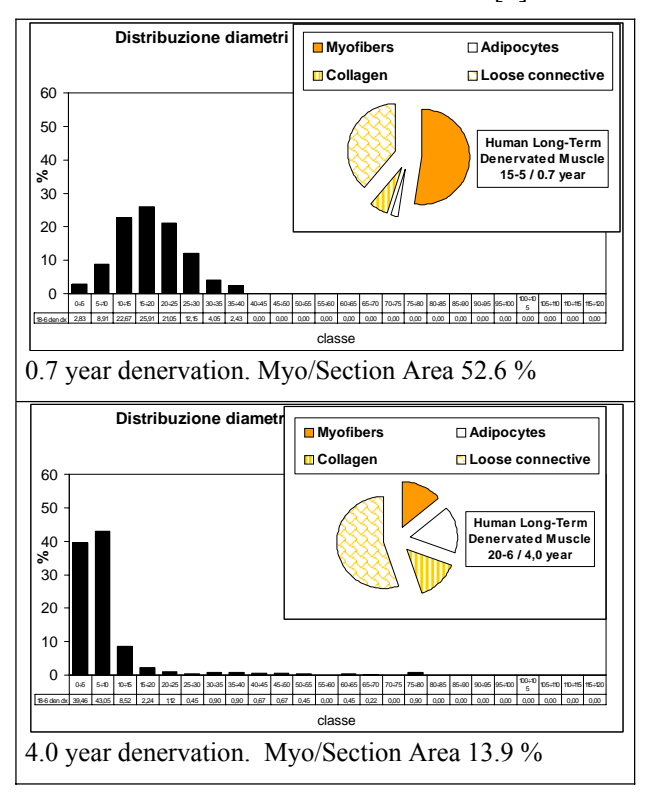


Fig.1: Human long-term denervated muscle. Fiber size spectrum and percentual area of myofibers.

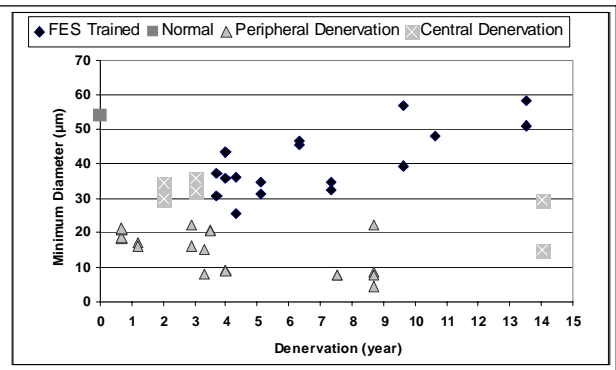


Fig. 2: Myofiber sizes of long-term denervated human muscle without and with FES-training.

Figure 2 shows the time-course of long-term denervated human muscle atrophy and recovery by FES-training according to Kern protocol [6]. Several years of FES-training increase myofiber size to values higher than those of both lower and upper motorneuron lesions. Indeed, they reach the value of sedentary normal subjects.

Anti-MHCemb positive fibers were present in all the biopsies we studied. Table 1 shows that about 10 myofibers per biopsy were stained by anti-MHCemb, while only 5 myofibers were recently regenerated in the muscle biopsy of FES-trained subjects.

	Denervation	FES-training	
	(# 20)	(# 17)	
Denervation Range (year	0.7 – 8.7	3.7 – 13.5	
	Mear	n +/- SD	p
•Cryosection Area (mm²)	4,9+/- 1,8	6,4+/-2,0	0,006
•Regenerated Fiber/mm²	2,3+/-2,3	0,8+/-1,3	0,011
•Regenerated Fiber/Fiber	4,1+/-5,2	1,6+/-2,1	0,058

Table 1: Regenerative myogenic events in long-term denervated human muscle without and with FES-training.

Discussion

Over the last 30 years there has been a good deal of interest in the use of functional electrical stimulation (FES) to restore movement of the limbs of patients paralysed by upper motor neuron lesion in the spinal cord. There is, however, another group of patients that, due to the marked atrophy of the denervated muscle, present severe secondary medical problems of bone and skin, and that are more difficult to treat successfully. In these patients, the spinal cord injury (SCI) results in irreversible loss of the nerve supply to some or all of the muscles of the affected limbs (conus cauda lesion). The absence of functional nerve fibers makes it more difficult for surface electrodes to recruit a sufficient population of myofibers needed

to regain functional movements. Indeed, using clinically approved stimulation devices the long-term denervated degenerated muscle (DDM) is poorly excitable from six months after injury.

Despite these difficulties, pilot studies on FES of human long-term DDM have been published. Especially encouraging are some of our previous results [6-9], which have shown that electrical stimulation by long impulses can be used to restore muscle mass and force production. This clinical work strongly supports the idea that FES is a powerful tool for functional restoration of long-term DDM, a fact that, for various reasons, was not recognized until recently.

In the present work we analyzed biopsies from long-term denervated human legs and from muscle stimulated using a particular FES protocol.

We have here shown that about 4 % of the myofibers stains positive by the antibody to MHCemb, indicating that they are fibers, which had regenerated during the last few weeks. Embryonic myosin is expressed in myotubes and young myofibers and represents the soundest molecular marker of early myogenic events in both developing and adult muscles [3]. When reinnervation of regenerated myofibers occurs in adulthood, either slow or fast types of adult myosin may substitute the embryonic myosin 5-7 days post-damage. On the other hand, if not reinnervated [3], the regenerated myofibers undergo atrophy and degeneration, as we have see here in human byopsies. In the human muscle biopsies up to 19-year post SCI, about 4 percent of fibers are positive to immunostaining with an antibody for MHCemb indicating recent regeneration. The fact that the percentage of regenerated myofibers decreases in muscle biopsies of subjects that performed FES-training from 2.3 to 9.3 years is in our opinion a further evidence of effectiveness of the Functional Electrical Stimulation Therapy.

Electron microscopy analysis of DDM biopsies confirms the immunocytochemistry findings [4]. During the next years, the goals of the EU supported RISE project will be to identify, using experiments in animals and clinical research, safer stimulation protocols needed to induce early effects with, hopefully, a reduced stimulation burden for the patients. If all myofibers in the thigh could be consistently reached, the increased muscle mass and fatigue resistance will rise

References

patients and their quality of life.

[1] Carlson B.M., Borisov A.B., Dedkov E.I., Dow D., Kostrominova T.Y.: The biology and restorative capacity of long-term denervated skeletal muscle. Basic Appl Myol 2002;12:247-54

- [2] Carraro U., Morale D., Mussini I., Lucke S, Cantini M., Betto R., Catani C. Dalla Libera L., Danieli-Betto D., Noventa D.: Chronic denervation of rat diaphragm: maintenance of fiber heterogeneity with associated increasing uniformity of myosin isoforms. J Cell Biol 1985;100:161-174
- [3] Mussini I., Favaro G., Carraro U.: Maturation, dystrophic changes and the continuous production of fibers in skeletal muscle regenerating in the absence of nerve. J Neurophatol Exp Neurol 1987;46:315-31
- [4] Kern H., Rossini K., Boncompagni S., Mayr W., Fanò G., Zanin M.E., Podhorska-Okolow M., Protasi F., Carraro U.: Long-term denervation in humans causes degeneration of both contractile and excitation-contraction coupling apparatus that can be reversed by functional electrical stimulation (FES). A role for myofiber regeneration. J Neuropathol Exp Neurol, in press.
- [5] Rossini K., Zanin M.E., Carraro U.: Stage and quantify regenerative myogenesis in human long-term permanent denervated muscle. Basic Appl Myol 2002; 12; 277-287
- [6] Kern H., Hofer C., Strohhofer M., Mayr W., Richter W., Stohr H.: Standing up with denervated muscles in humans using functional electrical stimulation. Artif Organs 1999;23:447-52
- [7] Kern H., Hofer C., Modlin M., Forstner C., Raschka-Hoegler D., Mayr W., Stoehr H.: Denervated muscles in humans: limitations and problems of currently used functional electrical stimulation training protocols. Artif Organs. 2002;26:216-8
- [8] Hofer C., Mayr W., Stöhr H., Unger E., Kern H.: A stimulator for functional activation of denervated muscles. Artif Organs 2002;26:276-9
- [9] Mayr W., Hofer C., Bijak M., Rafolt D., Unger E., Sauermann S., Lanmueller H., Kern H.: Functional Electrical Stimulation (FES) of denervated muscles: existing and prospective technological solutions. Basic Appl Myol 2002;12:287-90

Acknowledgements

Supported by EU Commission Shared Cost Project RISE (Contract no. QLG5-CT-2001-02191).

Author's Address

Prof. Ugo Carraro, Department of Biomedical Science, University of Padova. Via G.Colombo, 3; 35121 Padova (Italy). Tel +39 049 8276030; fax +39 049 8276040. e-mail: ugo.carraro@unipd.it.

Session 4

FES of Denervated Musculature 2

Chairpersons:

U. Carraro (Padova, Italy)

H. Kern (Vienna, Austria)

DEGENERATION OF CHRONICALLY DENERVATED HUMAN MUSCLE IS REVERSIBLE.

Simona Boncompagni¹, Helmut Kern², Winfried Mayr³, Ugo Carraro⁴ and Feliciano Protasi¹.

¹Istituto Interuniversitario di Miologia, CeSI, University G. d'Annunzio School of Medicine, I-66023 Chieti, Italy.

 ²Ludwig Boltzmann Institute of Electrostimulation and Physical Rehabilitation, Dept of Physical Medicine, Wilhelminenspital A-1171 Vienna, Austria.
 ³Dept of Biomedical Engineering and Physics, Univ. of Vienna A-1171 Vienna, Austria.

⁴Dept of Biomedical Sciences, Univ. of Padova Medical School I-35121 Padova, Italy.

Introduction

Muscle contraction is triggered by electrical impulses, i.e. action potentials, which are transmitted by the motoneurons to individual skeletal muscle fibers at the level of the neuromuscular junctions. This electrical signal propagates along the fiber surface and enters its interior via special invaginations of the sarcolemma called transverse-tubules (TTs). The TTs are closely apposed to the sarcoplasmic reticulum (SR) and these two membrane systems are highly ordered and organized: in fact, TTs invaginate at precise locations along the myofibrils (either at the Z-line or at the A-I junction) bringing the external membrane in proximity to the SR terminal cisternae and forming specialized junctions called calcium release units (CRUs), or This precise morphological relation triads. between CRUs and myofibrils is essential for excitation-contraction coupling (ECC), mechanism that allows transduction of the action potential into muscle contraction (Franzini and Jorgensen, 1994; Flucher and Franzini Armstrong, 1996).

Structural and functional properties of muscle fibers are strictly dependent upon nervous system innervation. In fact, in case of spinal-cord injury (SCI), skeletal muscle fibers undergoes a rapid disorganization accompanied by loss of mass (atrophy), contractile force, and by a series of biochemical and physiological changes. For many years the general belief has been that severely atrophic muscle fibers are irreversibly lost and that no effective treatment is available for those muscles that have undergone severe atrophy as a result of a long-standing denervation injury. For this reason over the last 30 years there has been a good deal of interest in the use of functional electrical stimulation (FES) to restore movement of the limbs of patients immobilized by SCI, i.e. upper motor neuron lesion, spastic paralysis, etc. Just recently an innovative rehabilitation procedure based on a particular FES protocol have been specifically developed to stimulate a response in human long-term denervated and degenerated muscles (DDM) with the aim of reversing muscle atrophy and degeneration in patients with complete lower motoneuron lesions (Kern et al., 2002). The results obtained with this particular FES protocol are extremely encouraging since they have shown that electrical stimulation by long impulses can indeed restore muscle mass, force production and movements even after long lasting complete denervation (Hofer et al., 1999; Carraro, 2002; Kern et al., 2002; Mayr et al., 2002). Surprisingly, muscle function in the FES trained extremities was restored sufficiently to allow for supported standing up, standing, and even for a few steps to be taken (Kern et al., 1999).

While the mechanical and electrical properties of mammalian denervated muscle, together with the structural alterations of the contractile apparatus following early and mid-term denervation, are well described in the literature, not much is known about the effect of long-term denervation on the ultra-structure of myofibrils and of membranes involved in ECC in human muscle fiber.

Material and Methods

The samples obtained via biopsies were fixed in 2.5% glutaraldehyde in 0.2 M sodium cacodylate buffer, pH 7.2, for 2h on ice followed by buffer rinse and fixation for 1h in 1% osmium tetroxide. The specimens were dehydrated in a graded series of ethanol solutions and embedded in epoxy resin. Ultrathin sections (about 40 nm) were cut in Leica Ultracut R (Leica Microsystem, Austria) using a Diatome diamond knife (DiatomeLtd. CH-2501 Biel, Switzerland) and stained in 4% uranyl acetate and lead citrate. Sections were examined with a FP 505 Morgagni Series 268D electron microscope (Philips), equipped with Megaview III digital camera and Soft Imaging System (Germany).

Results

Using electron microscopy (EM), we have performed a detailed analysis of human long-term DDM and studied the effect of FES on the ultrastructure of both contractile and ECC apparatuses. Our results shows that lack of innervation in muscle fibers results in the parallel degeneration of both contractile and ECC apparatuses. Myofibrils are very disorganized in most of the fibers, while some healthy myofibrils can still be found in few regenerating ones. CRUs are rare and generally misshapen and ryanodine receptors (RyRs), the Ca2+ release channels of the SR, are also missing from most of the junctions (Kern et al., 2004). Since effects of long term denervation have not been described in detail in human muscle fibers, these results are novel but not surprising since similar results have been described in animal models. Definitely more interesting are the observation made in the restimulated muscle fibers: in fact, FES promotes a surprising restoration of both contractile and ECC apparatuses. The level of recovery ultrastructural properties of myofibrils (Fig. 1) and of membranes involved in ECC (Fig. 2) is striking: CRUs and sarcomeres re-associate with each other in way that triads are located at sarcomere I-A junction, as in normal human muscle (arrows in Fig. 2 A). Triads are frequent and well distributed within the fiber and RyRs re-appear in the junctional gap (arrows in Fig. 2 B).

Discussion

The present structural studies are extremely encouraging since they demonstrate that: i) the severe muscle fibers degeneration that follows long-term denervation is reversible, and ii) the protocol used during FES training is effective in reverting this atrophy in human muscle of patients affected by long-term lower motoneuron lesion. The reorganization of the contractile and ECC apparatuses appears to occur in parallel, but it is not yet clear which is the leading process. However, since the reorganization of the muscle fiber starts from the periphery, it is possible that the leading event is the re-organization of the TT apparatus, which could be promoted by the spreading of the electrical signal along the denervated fiber. This structural work strongly supports the idea that FES may be a powerful tool in the structural and functional restoration of longterm DDM, a fact that for various reasons was not recognized until recently.

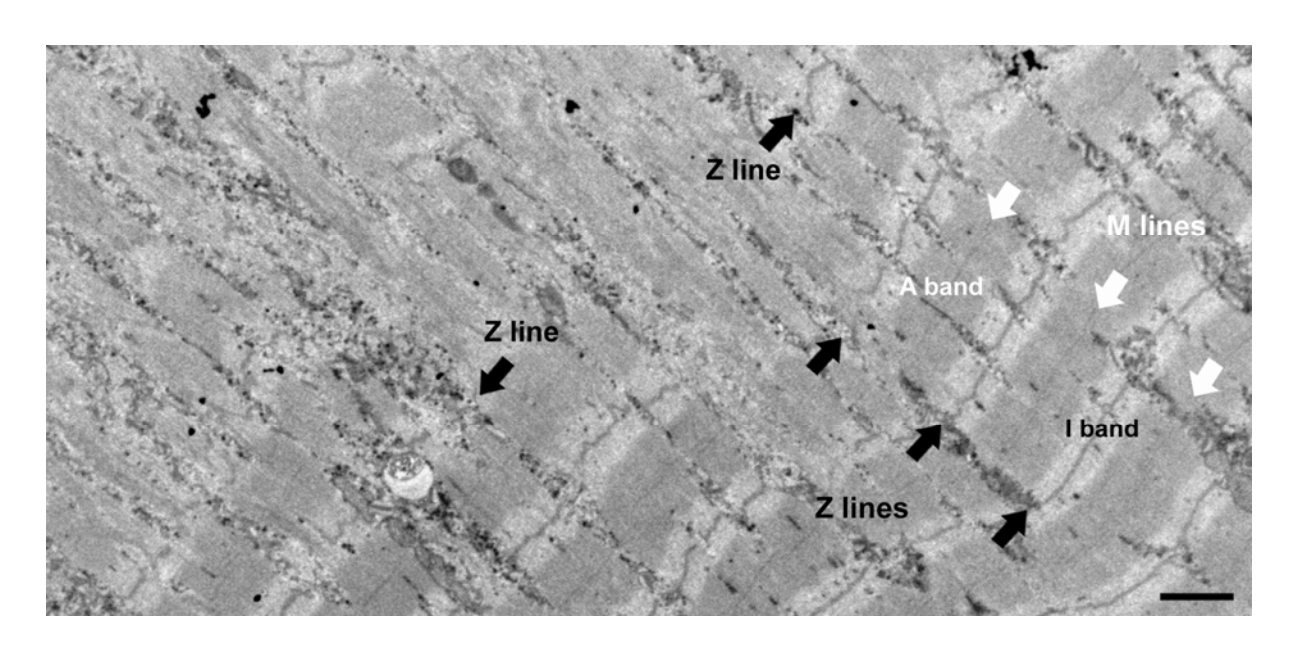


Figure 1: FES restores the ultrastructure of long-term denervated myofibrils. The micrograph shows a fiber from a patient that was denervated for 48 months and treated with FES for 26 months. The restoration of myofibrils starts usually at the fiber periphery: shown in this micrograph is an area (right side) in which myofibrils are very well organized next to a region (left side) in which the filaments are still quite disordered, but clearly already aligning in the direction of the re-arranging myofibrils. Scale bar: 1μm.

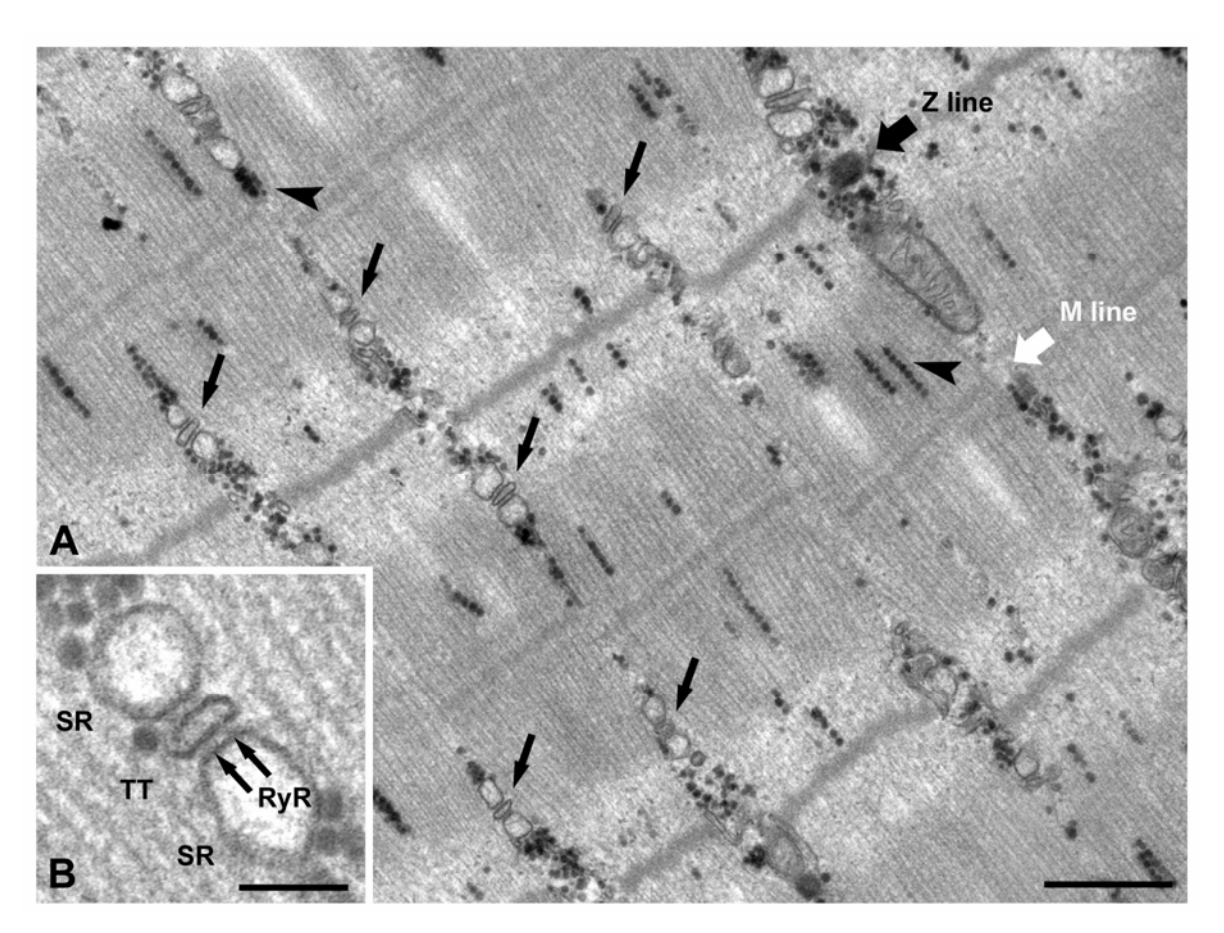


Figure 2: FES restores the ultra-structure of the ECC apparatus. A) ECC apparatus re-associate to the A-I junction of the sarcomere and the frequency of CRUs is also restored in a way that almost every sarcomere has two triads on each side (small black arrows). B) triads now exhibit a normal profile and now contain two rows of RyRs on each side of the TT (arrows) as in normal skeletal muscle junctions.

A, scale bar: 0.5 μm; B, scale bar: 0.1 μm.

References

Carraro, U. 2002. Modulation of trophism and fiber type expression of denervated muscle by different patterns of electrical stimulation. Basic Appl. Myol. 12: 263-272.

Franzini-Armstrong, C., and Jorgensen, A. O.1994. Structure and development of e-c coupling units in skeletal muscle. Annu. Rev. Physiol. 56:509-534.

Hofer, C., Mayr, W., Stöhr, H., Unger, E., and Kern, H. 1999. A stimulator for functional activation of denervated muscles. Artif. Organs. 26:276-279.

Kern, H., Hofer, C., Strohhofer, M., Mayr, W., Richter, W., and Stohr, H. 1999. Standing up with denervated muscles in humans using functional electrical stimulation. Artif. Organs. 23: 447-452.

Kern, H., Christian, H., Michaela, M., Claudia, F., Winfried, M., and Wolfgang, R. 2002. Functional electrical stimulation (FES) of long-term denervated muscles in humans: Clinical

observations and laboratory findings. Basic Appl. Myol. 12: 291-297.

Kern, H., S. Boncompagni, K. Rossini, W. Mayr, G. Fano', M. E. Zanin, M. Podhorska-Okolow, F. Protasi, and Ugo Carraro. 2004. Long-term denervation in humans causes degeneration of both contractile and excitation-contraction coupling apparatus that can be reversed by functional electrical stimulation (FES). A role for myofiber regeneration? J. Neuropath. Exp. Neurol. In press.

Mayr, W., Christian, H., Manfred, B., Dietmar, R., Ewald, U., Stefan, S., Hermann, L., Helmut, K. 2002. Functional Electrical Stimulation (FES) of denervated muscles: existing and prospective technological solutions. Basic Appl. Myol. 12: 287-290.

Author's Address

Prof. Dr. Simona Boncompagni

Istituto Interuniversitario di Miologia, CeSI, University G. d'Annunzio School of Medicine, I-66023 Chieti, Italy.

METABOLIC CAPACITY OF HUMAN LONG-TERM DENERVATED MUSCLES

W. Rossmanith, K. Moser-Thier, H. Gruber, R. E. Bittner

Center for Anatomy and Cell Biology, Medical University of Vienna, Vienna, Austria

Metabolic capacity of skeletal muscle displays a remarkable plasticity in response to physical activity. Changes in mitochondrial density and activity are a central phenomenon of these adaptations. Yet, little is known about the restorability of mitochondrial capacity in highly degenerated long-term denervated muscle by means of functional electrical stimulation. We are following mitochondrial parameters of a cohort of patients with long-term flaccid paraplegia undergoing functional electrical stimulation. Up to now we have analyzed mitochondrial function and total amount of mitochondria before the onset of stimulation of the bilateral muscle biopsies of 23 patients. Mitochondrial function was determined by respiratory physiology of permeabilized muscle fibers and mitochondrial density by measurement of a marker enzyme activity (citrate synthase) in homogenates. Our results indicate a generally low respiratory capacity of denervated muscles. This reduction appears to be the result of the low mitochondrial density of these highly degenerated muscles, whereas remaining mitochondria appear to be functional. Mitochondrial density and cellular respiratory activity are negatively correlated with the length of the preceding denervation period of the analyzed muscles and the extent of degeneration (as evaluated by routine histology). These results will be a reference for the comparison of the effects of 2-3 years of functional electrical stimulation on muscle mitochondrial capacity.

Author's Address

Rossmanith Walter, Univ.Ass. Univ.-Doz. Mag. Dr. Institut für Anatomie Währinger Straße 13 A- 1090 Wien

e-mail: walter.rossmanith@meduniwien.ac.at

EVALUATION OF FES-INDUCED ELASTIC AND VISCOUS MOMENTS IN PARAPLEGICS WITH DENERVATED MUSCLES

E. Gallasch*, D. Rafolt**, G. Kinz**, M. Fend*, H. Kern***, W. Mayr**

* Department of Systems Physiology, Medical University of Graz

** Department of Medical Physics and Biomedical Engineering, Medical University of Vienna

*** Department for Physical Rehabilitation, Wilhelminenspital, Vienna

Abstract

The pendulum test was applied to evaluate FES induced joint moments in paraplegics with denervated muscles. Therefore a manipulandum was connected to the knee joint and programmed to elicit gravity induced leg oscillations. The FESinduced output torque was compensated before in order to keep the leg in a mean vertical position (knee angle 90°). A second order dynamical model was applied to extract the elastic and viscous moments from the recorded leg oscillations. This model provided an almost adequate description of relaxed and FES contracted states. In the relaxed state the elastic moment was 15.3 ±2.37 Nm/rad and the viscous moment 0.41 ±0.21 Nms/rad. The FES induced elastic moment was 29.4 ±28.5 Nm/rad and the FES induced viscous moment 1.53 ± 1.03 Nms/rad (N = 10, before FES-training).

Introduction

In paraplegics with denervated and long term degenerated muscles FES-training is probed as therapeutic countermeasure (objective of the EU-RISE project) [1]. To elicit tonic contractions, and to induce muscle growth in such patients, high current repetitive stimulation is applied via large transcutaneus electrodes over quadriceps muscles [2]. As a side-effect of this technique, considerable co-contraction is produced in antagonistic muscles inducing joint stiffening. Especially in the early phase of the training joint stiffening dominates over output torque. Therefore, to evaluate the stimulation and training effects, an objective method to sense the FES-induced stiffness in the knee joint was needed.

As joint stiffness is given by the ratio between torque and deflection, a tensile technique has to be applied. Basically three approaches exist to sense stiffness at the joint level: programmed limb deflections, programmed external torques and gravity induced limb oscillations. Programmed limb deflections are delivered by isokinetic devices. Although commercial available, these devices are less suited to sense the weak FES-induced stiffening effects. Programmed torques on the other hand allow the superposition of weak test forces [3], but this tentile test has to be performed

at horizontal limb position in order to avoid gravity induced oscillations.

The third approach utilises the oscillations as produced by gravity. In the pendulum test, further known as "Wartenberg Test" [4], the leg is dropped and the responding oscillation frequency is analysed to extract joint stiffness. The pendulum test was probed on paraplegics with innervated muscles [5, 6]. As the response of these muscles highly depend on spinal feedback, this test showed less reliable in contrast to isokinetic constant velocity tests [7]. For denervated muscles, however, no spinal feedback exists, therefore the oscillations solely will mirror the properties of the muscles interacting at the joint.

Material and Methods

Experimental Procedure

In the classical pendulum test [5,6] the leg is raised 60° from the vertical and then released, resulting in oscillatory motions around an resting point of 0°. With our denervated patients this protocol works quite well at relaxed muscles. During FES however an output torque is produced, shifting the resting point into vertical direction. Therefore, for comparisons at defined knee angles, it showed advantageous to compensate these torques with a manipulandum.



Fig. 1: Experimental setup with electrical stimulation and manipulandum connected to the lower leg.

Fig.1 shows the setup for the pendulum tests. The manipulandum was connected to the knee joint via an adjustable lever to hold the subject's leg and foot in a rigid position. The manipulandum consists of a realtime controlled torque motor with an embedded angular displacement sensor [8] to control and to record the leg motions. Test oscillations were elicited by raising the leg 12° from the vertical via programmed torques.

FES was applied over the quadriceps muscle group via large wet electrodes (biphasic pulses, width 2 x 20 ms, repetition rate 20 Hz). Each test session started with relaxed muscles, then the stimulation amplitude (0 to 80 Volt) was slowly increased. The curve in Fig. 2 shows typical damped oscillations during such a session. With stimulation amplitude the oscillation frequency increases and the leg extends. If the extension from the resting point exceeded an angle of 5°, the contraction torque was compensated automatically.

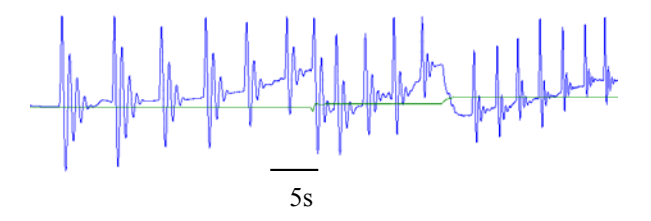


Fig. 2: Test recordings of leg oscillations while the stimulation voltage continuously was increased and leg extension stepwise was compensated (from subj.2)

Modeling and Analysis

Considering tonic contractions in agonist and antagonist muscles, we can assume that the mechanical properties at the joint are lumped together. The oscillation dynamics of the vertical leg then is described by the following differential equation:

$$J\ddot{\varphi} + D(\varphi, t)\dot{\varphi} + C(\varphi, t)\varphi + mgl_c \sin \varphi = 0$$
 (1)

In (1) J denotes the inertial moment of the leg and the manipulandum, D the lumped viscous moment, C the lumped elastic moment, C the lumped elastic moment, C the lower leg, C the acceleration due to gravity and C the center of mass from the knee axis. Parameters C and C are computed from an antropometric model of leg and foot [9] and the manipulandum mechanics. For small C around the vertical (<15°) and stationarity for the duration of the test, equation (1) becomes:

$$J\ddot{\varphi} + D\dot{\varphi} + C'\varphi = 0 \qquad \text{with} \qquad (2)$$

$$C' = C + C_g$$
 and $C_g = mgl_c$ (3)

Equation (2) can be solved analytically, for damped oscillations the solution is:

$$\varphi(t) = C'e^{-\delta t}\cos\omega t \qquad \text{with} \qquad (4)$$

frequency:
$$\omega = \frac{2\pi}{T} = \sqrt{\frac{C'}{J} - \delta^2}$$
 (5)

and damping:
$$\delta = \frac{D}{2J} = \frac{\ln R}{t_2 - t_1} = \frac{\ln R}{T}$$
 (6)

The damping coefficient δ further can be estimated from the experimental data, whereby R is the ratio of the peak angle of one cycle to the peak angle to the next cycle, and T is the cycle length, see Fig. 3.

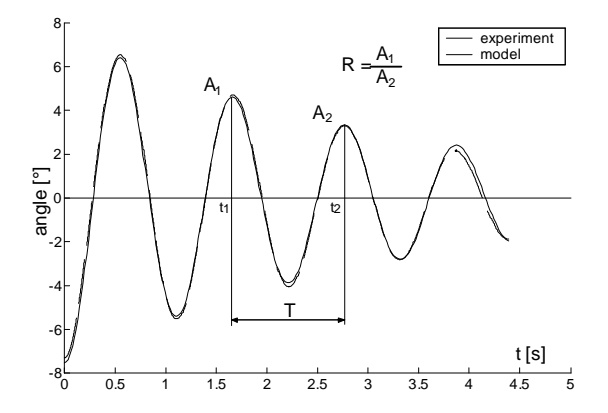


Fig. 3: Estimation of R and T from experimental data

After estimation of δ the viscous moment D can be computed from equation (6), and after insertion of (6) into (5) and some algebraic operations the elastic moment C is given by:

$$C = J \frac{4\pi^2 + (\ln R)^2}{T^2} - C_g \tag{7}$$

For relaxed and stimulated muscles the pendulum frequencies *are*:

$$\omega_{rel} = \sqrt{\frac{C'_{rel}}{J} - \delta_{rel}^2}$$

$$\omega_{stim} = \sqrt{\frac{C'_{rel} + C_{FES}}{J} - \delta_{stim}^2}$$
(8)

After squaring both equations and insertion of C'_{rel}/J into (8) the FES-induced stiffness C_{FES} then is given by:

$$C_{FES} = J(\omega_{stim}^2 - \omega_{rel}^2 + \delta_{stim}^2 - \delta_{rel}^2)$$
 (9)

By repeating the pendulum test in relaxed and stimulated states, C_{FES} now is obtained without explicit knowledge of C'_{rel} .

Subjects

Until now 17 paraplegics were tested before the beginning their FES-training. Only in 10 of these subjects markable increases of joint stiffness (> 10%) had been observed, in the other 7 subjects

FES practically showed no effect. From all subjects anthropometric measures were taken to calculate the inertial parameters. For the clinical study the stimulation amplitude was increased in 10% steps from 0 to 80 Volts. After each step increase the produced output torque was compensated, than the pendulum test was performed twice, in both directions.

Results

Table 1 shows the relevant patient data and the joint moments in the relaxed state. Only the 10 patients responding to FES are shown. According to (3) C_G is produced by gravity and C in the knee joint. Mean values are 0.65 ± 0.19 for J_{leg} , 10.6 ± 2.4 for C_G , 15.3 ± 9.4 for C and 0.41 ± 0.27 for D.

Subj	age	size	wght	time	J_{leg}	C_{G}	С	D
1 m	37	1.75	55	2	0.39	7.6	4.9	0.15
2 m	21	1.94	75	2	0.93	12.8	28.8	0.77
3 m	48	1.74	86	6	0.61	11.2	12.6	0.36
4 m	53	1.80	60	4	0.46	8.4	10.8	0.28
5 m	31	1.93	70	1	0.76	9.8	11.4	0.21
6 m	48	1.77	70	2	0.54	9.4	8.4	0.24
7 m	25	1.86	72	1	0.57	10.2	20.7	0.40
8 m	44	1.77	118	6	0.95	16.0	32.9	0.99
9 m	20	1.84	70	1	0.67	10.8	6.7	0.27
10 m	31	1.75	75	1	0.60	10.1	15.4	0.44

Table 1: Patient data and parameters from relaxed state (0% stimulation level) Item "time" are the number of years since the denervation occured. C [Nm/rad], D [Nms/rad] and J [kgm²].

Table 2 shows the contraction output torque in dependence of the stimulation level. Due to the different states of muscle degeneration there was a high variation in FES responsibility. To reduce muscle fatique the test contractions were started at the 50% stimulation level. Only if a response was detected at that level, the test was performed at lower levels.

Subj	10	20	30	40	50	60	70	80	90	99%
1	0	0	0	0	0	0	0	0	0	0
2	0	0	0	0	.15	.27	.36	.41	.45	.45
3	0	0	0	0	0	0	0	0	0	0
4	0	0	0	0	0	0	0	0	0	0
5	0	0	0	0	0	0	0	.27	.45	.45
6	0	0	0	0	0	0	0	0	0	.15
7	0	0	0	0	0	.03	.26	.90	1.8	2.3
8	0	0	.30	1.8	2.2	3.1	4.8	5.1	3.1	2.9
9	0	.21	.66	3.5	5.3	4.0	.70			
10	0	0	0	0	0	0	0	0	0	0

Table 2: Output torque in dependence of the stimulation level (10 to 99%) as measured by the compensation torque [Nm].

Table 3 shows the elastic moment in dependence of the stimulation level (= FES-induced stiffness C_{FES}). At higher levels C_{FES} saturated or even decreased, indicating muscle fatigue. Maximal C_{FES} therefore showed a high standard deviation (29.4 ±28.5 Nm/rad). C_{FES} however showed stable for swing angles between 3- 15°, for angles < 3° C_{FES} slightly increased.

subj	10	20	30	40	50	60	70	80	90	99%
1	0	0	0	0	0	0.2	1.9	5.8	9.5	11
2	0	0	0	0	2.3	3.2	5.7	11	62	54
3	0	0	0	0.6	0.9	9.0	16	20	19	20
4	0	0	0	0	0	0	1.5	2.8	4.4	5.6
5	0	0	0	0	0.3	0.9	7.1	32	33	34
6	0	0	0	0	0.3	0.7	2.1	2.8	8.6	7.2
7	0	0	0	0	0	0.9	2.8	3.8	7.1	8.8
8	1.5	2.5	12	10	27	50	75	88	79	74
9	0.4	0.7	1.6	6.7	20	19	50			
10	0	0	0	0	0	0	0.4	1.9	4.2	6.2

Table 3: FES-induced elastic moment (C_{FES}) in dependence of stimulation level (10 to 99%).

Table 4 shows the viscous moment in dependence of the stimulation level (= FES-induced viscosity D_{FES}). The mean of maximal D_{FES} was 1.53 \pm 1.03 Nms/rad.

subj	10	20	30	40	50	60	70	80	90	99%
1	0	0	0	0	.01	.06	.31	.60	.97	.95
2	0	0	0	0	.08	.38	.75	1.2	2.7	2.9
3	0	0	0	.14	.26	.85	1.1	1.1	1.0	1.0
4	0	0	0	0	0	0	.13	.18	.28	.30
5	0	0	0	0	.04	.10	.83	1.9	2.0	2.1
6	0	0	0	0	.02	.07	.21	.39	.65	.76
7	0	0	0	0	0	.14	.12	.54	.84	1.0
8	.03	.06	.24	.27	.39	.94	1.9	3.2	1.7	1.4
9	.03	.07	.07	.43	1.2	1.1	2.4			
10	0	0	0	0	.01	.02	.19	.31	.50	.59

Table 3: FES-induces viscous moment (D_{FES}) in dependence of stimulation level (10 to 99%).

Discussion

The results of this study show, that the pendulum test is a helpful tool to assess muscle performance in denervated paraplegics. The pendulous motion was well described the second order model, both in the relaxed and FES-contracted state, which allowed the extraction of elastic and viscous moments. With contraction level the number of oscillations decreased, a fact resulting from the quadratic term of the damping coefficient in equation (5). Therefore with FES-trained subjects it might be better to apply a model-adjustment technique for extraction the joint moments.

In the present study the values of C and D in the relaxed state were considerable smaller as reported for the normal leg (35.7 \pm 7.8 Nm/rad and 1.85 \pm 0.16 Nms/rad from [10]). Muscle atrophy and degeneration (replacement of muscle tissue by connective tissue) is held responsible for this effect. Degeneration on the other hand could lead to increased stiffness in the relaxed musculature, an effect termed as "contracture". Actually this effect was not observed as in all patients C was lower than in the normal leg.

An other effect that could influence passive muscle stiffness is the formation of a rigor complex in the crossbridges due to a lack of ATP. In the normal muscle such a rigor sometimes is observed after exhausting contractions or fatiguing electrical stimulation. To clarify the formation of a FES-induced rigor in the denervated musculature, it would be necessary to repeat the relaxed test after the FES-training.

In the FES-contracted state, C_{FES} and D_{FES} highly depend on individual factors, obviously reflecting the differences in patient history. Consequently the calculated mean values showed considerable variation and are not very representative. However compared to the produced output torque, the two joint moments showed a higher responsibility to FES. Even from the other 7 subjects from which no one produced an output torque, small increases of C and D were observed. It is therefore concluded that the two joint moments are the better indicator to detected weak contractions in the denervated musculature.

The main problem in the clinical application of the pendulum test was FES-induced fatigue. Specifically in the non-trained musculature as studied here, signs of fatique often are observed 50 seconds after induction of repetetive stimulation. The reasons for fatigue are multiple such as limited aerobic/ anaerobic capacity, local acidosis, depletion of calcium and tissue heating due to power absorption from high current stimulation.

To reduce the effect of fatigue on measurement, the total observation time has to be reduced to less than 50 seconds. Actually the typical duration of one oscillation is 10 seconds including a pause to ensure that an oscillation has died out before the next oscillation starts. However as the analysis showed, the main information lies in first two or three oscillations with large amplitudes. Therefore the later oscillations may be reduced by braking or active damping with the manipulandum. Further it showed not necessary to perform the test twice at each stimulation level (in both directions), as the directional asymmetries were small.

References

- [1] Mayr W., Hofer C., Bijak M., Lanmüller H., Rafolt D., Reichel M., Sauermann S., Unger E., Kern H.: EU-Projekt RISE, FES denervierter Muskulatur. Biomed. Technik 48 (Suppl.1), 2003, 52-53
- [2] Kern H., Hofer C., Strohhofer M., Mayr W., Richter W., Stöhr H.: Standing up with denervated muscles in humans using functional electrical stimulation. Artif. Org. 23, 1999, 447-452
- [3] Walsh E.G.: Muscles, Masses & Motion, Physiology of Normality, Hypotonicity, Spasticity & Rigidity. Mac Keith Press, USA, 1992
- [4] Wartenberg R.: Pendulousness of the leg as a diagnostic test. Neurology 1, 1951, 18-24
- [5] Badj T., Vodovnik L.: Pendulum testing of spasticity. J. Biomed. Eng. 6, 1984, 9-16
- [6] Lin D.C., Rymer W.Z.: A quantitative analysis of pendular motion of the lower leg in spastic human subjects. IEEE Trans. BME 38(9), 1991, 906-918
- [7] Firoozbakhsh K.K, Kunkel C.F., Scremin A.M. Moneim M.S.: Isokinetic dynamometric technique for spasticity assessment. Am. J. Phys. Med. Rehab. 72, 1993, 379-385
- [8] Fend M., Rafolt D., Gallasch E.: Momentengeregelte Testaktuatorik für muskelgelenkmechanische Untersuchungen. Biomed. Technik 48 (Suppl.1), 2003, 410-411
- [9] Pavol M.J., Owings T.M., Grabiner M.D.: Body segment inertial parameter estimation for the general population of older adults. J. Biomech. 35, 2002, 707-712
- [10] Zhang L.Q., Nuber G., Butler J., Bowen M., Rymer W.Z.: In vivo human knee joint dynamic properties as functions of muscle contraction and joint position. J. Biomech. 31, 1998, 71-76

Acknowledgements

Supported by the European Union, Grant RISE EC/QLG5-CT-2001-02191

Author's Address

Prof. DI. Dr. Eugen Gallasch Department of Systems Physiology A-8010 Graz, Harrachgasse 21/5 e-mail: eugen.gallasch@meduni-graz.at

FUNCTIONAL ELECTRICAL STIMULATION OF DENERVATED SKELETAL MUSCLE FIBERS IN 3D HUMAN THIGH - MODELING AND SIMULATION

M. Reichel*, J. Martinek*, W. Mayr*, F. Rattay**

* Department of Biomedical Engineering & Physics, Medical University of Vienna, Austria

** TU-BioMed, Vienna University of Technology, Austria

Abstract

A finite difference model of the human thigh is used to analyze the excitation process in the fibers of denervated skeletal muscles which are treated by Functional Electrical Stimulation (FES) via surface electrodes. The MATLAB research tool FES-FIELD was developed to simulate the stationary electrical field for real human 3D geometry.

The first part of this computer simulation study was to compare the excitation effect of the FES via an extracellular point source in relation to the longitudinal position of the electrode above a single denervated skeletal muscle fiber. Action potential initiation is simulated with a muscle fiber model of the Hodgkin Huxley type and with a generalized form of the activating function. Results showed that there is an optimal longitudinal position of the electrode at the muscle-tendon junction with strongest excitation effect.

The second part, being the purpose of this study, was to analyze the entire amount of skeletal muscle fibers in the 3D electrical field. Therefore another MATLAB research tool (FES- ANALYSE) was developed to give a first estimate of suprathreshold regions. At the endings of a target fiber the activating function is proportional to the first derivative of the extracellular voltage, whereas the second derivative is the driving element for the central part. The analysis demonstrates that it is generally easier to initiate action potentials at the fiber endings especially for fibers in deeper regions.

Introduction

Most of the knowledge on Functional Electrical Stimulation (FES) of denervated (flaccid paralyzed) muscle is the product of more than 30 years of experimental use [1], i.e. it is empirical and subjective. Excitation of denervated skeletal muscle fibers depends either on electric field distribution in muscle tissue or on membrane properties and the microscopic morphological features of muscle cells [2]. The whole simulation of the combined models is necessary to quantitatively observe all the processes which

happen during FES and to optimize the effects caused by the applied voltage.

With the potential distribution along one muscle fiber the activating function [3], calculated along a nerve fiber, can be determined. A useful membrane model [4], caused by the use of voltage-clamp techniques, is available and the early model study of Adrean & Peachey [5] showed that the transversal tubular system (T-system) exerts an important loading effect in the form of a tubular outlet current.

For quantitatively observation a 2D-model of the distribution of the extracellular electric field in a length section of the human thigh has been established in 1997 and 1999 [4]. It focuses on denervation of the lower extremities. The major target muscle for FES that causes knee extension is the m. quadriceps femoris. Distribution of the electrical potential along its fibers is representative for its functional contraction caused by its electrical activation. In this 2D-model, where the femur is of low conductivity compared to the surrounding tissue, the current - applied through surface electrodes covering the m. quadriceps femoris - cannot be passed on to the hamstrings below the femur. However, in a 3D-simulation [6] the stimulation current can be passed on to the hamstrings through the muscles enclosing the femur. Voltage distribution changes considerably compared to the 2D-model.

In comparison to the stimulation of motorneurons functional electrical stimulation of denervated skeletal muscle fibers needs essentially stronger stimuli in voltage as well as in pulse duration. Therefore, optimization of the stimulation parameters including shape and positioning of surface electrodes are important topics for the treatment of paraplegic patients with denervated muscles.

Material and Methods

Muscle fiber compartment model

A muscle fiber is a cylindrical cell which essentially consists of the sarcolemma, the transverse tubular system (T-system), the

myofibrils and the intracellular fluid. The electrical excitation of a target fiber is simulated with a compartment model of Hodgkin Huxley type that is extended to include the current flow i_T into the T- system, i.e. membrane current im becomes

$$i_m = i_{ion} + i_T + C_m \frac{dV}{dt} \tag{1}$$

The ionic currents across the membrane consists of sodium i_{Na} , potassium i_K and leakage current i_L with a shift of the sodium current characteristics towards hyperpolarization, depending on the status of the denervation [1]. i_T results from the potential difference between the membrane potential V and the outermost (at radius a) tubular potential $V_T(a)$, which causes a current over the access resistance R_S of the T-system. The tubular potential is determined from the differential equation [2]

$$G_{L,T}\left(\frac{\partial^2 V_T}{\partial \rho^2} + \frac{\partial V_T}{\rho \partial \rho}\right) = c_T \frac{dV_T}{dt} + i_{ion,T}$$
 (2)

where c_T is the capacity of the T-system. The calculation of the ionic currents of the T-system $i_{ion,T}$ is analogue to those of the sarcolemma with corresponding parameters. $G_{L,T}$ denotes the lumen conductivity of the T-system and ρ is the fiber radius. The current relation along the fiber is

$$\frac{a}{2\rho_i} \left(\frac{\partial^2 V}{\partial x^2} + \frac{\partial^2 V_e}{\partial x^2} \right) = i_m \tag{3}$$

with fiber radius a, the intracellular conductivity ρ_i , the second derivation of the transmembrane and the extracellular potential V and V_e as functions of the fiber's length co-ordinate x.

With constant compartment length Δx the numerical form of (1) and (3) for the central compartments results in

$$\frac{a}{2 \cdot \rho_{i}} \left[\frac{V_{n+1} - 2 \cdot V_{n} + V_{n-1}}{\Delta x^{2}} + \frac{V_{e,n+1} - 2 \cdot V_{e,n} + V_{e,n-1}}{\Delta x^{2}} \right] = c \frac{dV_{n}}{dt} + i_{ionn} + i_{T,n} (4)$$

where the exciting effect of a denervated muscle fiber can be obtained by the classic activating function

$$f = \frac{\partial^2 V_e}{\partial x^2} \tag{5}$$

which was introduced to calculate the extracellular influence of the electrical field V_e along a nerve fiber x.

The junction between skeletal muscle and tendon (Fig. 1) consists of hemidesmosomes at the end of each muscle fiber as a mechanical connection to the collagen bundles of fibers of the tendon. At this location a very strong inhomogeneity referring to the muscle fiber can be observed because there is

no continuity between muscle fiber and collagen fibrils.

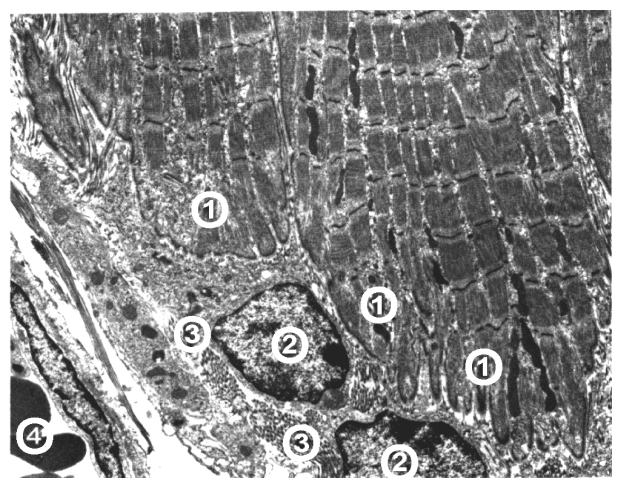


Fig. 1: Muscle-tendon junction (enlargement 4000); 1...finger-shaped endings of muscle fibers, 2...fibrocyts, 3...collagen fibrils, 4...erythrocyte.

It can be assumed, that no intracellular current is able to flow across the barrier between muscle fiber and collagen fibrils of tendon tissue. This consideration can lead to a substantial contribution of activating effect at the terminal region of the muscle fiber (Fig. 1), where the classic activating function for quasi infinite fiber length is negligible small. For that reason (4) is reduced to

$$\frac{a}{2 \cdot \rho_{i} \cdot \Delta x} \cdot \left[\frac{V_{2} - V_{1}}{\Delta x} + \frac{V_{e,2} - V_{e,1}}{\Delta x} \right] = c \cdot \frac{dV_{1}}{dt} + i_{ion,1} + i_{T,1}$$

$$\frac{a}{2 \cdot \rho_{i} \cdot \Delta x} \cdot \left[\frac{V_{N-1} - V_{N}}{\Delta x} + \frac{V_{e,N-1} - V_{e,N}}{\Delta x} \right] = c \cdot \frac{dV_{N}}{dt} + i_{ion,N} + i_{T,N}$$
(5)

This means that the activating function [3,4] becomes proportional to the first derivative of the extracellular voltage at the endings of a fiber

$$f' = \frac{\partial V_e}{\partial x} \tag{6}$$

(terminal activating function), whereas the second derivative is the driving element for the central part (5).

Electrical field

The geometric information is available as a number of CT cross-sections from patient data (Fig. 2). The MATLAB application FES-FIELD provides an input filter for DICOM format, which first converts the files into gray scaled 16bit images, then finds the outermost contour (skin) and last colors the contour-pixels white and all outlying pixels black (air). Depending on their gray values, the pixels inside the contour (skin) represent the basic types of tissue (conductivities in S/m): fat (0.03), muscle (0.1 transv. and 0.7 longitud. to fiber direct.), bone (0.016) and connecting tissue (0.06). The entire gray scale can be divided into

several groups where each group stands for a type

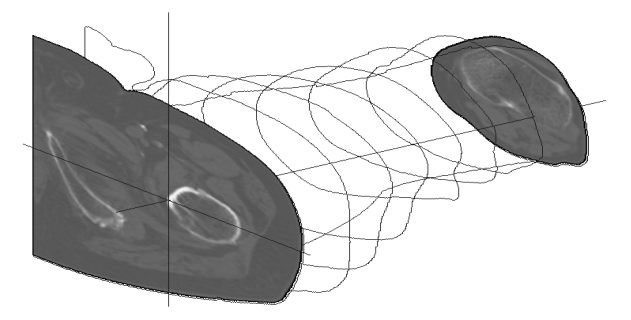


Fig. 2: Geometric 3D-Model of a right human thigh built by 51 CT cross-sections between hip and knee.

of tissue. The potential distribution is evaluated with the finite difference method considering a

conductivity of 10S/m for the electrode material (for details see [4, 6]).

Results

An example shows the stationary electrical field calculated by FES-FIELD in one length-section applied by large electrodes of 2 different locations (Fig. 3). The electrodes (black) are of rectangular shape (8 by 10cm) and placed centered onto the thigh. The distance from the center of the proximal to the center of the distal electrode is 10cm in case 1 (Fig. 3, left) and 15cm in case 2 (Fig. 3, right). The position of the proximal electrode is kept constant in the two cases and the distal electrode is shifted 5cm towards distal in the second case.

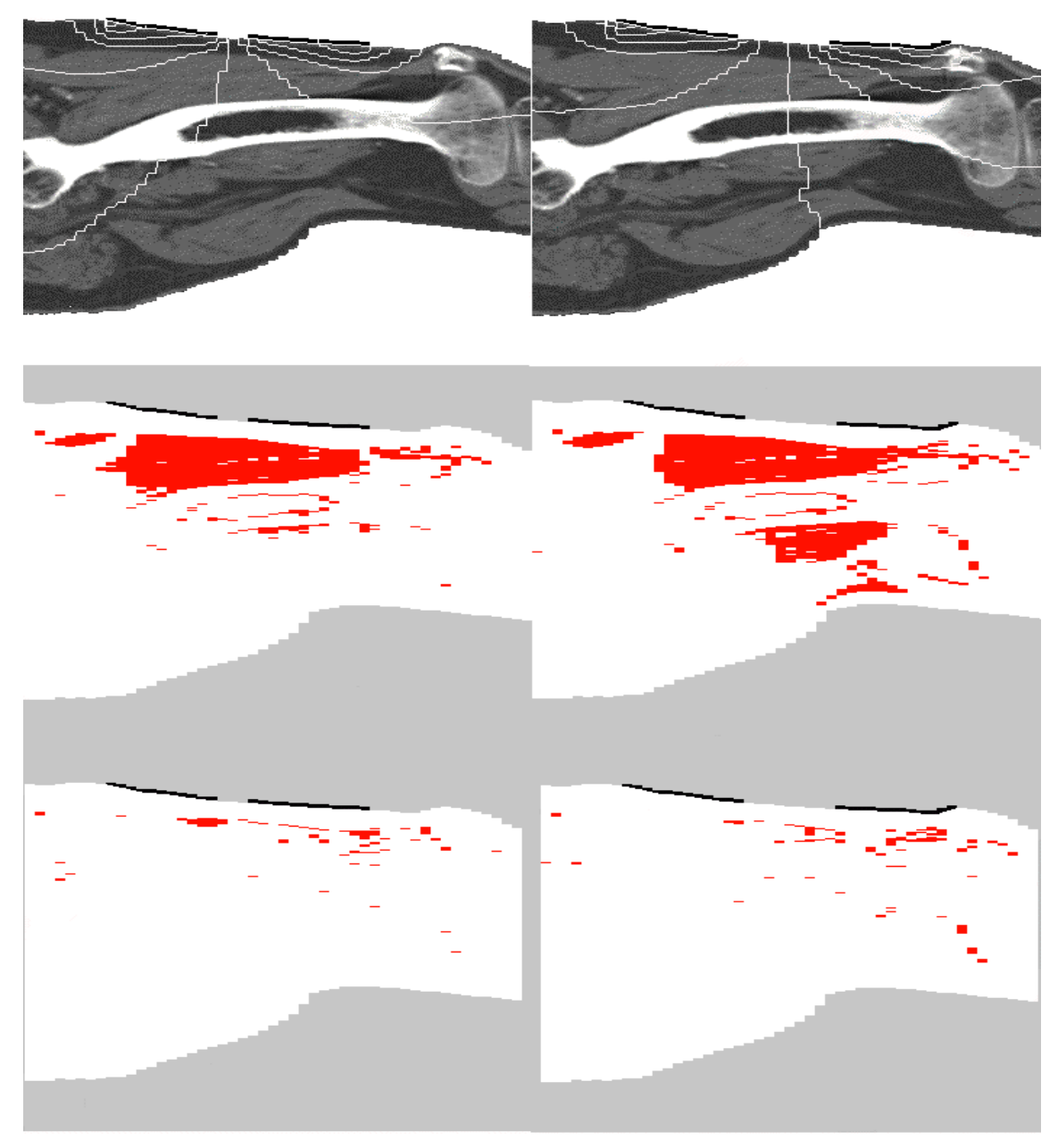


Fig. 3: Analyse of the electrical field in a CT length section of a human thigh applied by 2 electrodes (black) in 2 different cases (left: small distance; right: large distance). The electrical field is indicated by equipotential lines (top). Activation areas of the muscles (red) are determined either by the terminal activating function (middle) or by the classic activating function (bottom).

The stationary electrical field applied by a stimulator with pulse parameter of 80V and 20ms is shown by equipotential lines on gray scaled CT length sections from the middle of the thigh (Fig. 3, top). The equipotential lines are equally spaced by approx. 7V. In case 2 the electrical field distribution over the muscles of the thigh is more symmetrically in contrast to case 1 due to electrode position.

The terminal activating function is higher in case 2 than in case 1 (Fig. 3, middle). The red area indicates all possible muscle fiber endings which would be over threshold and therefore excited due to the stimulation parameter and the field distribution. In case 1 the area of activation is mostly in quadriceps femoris and would be an optimum for knee extension to stand up. In case 2 also the area of hamstrings are activated, which would lead to co-contraction of hamstrings and would reduce knee extension force despite of more activation in the area of quadriceps than in case 1.

The classic activating function (Fig. 3, bottom) is nearly equal in case 1 and case 2. In case 1 the largest area of activation can be observed very superficial direct under the fatty tissue near the distal edge of the proximal and the distal electrode caused by a stronger field distortion than in other areas due to the effect of the electrodes itself. In case 2 the activation is shifted towards distal and is reduced at the distal edge of the proximal electrode caused by lower current density due to larger electrode distance. The sum of all activated areas is very small an would not lead to a proper knee extension force for standing up neither in case 1 nor in case 2.

Discussion

In this research the stationary electrical field in the human thigh while applying functional electrical stimulation to paraplegic patients was simulated. One of the initial motivations for developing this simulation was being able to determine voltage distribution along muscle fibers. Using the 3D-matrix giving a voltage value for each pixel, the voltage distribution along any fiber or path can be determined whereof the activating function can be calculated. In difference to the classic activating function f the terminal activating function f effects only in the first or the last segment of the muscle fiber; everywhere else it is zero.

The classic activating function alone is useful for calculating the excitation of long nerve fibers. In contrast to typical muscle fiber stimulation in many FES applications the structure of an involved nerve fiber is homogeneous and seems to be of infinite length at the region of interest. Also for

single muscle fibers the classic activating function can be used, but only in the case of a very short distance [7] (up to 1-2mm) of the electrode to the fiber. For larger distances the exciting effect from an electrode placed over the end of the muscle fiber, calculated by the terminal activating function is stronger than the effect from an electrode positioned in the middle with equal amplitude.

Most cases for FES in denervated muscle are similar to the results in Fig. 3. The electrodes are much farther than 2mm from the target fibers, which means that the thickness of the fatty tissue is more than 1cm. For this reason the exciting effect at the muscle-tendon junction is stronger than anywhere else along the muscle fibers to force action potential and this is the only way to produce enough knee extension force for standing up.

References

- [1] Kern H., 1995. Funktionelle Elektrostimulation paraplegischer Patienten, Österr. Z. Phys. Med. Heft 1, Supplementum.
- [2] Henneberg K.A., Roberge F.A., 1997. Simulation of propagation along an isolated skeletal muscle fiber in an isotropic volume conductor, Ann. Biomed. Eng. 25: 15-28
- [3] Rattay F. 1999. The basic mechanism for the electrical stimulation of the nervous system. Neuroscience 89, 335-346.
- [4] Reichel M., 1999. Funktionelle Elektrostimulation denervierter Skelettmuskulatur Modellbildung und Simulation, (in German), Dissertation TU-Wien.
- [5] Adrean R.H. and Peachey L.D. 1973. Reconstruction of Action Potential of Frog Sartorius Muscle. J. Physiol. Lond. 235:103-131.
- [6] Reichel M., Breyer T., Mayr W., Rattay F., 2001. Simulation of the three dimensional electric field In The course of functional electrical stimulation. Artificial Organs 26 (3):252-255.
- [7] Reichel M., Mayr W. and Rattay F. 2002. Simulation of Exitation Effects at the Muscle-Tendon Junction in Denervated Muscle Fiber. Proceedings of the 7th Annual Conference of the International Functional Electrical Stimulation Society (IFESS), 152-154.

Author's Address

Martin Reichel, PhD

Department of Biomedical Engineering & Physics, University of Vienna, Austria

Währinger Gürtel 18-20, 1090 Vienna e-mail: martin.reichel@univie.ac.at

INDUCING MUSCLE HYPERTROPHY AS A THERAPEUTIC STRATEGY FOR MUSCLE WASTING: ROLE OF IGF-1

Antonio Musarò, Cristina Giacinti, Gabriella Dobrowolny, Laura Pelosi, Laura Barberi, Mario Molinaro

Department of Histology and Medical Embryology; University of Rome La Sapienza.

Abstract

The prolongation of skeletal muscle strength in aging and neuromuscular disease has been the objective of numerous studies employing a variety of approaches.

The characteristic loss in muscle mass, coupled with a decrease in strength and force output, has been associated with a selective activation of apoptotic pathways and a general reduction in survival mechanisms. Aging and genetic diseases, such as muscular dystrophies, amyotrophic lateral sclerosis, cancer and AIDS, are characterized by alterations in metabolic and physiological parameters, progressive weakness in specific muscle groups, modulation in muscle-specific transcriptional mechanisms and persistent protein degradation.

Although considerable information has accumulated regarding the physiopathology of muscle diseases, the associated molecular mechanisms are still poorly understood.

In this context, where direct therapeutic approaches to redress the primary disease are still sub-optimal, it may be more effective to focus on strategies for improving skeletal muscle function. In this review we will discuss the potential therapeutic role of Insulin-like Growth Factor 1 (IGF-1) in treatment of muscle wasting associated with several muscle diseases.

Text

While much has been learned about skeletal muscle formation in the embryo, less is known about the molecular pathways controlling skeletal myocyte survival and plasticity in the adult. Tissue remodeling is an important physiological process which allows skeletal muscle to respond to environmental demands. In particular, the complex contractile properties of skeletal muscle depend upon a heterogeneous population of myofibers that confer the functional plasticity necessary to modulate responses to a wide range of external factors, including physical activity, change in hormone levels and motor-neuron activity, oxygen and nutrients supply [1]. Fiber type is an essential determinant of muscle function and alteration in fiber composition represents a major component in the muscle degeneration associated with muscle diseases.

Chronic protein degradation is one of the most devastating consequences of defects in muscle survival mechanisms. For example, one of the most severe characteristics of muscular dystrophy is the progressive loss of muscle tissue due to chronic degeneration of muscle and to the exhaustion of satellite cells that replace damaged fibers [2].

Thus, the persistent protein degradation observed in neuromuscular diseases reflects a pathological muscle catabolism.

To date however, efforts to prevent or attenuate age- or disease-related muscle degeneration have been largely unsuccessful. Cell-based therapies have been stalled by the difficulty in obtaining sufficient numbers of autologous myoblasts and by inefficient incorporation into host muscle [3,4].

The identification of multi-potent stem cells residing in extrahematopoietic adult tissues has offered new perspectives in cell-mediated therapy for genetic diseases. Small numbers of haematopoietic stem cells (HCS) reside in the muscle beds of non-injured animals and more migrate into sites of injury, suggesting a mechanism by which damaged tissues are repaired [5]. However this seems a rare event and presents limitations for an efficient tissue repair.

Administration of growth hormone prevents age-related loss of muscle mass, but has failed to increase muscle strength.

Experimental models of muscle growth and regeneration have implicated Insulin-like Growth Factor-1 (IGF-1) as an important mediator of anabolic pathways in skeletal muscle cells [6]. In particular, IGF-1 is a key factor in the induction of muscle hypertrophy, thus a potential therapeutic approach that could counteract muscle atrophy observed in aged and pathological muscle is the induction of an increase in muscle mass.

We have generated a transgenic mouse carrying a local isoform of IGF-1 (mIGF-1) under the control of the muscle-specific regulatory elements from the MLC1/3 locus [7]. These mice display increased muscle mass associated with increased force generation compared to age-matched wild type littermates. Examination of older mice revealed that expression of the mIGF-1 transgene is protective against normal loss of muscle mass, promoting muscle regeneration [7].

In addition, high levels of mIGF-1 transgene expression in the mdx mouse model of muscular dystrophy also preserves muscle function in the absence of dystrophin, inducing significant hypertrophy and hyperplasia at all ages observed, reducing fibrosis and myonecrosis, and elevating signaling pathways associated with muscle survival and regeneration [8].

In addition, we analyzed whether muscle regeneration involved the recruitment of uncommitted cell populations. We demonstrated that the capacity of the transgenic muscle to regenerate is also associate to an increase in the recruitment of circulating stem cells expressing Sca1, CD45 and c-Kit, general markers of hematopoietic stem cells [9]. The recruited uncommitted cells homing the damage muscle, contribute to muscle regeneration and guarantee a reserve of muscle stem cells.

IGF-1 can therefore act, in combination with other regenerative factors, as a homing signal attracting circulating stem cells to repair injured muscle.

All of these evidences suggest that IGF1 activates regenerative processes and survival pathways leading to maintenance of muscle phenotype and attenuation of muscle atrophy and disease.

Reference

- [1] Buonanno A., Rosenthal N.: Molecular control of muscle diversity and plasticity. Dev. Genet. 1996, 19:95-107.
- [2] Musarò A, Rosenthal N. Attenuating muscle wasting: cell and gene therapy approaches. Current Genomics 2003; 4:575-585.
- [3] Grounds, M.D. Myoblast transfer therapy in the new millennium. Cell Transplant., 2000, 9: 485-487.
- [4] Grounds, M.D., White, J.D., Rosenthal, N., Bogoyevitch, M.A. The role of stem cells in skeletal and cardiac muscle repair. J. Histochem. Cytochem., 2002, 50: 589-610.
- [5] Blau, H.M., Brazelton, T.R., Weimann, J.M. The evolving concept of a stem cell: entity or function? Cell, 2001, 105: 829-841.
- [6] Musarò A.,Rosenthal N: The role of local Insulin-like Growth Factor-1 isoforms in the pathophysiology of skeletal muscle. Current Genomics 2002; 3: 149-162.
- [7] Musarò A, Mc Cullagh K, Paul A, Houghton L, Dobrowolny G, Molinaro M, Barton ER, Sweeney LH, Rosenthal N: Localized Igf-1 transgene expression sustains hypertrophy and regeneration in senescent skeletal muscle. Nature Genetics 2001; 27: 195-200.
- [8] Barton ER, Morris L, Musaro A, Rosenthal N, Sweeney HL: Muscle-specific expression of insulin-like growth factor I counters muscle decline in mdx mice. J Cell Biol. 2002; 157: 137-48.
- [9] Musarò A, Giacinti C, Borsellino G, Dobrowolny G, Pelosi L, Cairns L, Ottolenghi S, Bernardi G, Cossu G, Battistini L, Molinaro M, Rosenthal N. Muscle restricted expression of mIGF-1 enhances the recruitment of stem cells during muscle regeneration. PNAS 2004; 101: 1206-1210.

Author's address:

Dr. Antonio Musarò Department of Histology and Medical Embryology; Interuniversity Institute of Myology, University of Rome La Sapienza, Via A. Scarpa, 14 00161 Rome e-mail: antonio.musaro@uniroma1.it

Keynote lecture

S. Salmons (Liverpool, UK)

FES OF DENERVATED MUSCLES: BASIC ISSUES

S. Salmons, Z. Ashley, H. Sutherland, M.F. Russold, F. Li, J.C. Jarvis

Muscle Research Group, Department of Human Anatomy and Cell Biology University of Liverpool, Liverpool L69 3GE, UK

Abstract

Denervating injuries result in flaccid paralysis and severe atrophy of the affected muscles. We review here the potential for functional restoration of such muscles by electrical stimulation, focusing on the basic scientific issues.

Introduction

Over the last 30 years there has been much interest in the use of Functional Electrical Stimulation (FES) to restore posture and movement to paralysed limbs. This has focused largely on patients who have sustained an upper motor neuron lesion, resulting in spastic paralysis. There is, however, another group of patients whose problems are more severe and more difficult to treat: those who have sustained an irreversible lower motor neuron injury, resulting in flaccid paralysis of the affected limbs. The condition is more severe because of the marked atrophy of the denervated muscles and the associated deterioration of joints and skin. It is more difficult to treat because direct stimulation of muscles requires more electrical energy, particularly if parts of the muscle distant from the electrodes are to be recruited. Nevertheless it has been shown contrary to widely held opinion—that an intensive regime of electrical stimulation can have a marked influence in such patients, even after long-standing denervation [1, 2]. Electrical stimulation improved the excitability of the denervated tissues, reversed much of the loss of mass, and in some cases restored quadriceps muscle function sufficiently to support standing up.

A more extensive investigation is now under way, involving bioengineers, basic scientists, and clinicians, supported by the EU Project 'RISE'. One objective of this project is to seek a better scientific understanding of the phenomena surrounding long-term denervation and stimulation of skeletal muscle, one which can be used as a starting-point for stimulation techniques that are safe, effective and patient-friendly.

What are the potential therapeutic benefits of this approach in these patients? The following would be regarded as satisfactory clinical outcomes:

- 1. Restoration of muscle mass. For cosmetic reasons and to improve skin cushioning.
- 2. Restoration of muscle force. For standing up and standing of short duration, with associated improvements in local blood flow, skin condition, and general cardiovascular fitness.
- 3. Improved fatigue resistance. For standing of longer duration.

Whether these outcomes are achievable depends on more than just the nature of the response of the tissue to long-term denervation and stimulation. What is equally important in practice is the motivation that can be expected from the patient and the extent to which they are prepared to integrate the therapeutic regime into daily life. If, for example, we were to show that the desired results could be achieved in animals by stimulating each muscle for more than one hour per day, this would be scientifically interesting but clinically irrelevant: few patients would agree to a regime that interfered to this extent with their normal activities. Conversely, if restoration of mass turned out to be the only feasible outcome, we could try to achieve it with fewer impulses, arriving at a protocol that was more acceptable to the patient.

In the following we will examine some of the basic issues that we and other participants in the 'RISE' project have encountered. At this stage more questions will be raised than answers given. The reason is that, with a few exceptions, the experimental literature tends to focus on denervation of relatively short duration. By investigating the effects of long-term denervation, with and without chronic supramaximal stimulation, we are entering largely unknown territory.

Excitability

When a muscle is denervated it becomes less responsive even to direct stimulation. This

reduction in excitability presents a major practical difficulty. In patients it has been necessary to use biphasic rectangular current pulses with a duration as long as 120 ms to recruit fibers throughout the quadriceps femoris muscles. These long durations preclude the use of tetanic stimulation, and initial training has to be confined to twitch contractions. Kern and his colleagues found, nevertheless, that muscles subjected to this type of training for several months became more excitable. Pulses of shorter duration (such as 40 ms) could then be used, and this allowed low-frequency tetani to be introduced into the regime [3].

We wanted to set up an animal model of these changes in excitability. With Hermann Lanmüller and his colleagues we developed a technique for monitoring the rheobase and chronaxie in conscious rabbits (chronaxie is the pulse duration needed to excite the muscle at twice the threshold amplitude, or rheobase). A selective motor denervation was performed on the tibialis anterior muscle of one hind limb; foil electrodes placed on the muscle were connected to an implanted stimulator. After the animal had recovered from anaesthesia, the muscle could be palpated for threshold contractions while the implanted stimulator was controlled by a PC via a radiofrequency link. The results will be presented in more detail at this conference by Dr Zoe Ashley, on behalf of the Liverpool group. Chronaxie lengthened to about 15 ms within days of denervation, but did not increase more than this, even after denervation for 24 weeks. Chronic stimulation of 10-week-denervated muscles for 6 weeks had no apparent effect on chronaxie. How do we explain these differences between clinical and experimental findings?

It seems unlikely that rabbit muscle differs fundamentally from human muscle in its response to denervation. It also seems unlikely that the period of denervation was too short to model the human response; phenomena in smaller laboratory animals tend, if anything, to occur on a more rapid time scale than those in large animals, including man. The denervation period is being extended to 36 weeks, but so far the chronaxie seems not to differ from that obtained at 24 weeks.

It remains possible that the changes in excitability observed in the clinical situation occurred outside of the muscle itself. In the patients the stimulating electrodes were placed on the skin, and changes in the composition of subcutaneous tissues could have affected the measurement of excitability. In the rabbits, the electrodes were placed directly on the surface of the muscle, and measurements would not be affected by changes in surrounding tissues. This explanation gains some support from our colleagues in Padua, who have looked at the excitability of denervated muscles in the anaesthetised rat; they found that chronaxie was considerably longer when measured with skin electrodes than with intramuscular electrodes.

Muscle mass and cross-sectional area

The thighs of trained patients acquired an external appearance that, while still not normal, was much more acceptable cosmetically to the patient. Cross-sectional areas were measured by computerised tomography; in one patient (V.Z.) training for 26 months increased the cross-sectional areas of the two quadriceps muscles to 94.7% (right) and 85.7% (left) of the areas typical of a healthy subject [2]. This is in striking contrast to the severely wasted appearance that is seen in untrained, long-term denervated limbs.

The denervated rabbit muscles showed a similar response. The stimulated muscles were markedly larger, in both mass and cross-sectional area, than denervated controls. Histological examination showed that the fibres in these muscles were larger in diameter and more tightly packed. Although there was some inter-animal variability, some of the muscles had a histological appearance that was close to normal, something never seen in muscles subjected to denervation alone.

Force-generating capacity

Before training, the quadriceps muscles of the patients could not develop measurable torque at the knee. The increase in muscle size brought about by long-term stimulation was accompanied by a return of force, sufficient in some cases to support standing up. The force was, however, a small fraction of what might have been expected from the cross-sectional area—only 10% that of a normal subject in the case study referred to above.

Rabbit muscles that had been denervated and stimulated also showed a shortfall in force-generating capacity. The force per gram wet weight for a maximum tetanic contraction was 5.6 N/g, against the 7.7 N/g of the control innervated muscles.

What is the reason for this underperformance?

In the patients, only net knee torque has been measured; this gives an artefactually low estimate of the torque exerted by the quadriceps muscles because of co-contraction of antagonists. A new non-invasive technique developed by Dr D. Rafolt should overcome this problem. It is also difficult to recruit the entire muscle by surface stimulation in man. However, neither of these factors can explain the abnormally low forces developed by denervated muscles in the rabbit.

In both human and rabbit denervated muscles, the long duration of the stimulus pulses places an upper limit on the frequency used to generate a tetanus. However, examination of force-frequency curves in the rabbit (Fig. 1) shows that the tetanic force is already asymptotic at 50 Hz, so it is unlikely that the tension shortfall is due to low stimulation frequencies. Moreover, the tetanus elicited at 50 Hz is sustained and shows a slight ripple corresponding to individual stimuli; this would argue against a failure of excitation-contraction coupling, at least in the population of fibres that is developing tension.

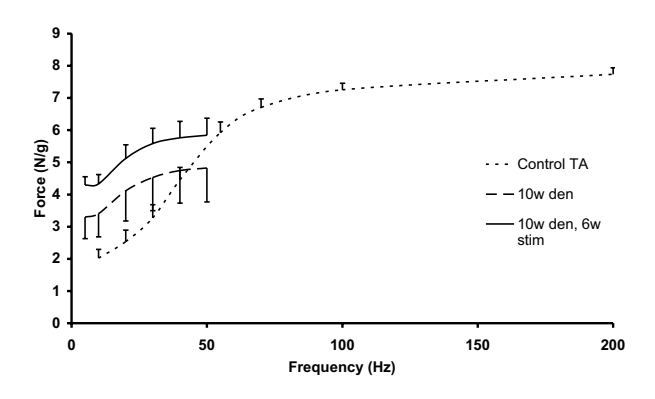


Fig. 1: Effect of denervation, and denervation with stimulation, on rabbit tibialis anterior muscles. The stimulation pattern illustrated was as follows: pulse duration, 20 ms; burst frequency, 20 Hz; on time, 2 s; off time, 1 s; stimulation delivered for 1 h/day. w=weeks.

It remains possible that tension development is affected by abnormalities at the fibre or the whole muscle level. At the fibre level the myofilament arrays could be disrupted or myofibrillar occupation of the fibre cross-section could be reduced by the presence of mitochondria or other structures. At the whole muscle level, the cross-sectional area occupied by contractile tissue could be reduced by oedema, fat, or fibrous connective tissue. Microscopic examination of stimulated denervated

muscle tissue from both patient biopsies and the experimental rabbits reveals a substantially normal appearance, and this currently favours explanations based on changes at the fibre level. Investigations in progress should help to throw further light on this question.

Contractile speed

The contractile speed of the human muscles is not known, although the non-invasive technique already mentioned should provide information on this. In the rabbits, the denervated muscles contract more slowly than their innervated counterparts in the contralateral hind limb, and this difference remains after chronic stimulation. Although the denervated muscles have a low maximum shortening velocity, this alone does not entirely explain the differences in contractile speed. The muscles show a very high twitch:tetanus ratio, which points to prolonged activation. This may be due to deficiencies in the mechanisms for calcium ion reuptake or other abnormalities in the sarcoplasmic reticulum membrane.

The slowness of the muscles is not necessarily a disadvantage. Although it reduces the available power, it permits substantial fusion, even of low-frequency tetanic contractions, and the force developed is correspondingly greater.

Fatiguability

Although some of the trained patients can stand with quadriceps stimulation, the muscles quickly fatigue. There is no evidence of this in the rabbit model. The fatigue resistance of a 10-week-denervated muscle is not substantially different to that of a normal, innervated muscle and undergoes no change in response to 6 weeks of stimulation. After denervation and stimulation, therefore, the rabbit muscle is neither more nor less fatigue-resistant than an innervated control muscle. This is somewhat unexpected, for an innervated muscle would show a marked increase in fatigue resistance after 6 weeks of stimulation.

Examination of sections stained histochemically for the demonstration of NADH tetrazolium reductase indicates that the denervated rabbit muscle fibres have a greatly increased mitochondrial population. Such an appearance would normally be associated with a highly fatigue-resistant character. This suggests either that the mitochondria do not function normally, or that oxidative metabolism is rate-limited by the blood supply to the muscle or oxygen transport to the fibres. These putative mechanisms are currently under investigation, but preliminary evidence from our colleagues in Vienna (Dr F. Bittner, Prof H. Gruber) suggest that there may be some decoupling of oxidative-phosphorylation.

Degeneration-regeneration

Biopsies from the patients' quadriceps muscles have been examined in Padua by Professor U. Carraro and Dr K. Rossini. Using antibodies to embryonic myosin isoforms they have demonstrated a higher than normal incidence of ongoing regeneration in the denervated muscles. We will be applying similar techniques to the examination of the denervated rabbit muscles, but quantitative morphology on the samples obtained to date indicates that the total number of fibres in the muscle is not changed by denervation with or without stimulation. This suggests either that degenerative-regenerative phenomena take place at a low level, or that the degenerative loss of fibres is balanced by the generation of new fibres. It remains possible that muscle degeneration takes place on a larger scale in the patients after denervation for some years, and that this stage has not yet been reached in the experimental rabbit muscles.

Conclusions

To date, the rabbit experiments offer no evidence that long-term stimulation can change the excitability of the muscle. It would seem that the training regime will continue to be limited to twitch or low-frequency tetanic stimulation. Considerable restoration of muscle mass is achievable through stimulation. However, the force-generating capacity of these muscles does not increase commensurately, possibly because of abnormalities at the ultrastructural level. There is no indication, so far, that this situation can be improved by stimulation. In the rabbits the denervated muscles remain slow after stimulation. Although this limits the available power, it enhances the force that can be generated in lowfrequency tetanic contractions. There is currently no explanation for the fatiguability of the trained human muscles, although the rabbit experiments point to possible abnormalities in oxidative metabolism. Regenerative phenomena clearly play a part in the processes of denervation and stimulation, but their importance remains to be established. We should emphasize that these are very preliminary conclusions; a good deal of experimental work and analysis has still to be done.

Long-term denervation of muscles is accompanied by a number of changes at the tissue and subcellular level. It is by no means certain at this stage that we can reverse all of these changes by stimulation, particularly with regimes that would be acceptable to patients. However, it is both the clinical and the laboratory experience that long-term stimulation of denervated muscles produces a highly significant increase in mass and cross-sectional area. In patients this offers the prospect of an improved cosmetic appearance of the denervated limb and better cushioning, with a reduced risk of pressure sores. This alone would be a worthwhile outcome.

References

- [1] Kern, H.: Funktionelle Elektrostimulation paraplegischer Patienten. Oster. Zeit. Phys. Med. 5, 1995, 1-79
- [2] Kern, H., Salmons, S., Hofer, C., Mödlin, M., Richter, W., Mayr, W., Rossini, K., Carraro, U.: Recovery of long-term denervated human muscles induced by electrical stimulation. Muscle Nerve, 2004, in press
- [3] Kern, H., Hofer, C., Mödlin, M., Forstner, C., Raschka-Höger, D., Mayr, W., Stöhr, H.: Denervated muscles in humans: limitations and problems of currently used functional electrical stimulation training protocols. Artif. Org. 26, 2002, 216-18

Acknowledgements

This study is supported by EU Commission Shared Cost Project ('RISE', Contract No. QLG5-CT-2001-02191).

Author's Address

Prof. S. Salmons
Department of Human Anatomy and Cell Biology
The Sherrington Buildings
Ashton Street
University of Liverpool
Liverpool L69 3GE, UK
Email: s.salmons@liverpool.ac.uk

Session 5

FES of Denervated Musculature 3

Chairpersons:

H. Gruber (Vienna, Austria) W. Girsch (Vienna, Austria)

DETERMINATION OF THE CHRONAXIE AND RHEOBASE OF DENERVATED LIMB MUSCLES IN CONSCIOUS RABBITS

- Z. Ashley*, H. Sutherland*, H. Lanmuller**, E. Unger**, F. Li*, W. Mayr**, H. Kern***, JC. Jarvis*, S. Salmons*
- * Muscle Research Group, Department of Human Anatomy & Cell Biology, The Sherrington Building, University of Liverpool, Liverpool, L69 3GE, UK
- ** Department of Biomedical Engineering & Physics, Medical University, AKH, A-1090, Vienna, Austria
- *** Ludwig Boltzmann Institute of Electrostimulation and Physical Rehabilitation, Department of Physical Medicine, Wilhelminenspital, Vienna, Austria

Abstract

Measurements of the rheobase and chronaxie can be used to define the excitability of nerves and muscles. The aim of this study was to obtain a record over many weeks of changes in the rheobase and chronaxie of denervated rabbit tibialis anterior muscle (TA).

A custom-built electronic stimulator was implanted into the peritoneal cavity of New Zealand White rabbits. Large stainless steel electrodes were placed on the denervated TA muscle. Rheobase and chronaxie were measured non-invasively at weekly intervals by means of a laptop PC, which communicated with the stimulator via a radiofrequency link. At each setting the denervated TA was palpated manually to detect the response of the muscle.

During the first few days after denervation the rheobase increased transiently to 0.8 ± 0.13 mA, approximately twice the value for normal innervated muscle, then decreased to normal for the remainder of the experimental period. Chronaxie underwent a significant 3-fold increase from 4.5 ± 1.1 ms to 14.1 ± 1.1 ms during the first two weeks of denervation and remained elevated throughout.

The custom-built implantable electronic stimulator allowed changes in muscle excitability to be studied over a long period of denervation within individual animals, providing an accurate assessment of the time course of denervation-induced changes in muscle excitability.

Introduction

The excitability of a tissue can be defined by the relationship between stimulation amplitude and stimulation duration, otherwise known as the strength-duration curve. There are two points on this curve that can be used to define the excitability of the tissue, the rheobase and the chronaxie.

The rheobase of an excitable tissue is the minimum stimulus amplitude needed to elicit a response at infinitely long pulse durations; the chronaxie is the minimum pulse duration for a response when the stimulus amplitude is twice the rheobase (Fig. 1).

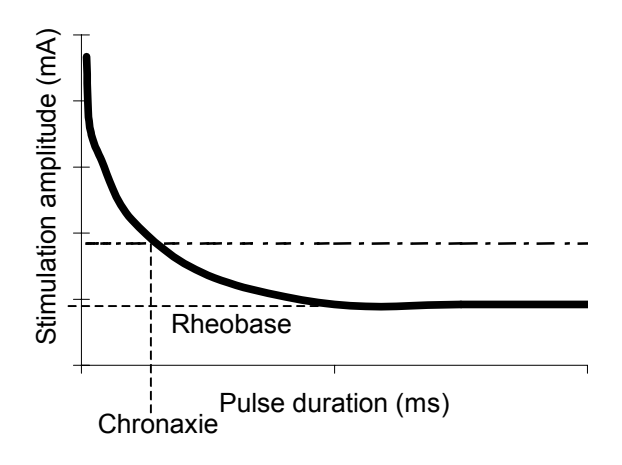


Figure 1: Typical strength-duration curve obtained from skeletal muscle. The rheobase is the asymptote to the lower portion of the curve. The chronaxie is the pulse width required to produce a response at twice the rheobase.

Denervation of skeletal muscles has been shown to result in many changes in structure and function. One of these changes is the decrease in the excitability of the muscles, associated with a large increase in the chronaxie [1]. Denervated muscles do not respond at all to short stimulating impulses; they require pulses of longer duration than those that are adequate for innervated muscles.

The use of electrical stimulation to alleviate the severe atrophy arising from denervation must take account of changes in muscle excitability. This study was designed to investigate the long-term changes in excitability of denervated muscle in order to elucidate the stimulation pattern that is necessary for the restoration of denervated muscle by electrical stimulation.

Material and Methods

Surgical procedures

All procedures were carried out in accordance with the Animals (Scientific Procedures) Act 1986, which governs the use of experimental animals in the UK.

Six New Zealand White rabbits (2.5 - 3 kg) were operated under inhalational anaesthesia (2% Isoflurane). All surgical procedures were carried out with full aseptic precautions.

The ankle dorsiflexor muscles of the left hind limb were denervated by avulsion and ligation of the motor portion of the common peroneal nerve. The proximal stumps were placed into a silicone rubber tube, with two ligatures placed tightly around the nerve. The tube was then reflected 90° from its original position and secured to underlying fascia. A custom-built electronic stimulator was placed into the peritoneal cavity and secured to the abdominal wall. Leads were routed subcutaneously to large stainless steel foil electrodes on the proximal superficial and deep distal surfaces of the TA muscle. The animals were allowed to recover from anaesthesia and inspected daily.

Measurements

The rheobase and chronaxie were determined by means of the implanted stimulator. Measurements were managed by a laptop PC, which communicated with the implanted stimulator via a radiofrequency link. At each setting the denervated TA was palpated manually for a response.

The pulse duration used to determine the rheobase was 100 ms. The amplitude was resolved to 0.04 mA in a 3-stage protocol. The pulse amplitude was then set at 2x rheobase, and the chronaxie resolved to 0.5ms in a 2-stage protocol. At each step 10 bipolar constant-current pulses were delivered while the muscle was palpated.

Immediately after completion of the surgical procedure, while the animals were recovering, measurements were taken to give a baseline reading. The measurements were then repeated at weekly intervals over the 24-week denervation period. The animals were lightly restrained during the measurements, but were fully conscious.

At the end of the denervation period physiological tests were carried out under terminal general anaesthesia (continuous intravenous Hypnorm infusion). In the course of these measurements a full strength-duration curve was obtained, from which the rheobase and chronaxie could be determined.

Data analysis

Data shown are mean \pm SEM, n = 6. Alterations in the values over the period of denervation were assessed for significance by ANOVA. Statistical significance was set at p<0.05.

Results

Rheobase

During the first few days of denervation the rheobase increased significantly (p<0.05) to 0.80 ± 0.13 mA (Fig. 2). This increase was transient and values then decreased and normalised for the remainder of the experimental period.

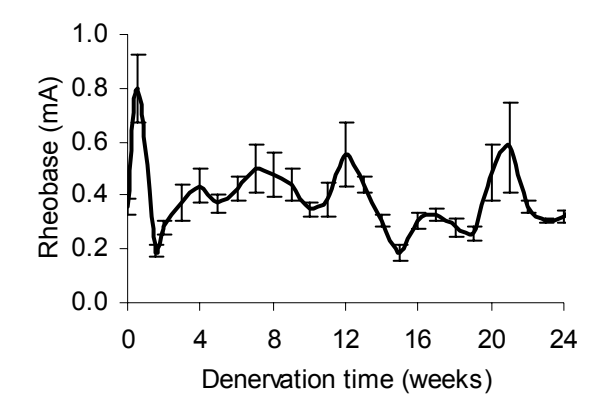


Figure 2: Rheobase values obtained from conscious rabbits over a 24-week period of denervation. Data shown are mean \pm SEM for n = 6 animals.

Chronaxie

Chronaxie increased 3-fold from 4.5 ± 1.1 ms to 14.1 ± 1.1 ms (p<0.01) over the initial 2 weeks of the denervation period (Fig. 3), and remained at this elevated level throughout the 24-week experimental period.

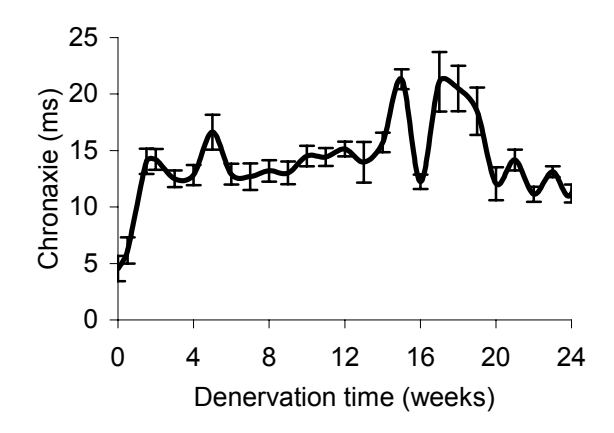


Figure 3: Chronaxie values obtained from conscious animals over the 24-week denervation period. Data shown are mean \pm SEM for n = 6 animals.

To see if there was any relationship between the rheobase and chronaxie values the data was compared by time point within individual animals (Fig. 4). There was a tendency for chronaxie to decrease when rheobase increased, and vice versa.

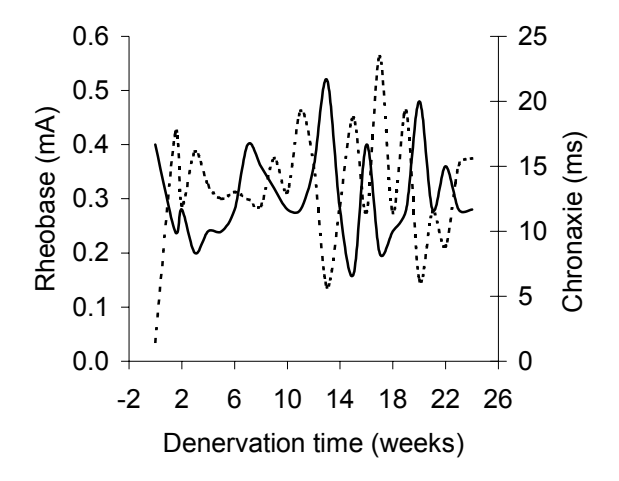


Figure 4: Rheobase (solid line) and chronaxie (dotted line) values obtained from an individual conscious rabbit over the 24-week denervation period.

Validation of conscious measurements

Comparison of the rheobase and chronaxie measurements from the conscious animals and measurements obtained during physiological assessment showed a clear correlation. Neither the rheobase (Fig. 5) nor the chronaxie (Fig. 6) were significantly different between the last measurement in the conscious animals and the values derived from the strength-duration curve measured under terminal anaesthesia.

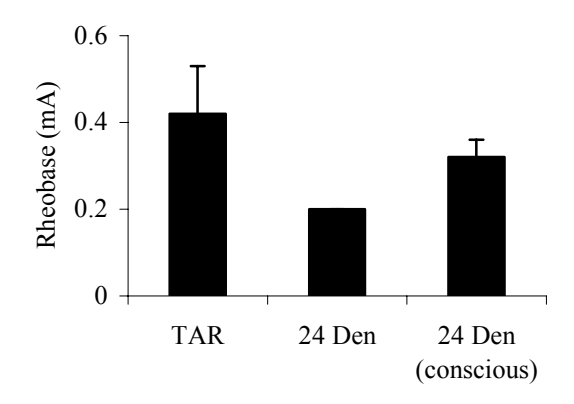


Figure 5: Rheobase values obtained from innervated contralateral control muscles (TAR) and 24-week denervated muscles (24 Den) under general anaesthesia, and values from 24-week denervated muscles in conscious animals (24 Den conscious). Data are shown as mean \pm SEM for n = 3 animals.

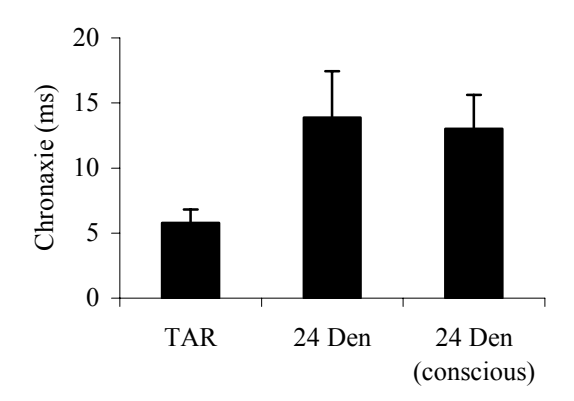


Figure 6: Chronaxie values obtained from innervated contralateral control muscles (TAR) and 24-week denervated muscles (24 Den) under general anaesthesia, and values from 24-week denervated muscles in conscious animals (24 Den conscious). Data are shown as mean \pm SEM for n = 3 animals.

Discussion

This is, to the best of our knowledge, the first study to provide a detailed time course of changes in the excitability of denervated skeletal muscle over an extended period within individual animals.

The initial baseline measurements were essentially those for normal innervated muscle, and they were very similar to those obtained from the innervated contralateral control TA muscle. The values for chronaxie were higher than expected from the literature [2] $(3.7 \pm 1.0 \text{ ms}, \text{ compared to } 0.43 \pm 0.02 \text{ ms})$. This may be an effect of anaesthesia resulting in a prolongation of the measured chronaxie.

The transient increase in rheobase in the first 3 days following denervation may be the result of post-operative oedema. This could have produced some shunting of the stimulation current around the fibres, and may also have made the muscle response less easy to palpate. The rheobase has returned to normal values within 1-2 weeks.

The significant 3-fold increase in chronaxie occurred between 7 and 10 days after denervation, with a small increase already seen after 3 days. Degeneration of the motor endplates takes between 30-70 hours [1]. Once the endplates are no longer functional the sarcolemma has to be stimulated directly, to elicit a twitch response with electrical stimulation.

A relationship was observed between the rheobase and chronaxie: if the rheobase was lower the chronaxie tended to be higher. This is to be expected since the measurement of chronaxie depends on the prior determination of rheobase. A slight overestimation of the rheobase value will tend to reduce the measured chronaxie. The measurements were made throughout by the same team in the same way to minimize subjective variation in assessing the response. Nevertheless, inter-week variability was observed in the rheobase values, and this was probably attribuitable to variation in the sensitivity with which the experimenter was able to palpate the twitch response. Some variation may also have resulted from small differences in the location of the twitch response or the animal's limb position.

This study was conducted with a custom-made implanted electronic stimulator that is capable of repeatedly measuring the excitability of a denervated muscle over an extended period of denervation (24 weeks). These data allow changes in excitability to be tracked within individuals, improving the scientific value of the data and reducing the number of animals used.

References

- [1] Gutmann E, Zelena J: Morphological changes in the denervated muscle. The denervated muscle, Chapter 2 pg 57-102. Ed: Gutmann E. 1962 Czechoslovak Academy of Sciences
- [2] Kiernan MC, Burke D, Andersen KV, Bostock H: Multiple measures of axonal excitability: A new approach to clinical testing, Muscle & Nerve, 23(3): 399-409, 2000.

Acknowledgements

Research was supported by EU project "RISE" (Contract No: QLG5-CT-2001-02191).

Author's Address

Dr Zoe Ashley Muscle Research Group Department of Human Anatomy & Cell Biology University of Liverpool, L69 3GE, UK e-mail: zoeash@liverpool.ac.uk

FES OF DENERVATED TIBIALIS ANTERIOR IN THE PIG MODEL

W. Girsch *, C. Hofer **, D. Rafolt ***, W. Rosmanith ****, G. Weigel***, E. Unger ***, W. Mayr ***

* Orthopaedic Hospital Speising, Vienna, Austria

** LBI of Electrical Stimulation & Physical Rehabilitation, Wilhelminenspital Vienna, Austria

*** Center of Biomedical Engineering & Physics, Medical University of Vienna, Austria

**** Center of Anotomy and Cell Biology, Medical University of Vienna, Austria

Introduction

Currently experiments are carried out in Liverpool to evaluate stimulation parameters and protocol for effective and safe stimulation of long-term denervated muscles. These basic experiments are carried out in rabbits using implanted stimulation electrodes. Obviously experiments from rabbits cannot be transferred directly to human application. Therefore a small series of animal experiments in pigs is scheduled to "bridge" results from rabbit to human.

Material and Methods

Animals:

12 "Göttinger minipigs" of the same sex will be used for investigation.

Denervation:

In a first surgical procedure the left common peroneal nerve will be dissected to denervate the left Tibialis anterior (TA) and Extensor digitorum longus (EDL) muscle. A period of minimum 6 months will be kept to achieve long term denervation. After that time periode neurophysiological investigations and muscle biopsies will be performed monthly in order to detect the desired denervation state which means more than 50% reduction of muscle mass and loss of mitochondrial function.

Prior to stimulation the left leg has to be denervated partly or totally in a second surgical procedure performing either local denervation of peripheral sensible nerves or rhizotomy of dorsal rootlets vie hemilaminectomy.

Stimulation:

Chronical stimulation will be performed over a time period of 6 months:

Surface electrodes will be fixed to the anterior surface of the left lower leg for 30 to 60 minutes, once daily for five days per week. Stimulation will be started when the animals are trained to accept the electrodes. Stimulation parameters will be set according to the findings from rabbit experiments.

Investigation:

Under general anesthesia the denervated and stimulated TA muscles will be connected to force transducers for physiological examination. After sacrification of the animals the entire TA and EDL muscles will be excised for investigation according to the rabbit experiments.

Discussion

The scheduled pig experiment should be appropriate to "bridge" results from rabbit experiments to human application: Pig skin is comparable to human skin. "Göttinger minipigs" grow up to about 80kg which is comparable to human bodyweight. Stimulation once a day for half an hour is an accepted protocol for human application. Moreover the experiment should not only allow to answer the scientific questions about efficacy and safety of stimulation of long-term denervated muscles but also to test the technical equipment for human use.

Acknowledgements

Supported by EU Commission Shared Cost Project RISE, Contr. Nr. QLG5-CT-2001-02191 and Austrian Ministry of Education, Science and Culture.

Author's Address

Univ.-Doz. Dr. Werner Girsch Orthopaedic Hospital Speising Speisinger Strasse 106 A-1134 Wien, Austria

e-mail: werner.girsch@meduniwien.ac.at

DISTRIBUTION OF REST PERIODS BETWEEN ELECTRICALLY GENERATED CONTRACTIONS IN DENERVATED MUSCLESOF RATS

D.E. Dow, J.A. Faulkner, R.G. Dennis

Institute of Gerontology, Dept. of Biomedical Engineering, Univ. of Michigan, Ann Arbor, MI, 48109, USA

Abstract

Stimulation protocols for denervated muscles typically distribute the generated contractions either within treatment sessions followed by hours of rest, or repeated 24 hours per day with each contraction followed by a constant interval of rest. Our purpose was to directly compare the effects of the same number of identically generated contractions having different distributions throughout the 24 hour day. For 5 weeks in denervated muscles of rats, implanted stimulators generated between 100 to 800 contractions daily, distributed either within worksets that alternated periods of activity and rest, or separated by constant intervals of rest. Most of the tested protocols maintained muscle mass and maximum force near values for control Although 100 contractions daily muscles. generated at constant intervals were sufficient to maintain mass and force, 100 contractions during a 4-hour treatment session followed by 20 hours of rest were not sufficient, and mass and force were not different from values of denervated muscles.

Introduction

The contractile and cellular properties of skeletal muscles are influenced by the amount and pattern of contractile activity [1]. Denervated muscles undergo no contractile activity, and rapidly lose muscle mass, maximum force and even specific force that is normalized for the physiological cross sectional area (CSA) of the muscle [2]. We have developed a protocol of electrical stimulation for denervated extensor digitorum longus (EDL) muscles of rats that maintains muscle mass, maximum force, specific force and mean fiber CSAs at values close to those for control muscles

after 5 weeks of stimulation [3,4]. This protocol generates short, tetanic contractions separated by a constant interval of rest, repeated 24 hours per day. In this earlier study, the effect of the distribution of the generated contractions and periods of rest was not studied.

Mammals have periods of more or less intense muscular activity related to the 24 hour circadian Exercise training alters contractile activity and is accomplished within the circadian cycle that includes long periods of rest. The timing of the periods of rest between contractions or sets of contractions in resistance training affects fatfree mass, maximum force and power output [6]. For training of muscles in paraplegics with electrical stimulation, muscle force was affected by the length of the treatment session, the ratio of work to rest periods within the treatment session, and the number of treatment sessions per week [7]. The timing of the periods of rest between contractions or sets of contractions may also affect electrically stimulated-denervated Certain stimulation-denervation studies grouped all electrically generated contractions for one day into one or more treatment sessions, and those sessions were repeated a number of times per week [8,9]. Other studies separated each contraction by a constant interval of rest, repeated 24 hours per day, 7 days per week [3,4,10,11]. Our purpose was to directly compare the effects of the same daily number of identically generated contractions that had different temporal distributions of the rest periods between contractions.

Material and Methods

The experiment utilized 63 adult male WI/HicksCar rats (Harlan, Indianapolis, IN, USA).

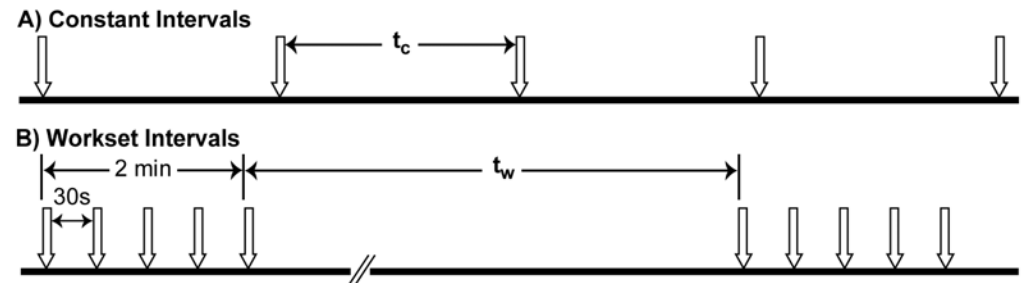


Fig. 1: Distribution of the periods of rest between muscle contractions for protocols of A) constant intervals or B) workset intervals. Each down-arrow symbol represents a train of 20 pulses at 100 Hz to generate one tetanic contraction. In constant intervals (A), each contraction was separated by exactly the same period of rest $(\mathbf{t_c})$ throughout each period of 24 hours. In each set of workset intervals (B), 5 contractions were separated by 30 seconds of rest, followed by a longer period of rest $(\mathbf{t_w})$. These worksets of 5 contractions followed by $\mathbf{t_w}$ of rest were repeated for a 4 hour period designated a workout.

All procedures were conducted in accordance with the guidelines established in the U.S. Public Health Service Guide for the Care of Laboratory Animals and with the approval of the University Committee on the Use and Care of Animals.

Rats were assigned to one of the following three groups: 1) denervated (n, 5; final age, 6.1 ± 0.3 mo; weight, 373±10 g), 2) constant intervals stimulated-denervated (n, 31; final age, 6.8±0.1 mo; weight, 382±4 g) or 3) workset intervals stimulated-denervated (n, 28; final age, 7.2±0.4 mo; weight, 381±5 g). The EDL muscle of the right hindlimb of each rat underwent the experimental interventions involving denervation and stimulation. The left EDL muscle of each rat remained unoperated and innervated, received no stimulation prior to final evaluation, and acted as a control muscle [4]. An initial surgery permanently denervated the right EDL muscle in each rat according to the procedure described by Carlson and Faulkner [12]. Immediately following, rats in either of the stimulated-denervated groups had a stimulator and electrode wires implanted according to the procedure described by Dow [4]. After a 5 week period following the initial surgery, the denervated or stimulated-denervated muscles were evaluated in vitro according to the procedure of Faulkner et al. [2,3,12] to determine muscle mass, maximum force for isometric, tetanic contractions, and specific force that was normalized for the physiological CSA of the muscle.

To generate a tetanic contraction, the stimulator generated 20 bipolar pulses at 100 Hz, with 8 V pulse amplitude that generated a current of 6-12 mA [3,4]. The number of contractions generated each day (C_d) was set at a value between 100 and 800. Fig. 1 contrasts the two types of distributions of contractions and rest periods over each 24 hour period. In the constant intervals distribution, each individual contraction was separated by an equal period of rest (t_c), and this was repeated 24 hours per day (Fig. 1A). The value of t_c was determined

by the desired value of C_d , and ranged from 14.4 minutes for C_d of 100 to 1.8 minutes for C_d of 800 contractions daily.

In the workset intervals distribution, the generated contractions were distributed into layered sets of work and rest. Five contractions, each separated by 30 seconds of rest, were generated during a set (Fig. 1B). Then, a longer period of rest (t_w) was allowed before the next set began (Fig. 1B, Table 1). These sets of five contractions followed by t_w minutes of rest were repeated throughout a 4 hour period called a workout. Each 4 hour workout was followed by 2 hours of rest during which no contractions were generated. This allowed a maximum of 4 workouts per day. diagrams a protocol having 4 workouts per day, designated WWWW. Fig. 2B diagrams a protocol, designated WRRR, having only 1 workout per day with rest over the remaining 20 hours. Table 1 lists the values for C_d, t_w, pattern of workouts, and maximum period of continuous rest between contractions during each 24 hour day.

C _d	t _w	Pattern	Max Rest	
100	10.0	WRRR	20 hr	
200	10.0	WRWR	8 hr	
300	10.0	WWWR	8 hr	
400	10.0	WWWW	2 hr	
600	4.0	WWWR	8 hr	
800	4.0	WWWW	2 hr	

Table 1: Protocols of workset intervals.

Following the 5 week treatment period, each rat was anesthetized, the stimulator was checked *in vivo* with use of an oscilloscope for proper functioning, the EDL muscles were removed and evaluated *in vitro* for determination of muscle properties. A stimulator was considered defective if the pulses were mono-polar, if the pulse width was longer than 0.6 ms, if the voltage amplitude was less than 5 volts or if the current was less than 1 mA. Physiological data recorded from a muscle with a defective stimulator were discarded without

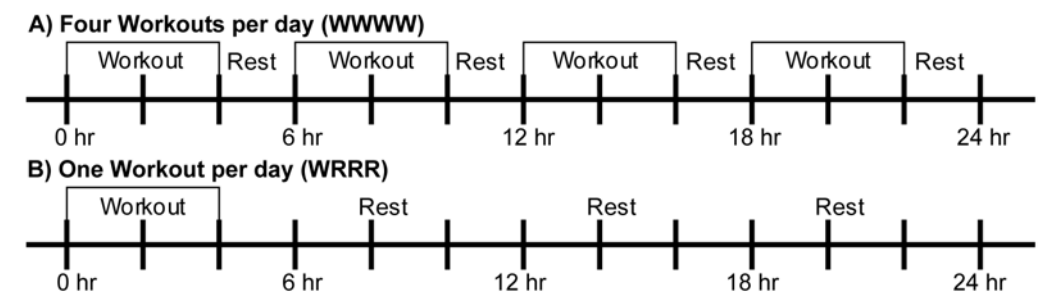


Fig. 2: Examples of workout patterns. Depending on the protocol of workset intervals, each 6 hour period of the 24 hour day may have had either a workout lasting 4 hours followed by 2 hours of rest (designated W), or a full 6 hours of rest (designated R). A) shows a *WWWW* pattern, where each 6 hour period contained a 4 hour workout (W), each followed by 2 hours of no stimulation. B) shows a *WRRR* pattern, where the first 6 hour period contained a 4 hour workout (W) followed by 2 hours of no stimulation, and the other three 6 hour periods contained no workouts, only rest (R), resulting in a daily rest period of 20 hours having no contractions.

further analysis.

Statistical analysis was performed using SPSS software (SPSS Inc., Chicago, IL, USA). For the dependent variables of muscle mass, maximum force and specific force, a one-way ANOVA was used to compare differences between the different experimental groups. When a significant main effect was found, the Bonferroni t-test was used for Post Hoc analysis and the 0.05 level of probability was used to signify statistical significance. All data are presented as means ± standard error (SE).

Results

Of the 63 rats utilized for this experiment, data were discarded for the right EDL muscles from 5 of the 30 rats with constant intervals and 5 of the 28 rats with workset intervals because the stimulator had become defective as determined by the procedure described above. Data were also discarded for 3 of the 63 left control EDL muscles because the muscle evaluation procedure was inadvertently not completed correctly. Of the 53 implanted stimulators, 17% became defective prior to final evaluation.

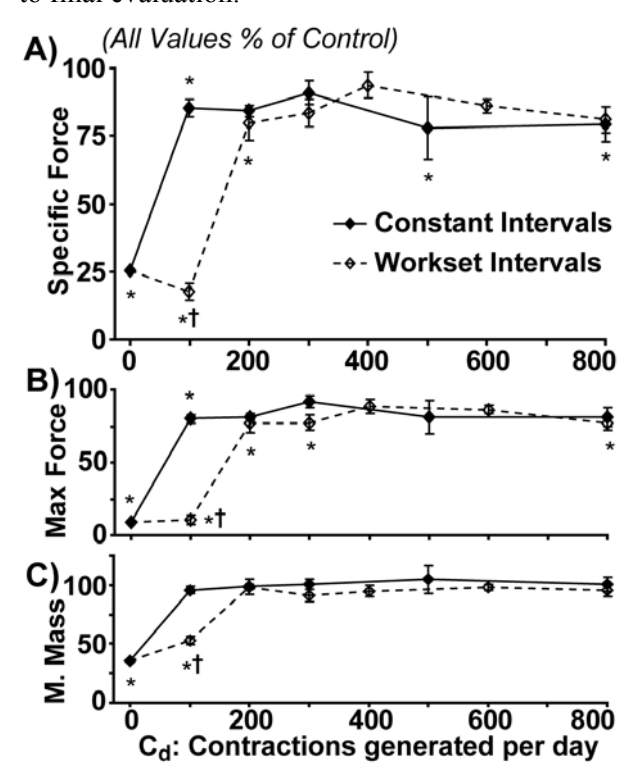


Fig. 3: Specific force (A), maximum force (B) and muscle mass (C) following 5 weeks of denervation and stimulation for different numbers (C_d) and distributions (constant intervals or worksets) of contractions generated daily. C_d of 0 plots the outcome of denervated muscles that received no stimulation. Error bars are SE. The * indicates difference with values of control muscles (p<0.05). For the workset intervals, the † indicates difference with values of the constant intervals having equal C_d contractions daily (p<0.05).

The EDL muscle of rats maintained only 36% of muscle mass, 9% of maximum force (P_o) and 25% of specific force (sP_o) after 5 weeks of denervation (Fig. 3). Denervation not only induced atrophy in the muscle, but the remaining muscle tissue was weaker, generating lower values of force, even when normalized by the smaller CSA of the atrophied muscle. In contrast, if stimulated with either of the protocols having C_d of between 200 and 800 contractions daily, values for these properties were maintained close to those for control muscles, such that mass was above 90%, and both P_o and sP_o were above 75% (Fig. 3). For the tested protocols having C_d of 200 to 800, mass, Po or sPo were not different whether the contractions were separated by constant intervals or workset intervals (Fig. 3). In contrast, at C_d of 100 the constant intervals maintained 95% of mass, 80% of Po and 85% of sPo, but the workset intervals maintained only 53% of mass, 11% of Po and 18% of sP₀. These low values for the workset intervals (C_d, 100) were not different than values for denervated muscles that had received no electrical stimulation (Fig. 3).

Discussion

The maintenance of mass and force were influenced not only by the number of electrically generated contractions, but also by the distribution of these contractions throughout the day (Fig. 3). One difference between the protocols that did maintain mass and force, and the protocol that did not is the maximum continuous period of rest between contractions during each 24 hour day. Of the protocols that did maintain mass and force, the constant intervals at C_d of 100 had a maximum rest of 0.24 hours, the workset intervals at C_d of 400 and 800 had maximum rest of 2 hours, and the workset intervals at C_d of 200, 300 and 600 had maximum rest of 8 hours (Table 1). The workset intervals at C_d of 100 that failed to maintain mass and force had a maximum period of continuous rest each day of 20 hours (Table 1, Fig. 2 & 3). For mass and force of denervated-stimulated muscles to be maintained by a protocol of 100 contractions per day, a key factor may be the maximum tolerable period of rest per day, which appears to be greater than 8 but less than 20 hours.

An overly long period of rest between contractions may be enough to initiate changes in the regulation of gene and protein expression that leads to denervation atrophy in skeletal muscle. Action potentials and the resulting contractions are key regulators of denervation atrophy [11,13]. Buffelli et al. have shown that the prevention of action potentials by a nerve block, and the resulting lack of contractions, was sufficient to induce changes to

skeletal muscle that appeared identical to denervation [13]. Following the onset of denervation, action potentials from the nerve and resulting contractions cease, and Eftimie et al. have shown that the expression of specific molecular signals changes within hours [14]. For example, myogenin mRNA is up-regulated within 8 hours and MyoD mRNA is up-regulated within 16 hours [14]. Thereafter, within 4 hours of the onset of chronic electrical stimulation, the expression of myogenin is down regulated [15]. An excessively long period of rest between contractions may initiate the cascade of changes in mRNA and protein expression levels that initiate the processes of denervation atrophy. A protocol of stimulationdenervation having a sufficient number (C_d of 100) of contractions per day, but distributed such that an excessively long period of rest (20 hrs) occurred and repeated for 5 weeks, was insufficient to maintain the mass and force above levels of denervated and unstimulated muscles. Further research will be required to determine the maximum period of rest during each 24 hour period that would not hinder maintenance of muscle mass and force. Such findings may give insight useful for basic research in muscle disuse and for applied research to guide the design and timing for treatment sessions of electrical stimulation for denervated muscles.

References

- [1] Fitts RH: Effects of regular exercise training on skeletal muscle contractile function. *Am J Phys Med Rehabil*, 82(4), 2003, 320-331
- [2] Carlson BM, Billington L, Faulkner J: Studies on the regenerative recovery of long-term denervated muscle in rats. *Restor Neurol Neurosci*, 10, 1996, 77-84
- [3] Dennis RG, Dow DE, Faulkner JA: An implantable device for stimulation of denervated muscles in rats. *Med Eng Phys*, 25(3), 2003, 239-253
- [4] Dow DE, Cederna PS, Hassett CA, Kostrominova TY, Faulkner J.A., Dennis R.G. Numbers of Contractions to Maintain Mass and Force of a Denervated Rat Muscle. *Muscle Nerve* 2004. (In Press)
- [5] Hodgson JA, Wichayanuparp S, Recktenwald MR, Roy RR, McCall G, Day MK, Washburn D, Fanton JW, Kozlovskaya I, Edgerton VR: Circadian force and EMG activity in hindlimb muscles of rhesus monkeys. *J Neurophysiol*, 86, 2001, 1430-1444
- [6] Kraemer WJ, Ratamess N, Fry AC, Triplett-McBride T, Koziris LP, Bauer JA, Lynch JM, Fleck SJ: Influence of resistance training volume and periodization of physiological and performance

- adaptations in collegiate women tennis players. Am J Sports Med, 28(5), 2000, 626-633
- [7] Petrofsky JS, Stacy R, Laymon M: The relationship between exercise work intervals and duration of exercise on lower extremity training induced by electrical stimulation in humans with spinal cord injuries. *Eur J Appl Physiol*, 82(5-6), 2000, 504-509
- [8] Salerno GM, Bleicher JN, Stromberg BV: Blink reflex recovery after electrical stimulation of the reinnervated orbicularis oculi muscle in dogs. *Ann Plast Surg*, 25(5), 1990, 360-371
- [9] Kern H, Hofer C, Strohhofer M, Mayr W, Richter W, Stohr H: Standing up with denervated muscles in humans using functional electrical stimulation. *Artif Organs*, 23(5), 1999, 447-452
- [10] Al-Amood WS, Lewis DM: Fast-to-slow transition in myosin heavy chain expression of rabbit muscle fibres induced by chronic low-frequency stimulation. *J Physiol (Lond)*, 392, 1987, 377-395
- [11] Gundersen K, Eken T: The importance of frequency and amount of electrical stimulation for contractile properties of denervated rat muscles. *Acta Physiol Scand*, 145, 1992, 49-57
- [12] Carlson BM, Faulkner JA: Reinnervation of long-term denervated rat muscle freely grafted into an innervated limb. *Exp Neurol*, 102, 1988, 50-56
- [13] Buffelli M, Pasino E, Cangiano A: Paralysis of rat skeletal muscle equally affects contractile properties as does permanent denervation. J Muscle Res Cell Motil, 18, 1997, 683-695
- [14] Eftimie R, Brenner HR, Buonanno A: Myogenin and MyoD Join a family of skeletal muscle genes regulated by electrical activity. *Proc Natl Acad Sci U S A*, 88(4), 1991, 1349-1353
- [15] Neville CM, Schmidt M, Schmidt J: Response of myogenic determination factors to cessation and resumption of electrical activity in skeletal muscle: a possible role for myogenin in denervation supersensitivity. *Cell Mol Neurobiol*, 12(6), 1992, 511-527

Acknowledgements

This work was supported by NIH grant PO1-AG10821, NIA training grant AG00114-17 and NIDCR training grant DE07057. The authors thank Cheryl A. Hassett for surgical procedures.

Author's Address

Dr. Douglas E. Dow

Institute of Gerontology, 300 North Ingalls, Ann Arbor, MI, 48109-2007, USA.

e-mail: ddow@umich.edu

home page: www.umich.edu/~ddow

MORPHOLOGY OF THE 2-MONTHS DENERVATED RAT LEG MUSCLE

A Jakubiec-Puka*, K Krawczyk*, H. Chomontowska*, D Biral**, U Carraro**

* Nencki Institute of Experimental Biology, Warsaw, Poland

** C.N.R. Institute of Neuroscience, Neuromuscular Section, Laboratory of Applied Myology, Department of
Biomedical Science, University of Padova, Italy

Abstract (shorter version)

Mechanism of denervation atrophy progress is not fully clear, especially in some later stages of atrophy. In the present work ultrastructure of slow (soleu, SOL) and fast (extensor digitorum longus, EDL) rat leg muscles were examined two months after denervation, when progress of atrophy slow down, and it enter in some stabilised stage. In the muscles here observed, the mass decreased to about 25% of the control value. Muscle fibres were decreased in size considerably, but not uniformly. The most muscle fibres were preserved showing features of denervation atrophy. However, about 1.4% muscle fibres, both in SOL and EDL, were seriously damaged: "necrotic" or resembling cells undergoing "programmed cell death". The last showed generally increased electron-density, disorganised contractile structure, damaged or not recognisable mitochondria and large vacuoles. Such fibres were grouped or situated close to preserved ones or to myotubes. Myotubes constituted about 2% of muscle fibres. Some of them were degenerating or dying. Large accumulations of collagen fibrils were common among muscle fibres, surrounding often blood vessels or myotubes. Thus, just as early as in 2-monthdenervation, muscle shows some "degenerative" changes and dying and regenerating fibres are present, in addition to "simple" muscle atrophy,

Introduction

Mechanism of denervation atrophy progress is not fully clear, especially in some later stages of atrophy. In the early stage of denervation atrophy loss of muscle mass and diminishing of fibre diameters are the highest. Several changes, as diminishing of the contractile structure, progressive loss of mitochondria, anomalies of nuclei, formation of myelin figures and lipofuscin granules and folds of sarcolemma are the main features of muscle fibres in first month after denervation. Some moderate increase of collagen among muscle fibres is also observed. In this stage of atrophy the seriously damaged or necrotic muscle fibres and signs of regeneration were hardly seen [3,5]. Those characteristics of "simple" atrophy are reversible when the muscle is reinnerveted on the $14 - 30^{th}$ day after denervation [3, 4 and unpublished observations].

In the long-term denervated muscle (several months) atrophy is very advanced and its progress is negligible. The number of muscle fibres is reduced and their cross-

sectioned area highly decreased. The number of satellite cells and vessels is evidently reduced. Simultaneously, degenerating and dying fibres are observed and connective tissue is increased considerably [1,2,7,8]. In the long-term-denervated muscle a restorative capacity becomes progressively poorer [8] and the muscle, contrary to the early stage of atrophy, is not able to restore fully its structural and functional state. Reason(s) of this is not clear, especially that muscle fibre keeps ability to be reinnervated for years and formation of new muscle fibres takes place even in the very long-time-denervated muscle [2,8].

In the present work muscle ultrastructure was examined two moths after denervation, when progress of atrophy slow down, and it enter in some stabilised stage. In the 2-months-denervated muscle the total number of fibres per muscle remains still constant and muscle keeps its restorative capacity [8], however fibre loss and regeneration begin [7].

Material and Methods

In this work 3-months of age female Wistar rats were used. Slow (soleus, SOL) and fast (extensor digitorum longus, EDL) rat leg muscles were denervated by cutting the sciatic nerve as describe earlier [3,4]. Both nerve stumps were strongly ligated; the proximal stump was implanted in subcutaneous dorsal region. All procedures of sample preparation for study of ultrastructure were performed as previously [5,6].

Results and Discussion

In the muscles here observed, the mass decreased to about 25% of the control/contralateral value. Muscle fibres were reduced in size considerably, but not uniformly - some large fibres were present; also "angulated" and split fibres were frequent. Electron microscopic examination showed in the most muscle fibres a preserved contractile structure, however with some anomalies. Myofibrils were small and separated, devoid of hexagonal arrangement of filaments, but keeping tetragonal order of the Z-line. Disorganization of myofibrils and contraction bands appeared occasionally. Regularity of the contractile structure was more disturbed in SOL than in EDL muscle. Triads were properly arranged within regions of the regular contractile structure. Otherwise they were abnormally situated or absent. Nuclei, normal looking or of abnormal morphology, were often situated in central

fibre regions or in rows. Sparse mitochondria, small and dark, were grouped in areas free of myofibrils (Figs1,2). Ultrastructure of muscle fibres in general resembled that in the first month after denervation, but fibre organelles and structures seemed to be more stabilised. Degenerating mitochondria, myelin figures, lipofuscin bodies or folds of sarcolemma and basement lamina were much less frequent than in the first month after denervation.

Among the majority of described above atrophying muscle fibres, some seriously damaged ones were seen. Several muscle fibres resembled cells undergoing "programmed cell death". Those fibres showed generally increased electron-density, disorganised contractile structure with the Z-line hardly seen, damaged or unrecognisable mitochondria and large vacuoles (Figs.3,4). Some fibres were "necrotic", with myofibrils devoid of the Z-line and considerably swollen and disrupted mitochondria (Fig.5). "degenerating" or necrotic muscle fibres constituted 1.4% of about 1800 fibres randomly taken for observation (from SOL and EDL muscles of 6 rats). Heavily damaged or dying muscle fibres were situated close to other damaged ones (Fig. 3) or intermixed to preserved fibres and to myotubes. Myotubes appeared beneath of basal lamina in viable muscle fibres or developed individually resembling those in muscle regeneration. Myotubes constituted about 2% of muscle fibres. They appeared evidently more frequent in regions containing damaged fibres Additionally, about 2% of muscle fibres were of very small size. Those fibres perhaps develop from myotubes or they appear as an effect of muscle fibre splitting. Some of myotubes and small fibres were degenerating or dying (Figs. 1,2). Large accumulations of collagen fibrils were common among muscle fibres, especially in regions of damaged fibres (Figs. 3,4) where fat cells were occasionally observed as well. Collagen fibrils surrounded often blood vessels or myotubes (Fig. 6). Those anomalies were observed both in SOL and EDL muscles.

Thus, just as early as in 2-month-denervation, muscle shows some "degenerative" changes and dying and regenerating fibres are present, in addition to "simple" muscle atrophy. It seems that some irreversible damage of muscle tissue begins already in the second months after denervation.

References

- [1] Dedkov EI, Kostrominova TY, Borisow AB, Carlson BM: Reparative myogenesis in long-term denervated skeletal muscle of adult rats results in a reduction of the satellite cell population. Anat Rec 2001;263:139-154.
- [2] Gutmann E, Zelena J: Morphological changes in the denervated muscle. In "The denervated muscle", Ed. Gutmann E., 1962, Prague: 57-126.
- [3] Jakubiec-Puka A, Laskowska-Bożek H: Morphological changes in rat skeletal muscle following reinnervation. Folia Histochem Cytochem 1977;15:333-342.

- [4] Jakubiec-Puka A, Drabikowski W: Influence of denervation and reinnervation on autolytic activity and on protein composition of skeletal muscle in rat. *Enzyme* 1978;23:10-21.
- [5] Jakubiec-Puka A, Kulesza-Lipka D, Kordowska J: The contractile apparatus of striated muscle in the course of atrophy and regeneration. II. Myosin and actin filaments in mature soleus muscle regenerating after reinnervation. *Cell Tissue Res* 1982;227:641-650.
- [6] Jakubiec-Puka A., Biral D. Caveolae in the muscle overloaded in an extended position. *Basic Appl Myol* 2000;10:191-195.
- [7] Schmalbruch H, Lewis DM. A comparison of the morphology of denervated with aneurally regenerated soleus muscle of rat. *J Muscle Res Cell Motil* 1994;15:256-266.
- [8] Viguie CA, Lu D-X, Huang S-K, Rengen H, Carlson BM: Quantitative study of the effects of long-term denervation on the extensor digitorum longus muscle of the rat. *Anat Rec* 1997;248:346-354.

Acknowledgements

The authors wish to thank to Mrs Justyna Osmulska for their expert assistance.

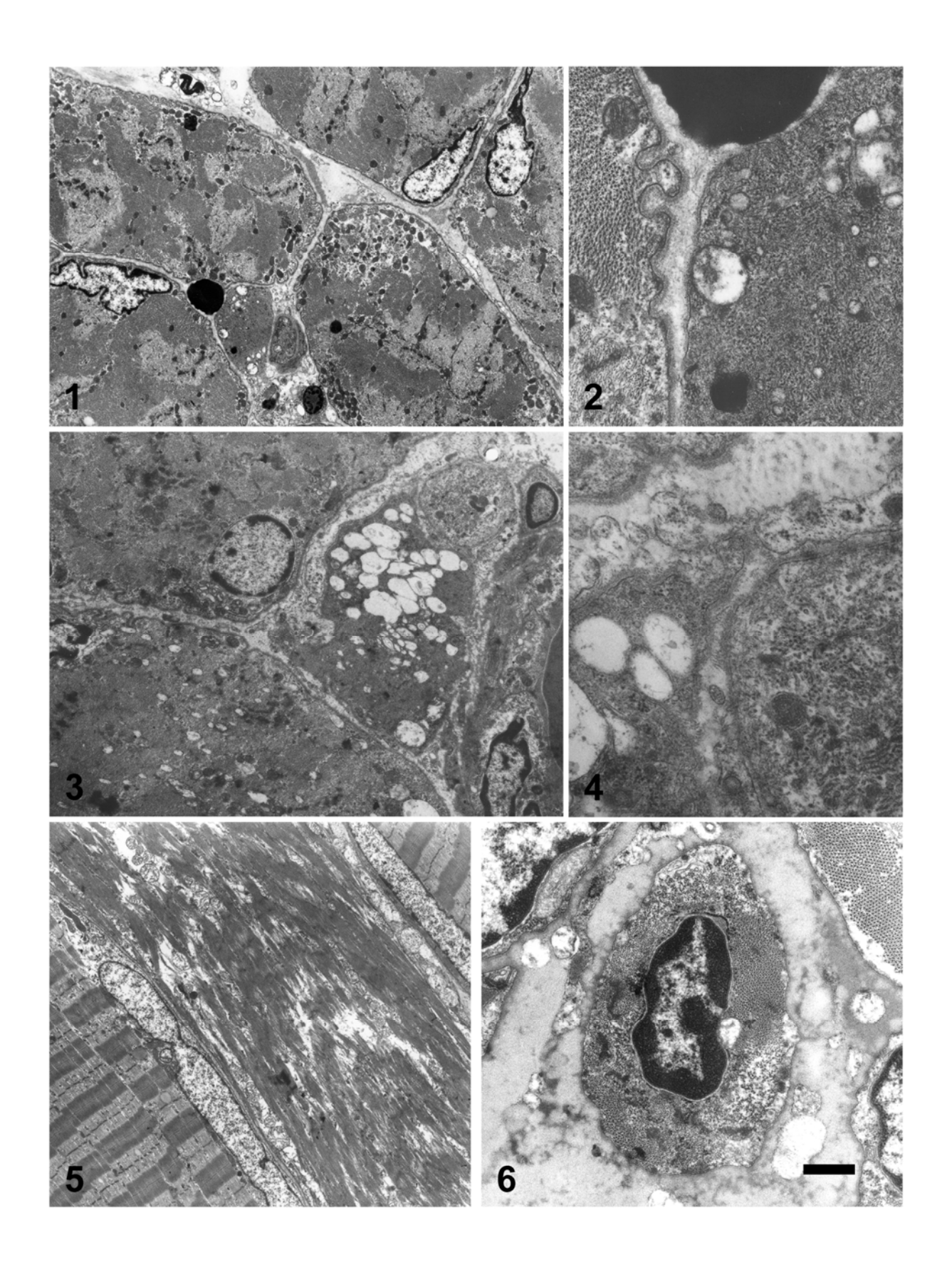
Author's Address

Dr Anna Jakubiec-Puka, Nencki Institute of Experimental Biology, ul Pasteura 3, Warszawa, Poland. Tel +48 22 6598571; fax: +48 22 8225342; e-mail: anna.jakubiec@wp.pl Prof.

Legends

- **Fig. 1.** SOL, transverse section. Muscle fibres are decreased in size. The contractile structure is recogniszble, with exception of the small fibre close to the dark body (see Fig.2) resembling apoptotic body; some nuclei of unusual shape.
- **Fig. 2.** Part of the Fig. 1. Left fibre with well preserved contractile structure, preserved mitochondria and folded sarcolemma. Right fibre with remnants of the contractile structure and vacuoles. The dark body in the upper part.
- **Fig. 3.** SOL, transverse section. Group of muscle fibres: two of them, right (perhaps dying, see Fig. 4) and lower situated containe numerous vacuoles. The left-up-situated fibre looks almost normal. Two myotubes are seen in the right-upper corner.
- **Fig. 4.** Part of Fig. 3. Left fibre, perhaps dying, contains remnants of the disorganized contractile structure and large vacuoles. Right fibre is myotube with well recognisable contractile structure. Accumulation of collagen fibrils in the upper region.
- **Fig. 5.** EDL, longitudinal section. Left and right fibres look like normal. In the central fibre the Z-line is lost; damaged, swollen mitochondria are seen.
- **Fig. 6.** EDL, transverse section. Myotube, with central nucleus and well recognisable contractile structure, is surrounded by masses of collagen fibrils.

Bar is: $1-2.6 \mu m$; $2-0.45 \mu m$; $3-1.5 \mu m$; $4-0.35 \mu m$; $5-3.3 \mu m$; $6-0.62 \mu m$.



THE LONG-TERM DENERVATED RAT MYOFIBER: A NEW CONTRACTILE CELL TYPE

D Danieli*, E Germinario*, D Biral**, M Fabbian**, ME Zanin**, V Vindigni**, A Megighian*, Ch Hofer***, M Moedlin ***, H Kern***, W Mayr***, U Carraro**

* Department of Human Anatomy and Physiology, University of Padova, Italy

** C.N.R. Institute of Neuroscience, Neuromuscular Section, Laboratory of Applied Myology, Department of Biomedical Science, University of Padova, Italy

*** Ludwig Boltzmann Institute of Electrostimulation and Physical Rehabilitation, Vienna, Austria

Abstract

In spite of a large numbers of clinical and experimental studies on effects of denervation on the properties of skeletal muscle, little is known on electrophysiological and mechanical characteristics of long-term denervated muscles. We studied in rat (2-8 months after sciatectomy) excitability in vivo and excitability and mechanical properties in vitro of isolated EDL and soleus muscles. Chronaxie of the leg muscles increased with denervation time up to values higher than 30 msec. Intracellular recordings in 6-month denervated EDL muscle fibers showed a strongly reduced Resting Membrane Potential and very poor excitability to depolarizing current injection. The long-term denervated muscles showed a significant increase of contraction and relaxation Twitch tension was small. Tetanic times. stimulation produced only a little increase of the tension with respect to twitch tension. Cryosection analyses allow to distinguishing three stage during long-term denervation: 1. Up to three-month: myofiber atrophy with distinct ATPase fibertyping; 2. Up to six-month: myofiber atrophy with increased loose connective tissue; 3. After 7-month: lipodystrophy, i.e. adipocytes replace fibers, which had lost ATPase typing (fast-like characteristics prevails also in long-term denervated soleus). The overall picture is complicated by low-rate, but continuous late accumulation of death/regeneration events. Our results indicate that the poor contractility of the long term denervated muscle is not only related to myofiber atrophy, but also to Excitation-Contraction Coupling (ECC) failure.

Introduction

In spite of a large numbers of clinical and experimental studies on effects of denervation on the properties of skeletal muscle, little is known on the electrophysiological and mechanical characteristics of long-term denervated muscles. In a recent review on restorative capacity of long-term denervated muscle [1], Bruce Carlson shows that the decline of maximum tetanic force in the denervated rat muscle precedes severe atrophy

(Fig.1). Indeed maximum force is less than 5% of normal one month after sciatectomy, while the muscle weight is still 35% of the controlateral innervated muscle.

Here we will show that this is the result of a severe decline in muscle excitability, which precedes many months the final dystrophy of the denervated myofibers.

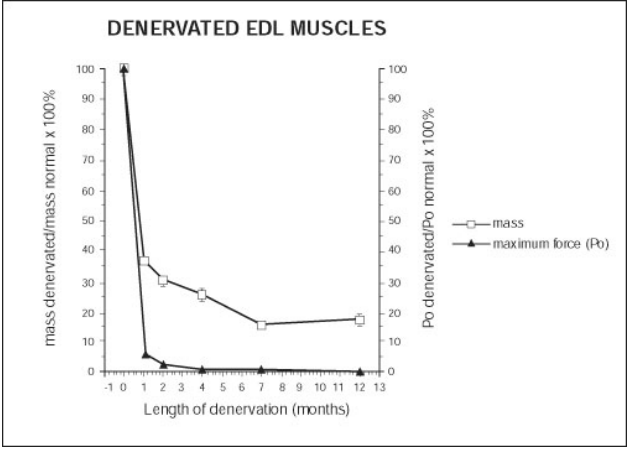


Fig.1: Curves showing the rapid decline in mass and maximum tetanic force in the denervated rat extensor digitorum longus muscle (from Carlson et al. 2002 [1]).

Material and Methods

We studied in rat (2-8 months after leg denervation by sciatectomy) excitability in vivo (by surface electrodes) [2] and in vitro excitability and mechanical properties of isolated muscles [3]. Muscle cryosections were stained by Hematoxilin-Eosin and Myosin ATPase for determination of fibre dimension and composition [4].

Results

As expetcted, if the tight muscle contraction was elicited by surface electrodes the chronaxie of the leg muscle increased with denervation time up to values of 30 msec at 4-6 months. This is the maximum that was possible to measure without eliciting in the sciatectomy model contraction of innervated thigh muscles. In vitro studies by intracellular recordings in 6-month denervated muscle fibres showed a strongly reduced Resting Membrane Potential and very poor excitability to

depolarizing current injection. Rinput was also reduced, suggesting a decreased membrane resistance, which could in part justify the reduced excitability shunting membrane currents.

Analyses in vitro of the mechanical characteristics of the long-term denervated EDL muscles showed a significant increase of contraction and relaxation times. Twitch tension was small. Low-frequency tetanic stimulation produced an incomplete fusion of the single twitches and only a little increase of the tension with respect to twitch tension. High-frequency stimulation (60 Hz) caused an initial transient tension increase followed by a tension decrease to about that of twitch, or less.

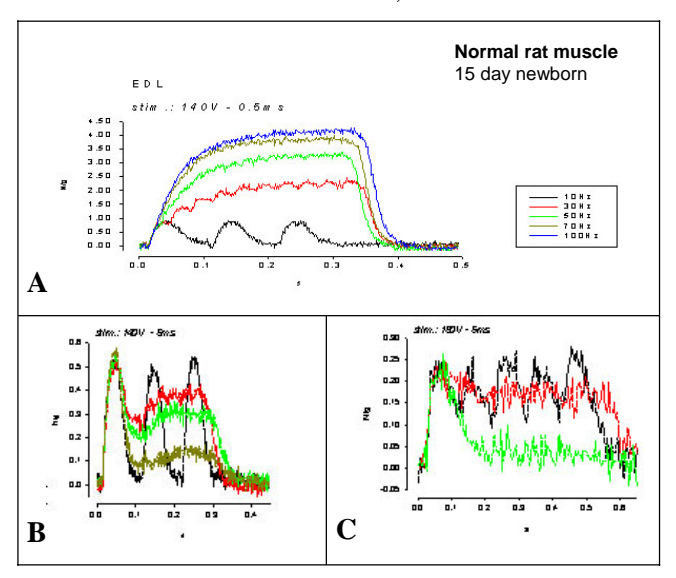


Fig.2: Mechanical characteristics of long-term denervated rat muscle. A, normal muscle; B, EDL 4-month denervation; C, Soleus 4-month denervation. High-frequency stimulation sustains tetanic contraction at lower than twitch force. Note in A that normal muscle tetanic force is four time higher than twitch contraction.

Though the analyses in vitro on isolated rat muscles are optimised to electrophysiological characteristics of normal muscles, and then do not allow long-impulses and high-current stimulation, the behaviour of the long-term stimulated muscles is a sound evidence of excitation-contraction coupling (ECC) failure.

Soleus muscle twitch was very small and slower than normal muscle, whereas tetanic tension was not higher than that of twitch. In some preparations, high frequency stimulation (40 Hz) elicits only the first twitch, which is followed by a plateau of very low tension as long as the stimulation train.

Figure 3 confirms that the denervated myofibers, which still have 20 μ m diameter at 2-month, level of at 10 μ m from 3- up to 9-month denervation. Light microscopy (Fig. 4) allows to distinguish three stages during long-term denervation: 1. Up to

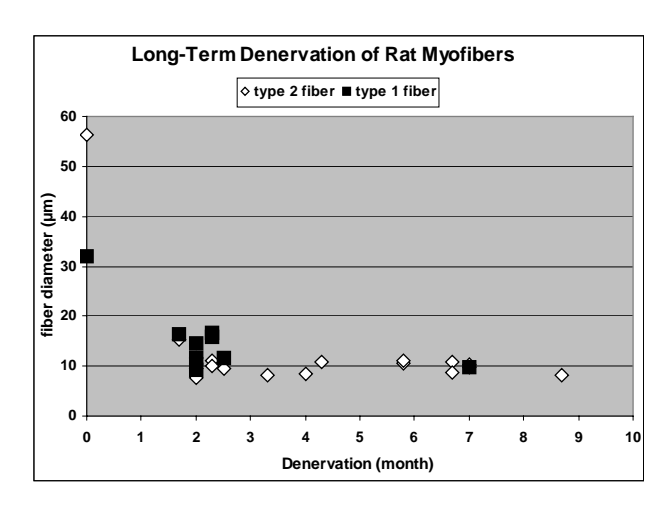


Fig. 3: Post-denervation atrophy of rat myofibers.

three-month: myofiber atrophy with distinct ATPase fiber-typing (Fig. 4 C, D); 2. Up to six-month: myofiber atrophy with increased loose connective tissue (Fig. 4 E, F); 3. After seven-month: lipodystrophy, i.e. adipocytes replace fibers, which had lost ATPase typing (fast-like characteristics

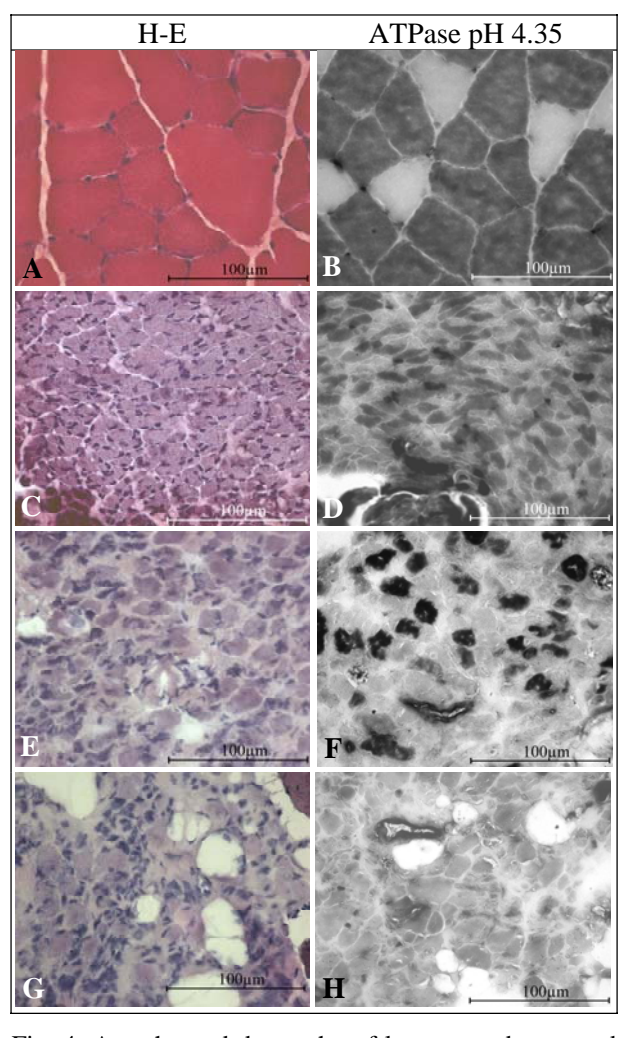


Fig. 4: Atrophy and dystrophy of long-term denervated rat soleus. A,C,E,G: H-E stain; B,D,F,H: Myosin ATPase pH 4.35. (A-B) Normal muscle; (C-D) 2-month denervation; (E-F) 4-month denervation; (G-H) 9-month denervation.

prevails also in long-term denervated soleus) (Fig. 4 G, H). The overall picture is complicated by low-rate, but continuous late accumulation of myofiber death/regeneration events [1, 5, 6].

Discussion

Our results in the rat model show that the poor contractility of the long-term denervated muscle is not only related to myofiber atrophy/dystrophy, but also to ECC failure. Results of our myofiber diameter analysis is in line with published data (compare figure 1 and 3). The only major difference is the time scale of changes. In small rodents the main events occur in months, while the same stage transitions take years in humans [7]. Whether these differences are the result of size and/or metabolic characteristics is still unknown. We are awaiting the results of the Liverpool Unit on rabbit muscle denervation and continuous FES stimulation, which will add basic knowledge and hopefully clinically relevant suggestions on how to speed up the process of muscle recovery. Experiments in large mammals (pigs) are also underway in Vienna under the auspices and support of the EU project RISE.

We are confident that all together these researches will provide safer stimulation protocols needed to induce early effects with, hopefully, a reduced stimulation burden for the SCI patients. If all myofibers in the thigh could be consistently reached, the increased muscle mass and fatigue resistance will rise patients and their quality of life.

References

- [1] Carlson B.M., Borisov A.B., Dedkov E.I., Dow D., Kostrominova T.Y.: The biology and restorative capacity of long-term denervated skeletal muscle. Basic Appl Myol 2002;12:247-54
- [2] Kern H: Functional electrical stimulation (FES) of long-term denervated muscle in humans. Basic Appl Myol 2002; 12 (6):53-63.

- [3] Germinario E, Esposito A, Megighian A, Midrio M, Betto R, Danieli-Betto D. Effects of modulators of sarcoplasmic Ca2+ release on the development of skeletal muscle fatigue. J Appl Physiol. 2004 Feb;96(2):645-9.
- [4] Rossini K., Zanin M.E., Carraro U.: Stage and quantify regenerative myogenesis in human long-term permanent denervated muscle. Basic Appl Myol 2002; 12; 277-287
- [5] Carraro U., Morale D., Mussini I., Lucke S, Cantini M., Betto R., Catani C. Dalla Libera L., Danieli-Betto D., Noventa D.: Chronic denervation of rat diaphragm: maintenance of fiber heterogeneity with associated increasing uniformity of myosin isoforms. J Cell Biol 1985;100:161-174
- [6] Mussini I., Favaro G., Carraro U.: Maturation, dystrophic changes and the continuous production of fibers in skeletal muscle regenerating in the absence of nerve. J Neurophatol Exp Neurol 1987;46:315-31
- [7] Kern H, Rossini K, Boncompagni S, Mayr W, Fanò G, Zanin ME, Podhorska-Okolow M, Protasi F, Carraro U. Long-term denervation in humans causes degeneration of both contractile and excitation-contraction coupling apparatus that can be reversed by functional electrical stimulation (FES). A role for myofiber regeneration. J Neuropathol Exp Neurol, in press.

Acknowledgements

Supported by EU Commission Shared Cost Project RISE (Contract no. QLG5-CT-2001-02191).

Author's Address

Prof. Ugo Carraro, Department of Biomedical Science, University of Padova. Viale G. Colombo, 3; I-35121 Padova (Italy). Tel +39 049 8276030; fax +39 049 8276040. e-mail: ugo.carraro@unipd.it.

A NEW FAST AND RELIABLE SDS PAGE TO QUANTIFY TOTAL PROTEIN AND MYOSIN HEAVY CHAIN IN CRYO-SECTIONS OF NEEDLE BIOPSY SHOWS THAT LONG-TERM PERMANENT DENERVATED HUMAN MUSCLES RECOVER BY FES TRAINING

U Carraro*, K Rossini*, ME Zanin*, M Fabbian*, W Mayr**, Ch Hofer***, H Kern***

* C.N.R. Institute of Neuroscience, Neuromuscular Section, Laboratory of Applied Myology, Department of Biomedical Science, University of Padova, Italy

** Department of Biomedical Engineering and Physics, University of Vienna, Austria.

*** Ludwig Boltzmann Institute of Electrostimulation and Physical Rehabilitation, Vienna, Austria

Abstract

We describe a new gel electrophoretic method, which quantify total protein and Myosin Heavy Chain in cryo-sections of needle muscle biopsies. Severe atrophy of skeletal muscles occurs during long-term permanent denervation. We studied 21 human muscle biopsies taken from patients' suffering lower motoneuron denervation from 6month to 30-year and SCI subjects trained with Functional Electrical Stimulation (FES) for different periods of time (0.5 to 6 years). Electrical stimulation of denervated muscles increase size of the myofibres and maintains sarcomeres, by preventing/reversing secondary degeneration of the long-term denervated tissue. Here we show results of the quantitation of myosin content in permanent denervated long-term muscles. Additional markers of muscle damage / apoptosis / necrosis / inflammation / myogenesis could be quantitatively assesed bvimmunoblotting approaches.

Introduction

The main goal of FES is providing muscular contraction and producing a functionally useful movement, but it could be used just to obtain recovery of myofiber size [1]. The electrical stimulation is believed to promote muscle growth, neuron sprouting, and increased sensation. Previous published results [2, 3] shown worthwhile restitution of muscle trophism using FES. In this work we analyze and quantify muscle re-growth due to electrical stimulation by measuring myosin content in biopsies of muscle tissue after lower-motorneuron long-term permanent denervation (LT-PD) without and with FES training.

Material and Methods

Biopsies

Subjects were either LT-PD (4 - 8.7 years), or LT-PD after FES training (2.3 - 7 years). Needle

biopsies of human muscles were taken from right and left leg.

Molecular markers and quantification of total protein in cryostatic sections of these human biopsies were as described in [4].

4% Stacking Gel – SDS PAGE to determine total protein in cryosections of human biopsies

The total protein quantities is determined using a short run in 4% stacking gel SDS PAGE, prepared according to [4]

5% Stacking Gel – SDS PAGE to determine Myosin/Total protein ratio in cryosections of human biopsies

When stacking gel concentration was increased from 4% to 5% in the stacking gel, in the running condition above described myosin heavy chains separated from protein front during the stacking period of gel electrophoresis. After staining and destaining, MHC/Total protein ratio was determined by gel densitometry.

Gel Densitometry

Protein contents in slab gels were quantitated by densitrometry using an Epson Perfection 1650 scanner connected to a PC. Data were computed using Scion Image for Windows version 4.0.2. by Scion Image software (PC version) of Scion Corporation.Page Layout

Results

Protein content of skeletal muscle biopsies

Figures 1 and 2 show results of the molecular analyses by SDS-PAGE of protein from LT-PD skeletal muscle biopsies. Figure 1 shows total protein content in 6 representative samples.

Figure 1. Total protein by stacking gel 4%

When stacking gel concentration was increased from 4% to 5%, myosin heavy chains separated from protein front during the stacking period of gel electrophoresis (Figure 2). By the new 5% **PAGE** stacking-gel **SDS** we determined myosin/total protein ratio. In accordance to previous data, skeletal muscle contains about 200 mg of total protein and 100 mg of myosin per gram of fresh muscle weight, i.e., myosin heavy chains represent 50 percent of total muscle proteins. Table 1 shows that the 4 to 8.7 year denervated muscle have a mean percentual of MHC of 13.6±5.6, while after FES the percent increases to 29.4 ± 12.7 .

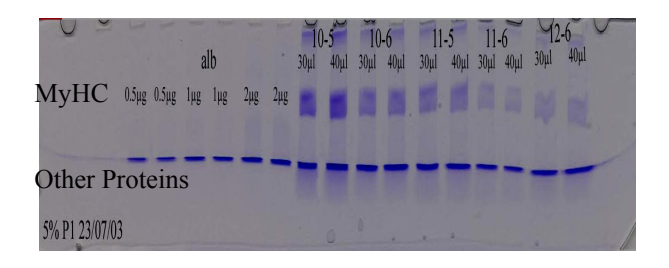


Fig. 2: 5% stacking gel SDS-PAGE. From left to right, known increasing amounts of BSA (alb) and then proteins fron cryo-sections of human muscle biopsies. The low-migrating bands are MyHCs. The total protein: MyHC ratio returns to almost normal value after FES.

Discussion

Biopsy	Denervation	FES	MHC in total
	time	Time	protein
	(years)	(years)	(%)
D1	4		16.9
D2	4		15.7
D3	7.5		18.7
D4	7.5		18.1
D5	7.7		2.6
D6	8.7		12.1
D7	8.7		11.2
Mean ± st dev			13.6 ± 5.6
FES 1	4	2.3	20.4
FES 2	4	2.3	17.8
FES 3	5	2.3	26.6
FES 4	6.3	4.3	19.7
FES 5	6.3	4.3	26.6
FES 6	7.5	7	48.1
FES 7	7.5	7	46.5
Mean ± st dev			29.4 ± 12.7

Table 1. Percentual content of MHC in Total Protein. D(1-7), Denervated muscle; FES(1-7), denervated and stimulated muscle.

We here studied influence of functional electrical stimulation training on long- term paralyzed human muscle. We shown that the gel electrophoretic method wich allows to determine the percentual content of myosin heavy chain in

the human biopsies provide good evidence that the atrophic LT-PD muscles recover after FES training and some biopsies reach almost normal values. Thus molecular analyses confirm results we shown by morphological approaches [5].

During the next years, the goals of the EU supported RISE project will be to identify, using experiments in animals and clinical research, safer stimulation protocols needed to induce early effects with, hopefully, a reduced stimulation burden for the patients. If all myofibers in the thigh could be consistently reached, the increased muscle mass and fatigue resistance will rise patients and their quality of life.

References

- [1] Carraro U, Dalla Libera L, Catani C: Myosin light and heavy chains in muscle regenerating in absence of the nerve. Transient appearance of the embryonic light chain. Exp Neurol 1983; 79: 106-117
- [2] Carraro U, Rossini K, Zanin ME, Rizzi C, Mayr W, Kern H: Induced myogenesis in long-term permanent denervation: perspective role in functional electrical stimulation of denervated legs in humans. Basic Appl Myol 2002; 12 (2):53-63.
- [3] Kern H: Functional electrical stimulation (FES) of long-term denervated muscle in humans. Basic Appl Myol 2002; 12 (6):53-63.
- [4] Bielewicz J, Zanin ME, Galbani A, Carraro U. Contractile Proteins Content of Long Term Permanent Denervated Human Muscle after Functional Electrical Stimulation. Basic Appl Myol 2004; 14 (2):83-86.
- [5] Kern H, Rossini K, Boncompagni S, Mayr W, Fanò G, Zanin ME, Podhorska-Okolow M, Protasi F, Carraro U. Long-term denervation in humans causes degeneration of both contractile and excitation-contraction coupling apparatus that can be reversed by functional electrical stimulation (FES). A role for myofiber regeneration. J Neuropathol Exp Neurol, in press.

Acknowledgements

Supported by EU Commission Shared Cost Project RISE (Contract no. QLG5-CT-2001-02191).

Author's Address

Prof. Ugo Carraro, Department of Biomedical Science, University of Padova. Via G.Colombo, 3; 35121 Padova (Italy). Tel +39 049 8276030; fax +39 049 8276040. e-mail: ugo.carraro@unipd.it.

Keynote lecture

A. Wernig (Bonn, Germany)

LITTLE EVIDENCE FOR CONTINUAL MUSCLE FIBER REPAIR BY PRESUMED CIRCULATING STEM CELLS.

Wernig A ¹, Schäfer R ¹, Knauf U ¹, Zweyer M ¹, Högemeier O ¹, Mundegar R ¹, Wernig G¹, Wernig M²

> Dept. of Physiology, University of Bonn, Germany (1) MIT Boston, USA (2)

It has recently been claimed that bone marrow derived blood cells can contribute to the myogenic compartment. Such occurrence would bear considerable therapeutic potential in genetically determined muscle diseases like Duchenne Muscular Dystrophy due to a loss in the structural muscle protein dystrophin.

In order to identify circulating stem cells we transplanted male bone marrow carrying EGFP reporter and intact dystrophin genes into female MDX mice. Throughout life MDX mice suffer muscle fiber damage, thus, if circulating cells do repair damaged muscle fibers (by fusing), the frequency of green fluorescent protein (GFP) and dystrophin positive muscle fibers should continually increase with time.

Upon sacrifice at 16 to 46 weeks after bone marrow transplantation, soleus and e.d.l. muscles typically contained some 0.5 - 2% GFP-positive muscle fibers (n=44), TA muscles around 1 -5% (n=24). However, no increase with time in the frequency of GFP labelled muscle fibers was detectable. On frozen sections, dystrophin positive muscle fibers were present in all muscles, but there was no increase in frequency with age either and no difference between experimental and untreated MDX mice. Thus, most dystrophin positive fibers are probably revertant fibers, rather than fibers which have acquired the donor gene.

Also, Y-chromosome specific DNA (a separate marker of the male donor cells in female recipients) extracted from whole muscles did not increase with time (n=18). These findings and the lack of increase in both GFP and dystrophin positive fiber numbers speaks against the existence of circulating stem cells which would enter damaged skeletal muscle fibers and acquire the myogenic program.

Similarly, cryodamaging or crushing muscles 8 and 16 weeks after transplantation did not produce more GFP or dystrophin positive muscle fibers. There was, however, a higher yield in Y-chromosome related DNA in the damaged versus undamaged muscles and in untreated MDX versus non-MDX muscles due to accumulation of donor derived cells in the interstitial space. The finding of donor derived nuclei within structurally intact GFP negative or dystrophin negative muscle fibers indicates that donor cells enter (damaged) muscle fibers but may remain there without expressing or acquiring a myogenic program.

This work has been supported by BMBF grant 01GO122 to A.W.

Author's Address

Anton Wernig, Univ.- Prof. Dr. Medizinische Fakultät der Rheinischen Friedrich-Wilhelms-Universität Bonn Institut für Physiologie II Wilhelmstrasse 31 53111 Bonn Deutschland email: anton.wernig@ukb.uni-bonn.de

FOLLOW UP OF HUMAN MYOGENIC CELLS FROM DONORS AGED 2- 82 YEARS

Wernig A¹, Knauf U¹, Schäfer R¹, Zweyer M¹, Mundegar R¹, Partridge T²

Deptm. of Physiology, University of Bonn, Germany (1) MRC London, Hamersmith Hospital, UK (2)

We investigated whether the lifelong turnover of the organotypic muscle stem cells, the satellite cells, might lead to their exhaustion in aged people. Human myogenic cells derived from donors aged 2-82 years (n=12) were implanted into soleus muscles of immunincompetent mice.

In addition, we studied myogenic cells from biopsies of 3 children suffering from Duchenne muscular dystrophy (DMD), a disease in which satellite cells are proposed to suffer premature ageing due to continuous demand for muscle regeneration.

Seven to 12 weeks after implantation, grafted cells were quantified by structural features (muscle fibres expressing human protein and human nuclei/myonuclei) and by the amount of human DNA extracted from these muscles.

When considering highly pure myogenic cell preparations, we observed an inverse relation between the donors' age and the proliferative capacity in vitro as well as in vivo with about 2 divisions of each satellite cell per 10 years of life. Myogenic cells from the oldest donors still grew human muscle tissue, indicating a residual proliferative capacity even in aged donors in spite of a continual loss of growth capacity of satellite cells in the living muscle.

On the other hand, cell preparations with initially low or decreasing myogenicity during expansion in vitro showed completely different growth characteristics, e.g. increased proliferative capacity, longer telomeres and lower myogenicity of the tissue formed upon implantation.

We suggest a "Desmin Factor" (DF) to predict myogenicity of the human tissue formed in vivo from the growth characteristics during expansion in vitro. This may serve as a prognostic tool for transplantation efficacy in human trials.

Author's Address

Anton Wernig, Univ.- Prof. Dr.
Medizinische Fakultät der Rheinischen Friedrich-Wilhelms-Universität Bonn
Institut für Physiologie II
Wilhelmstrasse 31
53111 Bonn
Deutschland
email: anton.wernig@ukb.uni-bonn.de

Session 6

Lower Extremities: Basics

Chairpersons:

H. Cerrel-Bazo (Arcugnano, Italy) M. Bijak (Vienna, Austria)

ATTEMPTS TO REDUCE MUSCLE FATIGUE BY RANDOMIZING FES PARAMETERS

T.A. Thrasher^{1,2}, G.M. Graham¹, M.R. Popovic^{1,2}

¹ Institute of Biomaterials and Biomedical Engineering, University of Toronto, Canada
² Lyndhurst Centre, Toronto Rehabilitation Institute, Canada

Abstract

Muscles tend to fatigue very rapidly when undergoing functional electrical stimulation (FES). FES-induced muscle fatigue occurs much more quickly than normal fatigue, and this greatly limits activities such as FES-assisted walking. It has been hypothesized that FES-induced muscle fatigue can be reduced by randomly modulating parameters of the electrical stimulus, such as pulse frequency, pulse width and current amplitude. Seven paraplegic subjects participated in this study. While subjects were seated in a neutral posture, FES was applied to the quadriceps and tibialis anterior muscles using surface electrodes, one muscle at a time. The resulting isometric force was measured, and the time for the force to drop by 3 dB (fatigue time) was determined. Also determined was the force time integral (FTI). Four different modes of FES were applied in separate trials: (1) constant stimulation, (2) randomized frequency, (3) randomized current amplitude, and (4) randomized pulse width. In randomized trials (2 to 4), stimulation parameters were modulated in a range of +/- 15% using a uniform probability distribution. There was no significant difference between the fatigue time measurements for the four modes of stimulation. There was also no significant difference in the FTI measurements. Therefore, random modulation of the stimulation frequency, current amplitude and pulse width appeared to have no effect on muscle fatigue.

Introduction

It is well known that muscle contractions induced by FES tend to fatigue more quickly than natural contractions [1]. Fatigue limits the role of FES in applications such as standing and walking after Spinal Cord Injury (SCI). The goal of this study was to reduce the rate of muscle fatigue by modulating the three main FES parameters. We hypothesized that by randomly modulating frequency, current amplitude and pulse width, the resulting firing rate and level of recruitment of individual motor units, or groups of motor units, would vary over time.

Graupe et al. addressed the problem of muscle fatigue associated with FES by applying stochastic

modulation to the inter-pulse interval of the electrical stimulus, which amounts to frequency randomization [2]. They found the maximum increase in leg extension time as compared to stimulation with no inter-pulse interval modulation to be 37%. These results were significant but limited to only one subject. Other methods to reduce FES induced muscle fatigue have been explored, with varying success. The use of doublets (pairs of closely spaced pulses) has been shown to reduce fatigue in some activities [3,4] and increase fatigue in others [5,6]. Fatigue has been reduced by stimulating multiple motor points (distal and proximal) in a sequential manner [7], and alternating between trains of high and low frequency stimulation [8]. There remains a clear a need for much clarification in the area of fatigue reduction associated with FES stimulation.

Materials and Methods



Fig. 1: Experimental setup for tibialis anterior force measurement. Electrodes placed for quadriceps and tibialis anterior stimulation. Load cell attached to floor.

Seven subjects with SCI participated in this study. One was female and 6 were male (mean age of 31.2 ± 6.2) and their level of injury ranged from

C6/C7 to T8. The time since injury ranged from 3 months to 13 years with a mean of 7.2 ± 4.3 years. Four subjects were firt-time FES users, while three subjects had 3 to 12 months of prior FES training.

Subjects were seated in an upright position on a padded bench, as shown in Fig. 1. Self-adhesive electrodes were placed on the skin for stimulation of the quadriceps and tibialis anterior. FES was applied to the muscles using a Compex 2 programmable stimulator (Compex SA, Ecublens, Switzerland). The stimulation signal consisted of biphasic, bipolar, current controlled pulses with a mean pulse width of 250 µs and a mean frequency of 40 Hz. Pulse amplitude was set between 34 and 110 mA, varying with each subject and muscle group. Stochastic modulation of the amplitude, frequency and pulse width was achieved using a uniform probability distribution from -15 to +15%. Values for pulse amplitude, width, and frequency were refreshed every 100 ms.

Muscles were tested one at a time. The limb force was measured using a strain gauge based, tension/compression pancake load cell (Honeywell Sensotec, Columbus, Ohio, USA) with a range of -1100 to 1100 N. The load cell was mounted on the base of the apparatus in one of two positions (depending on which muscle was being tested). When knee extension moment was being measured, the load cell was mounted anterior to the subject's ankle, and a strap connected in series to the load cell was fixed to the ankle. In the second configuration, the load cell was mounted below the foot rest, and the strap was attached to the foot over the metatarsus. The strap was inelastic, and the load cell was thus used to measure isometric knee extension and isometric dorsiflexion moments.

Four trials were performed on each muscle group; no random modulation of any parameters (control trial), random modulation of pulse amplitude (amplitude trial), random modulation of pulse frequency (frequency trial), and random modulation of pulse width (pulse width trial). A 10-minute rest time was administered between each test, which was considered to be adequate for repeatable results [4,5,6]. The order of the trials was randomized.

Two indices of muscle fatigue were considered in this study: fatigue time, and fatigue time integral (FTI). Fatigue time was defined as the time from onset of stimulation until the force decreased to below 70.8% of the maximum force for that trial, equivalent to a drop of 3dB (the -3dB force). FTI was calculated as the integral of the force during the period defined as fatigue time. FTI is regarded

by some researchers to be the most suitable measure of sustained muscle power [4,5].

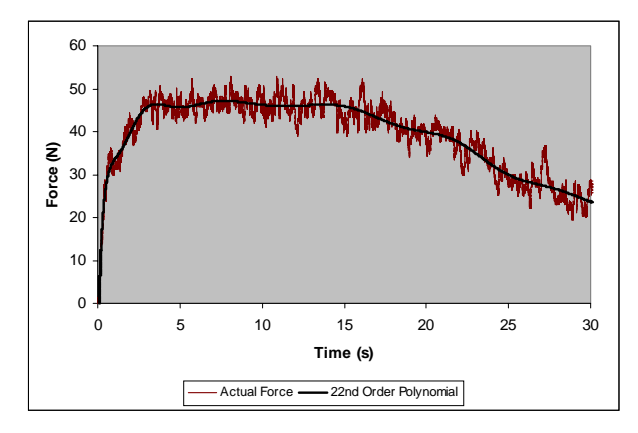


Fig. 2: Force-time curve for stimulation of subject 3's right tibialis anterior with amplitude randomization..

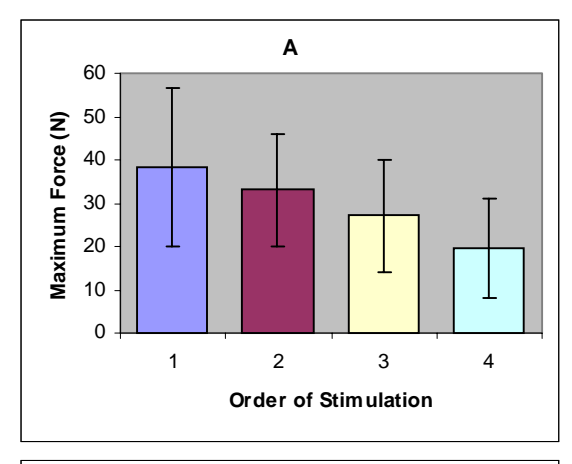
To facilitate data analysis, a 22nd order polynomial was fitted to each curve using a least squares algorithm (see Fig. 2). The order of the polynomial was determined using an iterative method on a representative sample of curves by increasing the order until the R²-value remained the same (to 3 significant digits) for consecutive iterations.

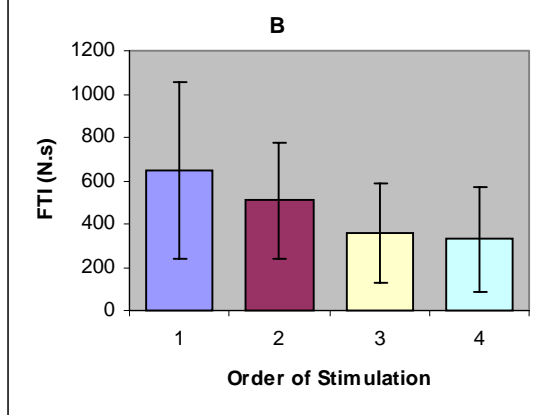
The results from the four trials were compared using a two-way Analysis of Variance (ANOVA) without replication. The two factors considered were the individual muscles and the modes of stimulation. Separate tests were performed using measurements of fatigue time and FTI. The order of trials was also tested for bias, and the maximum forces were considered as well. Statistical significance was set at p < 0.05.

Results

No significant differences were found in terms of fatigue time between the control trials and the random modulation trials (p-value = 0.1911). There was also no significant effect of random modulation on FTI (p-value = 0.7649). Unsurprisingly, there was a highly significant bias for individual muscles on fatigue time and FTI (p-value < 0.0001), i.e. some muscles performed significantly differently from other muscles over all trials. There was no difference seen in the fatigue time or FTI measurements between subjects with previous FES training and subjects with no previous FES training (p-value = 0.4164).

The order of stimulation trials was found to have a very significant effect on the maximum forces recorded and the FTI. As shown in Fig. 3, there is a downward trend in maximum force and FTI the more a muscle is stimulated. This trend is not seen in the fatigue time measurements.





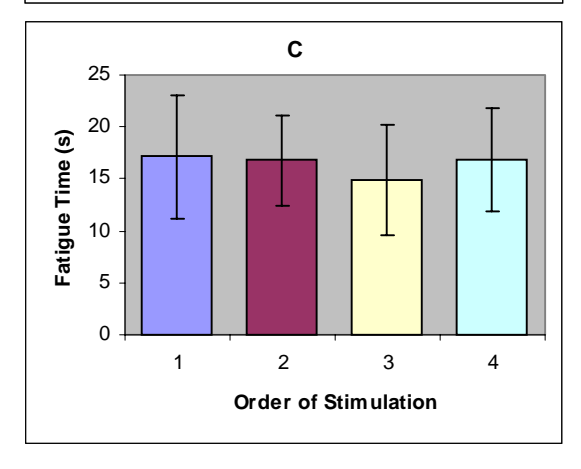
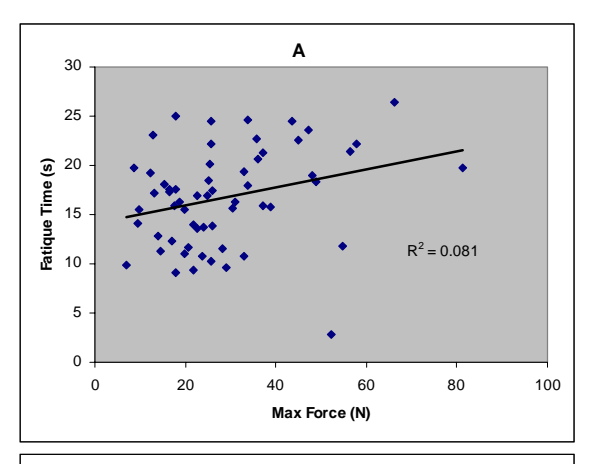


Fig. 3: Data averages arranged in order of trial. Stimulation order appeared to have no effect in terms of fatigue time (p=0.1354), however it had a clear, diminishing effect on maximum force (p<0.0001) as well as FTI (p<0.0001). Error bars indicate \pm one standard deviation.

An ad hoc analysis of the correlations between fatigue time and maximum force was performed. A similar analysis was performed on FTI and maximum force. As shown in Fig. 4A, there was very little, if any, correlation between the maximum force and the fatigue time ($R^2 = 0.081$). There was a high level of correlation between FTI and maximum force (linear relationship, $R^2 = 0.728$), in force translated into variation in the FTI measurement, which resulted in an unreliable measure of muscle fatigue.



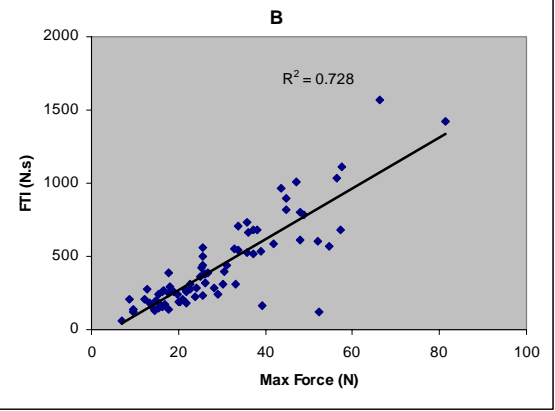


Fig. 4: Linear correlation between (A) FTI and maximum force; and (B) fatigue time and max. force.

Discussion

In this study, stochastic modulation of frequency, amplitude and pulse width did not result in a statistically significant increase in fatigue time. It was found, however, that maximum force decreased significantly on successive trials, suggesting that the 10 minutes was not a sufficient amount of time for fatigued muscles to recover to full strength. This was surprising, since 10 minutes rest was suggested in several previous fatigue studies [4,5,6]. It remains unclear how long an electrically stimulated muscle requires to return to full strength after FES.

A ten minute rest time was chosen due in part to time constraints and in part because repeatable results have been achieved using a ten minute rest time in previous studies. In addition, studies have demonstrated a full recovery in peak force and endurance from short high intensity stimulation after only ten minutes [9] and 95% recovery in peak force from continuous maximum voluntary contractions after only three minutes [10]. Our results did not indicate a full recovery in muscles potential to reach peak force since the peak force was highly dependent on stimulation order. FTI, which incorporates muscle force, was also highly dependent on stimulation order and was therefore not a reliable measure of muscular fatigue. With a

longer rest time of perhaps 30 minutes or several hours, FTI would not be influenced by previous testing and could be an effective tool for measuring fatigue. Fatigue time was not highly influenced by the order of stimulation, matching only 33% of the time. For this measurement a 10-minute rest time appears to be adequate.

The FTI was an appealing measure of fatigue since it includes a combination of fatigue time and level of sustained force. However, none of the FTI measurements from any of the three random modulation trials exhibited significant difference when compared to the control trials. In this study, the FTI was a poor measure of muscle fatigue since it showed a high level of correlation with the order of stimulation. This bias could have confounded the results of the study, and any positive effect that random modulation was having would have been obscured.

Isometric muscle force is a critical factor in many daily activities such as standing and grasping and therefore effort is justified in trying to reduce isometric fatigue. A limitation of isometric force as an index for fatigue is that it cannot be directly compared to dynamic fatigue indexes such as the number of achievable leg lifts. Nor can results from this study be extrapolated to conditions where dynamic muscle force is the most important factor, such as the swing phase of walking. FES induced muscle contractions have been shown to be more prone to fatigue under dynamic conditions than under isometric conditions [11], so there are clear differences in the two mechanisms of fatigue.

Despite significant efforts to reduce and eliminate the problem of muscle fatigue associated with FES, it remains a major limitation for applications of FES such as walking and grasping. It seems logical to investigate a combination of doublet and frequency modulated stimulation with long-term stimulation in an effort to further reduce muscle fatigue associated with FES.

References

- [1] Baker LL et al. Neuromuscular electrical stimulation: a practical guide, 3rd Edition. Rancho Rehabilitation Engineering Program. Ranch Los Amigo Medical Centre, Downey, CA, 1993.
- [2] Graupe D, Suliga P, Prudian C, Kohn KH. Stochastically-modulated stimulation to slow down muscle fatigue at stimulated sites in paraplegics using functional electrical stimulation for leg extension. *Neurol Res* 2000; 22: p 703-704.

- [3] Karu ZZ, Drufee WK, Barzilai AM. Reducing muscle fatigue in FES applications by stimulating with N-Let pulse trains. *IEEE Trans Biomed Eng* 1995; 42: 809-817.
- [4] Bigland-Ritchie B, Zijdewind I, Thomas CK. Muscle fatigue induced by stimulation with and without doublets. *Muscle Nerve* 2000; 23: 1348-1355.
- [5] Thomas CK, Griffin L, Godfrey S, Ribot-Ciscar E, Butler JE. Fatigue of paralysed and control thenar muscles induced by variable or constant frequency stimulation. *J Neurophisiol* 2003; 89: 2055-2064.
- [6] Kebaetse MB, Turner AE, Binder-Macleod SA. Effects of stimulation frequencies and patterns on performance of repetitive, nonisometric tasks. *J Appl Phisiol* 2002; 92: 109-116.
- [7] Lau et al. Fatigue reduction by sequential stimulation of multiple motor points in a muscle. *Clin Ortho Rel Res* 1995; 321: 251-258.
- [8] Matsunaga T, Shimada Y, Sato K. Muscle fatigue from intermittent stimulation with low and high frequency electrical pulses. *Arch Phys Med Rehabil* 1999; 80: 48-53.
- [9] Lariviere C, Gravel D, Arsenault AB, Gagnon D, Loisel P. Muscle recovery from a short fatigue test and consequence on the reliability of EMG indices of fatigue. *Eur J Appl Physiol*, 2003; 89: 171-176.
- [10] Bigland-Ritchie et al. Reflex origin for the slowing of motoneurone firing rates in fatigue of human voluntary contractions. *J Physiol* 1986; 379: 451-459.
- [11] Yu NY, Chen JJ, Ju MS. Study of the electrically evoked EMG and torque output during the muscle fatigue process in FES-induced static and dynamic contractions. *Basic Appl Myol* 1999; 9: 11-18.

Acknowledgements

This study was funded in part by the Natural Sciences and Engineering Research Council (NSERC) of Canada, and the Canadian Paraplegic Association Ontario (CPA Ontario).

Author's Address

Dr. Adam Thrasher Rehabilitation Engineering Laboratory 520 Sutherland Drive Toronto, Ontario, Canada M4G 3V9 e-mail: adam.thrasher@utoronto.ca

REPETITIVE PAINFUL STIMULATION PRODUCES AN EXPANSION OF WITHDRAWAL REFLEX RECEPTIVE FIELDS IN HUMANS

E.G. Spaich, L. Arendt-Nielsen, O.K. Andersen

Center for Sensory-Motor Interaction, Department of Health Science and Technology
Alborg University, Denmark

Abstract

The aims of the present study were to investigate whether temporal summation of the nociceptive withdrawal reflex depends on the stimulation site on the sole of the human foot, and to characterise the reflex receptive fields (RRF) of lower limb muscles to repetitive stimulation. The cutaneous RRFs were assessed in 15 subjects in sitting position by recording the EMG from five lower leg muscles and the kinematic responses (ankle, knee, and hip joints) to repetitive painful electrical stimulation. The stimulus consisted of a series of five stimuli (frequency: 3 Hz) delivered randomly at 10 different sites on the sole of the foot.

The size of the reflexes increased generally between the first and the second stimulus, however, the increment depended on the stimulation site. In tibialis anterior, the RRF covered the distal sole of the foot and gradually expanded during the stimulus train. No expansion towards the heel area was detected. In soleus, the reflexes were facilitated after the second stimulus at all sites and remained in this state until the last stimulus. In vastus lateralis, biceps femoris, and iliopsoas a gradual expansion of the RRF was seen, resulting in RRFs covering the lateral, distal foot, and part of the proximal foot (iliopsoas). Knee and hip flexion were evoked at all sites. Ankle dorsiflexion was evoked at the distal foot, while ankle plantarflexion was evoked at the heel.

The enlargement of the RRF reflects spinal temporal summation leading to gradually stronger reflex responses. The degree of temporal summation was dependent on stimulation site. The facilitation of the withdrawal reflex responses due to repetitive stimulation might have potential applications in the rehabilitation engineering field, where these reflexes could be used to assist gait of patients with central nervous system injuries.

Introduction

Repetitive stimulation has been shown to facilitate the human nociceptive withdrawal reflex response for interstimulus intervals ranging between 50 ms and approximately 330 ms [1] [2]. In intact rats,

facilitated responses were observed only during few seconds (5-7 s), then the responses reached a plateau and decreased [3]. Gozariu et al. [3] suggested that supraspinal structures are likely responsible for the delayed suppression of the responses. The mechanism mediating the gradual increase in pain intensity and reflex response is denoted temporal summation and likely reflects neuronal integration of excitatory potentials at the spinal level. There is a high correlation between reflex build up and induction of pain indicating that activation of nociceptive fibers is needed for neuronal integration to happen [2].

Stimulation of areas within the cutaneous reflex receptive field (RRF) of a muscle may evoke a reflex response in the muscle that will ultimately result in withdrawal of the stimulated area [4] [5]. The RRF of different muscles overlap [5] [6] and therefore the final movement results from the combined response of all the muscles with RRF covering the stimulated area. The sensitivity of the RRF is high within the focus of the RRF and gradually decreases toward the border of the RRF [4]. In addition, the latency of the reflexes is shortest in the RRF focus and longer towards the border of the RRF in animals [4] and in humans [7] indicating graded RRF sensitivity. It is therefore hypothesised that repetitive stimulation within the focus of the RRF may lead to robust temporal summation while stimulation in the periphery evokes less temporal summation at identical stimulus intensities.

The aims of the present study were to investigate whether temporal summation of the nociceptive withdrawal reflex depends on stimulation site, and to characterize the RRF of lower limb muscles to repetitive stimulation of the sole of the foot..

Material and Methods

Fifteen volunteers (nine males and six females, mean age 24.5 years, range 20-32 years) participated in this study. The protocol was approved by the local ethical committee and was in accordance with The Declaration of Helsinki. All volunteers provided written informed consent before participating in this study.

Electric stimulation

Ten electrodes (15×15 mm, Medicotest, Denmark) were mounted on the sole of the right foot (Fig. 1). A common anode (7×14 cm electrode, Pals, Axelgaard Ltd., USA) was placed on the dorsum of the foot. This electrode configuration ensured that the stimulus was always perceived as coming from the sole of the foot. Each stimulus consisted of a constant current pulse train of five individual 1 ms pulses delivered at 200 Hz. For each electrode position, the stimulus intensity was adjusted based on the pain thresholds to ensure equal sensory intensity irrespective of the stimulation site. To assess the effect produced by repetitive stimulation, five stimulations were delivered as a stimulus train with a frequency of 3 Hz. Each train was delivered randomly to one of the ten electrodes by a computer-controlled constant current electrical stimulator (Noxitest, Aalborg, Denmark). Each stimulation site was tested five times resulting in a total of 50 stimulation trains. The inter-stimulus interval was between 15 and 20 seconds.

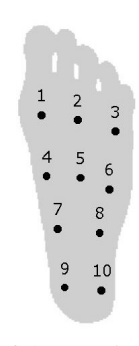


Figure 1. Placement of the 10 stimulation electrodes.

Kinematics

Three goniometers (Biometrics Ltd, type XM180, Gwent, United Kingdom) were mounted on the lateral side of the right ankle, knee, and hip joints to monitor the kinematic response. The goniometric signals were filtered (20 Hz low pass filter), sampled (2000 Hz), displayed, and stored.

EMG recordings

Surface electromyogram (EMG) was recorded from the following ipsilateral muscles: tibialis anterior (TA), soleus (SOL), vastus lateralis (VL), biceps femoris (BF), and iliopsoas (IL). The EMG signals were amplified, filtered (5-500 Hz, 2nd order), sampled (2000 Hz), displayed, and stored from 200 ms before stimulation and until 2800 ms after the stimulation onset.

Experimental protocol

First, EMG, stimulation electrodes, and goniometers were mounted. Then, the pain

threshold (PTh) to electrical stimulation was determined at each site while sitting. During the reflex recordings the stimulus intensity was set as a fixed factor multiplied by the pain thresholds determined at the individual stimulation sites. A multiplication factor of 1.5 was first chosen, however, it was later adjusted individually for all subjects by assessing the build up in the reflex size while taking the reported pain into consideration. This resulted in one individual factor for each subject. The sequence of stimulation positions was then randomised and the actual reflex recordings took place. The reflexes were recorded with the subjects sitting in an elevated chair with knees and hips flexed approximately 90 degrees and the lower leg hanging free.

Data analysis

The size of the EMG reflex response was assessed in all muscles by the root mean square (RMS) amplitude of the individual reflexes in the 60-250 ms post-stimulation interval, except for SOL where an interval of 110-250 ms was chosen as a silent period is often seen prior to the excitatory reflex. The reflex sizes were calculated separately for all five stimuli in the train. The reflex size for the five assessments was then averaged for each stimulation site. Temporal summation assessed by comparing the reflex size evoked by stimulus number two to five with the reflex size evoked by the first stimulus in the train. The peak angle change, relative to the pre-stimulus position, in a time interval from 100 ms after the first stimulus and until 500 ms after the last stimulus was found for the three joints. The pre-stimulus position was determined as the mean goniometer signal during 100 ms prior to the onset of the first stimulus.

Statistics

The EMG reflex responses were analysed using two-way repeated measures ANOVA (factors: stimulation site and stimulus number in the train of five stimuli). Student Newman-Keuls statistics (SNK) were used for post-hoc pairwise comparisons. *P*<0.05 was regarded as statistically significant. All values are presented as mean and standard error of the mean (SEM).

Results

The mean PTh for all 10 sites was 14.9±0.39 mA. The lowest PTh was detected at the arch of the foot (12.3±1.1 mA). Based on the pain thresholds, the multiplication factor was determined to ensure stable reflexes resulting in a mean stimulus intensity of 1.51±0.08 times the PTh ranging from 0.9×PTh to 2.2×PTh.

EMG reflex responses

In general, the reflexes increased in size between the first and second stimulus of the train, however, they were dependent on the stimulation site. The TA RRF covered the distal sole of the foot, with a gradual expansion of the RRF during the stimulus train (Fig. 2). Reflexes evoked at sites 1 and 2 were larger than reflexes evoked at sites 3, 7-10 while reflexes evoked at sites 4 and 5 were larger than reflexes evoked at sites 8-10 after the fourth stimulus in the train (ANOVA interaction, p<0.001, SNK p<0.05, Fig. 2). Reflexes in SOL were facilitated after the second stimulus at all sites (Fig. 2) (ANOVA p<0.001) and were of identical size during stimulus 2-5.

A gradual expansion of the RRF was seen in both BF and VL. In BF, the reflex receptive fields covered the distal, lateral part of the sole of the foot (sites 1-3, 5,6, and 8) after the second stimulus while facilitated reflexes were seen at sites 1-8 in VL at stimulus five (Fig. 2). The IL RRF covered the distal, lateral part of the sole and gradually expanded to proximal sites (Fig. 2).

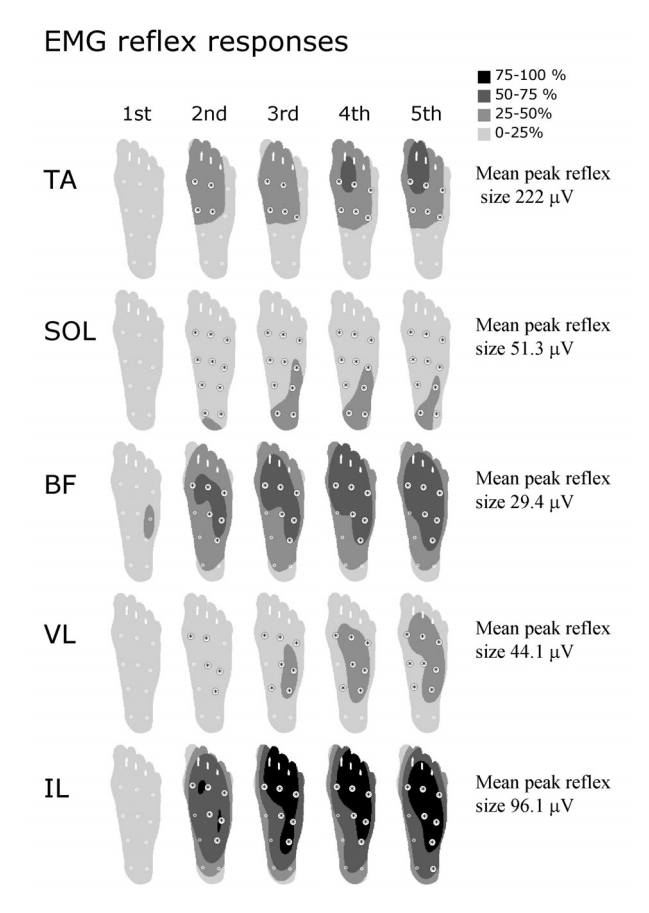


Figure 2. The RRF after each stimulus are shown. Two-way interpolation of grand mean RMS values was used to represent the RRF. * indicates that the reflexes are significantly larger than the reflexes evoked by the first stimulus at this stimulation site.

In all muscles, there were no statistically differences between reflexes evoked by stimulus four and five, which indicate that the reflex size reached a plateau.

Kinematic reflex responses

Knee and hip flexion were evoked at all sites (Fig. 3). At the ankle joint a mean dorsi-flexion of 8.7±1.3° was recorded. Ankle dorsi-flexion was evoked at skin sites distal to the ankle joint, whereas significant plantar flexion was evoked at sites 9 and 10 on the heel (Fig. 3).

Kinematic reflex responses

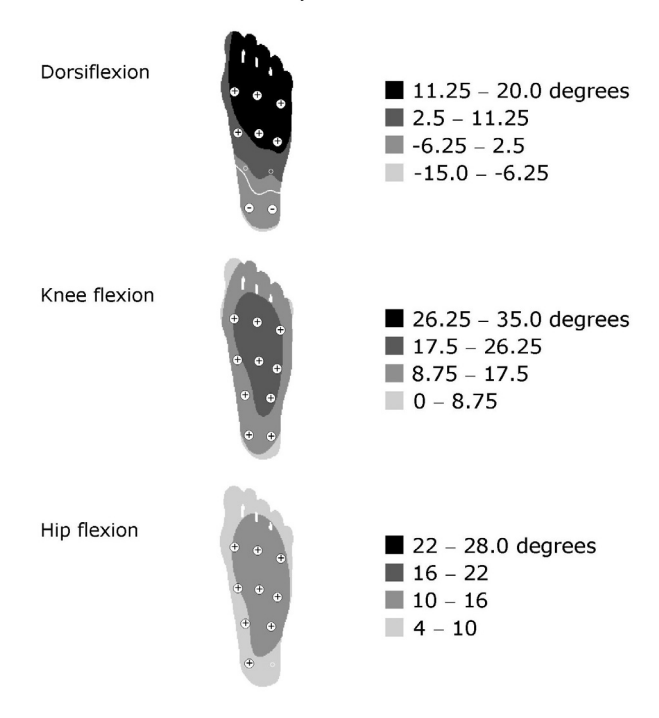


Figure 3. Mean reflex angle changes during the stimulus train for the ankle, knee, and hip joints. For the ankle joint, a white line indicates the transition from dorsiflexion to plantarflexion. Angle changes statistically different (95% confidence intervals) from 'no reflex movement' (0 degrees) are indicated by either \oplus or \bigcirc to indicate dorsi-flexion/plantar flexion of the ankle, and flexion/extension of the knee and hip joints.

Discussion

In the present study, the RRF gradually expanded during the stimulus train for stimulus intensities of approximately 1.5 times the pain threshold. The largest increment was observed after the first stimulus, while only marginal changes where observed between stimulus four and five, suggesting the reflex response reached a plateau. The immediate facilitation of the reflex response at the center of the RRF and the gradual increase of the size of the reflexes at the borders of the RRF could indicate a graded sensitivity of the RRF.

Withdrawal reflexes to repetitive nociceptive stimulation have been investigated in many human studies [8] [9] [2]. During the initial part of a train, the reflex size gradually becomes larger and the duration of the reflex becomes longer. After approximately 1 to 2 seconds of repetitive stimulation, the reflex size saturates or even decreases probably due to an inhibitory circuit, which may involve supra-spinal structures [3].

Interneurons located in the deep dorsal horn (WDR neurons) present spatial patterns of response similar to those of various single muscles [10] and are likely involved in encoding the nociceptive withdrawal reflex RRF. Deeply located WDR neurons are also the most sensitive neurons to repeated stimulation at C-fiber strength [11]. An increase in the excitability of the WDR neurons, to both A δ - and C-fiber inputs, was observed after conditioning by repetitive stimulation at C-fiber strength [11].

The kinematic responses are in agreement with previous observations evoked by a single stimulus [5]. The responses were however facilitated by the repetitive stimulus.

In conclusion, temporal summation with site-dependant sensitivity was detected in the reflex responses from all muscles. This led to a gradual expansion of the RRF during the train of five stimuli. The facilitation of the withdrawal reflex responses due to repetitive stimulation might have potential applications in the rehabilitation engineering field, where these reflexes could be used to assist gait of patients with central nervous system injuries.

References

- [1] Price D.D., Hu J.W., Dubner R., Gracely R.H.: Peripheral suppression of first pain and central summation of second pain evoked by noxious heat pulses. Pain, 3, 1977, 57-68.
- [2] Arendt-Nielsen L., Sonnenborg F.A., Andersen O.K.: Facilitation of the withdrawal reflex by repeated transcutaneous electrical stimulation: an experimental study on central integration in humans. Eur.J.Appl.Physiol, 81(3), 2000, 165-173.
- [3] Gozariu M., Bragard D., Willer J.C., Le Bars D.: Temporal summation of C-fiber afferent inputs: competition between facilitatory and inhibitory effects on C-fiber reflex in the rat. J.Neurophysiol., 78(6), 1997, 3165-3179.

- [4] Schouenborg J., Kalliomäki J.: Functional organization of the nociceptive withdrawal reflexes. I. Activation of hindlimb muscles in the rat. Exp.Brain Res., 83(1), 1990, 67-78.
- [5] Andersen O.K., Sonnenborg F.A., Arendt-Nielsen L.: Modular organization of human leg withdrawal reflexes elicited by electrical stimulation of the foot sole. Muscle Nerve, 22(11), 1999, 1520-1530.
- [6] Sonnenborg F.A., Andersen O.K., Arendt-Nielsen L., Treede R.D.: Withdrawal reflex organisation to electrical stimulation of the dorsal foot in humans. Exp.Brain Res., 136(3), 2001, 303-312.
- [7] Andersen O.K., Sonnenborg F.A., Arendt-Nielsen L.: Reflex receptive fields for human withdrawal reflexes elicited by non-painful and painful electrical stimulation of the foot sole. Clin.Neurophysiol., 112(4), 2001, 641-649.
- [8] Shahani B.T., Young R.R.: Human flexor reflexes. J.Neurol.Neurosurg.Psychiatry, 34(5), 1971, 616-627.
- [9] Hugon M.: Exteroceptive reflexes to stimulation of the sural nerve in man. 1973, 713-729.
- [10]Schouenborg J., Weng H.R., Kalliomäki J., Holmberg H.: A survey of spinal dorsal horn neurones encoding the spatial organization of withdrawal reflexes in the rat. Exp.Brain Res., 106(1), 1995, 19-27.
- [11]Schouenborg J., Sjölund B.H.: Activity evoked by A- and C-afferent fibers in rat dorsal horn neurons and its relation to a flexion reflex. J.Neurophysiol., 50(5), 1983, 1108-1121.

Acknowledgements

This study was supported by The Danish Technical Research Council.

Author's Address

Erika G. Spaich Center for Sensory-Motor Interaction Aalborg University Fredrik Bajers Vej 7 D3, DK-9220 Aalborg, Denmark e-mail: espaich@smi.auc.dk

EFFECTS OF GAIT TRAINING WITH NEUROMUSCULAR ELECTRICAL STIMULATION ON THE ELECTROMYOGRAPHIC ACTIVITY IN PARAPLEGIC PATIENTS

E.W.A. Cacho,* A. Cliquet Jr.* *

* Dept. of Orthopedics & Traumatology, Fac. of Medical Sci., UNICAMP

*Dept. of Electrical Engr, USP.

Abstract

The useful effect of locomotion training through neuromuscular electrical stimulation (NMES) in patients with spinal cord injury has already been established. The human spinal cord recognizes the appropriate sensorial information and can modulate responses about the motor pool which facilitates walking under NMES training. The actual model towards the effect of gait training, via NMES, in the spinal locomotion centre is still unclear. In this work, ten male patients (21 - 36 yrs. old) with chronic spinal cord injury (seven complete, three incomplete, neurologic level below T2) were evaluated at the Biomechanics & Rehabilitation Lab./University Hospital: first as soon as the patients joined the Programme and after 30 NMES based gait sessions, alternating quadriceps/peroneal stimulation. Clinical protocols of the American Spinal *Injury* Association (ASIA), Ability Ambulation Scale as well as Electromyography (EMG) of muscle soleous (SO), gastrocnemious medialis (GA) and tibialis anterior (TA) were assessed. Motor recovery was improved with two incomplete subjects (ASIA) and lower limb (SO,GA,TA) EMG stance and swing coordination gait patterns were also improved in the incomplete ones. For the complete spinal cord lesions, EMG activity increased during the stance phase and SO and GA muscle patterns were improved. Results suggest that gait training with NMES does induce changes in the spinal cord neural center, thus triggering the recovering of functional abilities/gait paraplegics.

Introduction

The lost of gait ability is a major problem in individuals with Spinal Cord Injury (SCI)[1] and its restoration has been intensively studied. The development of rehabilitation strategies towards gait based in the locomotor control of mammal is highly dependent on the central pattern generator (CPG) that is responsible for a large part of gait control. In humans, CPG is not too robust if compared with other mammals. It is able to recognize appropriate sensorial information and modulate motoneuron responses that facilitate locomotion [2].

The capacity of the spinal cord in interpreting the sensorial influx and modulate the paths that generate the step can be improved by a gait task-specific training [3, 4].

The gait task-specific training thru NMES in subjects with SCI presents an effective potential in the recovery mobility process and ambulation [5].

Gait training with NMES might be like a therapeutic way to inducing gait in paraplegic patients and modulate responses at the spinal level. In this study the improvement of gait in such individuals, was analysed thru the effects of training with NMES-assisted gait on the electromyographic (EMG) activity at the leg muscles in paraplegic patients.

Material and Methods

Ten patients, 10 male, age 21-36 years (mean of 30.3 years, sd ± 7.10), with chronic SCI (> one year of lesion) were recruited. The subjects were evaluated and treated in the Biomechanical and Locomotion Rehabilitation Laboratory of the University Hospital at UNICAMP, from January 2002 to December 2003 (Table 1). The research was approved by the Ethics Committee of the Faculty of Medical Sciences-UNICAMP (Protocol n° 381/2001).

Table 1- Subject Characteristics

	Level of	AC*	Muscle		
Code	Lesion	Pre/	Tone** $R-L^+$		Distance
	Impairment	Post			
	Scale		Pre/Post		
1	T8-ASIA A	1	1	1	40 m
2	T10-ASIA C	1 / 2	1/+1	1	70 m
3	T8-ASIA A	1	1/+1	1/+1	70 m
4	T6-ASIA A	1	1/0	1	36 m
5	T8-ASIA A	1	1	1/+1	58 m
6	T9-ASIA C	1 / 2	+1/1	+1/1	90 m
7	T5-ASIA A	1	1/0	1/0	40 m
8	T3-ASIA A	1	0	1	100 m
9	T8-ASIA A	1	+1/2	+1/2	70 m
10	T6-ASIA C	1 / 2	+1/1	1	120 m

^{*}AC, ambulatory capacity; **According to the Modified Ashworth Scale; *R/L, right/left.

Instrumentation

Neurologic examinations of all patients were performed according to ASIA standards [6]. The motor (maximum 100 points) and sensory (maximum for both anesthesia and algesia 112 points) scores indicated the severity of the spinal cord lesion. The impairment scale classified as (A) no motor or sensory function below the lesion; (B) sensory function only below the lesion; (C) "useless" motor function below the lesion; (D) "useful" motor function below the lesion; and as (E) recovered.

The ambulation capacity of patients was assessed as being in one of four categories: (1) no ambulatory capacity, with the patient unable to walk or stand; (2) therapeutical ambulatory capacity, with standing and walking possible but only with the support of either two crutches and the help of an accompanying person (such patients could perform these procedures only as a therapeutical approach); (3) functional ambulatory capacity, with daily walking possible over short distances without the aid of physiotherapists or braces (a category of ambulatory capacity used regularly in the activities of daily living and at work); and (4) full ambulatory capacity, with little or no disturbance in walking (a categorization corresponding to that used in earlier studies)[7].

The Modified Ashworth Scale [8] determined spasticity of the plantar flexors, which presents a score from 0 to 4 where 0 is normal tonus and 4, is complete rigidity of the segment.

Multichannel surface EMG recordings used a device of Noraxon USA, with bipolar surface electrodes (5 cm apart) on the tibialis anterior (TA), medial gastrocnemius (GM), and soleus (SO) muscles of both legs: SO, distal to the gastrocnemius muscle and medial to the achilles tendon; GM, below the popliteal crease; and TA, below the tibial tuberosity and lateral to the tibial crest.

Procedure

The subjects were evaluated in the first and after thirty sessions of gait training with the instruments cited above.

The gait training programme consisted of a strengthening period for the quadriceps muscle, with the patient seated, followed by standing and gait training which consisted of 30 sessions. The patients walked during 40 minutes, with rest periods and the distance walked was measured.

For training, a four channel NMES system with surface electrodes was used to enable standing and walking with a reciprocal gait in paraplegic patients [9].

EMG data acquisition was done with the subjects walking without NMES but with the lending support and an extensor splint knee united to an ankle foot mechanical orthosis (AFO) along six meters approximately.

Data analyses

The collected data of EMG were manually analysed, beginning with the identification and marking of gait phases, through signals (on/off) from the pressure sensors on the plantar foot. Quantitative representation of intramember coordination was achieved thru amplification (band pass filters, 30 to 300 Hz), analog-to-digital conversion and sampling at 1000Hz. EMG signal was rectified (RMS) about an average of five steps.

A descriptive analysis of variable studies comparing with each measure of EMG (muscle – TA, GM, SO; period – pre and post-training; phase – swing and stance) was done.

To explain the variability of each measurement in the EMG activity Variance Analysis with 3 repeated factors and with RANK transformation [10] was performed. When the factor was significative comparison multiple tests (Contrast Tests) to identify the differences were done.

Results

Effect of level gait training

Relative to the periods pre and post-training, in the right leg, intramember coordination significant values were obtained for the SO muscle which showed major values in the stance phase and minor values in the swing phase (pre: p-values = 0.0122; e post: p-values = 0.0111). About this aspect, the SO muscle demonstrated smaller values in the swing phase in the post-training period (p-value = 0,0046) (Fig. 1).

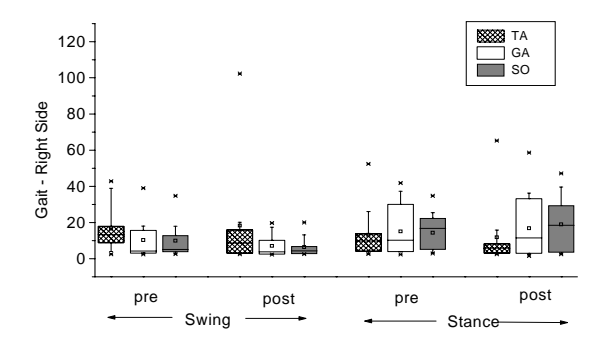


Fig. 1: Gait variables for the right leg.

For TA e GA right muscles, statistical differences were not observed, possibly due to the large variability of EMG activity. Therefore, when evaluating separately the right leg muscles of

subjects with incomplete lesions, a more coordinated EMG intramember pattern (Fig 2) was found.

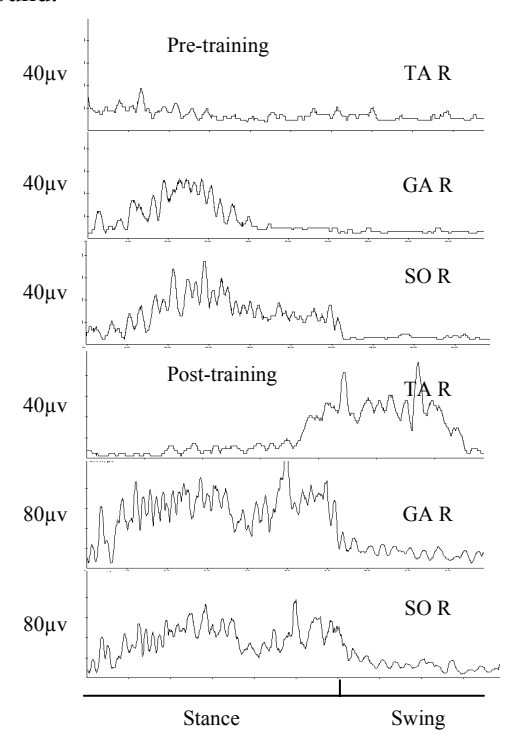


Fig. 2: EMG pattern for subject 10. Pre and post training.

In the left leg it was noticed that the TA muscle presented an increase in the EMG activity in the post- training period for the swing phase (p-value = 0.0382) (Fig. 3). GA and SO muscles of the left leg, referred a larger EMG activity in the stance phase when compared to the swing phase (P = .0028; P = .0378, respectively), including the pre and-post training period.

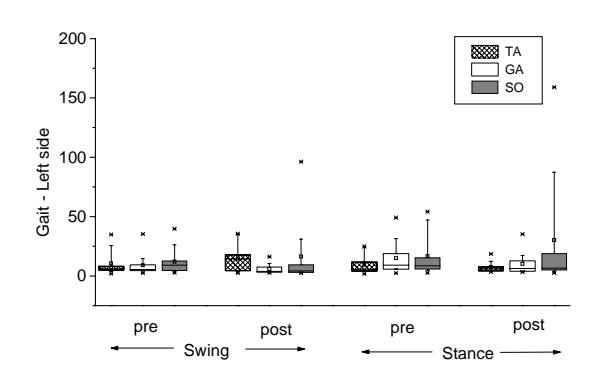


Fig. 3: Gait variables of the left leg.

During that same phase (stance), in the post-training period, differences between the leg muscles were noticed when the TA muscle presented lower EMG activity than that of the GA and SO (P = .0430; P = 0.0038, respectively).

Discussion

The selection of an appropriate locomotor pattern depends upon a combination of central programs and afferent inputs, moreover instructions to a respective motor condition. This information determines the organization way of muscular synergies [11] designating multiple conditions of stance and swing [12]. Prior investigations have demonstrated that it is possible to induce locomotor activity in complete and incomplete paraplegic patients [13].

In this study improvements were obtained relatively to ambulatory capacity of subjects 2, 6 and 10, which went from category 1 (no ambulatory capacity) to 2 (therapeutic ambulatory capacity). All subjects obtained gains in the NMES-assisted gait (Table 1). Other studies have documented positive results in the NMES-assisted training [14], mainly with incomplete paraplegic patients. Therapeutic effects of NMES-assisted level gait training involve central and peripheral factors [5], like changes in the muscular fibre properties [15] and in the plasticity of motor gait behavior during chronic stages of the spinal lesion.

In the present study alterations in muscle tone were not observed (Table 1). Granat et al (1993) [14] found a significant reduction of spasticity after a NMES exercise and gait programme for patients with incomplete SCI with evaluation being done by a pendulum test but not with the Asworth Scale.

Three aspects are rather relevant: (1) some studies have shown that electrical stimulation of the common peroneal nerve reduces the amplitude of the H-reflex in the SO muscle [16]. This change in the H-reflex could be related with the intrinsic modulation capacity of the spinal cord [17] evidencing plasticity in the level of spinal reflexes in primates after a period of task-dependent training [18]; (2) NMES excites the quadriceps Ia afferent fibres thus contributing for the excitation of their α -motoneurones as well as the α motoneurones of the SO muscle, thus leading the muscles to act as anti-gravity synergists [19]; (3) the spinal CPGs might be the active in paraplegic patients through influx of afferent task-specific information. The NMES-assisted training can contribute to some afferences to the CPGs in SCI patients as the afferent inputs from load receptors [11] and from the stretch receptors Ia of the hip [20]. Thus, the discharge weight during the NMES-assisted gait training can contribute to the spinal circuitry.

NMES-assisted gait training allows a modulation of the H-reflex through the peroneal nerve stimulation and offer correct information about the

task-dependent coordination, thus facilitating the gait performance and EMG coordination patterns. Therefore, such therapeutic approach is capable of yielding satisfactory results towards the ambulatory rehabilitation.

References

- [1]Rowley, S., Forde, H., Glickman, S., et al: Lesão de Medula Espinhal in Stokes, M.: Neurologia para Fisioterapeutas. São Paulo, Premier, 2000, 117-133.
- [2]Field-Fote, E.C.: Spinal cord control of movement. Implications for locomotor rehabilitation following spinal cord injury. Phys Ther., 80 (5), 2000, 477-484.
- [3]Richards, C.L., Malouin, F., Wook-Dauphince, S., et al: Task-specific physical therapy for optimization of gait recovery in acute stroke patients. Arch Phys Med Rehab., 74, 1993, 612-620.
- [4]Dietz, V.: Spinal cord pattern generators for locomotion. Clin Neurophys., 114, 2003, 1379-1389.
- [5]Ladouceur, M., Barbeau, H.: Functional electrical stimulation-assisted walking for person with incomplete spinal cord injury; longitudinal changes in maximal overground walking speed. Scand J Rehab Med., 32, 2000, 28-36.
- [6]American Spinal Injury Association. Standard for Neurological and Functional Classification of Spinal Cord Injury, Chicago, ASIA, 1992.
- [7]Curt, A., Dietz, V.: Ambulatory capacity in spinal cord injury: significance of somatosensory evoked potentials and ASIA protocol in predicting outcome. Arch Phys Med Rehab., 78, 1997, 39-43.
- [8]Haas, B.M., Bergström, E., Jamous, A. et al: The interrater reliability of the original and of the modified Ashworth scale for the assessment of spasticity in patients with spinal cord injury. Spinal Cord., 34, 1996, 560-564.
- [9]Sepúlveda, F., Cliquet Jr., A.: Gait restoration in a spinal cord injured subject via neuromuscular electrical stimulation controlled by an artificial neural network. Inter J Art Org., 21 (1), 1998, 49-62.
- [10]Montgomery, D.C.: Design and Analysis of Experiments. New York, John Wiley & Sons, 1991, 649.
- [11]Horak, F.B., Nashner, L.M.: Central programming of postural movements adaptation

- to altered support –surface configurations. J Neurophys., 55, 1986, 1361-1381.
- [12]Mackay-Lyons, M.: Central pattern generation of locomotion: a review of the evidence. Phys Ther., 82, 2002, 69-83.
- [13]Harkema, S.J., Hurley, S.L., Patel, U.K, et al: Human Lumbosacral Spinal Cord Interprets Loading During Stepping. J Neurophys., 77, 1997, 797-811.
- [14] Granat, M. H., Ferguson, A. C., Andrews, B. J., et al: The role of functional electrical stimulation in the rehabilitation of patients with incomplete spinal cord injury observed benefits during gait studies. Paraplegia., 31, 1993, 207-215
- [15]Salmons, S., Henriksson, J., The Adaptive Response of Skeletal Muscle to increased Use. Muscle Nerve., 4 (2), 1981, 94-105.
- [16] Stein, R.B., Yang, J.F., Bélanger, M., et al: Modification of reflex in normal and abnormal movements. Prog Brain Res., 97, 1993, 189-196.
- [17]Zehr, E. P., Hesketh, K. L., Chua, R.: Differential Regulation of Cutaneous and H-Reflexes During Leg Cycling in Humans. J. Physiology, 2000, 1178-1184.
- [18] Wolpaw, J.R.: Acquisition and maintenance of the simplest motor skill: investigation of CNS mechanisms (review). Med Sci Sports Exerc., 26, 1994, 1475-1479.
- [19]Meunier, S., Penicaud, A., Pierrotdeseilligny, E., et al. Monosynaptic Ia excitation and recurrent inhibition from quadriceps to ankle flexors and extensors in man. J Physiol., 423, 1990, 661-675.
- [20]Dietz, V., Roland, M., Colombo, G.: Locomotor activity in spinal man: significance of afferent input from joint and load receptors. Brain, 125, 2002, 2626-2634.

Acknowledgements

The State of São Paulo Foundation for Research (FAPESP), FAEP-UNICAMP and CNPq.

Authors' Addresses

Professor Alberto Cliquet Jr., PhD.
Dept. of Orthopedics & Traumatology-UNICAMP cliquet@fcm.unicamp.br & Dept. of Electrical Engr.-USP.
13560970, S.Carlos, Brazil cliquet@sel.eesc.usp.br Enio Walker Azevedo Cacho, MSc. Student Dept. of Orthopedics & Traumatology-UNICAMP.
13083970, Campinas, Brasil enio@fcm.unicamp.br

NEUROLOGICAL REHABILITATION, PLASTICITY AND ACTIVITY— MEDIATED ASPECTS: A ROLE FOR LOCOMOTOR GENERATING ACTIVITY AND THE RESIDUAL POTENTIAL ON SCI INDIVIDUALS THROUGH FES WALKING?

Cerrel Bazo H 1

Centro di Neuroriabilitazione e Ricerca di Villa Margherita, Arcugnano, Vicenza, Italy (1)

New scientific work has given the idea of a grown potential to reduce the neurological impairments and functional disabilities of people with SCI (spinal cord injury). As a result patients and families have become forceful advocates for SCI cure. This has posed a challenge for ETHICS compelling researchers and clinicians to promise only for concrete results.

Developmental & experimental neurobiology has enable axons to grow and stem cells to differentiate and migrate. We are learning about the flexibility and plasticity of the sensorimotor system above and below the level of spinal injury [brain-spinal cord-motor unit], and about the residual activity of muscle-skeleton, bladder, bowel, cardio-respiratory and general autonomic system responses feasible for functional use by a NEW CIRCUITRY and/or by ARTIFICIAL means.

In this paper, we briefly comment the possibilities of CNS plasticity in animals and humans. We describe the sacral sparing theory as a tool for human SCI clinical outcome prognosis related to walking performance. By means of functional electrical stimulation (FES), we show some promising clinical results that can be associated with plasticity in the CNS organization nurturing interesting thoughts about the integration of different systems (below and above the level of injury). We demonstrate that it may be possible for FES to potentiate the effects of the residual potential on chronic SCI subjects to generate a pattern of movement that can be useful for standing, stepping and or cycling.

Dormant long-term SCI residual activity may lose the awareness to support above and below the level of injury activity. The sensorimotor system if properly stimulated may generate activity useful for the functional integration of different systems. In this sense; FES, the awareness learning process and training mediated-activities may open real pathways of communication between the above and below level of injury encouraging us to prepare for structural, methodological and neurophysiological studies to proof for the effectiveness of this mediated-approach proposed as a new neurorehabilitation gaining technique.

Key words: CNS organization and plasticity, functional electrical stimulation, human long-term SCI, locomotor-generated pattern activities, spinal-cord injury.

Author's Address

Humberto Cerrel Bazo, Medical Dirctor Dr. Centro di Neuroriabilitazione e Ricerca di Villa Marherita Via Costacolonne 20 36057 Arcugnano, Italy e-mail: hcb57@yahoo.com

Session 7

Lower Extremities: Gait

Chairpersons:

T. Bajd (Ljubljana, Slovenia) M. Popovic (Toronto, Canada)

STIMULATION PARAMETER OPTIMISATION FOR FES SUPPORTED STANDING UP AND WALKING IN SCI PATIENTS

M. Bijak¹, M. Rakos², C. Hofer³, W. Mayr¹, M. Strohhofer³, D. Raschka³, H. Kern³

- Department of Biomedical Engineering and Physics, Medical University of Vienna, Austria
 Otto Bock Healthcare Products GmbH, Vienna, Austria
- 3) Department of Physical Medicine and Rehabilitation, Wilhelminenspital, Vienna, Austria

Abstract

Functional Electrical Stimulation (FES) to restore leg movement for standing up and walking (stepping) in SCI patients with intact lower motor neuron is used by several groups. Usually quadriceps muscles are stimulated for hip and knee extension, gluteus muscles for hip stabilization and common peroneal nerve to elicit the flexion reflex.

The demand to get a natural movement would require a huge amount of stimulation channels – a request that could be easily fulfilled from the engineer's point of view but not from the point of practicability since each stimulated muscle requires two skin attached electrodes resulting in a prolonged time for donning and doffing.

In the described project a newly developed eight channel stimulator that can vary the stimulation parameters in many ways and over a wide range is used. The goal is to achieve a natural movement with a minimum of surface electrodes by optimising the stimulation parameters

Seven experienced FES users and five unexperienced persons (all between Th46-Th11) participate in this study.

Standing up can be significantly improved by optimising the time delay between the onset of quadriceps and gluteus muscles (0.2-0.4~s) and the duration of the ramp. A 0.2s delay gives good results in heavy patients while slower ramps (0.4s) are required in slim patients. During stepping gluteus muscle timing is not very crucial. He is turned off 0.1-0.2s before quadriceps muscle and with the same delay turned on again. Of major influence on the gait quality is the timing during heel strike when peroneal stimulation is switched of and quadriceps stimulation is turned on. 6 patients require 0.0-0.1s where neither peroneal nor quadriceps stimulation is applied, the others require an overlap of 0.1-0.2s.

Activation of adductor muscles during standing up and during the swing phase helps to avoid hip abduction and improves knee trajectories.

Introduction

Functional Electrical Stimulation (FES) can be used to activate lower extremities in paraplegic persons. Mainly three approaches can be found: Stimulation of leg muscles via skin attached electrodes [1], implanted electrodes attached to an external stimulator [2] and implanted electrodes in combination with an implanted pulse generator [3]. Electrical stimulation used in combination with orthoses is also reported [4; 5].

This paper focuses on surface stimulation because it can be easily applied and the patient can enter the FES program in any stage of the rehabilitation process. The functionality standing up, standing and stepping/walking is provided by electrodes placed over the quadriceps muscles to get hip and knee extension, gluteal muscles for hip stabilisation and common peroneal nerve to elicit withdrawal reflex for hip flexion, knee flexion and ankle dorsiflexion.

For basic functions six electrodes are required per leg. Better results could be expected if more muscles are selectively stimulated [6]. In the case of surface stimulation more channels would result in a longer time for donning and doffing (attach electrodes, hide cables, connect device, check for proper electrode placement), lowering the usability of such a stimulation system in daily life.

An eight channel stimulation system with a high degree of freedom in stimulation parameter range was developed [7]. Individual parameter optimization shall improve the outcome of the described stimulation strategy.

User friendliness played an important role during the hard- and software design phase.

Material and Methods

Seven FES experienced paraplegic patients and five unexperienced (all between Th4 to Th11), volunteered to participate in this study and to test the new eight channel stimulation system.

Stimulation device

An eight channel stimulation system (subject of cooperation between the Medical University Vienna and Otto Bock Healthcare Products GmbH) was used. The system consists of two four channel stimulation modules, one for each leg, and one master module holding the batteries and the components for bus management.

The user interface and the handling of the stimulation sequences are provided by a PocketPC (Comapq, Ipaq Model 3950, HP, Houston, Texas, USA). Equipped with a wireless LAN card the PocketPC is able to communicate with a PC for data upload, data download data synchronization and to open a channel for stimulator control directly from the PC.

All modules, two stimulation modules, the master module and the PocketPC are stored in a custom made belt to wear the stimulation equipment around the waist. Connection cables are hid in the belt (Fig. 1).

A wireless (433MHz) remote control offers access to the stimulators basic functions. Buttons are mounted close to the supporting handle so they can be reached by thumb without releasing the handle.

PC Software

Special software for the PC was written for data management and to build stimulation sequences. A graphical user interface helps the therapist to control stimulation timing and amplitude, pulse width and pulse frequency. The latter two parameters can be set individual for attack, plateau and decay of stimulation burst and for continuous stimulation.

Patient session

When the patient comes to the rehabilitation centre electrodes are attached over quadriceps muscles, gluteus muscles and peroneal nerve. In the following five minutes a warm-up program with weak contraction for quadriceps and gluteus muscles is performed.

Under control of the PC the stimulation amplitude is increased for each single channel under supervision of the therapist until a strong contraction is observed. Electrode position of the peroneal electrodes and stimulation parameters are changed until a sufficient reflex response is noticed.

Based on the previous findings the patient starts to practice FES evoked standing up and sitting down. A physiotherapist watches carefully the movement and advises the patient to correct his posture, balancing, grip force and so on if necessary.

Next, walking training is started. Parameters are optimized for smooth stepping movements.

In patients tending to have knee abduction during standing up and having problems to swing the leg forward in a linear way electrodes are placed on the inner thigh to activate adductor muscles.

As soon as the session is completed the stimulation sequences for home use are selected and transferred into the PocketPC.

In general stimulation parameters are: 27Hz pulse frequency, biphasic pulses, pulse duration 0.6µs+0.6µs.



Fig. 3: FES supported stepping. Patient is wearing an eight channel stimulator consisting of two four channel stimulation modules (left and right) and a master module .with PocketPC (middle). Stimulation is triggered with the right thumb.

Results

In general the introduction of ramps when the stimulation is activated or deactivated leads to a more natural movement in comparison to simply switching stimulation on and off.

To stand up the patient checks for proper foot forward and position. leans triggers stimulation. A pattern (according to figure 1) for standing up is shown in figure 2. For a smooth upwards movement heavy patients request a steep ramp for quadriceps stimulation onset (0.2s), slim patients request slow ramps (up to 0.4s). A time delay between quadriceps activation and gluteus activation is necessary to first lift the body from the seat and then, when the knees are nearly extended, to push the hip forward and stabilize it. 0.2-0.4s time delay gives good results. After an upright posture is taken, the stimulation amplitude can be reduced by 10 to 25 percent, to lower muscle fatigue. In two cases (the heaviest patients) the stimulation frequency during standing up is increased to 70Hz.

Adductor stimulation was effective in improving knee trajectories during standing up by reducing knee abduction.

The corresponding walking sequence is outlined in figure 3. When a step is triggered quadriceps and gluteus stimulation is turned off, flexion reflex is provoked and at the end of the swing phase extensors are turned on again.

During stepping the most critical part is the timing during heel strike when peroneal stimulation is switched of and quadriceps stimulation is turned on. Four patients require 0.0-0.1s where neither peroneal nor quadriceps stimulation is applied, the others require an overlap of 0.1-0.2s. The gluteus timing had no major influence on the gait quality. In all patients gluteus was turned off at the beginning of the swing phase 0.1s before quadriceps and turned on again at the end of the swing phase 0.1s after quadriceps.

Sitting down is an uncritical task: Releasing the hip and then turning off quadriceps stimulation. Heavy patients need slow ramps, the others prefer steep ramps.

Patients can perform 15-25 steps per minute with a step length of 20-30cm. The walking distance until exhaustion or muscle fatigue occurs is 4-60m.

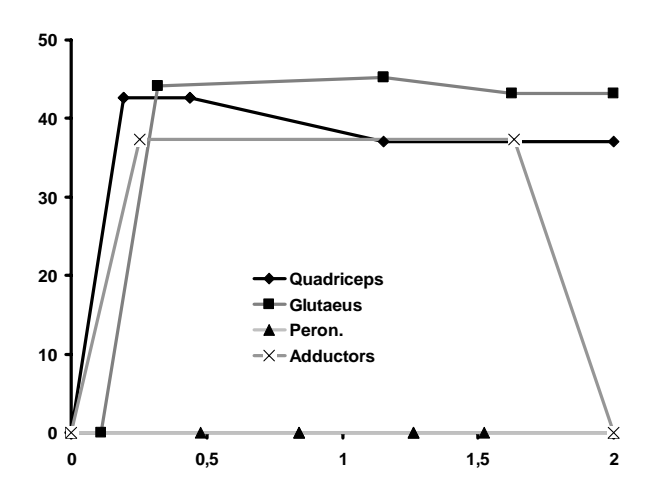


Fig 2: Envelope of the stimulation impulse amplitudes for standing up for one leg. X-axis: Time in seconds, Y-axis: Peak voltage in volt

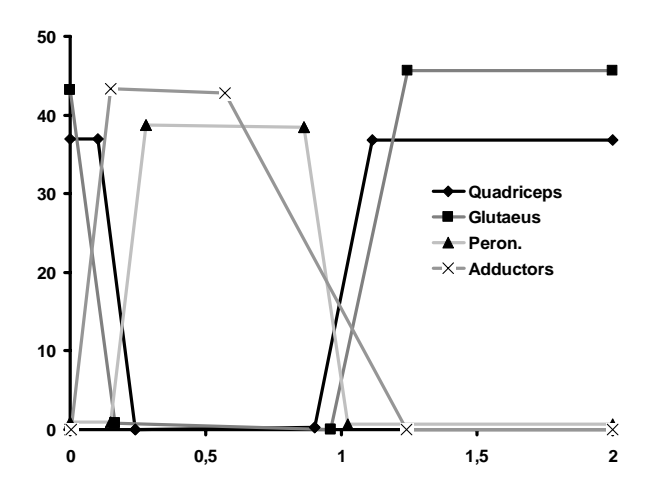


Fig 3. Fig: Envelope of the stimulation impulse amplitudes for stepping for one leg. X-axis: Time in seconds, Y-axis: Peak voltage in volt

Discussion

The eight channel stimulation system was well accepted by the patients and worked reliable.

After an introduction and three patient sessions under supervision the therapists were able to handle the PC and PocketPC software independently.

In all patients a smooth course of motions for standing up and stepping could be reached by individual parameter optimization.

Somehow disappointing is the short walking distance. Of course the endurance is considerably influenced from the experience and rehabilitation status of the patient. Mainly two factors limit the walking distance: muscle fatigue of stimulated muscles and exhaustion due to applied arm support. Muscle fatigue can be improved by trainings strategies. A high arm support may have several reasons. Every factor that causes leaning forward induces higher arm support. Hip contracture inhibits an upright posture resulting in leaning forward. Fear of falling backwards or fear of device failure provokes the same problem. A higher arm support is also applied if the steps are too long and the major work of moving the body forward is done by pulling with the arms. Heavier patients in general use more arm support to stay balanced.

It was observed that the patients request higher stimulation amplitudes than necessary for the required functionality because they feel much safer if legs and hips are very stiff. This overstimulation advances muscle fatigue.

Author's Address

Manfred Bijak, Ph.D.
Medical University Vienna
Vienna Medical School
Waehringer Guertel 18-20/4L
A-1090 Vienna, Austria

e-mail: manfred.bijak@meduniwien.ac.at

References

- [1] Bajd, T., Kralj, A., Turk, R., Benko, H., and Sega, J.: The use of a four-channel electrical stimulator as an ambulatory aid for paraplegic patients. Phys. Ther., Vol. 63, No.7, 1983, pp 1116-1120.
- [2] Marsolais, E. B. and Kobetic, R.: Functional electrical stimulation for walking in paraplegia. J. Bone Joint Surg. Am., Vol. 69, No.5, 1987, pp 728-733.
- [3] Holle, J., Frey, M., Gruber, H., Kern, H., Stohr, H., and Thoma, H.: Functional Electrostimulation of Paraplegics; Experimental Investigations and First Clinical Experience with an Implantable Stimulation Device. Orthopedics, Vol. 7, 1984, pp 1145-1155.
- [4] Yang, L., Granat, M. H., Paul, J. P., Condie, D. N., and Rowley, D. I.: Further development of hybrid functional electrical stimulation orthoses. Artif. Organs, Vol. 21, No.3, 1997, pp 183-187.
- [5] Kobetic, R., Marsolais, E. B., Triolo, R. J., Davy, D. T., Gaudio, R., and Tashman, S.: Development of a hybrid gait orthosis: a case report. J. Spinal Cord. Med., Vol. 26, No.3, 2003, pp 254-258.
- [6] Kobetic, R., Triolo, R. J., and Marsolais, E. B.: Muscle selection and walking performance of multichannel FES systems for ambulation in paraplegia. IEEE Trans. Rehabil. Eng, Vol. 5, No.1, 1997, pp 23-29.
- [7] Bijak, M., Hofer, C., Lanmuller, H., Mayr, W., Sauermann, S., Unger, E., and Kern, H.: Personal computer supported eight channel surface stimulator for paraplegic walking: first results. Artif. Organs, Vol. 23, No.5, 1999, pp 424-427.

Acknowledgements

This project is supported by Forschungsförderungsfonds, Vienna (FFF)

QUALITY AND SAFETY OF GAIT IN STROKE PATIENTS USING A DROPPED FOOT STIMULATOR.

J.Van Vaerenbergh^{1,2,3}, A. De Kegel¹, S. De Ruijter¹, S. Vandenberghe¹, Y. D'Hont¹, L.Briers²

Department of Physiotherapy, Arteveldehogeschool, Gent, Belgium.
 Centre for Movement Analysis and Therapy, Brussels, Belgium.
 Faculty of physical education and physiotherapy, Katholieke Universiteit Leuven, Belgium

Abstract

In this study a reduced spring like model of walking was used to demonstrate the effect of FES on the quality and safety of gait. The acceleration profile of the COF was considered as a good quality estimator of the spring system. FES optimized the spring properties in most of the participating patients but especially in those reporting a reduced fear of falling

Introduction

To understand and describe the functional benefit of FES, the use of a reduced model is advisable. The simplification helps to derive better applications to customize them to fit a particular stroke patient. If we reduce walking to wheel like propulsion, generated by a counterbalancing mechanism symbolically represented by a system of springs, the latter might be replaced by the muscle model of Hill [1] [2]. Hence force is generated by nonlinear components that depend on neural activation (Q), length (L) and its derivative (dL/dt). (Fig. 1)

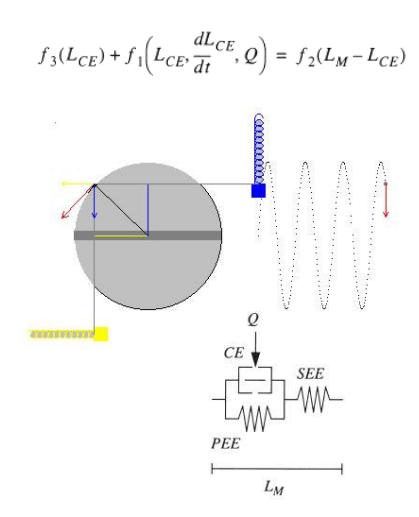


Fig. 1: walking represented as a reduced non linear model. CE (contractile element), SEE (series elastic element) and PEE (parallel elastic element)

The reduction model simulates a uniformly circular movement with a constant speed and responds to Newton's law. However in-shoe plantar pressure measurements recording ground reaction forces during walking at constant speed don't show a perfect sinusoidal behaviour as represented in fig.1. This is because the potential and kinetic energy curves generated during heel strike, foot flat and push off are generally out of phase and submovements. responsible for submovements are demonstrable in the centre of force trajectory (COF). The frequency spectrum of them can be revealed by harmonic or Fourier analysis, converting the signal from the time to frequency domain.[3] The most dominant frequency shows up as a large wave at a position along the horizontal axis corresponding to its frequency. Anv other frequencies harmonics) show up as smaller peaks at different positions according to their frequency. Fig.2 shows the existence of higher harmonics, responsible for the acceleration variations of the COF during the foot support phase.

Hemiparesis has far reaching consequences for the proposed model. In fact the Hill model is highly sensible for changes in muscle excitability and structural shortening. If FES is successful it will show a strong influence on the harmonics by improving the spring characteristics.

The following research will demonstrate that FES is perceived as comfortable and safe when this kind of optimisation takes place.

Material and Methods

The COF acceleration profile of the affected and non affected foot was investigated during walking in new FES users having a first stroke for at least six months and presenting with an obvious dropped foot. The Odstock one channel dropped foot stimulator was used to correct abnormal gait in 22 patients (mean age was 69 years).

The Fscan system (Tekscan Inc.) was used to record the COF trajectories. Ultra-thin flexible insole sensors were placed in the shoes of the subjects. Measurements were done during walking at a self-generated, comfortable speed and data with and without FES were compared. The acceleration of the COF trajectories in X and Y direction was obtained by a double derivative. These data were smoothed by a running average using 10 samples and low pass filtered with a 14 Hz 8 order Butterworth filter. Finally a Fourier

analysis was performed to calculate the power density spectrum. The 2.34, 4.69, 7.03 and 9.38 Hz frequency ranges were further studied. The respectively power in each frequency bandwidth was compared with and without the use of FES. A Student t-test for paired samples was used to compare means. Significance level was set at $p \le 0.05$

At the same time the 'go up and downstairs', 'walk around neighbourhood', 'housecleaning', and simple shopping items from the Falls Efficiency Scale were recorded one week before the gait study and after six weeks of FES use.[4] The Wilcoxon matched-pairs signed ranks test was used to compare these results.

Results

In all investigated stroke patients the unrolling of the affected and unaffected foot was clearly disturbed. This coincided with superimposed irregularities or submovements to the normal acceleration curve, a high power at the sound side and a very low power at the affected side in most frequencies.

FES reduced power (X en Y direction) in the non affected limb and increased the power in the affected limb. However the difference was only significant for the accelerations in X direction. (Fig. 3-4)

The average score on the Falls Efficiency Scale rose with 5.35 points ($p \le 0.001$) after six weeks of FES use.

Recalculating the power density spectrum statistics for those patients having an increase in the Falls Efficiency Scale higher than the average showed a strong influence on the acceleration characteristics especially in the Y direction. (Fig. 5)

Discussion

Stroke patients very often complain about an unsafe, low quality gait and fatigue during walking.[5] In many cases this is a consequence of an inefficient gait. In this study walking was simulated as wheel like propulsion, steered by counterbalancing mechanisms symbolically represented by springs driven by the Hill model.

The movement of the COF was the fingerprint of this spring system and Fourier analysis showed a superposition of several harmonics dealing with the specific spring capacities during heel strike, foot flat and push off. (fig 2)

According to the Hill model it is important to distinguish in stroke stiffness due to spasticity from that due to rheologic adaptations.

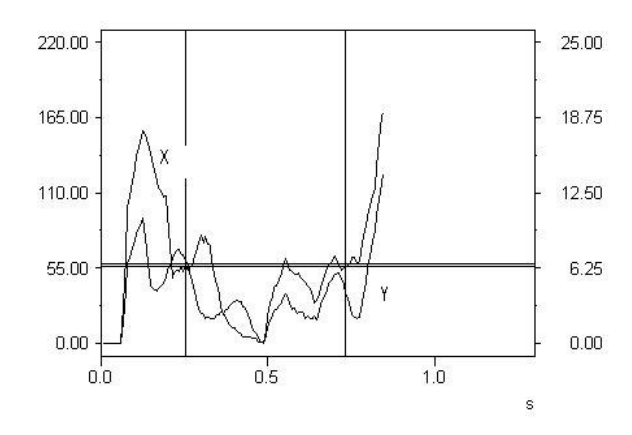


Fig. 2: COF X -Y acceleration profile of a stroke patient

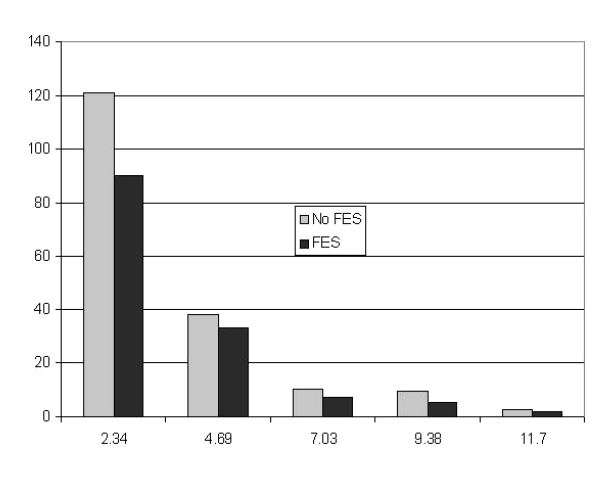


Fig. 3: Sound leg power spectrum for the X-COF accelerations. p=0.039 for 2.34 Hz and p=0.045 for 9.38 Hz

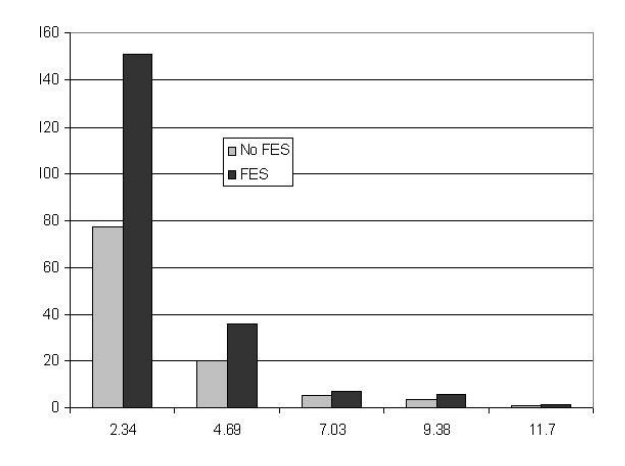


Fig. 4: Affected leg power spectrum for X-COF accelerations. p=0.049 for 2.34 Hz and p=0.02 for 4.69 Hz

The first is caused by disorganised reflexes, the latter by intrinsic changes in connective tissue arising from disuse secondary to hemiparesis.[6] This may be compounded by increased actinmyosin cross-bridge linkages, which are thought to

be associated with reduced rates of cross-bridge detachment.[7]

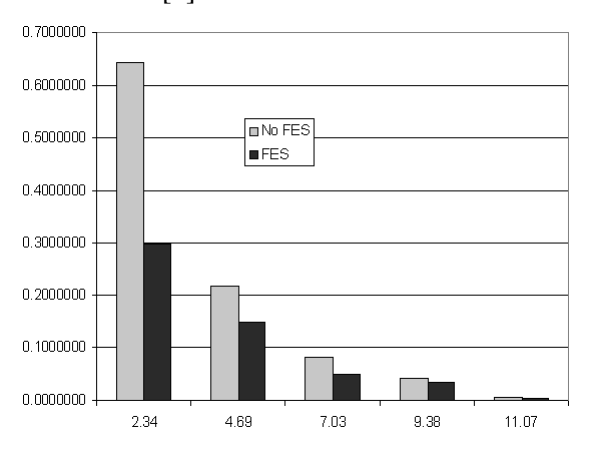


Fig. 5: Sound leg power spectrum for Y-COF accelerations. p=0.0001 for 2.34 Hz and p=0.05 for the higher frequencies.

Mirbagheri e.a [8] found a decreased reflex stiffness of 53% after FES assisted walking, and also intrinsic stiffness dropped by 45%. In contrast, both reflex and intrinsic stiffness increased in the non-FES control subjects. These findings suggest that FES-assisted walking has an important influence on the passive and active components of the muscle respectively represented by the SEE, PEE and CE elements in the Hill model. These findings are consistent with our study, which shows that FES for a dropped foot restores some feature of the spring mechanism. However our study only addressed temporary effects in chronic stroke.

Indeed the electrical induced contraction in the anterior Tibial Muscle of the affected limb is not only responsible for a better clearance during swing with an improved balance at the sound side, it also stretches the calf muscles during heel strike, which facilitates the storage of potential energy needed for the kinetic release during the powerful push off. This is visible in the normalisation of the 2nd harmonic in both affected and non affected limbs. At the same time, movement fragmentation is reduced which adheres the minimum jerk theory in control optimization.[9]

The fact that the acceleration scheme for the Y direction is only improved in patients who had the impression of an improved safety with the dropped foot stimulator makes us believe that in some cases FES is fighting against some remaining or altered spring properties. This is perceived by the patient as a less comfortable way of walking even when visual inspection of their gait gives the impression of an overall improvement. It is even not excluded that in those patients safety is on its turn compromised.

There is also the possibility that FES was not optimally tuned for each patient. If this is true, our approach will be an attractive method to guide this process. However the need for normative data is requested. In an unpublished study we found a positive relationship between power and speed in the 2.34 Hz frequency range.(fig.6) The increased walking speed seen in FES users can explain partly our observations, but seemingly it looks more complicated than that.

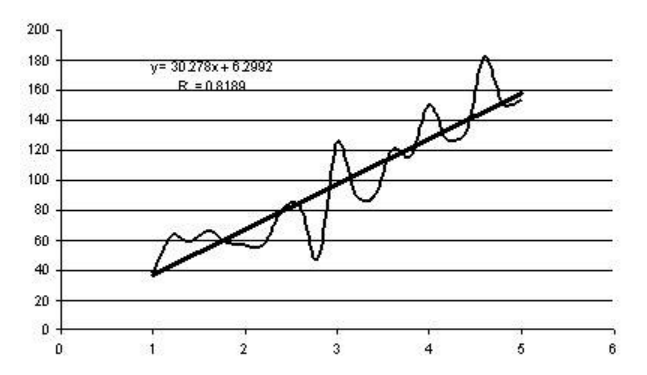


Fig. 6: Relationship between walking speed and power in 2.34 Hz frequency range

If we interpret the mean power values of our investigated stroke patients in accordance to the normal curve, we should expect a speed of 4 km/h for them, which is of course completely absurd. In the most case it was only between 1 and 2 km/h. With FES the speed increases but the power decreases in the sound limb. This might suggest an regained optimised relation between speed and energy input.

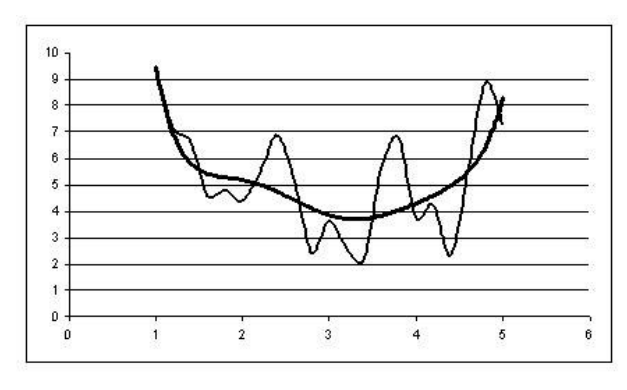


Fig. 7: Relationship between the power in the higher frequencies (>7.03Hz) and walking speed.

The higher frequencies, which are the indicators for the number of submovements don't show this linear relation between speed and power; but argue for the existence of a advantageous speed, with an optimal signal/noise ratio.(fig.7)

Under those circumstances FES can bring patients to a better signal/noise ratio by increasing speed. This optimization could be the prime factor for an improved feeling of safety.

However these interpretations should be treated very cautiously and further research is necessary. Also more clarifications explaining which factors are exactly influenced in the Hill equation by the dropped foot stimulator in stroke are needed.

References

- [1] Winters JM. Hill-based muscle models: a systems engineering perspective, In: Multiple Muscle Systems Biomechanics and Movement Organization, eds.Winters JM and S. L. Y. Woo, pp. 69-73, Springer-Verlag, New York, 1990.
- [2] Zajac FE. Muscle and tendon: properties, models, scaling and application to biomechanics and motor control. Crit Rev Biomed Eng 1989;17:359-411.
- [3] Alexander RM, Jayes AS. Fourier analysis of forces exerted in walking and running. J Biomech 1980;13:383-390
- [4] Hellstrom K, Lindmark B. Fear of falling in patients with stroke: a reliability study. Clin Rehabil 1999;13(6):509-17
- [5] Taylor PN, Burridge JH, Dunkerley AL, Wood DE, Norton JA, Singleton C et al. Clinical use of the Odstock dropped foot stimulator: its effect on the speed and effort of walking. Arch Phys Med Rehabil 1999;80(12):1577-83.
- [6] Mayer NH. Clinicophysiologic concepts of spasticity and motor dysfunction in adults with an upper motoneuron lesion. Muscle Nerve Suppl 1997;6:S1-13
- [7] Friden J, Lieber RL. Spastic muscle cells are shorter and stiffer than normal cells. Muscle Nerve 2003;27:131-132
- [8] Mirbagheri MM, Ladouceur M, Berbeau H, Kearney RE. The effect of long-term FESassisted walking on intrinsic and reflex dynamic stiffness in spastic spinal-cord-injured subjects. IEEE Trans Neural Syst Rehabil Eng. 2002;10:280-289
- [9] Hogan N. The mechanics of multi-joint posture and movement control. Biol.Cybern 1985;52:315-231

Acknowledgements

This study is financially supported by the Compahs research foundation— Gent, Belgium and the CMAT-Brussels, Belgium

Author's Address

Drs. Jo Van Vaerenbergh Center for movement analysis and therapy R.Reniersstraat 11 B-1090 Brussels

E-mail: jo.vanvaerenbergh@cmat.be

STUDYING GAIT PATTERN WHEN EMULATING MUSCLE CONTRACTURE

Andrej Olenšek*, Zlatko Matjačić*, Tadej Bajd**

* Institute for Rehabilitation, Republic of Slovenia ** Faculty of Electrical Engineering, University of Ljubljana

Abstract

In pathological gait it is very important to correctly identify primary gait anomalies originating from damage to the central nervous system and not mistaken them for compensatory changes of gait pattern. For that purpose a mechanical system consisting of specially sewed trousers, special shoes arrangement and elastic ropes attached to the designated locations on the trousers was designed that allows repeatable emulation of muscle contractures of soleus (SOL) gastrocnemius (GAS)muscles. neurologically and orthopaedically intact subjects instrumentally participated insupported kinesiological evaluation. Results show that subjects developed compensatory mechanisms according to the type of artificially imposed muscle contracture

Introduction

Often in clinical studies and praxis we meet cases where damage to the central nervous system manifests in gait anomalies, leading to less efficient gait compared to normal gait. Patient's abilities to properly exert synchronised muscle activation for energy optimal gait are disturbed resulting in greater energy dissipation and efforts required for preservation the body in the upright position. It is a challenging task to establish appropriate diagnosis. Namely it is necessary to identify primary anomalies, which are directly attributable to the damage to the central nervous system or musculoskeletal system and not mistaken them for secondary anomalies, which the individual develops to compensate for unwanted effects arising from primary anomalies. For this purpose instrumented kinesiological assessment and analysis of joint kinematics, kinetics and muscle dynamic EMG signals are indispensable

Very common example of pathological gait represents toe-walking. It is most frequently present in cerebral palsied children and is a result of either prolonged and premature ankle plantarflexors activity, plantarflexor spasticity and/or plantarflexor contractures leading also to bone and soft tissue deformities. Recently two studies investigated the kinematic, kinetic and

EMG characteristics of toe-walking [2.3]. Participants in both studies were able-bodied subject who were asked to induce toe-walking by self-restricting their walking. Comparing heal-toe walking and toe-walking Kerrigan et. al. [2] reported of significant reduction in the peak ankle plantarflexor torque and power generation during terminal stance and preswing, whereas in loading response, the moments of the ankle dorsiflexor and knee extensors were absent. Furthermore, during toe-walking Perry et. al. [3] also recorded greater plantarflexion during stance, higher peak and mean plantarflexor moments during loading response and midstance, lower mean plantarflexor moments during terminal stance and lower peak extensor moment in midstance. However it seems that the methodology of inducing toe-walking by asking subjects to self-restrict their walking can not pathological adequately approximate biomechanical conditions where the equinus is induced due to plantarflexor spasticity or contractures. Furthermore, since plantarflexors are constituted by a monoarticular soleus muscle as well as by a biarticular gastrocnemius muscle we can assume that spasticity or contracture of each muscle may have different biomechanical effects on resulting gait pattern in the joints of both lower extremities. Therefore, we need a more refined methodology, which will enable more detailed study into toe-walking gait patterns.

In this paper we present novel mechanical system, which is designed to ensure well-controlled conditions for repeatable emulation of artificially induced toe-walking gait in neurologically intact subjects. The system enables emulation of soleus muscle contracture, gastrocnemius muscle contracture or combination of both muscles contractures. We further present a study on the effects of emulated muscle contractures on gait patterns of six neurologically intact individuals.

Materials and Methods

Contracture emulation system

Fig. 1 shows schematic drawing of the proposed system consisting of specially sewed trousers, special shoes arrangements and elastic ropes attached at the proximal end to the designated locations on the trousers and at the distal end to the

fixation frame at the heels of shoe. Trousers are made of durable material able to withstand mechanical loading due to stretching of the elastic ropes. To prevent trousers from moving vertically during walking four leather patches are longitudinally and transversally sewed to the inner side of left and right trouser legs.

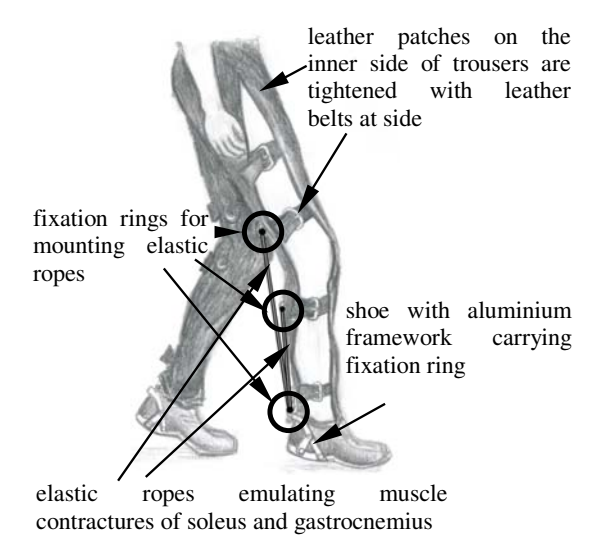


Fig 1: schematics of a subject during walking with emulation of SOL and GAS muscle contracture. The system consists of specially designed trousers and shoes and elastic ropes, representing emulated muscle contractures.

Additionally, fastening four leather belts on each leather patch keeps the whole arrangement firmly embraced to the thigh and shank of the lower extremity. Trouser legs on outer sides up to the pelvis level remain unstitched, providing enough space for fastening the belts and at the same time leaving hip, knee and ankle joint uncovered and freely movable. Iron fixating rings are mounted directly on trousers and leather patches at the approximate positions where particular muscles are attached to the bone. Iron nuts, tightening fixating rings on both sides of leather patches, were covered with soft leather tissue ensuring soft skin contact and firm attaching points for elastic ropes. Located beneath and posterior and above and posterior to the knee joint axis first and second fixating rings correspond to proximal ends of SOL and GAS muscles respectively. Distal ends of both muscles are attached to the heel arrangement of the shoe proximal to the ankle joint axis on the third and final fixating ring. Two aluminium bars are bent in the shape of shoe and mounted on shoes with iron screws and nuts trough shoes heels. Carrying the third fixating ring the first bar is on both sides of the shoe supported by the second bar, together forming triangles and thus preventing the frame from moving. Muscle contracture is emulated with one or more elastic ropes connected in parallel. When choosing appropriate length and stiffness of elastic ropes we had to prevent elastic rope to exceed it's elastic limits, which would induce unwanted perturbation in walking. Decision which elastic rope is appropriate to satisfy this condition and at the same time induce well-controlled changes in gait pattern was reached according to the trial and error tests.

Participants

Six subjects of similar age, height and mass (mean age \pm standard deviation, 22.5 \pm 1.87 y; mean height, 175.0 \pm 4.2 cm; mean mass, 64.2 \pm 4.2 kg) participated in this study. Subjects were free from any muscoloskeletal or neurological impairments that would affect their gait.

Experimental conditions

Providing good possibilities to emulate several constraining conditions the study was limited to emulation of muscle contractures of soleus and gastrocnemius individually (in text referred as SOL or GAS muscle contracture) or in combination (in text referred as SOL-GAS muscle contracture) each time using two elastic ropes emulating muscle contractures. Recordings when subjects were equipped with proposed system but with no elastic ropes attached (referred as normal gait) were taken for comparison. We used VICON motion analysis system consisting of six 50 Hz cameras with infrared strobes for capturing threedimensional motion of lower extremity and pelvis and two AMTI force platforms for recording ground reaction forces. By means of VICON Clinical Manager we calculated ankle, knee and hip joint angles, moments and powers for the movement in the sagittal plane. Participants were instructed to walk at average walking speed of approximately 1 m/s. Using a time watch trials were excluded from further analysis if the time taking the subject to overcome the distance of seven meters differed for more than one half of a second from the expected time of seven seconds. In each experimental condition i.e. type of emulated muscle contracture at least four clear steps with the left leg (equipped with elastic ropes in the second experimental condition) were recorded and averaged in each sample of gait cycle.

Data analysis

Resulting gait pattern recordings for six participants were included in the further statistical

analysis. Comparing particular type of artificially induced pathological gait to subject's normal gait differences in joint moments were examined. Focusing on the differences in ankle and knee peak and average moment values in midstance (10-30% of GC) and terminal stance (30-55% of GC) we performed one-tailed t-test pair-wise comparison between particular experimental conditions. The level of statistical significance was set to p < 0.05.

Results

Figure 2 shows representative recordings of a gait pattern measured in one of the subjects. Each graph shows trajectories measured under all four experimental conditions. There is a selected considerable difference between the resulting kinematic and kinetic patterns. Artificial constraint imposed by elastic ropes emulating SOL and SOLGAS muscle contracture forces ankle in excessive plantarflexion throughout gait cycle whereas in case of GAS muscle contracture the difference is not so explicit. Likewise the knee was flexed throughout stance phase and the range of motion in hip decreased, which resulted in shortened step as opposed to normal walking. Noticeable differences are present also in joint moment patterns Characteristic two-teeth profile occurs in the ankle when SOLGAS muscle contracture present opposed to not so extensive ankle plantarflexor moment increase in other two cases. Furthermore opposite effect on knee extensor moment could be noticed

comparing SOL and GAS muscle contracture. Whereas in SOL muscle contracture reduction of knee extensor moment in midstance was recorded in GAS muscle contracture knee extensor moment markedly increased in terminal stance. In most constrained situation of SOL-GAS contracture characteristic behaviour of both cases is summarised, namely midstance is characterised with knee extensor moment reduction whereas terminal stance with knee extensor moment increase. The power trajectories characteristic power absorption pattern in the ankle in the early stance phase accompanied by decrease of power absorption at the knee. During push-off there is increased power absorption in the knee joint. Power generation in the hip joint in the early stance phase is somewhat increased.

Statistical analysis including results of all six subjects results supported these findings (figure 3). Regardless of type of muscle contracture greater peak and mean ankle plantarflexor moment was recorded in midstance compared to normal gait at the same time indicating statistical significant difference between SOL and GAS muscle contracture and SOLGAS muscle contracture whereas in terminal stance differences are less evident. In knee joint the differences are less evident in midstance and more explicit in terminal stance when compared to normal walking, as results show considerable greater peak and average knee extensor moment.

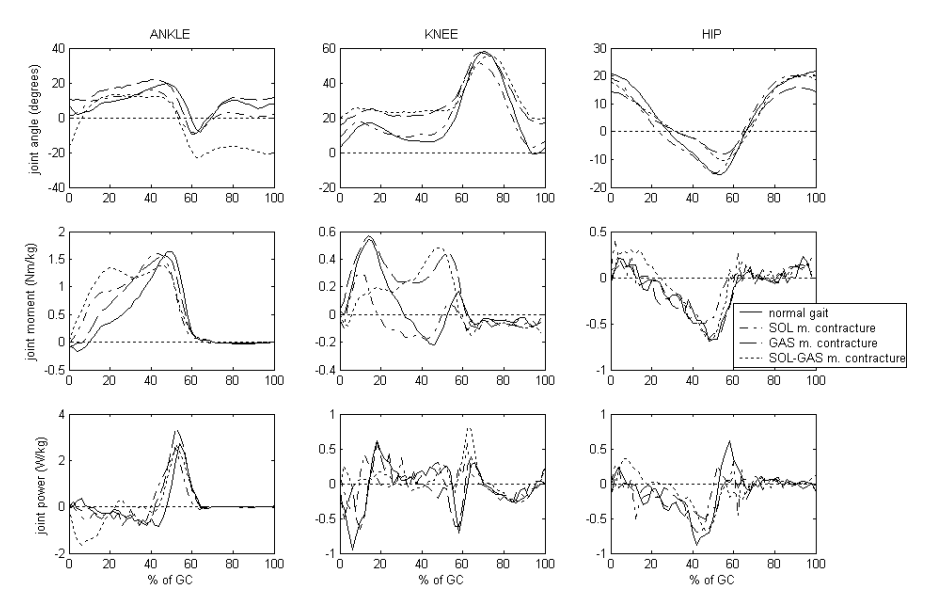


Fig 2. representative gait patterns of subject's left leg when normally walking and when emulating SOL and GAS muscle contractures separately and in combination on the left leg

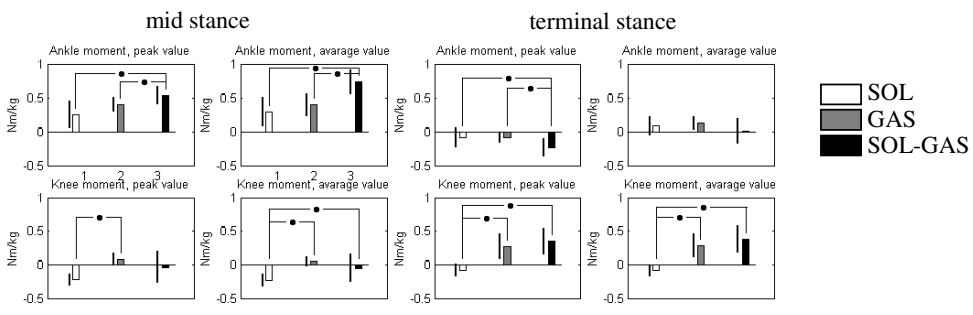


Fig. 3: For left leg comparing ankle and knee peak and average moment deviations from normal gait between different experimental conditions

Discussion

We have developed a mechanical system, which enables well-controlled imitation of SOL and GAS muscle contractures in neurologically and orthopaedically intact subject. The created biomechanical conditions are good approximation for spastic or contracted muscle. By varying the stiffness of the elastic ropes and also by utilizing various combinations of plantarflexor muscles contractures we are in position to investigate the role of each pathological combination in controlled conditions. Since the primary cause of altered gait pattern is known we can identify secondary, compensatory changes.

The main goal of this paper was to study the resulting gait patterns of emulated toe-walking, and compare our results with those of Kerrigan and Perry [2,3]. There are substantial similarities between the results for the ankle joint. The ankle is in pronounced plantarflexion, the ankle moment has characteristic double tooth shape and the power absorption in the ankle at the initial contact is evident. For the knee joint the results presented in fig. 2 and 3 are in agreement with [2,3] for the SOL condition and in for the GAS and SOL-GAS restraining conditions where knee joint is in marked flexion throughout stance and the knee extensor moment is substantially higher throughout the stance phase. The behaviour in the hip joint is similar to the one reported in Kerrigan. The differences observed in the knee joint indicate that there exist several toe-walking kinematic and kinetic patterns that must depend on degree of each plantarflexor muscle pathological Furthermore results in figure 3 support these findings and additionally emphasize that the differences in ankle and knee moment values show significant differences between particular restraining conditions.

The single disadvantage of the developed system is that the subjects needs to be of similar height and weight due to the size of trousers and shoes. Also a subject with substantially greater power generation capacity could overwhelm the strength of elastic ropes, therefore a direct comparison

between the subjects would not be possible. For these reasons subjects of similar height, weight and physical condition needs to be chosen to participate in the experiments, making the results between subjects directly comparable.

The developed system in its present form can be used only for emulation of SOL and GAS contractures, however, it can easily be expanded to allow emulation of contractures of other muscles of lower extremity. by mounting mechanical rings at the appropriate anatomical sites on the leather patches of the trousers. A variety of combinations can be studied and compared to gait patterns recorded with a single muscle contracture emulation.

References

[1] HANSON C. J., and JONES L. J.: Gait abnormalities and inhibitive casts in cerebral palsy. J. Am. Podiatr. Med. Assoc., 79, 1989, 53-59

[2] KERRIGAN D. C., OILEY P. O., ROGAN S., and BURKE D. T.: Compensatory advantages of toe walking. Arch. Phys. Med. Rehabil., 81, 2000, 38-44

[3] PERRY, J., BURNFIELD, J. M., GRONGLEY, J. K. and MULROY, S. J.: Toe walking: muscular demands at the ankle and knee. Arch. Phys. Med. Rehabil., 84, 2003, 7-16

Author's address

Andrej Olenšek Institute for rehabilitation, Republic of Slovenia Linhartova 51, SI-1000 Ljubljana Slovenia e-mail:andrej.olensek@mail.ir-rs.si

FUNCTIONAL ELECTRICAL STIMULATION PROPELLED CYCLING OF PARAPLEGICS-AN OCCUPATIONAL PHYSIOLOGICAL APPROACH

J. Szecsi*, S. Krafczyk*, A. Straube*, J. Quintern*

* Dept. of Neurology, Ludwig Maximillians University Munich, Germany

Abstract

Cardiovascular adaptation processes can be induced by FES-ergometer training, and useful distances can be covered during FES-cycling. However, this is only possible, if a minimum amount of mechanical output power is generated. As a rule this cannot be achieved in the case of untrained patients due to a number of causes. This study concentrated on the work physiological aspect of FES-cycling, which although often overlooked is very important from the viewpoint of the paraplegic's limited endurance. power and *Isometrical* measurements were made in seven completely untrained and one exceptionally strong patient. Subsequently the patients performed cycling exercises, and the drag torques and the cadences were recorded. *Graphic* representation of the cadence/muscle stress values unrevealed a work physiological interpretation of the individual cycling capability and the effort of the paraplegic patient in a particular cycling situation.

This approach shows that the excessive fatigue observed in paraplegic cyclists is due to the fact that they work in the fatigue mode rather than the steady-state mode. The analysis shows that training under load can improve the performance of the SCI-cyclist so that he/she is able to work in the steady-state region.

Introduction

A minimum of generated mechanical output power and endurance are the prerequisites for the onset of the cardiovascular adaptation processes that FES-ergometer training induces as well as for useful distances to be covered during FES-cycling. As a rule this cannot be achieved in the case of untrained patients.

Cycling causes dynamic contractions that periodically hinder the passage of blood,

partially or totally. Local fatigue is of extreme importance in FES cycling. To avoid it, the load and rate of contraction have to be adjusted to the actual muscle strength. Our aim was to propose a measure for the individual effort of the paraplegic patient in terms of load and contraction rate

Material and Methods

Eight completely paraplegic patients participated in the study. While seven had had no previous training (No. 1-7 = the "weak" group), one (No. 8, the "strong" patient) was exceptionally well trained (able to cycle more than 10 km). To reach such a condition, patient No. 8 had stimulated the quadricep muscles for years on an average of 6 hours daily (!), under high intensity and load. The "weak" group included 5 men and 2 women (mean age of 30.7 ± 5 years) who had lesions at levels Th 4 - 12. Patient 8, a 33-year-old woman, had been paralyzed by an accident 15 years previously and had a lesion at level Th 6. First, the individual isometrical torque profiles of the six stimulated muscle groups (quadriceps, gluteus, hamstrings) were determined for all patients with a six-component sensor (ATI, Garner, USA).

The cycling situations of the patients are characterized by the two values, cadence and muscle stress.

The muscle stress k is computed by means of the formula k = Load/Drive, whereas Load is provided essentially by the drag torque and the crank revolution speed and Drive is the averaged isometrical torque [2].

Indoor cycling exercises on the ergometer (Motomed Viva 1, Reck GmbH, Betzenweiller, Germany) were used to find cycling situations that could be continued for at least 20 minutes without reducing the

cadence by more than 10 rpm (no local fatigue) by constant resistive torque. These situations occurred on the border between steady-state and the fatigue regions. The patients performed on average 6±3 ergometer trials.

In subsequent outdoor cycling exercises (OVG tricycle, Munich, Germany) the cadence and the drag-torque of each of the patients were recorded. The patients freely chose their cycling situations. There were performed on average 15±5 cycling sessions pro patient.

A graphical representation of the cycling situations of the patients allowed the definition of the individual borderline of the paraplegic separating the steady-state region from the fatigue region by means of the least squares method on the basis of border points obtained in the ergometer trials (Fig.1).

The region delimited by the normalized power, given by $k \times \omega$ (muscle stress times rotation speed of crank), is the area where cycling of the individual patient on the particular OVG tricycle has to take place. We introduced the distance between the normalized power curve and the steady state region as *cycling capability* of the individual patient with respect to the particular available tricycle.

The distance of the cycling situation from the steady state region was called the *individual effort*. We assume that the individual effort and the cycling capability correlate negatively with the patients endurance or the covered distance.

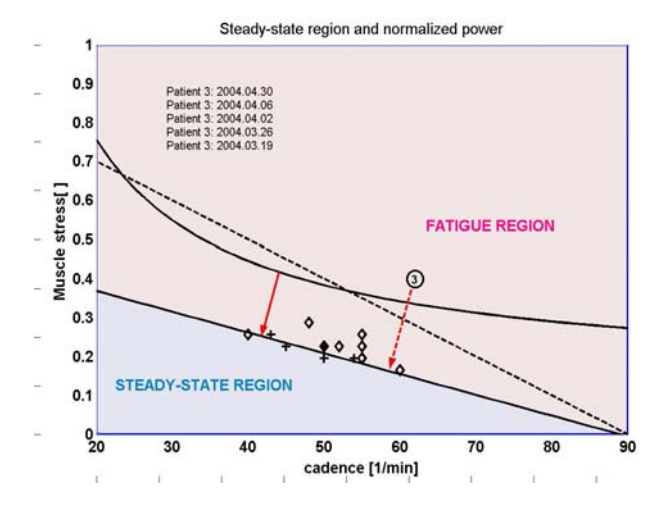
Results

Construction of the borderline in the case of the individual paraplegic patient

We defined for each of the eight paraplegic patients individually the borderline delimiting the steady-state and fatigue regions by the method illustrated by Fig.1. It could be established that the "paraplegic" borderline varies in steepness and position with respect to the "normal" borderline, nevertheless it is always shifted to the south of the graphic.

The borderline for healthy persons was taken from the literature [1]. The individual effort (in this case -0.25 1/min) is always greater than

the driving capability (in this case -0.17 1/min).



Exemplification of the Fig.1 borderline construction in case of patient 3. The diamonds represent ergometer exercise tests holding at least 4 minutes their revolution speed but loosing it eventually later. The crosses show steady-state ergometer tests performed at constant revolution speed during at least 20 minutes. Solid straight line: "paraplegic" boderline, dashed line: "normal" borderline, solid curve: normalized power. The outdoor cycling situation is represented by the encircled figure 3. The arrows represent the individual effort in the case of the cycling situation (dashed) and the cycling capability of the patient (solid).

Strong vs. weak patients

The relative position of the borderline and power curves describes the FES-cycling capability of the patients. In Fig. 2 we depicted the averaged cycling situations of the "weak" patient 1, the "very strong" patient 8 and the "strong" patient 2.

We observe that the strong (the strongest of the "weak" group) patient 2 has an intersection of his curves and the extraordinary strong patient shows an extremely large intersection area. The curves of the weak patient 1 have no intersection.

We realize that borderline and normalized power represent the two facets of the conditional properties of the patient: force (power) and endurance (borderline). In consequence force and endurance exercise have to influence these curves.

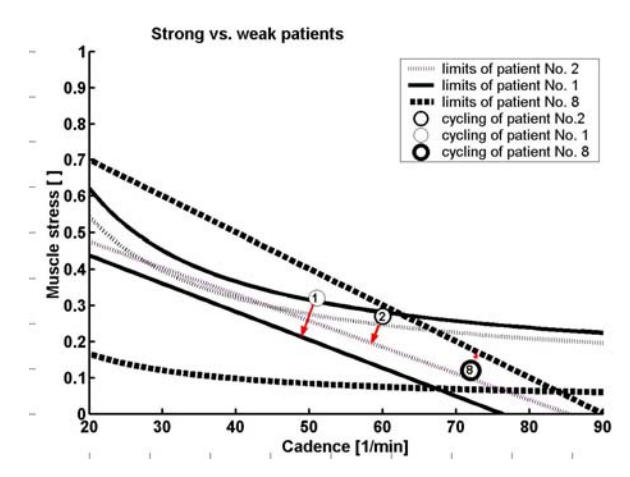


Fig.2. Cycling situations of patients 2,1 and 8 (circles) together with their borderlines and normalized power curves. Arrows represent the individual efforts of the respective cycling situations.

Individual effort, cycling capability and covered distance

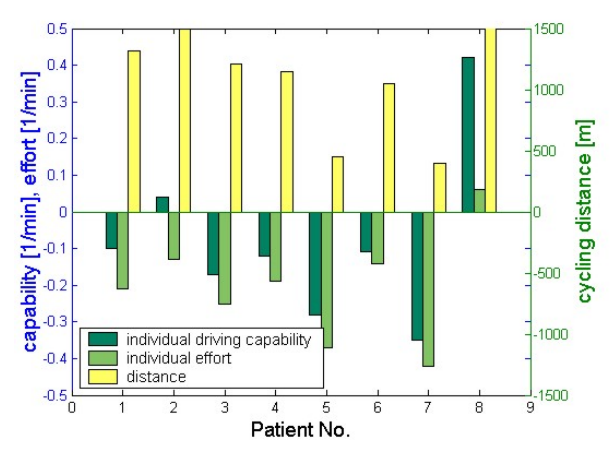


Fig. 3 The relationship between individual effort and driving capability on the one hand and covered distances on the other hand. The distance in the case of patient 8 is actually above 10 km!

Fig.3 shows that only patient 8 cycles with a positive individual effort, i.e. in the steady-state region. The calculated correlation coefficients are 0.92 (distance/effort) and 0.79 (distance/capability).

Discussion and conclusion

The work physiological approach revealed that the excessive fatigue observed in the untrained paraplegic cyclist can be attributed to the fact that he or she works in the fatigue mode rather than in the steady-state mode. Training performed under load can bring the performance of the SCI cyclist into the region of steady-state work.

Based on isometrical measurements and ergometer tests, the method of individual effort provides a performance measure for the control of the training progress of the paraplegic cyclist. Further it provides a tool for the cycling distance in the modelling of paraplegic cycling.

6 References

- Astrand P O, Rodahl K (1989)
 Textbook of Work Physiology,
 McGraw-Hill Book Company
- Szecsi J, Fiegel M, Krause Ph,
 Quintern J (2004) Individual adaptation
 of functional electrical stimulation of
 paraplegics in different cycling tasks.
 Tech. Health Care, Vol. 12, No. 2, pp

 89-93.

Acknowledgements

This work was supported by the Deutsche Forschungsgemeinschaft für Sonderforschungsbereiche (Grant SFB 462).

Author's Address

Dipl. Ing. Johann Szecsi, MD Department of Neurology University of Munich D-81377 Munich, Marchioninistr. 23 e-mail: jszecsi@nefo.med.uni-muenchen.de

METHODS FOR DYNAMIC BALANCE TRAINING DURING STANDING AND STEPPING

Zlatko Matjačić, Špela Rusjan, Irena Stanonik, Nika Goljar, Andrej Olenšek

Institute for Rehabilitation, Republic of Slovenia

Abstract

Regaining of walking ability is one of the main goals of rehabilitation following stroke. An important aspect of bipedal locomotion is efficient balancing of the trunk. In this paper we present novel methodology for dynamic balance training during standing and stepping in commercially available mechanical balance training device. A case study involving a single subject with chronic hemiparesis investigated effects of proposed dynamic balance training that lasted for two-weeks with two half an hour per dav. training sessions Instrumented kineziological evaluation of subject's gait indicated important improvement in subject's postural control during walking.

Introduction

One ofthe major consequences cerebrovascular insult is the impaired walking ability [1]. Various neurotherapeutic techniques and methods combined with strength training is traditionally used in rehabilitation. In the last couple of years a philosophy of task-oriented therapy has been proposed as a result of recent findings from basic research studies on reorganization of impaired brain subjected to a repetitive and intense practice of various functional movements [2]. Several techniques, such as partial body weight supported (BWS) treadmill and overground walking, functional electrical stimulation supported gait training and development of robotized gait trainers were developed and evaluated [1]. Common denominator of all listed techniques is that they assist in obtaining repetitive cyclical activity of both lower extremities in very early stages post stroke, thus allowing rehabilitation of also in nonambulatory subjects. walking Simultaneously trainees use upper extremities holding onto firm support of i.e. parallel bars to control equilibrium of the trunk and to provide assistive forces required for generation of propulsive forces. Bipedal walking requires harmonization of three basic gait components: cyclical movement of lower extremities, generation of propulsive forces and maintaining balance and upright posture of the upper body consisting from the pelvis, trunk, head and arms,

which represent approximately two thirds of the total body mass. As the above mentioned gait training techniques address fully only the first component, partially the second component and not at all the third component, because of the use of upper extremities, we can question whether any of the existing methods optimally exploits the residual capacity of damaged brain to re-learn the skills necessary for independent, bipedal walking. It seems that at this stage of development a training modality, focusing on improving the control mechanisms to maintain balance of the trunk without using the upper extremities, which would complement the existing techniques for training of the cyclical activity of both lower extremities, is missing. In the recent years we have developed mechanical apparatus and methodology, which enables neurologically impaired population fallsafe balance training during standing while having feet positioned in parallel or tandem stance [3]. The device enables also balance training while practicing different components of walking such as accomplishing the whole step where the sequence of push-off, swing and weight acceptance of one extremity and complementary stance phase weight bearing activity of the other extremity is repetitively executed. While performing these maneuvers the trunk needs to be maintained erect. which should facilitate re-organization of the postural control system. In this paper we report on dynamic balance training of various gait components during standing in mechanical balance training device [3] and it's evaluation in a case study.

Materials and methods

Device

Dynamic balance training program is based on previously developed mechanical apparatus [3], which is commercially available as Balance Trainer (medica Medizintechnik GmbH, Hochdorf, Germany). Balance Trainer looks very much like an ordinary standing frame. It consists from two parallel bars that are connected to a base plate via a two degrees of freedom mechanical joint. This joint consists from two helical springs positioned within two steel cylinders. Another cylinder made of durable plastic material slides between the inner walls of the steel cylinder and the outer walls of the

spring. By changing the vertical position of the plastic cylinder we also change the active length of the spring, thereby changing also the effective length and stiffness of the whole joint. One end of the helical spring is firmly mounted on the base plate while the other connects to the vertical bar. Knee support bar and the pelvis support table are connected to both parallel bars via simple hinge joints. By the way of described mechanical joints the device allows for physiological movement of a standing person while standing as well as performing a single step. The device is also equipped with a simple mechanical locking system that enables locking of both parallel bars into vertical position. In this way the device becomes an ordinary standing frame.

Training procedures

An overview of the derived balance training procedures is encapsulated in nine photographs as shown in Figure 1. All photographs show a neurologically intact subject while performing various tasks during standing on Balance Trainer and a physiotherapist guiding, correcting and facilitating movement and proper posture of the trunk. Fig. 1a shows a parallel stance, which is an initial and final posture for all training tasks. Fig. 1b shows inclination of the subject to the right while therapists monitors the posture of the trunk. In a similar manner the subject can incline also to the left, forward and backward. Thus, the device enables circular movement of pelvis in the transversal plane. Described movement of lower extremities can be complemented with associated movement of upper extremities as shown in Fig. 1c and 1d. Fig. 1e and 1f show training of a functional activity during parallel stance. In all six described exercises the knee pellots were adjusted equally for both extremities. They can be displaced to control the degree of allowable knee flexion, which is useful for avoiding excessive knee hyperextension that is common in chronic hemiparesis. However, the knee pellots can also be positioned in such a way to allow for a tandem stance of both extremities, thereby creating a posture which is similar to a double stance during walking. Similar exercises as shown in Figs. 1a – 1f can be exercised as well in tandem stance, which facilitates weight shifting activities. The last three photographs show a situation where the knee pellot bar is completely removed, which allows a standing subject to practice the whole step. Fig. 1g shows a push-off of the left lower extremity and gradual weight acceptance of the right extremity. Pelvis and the trunk are held in

the upright posture. In Fig. 1h the left lower extremity proceeds into a swing phase, while the right lower extremity fully supports the body weight. Hip abductors and extensors control the posture of pelvis and trunk in the frontal and sagittal planes, respectively. Fig. 1i shows the conclusion of the step with beginning of the weight acceptance of the left leg. The training procedures as outlined in the Fig. 1 can be exercised with an adjustable level of mechanical support, originating from the action of adjustable stiffness action of both two degrees of freedom mechanical joints. The judgment on the needed level of mechanical support for each individual patient resides on a physiotherapist.

Case description

Participant that was selected for a case study evaluation was a 57 years old man who had a stroke resulting in a right-sided chronic hemiparesis 14 months before participating in the study. The level of mechanical support was minimal as the subject could stand and walk independently, however his balancing abilities were impaired. Therapeutical program lasted for 10 days with two days break during the weekend of intensive practice. The duration of one session was approximately half of an hour, with two sessions per day. Kinesiological gait analysis was carried out before initiation of therapeutic intervention, at the end of two-week training period and at follow-up, three weeks after the closure of treatment. We used VICON 370 (Oxford Metrics Ltd, Oxford, UK) threedimensional motion capturing and analysis system consisting of six 50 Hz cameras with infrared strobes and two force platforms AMTI OR6-5-1000 (Advanced Mechanical Technology Watertown, MA). The participant, who was barefooted, was instructed to walk with self-paced velocity. At least six steps per leg were recorded for each measurement session and at least three steps per measurement per each leg were suitable for further analysis. Clinical Manager software, supplied by the same producer, was used for calculation of hip flexion/extension moment of force, which is prime vehicle for postural control of trunk in the sagittal plane[4]. We also performed a spectral power density analysis of hip moments of force in order to explore the underlying balance control aspects of walking. Participant's gait was also evaluated by means of clinical assessment tools: Functional Ambulation Category, 10-m walk and 9-minutes walk. These assessments performed only before and therapeutical intervention.

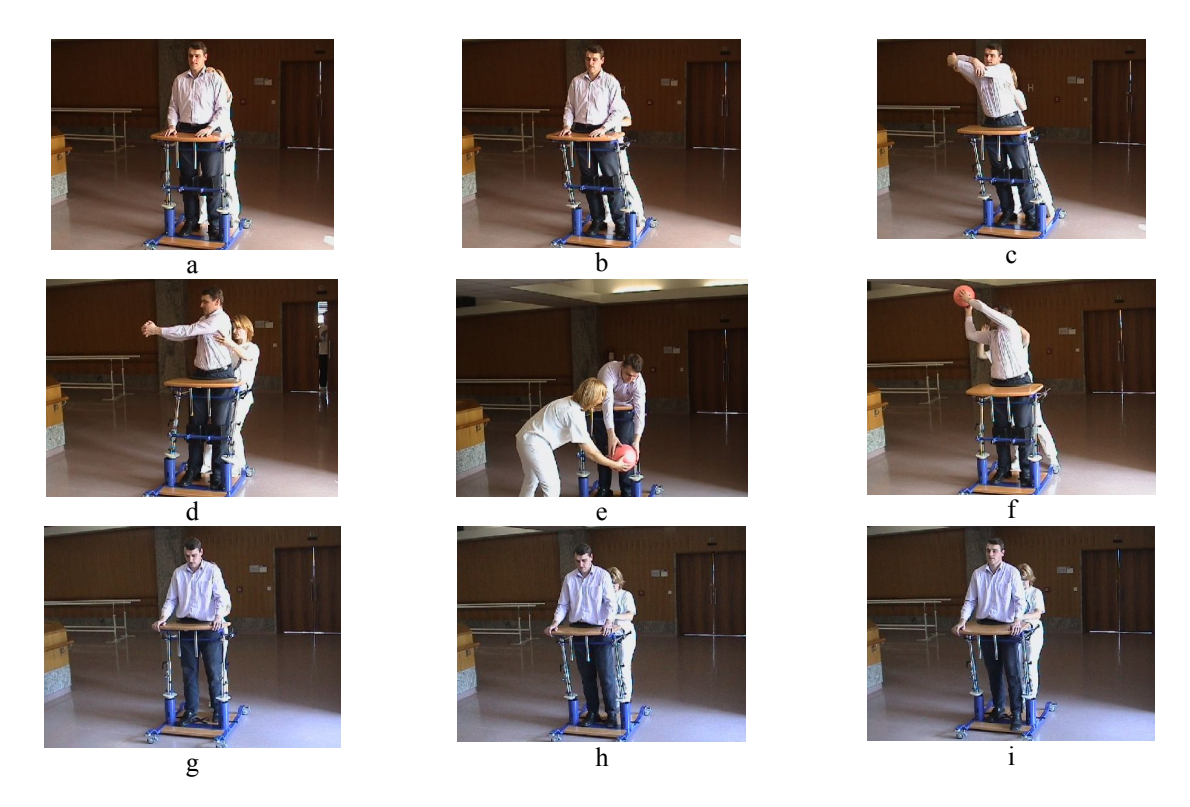


Figure 1. Elements of dynamic balance training during standing and executing a step as demonstrated in a neurologically intact person.

Results

Figure 2 shows hip joint flexion/extension moments for the impaired right extremity for all three measurements. The hip flexion/extension assessed before therapeutical moment as intervention is similar to the one observed in normal gait for almost whole gait cycle with important exception in the first 10% of the gait cycle. We can notice a rapid rise of hip extension moment, which in the very short time rapidly falls and then again rises. If we compare the hip flexion/extension moment as assessed in the measurement sessions after the therapeutic intervention and at follow-up, no such behavior can be observed. Figure 3 shows power density spectra for hip flexion/extension moments of the right extremity for all three measurements in the frequency range from 2.5 Hz up to 20 Hz. Comparing the mean values at different discrete frequencies and between the three measurement sessions we can see the reduction of amplitude ranging from 100% and up to 500% after the end of therapy and at follow-up. FAC score before and after therapeutic intervention was 5. Before therapeutic intervention the results for 10-m walk was 8 seconds and for 9-minutes walk 585 meters. After therapeutic intervention these values were 8 seconds and 600 meters.

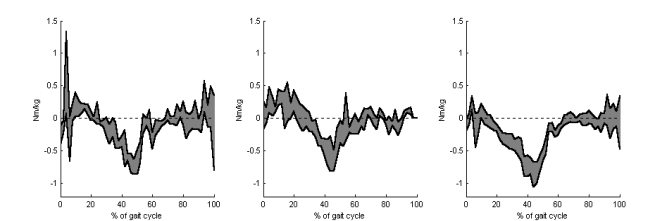


Figure 2. Flexion/extension hip moment in the impaired right extremity shown within the boundaries of one standard deviation. Left graph – before intervention, middle graph – after intervention, right graph – at follow-up.

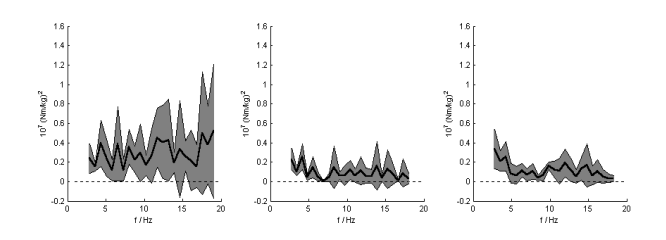


Figure 3. Spectral power density plots for flexion/extension hip moment in the impaired right extremity shown within the boundaries of one standard deviation and for the frequency range from 2.5 Hz to 20 Hz. Left graph – before intervention, middle graph – after intervention, right graph – at follow-up.

Discussion

The main purpose of this paper was to present novel dynamic balance training techniques during standing and stepping and to explore whether training of various gait components during standing in previously developed mechanical balance training device improves balance mechanisms that control the posture of the trunk during level ground walking of a selected subject with chronic hemiparesis. The results of detailed analysis of instrumented gait assessment indicate improvement of postural mechanisms that are the prime vehicles for balancing the trunk during walking in the selected patient that underwent the developed training intervention. This improvement was retained also beyond the training period as suggested by the results of follow-up assessment.

We have focused in our analysis onto the moments produced by the hip flexor/extensor muscles, which were shown to be the main mechanisms for trunk posture regulation in the sagittal plane during walking [4]. Marked difference was seen in hip moment trajectories of the right extremity before our therapeutic intervention. This difference was mainly reflected in a large jerk in hip moment immediately after the foot contact that started stance phase. The observed oscillation was likely due to a highly sensitive postural reflex response. Since the duration of this jerk was too short to have any noticeable effect on hip and trunk movement it was not functional and only resulted in significant loading of the hip joint via the compressive forces that accompany the observed moment jerk. The oscillatory behavior in the flexion/extension hip moment could be observed also throughout the whole gait cycle in power density spectra. This complements the observations made in the time domain and further demonstrates the high gain in the hip flexion/extension postural mechanisms. The results assessed immediately after the therapeutic intervention and at follow-up show marked decrease in the gain indicated by reduction of power density spectra. From the clinical point of view we can pose a question of clinical relevance of the observed improvement, especially because the accompanying assessment of clinical outcome measures did not show any improvement. Firstly, the reduction of the jerk in hip moments is beneficial as reduces the unnecessary stress onto the musculo-sceletal

structures. Secondly, the patient as well as his therapists observed much more confident walking following the intervention, which has a positive effect on self-confidence, self-image and reduced fear of falling. Thirdly, we need to take into account that the patient we selected for this case study was in terms of walking abilities exceptionally good. This choice was necessary because the selected subject had to be capable of independent walking in order to be eligible for instrumented gait analysis procedures. In such patients it is fairly difficult to improve any aspect of walking, which was confirmed also by the results of clinical assessment. If we had not undertaken also objective gait analysis measures we could not see significant difference in patient's gait performance. Also the patient was well in the chronic stage of hemiparesis, which ruled out otherwise possible effects of spontaneous recovery.

Acknowledgements

The authors express their gratitude to the volunteer subject and acknowledge financial support of Ministry of Education, Science and Sport, Republic of Slovenia.

References

- [1] Teasell RW, Bhogal SK, Foley NC, et al. Gait retraining post stroke. Top Stroke Rehabil 2003; 10: 34-65.
- [2] Liepert J, Bauder H, Wolfgang HR, et al. Treatment-induced cortical reorganisation after stroke in humans. Stroke 2000; 31: 1210-1216.
- [3] Matjačić Z, Hesse S, Sinkjaer T. BalanceReTrainer: A new standing-balance training apparatus and methods applied to a hemiparetic subject with a neglect syndrome. NeuroRehabilitation 2003; 18:251-259.
- [4] Winter DA, Ruder GK, MacKinnon CD. Control of Balance of upper body during gait. In: Winters JM and Woo SL-Y (eds) Multiple muscle systems. Springer Verlag, New York, 1990: 535-541.

Author's Address

Dr. Zlatko Matjačić Institute for rehabilitation Linhartova 51, SI-1000 Ljubljana Slovenia e-mail:zlatko.matjacic@mail.ir-rs.si

CONTROL OF THE KNEE JOINT UNDER FUNCTIONAL ELECTRICAL STIMULATION-SIMULATION RESULTS BASED ON A NEW PHYSIOLOGICAL MUSCLE MODEL

H. El Makssoud, P. Fraisse, S. Mohammed, D. Guiraud, P. Poignet

DEMAR Project – Department of Robotics
LIRMM / INRIA, 161 Rue Ada - 34392 Montpellier Cedex 5, France

Abstract

The implantation of an advanced neuroprosthetic device on two patients in 1999-2000 (SUAW project, Biomed II) has encouraged us to develop in a first step a physio-mathematical model of the skeletal muscle and afterwards synthesise the stimulation patterns of the whole dynamic lower limb model. The main issues concern the muscle modelling and its applications in controlling the movement of the human knee by Functional Electrical Stimulation (FES).

Introduction

The Mathematical model describes the complex physiological system of the skeletal muscle based on the macroscopic Hill and microscopic Huxley concepts. A new study published by Sorine [1] opened the possibility of controlling the heart muscle model by using a chemical control input to stimulate the contractile element of the model. Starting with this concept, we have proposed a new physiological skeletal muscle model. This model leads us to define the signal input and to characterize the parameters of the muscle model presented by two differential equations where the outputs are the muscle force and length. The input model represents the actual electrical signal as provided by the stimulator "PROSTIM" offering the possibility of tuning three independent parameters: amplitude, pulse width and frequency. We have integrated this model within a control loop of the human knee joint simulator including two skeletal muscles quadriceps and hamstrings. The parameters of the above model were identified by means of experimental measures on the agonist/antagonist knee muscles of the paraplegic patient by using a multi moment platform. Consequently, a control strategy can be performed and validated on this simulator. Some simulation results of the movement of the knee joint relying on theory of High Order Sliding Modes are presented.

Material and Methods

Biomechanical model

The biomechanical model consisted of two segments representing respectively the femur and the tibia bones, a pulley modelling the knee articulation and two agonist antagonist muscles. The femur is supposed to be fixed corresponding to the patient laying supine. Two forces $F_{\rm ext}$ and $F_{\rm flex}$ act on the swinging segment at the insertion point I and which represent respectively the extension and the flexion forces. These forces are supposed to be constant along their directions. ($\theta = 0$ corresponds to full extension of the knee)

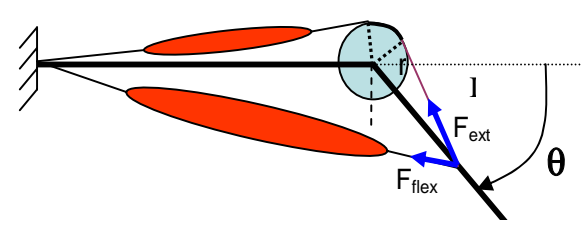


Fig. 1: biomechanical model of the knee

Muscle model

A physiological based muscle model is required to better understand its internal behaviour and to develop strategies for simulation, motion synthesis or motor control during clinical restoration of movement. The muscle model, described in [2], represents the complex physiological system of the skeletal muscle based on both macroscopic Hill and microscopic Huxley concepts. Fig.2 shows the parallel element E_P with the two elements in series E_S and E_C .

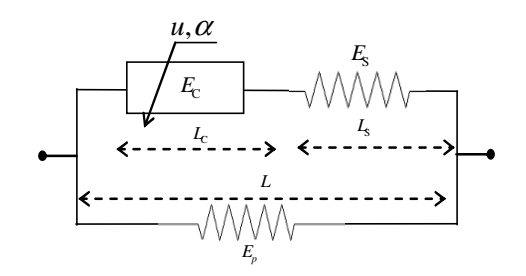


Fig. 2: model of muscle and particularization of E_{C}

The muscle model is controlled by two variables: u, a chemical control input and α , the ratio of recruited fibres. This model can be presented by two differential equations where the outputs are k_c and F_c representing, respectively, the stiffness and the force generate by the contractile element. k_0 and F_0 are the maximum values of k_c and F_c .

$$\begin{cases} \dot{k}_{c} = \left(s_{0} \alpha k_{o} - s_{u} k_{c} + s_{v} \frac{s_{0} \alpha F_{o} - s_{u} F_{c}}{1 + p k_{c} - s_{v} q F_{c}} q k_{c} \right) \mathbf{u} - s_{v} \frac{a k_{c}}{1 + p k_{c} - s_{v} q F_{c}} \dot{\varepsilon} \end{cases} (1)$$

$$\dot{F}_{c} = \frac{s_{0} \alpha F_{o} - s_{u} F_{c}}{1 + p k_{c} - s_{v} q F_{c}} \mathbf{u} + \frac{b k_{c} - s_{v} q F_{c}}{1 + p k_{c} - s_{v} q F_{c}} \dot{\varepsilon}$$

$$a = \frac{L_0}{L_{c0}}; \quad b = L_0; \quad p = \frac{1}{k_s}; \quad q = \frac{1}{L_{c0}k_s}; \quad L_0 = L_{c0} + L_{s0}$$

 S_u , S_0 and S_v are the sign of the control and velocities of the contractile element. The parameters used in simulation are issued from the literature [1] and presented in table 3.

Muscle model parameters	variable	Numeric value	unit
stiffness of E _S	k _S	5 10 ⁴	N/m
Contractile elements length	L_{C0}	40 10-2	m
Elastic elements length	L_{S0}	10 10-2	m

Table 3: Specific parameters of the muscle model.

Biomechanical model of the knee

Let us consider the model of the muscles and knee joint as a non-linear state model:

$$\dot{\mathbf{x}} = \mathbf{f}(\mathbf{x}, t, \mathbf{U}) \tag{2}$$

Where $\mathbf{x} = [X_1 \dots X_6]^T = [k_{c1} \quad k_{c2} \quad F_{c1} \quad F_{c2} \quad \theta \quad \dot{\theta}]^T$ is the state vector and $\mathbf{U} = [u_1 \quad \alpha_1 \quad u_2 \quad \alpha_2]^T$ the control vector. The variable θ represents the joint of the knee. The state variables k_{c1} , F_{c1} , u_1 , α_1 and k_{c2} , F_{c2} , u_2 , α_2 are respectively the state variable of the quadriceps and hamstring. The state model of the biomechanical model of the knee can be expressed as:

$$\begin{split} \dot{X}_{1} &= \left(S_{0_{1}}\alpha_{1}k_{m_{1}} - S_{u_{1}}X_{1} + S_{v_{1}}q_{1}\frac{S_{0_{1}}\alpha_{1}\sigma_{m_{1}}X_{1} - S_{v_{1}}q_{1}X_{3}}{1 + p_{1}X_{1} - S_{v_{1}}q_{1}X_{3}}\right)u_{1} - \frac{S_{v_{1}}a_{1}X_{1}rX_{6}}{L_{01}\left(1 + p_{1}X_{1} - S_{v_{1}}q_{1}X_{3}\right)}\\ \dot{X}_{2} &= \left(S_{0_{2}}\alpha_{2}k_{m_{2}} - S_{u_{2}}X_{2} + S_{v_{2}}q_{2}\frac{S_{0_{2}}\alpha_{2}\sigma_{m_{2}}X_{2} - S_{u_{2}}X_{4}X_{2}}{1 + p_{2}X_{2} - S_{v_{2}}q_{2}X_{4}}\right)u_{2}\\ &+ \frac{S_{v_{2}}a_{2}X_{2}L_{0}L_{ii}\sin(X_{5})}{L_{02}\sqrt{L_{0}^{2} + L_{ii}^{2} + 2L_{0}L_{ii}\cos(X_{5})}\left(1 + p_{2}X_{2} - S_{v_{2}}q_{2}X_{4}\right)}\\ \dot{X}_{3} &= \frac{S_{0_{1}}\alpha_{1}\sigma_{m_{1}} - S_{u_{1}}X_{3}}{1 + p_{1}X_{1} - S_{v_{1}}q_{1}X_{3}}u_{1} + \frac{\left(b_{1}X_{1} - S_{v_{1}}a_{1}X_{3}\right)rX_{6}}{L_{01}\left(1 + p_{1}X_{1} - S_{v_{1}}q_{1}X_{3}\right)}\\ \dot{X}_{4} &= \frac{S_{0_{2}}\alpha_{2}\sigma_{m_{2}} - S_{u_{2}}X_{4}}{1 + p_{2}X_{2} - S_{v_{2}}q_{2}X_{4}}u_{2} - \frac{\left(b_{2}X_{2} - S_{v_{2}}a_{2}X_{4}\right)L_{0}L_{u}\sin(X_{5})}{L_{02}\sqrt{L_{0}^{2} + L_{u}^{2} + 2L_{0}L_{u}\cos(X_{5})\left(1 + p_{2}X_{2} - S_{v_{2}}q_{2}X_{4}\right)}}\\ \dot{X}_{5} &= X_{6} \end{split}$$

$$\dot{X}_{6} &= \frac{1}{J}\left(X_{3}r - X_{4}\frac{L_{0}L_{ii}\sin(X_{5})}{\sqrt{L_{0}^{2} + L_{u}^{2} + 2L_{0}L_{u}\cos(X_{5})}} - mg\cos(X_{5})\beta L_{1} - F_{v}X_{6}\right) \end{split}$$

Control strategy based on HOSM

The control strategy we propose is based on the High Order Sliding Modes method [3]. This method generalizes the basic sliding mode approach and acts on the higher order time derivatives of the system. Thus, the discontinuity of the control vector does not appear in the first (r-1)th total time derivative (see Equation 4).

$$s = \dot{s} = \ddot{s} = \dots = s^{r-1} = 0$$
 (4)

The relative degree r can be defined as:

$$\frac{\partial s^{(i)}}{\partial u} = 0, (i = 1, 2, ..., r - 1), \frac{\partial s^{(r)}}{\partial u} \neq 0$$
 (5)

The classical VSS approach provides a solution for a relative degree r=1. We also use the 2-sliding mode control in this case in order to remove the well-known chattering phenomenon. In the other cases (r>1), the discontinuous control vector is on the (r-1)th time derivative of s and chattering phenomenon disappears while keeping the robustness properties of the sliding modes.

Position control law strategy

The sliding surface used to constraint the dynamic behaviour of the knee joint is a first order differential equation chosen as:

$$s = (\dot{\theta}_{J} - \dot{\theta}) + \lambda(\theta_{J} - \theta) \tag{6}$$

Where $\dot{\theta}_d$, θ_d are respectively the desired velocity and desired position, λ is a positive coefficient. Let us consider the sliding surface equation (6) in order to determine the relative order of the controlled system. We obtain the following result:

$$\frac{\partial \dot{s}}{\partial u} = 0, \ \frac{\partial \ddot{s}}{\partial u} \neq 0 \tag{7}$$

Therefore, the relative degree of the sliding control is r=2. Considering the step response case $(\ddot{\theta}_d = \dot{\theta}_d = 0)$, the second time derivative of the sliding surface can be written as:

$$\ddot{s} = -\ddot{X}_6 - \lambda \dot{X}_6 \tag{8}$$

The expression of the second time derivative of the state variable X_6 is given by:

$$\begin{split} \ddot{X_{6}} = & \frac{1}{J} \frac{rS_{0} \alpha_{i} \alpha_{m}}{(1 + p_{i} X_{i} - S_{n_{i}} q_{i} X_{3})} \frac{u_{i}}{1 + p_{i} X_{i} - S_{n_{i}} q_{i} X_{3}} \frac{u_{i} + r \frac{\left(b_{i} X_{i} - S_{n_{i}} q_{i} X_{3}\right) r X_{6}}{L_{0} \left[1 + p_{i} X_{i} - S_{n_{i}} q_{i} X_{3}\right]} \frac{u_{i}}{(1 + p_{i} X_{i} - S_{n_{i}} q_{i} X_{3})} \frac{S_{0} \alpha_{i} \alpha_{m} L_{0} L_{i} \sin(X_{5})}{\left(1 + p_{2} X_{2} - S_{2}, q_{2} X_{4}\right) \left(L_{0}^{2} + L_{i}^{2} + 2 U_{0} L_{i} \cos(X_{5})\right)} \frac{u_{2}^{2} + \frac{S_{0} \alpha_{m} L_{0} L_{0}^{2} \sin(X_{5})}{\left(1 + p_{2} X_{2} - S_{2}, q_{2} X_{4}\right) \left(L_{0}^{2} + L_{i}^{2} + 2 U_{0} L_{i} \cos(X_{5})\right)} \frac{u_{2}^{2}}{L_{0} \left(1 + p_{i} X_{i} - S_{n_{i}} q_{i} X_{3}\right) r X_{0} L_{0}^{2} + L_{i}^{2} + 2 U_{0} L_{i} \cos(X_{5})}} - X_{4} \frac{L_{0} L_{i} L_{0} C_{0} \left(X_{5}\right) \sqrt{L_{0}^{2} + L_{i}^{2} + 2 U_{0} L_{i} \cos(X_{5})}}{L_{0}^{2} L_{i}^{2} + L_{i}^{2} + 2 U_{0} L_{i} \cos(X_{5})} + mg \mathcal{I}_{1} X_{6} \sin(X_{5}) - F X_{6}} \end{split}$$

Inserting the expressions of \dot{X}_6 and \ddot{X}_6 within the equation (8) allows writing the second time derivative of s as:

$$\ddot{s} = \varphi(x, t) + \gamma(t, x)u \tag{9}$$

It is assumed that $\Phi > 0$, $|\varphi| \le \Phi$, $0 < \Gamma_m \le \gamma \le \Gamma_M$

We express the equation (9) as:

$$\begin{cases} \dot{y}_1 = y_2 \\ \dot{y}_2 = \varphi(t, x) + \gamma(t, x)u \end{cases}$$
 (10)

Where $y_1 = s$. In that case, the problem is equivalent to the finite time stabilization problem for the uncertain second-order system. Most of 2-sliding controllers have been proposed in [3]. We have chosen an algorithm with a prescribed convergence law. The general formulation of such a class of a 2-sliding control algorithm is:

$$\dot{u} = \begin{cases} -u & \text{if } |u| > 1 \\ -V_M sign(y_2 - g(y_1)) & \text{if } |u| \le 1 \end{cases}$$
 (11)

Where V_M is a positive constant, g is a continuous function. Moreover, this function must verify some specific conditions (see [3]).

$$g(y_1) = -\lambda_1 |y_1|^{\rho} sign(y_1), \quad \lambda_1 > 0, \quad 0.5 \le \rho < 1$$
 (12)

A substitution of y_2 by Δy_1 is theoretically possible whether y_2 is not available.

The sufficient condition for the finite time convergence to the sliding manifold is defined by the following inequality:

$$V_{M} > \frac{\Phi + \sup[g'(y_{1})g(y_{1})]}{\Gamma_{\dots}}$$
(13)

Results

We have implemented this control algorithm defined by equation (11) on the simulator of the biomechanical model of the knee joint (cf. equation (3)). The components of control vector U are the chemical inputs (u_1, u_2) and ratios of the recruitment fibres (α_1, α_2) . These coefficients depend on the Electric Stimulation Current (I) and Pulse Width Modulation (PW) values, (see [4]). In our case, the biomechanical model of the knee joint is controlled by two muscles: Quadriceps and Hamstring. Consequently, there are two Electric Current, I_q and I_h as well as two Pulse Width Modulations values, PW_q and PW_h which have to be deduced from the control vector u.

Therefore, we propose a method to define the contribution of control vector u stemming from the

2-sliding controller to calculate the Electric Currents and PWM values. We have selected the following algorithm:

If u > 0:

$$I_{q} = uI_{Max}, I_{h} = 0, PW_{q} = uPW_{qmax}$$

If u<0:

$$I_q = 0$$
, $I_h = |u|I_{Max}$, $PW_h = |u|PW_{hmax}$

The Electric Current and Pulse Width Modulation values enable to deduce the ratios of the recruitment fibre (α_1, α_2) by using the results presented in [4]. The control vector u is defined as:

The chemical inputs u_1 and u_2 are automatically activated when the Electric Currents are respectively superior to zero.

We have implemented this algorithm on the simulator built with SimulinkTM software. We applied two different desired positions as:

1)
$$t < 2s : \theta_d = 100 \deg$$
,

2) t>2s:
$$\theta_d = 80 \deg$$
,

The coefficients of the 2-sliding controller are chosen to verify the condition equations (12) and (13). We determined the following values: $\lambda = 10$, $\lambda_1 = 10$, $\rho = 0.5$, $V_M = 1$.

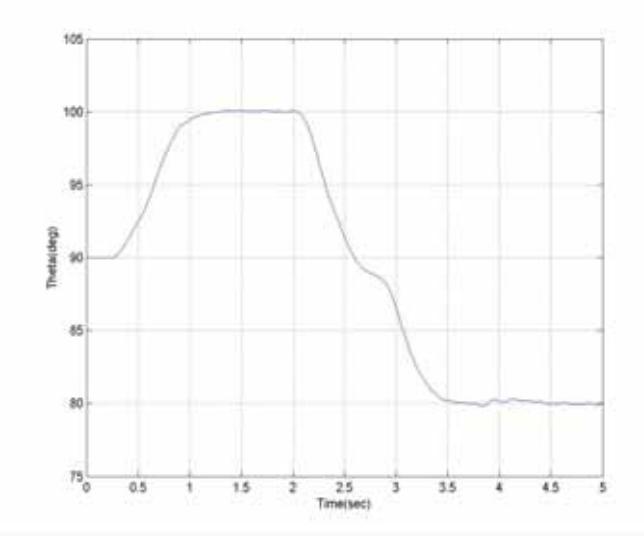


Fig. 2: Trajectory of the knee joint

Figure 2 is the first control result with the new muscle model. Focusing on the first step response, we can discover the sliding surface and finite time convergence figure 3.

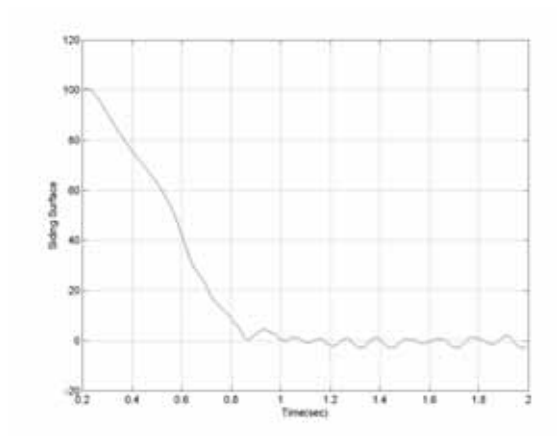


Fig. 3: Sliding surface response

The figure 4 is the experimental step response obtained for the first time period (t<2s). We added the theoretical step response we should obtain if the constraint s=0 was always verified. The two curves match (t~0.85s) when the sliding surface reaches zero (cf. figure 3).

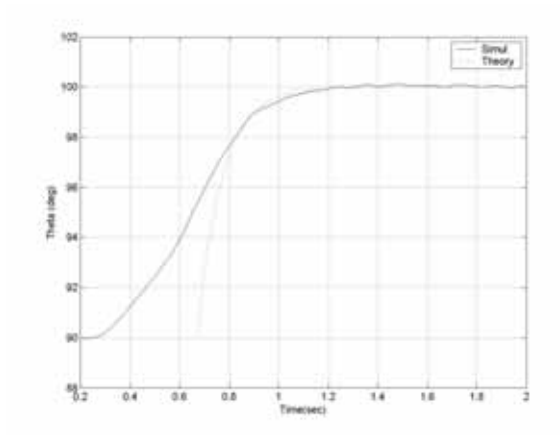


Fig. 4: Experimental step response versus theoretical step response

Figures 5 and 6 present respectively the control vector u computed by the equation (14) and the Pulse Width Modulation (PW_q and PW_h).

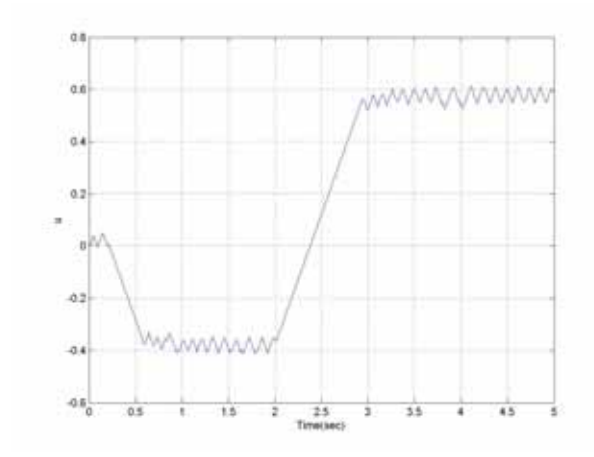


Fig. 5: Control vector

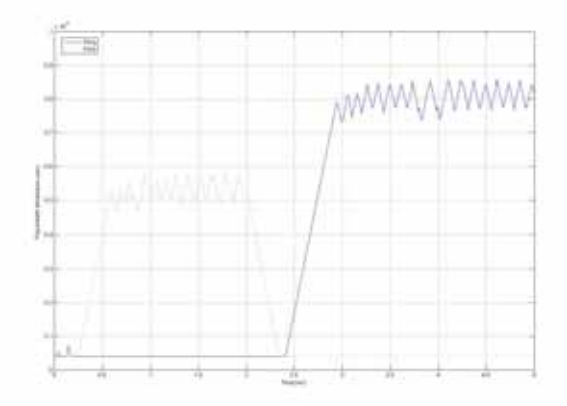


Fig. 6: Pulse Width Modulation (quadriceps and hamstring).

Discussion

This paper presented the first step of muscle control study by using the new multiscale model developed within the DEMAR project. The simulation results obtained with the control algorithm based on the HOSM seems to be efficient. We are able to control two antagonist muscles with the same control vector and force dynamically the behaviour of the system as a first order time response. The future work will concern the validation on patients. We plan to perform and validate the 2-sliding controller by using the multi moment platform on a paraplegia patient.

References

- [1] Bestel J., Sorine M., "A differential model of muscle contraction and applications", In Schloessman Seminar on Mathematical Models in Biology, Chemistry and Physics, Max Planck Society, Germany, May 19-23 2000.
- [2] El Makssoud H., Guiraud D., Poignet P., Mathematical muscle model for Electrical Stimulation control strategies IEEE International Conference on Robotics & Automation New Orleans, LA, USA, April 26 May 1, 2004.
- [3] L. Fridman, A. Levant, "High-Order Sliding Modes", Sliding Modes Control in Engineering, Ed. W. Perruquetti, J.P. Barbot, Marcel Dekker, Inc. New-York, pp. 53-101, 2002.
- [4] El Makssoud H., Guiraud D., Poignet P., Enhancement of physiological and mechanical modelling of the skeletal muscle controlled by Functional Electrical Stimulation, 9th IFES Society, September 2004, Bournemouth, UK.

Author's Address

Hassan El Makssoud, Philippe Fraisse e-mail:makssoud@lirmm.fr, fraisse@lirmm.fr Department of Robotics LIRMM, 161 Rue Ada 34392 Montpellier Cedex 5, France Home page: http://www.lirmm.fr/

THE MOTION MAKER TM : A REHABILITATION SYSTEM COMBINING AN ORTHOSIS WITH CLOSED-LOOP ELECTRICAL MUSCLE STIMULATION

C. Schmitt*, P. Métrailler*, A. Al-Khodairy**, R. Brodard***, J. Fournier*, M. Bouri*, R. Clavel*

* Laboratoire de Systèmes Robotiques, Ecole Polytechnique Fédérale de Lausanne, Switzerland ** Clinique Romande de Réadaptation - suvaCare, 1951 Sion, Switzerland *** Fondation Suisse pour les Cyberthèses, 1844 Villeneuve, Switzerland

Abstract

The aim of this paper is to present an active functional device using Closed-Loop Electrical Muscle Stimulation liable to rehabilitate spinal cord iniurv and hemiplegic individuals. "MotionMakerTM" is a stationary programmable test and training system for the lower limbs developed at the Ecole Polytechnique Fédérale de Lausanne. It is composed of two orthoses comprising motors and sensors, and a control unit managing the electrical stimulation with real-time regulation. This allows leg movements with the desired characteristics of position, speed and torque. Initial tests have been carried out. The results provide elements for an objective and quantitative evaluation of the performances of the MotionMakerTM, which ensure a reliable contribution to the diagnosis, assessment and recovery of functions during the rehabilitation process.

Introduction

Paralysis resulting from spinal cord injury (SCI) cause extensive medical secondary complications [1]. These may slow down the rehabilitation program and can be prevented by moving the paralysed limbs and maintaining muscular trophicity with functional electrical stimulation (FES). Moreover, to be efficient, especially in the incomplete lesion, FES must stimulate the muscles as faithfully as possible in accordance with the sequence of muscle contraction for a given movement. The kinematics and the dynamics of the movement must be respected at best. Therefore, a closed-loop control of the FES is essential to achieve complex and repetitive movements such as press-leg and cycling. For this, the FES must be combined with an orthosis including motors or brakes and sensors. Such an orthosis is called a hybrid orthosis [2].

Adding closed-loop electrical muscle stimulation (CLEMS), the hybrid orthosis becomes a "Cyberthosis" which is the contraction of the words cybernetic and orthosis, concept proposed by the Swiss Foundation for Cyberthoses (FSC: Fondation Suisse pour les Cyberthèses). The

advantage of using a cyberthosis is to be able to create an active and progressive muscle participation which passive mobilization exercises made by therapists do not allow.

Our group first developed a knee orthosis to verify the feasibility of CLEMS applied selectively and simultaneously to the rectus femoris, vastus lateralis and vastus medialis [3]. The results of simple knee joint extension with valid and incomplete SCI individuals has given the essential information needed in order to design a complete lower limb hybrid orthosis with three degrees of freedom (DOF): hip, knee and ankle.

The purpose of this paper is to present a stationary programmable test and training system for the lower limbs activated by electrical stimulation. This device is called "MotionMakerTM" (Fig. 1). It is composed of two orthoses with 3 DOF comprising motors and sensors, a control unit managing the electrical stimulation and the motors with real-time regulation, a multi-channel electrostimulator and a worktable. This allows SCI individuals to sustain or make leg movements with the desired characteristics of position, speed and torque. The aim is efficient strengthening of the muscles, the development of endurance, as well as joint mobility and movement coordination.

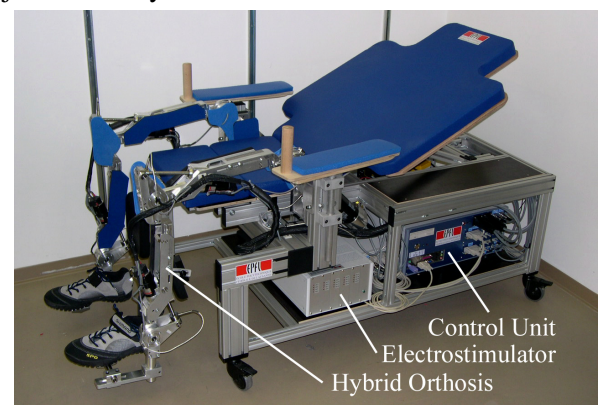


Fig. 1: MotionMakerTM prototype

Material and Methods

MotionMakerTM design description

The version of the MotionMakerTM described here is the first prototype (Fig. 1) used as a research tool for study on valid subjects (in our laboratory) and

SCI individuals in a specialized clinic which is collaborating in the project (CRR: Clinique Romande de Réadaptation - suvaCare). It was built for functionality evaluation and data acquisition. The product design issues will be addressed after the results of the first clinical trials in order to optimize the device and thus warrant a further development. The MotionMakerTM was designed to meet requirements of adjustment to fit people from 150 to 190 cm in height. Comfort was also taken into account with an adequate foam mattress. The control unit and the electrostimulator are placed inside the frame. The patient transfers from the wheelchair to the device at the front or slightly beside it. He must be assisted in this operation.

Orthosis

The orthosis (fig. 2) is an exoskeleton placed on the external side of the leg. It includes three joints: hip, knee and ankle. Crank systems activated by a screw jack controlled by a DC motor drive each joint motion. The joints being pin axis, the orthosis runs only in a sagittal plane. Although the knee joint is polycentric, inducing a sliding instantaneous center of rotation and a slight movement of the sagittal plane, the pin axis is a good approximation of the knee motion.

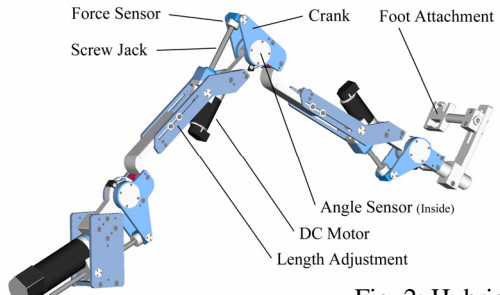


Fig. 2: Hybrid Orthosis

The lengths of the leg segments can be manually adjusted. The joint ranges of motion as well as the applicable human torque are resumed in Table 1.

Motion [deg], Velocity [deg			Knee	Ankle		
Range of Moti	on: Ext. / Flex.	5 / 120	10 / 130	45 / 25		
	Velocity	110	110	110		
Torque: motion way	Muscle Work	Isotonic max. strength at isokinetic velocity of 110				
Extension	Concentric	Gluteus Maximus 50	Quadriceps 50	Gastrocnemius 50		
Extension	Exentric	Rectus Femoris 80	Hamstrings 30	Tibialis anterior 30		
Flexion	Exentric	Gluteus Maximus 50	Quadriceps 50	Gastrocnemius 50		
Flexion	Concentric	Rectus Femoris 80	Hamstrings 30	Tibialis anterior 30		
Max	cimum Torque		190 at 40°	190 at 0°		

Table 1: Joint range of motion and torque (0°= straight leg)

In addition, for safety reasons, manual adjustable joint stops can limit the range of movement of every single joint whenever indicated.

Worktable

The main function of the worktable is to place the patient in a good and comfortable position for the exercise and to adjust both orthoses to the subject. Fig. 3 shows the different adjustments (DOF). Currently these are made manually; for the next version they will be automated.



Fig. 3: Worktable DOF

Control unit

The controller consists of an intelligent central unit, namely an industrial PC with a real-time extension and an axis interface board and amplifiers. The control architecture adopted to control the MotionMakerTM is composed of a motion control and electrostimulation management. The controller synoptic is shown in Fig. 4. It is highly flexible and is built with different modules, some of them working as real-time processes composing the real time controller (RTC). The software modules composing the control unit are as follows:

- The Graphical User Interface (GUI) used to communicate with the real-time motion server (RTMS) by using the communication library (dll).
- The Communication Library. This interface, provided as a *dll*, allows communication with the RTC and renders it invisible to the user. Thus, all the high-level instructions necessary to set up the motion and the CLEMS control are made available.
- *Real-Time Motion Server*. The RTMS is the main door of the RTC. It receives orders and parameters from the GUI via the *dll* and dispatches them to the processes concerned (motion generator, motion controller or CLEMS controller).
- *Motion generator*. It generates the trajectories with specified geometry and given dynamics. This motion generator (MG) also communicates with the CLEMS control to carry out the movement or not.
- *Motion controller* (MC). It attends to the regulation of the set-points on each axis.
- Library of Forward and Inverse Kinematics.
- *CLEMS controller*. It carries out the regulation of force values using muscle stimulation.
- Library of Input/Output Functions.

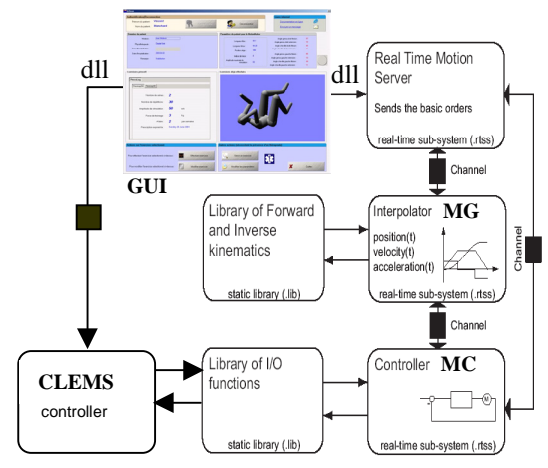


Fig. 4: Motion control principle and software

Electrostimulator StimWaveTM

In order to fulfil the MotionMakerTM FES requirements, a high-performance electrostimulator has been developed. It consists of 20 independent modular channels. The parameters of each are realtime controllable by the central unit via a common serial link. Each channel is able to generate rectangular biphasic symmetrical current pulses up to 100 mA. The compliance voltage is about 200V. The frequency and the pulse width are adjustable within a range of 10 to 85 Hz and 100 to 300 µs respectively. To avoid parasitic current flow between the electrode pairs, each channel output is electrically floating. The main concern was patient security. Therefore different sorts of hardware and software security systems have been implemented, such as pulse timeouts, programmable current limitation. command relevancy communication checksum.

FES control

Self-adhesive electrodes of different shapes are placed on the principal muscles of both limbs; Rectus Femoris (RF), Vastus Medialis (VM), Vastus Lateralis (VL), Gluteus Maximus (GM), Hamstrings (H), Tibialis Anterior (TA) and Gastrocnemius (G). This allows us to give active torques to all joints.

Pulse width is kept constant at 300 μs to ensure optimal stimulation and frequency is set in regard to the subject's muscle reaction. Current amplitude is adjusted up to 100 mA by the CLEMS control so muscle strength follows the control command.

Protocol

After 10 minutes of warm-up stimulation at 10 Hz-frequency, we started with isometric stimulation of all muscles at 30 Hz or 50 Hz to observe the subject's tolerance and muscle response to electrical stimulation (Fig. 5). Press-leg exercises with controlled strength and velocity followed in the test.

Subjects

#	IN	Sex	Age	NL	IS	TSI	MP	SP	S
1	RF	M	48	Т9	Α	4	0-1	2	1
2	EA	M	60	T8 R, T5 L	D	8	2-4	0	2
3	JB	M	77	C5	D	2.5	1-4	1	1
4	PG	F	79	T2	С	3	1-4	1	1

Table 2: Subjects. IN: Initials, NL: Neurological Level, IS: Impairment Scale, TSI: Time Since Injury [month], MP: Muscle Power (min & max), Sp: Spasticity, S: # of sessions, R: right, L: left.

SCI patients were screened during a three-month period (February-May 2004). Four eligible spinal cord inpatients (3 males and one female), 48 to 79 years old (mean 66) gave their written consent. Subjects were classified according to the NISCI-92 nomenclature [4]. Spasticity was measured

according to the modified Ashworth scale [5]. All but one had incomplete spinal cord lesions. Table 2 resumes the characteristics of the patients.

Clinical observation

Three patients had one session and one had two sessions. There were no drop-outs during the study. The sessions lasted 100-120 minutes. The duration was closely related to electrode application on both legs and individual performance in transfer from the wheelchair to comfortable installation on the MotionMakerTM. None of the four patients complained of pain during the test period nor developed pelvic or leg pressure sores, or fractures, or had increased spasticity. One patient had a lumbar brace and 2 cervical collars. None complained of pain or discomfort. All subjects agreed to participate in further sessions.

Results

Preliminary valid subject testing

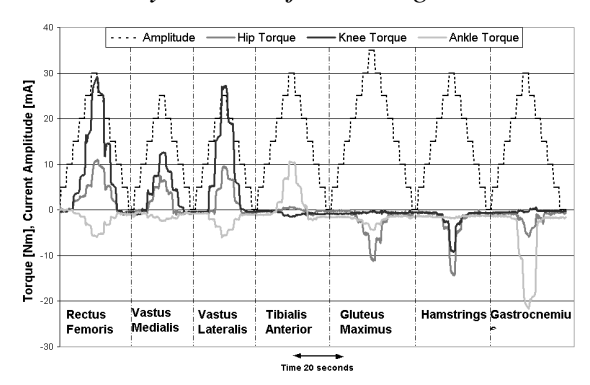


Fig. 5: Isometric stimulation valid subject (CS)

Fig. 5 shows a result of an isometric stimulation. Each muscle is activated with increasing-decreasing amplitude steps. Torques due to muscle contraction are plotted in function of time. A horizontal movement of the ankle defines the press-leg trajectory. The aim is that the resulting force applied by all muscles follows the value of 30 N (*Force Order*) in horizontal direction (*Force X*) and 0 N in vertical direction (*Force Y*). Fig. 6 shows a result of five FES press-leg extensions.

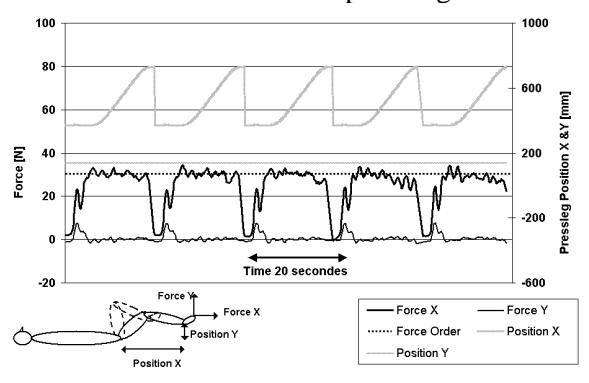


Fig. 6: Press-leg with CLEMS, valid subject (PM)

Preliminary SCI individuals testing

Due to muscle atrophy and no FES adaptation of our SCI individuals, stimulated strengths were low and difficult to control. A long training program with the MotionMakerTM will demonstrate its ability to overcome these phenomena. On the other hand, our device allowed us to measure the residual voluntary strength of our SCI subjects during press-leg movement. JPB performed two extensions with approx. 150 N.

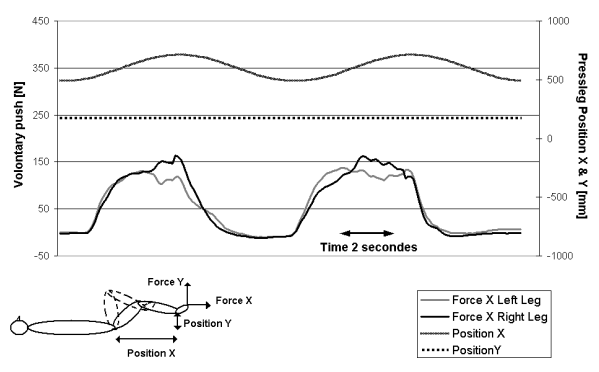


Fig. 7: Press-leg measurement of residual voluntary strength of incomplete SCI subject.

The next step will be to increase muscle strength by adding CLEMS stimulation with voluntary contribution.

Discussion

Using the MotionMaker TM , complications due to immobilization should be prevented more effectively and rehabilitation to restore gait should speed up.

Cyberthosis with its CLEMS real-time control can resolve two basic concerns restricting the capacity of FES system for fitness movement or assisted gait. The first is the difficulty to control selectively and simultaneously the contractions of several muscles by means of FES. This is mainly because of the non-linear response of the muscle contraction by FES and the inconsistent behavior of the electrically-induced muscle contraction. The second is a rapid muscle fatigue, which could be a consequence of the first concern. The CLEMS provides pulse amplitude modulation by a feedforward controller including proportional, integral and derivative (PID) algorithm to achieve just-sufficient muscular contractions. This is a solution to get just enough joint torque to produce a correct, desired limb trajectory, with or without external loads created by the orthosis motors themselves. Force and position sensors give the necessary feedback to the CLEMS controller.

The MotionMakerTM is the first device of an innovative three-stage rehabilitation program initiated and managed by the Swiss Foundation for Cyberthoses. When the patient has recovered a

condition sufficient physical with MotionMakerTM, it will be possible to begin specific walk training on a device which must respect gait kinematics and dynamics (momentum conservation). The "WalkTrainerTM" (Fig. 7), a mobile system providing training and assistance for gait in a vertical position, will do this. Paralyzed patients, properly prepared and trained, could, at this stage, be fitted with a walking cyberthosis: the "WalkMakerTM" (Fig. 8). This device, enabling an autonomous gait, will be aimed at patients for whom SCI does not allow a full gait recovery and who still need FES assistance. The WalkTrainerTM is in the process of development and the WalkMakerTM will be designed later, after acquisition of clinical data from the first two devices.

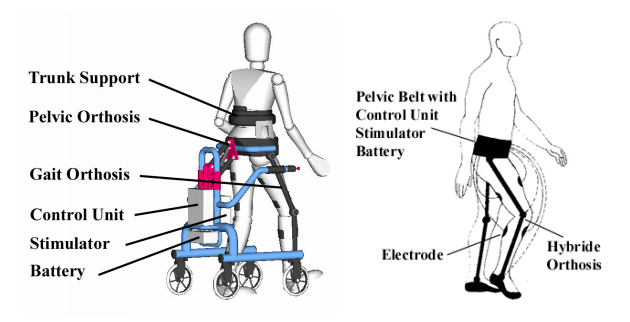


Fig. 7: WalkTrainerTM

Fig. 8: WalkMakerTM

References

- [1] Zejdlik, CP (Ed.) Management of Spinal Cord Injury. (2nd Ed.) Jones & Bartlett, Boston, 1992.
- [2] Popovic D, Sinkjear T. Control of movement for the physically disabled. *Springer*. 277-281, 2000.
- [3] Schmitt C, Métrailler P, Al-Khodairy A et al., A study of a knee extension controlled by a closed-loop functional electrical stimulation. *Proceedings*, 9th An. conf. of the IFESS, Bournemouth, 2004.
- [4] ASIA neurological standards committee 2000 (eds). *Int. standards for neurological classification of SCI.*
- [5] Bohannon RW, Smith MB. Interrater reliability of a modified Ashworth scale of muscle spasticity. *Physical Therapy*. 67 (2), 206-207, 1987.

Acknowledgements

We would like to express our sincere thanks to the SCI patients who volunteered to take part in the study. We are grateful to the FSC, the EPFL and to the Swiss Lottery (Loterie Romande) for their financial support.

Author's e-mail

carl.schmitt@epfl.ch, patrick.metrailler@epfl.ch, abdul.al-khodairy@crr-suva.ch, roland.brodard.fsc@bluewin.ch, jacques.fournier@epfl.ch, mohamed.bouri@epfl.ch, reymond.clavel@epfl.ch

Session 8

Sensors and Control

Chairpersons:

P. Meadows (Valencia, USA) D. Rafolt (Vienna, Austria)

SATURATION OF THE M-WAVE AMPLITUDE WITH INCREASING STIMULATION AMPLITUDE

Rafolt D.*, Mayr W.*, Vetter K.***, Gallasch E. **, Bijak M.*, Reichel M.*, Sauermann S.*, Lanmueller H. *, Unger E.*, Hofer C.****

*Department of Biomedical Engineering and Physics, Medical University of Vienna, Austria

** Department of Systemphysiologie, Medical University Graz, Austria

*** Otto Bock Inc., Austria; ****Wilhelminenspital Vienna, Austria

Introduction

The quantification of muscle fatigue is essential for the optimization of training in sports and rehabilitation. The measurement of blood gases like lactat concentration is widely used in serious sports, but such values are reflecting the total systemic status and therefore are not representative for a single fatigued muscle. Another approach is a biomechanical one: Using various protocols a decrease in the muscle performance characterizes fatigue. These methods need to measure the force output using more or less heavy equipment and therefore mobile measurements are complicated.

Looking for a simple to use methode to assess muscle fatigue during training, the recording and on-line analysis of the m-wave (synchronized EMG response on a electrical stimulation pulse) was considered. It is known that fatigue either caused by voluntary contraction or by FES leads to a decrease of the amplitude of the m-wave [1-7].

Moreover the latency of the m-wave response depends on the length of the muscle and therefore from the ankle of the joint under investigation. [8]. The shift of the latency is accompained with a change in the peak-to-peak amplitude of the m-wave. Thus one must know this relation in order to assign a change in the amplitude either to fatigue or to the change of the muscle length in the correct way.

As there are a number of physical and physiological parameters beside the stimulation amplitude that influence the excitability of the muscle (electrode position and size, electrode impedance, temperature of the muscle, sweating, polarity of the stimulus etc.) our aim was to find a measurement setup and protocol to compare pre and post fatigue data with minimum influences of these parameters. The investigation was done under the condition of using the same stimulation electrode setup for both FES training and m-wave measurement.

Material and Methodes

Exceeding a certain threshold level of the stimulation voltage the amplitude of the m-wave

increases very rapidly. Then at higher stimulation leves all the muscle fibers are activated and variations in the above-mentioned parameters do not change the excitation and therefore the amplitude of the m-wave saturate. The deciding factor for innervation of the muscle is the electrical field the nerve is exposed to. To keep this field above a level for supramaximal stimulation the voltage applied on the surface electrode must be sufficient high.

The question is: What amplitude of stimulation voltage is needed to detect the transition to a saturated state of the response.

From 10 persons from our university staff we recorded the twitch response (knee extension) on an isometric knee dynamometer built in our department and the EMG signal from the quadriceps muscle (vastus lateralis). The m-wave signal was measured with a commercial EMG-system (DISA-Neuromat 2000C; range 2mV/Dev.; 5-1000Hz). Ankle, knee and hip joints were immobilised for an angle of 90° each.

Stepwise increasing constant voltages pulses (biphasic, 2x300us) were applied to the muscle over self-adhesive stimulation electrodes (Schwa-Medico, 8x13cm). The positions of the stimulation electrodes was adjacent to the patella border for the distal electrode and 3cm distal to the inguinal fold for the proximal electrode - the lateral side of this electrode was turned about 30° more proximal. The stimulator was built in our department and the maximum output of the biphasic pulse was limited to 300Vpp. The orientation of the EMG-electrodes were varied and the polarity of the stimulation voltage was altered. Additionally in five subjects the angle of the knee was varied between 0° and 120° in steps of 10°. For data analysis Matlab 6 (Mathworks Inc.) was used.

Results

a. Orientation of the EMG electrodes:

In order to limit the hardware design for a transportable device (no special stimulation artifact rejection measures like blanking or filter circuits etc.) we desided to place the EMG electrodes perpendicular to the orientation of the stimulation

electrodes above the m.vastus lateralis. Lying more or less on a equipotential line of the electrical field arising from the stimulation voltage the crosstalk from the stimulus is a minimum. Nevertheless a typical m-wave curve can be detected as the vastus is a pennated muscle and has an orientation of the fibers of about 45 degrees.

In this arrangement the EMG measurement needs less space between the stimulation electrodes which could be advantageous for small or young people respectively or X-large FES electrodes. Fig.1 (left) shows the m-wave response from one subject using longitudinal electrodes. The m-wave is offset by the stimulus artefact. Fig.1 (right) shows a recording using perpendicular electrodes.

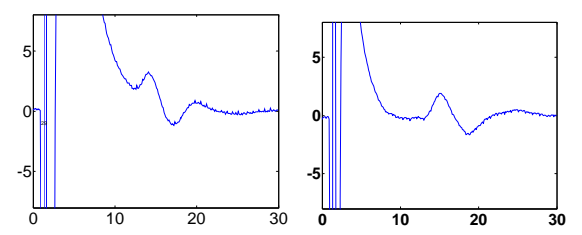


Fig:1: m-wave signals with longitudinal (left) and perpendicular (right) EMG bipolar electrodes (t in [ms]

b. Effect of knee angle:

Fig.2 shows the influence of the knee angle of the same subject with perpendicular arranged electrodes @60Vpp. The latency of the first maximum of the m-wave varies from 12ms for the stretched leg (0°) to 16ms (for a flexion of 120°). The corresponding peak-to-peak (PTP) amplitude of the m-wave shows a decrease with an increasing angle.

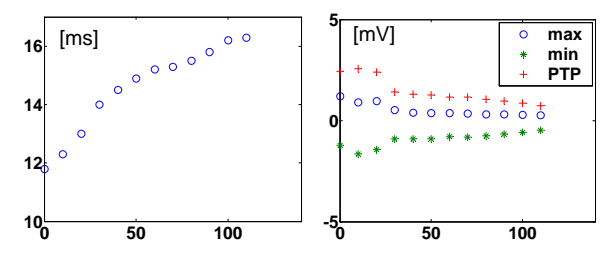


Fig.2 Latency and m-wave amplitude versus knee angle

c. m-wave amplitude in respect to the stimulation amplitude

In Fig.3 the peak-to-peak (PTP)-amplitude, the pos. and neg. maximum of the m-wave and the peak torque of the twitch was ploted against the PTP amplitude of the stimulation voltage.

For the description of the curves the following characteristic values were extracted: the threshold level (U_{th}) of the stimulation amplitude, the stimulation level (U_{sat}) at which the m-wave amplitude (M_{sat}) saturate, the stimulation level

 $(U_{Msat/2})$ at the half of $M_{sat}.$ Fatigue does not only manifest in a decreased EMG amplitude but also in a disproportional shift of the EMG/Stimulation curve to higher stimulation values in some subjects. Therefore $U_{Msat/2}$ is measured. For the quadriceps the saturation of the m-wave amplitude for stimulation was: $U_{sat} = 82 Vpp \pm 9.4 Vpp$ STD. For U_{th} we found $30V \pm 5.5V$ STD and for $U_{Msat/2} 52V \pm 7.4V$ STD respectively. The amplitude of the m-wave M_{sat} was found between 3mV and 9mV. (5.2mV±1.8mV STD).

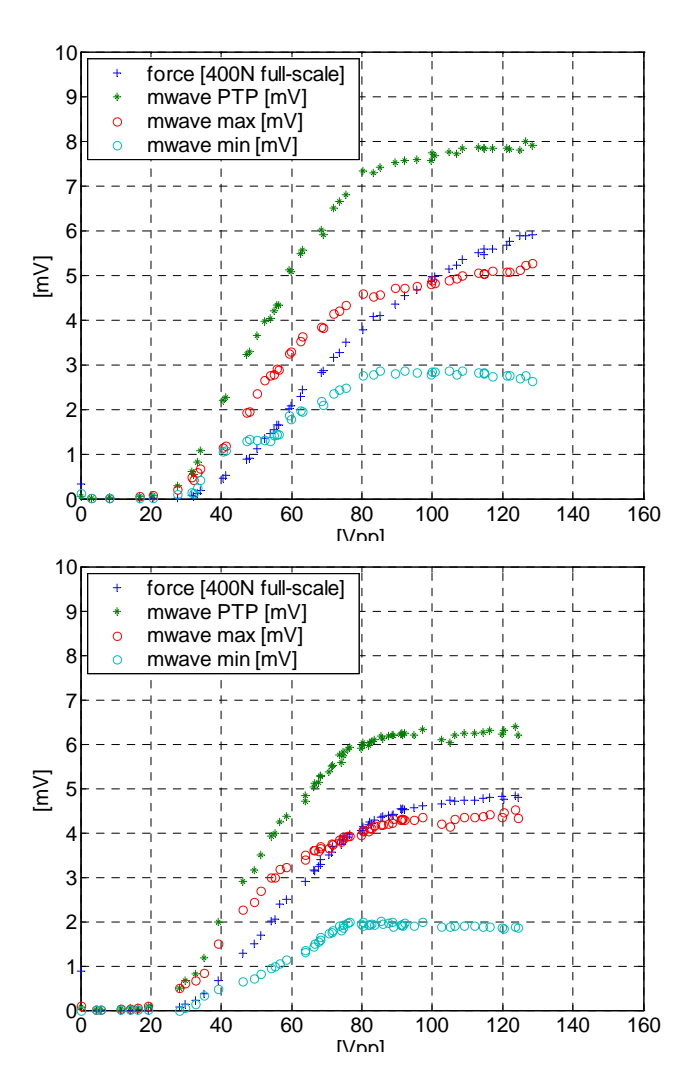


Fig.3 PTP, Max and Min of the m-wave before (upper diagram) and after (lower diagram) fatigue

d. Alteration of the polarity of the stimulation voltage: Changing the polarity of the stimulus leads to another synergy of motorunits and muscle groups respectifely as the different motorpoints are addressed in a different way. If we perform the measurements with both polarities the quadrizeps can be examined more detailed. We could found, that in most subjects the m-wave=f(stimulation) curve shifted to lower stimulation amplitudes for the cathode lateral (Fig.4).

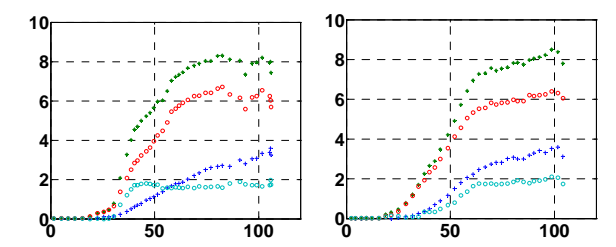


Fig.4 Cathode electrode distal (left), proximal (right) (from top to bottom: mwPTP, mwMax, Force, mwMin)

Discussion:

In sport physiology the m-wave is often monitored as an indicator for a supramaximal response of the force twitch. A saturation of the m-wave means a saturation of the twitch force response. This works for superficies muscle and small stimulation electrodes positioned over the motorpoint.

Using large electrodes (identical for m-wave test and FES training) co-contraction of synergistic muscles leads to a further increase of the twitch amplitude - even if the muscle under investigation is already stimulated supramaximal. Crosstalk of EMG signals also may lead to an increase in m-wave amplitude. If we plot the m-wave and twitch response respectively in relation to the stimulation amplitude the saturation level therefore is characterized by a higher slope below and a lower slope above this level.

Orientation of the bipolar EMG-electrodes: In the literatur we can find both: perpendicular orientation [4] and longitudinal orientation of bipolar EMG electrodes. The problem of the stimulation artefact is not the overriding of the EMG amplifier itself due to the galvanic crosstalk (input signal up to volt level – compared to the mV level for the m-wave signal). The big problem is the discharge process of the capacity of the stimulation electrode after the biphasic pulse. Due to the high gain of the amplifier, the discharge current is sensed even after milliseconds. (see exponential function in Fig.1).

Special attention must be paid for a sufficient period. In some warming previous measurements we found the m-wave amplitude higher before the fatigue test than after. As this occures also in the supramaximal stimulated muscle this fact must be addressed physiological processes in the muscle cell and therefore can't be distignuished from the fatigue process.

Conclusion:

To indicate muscle fatigue by the measurement of m-wave amplitudes we propose to use not only one teststimulus with a certain supramaximal amplitude but a series of increasing pulses up to 120V pp in steps of 5-10V in order to detect both the onset and saturation level. Repetition rate should be not higher then 2Hz to allow the mechanical response to return to zero in order to avoid movement artefacts for the following m-wave recording. The knee should be kept in a constant position as the relation between m-wave amplitude and knee angle differ very much and would demand a further calibration procedure. Last but not least the orientation of the EMG electrode perpendicular to the thigh is advantageous as the stimulation artefact is much smaller.

Literature:

- [1] Mizrahi J., Fatigue in Muscles Activated by Functional Electrical Stimulation. Crit. Reviews in Physical and Rehabilitation Medicine, 9(2):93-129, 1997
- [2] Mizrahi et. Al., EMG as an Indicator of Fatigue in Isometrically FES-Activated Paralyzed Muscle, IEEE Transaction on Rehabilitation Engineering, 2 (2), 1994
- [3] Chesler N. & Durfee W., Surface EMG as a Fatigue Indicator During FES-induced Isometric Muscle Contraction. J. Electromyol. Kiniesiol. Vol.7(1):27-37, 1997
- [4] Tepavac D. & Schwirtlich L., Detection and Prediction of FES-induced Fatigue, J. Electromyol. Kiniesiol. Vol.7(1):39-50, 1997
- [5] Dimitrova NA, Dimitrov GV., Amplituderelated characteristics of motor unit and Mwave potentials during fatigue. A simulation study using literature data on intracellular potential changes found in vitro. J Electromyogr Kinesiol. 12(5):339-49, 2002
- [6] Tanino Y. et.al., M wave and H-Reflex of soleus muscle before and after electrical muscle stimulation in healthy subjects. Electromyogr. Clin Neurophysiol. 43(6), 381-4, 2003
- [7] Shields RK, et. Al., Effects of electrically induced fatigue on the twitch and tetanus of paralyzed soleus muscle in humans. J Appl Physiol.;82(5):1499-507, 1997
- [8] Merletti R. et.al., Effect of ankle joint position on electrically evoked surface myoelectric signals of the tibialis anterior muscle, Arch-Phys-Med-Rehabil. 74(5): 501-6, 1993

Author's Address

DI. Dr. Dietmar Rafolt Department of Biomedical Engineering and Physic Vienna General Hospital A-1090 Vienna, Währinger Gürtel 18-20

e-mail: dietmar.rafolt@meduniwien.at

INTRAOPERATIVE RECORDING OF SACRAL ROOT NERVE SIGNALS IN HUMAN

G.A.M. Kurstjens*, N.J.M. Rijkhoff*, A. Borau**, A. Rodríguez**, J. Vidal**, T. Sinkjær*

* Center for Sensory-Motor Interaction, Aalborg University, Denmark.

** Institut Guttmann, Badalona, Spain.

Abstract

Electroneurographic signals were intraoperatively recorded from the S3 sacral nerve root in two SCI patients. The aim of this study was to record afferent nerve signals in response to mechanical stimulation of the urinary bladder, rectum and dermatome. Such signals could be used in an implantable neuroprosthesis to treat neurogenic detrusor overactivity. In both patients a neural response was recorded from the dermatome and the rectum, but from the bladder only in one patient. The results were consistent with results from animal and other human studies. Further studies are however needed because the number of subjects investigated remains low.

Introduction

Electrical stimulation of pudendal afferent nerves has an inhibiting effect on the micturition reflex [1]. Continues electrical stimulation of the dorsal penile/clitoral nerve [2, 3], pudendal nerve, and the dorsal sacral roots [4] has therefore been utilized to increase bladder capacity in SCI patients suffering from neurogenic detrusor overactivity (NDO). Because stimulation is only needed to inhibit a detrusor contraction, stimulation could be applied conditionally, i.e. when a contraction occurs. This approach has been shown to be at least as effective as continues stimulation [5, 6].

For clinical application of this treatment modality, a reliable technique for chronic monitoring of bladder activity is required. Biocompatibility and long-term reliability of artificial sensors can be a problem in implantation, but with the advent of methods for long-term electrical interfacing with nerves, recording from the natural sensors has become a realistic alternative [7]. Afferent electroneurographic (ENG) signals related to mechanical bladder activity have been recorded using cuff electrodes placed on (dorsal) sacral roots in the cat [8], pig [9], and human [10, 11].

The current study reports on two SCI patients investigated as part of an ongoing project to monitor mechanical bladder activity by recording ENG signals using cuff electrodes temporary placed on the (extradural) sacral roots in human.

Material and Methods

The study was approved by the local ethical committee of the Institut Guttmann and informed consents were obtained. Nerve signals were recorded in two spinal cord injury patients (Patient 1: male, 43 years, C6 incomplete, 17 years post injury, and Patient 2: female, 45 years, T3 complete, 6 years post injury).

Surgical preparations

Both patients underwent implantation of an extradural Finetech-Brindley sacral root stimulator. A dorsal laminectomy (L5-S4) was performed, and individual roots were identified anatomically and by the response of different muscle groups to electrical stimuation with a hook electrode. A bipolar cuff electrode (length 10mm, 25 µm platinum foil ring contacts 1mm width, and reference contact of the same material mounted on the outside of the cuff) was temporary placed on the extradural sacral nerve root that gave the best bladder response to electrical stimulation with a hook electrode, and the location of the cuff electrode was completely submerge in warm saline. The impedance of the electrode contacts was measured (±90nA sine wave at 1kHz), and finally a sterile telemeter [12] was connected to the cuff electrode.

Experimental protocol

The following protocol was used to study the relation between mechanical activity of the skin, rectum and bladder, and the ENG signals recorded:

- Neural interface The dorsal penile/clitoral nerve was electrically stimulated (1-50mA, 0.2ms pulse duration, 6 pulses/s) using surface electrodes, and elicited sensory compound action potentials (CAPs) were recorded from the sacral nerve root.
- Skin touching ENG was recorded when mechanically stimulating the relevant dermatome by hand (stroking and tapping).
- Rectal distension ENG was recorded during 4 consecutive injections of 50ml warm saline into a rectal balloon (latex condom mounted on a single lumen 18Ch catheter).

• Bladder distension - ENG was recorded during consecutive injections of 50ml warm saline into the bladder until a volume of 400ml was reached or the intravesical pressure exceeded 100 cm H_2O .

The ENG signal received from the telemeter and the bladder and rectal pressure were stored on digital tape (RD-135T, TEAC) for later analysis. After the measurements, the cuff electrode was removed and the normal surgical procedure resumed to implant the extradural stimulation electrodes.

Data processing and signal analysis

Recorded CAPs were averaged to reduce noise, the amplitude was measured peak-to-peak (Vpp), and the onset latency (To) was measured as the time to the first positive peak.

ENG signals were band-pass filtered (300Hz-3kHz) and the variance of the ENG signals and the time average of the pressure signals were calculated per time bin (Tbin = 40ms for cutaneous and Tbin = 100ms for bladder and rectal ENG). The SNR of an ENG response was quantified as the ratio between the variance of the ENG signal during peak neural activity and the variance of the noise and background activity when no stimulation as applied, corrected for the level of noise and background activity (average of 0.5s for bladder and rectal responses).

Results

Patient 1 received a cuff electrode with inner diameter of 3.4mm, and for Patient 2 a cuff electrode with inner diameter of 3.0mm was used because the nerve root was slightly smaller. In both patients, the cuff was placed on the right S3 sacral root and fitted snugly around the nerve. The impedance of the contacts inside the cuff electrode ranged from 1.0-1.3 k Ω (Patient 2) to 2.0-2.1 k Ω (Patient 1).

Sensory compound action potentials (CAPs)

The threshold for a CAP response in Patient 1 was 21mA (To = 6.30ms, N = 57) and 19mA in Patient 2 (To = 5.00ms, N = 58). The CAP responses in both patients to supra maximal stimulation is shown in Fig. 1. The amplitude of the evoked CAPs was similar in both patients: Vpp = $4.15\pm1.54\mu\text{V}$ (N = 58) for Patient 1 and Vpp = $4.35\pm2.38\mu\text{V}$ (N = 60) for Patient 2. However, the onset latency in Patient 2 (To = 3.85ms) was shorter than in Patient 1 (To = 6.30ms).

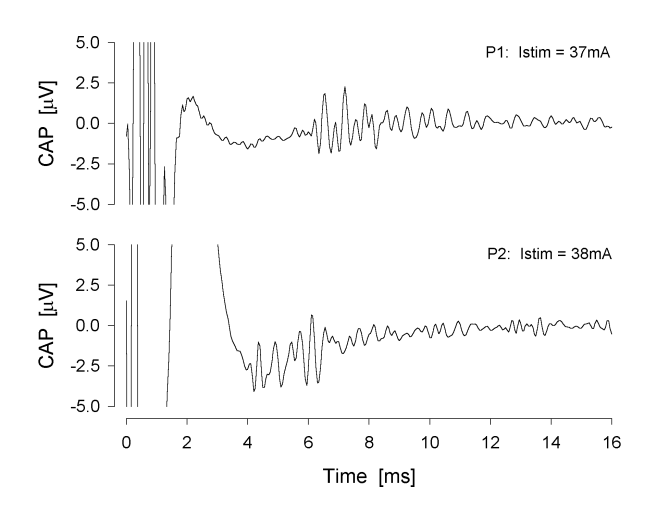


Fig. 1: Averaged CAPs elicited by supra maximal stimulation in Patient 1 (upper trace) and Patient 2 (lower trace). Onset of stimulation was at t=0, and stimulation artefact is present from t=0-4 ms.

Nerve signals from the dermatome

In both patients, clear increases in ENG were recorded when tapping and stroking the S3 dermatome. Although the amplitude of the ENG responses in the raw signal was not much larger than the level of background noise (see Fig. 2a), the presence of a response became much more clear after calculating the variance per time bin (see Fig. 2b).

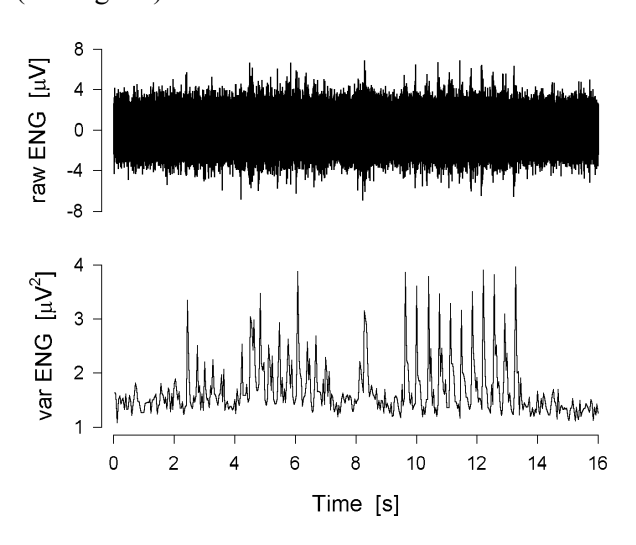


Fig. 2: Raw ENG (upper trace) and the variance per time bin (lower trace), recorded during touching and distinct tapping of the dermatome of Patient 1.

The first and last 2 seconds in Fig. 2 show the background noise. Between t = 2-7s, the skin was touched and stroked, and between t = 10-14s a series of distinct tapping was performed. Tapping the skin evoked ENG responses in Patient 1 with SNR = 1.37 ± 0.35 (N = 28 taps) and in Patient 2 responses with SNR = 1.52 ± 0.95 (N = 84 taps).

Nerve signals from the rectum

The increase in rectal pressure due to the consecutive saline injections in Patient 1 was small (15 cm H_2O). A small increase in ENG was only recorded during the last two injections (SNR = 0.09 and 0.11 respectively). During a series of extraction and rapid re-injection of 50ml from the full rectal balloon, pressure increases were larger (74 cm H_2O) and ENG responses with SNR = 0.10-0.26 (N = 5) were recorded.

The ENG and pressure signals recorded during rectal distension in Patient 2 are shown in Fig. 3. The subsequent 50ml saline injections (at t=35, 65, 95 and 130s) increased the rectal pressure by 17-27 cmH₂O, reaching a peak of 68 cmH₂O. The SNR of the ENG response ranged between 0.12 and 0.14. With the following rapid extractions and re-injections (from t=150s), changes in pressure of 23-37 cmH₂O and ENG responses with SNR = 0.08-0.21 were recorded.

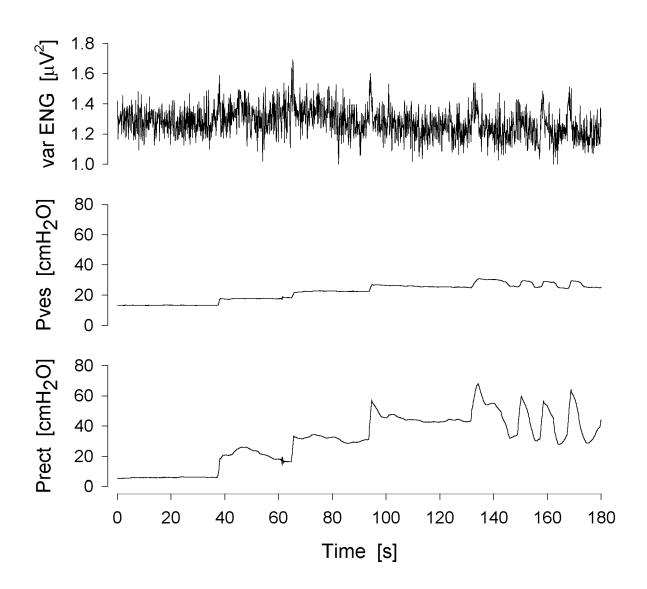


Fig. 3: Variance of the recorded ENG (upper trace), intravesical pressure (Pves, middle trace), and the rectal pressure (Prect, lower trace) during distension of the rectal balloon in Patient 2.

Nerve signals from the bladder

The consecutive saline injection in the bladder of Patient 1 failed to increase the pressure and no ENG response was recorded.

Fig. 4 shows the ENG and pressure signals recorded during eight consecutive 50ml saline injections in the bladder of Patient 2. Each injection increased Pves by 13-48 cm H_2O , clearly visible in the middle trace of Fig. 4, and the maximum Pves obtained was 102 cm H_2O during the fourth injection (t = 75s). ENG responses increased from the first (SNR = 0.10, t = 20s) till the fourth injection (SNR = 0.21, t = 75s), but did not increase more as following injections (t = 90-

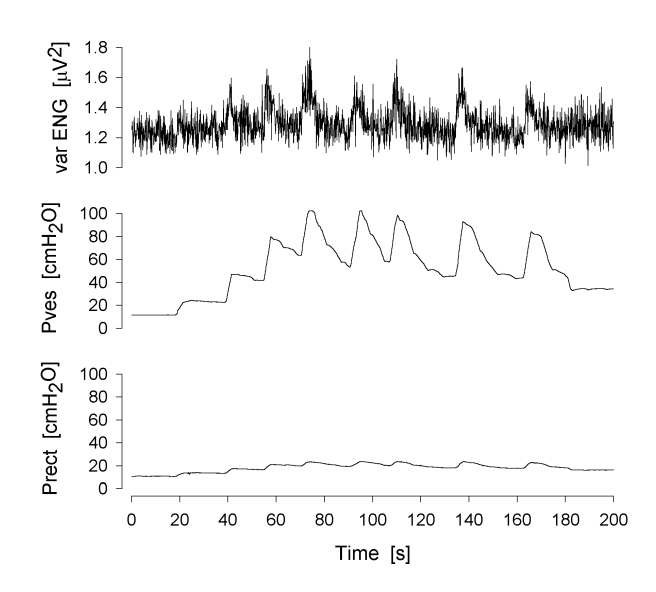


Fig. 4: Variance of the recorded ENG (upper trace), intravesical pressure (Pves, middle trace), and the rectal pressure (Prect, lower trace) during consecutive saline injections in the bladder of Patient 2.

170s) created similar changes in pressure: increases of 40-48 cmH₂O in Pves increased the ENG with SNR= 0.14-0.22 during each injection, after which both pressure and ENG declined rapidly.

Discussion

Sensory nerve signals originating from different pelvic organs were recorded from the extradural sacral root in both patients. The recorded ENG was very small in amplitude, which may be due to the relative large diameter of the cuff electrodes used. Alternatively, the cuff could be placed intradurally, where the dorsal and ventral roots are separated, smaller in diameter, and thus a larger signal would be obtained. Also, the amplitude of the recorded cutaneous ENG was much larger than ENG recorded from the bladder and rectum because the dermatomes are innervated by nerve fibers with much larger diameter compared to the nerve fibers innervating the bladder and rectum.

Furthermore, ENG signals were recorded while the dermatome, rectum and bladder were stimulated individually, and with the patients under general anesthesia. In clinical application however, the level of background neural activity will be much higher and there will be a continuously changing amount of afferent neural activity from different pelvic organs simultaneously. Improvement in recording selectivity and development of advanced signal processing techniques are therefore needed before the use of sensory ENG signals in a neural prosthetic device to control bladder function can be considered.

References

- [1] Fall M., Lindstrom S.: Electrical stimulation. A physiological approach to the treatment of urinary incontinence. Urol. Clin. North. Am. 18, 1991, 393-407.
- [2] Vudosek D.B., Light K.J., Libby J.M.: Detrusor inhibition induced by stimulation of pudendal nerve afferents. Neurourol. Urodyn., 5, 1986, 381-389.
- [3] Wheeler J.S.J, Walter J.S., Sibley P.: Management of incontinent SCI patients with penile stimulation: Preliminary results. J. Am. Paral. Soc., 17, 1994, 55-59.
- [4] Bosch J.L., Groen J.: Neuromodulation: urodynamic effects of sacral (S3) spinal nerve stimulation in patients with detrusor instability or detrusor hyperreflexia, Behav. Brain Res., 96, 1998, 141-150.
- [5] Kirkham A.P.S., Shah N.C., Knight S.L., Shah P.J.R., Craggs M.D.: The acute effects of continuous and conditional stimulation on the bladder in spinal cord injury, Spinal Cord, 39, 2001, 420-428.
- [6] Dalmose A.L., Rijkhoff N.J.M., Kirkeby H.J., Nohr M., Sinkjær T., Djurhuus J.C.: Conditional stimulation of the dorsal penile/clitoral nerve may increase cystometric capacity in patients with spinal cord injury, Neurol. Urodyn., 39, 2003, 130-137.
- [7] Sinkjær T., Haugland M., Struijk J.J., Riso R.: Long term cuff electrode recordings from peripheral nerves in animals and humans. In: Windhorst U., Johansson H, editors. Modern Techniques in Neuroscience Research, Springer-Verlag, 1999, 787-802.
- [8] Jezernik, S., Grill, W. M., Sinkjaer, T.: Detection and inhibition of hyperreflexia-like bladder contractions in the cat by sacral nerve root recording and electrical stimulation. Neurourol. Urodyn., 20(2), 2001, 215-230.
- [9] Jezernik, S., Wen, J.G., Rijkhoff, N.J.M., Djurhuus, J.C., Sinkjaer, T.: Analysis of bladder related nerve cuff electrode recordings

- from preganglionic pelvic nerve and sacral roots in pigs. J.Urol., 163(4), 2000, 1309-1314.
- [10] Grill W.M., Creasey G.H., Wu K., Takaoka Y.: Detection of hyperreflexia-like increases in bladder pressure by recording of sensory nerve activity in human spinal cord. Proceedings of the 5th Annual Meeting of the International Functional Electrical Stimulation Society (IFESS), Aalborg, Denmark, 2004, 234.
- [11] Sinkjær T, Rijkhoff N., Haugland M., Kurstjens M., van Kerrebroek P., Casey A., Kirkham A., Knight S., Shah J., Donaldson NdeN., Craggs M.: Electroneurograpic (ENG) signals from intradural S3 dorsal. Nerve roots in a patient with a suprasacral spinal cord injury. Proceedings of the 5th Annual Meeting of the International Functional Electrical Stimulation Society (IFESS), Aalborg, Denmark, 2004, 273-276.
- [12] Donaldson N. de N., Zhou L., Perkins T.A., Munih M., Haugland M., Sinkjær T.: Implantable telemeter for long-term electroneurographic recordings in animals and humans. Med. Biol. Eng. Comput., 41, 2003, 654-664.

Acknowledgements

This study was supported by grants from the Catalan network "Neuroprosthesis for rehabilitation" (Generalitat de Catalunya, Spain), the Danish National Research Foundation, and the European Commission (REBEC project).

Author's Address

G.A.M. Kurstjens, M.Sc. Center for Sensory-Motor Interaction Aalborg University Fredrik Bajers Vej 7D DK-9220 Aalborg Denmark

E-mail: mku@hst.aau.dk

Home page: http://www.smi.hst.aau.dk/~mku

SENSORY SUPPORTED FES CONTROL IN GAIT TRAINING OF INCOMPLETE SCI PERSONS

I.Cikajlo^{1,3}, Z.Matjačić¹, T.Bajd², R.Futami³ and N.Hoshimiya³

¹Institute for Rehabilitation Republic of Slovenia, Ljubljana, Slovenia ²Faculty of Electrical Engineering, University of Ljubljana, Slovenia ³Graduate School of Engineering, Tohoku University, Japan

Summary

Sensory supported electrical stimulation of the peroneal nerve during treadmill walking is proposed as a gait training modality in incomplete spinal cord injured (SCI) patients. Multisensor device provides the information on the tilt of the shank during the swing phase. The provided information significantly improves the triggering instant of the electrical stimulation. In the same time the swing phase estimation serves as a reference to determine the needed motor augmentation support. Both approaches, triggering as well as the intensity control of the functional electrical stimulation, were applied on healthy person and on C4-5 SCI patient.

State of the Art

In the last decades more incomplete than complete SCI patients are arriving to the spinal units. One of the primary goals of the rehabilitative program for the incompletely paralyzed subjects is to restore their walking patterns. The gait pattern can be restored in paralyzed persons by surface or implanted multi or single channel functional electrical stimulation (FES), by delivering electrical stimuli to the efferent and/or afferent nerves. The swing phase obtained by eliciting a synergistic flexion response through electrical stimulation of the common peroneal nerve was extensively used by our group [2]. The gait training modalities eliciting reflex responses result in complex and natural like movements which are in consequence provoking afferent signals in joints, tendons, and muscles, important for reeducation of walking. Treadmill walking is producing hip extension at the end of the stance phase which is inducing reflex hip flexion and thus initiating the swing phase of walking [1]. The treadmill training can be combined with electrical stimulation of the partially paralyzed extremities and may be used in combination with body weight support (BWS) [4]. The BWS helps the patient to concentrate on walking without having problems with maintaining stability. In the early gait training either physiotherapist or patient is manually triggering the electrical stimulation [2]. When the triggering is performed by the physiotherapist, then the patient is able to focus on the gait performance, while the physiotherapist's task remains to be the estimation of walking quality. Therefore, the instant of triggering is based on physiotherapist's experience and may vary from step to step. Consequently, the patient's walking performance depends on physiotherapist's skills. In order to overcome this undesired dependency, the FES triggering should be automatic, i.e. linked with a selected gait event or gait phase. There were described several attempts of using sensory information for direct control of FES to achieve the desired joint motion [6]. Hereby, we suggest the use of the tilt information of the shank in combination with an algorithm for gait evaluation [3]. The algorithm estimates the quality of the performed swing phase on the basis of the detected gait cycle and assessed acceleration time-course. Afterwards, the swing phase quality is classified into three levels and provided to the patient during treadmill walking as an audio cognitive feedback. The proposed method allows the patient to fully cooperate in the rehabilitation process and to take voluntary actions to improve his/her walking pattern.

In the paper we are proposing the use of the sensory information to trigger the surface peroneal nerve stimulation combined with treadmill walking as a modality for gait training in incomplete SCI persons [5].

Methods

The swing phase of walking in incomplete SCI patients is usually achieved by electrical stimulation of the peroneal nerve. Manual pushbutton or footswitch triggering was replaced by the proposed method based on the assessment of the tilt of the shank. Despite of the fact that the shank angle could be determined by two-axial accelerometer with low-pass filter, we had difficulties designing the efficient low-pass filter due to the time-delay of the high order filter. Therefore, we applied the gyroscope that was built in the multisensor device for the purposes of the swing phase estimation [3]. Using both sensor types and applying a recursive Kalman filter, we

were able to determine the shank angle irrespective of the sensor misplacement or strong heel strike, which were frequent sources of error.

The analysis of the gait cycle shows that the shank angle reaches its peak, in clinical terms the maximal knee flexion, in the pre-swing phase. This is the moment before the toe-off when the lower extremity goes into the swing phase. During the swing phase the knee joint moves toward extension. Therefore, the peak in the shank angle time-course was used to trigger the FES. We have also introduced an adjustable time delay to assure the appropriate instant of triggering for the patients with various motor disabilities.

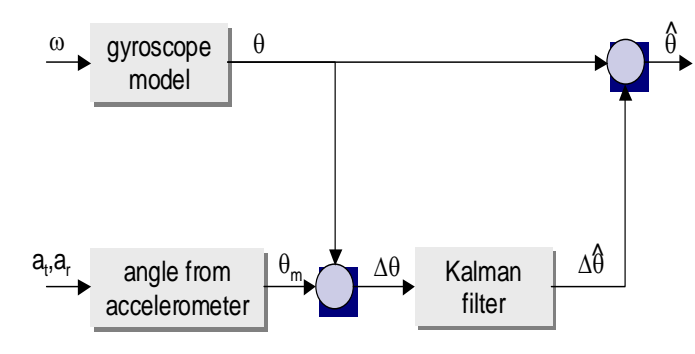


Fig. 1 A Kalman filter is implemented for accurate shank angle (θ) determination.

In the present investigation a healthy subject and a patient with C4-5 spinal cord lesion have participated. The role of the measurements in the healthy subject was to verify the assessed reference

shank angle trajectory, while the patient was involved into the FES treadmill walking. The surface electrodes were placed over the peroneal nerve with the aim to evoke the flexion reflex. A stimulation frequency of 20 Hz, a pulse duration of 0.2 ms and intensity of 35mA were used during the swing phase performance.

Results

The electrical stimulation was triggered by the help of the estimated shank angle as presented in fig.2. When the subject entered the pre-swing phase, the shank angle reached the peak value. Considering the predefined time-delay, the train of electrical stimulation pulses was delivered to the peroneal nerve. Before the gait training session also the duration of the train of stimuli, depending on patient's deficits and demands, was set up.

Our patient had difficulties performing a swing phase and was unable to make a progress of his lower extremity into the swing phase without stimulation. The applied peroneal nerve stimulation significantly increased hip and knee flexion and ankle dorsiflexion during the swing phase of walking. Consequently, the leg progressed into the swing phase efficiently as shown in fig.3. Even more, the patient was able to maintain the stability and walk on treadmill without arm support.

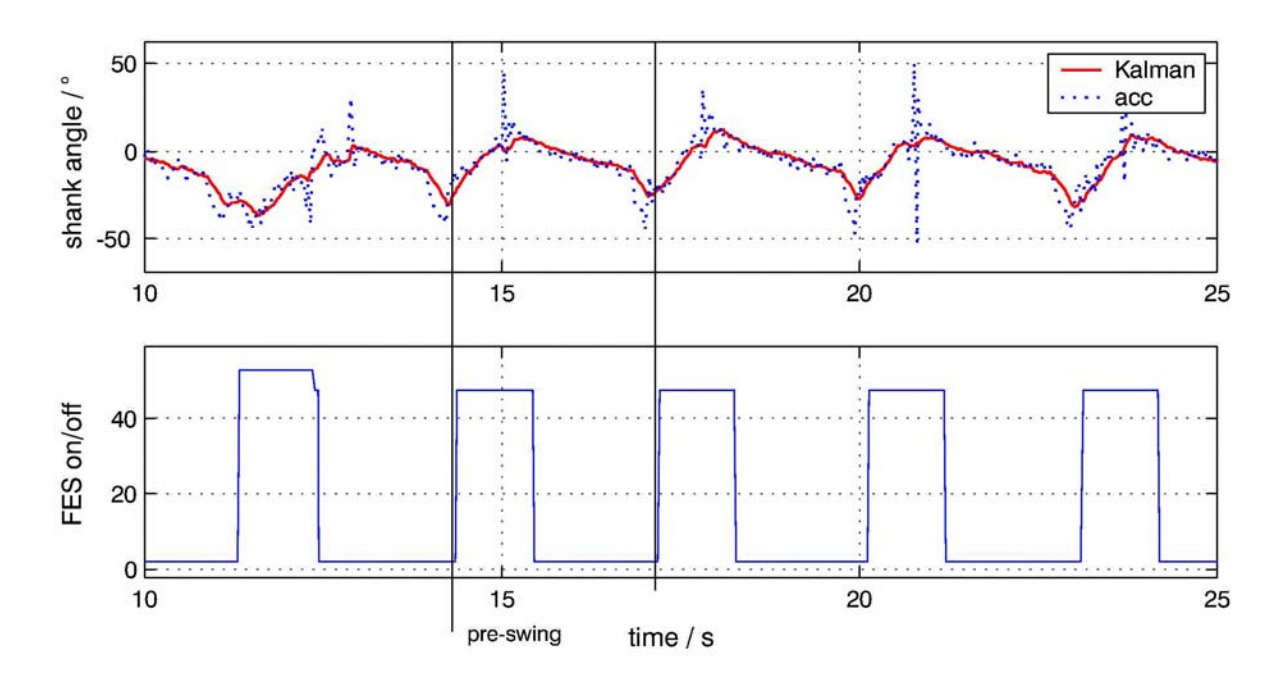


Fig. 2 The instant of FES triggering is determined with shank angle. A time-delay can be set manually.



Fig. 3. Record of an incomplete SCI patient's walking with the peroneal electrical stimulation.

Discussion

FES for lower extremities has been a research issue for several decades. Most of the conclusions were stating that permanent use of FES cannot be very efficient due to the muscular fatigue and patients' rejection of cumbersome devices. We can claim that therapeutic FES has proven successful, especially in combination with other rehabilitation techniques, such as treadmill walking. We have shown an efficient cooperation of the patient which is demonstrated by the successful combination of patients' voluntary action and the use of FES during treadmill walking [5]. The method proposed in the paper is also trying to point out the use of small, portable multifunction sensory system to control the FES for therapeutical purposes after incomplete spinal cord injury.

References

- [1] Wernig A, Müller S. Laufband locomotion with body weight support improved walking in persons with severe spinal cord injuries. *Paraplegia*, Vol. 30, 1992, 229-238.
- [2] Bajd T, Kralj A, Turk R, Benko H, Šega J. Use of functional electrical stimulation in the rehabilitation of patients with incomplete spinal cord injuries. *J Biomed Eng*, Vol 11, 1989, 96-102.
- [3] Cikajlo I, Bajd T. Swing phase estimation in paralyzed persons walking. *Technology & Health Care*, Vol 5, 2002, 425-433.
- [4] Hesse S, Maležič M, Schaffrin A, Mauritz KH. Restoration of gait by combined treadmill training and multichannel electrical stimulation in non-ambulatory hemiparetic patients. *Scand J Rehabil Med*, Vol 27, 1995, 199-204.
- [5] Cikajlo I, Matjačić Z, Bajd T. Development of gait re-education system in incomplete spinal cord injury. *J Rehab Med*, Vol 35, 2003, 213-216.
- [6] R. Dai, R. Stein, B. Andrews, K. James, M. Wieler. Application of tilt sensors in functional electrical stimulation. *IEEE Trans Rehab Eng*, Vol. 4, 1996, 63–72.

Author's Address

Dr. Imre Cikajlo, Institute for Rehabilitation Republic of Slovenia Linhartova 51 1000 Ljubljana, Slovenia e-mail: imre.cikajlo@mail.ir-rs.si home page: www.ir-rs.si

MICROPROCESSOR BASED INCLINOMETER SENSOR FOR USE IN FES

S. Sauermann*, E. Unger*, P. Protz**, M. Bijak*, D. Rafolt*

* Department of Biomedical Engineering and Physics, Medical University of Vienna, Austria

** Fachhochschule Technikum Wien, Vienna, Austria

Abstract

In this work an inclinometer type sensor device was developed. It is intended for measuring the tilt angles of body segments as feedback inputs for control systems in FES. The device is based on a two axis solid state accelerometer sensor, with a microcontroller for signal analysis. It provides 80 digital samples/s over the serial interface. The angular resolution is 0.5 degrees. The absolute error was always below ±4 degrees. There is no need for frequent calibration. Trial measurements of the shank angle during slow walking showed, that the output of the sensor is severely disturbed during fast movements. The system may therefore only be of use in slow movements that do not involve strong transient accelerations: for example standing up, standing, and sitting down. It is intended to use gyroscope sensors compensation in order to the system more generally applicable.

Introduction

Although an increasing number of commercial systems for Functional Electrostimulation (FES) have become available recently, only very few of them use feedback from sensors for monitoring and control. This may be in part due to the lack of proven sensor systems that support the use in everyday life without adding too much complexity.

Inclinometer sensors have been used in FES. Williamson describes the use of different acceleration sensors for gait event detection [1]. Cikajlo successfully used a combination of acceleration and gyroscope sensors for sensing the shank inclination angle during walking [2].

This work was aimed at a rigid, lightweight, easy to use, and reliable sensor system for measuring the tilt of body segments during FES. Multiple sensors on different body segments shall be used to measure joint angles. One main goal was to make the system as small and lightweight as possible, so that it may be fitted into an existing electrode trouser. It was therefore intended to study the feasibility of inclination measurements of body segments during walking with acceleration sensors alone. The static performance was to be tested, and

the sensor output should be compared with an optical gait analysis system.

Material and Methods

The gravitational acceleration is measured in two directions using a solid state acceleration sensor ADXL202 (Analog Devices, Norwood, MA, USA). The signals are analysed by a PIC16F876 microprocessor (Microchip Technology Inc., Chandler, AZ, USA). From the two calibrated acceleration values two inclination angles are calculated: (1) the angle alpha between the sensor x-axis and gravity, projected into the sensor plane, and (2) the angle gamma between the sensor plane itself and gravity. Up to four sensors may be monitored by a single decoder, in order to measure joint angles, e.g of the knee by calculating the tilt difference between the shank and the thigh.

Four sensors were manufactured. Each sensor was calibrated at production time, and the calibration parameters were stored into the EEPROM of the microprocessor. For static measurements the sensors were mounted on a testing device, and rotated over the full range of 360 degrees. The sensor outputs were compared to an absolute angle decoder (Art.Nr.: 07301312, Fa. Leine und Linde, Schweden). Regression curves were calculated and the maximum errors were calculated using Excel (Microsoft Corporation, Redmond, WA USA). This was repeated for different tilt angles gamma of the sensor plane. All measurements were repeated one week later, in order to test the long term stability.

Attempts were made to eliminate accelerations of the body segments themselves, for example during heel strike and heel off events. Low pass filters with cutoff frequencies from 45Hz down to 0.5 Hz were applied on the raw acceleration signals before calculating the inclination angles.

Results

The sensor provides 80 samples/s of both angles, alpha and gamma via the digital RS232 interface. It consumes 5 mA at a supply voltage of 6 V.

The angular resolution is 0.5 degrees (alpha) and 1-10 degrees (gamma). The maximal error of alpha

was always between \pm 4 degrees if gamma was between -75 and 75 degrees. The maximum error for the angle gamma was in the range of \pm 5 degrees for gamma greater than 20 degrees. The measurements were repeated one week later without recalibration, and showed no noteable changes. An example of the static tests of the four calibrated sensors are shown in Fig. 1, where the sensor plane was exactly vertical, gamma therefore being zero.

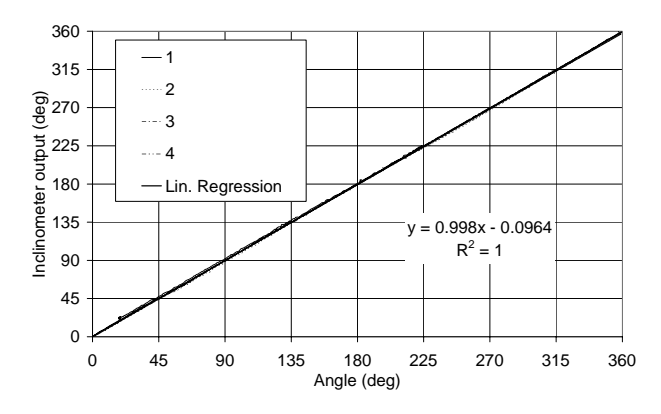


Fig. 1: Example of a static measurement of all 4 sensors. The inclination angle calculated by the inclinometer sensor resembles the tilt angle very closely over the complete 360 degree range.

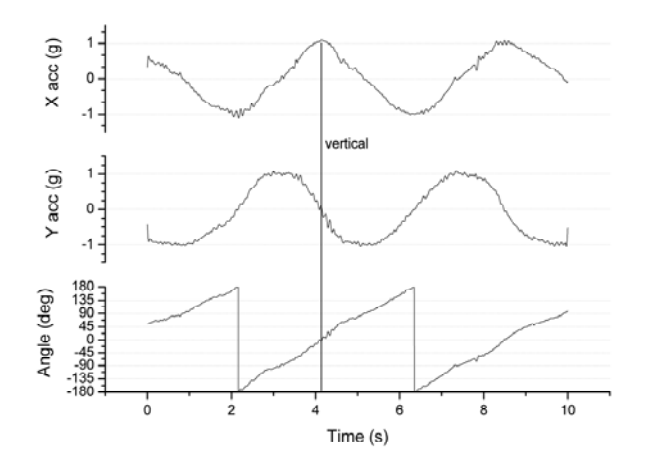


Fig. 2: The sensor output, as a testperson holds it in the hand and slowly rotates it over the full 360 degree range. The sensor plane is near vertical (gamma=0). The bottom trace shows the angle alpha between the x-axis and gravity, projected into the sensor plane.

Fig. 2 shows a trial measurement. The sensor is held by a testperson, which slowly rotates it over the full 360 degrees range. The acceleration signals in the upper two traces of Fig. 2 were filtered with a 45 Hz lowpass filters.

Fig. 3 shows the results of a first measurement of the shank angle on a healthy testperson during slow walking on an even surface, again with 45 Hz lowpass filters. The shank angle signal is distorted by dynamic accelerations. This is especially

obvious after the heel on and heel off events. In other trials the distortions were even more dramatic, so that no clean inclination angle signal could be derived.

Low pass filters with cutoff frequencies from 45 down to 0.5 Hz were tested. The inclination angle measurements were not significally improved.

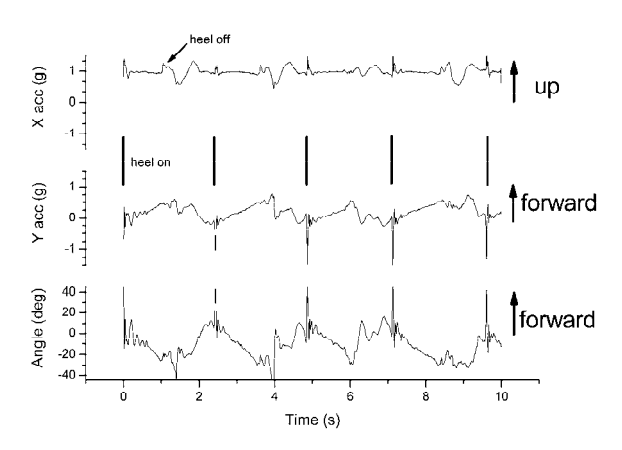


Fig. 3: Shank angle measured with an inclinometer sensor during slow walking. The heel on and off events are marked in the acceleration curves. The angle output is distorted by accelerations of the shank.

Discussion

In this work an inclinometer sensor was developed was tested in static measurements. The inclination angle measurements were found to be accurate and fast enough for applications in FES. First trial measurements of the shank inclination during walking resulted in inclination curves similar to those found in the literature [3]. However, accelerations of the shank disturbed measurements severely. These components could not be eliminated by low pass filtering, probably because the disturbing accelerations overlap the relevant inclination signal components very much. The comparison of the sensor output to the optical gait analysis system, as initially planned, was therefore not conducted.

We conclude that acceleration measurements alone the way they were used here were not sufficient for measuring body segment angles during normal and fast walking. The sensor in its present form is therefore limited to applications that involve slow movements, without strong transient accelerations: standing up, standing, and sitting down. Future work will involve gyroscope sensors in order to compensate for the accelerations of body segments, as it has been demonstrated by Cikajlo [2].

References

- [1] Williamson, R., Andrews, B.J.: Gait event detection for FES using accelerometers and supervised learning. IEEE Trans Rehab Eng, 8 (3), 2000, 312-319.
- [2] Cikajlo I., Matjacic Z., Bajd T.: Shank Angle Estimation in Locomotor Training of Incomplete Spinal Cord Injured Persons. Proceedings of the World Congress on Medical Physics and Biomedical Engineering, 2003, Sydney, Australia, 24-29.August
- [3] Perry, J.: Gait analysis: Normal and pathological function. Slack, USA, 1992, p89-130.

Acknowledgements

The authors wish to thank Gerhard Kirsch for his major contributions during the design of the circuit and the software.

Author's Address

Stefan Sauermann, PhD
Medical University of Vienna
Department of Biomedical Engineering and
Physics
Waehringer Guertel 18-20 / 4L
1090 Vienna, Austria
e-mail: stefan.sauerman@meduniwien.ac.at
home page: http://www.bmtp.akhwien.ac.at/bmt/home.htm

Multimodal, RF based Body Area Network for Device Control

S. Mina^a, S. Hanke^b

^aARC Seibersdorf Research GmbH ^bTechnische Universität Dresden

Abstract

Using electro-physiological signals like EMG or EOG for device control is a promising research area. The application in practice however has the disadvantage that electrodes have to be attached to the user and all electrodes have to be wired to biosignal amplifiers and the device to be controlled. To minimize the effort of electrode application and to avoid wiring at all a set of biosignal amplifiers with body area network connectivity is being developed. In the first stage an EMG module and the base station of the body area network is demonstrated.

Introduction

Usually body area networks (BAN) are associated either with exchanging electronic business cards by handshake [1] or with physiological monitoring [2]. Some projects focus on mobile telephony applications in conjunction with BAN technology for telecare [3] and other projects focus on local applications in hospitals [2, 4] e.g. intensive care units (ICUs).

This paper describes the application of body area network concepts in the field of rehabilitation technology to control devices like computer mouse emulators or nurse calling systems in hospitals.

One of the target user groups of the system could be patients with spinal cord injuries or equivalent diseases. By applying EMG activated devices on defined muscle groups the patients can interact with their surrounding using environmental control devices which are operated by the EMG device.

Materials and Methods

Due to the fact that the upper portion of the m. trapezius and the m. sternocleidomastideus use the n. accessorius (segment XI) as path of conduction, spinal cord injuries even at C7 or C6 will not affect the ability to activate this muscles [6].

For the development of signal processing algorithms and for the testing of algorithms and hardware a set of test EMG signals was recorded. The signals were derived from the m. trapezius with AgAgCl surface electrodes using Grass biosignal amplifiers and a 16 bit data acquisition system from IOtech. With this test data off-line simulation of signal processing and detection algorithms could be performed.

Before a threshold detection of the EMG signal is possible the envelope of the signal has to be calculated. Instead of using a simple rectifier it was decided to calculate the RMS (root mean square) of the EMG signal. The disadvantage of a peak rectifier could be that short spikes, with a small amount of energy, deliver the same peak value as a DC voltage of the same level but much higher energy. RMS calculation (1) delivers information of the effective voltage which is equivalent to the energy of the signal. RMS calculation of the EMG signal was chosen since very irregular waveforms of the signal can be expected and the RMS value provides a reflection of the effective voltage independent from the waveform.

$$RMS(x) = \sqrt{\frac{\sum_{i=1}^{n} x_i^2}{n}}$$
 (1)

To avoid unwanted triggering of the threshold detector caused by a permanent high muscle tonus an additional slope detection [7] was implemented. Only a slope with a certain amplitude can trigger the detector which can now not be influenced by high bias levels.

For an easy realization of the prototype ISM band RF modules seem to be a good choice because they minimize the engineering effort. To avoid disturbance by common 433MHz remote control devices the 868MHz ISM band was chosen. Similar technology could be identified in other experimental body area network setups [5] and seem to be, next to technologies like BlueTooth, a promising choice also in future since there are growing new stan-

dards for wireless control and sensor networks like IEEE 802.15.4 (ZigBee Alliance) operating in 868, 900 and 2450 MHz ISM bands that will become also interesting for medical applications.

The BAN protocol must provide a secure data transfer, device and net identification, exchange of device class, functions of the device and payload data transmission. For example it must be possible to distinguish between 'intelligent' sensors which perform all signal processing tasks themselves and send only trigger events and between sensors which transmit the raw data. With this information another device in the network could determine if a communication with the sensor is possible and the device can respond to transmissions of the sensor.

Results

The lab prototype setup consists of an EMG sensor with integrated signal processing, a relay box with five outputs and a PC unit with USB interface.



Figure 1. Base Station

All devices are equiped with an Adcon addLink868 half duplex RF module which already provides addressed network modes with up to 65536 different network identifications and up to 256 devices for each network ID.

The EMG sensor module uses a Texas Instruments MSP430 ultra low power 16bit microcontroller which handles all processing of the EMG signal and the BAN protocol. EMG is derived with disposable Ag-AgCl electrodes, an instrumentation amplifier and the on-chip ADC at a sample rate of approx. 400 samples per second and the RMS value is calculated over a rectangular window with a length

of 32 samples. A pushbutton on the module allows to send a request message on the net containing the device ID, the modality of the device and the device class. The example below shows a request from an EMG, binary class device with the ID 10.

10=R:EM:B

Binary class devices, like our EMG sensor, only send a trigger message to the network so that a binary mode reciver could perform an action when a trigger event is received.

The fact that the sensor modules should be miniaturized and may be hermetically sealed for some applications rise the problem of configuration of the modules. Compared with the relay box which allows a menu controlled setup of different parameters there is no space for comfortable displays or keypads on the sensor devices and also a plug to connect a programming device seem not suitable. Also an access via the BAN is not possible because the addressed mode impedes a communication between two networks with different ID.

The solution was found by using iButton[®] technology, which has it's origin at Dallas semiconductor. Small EEPROMs or other non volatile memories with OneWire[®] interface in small metal housings similar to watch batteries. A single iButton[®] with an EEPROM inserted into the sensor module holds parameters like device number and network ID and can easily be inserted and removed in the sensor device. The EEPROM can be loaded on the PC via a special software and a USB dongle.

The whole assembly can be powered with rechargeable NiMH, Li-Ion or Li Polymere batteries since it operates at voltages down to 3 VDC and has a power consumption of approx. 4 mA (mean value measured over a period of time of 5 minutes, device triggered every 10 seconds).

For monitoring BAN traffic, simulating devices and to receive payload data a PC module with USB interface has been developed. It can be operated in addressed modes to receive and transmit data in a BAN with a certain ID or it can be operated in a transparent mode to view raw data of the devices independent from their network number. The PC module acts only as bridge and all additional functionality comes from various test software modules programmed in LabView 6.1.

The relay box shown in figure 1 has five relay outputs and provides easy to use menus to set up parameters, assign devices and to invoke special modes of operation like the RF level monitoring. On a device request the module figures out if the request is from a device with a suitable device class, because the box provides no data processing and can act only on trigger messages from binary modules. If the class is identified and correct it is checked if the requesting device is allready assigned to an output. New devices can now be assigned to one of the five outputs and allready assigned devices can be deleted from the system. The module is based on an Atmel AVR® microcontroller since there is no need to minimize the power consumption because it is operated from mains.

Discussion

The prototype is going to be evaluated in clinical practice after it delivered promising results during lab testing. For the future the design of new modules like EOG amplifier devices for the operation of a mouse emulator is planned. In combination with the EMG modules it could be possible to navigate the mouse cursor by eye movements (measured with the EOG module) and to emulate the left and right mouse click with the help of the EMG modules. Evaluation of the system, miniaturization of the modules and efficient power sources will certainly be the most important tasks for future development and research.

In general assistive technology can be associated with an improvement of quality of life trough an increased autonomy of the user. The use of wireless, wearable sensor technology may bring and additional enhancement of quality of life [9] since the application of the device and the operation are easier compared with wired ones.

References

- [1] Zimmerman T.:Personal Area Networks: Nearfield intrabody communication. IBM Systems Journal Vol. 35, No. 3&4, 1996 - MIT Media Lab
- [2] Jovanov E., Raskovic D., Lords A.O., Cox P., Adhimi R., Andrasik F.: Synchronized physiological monitoring using a distributed wireless intelligent sensor system. IEEE Engineer-

- ing in Medicine and Biology Conference, Cancun, Mexico, 2003
- [3] Konstantas D., Jones V., Bults R.: MobiHealthinnovative 2.5G/3G mobile services and application for healthcare. 11th IST Mobile and Wireless Telecommunications Summit 2002 June 16-19, 2002; Thessaloniki, Greece
- [4] Noury N. et al.: Wireless ambulatory acquisition of high resolution physiological signals. European Congress an Telemetry, Garmisch-Partenkirchen, Germany, 2000
- [5] Coronel P., Schott W., Schwieger K., Zimmermann E., Zasowski T., and Chevillat P. (Editor): White Presentation on Wireless Body Area and Sensor Networks, 8th Wireless World Research Forum (WWRF8bis) Meeting, Beijing, China, Feb. 2004.
- [6] Mummenthaler M., Mattle H.:Neurology, Thieme, 2003
- [7] Mina S., Prazak B., Hochgatterer A.: A Dynamic Force Processing Input Strategy. 2nd Cambridge Workshop on Universal Access and Assistive Technology, March 22-24, 2004, Cambridge, United Kingdom
- [8] Baldus H., Klabunde K., Müsch G.: Reliable Set-Up of Medical Body-Sensor Networks. In Wireless Sensor Networks, Lecture Notes in Computer Science, Volume 2920/2004, Springer, 2004
- [9] Park S., Jayaraman S.: Enhancing the Quality of Life Trough Wearable Technology. IEEE Engineering in Medicine and Biology Magazine, Vol. 22, May-June 2003

Author's Address

Ing. Stefan Mina ARC Seibersdorf research GmbH Rehabilitation & Inclusion Research Group Viktor Kaplan Str. 2/1, A-2700 Wr. Neustadt e-mail: stefan.mina@arcsmed.at http://www.arcsmed.at

COMPUTER SIMULATION FOR MULTICHANNEL CLOSED-LOOP FES CONTROL OF THE WRIST JOINT

T. Watanabe*, M. Otsuka**, M. Yoshizawa*, N. Hoshimiya***

* Information Synergy Center, Tohoku University

** Graduate School of Engineering, Tohoku University

*** Tohoku Gakuin University

Abstract

A musculoskeletal model of the upper limb for FES research work was developed in this study. Movements of the elbow, the forearm and the wrist could be controlled by stimulating 15 muscles with the shoulder joint fixed at an arbitrary angle of flexion/extension. The muscle model had nonlinear length-force and velocity-force relation-ships, recruitment characteristics and activation dynamics. Nonlinear joint angle dependency of moment arm and passive viscoelastic property were also included into the model. The model was examined in multichannel closed-loop FES control of 2-DOF of movements of the wrist joint. Model predictions were qualitatively similar to results of experiments performed on neurologically intact subjects. Computer simulation studies using the developed model would be reasonable as an alternative to experiments in FES research work.

Introduction

In order to improve the current clinical FES system in Japan that is an open-loop control system, we have been developing a multichannel closed-loop FES control method [1, 2]. In studies of an FES control method, however, experiments with subjects, to whom electrical stimulation is applied, are required. Those experiments sometimes cause burdens on subjects and low reproducibility due to differences between subjects and so on.

Computer model simulation can be effective in FES research work because it makes it possible to evaluate new controllers or control methods without experiments on subjects. Since electrically stimulated musculoskeletal system shows complicated nonlinear and time variant properties, a musculoskeletal model at least including nonlinear properties has to be utilized for providing an alternative to experiments with subjects in FES studies.

In this paper, a musculoskeletal model of the upper extremity that would be used in FES study was developed. The developed musculoskeletal model was examined in closed-loop FES control of two degree-of-freedom (DOF) of movements of

the wrist joint through computer simulation comparing to experimental results obtained from neurologically intact subjects.

Material and Methods

Musculoskeletal Model for FES Study

A skeletal model of the upper extremity was constructed for FES control of elbow flexion/extension, forearm pronation/supination, and wrist dorsi/palmar flexions and radial/ulnar flexions. The shoulder joint was fixed at an arbitrary angle of flextion/extention. The 15 prime movers of those movements were modeled to be stimulated: biceps brachii long head, biceps brachii short head, brachialis, brachioradialis, triceps brachii long head, triceps brachii lateral head, triceps brachii medial head, pronator quadratus, pronator teres, supinator, extensor calpi radialis longus, extensor calpi radialis brevis, extensor carpi ulnaris, flexor carpi radialis and flexor carpi ulnaris.

The whole musculoskeletal model is outlined in Fig.1. Muscle force F_{CE} was described by the Hill type muscle model consisted of activation level determined by electrical stimulation a(t), length-force relationship k(l), velocity-force relationship h(v) and maximum force F_{max} as follows:

$$F_{CE} = a(t)k(l)h(v)F_{\text{max}}$$
 (1)

t showed time. l and v were muscle length and contraction velocity, respectively, which were functions of time. Active torque τ_{CE} developed by electrical stimulation was calculated by muscle force F_{CE} and moment arm $r_f(\theta)$. That is,

$$\tau_{CE} = F_{CE} \cdot r_f(\theta) \tag{2}$$

Moment arm $r_f(\theta)$ was represented by an approximated polynomial equation as a function of joint angle θ for each movement of each muscle [3]. Each element of the F_{CE} is described as bellow.

The recruitment property of electrically stimulated muscle u(s) was modeled by the following [4]:

$$u(s) = sc \cdot \tanh\left\{sh^{REC}\left(s - xc\right)\right\} + yc \tag{3}$$

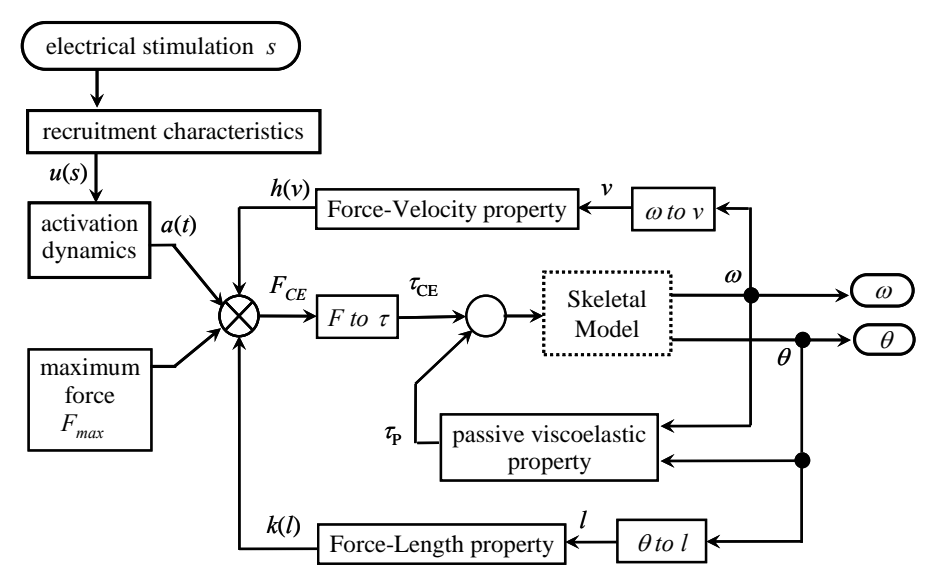


Fig. 1: Outline of the musculoskeletal model

where sc, sh^{REC} , xc and yc were parameters. Electrical stimulation was expressed by normalized stimulation intensity s as a function of time. The muscle activation a(t) was described by the following dynamics using recruitment level [5]:

$$\frac{da}{dt} = \frac{1}{t_r} \left\{ u(s) - a(t) \right\} u(s) + \frac{1}{t_f} \left\{ u(s) - a(t) \right\}$$
(4)

where t_r and t_f were time constants for rising and falling, respectively.

The length-force relationship k(l) was described by eq. (5) using muscle length l that was a function of time and optimum muscle length l_o [6].

$$k(l) = 1 - \left(\frac{l - l_o}{0.5l_o}\right)^2 \tag{5}$$

The velocity-force relationship h(v) during shortening of muscle was modeled by using muscle contraction velocity v that was a function of time and maximum contraction velocity v_{max} [6]. For lengthening of muscle, the relationship was described based on our previous work [7].

$$h(v) = \frac{v_{\text{max}} - v}{v_{\text{max}} + 2.5v} \quad (v \le 0 : shortening)$$

$$h(v) = 1.3 - 0.3 \cdot \frac{v_{\text{max}} + 2.5v}{v_{\text{max}} - 2.5^{2}v} \quad (v > 0 : lengthenig)$$
(6)

The maximum muscle force developed by electrical stimulation F_{max} was determined by PCSA (physiological cross sectional area) as follows [3].

$$F_{\text{max}} = PCSA \times 2.2 \tag{7}$$

The passive viscoelastic element developed passive torque τ_P calculated by eq. (8) for each joint movement [8]. The range of motion was also

represented by this property.

$$\tau_{n} = k_{0}\theta + b_{0}\omega + k_{1}\left\{\exp(k_{2} \cdot \theta) - 1\right\} \tag{8}$$

where θ and ω , which were functions of time, were joint angle and angular velocity, respectively. Parameters k_0 , b_0 , k_1 and k_2 were constants determined for each joint movement. In this study, same passive property was used for the wrist dosri/parmar and radial/ulnar flexions.

Validation of Musculoskeletal Model

The developed model was examined in multichannel closed-loop FES control of the wrist comparing to the experimental results that we performed with neurologically intact subjects [1, 2]. Two DOF of movements of the wrist joint, which dorsi/palmar flexions and radial/ulnar flexions, were controlled by stimulating the extensor calpi radialis (ECRL/B), the extensor carpi ulnaris (ECU), the flexor carpi radialis (FCR) and the flexor carpi ulnaris (FCU). Since surface electrodes were used in the experiments, ECRL and ECRB were assumed to be one muscle because of difficulty in selective stimulation to them. Target trajectory of the closed-loop control was circle trajectory in joint angle plane. Model simulations were performed under two different cycle periods (movement velocity) and two different shoulder positions.

Model parameters were adjusted to produce an experimentally acceptable delay time from the onset of electrical stimulation to a start of movement and a time constant in the first order delay approximation of step response. The input-output characteristics of the muscles were also roughly fitted to experimentally measured one through model parameters adjustments.

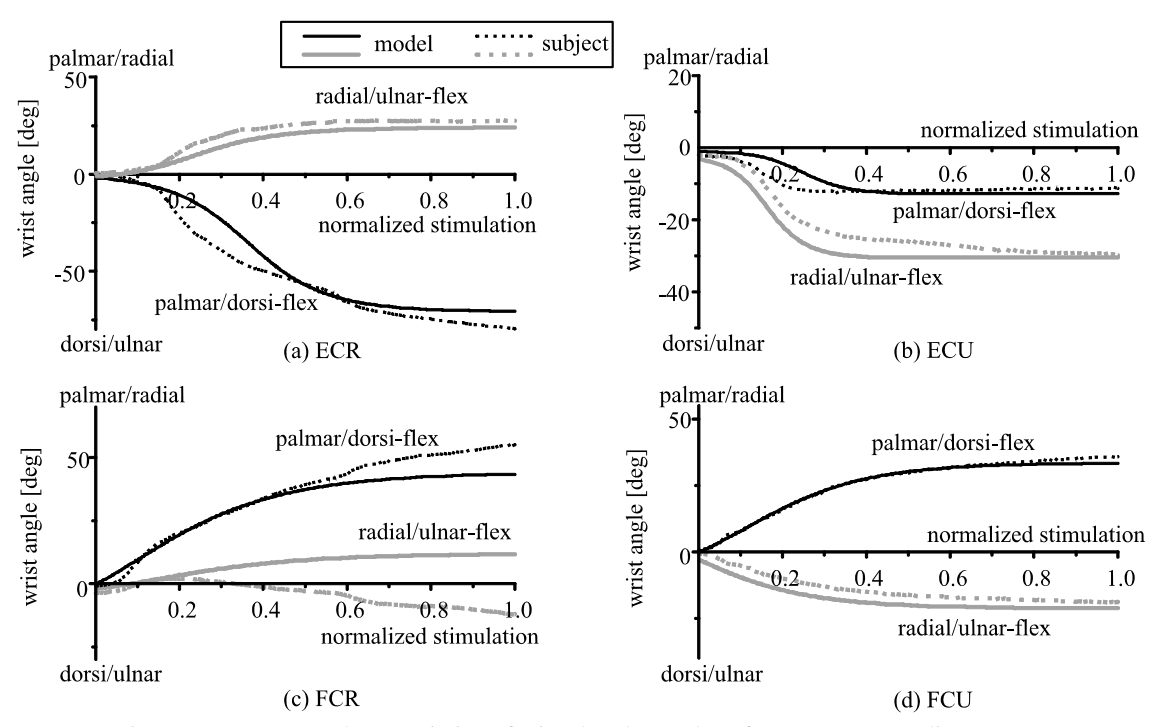


Fig. 2: Input-output characteristics of stimulated muscles after parameters adjustments.

Results

Fig.2 shows the input-output characteristics of the four muscles obtained from a normal subject and the model. Although it was difficult to make good fitting if a muscle had different nonlinearity in the characteristics of its functions, the model represented roughly similar characteristics.

An example of model simulation result of closed-loop FES control is shown in Fig.3 with the experimental result under the same condition. Stimulation pattern of the model was similar to the experimental one. That is, the stimulation intensities of ECR and FCU, those of ECU and FCR changed in reciprocal pattern as seen in antagonistic muscle pairs. However, stimulation intensities obtained from the model simulation were larger than those of the experiment.

Other model simulations also showed qualitatively similar responses to experimental results. For example, changing movement velocity or the shoulder joint angle (to put the upper limb in the horizontal plane) caused similar variation of stimulation intensities and joint angle trajectories between model simulations and the experimental results.

Discussions

Stimulation intensities of the model were larger than those of experiments as shown in Fig.3. This was mainly because the input-output characteristics of the model were not completely the same as the experimental one, but just roughly

fitted to them in model simulations.

In the model simulation result (Fig.3(a)), small oscillations of stimulation intensity was observed. Since the parameters of the PID controller were calculated by using slopes of approximated linear lines of the input-output characteristics [1], those oscillations were observed in experimental results if the linear approximations were insufficient. Even in those cases, the undesirable oscillation was suppressed by using an approximated line at the steepest part of the characteristic. In the model the simulation, same adjustment the approximated linear suppressed line the undesirable oscillation.

In this study, the aim of using model simulation is not to predict responses on a specific patient, but just to use it as an alternative to the nonlinear musculoskeletal system. For this purpose, model simulations will be accepted if it predicts qualitatively experimental results. Since most of experimental results obtained from normal subjects were reasonably predicted by the model, the developed model is considered to be sufficient for this purpose. The model will be effective as an alternative to human subjects in FES research work.

References

[1] Watanabe T., Iibuchi K., Kurosawa K., Hoshimiya N.: A method of multichannel PID control of 2-degree of freedom of wrist joint movements by functional electrical stimulation, Systems and Computers in Japan, 34(5), 2002, 25-36

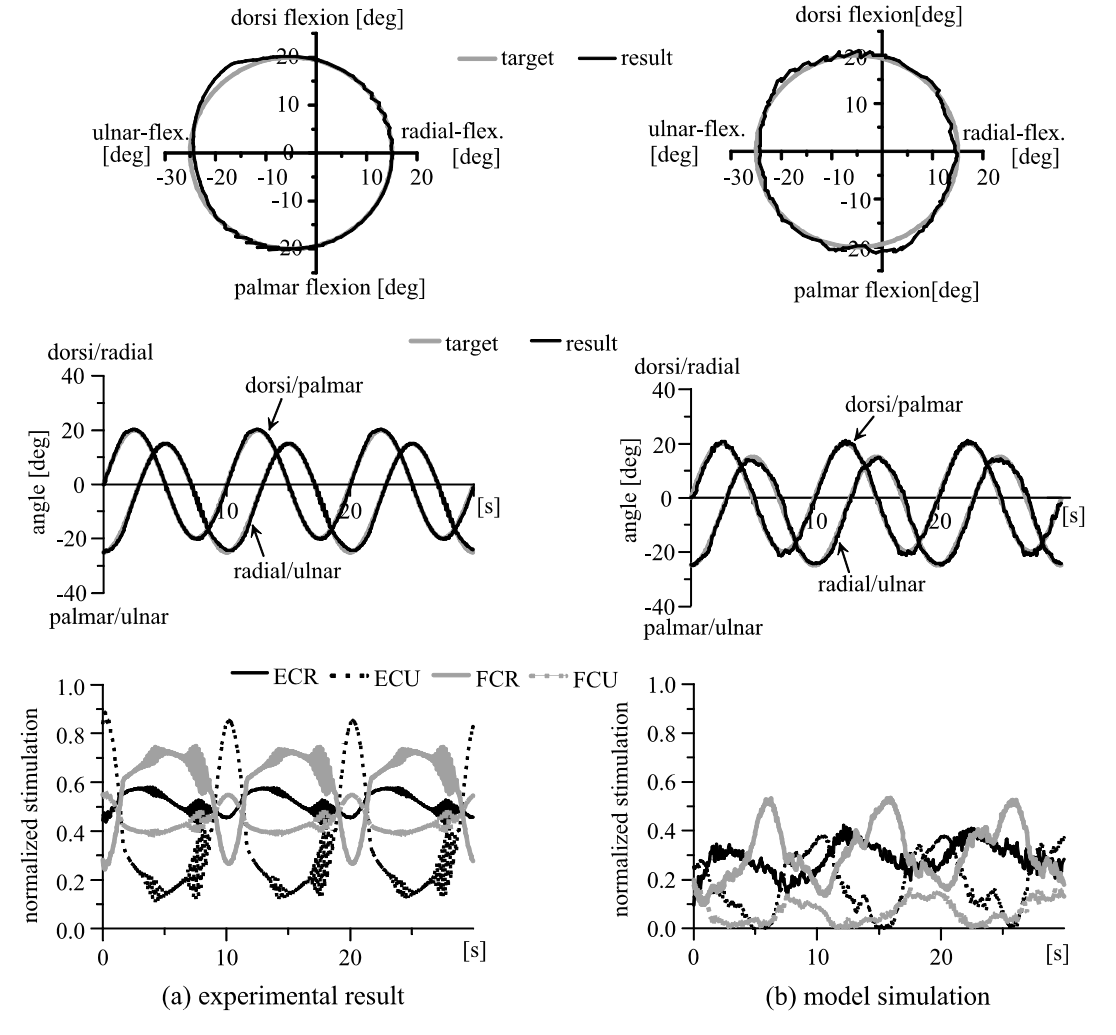


Fig. 3: Closed-loop FES control of 2-DOF movement of the wrist joint stimulating 4 muscles (the upper limb was in the direction of the gravity).

[2] Kurosawa K., Watanabe T., Futami R., Hoshimiya N., Handa Y.: Development of a closed-loop FES system using 3-D magnetic position and orientation measurement system, J. Automatic Control, 12(1), 2002, 23-30

[3] Lemay M.A, Crago P.E: A dynamic model for simulating movements of the elbow, forearm, and wrist, J. Biomech., 29(10), 1996, 1319-1330

[4] Levy M., Mizrahi J., Susak Z.: Recruitment, force and fatigue characteristics of quadriceps muscles of paraplegics isometrically activated by surface functional electrical stimulation, J. Biomed. Eng., 12, 1990, 150-156

[5] Pandy M.G, Ganer B.A, Anderson C.: Optimal control of non-ballistic muscular movements –a constant-based performance criterion for rising from a chair, J. Biomech. Eng., 37, 1995, 15-26

[6] Nigg B.M, Herzong W.: Biomechanics of the musculo-skeletal system, John Wiley & Sons Inc., NY, 1995

[7] Eom G., Watanabe T., Futami R., Hoshimiya N., Handa Y.: Computer-aided generation of stimulation data and model identification for functional electrical stimulation (FES) control of lower extremities, Frontiers Med. Biol. Eng., 10(3), 2000, 213-231

[8] Winters J.M, Stark L.: Analysis of fundamental human movement patterns through the use of in-depth antagonistic muscle models, IEEE Trans. Biomed. Eng., 32(10), 1985, 826-839

Acknowledgment

This study was partly supported by the Ministry of Education, Culture, Sports, Science and Technology of Japan under a Grant-in-Aid for Scientific Research.

Author's Address

e-mail: nabe@isc.tohoku.ac.jp

Dr. Takashi Watanabe Information Synergy Center, Tohoku University (In Dept. Electronic Eng, Tohoku University) Aramaki-aza-Aoba 05, Aoba-ku Sendai 980-8579, Japan

HIERARCHICAL HYBRID CONTROL FOR THERAPEUTIC ELECTRICAL STIMULATION OF UPPER EXTREMITIES

Mirjana B. Popović^{1,2}, Dejan B, Popović^{1,3}

¹Center for Sensory Motor Interaction, Aalborg University, DK ²Center for Multidisciplinary Studies, University of Belgrade, SCG ³Faculty of Electrical Engineering, University of Belgrade, SCG

Abstract

We describe the control applied for the Functional Electrical Therapy (FET) of the arm and hand in post-stroke hemiplegic patients. The controller implements two properties being characteristic for able-bodied humans when performing Reach / Grasp / Release (RGR) maneuvers: 1) Temporal synchrony, and 2) Spatial synergies. Temporal synchrony comprises the execution of RGR as a sequence of the following phases: 1) the hand transport to the object post (positioning or reaching), hand orientation and opening (prehension), hand closing (grasping of the object); 2) hold and move object; 3) using the object (the actual task); 4) returning the object; and 5) finally releasing it at the object post. Spatial synergy relates to rules establishing mappings among central control variables to individual joints of a limb, and the consequences are relations among performance variables. The kinematical data needed for the design of control was collected from 18 able-bodied subjects by using goniometers, and custom designed software LabVIEW environment. running incoordination control was designed by applying heuristics to determine temporal synchrony, and radial-basis function neural networks for determining spatial synergies. The validity of the control algorithm was tested in five post-stroke hemiplegic patients otherwise unable to grasp and release objects with their paretic arm.

Introduction

Clinical implementations of the Functional Electrical Therapy – FET [1] suggested that the functioning of post-stroke hemiplegic patients in the acute phase was improved to a higher level compared to patients who received conventional therapies only. The review [2] of the clinical studies which analyzed the recovery in hemiplegic post-stroke patients, that follows traditional therapeutic electrical stimulation suggests only modest recovery compared to the one that we found in the FET application. This is in accordance with the very promising reports obtained from the constraint induced movement therapy (CIMT)

studies [3]. The significant recovery after FET is likely benefiting from several elements: 1) intensive exercise that is augmented with the electrical stimulation; 2) provision of the function that is otherwise not available due to a paresis; 3) increased motivation to use the paretic arm; and 4) augmented activation of the afferent neural pathways due to electrical stimulation.

The control that we developed relies on a so-called coordination model of the Reaching / Grasping / Releasing (RGR) [4]. The hierarchical control for the RGR neural prosthesis comprises preprogrammed time sequencing and preprogrammed spatial synergies [4]. At the highest control level the user of a neural prosthesis selects voluntarily an action and the modality of operation, that is, she/he specifies the task. At the middle control level, the controller itself supplies temporal synchrony by applying a discrete rule-base algorithm. This rulebase controller operates as a finite automaton, and implements the state model of movement that was cloned by a heuristics of machine classification of the data acquired in able-bodied humans. At the lowest level, the controller implements spatial mapping determined by rule-based methods. The spatial synergies are performed in time windows established by temporal synchrony. The execution level, that is, stimulation pattern, directly matches the synergistic control laws.

A neural prosthesis that mimics biological control, most likely facilitates the recovery because of the external activation that is synchronized with the biological use of preserved sensory-motor systems.

Procedure for Designing the Control

Determination of temporal and spatial synergies. We studied 18 able-bodied subjects. The subjects were seated in front of a desk and performed five RGR tasks. The RGR tasks have been selected to include the following: 1) three grasping strategies (palmar grasp, lateral grasp, precision grip); 2) six different object positions within the working space defined with two attributes: distance and laterality, and 3) different sizes and masses of objects. The selection was accomplished by analyzing the following: 1) drinking from a 0.5-liter juice can; 2)

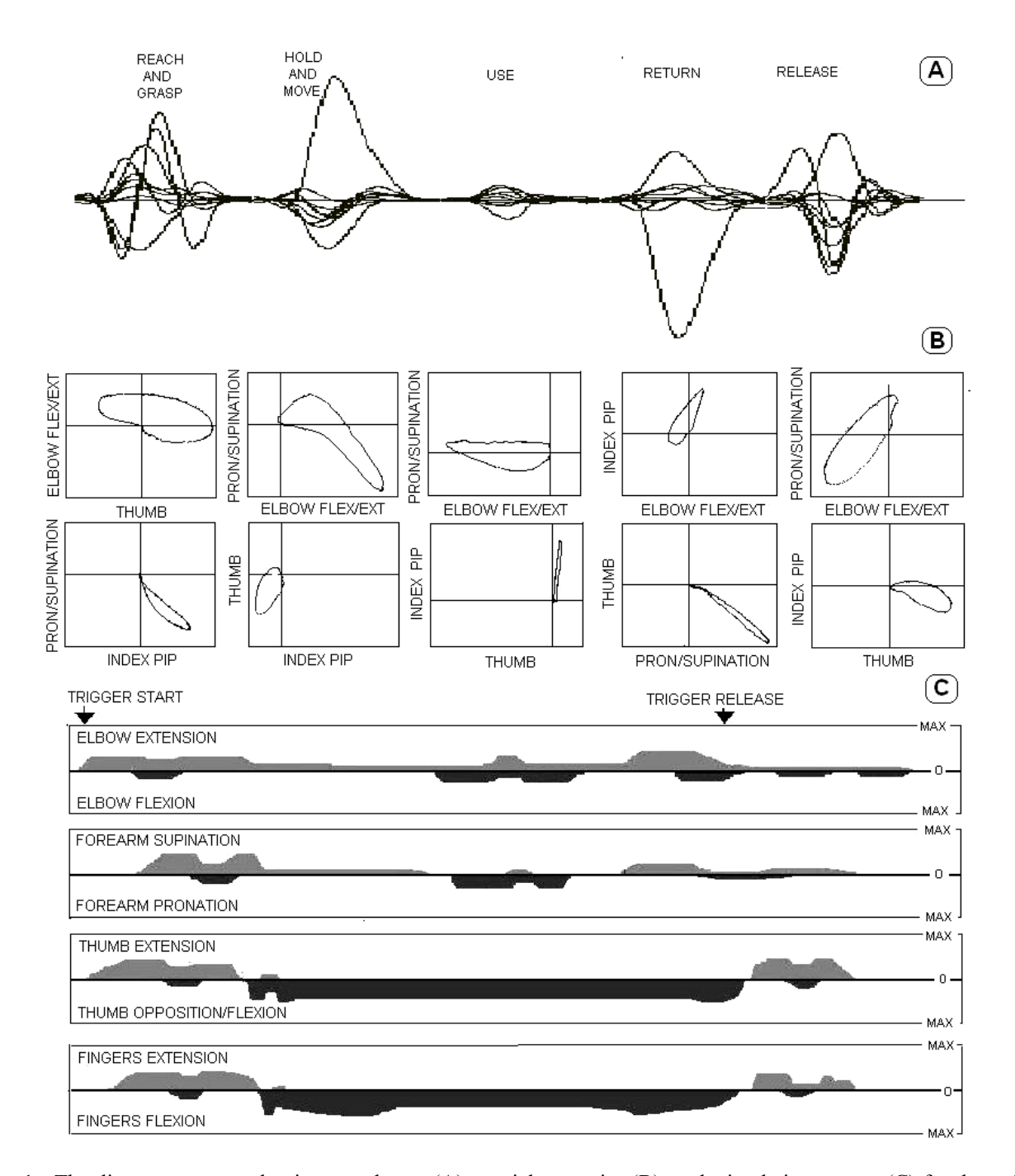


Fig. 1: The diagram presents the time synchrony (A), spatial synergies (B), and stimulation pattern (C) for the task of drinking from a 0,33-liter bottle proximal to the acromion. Temporal synchrony (A) shows that 9 joint angular velocities are divided into five successive phases (reach and grasp, hold and move, use, return and release the object). Spatial synergies (B) are presented by using joint angular velocity phase plots of the appropriate joint rotations. The synergies were determined by using radial basis function neural networks, and kinematics as inputs and outputs. Finally, the stimulation pattern (C) for this task was established based on the temporal synchrony and spatial synergies.

drinking from a 0.33-liter bottle, 3) inserting a VCR tape into a VCR machine; 4) writing on a paper positioned at the desk; and 5) eating finger food. The subjects repeated ten times each functional task with their dominant arm in three independent sessions. The order of tasks was randomly changed. Penny and Giles flexible goniometers (Biometrics, Gwent, U.K.) were mounted to measure the following: shoulder flexion/extension, abduction/adduction, elbow

flexion/extension, forearm pronation/supination, wrist ulnar/radial deviation, palmar/dorsal flexion, index finger flexion/extension, thumb adduction/adduction, and thumb flexion/extension. A custom designed acquisition program was used to capture the nine joint angles.

The sampling rate was 100 samples per second, and joint angles were low-passed filtered at 30 Hz with the 4th order Butherworth filters. All data were offline processed using a MatLab based program that

allowed determination of angular velocities The task was to determine the minimal number of unique couplings between joint angular velocities that characterize the task, object position and size, or their combination.

Two forms of couplings were of interest: 1) the time synchrony, and 2) the spatial mappings. These couplings were determined by a computerized matching that applied radial basis functions neural networks, and inductive learning.

One example for RGR task (0.33-liter bottle) is in Fig. 1 (top and middle panels).

Stimulation paradigm. We selected the frequency of 50 Hz, and pulses ($T = 250 \mu s$) with steep exponential rising edge to minimize unpleasant sensations typical for electrical stimulation *via* surface electrodes. The stimulation intensity was selected by varying the pulse amplitude between 5 and 40 mA in a manner that was acceptable by patients and resulted with functional movements.

Mimicking normal grasp and release of objects was provided by the newly designed multi-field electrode [5] that allowed activation of selected muscles *via* surface electrodes positioned over the forearm muscles.

The selection of the preferred stimulation sites did not necessarily lead to the "normal" grasp; yet, in all cases the grasp was functional. In addition to the control of finger and thumb flexion/extension (four channels), four channels of stimulation were applied to the following muscle groups of the arm: forearm supination (*Extensor Carpi Radialis Longus* m, *Supinator m*.); forearm pronation (*Pronator Teres m., Pronator Quadratus m.*); elbow flexion (*Biceps Brachii m, Brachioradialis m.*); and elbow extension (*Triceps Brachii m.*).

Fig. 1 (bottom) shows a typical stimulation pattern for the RGR of a small bottle (0.33 liter). The timing of the start and release commands is indicated with arrows pointing to the horizontal axis. The time has to be set according to the overall abilities of the user. The whole operation in average lasts about 10 seconds.

The described control for functional electrical stimulation systems was applied by using the custom designed 8-channel stimulator. The controller regulates the frequency, pulse duration, and charge balance, and executes triggered preprogrammed operation.

The PC compatible interface for setting the stimulation paradigm is realized *via* an IR serial communication channel.

The stimulator is described in details in Jorgovanović [6].

Implementation of the Control

The control system was tested in a case study that included 5 acute hemiplegic patients (Table 1).

The inclusion criteria were that patients had preserved wrist extension no more than 10 degrees; yet, no voluntary grasping and releasing. The study lasted three weeks. Subjects were asked to exercise for 30 minutes, five days, during three weeks. The treatment is described in details in Popovic *et al.* [1].

Subject	Age (years)	Period after CVA (weeks)	Diagnosis	MAS score
А	62	2.5	Hemi. L. Sin.	1+
В	50	3	Hemi. L. Sin.	2
С	62	3.5	Hemi L. Dex.	1+
D	65	3	Hemi L. Sin.	2
E	61	2	Hemi L. Sin.	3

Table I: Patients demographics; MAS –Modified Ashworth Scale; CVA-Cerebro Vascular Accident.

The Upper Extremity Function Test (UEFT) scores compared the effects of the neural prosthesis. The UEFT shows the ability to perform typical daily activities that require the grasping and releasing of various objects. The UEFT score was defined as the number of successful repetitions of a task that a subject could perform during a two-minute period. The successful operation was the one in which the

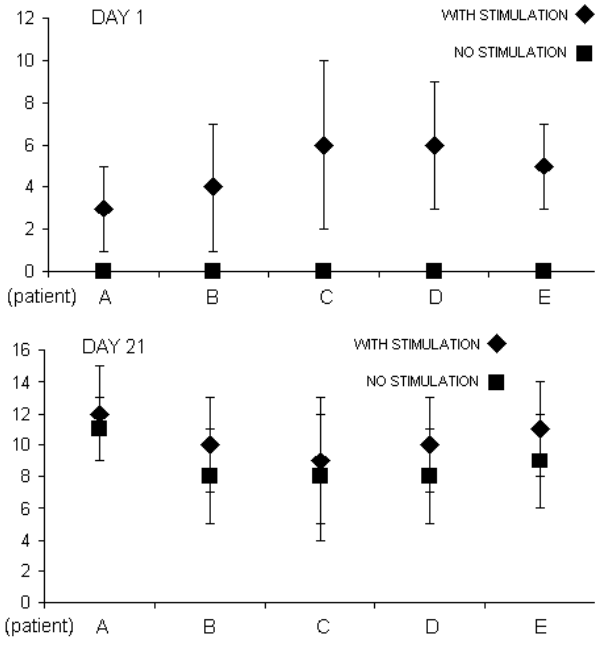


Fig. 2: The UEFT scores for the 5 post stroke patients on the day 1 and the day 21 of the study. The score is the averaged number of the grasps of various objects during two minutes. Square symbols show no stimulation, and the diamond symbols the scores with the stimulation. Vertical lines are the SD calculated for 11 tested tasks.

subject grasped, manipulated and used the object with his/her paretic arm. The same, trained individual evaluated the UEFT by analyzing the video recordings from a session when the UEFT was performed. The UEFT test was performed without and with the stimulation on the first and 21st day of the case study.

The results of the effects of the stimulation are presented in Fig. 2. The UEFT scores at the beginning (day 1) were 0 for all five patients without the stimulation (squares, top panel in Fig. 2) because patients were not able to perform any of the eleven functional tasks (handling can, pen, telephone, CD, etc.). During the same session the electrical stimulation allowed patients to functionally grasp between 3 and 6 objects in two minutes (diamonds, top panel in Fig. 2).

After the treatment, on the day 21, the patients improved their performance without the stimulation (squares, bottom panel, Fig. 2); they were able to effectively repeat task between 8 and 11 times during the period of two minutes. The performance with the electrical stimulation was still better; patients scored between 9 and 12 (diamonds, bottom panel in Fig. 2). The difference between the use of electrical stimulation and no stimulation became marginal after three weeks of the treatment due to the enhanced recovery as described in [2].

Conclusion

We describe here the control method for a neural prosthesis applicable for therapy that is appropriate for limited time application in the clinical environment. The aim of this control is to augment or generate missing functions of the paretic hand and arm in a manner that resembles to movements typical for able-bodied humans. The controller operates in the open-loop mode and response to two commands (trigger grasp and trigger release) that are issued by the user by a push-button interface.

The use of the controller was tested in five post stroke hemiplegic patients who were not able to perform simple daily tasks. All five subjects who participated in the study benefited immediately form the application; they could perform daily tasks assisted by a neural prosthesis. The benefit from the neural prosthesis could be seen also after three weeks (day 21 of the study); yet, the difference between the use and no use was very small.

The usage of this neural prosthesis requires that a patient use some preserved motor skills in order to compensate for the inexactness of the control. The control also needs that patients learn how to

integrate the externally assisted activity of muscles into their own voluntary activities.

In average, patients needed one session (30 minutes) to get used to the system operation because the stimulation schema mimics the movements that were typical before the CVA.

This control method is not yet suitable for home usage because of the complexity; it is intended for the therapy in the clinical environment.

References

- 1. Popović M.B., Popović D.B., Sinkjær T., Stefanović A., Schwirtlich L: Clinical Evaluation of Functional Electrical Therapy in Acute Hemiplegic Subjects J Rehab Res Develop, 40(5):443-454, 2003.
- 2. Popović D.B., Popović M.B., Sinkjær T: Neurorehabilitation of Upper Extremities in Humans with Sensory-Motor Impairment. Neuromod, 5(1):54-67, 2002.
- 3. Taub E., Uswatte G., Pidikiti R: Constraint-Induced Movement Therapy: a new family of techniques with broad application to physical rehabilitation-a clinical review. J Rehabil Res Dev, 1999, 36:3 237-51
- 4. Popović M.B: Control of Neural Prostheses for Grasping and Reaching. Med Eng Phys, 25(1): 41-50, 2003.
- 5. Bijelić G., Jorgovanović N., Bojanić D., Popović-Bijelić A., Popović D.B: ACTI-TRODE®: A new surface electrode-array for selective electrical stimulation. Proc 10th Medicon Conf, Ischia, Italy, July 30-Aug 2, 2004 (accepted).
- 6. Jorgovanović N: Control for Neural Prosthesis used in Neurorehabilitation contributing to Reaching and Grasping. PhD Thesis, Faculty of Engineering, University of Novi Sad, 2003.

Acknowledgment

Danish National Research Foundation, Denmark; Ministry for Science and Environmental Protection of Serbia, Belgrade supported the work on this project. We acknowledge the support of our clinical colleagues for the pilot experiments in post-stroke hemiplegic patients.

Author's address:

Dr. Mirjana Popović Center for Sensory Motor Interaction (SMI) Aalborg University Fredrik Bajers Vej 7 D-3, DK-9220 Aalborg e-mail: mpo@smi.auc.dk

PHYSICAL IMPLEMENTATION OF A PD CONTROLLER FOR IMPROVING HUMAN BALANCE DURING QUIET STANCE

Albert H. Vette*/**, Kei Masani*/***, and Milos R. Popovic*/**

* Institute of Biomaterials and Biomedical Engineering, University of Toronto

** Toronto Rehabilitation Institute

*** Department of Life Sciences, University of Tokyo

Abstract

Our studies have recently demonstrated that a proportional and derivative (PD) feedback controller, which takes advantage of the position and velocity information of the body sway, is capable of effectively generating a needed anticipatory control command in order to facilitate stable quiet standing. Furthermore, we identified gain pairs that ensured that the system behaved in a robust manner and that it had a dynamic behavior similar to the one observed in quiet standing experiments. The purpose of the present study was experimentally demonstrate that aforementioned PD controller can facilitate stable quiet standing. Our real-time closed-loop control system consisted of a center of mass position sensor, functional electrical stimulation regulated by the PD controller and a subject who had difficulty maintaining balance during quiet standing due to a neurological disorder called von Hippel-Lindau disease. The experiments were conducted in order to evaluate the subject's stability in the anterior-posterior plane only. In conclusion, the achieved results strongly suggest that the proposed feedback control system is capable of improving human balance during quiet stance in subjects with certain neuromuscular disabilities. The observed performance of the PD controlled feedback system supports our findings that the CNS adopts a control strategy that relies heavily on the velocity information.

Introduction

The improvement of standing capabilities has various therapeutic and functional benefits for subjects that suffer from spinal cord injuries and other neurological disorders. Therefore, open- and closed-loop applications of functional electrical stimulation (FES) for the purpose of facilitating stable standing have been subjects of research for many years. To compensate for significant time delays in the closed-loop control system of human bipedal quiet stance, it has been suggested that an anticipatory command to the body sway position can be achieved by using a feed-forward control system [1,2]. By contrast, a nested feedback system regulated by a torque controller has been

developed and evaluated by Hunt et al. [3,4]. Our team has recently demonstrated that a feedback system regulated by a simple proportional and derivative (PD) position controller is capable of providing the active torque component that is being applied by the CNS in order to regulate the body sway in spite of long neurological time delays [5,6].

The purpose of the present study was to evaluate our theoretical results experimentally and to investigate whether a PD controller can provide satisfactory control of balance during quiet standing. We applied and evaluated a real-time control system that was characterized by the following components: 1) a displacement sensor measuring the fluctuation of the approximated center of mass (COM), 2) a PD controller with Kp and Kd gains obtained in our theoretical studies (Kp = 750 Nm/rad and Kd = 350 Nms/rad) [6], and 3) the controlled level of ankle torque generated by means of FES.

Materials and Methods

Experimental Setup

Figure 1 shows a schematic of the experimental setup. The PD controlled system received its input from a laser displacement sensor (Keyence LK-2500, Japan), which recorded the fluctuation of the body sway in the anterior-posterior direction. The laser sensor was placed at the height of the subject's COM and used reflection to determine the distance to the reflection plate on the subject's back. Additionally, the subject stood on force plates (Kistler, Switzerland) that recorded the fluctuation of the center of pressure (COP). While only the COM was used for balance control, both COM and COP were used for stability analysis.

The laser displacement measurements were sent to the controller, which determined the level of active ankle torque that was needed to stabilize the system. After dividing the required torque into equal portions for each leg, the stimulator provided the necessary level of FES for both ankle extensors (Compex Motion, Switzerland). Please note that for safety reasons the two inputs to the stimulator were optically isolated from the rest of the system.

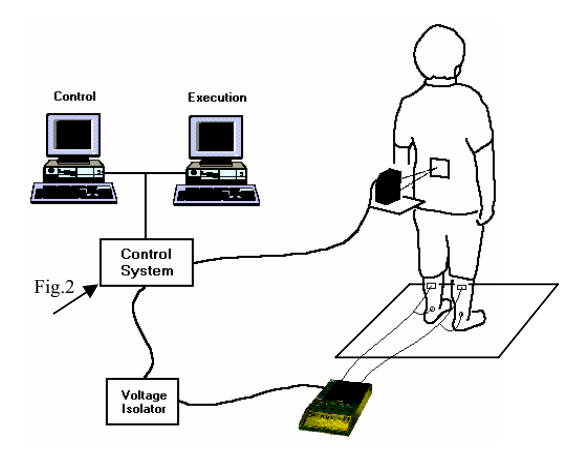


Figure 1: Feedback Circuit for Balance Control

The applied stimulation pulses had a constant frequency (35Hz) as well as pulse width (300µs), and were controlled by amplitude variation (mA). In order to produce the torque as calculated by the controller, we determined the amplitude-torque relationship of the subject in a preliminary experiment. The complete real-time system was executed by a C++-based kernel (MS Visual C++) that was controlled via a serial connection using the Matlab software (version 6.5) and the xPC toolbox (version 2.0). A National Instruments data acquisition board (PCI-MIO-16E-4) performed the necessary A/D and D/A conversions.

The closed-loop time delay of the feedback circuit consisted of the group delay time of the noise filter, the signal processing time within the circuit and the electromechanical response time of the plantar flexors. The delay was set within the range of 80-135ms to correspond with the physiological closed-loop time delay that is observed in able-bodied subjects during quiet standing.

Control System

Figure 2 shows the control system that was executed on the PC which regulated the level of muscle stimulation in real-time. The main components of this system were:

- A/D interface
- Butterworth 3rd order low-pass filter with 10Hz cut-off frequency
- PD controller with gains set to Kp = 750 Nm/rad and Kd = 350 Nms/rad
- Limits for minimum (0 Nm) and maximum torque (40 Nm)
- D/A Interface

In our setup, the positive values of the controller

output represented the torque that was expected to be generated by the plantar flexors. By contrast, the negative values represented the torque that the dorsiflexor muscles were meant to produce. Since we only stimulated plantar flexors, only positive values of the controller output were delivered whereas the negative values had no effect. Future research will consider the less dominant negative torque by including a stimulation branch for dorsiflexor muscles.

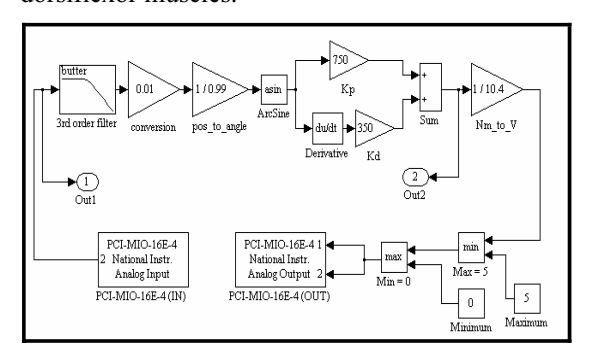


Figure 2: Control System for Balance Control

Procedure

In order to determine whether the proposed system was capable of improving balance during quiet standing, we compared the subject's performance for three different treatments:

- NTR: Natural performance without stimulation
- CST: Performance with constant stimulation
- CTR: Performance with controlled stimulation

For each treatment, three trials of equal length were recorded. During the 120 seconds of each trial, the subject was asked to stand still and maintain a balanced position (eyes open). The signals of the COM and COP fluctuation were logged at a sampling frequency of 1000Hz, filtered (4th order Butterworth, 5Hz cut-off frequency) and analyzed by means of a one-way ANOVA with a common significance level of $\alpha = 0.10$.

The fluctuation of the COM position and velocity was analyzed by means of the following *statistics*:

1) range of motion, 2) average amplitude, and 3) standard deviation. The COP fluctuation was analyzed by a method that was derived from the stability criterion for controlling standing in able-bodied subjects that has been suggested by Popovic et al. [7]. As a first part of the COP analysis, we determined the high preference and low preference zones for each recording. The high preference zone (HPZ) was defined by a circle that included 99% of the two-dimensional points. The circle that contained all two-dimensional points represented the low preference zone (LPZ). As a second part, the COP's HPZ and LPZ for the three

treatments were put into relation, allowing a statement on the subject's stability for each case: The smaller the respective preference zones, the higher the subject's balance control.

Subject

The proposed system was tested with a male subject that has difficulty keeping balance during quiet standing due to a neurological disorder called von Hippel-Lindau disease (VHL). The subject was 36 years of age, had height 173 cm, mass 59 kg, and suffered from VHL since birth. VHL is a rare genetic multi-system disorder characterized by the abnormal growth of tumors in certain parts of the body. The tumors of the central nervous system are called hemangioblastomas and may develop in the brain, the retina of the eyes, and other areas of the nervous system. Symptoms of VHL vary among patients and depend on the size and location of the tumors. The subject of our study had balance problems and impaired gait due to partial loss of sensation and proprioception. Furthermore, he experienced vision problems, dizziness and significant muscle weakness in the legs.

Results

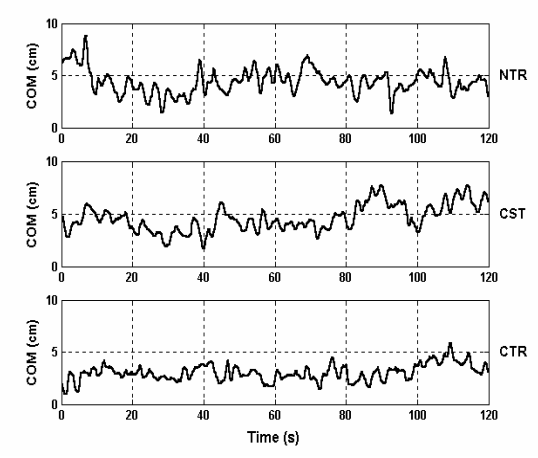


Figure 3: COM Fluctuation during Quiet Stance. COM fluctuation without stimulation (NTR), with constant stimulation (CST), and with controlled stimulation (CTR).

Figure 3 shows the time dependent COM displacement of the subject for three trials, each representing a different treatment. Already a visual inspection suggests that the body sway in CTR has a smaller magnitude than it does in NTR. The phase plots of the three COP recordings are shown in Figure 4, where each row represents the same treatment as in Figure 3. As with the COM, the smallest fluctuation is seen in CTR.

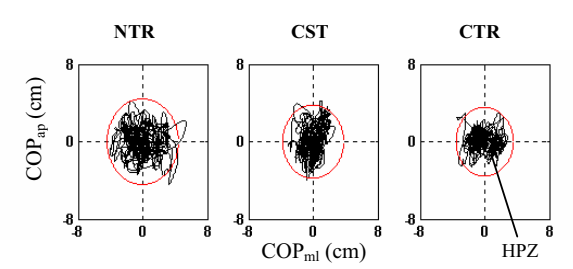


Figure 4: COP Fluctuation during Quiet Stance

Table 1 shows the results of the COM and COP analysis. Please note that the stated values represent the mean of three condition-specific results. For each of the eight statistics (range, amplitude, standard deviation, etc.), the smallest averaged value among the three treatments has been marked (bold font). It was revealed that the differences in treatment were significant for seven out of eight statistics.

Table 1: Average Stability Results for each Treatment

COM Position	NTR	CST	CTR
Range of Pos.	6.642 cm	6.795 cm	5.575 cm
Avg. Amplitude	0.852 cm	1.102 cm	0.701 cm
Std. Deviation	1.112 cm	1.321 cm	0.898 cm
COM Velocity	NTR	CST	CTR
Range of Vel.	11.812 cm/s	9.516 cm/s	7.615 cm/s
Avg. Amplitude	0.939 cm/s	0.882 cm/s	0.776 cm/s
Std. Deviation	1.240 cm/s	1.132 cm/s	1.020 cm/s
COP Position	NTR	CST	CTR
Radius of HPZ	4.807 cm	4.316 cm	3.756 cm
Radius of LPZ	6.339 cm	5.618 cm	4.745 cm

Discussion

The trials using a controlled level of stimulation had the smallest average value for all methods of analysis, suggesting a reduced body sway for this treatment. We also observed that the constant stimulation showed smaller values than the natural treatment for five out of eight statistics. Since the constant stimulation increases the level of stiffness around the ankle joint by providing additional muscle tonus, it improved the subject's balance in some regard. However, due to the findings that all statistics were larger for the constant stimulation than for the controlled stimulation, the role of the PD controller is clear: It is capable of effectively improving balance during quiet stance by mimicking the active part of the physiological control task. Hence, the feedback control system represents a valid setup for improving stability of subjects with certain neuromuscular disorders.

The question of whether a feedback system can control unsupported standing was also addressed by Hunt et al. They established and evaluated a feedback system that was regulated by a torque controller [3,4]. The inner loop provided feedback control of muscle moment, while the outer loop controlled the angle. The system performed reliably and according to the design formulation. Due to the fact that we applied a controller that emphasizes the velocity information of the body, we did not consider a nested structure: The information of the body angle - position and velocity - was sufficient to control the ankle moment. In spite of the different structures of the control systems, both studies agree that a feedback system is capable of stabilizing the human body during quiet stance, though several studies proposed the necessity of a feed-forward system [1,2].

Conclusion

The findings presented herein strongly suggest that human balance can be improved by means of a PD controlled feedback system that mimics the control task of an intact CNS. Furthermore, the system's effectiveness shows once more that the CNS adopts a control strategy that relies highly on the velocity information. Future research will test the proposed control system with a larger group of subjects who have poor control of balance due to age or neuromuscular disorders. Additionally, our system should incorporate stimulation of the dorsiflexor muscles. This allows the delivery of all control actions produced by the controller and not only the component in the posterior direction.

References

- [1] Gatev P, Thomas S, Kepple T, and Halett M: Feedforward ankle strategy of balance during quiet stance in adults. J Physiol, 1999, 514: 915-928.
- [2] Fitzpatrick R, Burke D, and Gandevia C: Loop gain of reflexes controlling human standing measured with the use of postural and vestibular disturbances. J Neurophysiol, 1996, 76: 3994-4008.
- [3] Hunt KJ, Munih M, and Donaldson N: Feedback Control of unsupported standing in paraplegia Part I: Optimal control approach. IEEE Trans. Rehab. Eng., 1997, 5(4): 331-340.
- [4] Hunt KJ, Gollee H, Jaime RP, and Donaldson N: Design of feedback controllers for paraplegic standing. IEEE Proc.-Control Theory Appl., 2001, 148(2): 97-108.

- [5] Masani K, Popovic MR, Nakazawa K, Kouzaki M, and Nozaki D: Importance of body sway velocity information in controlling ankle extensor activities during quiet stance. J Neurophysiol 2003a, 90: 3774-3782.
- [6] Masani K, Popovic MR, Nakazawa K, Kouzaki M, and Nozaki D: An estimate of control gains in human balance control system. Society for Neuroscience's 33th Annual Meeting, 272.10, 2003b.
- [7] Popovic MR, Pappas I, Nakazawa K, Keller T, Morari M, and Dietz V: Stability criterion for controlling standing in able-bodied subjects. J Biomechanics, 2000, 33: 1359-1368.

Acknowledgements

Canadian Fund for Innovation; Ontario Innovation Trust; Faculty of Medicine Dean's Fund, University of Toronto.

Author's Address

Prof. Dr. Milos R. Popovic Rehabilitation Engineering Laboratory Institute of Biomaterials and Biomedical Engineering, University of Toronto 4 Taddle Creek Road, Room 423, Toronto, Ontario M5S 3G9, Canada

E-mail: milos.popovic@utoronto.ca

http://www.utoronto.ca/IBBME/Faculty/Popovic_

Milos/index.html

Session 9

Therapeutic Effects

Chairpersons:

D. Popovic (Aalborg, Denmark) T. Keller (Zürich, Switzerland)

THERAPEUTIC EFFECTS OF SPINAL CORD AND PERIPHERAL NERVE STIMULATION IN PATIENTS WITH THE MOVEMENT DISORDERS

Huber J¹, Lisiński P², Kasiński A³, Kaczmarek M¹, Kaczmarek P³, Mazurkiewicz P³, Ponulak F³, Wojtysiak M¹

Department of Pathophysiology of Locomotor Organs, University of Medical Sciences in Poznań, Poland (1)

University of Medical Sciences in Poznań, Department and Clinic of Rehabilitation, Poland (2)

Institute of Control and Information Engineering, Poznań University of Technology, Poland (3)

Purpose: In the presented study we have investigated the therapeutic results of the modified FES and TENS programs applied to the patients with the treated degenerative spine disorders and the discopathy at the cervical and lumbar regions (group A, N=12), as well as to the patients after injuries and with the mielopathies at the cervical region of the spinal cord (group B, N=9).

Methods: The parameters of the electrostimulation programs (the pulse width, frequency and the train duration) have been modified in order to maximise the quality coefficients associated with the following criteria: functional evaluation of the limbs (upper and lower), examination of the physiological reflexes, examination of the perception of the superficial and deep receptors, evaluation of the muscles tension. The electrotherapeutic results have also been verified by the diagnostic examinations: EMG, ENG (M-wave) and SEPs of the selected muscles and nerves in the upper and lower limbs.

Results and Conclusions: It has been observed, that the one-side spinal stimulation (with anode-electrode placed above cathode) had the following effects: improved efficiency of the selected muscles (in case of groups A and B), improved afferent transmission to the spinal centres at the cervical region (B), as well as a slight improvement of the peripheral nerves conductivity at the upper and lower limbs (B). The local transcutaneous stimulation (with anode placed above cathode) of the peroneal nerve was characterised by the improved efferent conductivity to the innervated muscles, but had no effects on the afferent conductivity (A). The opposite electrodes placement (cathode above anode) resulted in the analgesic effects (A).

The optimisation procedure considered in this study allows to determine the progress and the directions of the physiotherapeutic treatment, aimed at the restoration of the patients' senso-motoric capabilities in the shortest time.

Author's Address

Filip Ponulak, MSc Poznań University of Technology Institute of Control and Information Engineering Piotrowo 3a 60-965 Poznań, , Poland

e-mail: Filip.Ponulak@put.poznan.pl

THE EFFECTS OF THE ELECTRIC STIMULATION WITH MIDDLE FREQUENCY ON CENTRAL AND PERIPHERAL PALSY

Rosselli D¹, Magliano M¹, Vrola M²

Gruppo Rieducazione Funzionale, Torino, Italy (1) Poliambulatorio Kibesiterapico Tesoriera, Torino, Italy (2)

The cause of motor lesion in central palsy mostly concerns the peripheral motoneurons and muscle fibers innervated by them. The affected motor units are only deprived of informations from the motor brain centers responsible for significant movement control. The muscles are "flabbily" paralyzed immediately ,the muscle tone is fastly reduced. After some time, the initially flabby palsy becomes increasingly spastic, with a progressive rising of reflex tone. The treatment goals of this kind of electrotherapy on these patients are to prevent the spastic mode, with acceleration of the axonal transport ,increased enzymic synthesis and challenge of metabolism(training effect),acceleration of the sprouting of regenerating axons, the maintenance of the range of motion of the joints involved.

This, in order to accellerate physiotherapeutic exercises. The effects of action impulses produced by middle frequency electrical stimulation in neural functional disorders, partially or totally denervated muscles due to peripheral palsy are:

Activation of the muscle pump to accelerate the centripetal transport of blood and lymph Activation of blood flow in the active muscle

Adaptation of the muscle fibers and their innervating motoneurons to the metabolic needs, i.e. increased repolarization activity and,in the muscle fibers additional contraction activity.

Thanks to this electrical stimulation therapy, what was once considered as a theoretical conclusion has now turned into reality. Of about 100 patiets examined, 30 (left side involved) were specifically treated with 2 electrical middle frequency circuits. The treatment started 10 days after the stroke. All the patients began the rehabilitation without articoular rigidity or spasticity evolution in the muscolar districts. Moreover, they experienced a relaxing feeling in their muscular groups and showed benefits since the very first applications. These considerations and these relevant results are the object of this study.

Author's Address

Diego Piero Rosselli, Chinestherapyst Gruppo Rieducazione Funzionale Via Susa,5 10094 Giaveno, Italy

e-mail: dirosystem@email.it

OVERCOMING ABNORMAL JOINT TORQUE PATTERNS IN PARETIC UPPER EXTREMITIES USING TRICEPS STIMULATION

T. Keller^{1,2}, M.D. Ellis^{3,4}, J.P.A. Dewald^{3,4,5}

Automatic Control Laboratory, Swiss Federal Institute of Technology Zurich, Switzerland
 Spinal Cord Injury Center, University Hospital Balgrist, Zurich, Switzerland
 Dept. of Physical Therapy and Human Movement Sciences, Northwestern University, Chicago IL, USA
 Sensory-Motor Performance Program, Rehabilitation Institute of Chicago IL, USA
 Biomedical Engineering Department, Northwestern University, Evanston IL, USA

Abstract

The goal of this research project was to quantitatively assess whether transcutaneous triceps stimulation can overcome the expression of abnormal torque patterns in the paretic upper limb of subjects with hemiparetic stroke. Abnormal torque patterns consist of strong coupling between shoulder abduction (SAB) and elbow flexion (EF) or between elbow extension (EE) and shoulder adduction (SAD) torques. Both patterns reduce the active range of motion during arm movements.

Eight chronic stroke subjects with moderate to severe (Fugl-Meyer assessment scores of 21/66 – 36/66) upper limb motor impairment participated in this study. Shoulder and elbow joint torques were measured with a 6 DOF load cell under isometric conditions, while the triceps muscle was stimulated to generate EE torques. At the same time the subjects were asked to lift up their arm to generate different SAB torque levels.

The obtained isometric results showed that electrical stimulation can overcome abnormal torque patterns in chronic stroke subjects while generating SAB. This is likely to have potential benefits to increase the reaching workspace of the paretic arm.

Introduction

Sensorimotor deficits and restricted mobility are among the more common problems following stroke. Clinically recognized motor deficits following stroke are weakness or paralysis and spasticity or hyperactive stretch reflexes. However, another more disabling deficit following stroke is a significant disturbance in movement coordination. Abnormal coordination is expressed in the form of abnormal muscle synergies and results in limited and stereotypic movement patterns, which are functionally disabling [1,2]. Abnormal coupling between SAB / EF and SAD / EE torques were quantitatively characterized [3,4] and are estimated

to be one of the main factors related to reaching deficits following stroke [5,6].

Transcutaneous functional electrical stimulation (FES) of the upper limb could provide the means to overcome abnormal torque coupling. Up to now FES in the upper extremities was mainly applied to improve or partially restore grasp function [7,8]. In addition to hand function a few laboratories investigated the control elbow extension movement in spinal cord injured (SCI) subjects using FES [9,10]. However, to date nobody has attempted to employ FES in hemiparetic stroke to reduce the effect of abnormal muscle and torque coupling between the elbow and shoulder.

The presented study was designed to investigate whether selective FES stimulation of elbow extensors can reduce the expression of the flexion synergy (i.e., SAB/EF coupling) thus potentially enhance the paretic arm's workspace during free reaching.

Material and Methods

Subjects

Eight subjects (5 male and 3 female; age 44-73) with a unilateral brain injury resulting from a stroke at least two years prior to participation in this study were selected. All subjects showed a moderate to severe upper limb motor impairment (Fugl-Meyer assessment scores of 21/66 - 36/66). Selection criteria for the hemiparetic subjects were the following: 1) Paresis confined to one side, with significant motor impairment of the upper limb; 2) Absence of muscle tone abnormalities and motor or sensory deficits in the unimpaired arm. 3) Absence of severe wasting or contracture of the impaired upper limb. 4) Absence of significant sensory deficits in the impaired upper limb. 5) Absence of severe cognitive or affective dysfunction. 6) Absence of severe concurrent medical problems. 7) Absence of brainstem lesions as determined from clinical or radiological reports. All subjects signed informed consent, which was

reviewed and approved by the Institutional Review Board of Northwestern University.

Setup

Subjects were seated in a Biodex chair with shoulder and waist strapped to restrain trunk and shoulder girdle movement during testing. The forearm, wrist, and hand were attached to a 6-DOF load cell (JR3 Inc., Woodland, CA, Model #45E15A) using fiberglass casting and a Delrin ring mounted at the wrist The attached arm was positioned in 75°SAB and 90°EF angle such that the middle finger was aligned to the medial sagittal plane of the body. Isometric shoulder and elbow torques were measured and the SAB torque was displayed in real-time on a computer monitor placed in front of the subject. The triceps brachii muscle was stimulated with a Compex Motion [11] transcutaneous electric stimulator using trapezoidal stimulation patterns with 1 s amplitude ramps and 5 to 12 s constant stimulation depending on the task. A stimulation frequency of 25 Hz was used in all trials. The stimulation amplitude was adjusted to generate the strongest EE torque without causing discomfort. The pulse duration that caused the highest EE torque was chosen from four durations i.e., 150, 200, 300, and 500 us.

Experiment

In the first part of the experiment the stimulation amplitude and pulse duration that generated the highest EE torque were determined. This was achieved by using the 1 s ramps to determine the maximum stimulation amplitude for a given pulse duration. Increasing the stimulation amplitude didn't always result in a higher EE torque because antagonistic muscles were activated at higher amplitudes (see Fig. 1). The highest stimulation amplitude that didn't generate co-contraction of antagonistic muscles was determined for each of the four pulse durations and the duration/amplitude pair that produced the highest EE torque was then chosen for the rest of the experiment.

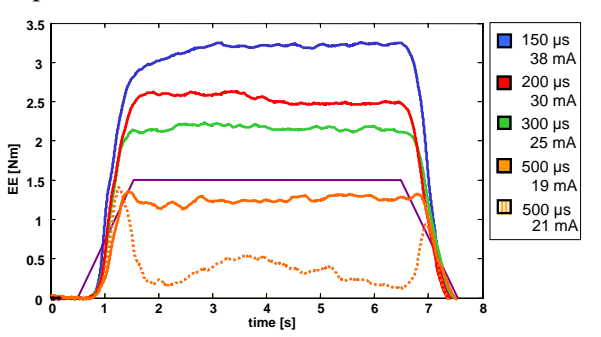


Fig. 1: In most subjects shorter pulse durations generated higher EE torques. The EE torque decreased when reaching greater stimulation amplitudes

presumably due to activation of antagonistic muscles (compare lowest plot (dashed - 500 µs and 21 mA) with 2nd plot from below (500 µs and 19 mA)

In the second part of the experiment the subjects were asked to lift their arms with different SAB torque levels while the triceps muscle was stimulated to produce an EE torque. Subjects could see on a dial on the screen displaying the actual SAB torque. They were asked to adjust and hold SAB torque for 12 seconds within a range of +/-10 %. For each trial the required SAB torque was randomly changed. During the holding phase the triceps muscle was stimulated for a duration of 7 seconds.

In the third part of the experiment the subjects had to perform different levels of SAB as in the previous paradigm, but in addition the subjects were instructed to generate voluntary EE torques during triceps stimulation.

Results

On average, without the subjects' volitional intervention a maximum EE torque of 6.3 (\pm 4.2) Nm or 25.8 (\pm 14) % of maximum voluntary contraction could be generated by triceps stimulation (n=8). It was generated with an average stimulation amplitude of 51 (\pm 15) mA and an average pulse duration of 181.25 (\pm 53) μ s.

El. stimulation & 10 Nm volitional SAB

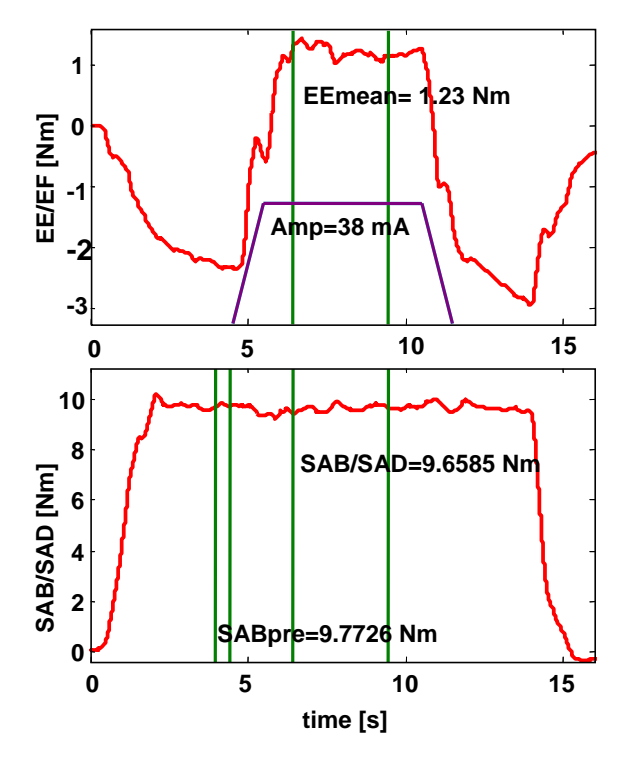


Fig. 2: The upper plot shows how the abnormal EF torque coupling generated by voluntary SAB of 10 Nm (lower plot) can be reversed applying triceps stimulation.

The maximum EE torque was calculated as the difference of the mean torque between 2 and 5 seconds after stimulation onset and the mean torque between 500 ms and 0 ms prior to triceps stimulation.

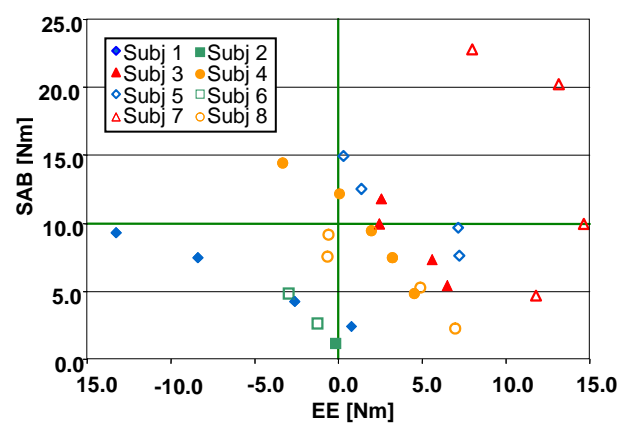


Fig. 3: The stimulated elbow torques of 8 subjects are plotted against the SAB torques the subjects were asked to generate voluntarily. Negative elbow torques are EF torques, occurring from abnormal torque coupling that couldn't be reversed by electrical stimulation.

When subjects were asked to lift up their arms in order to generate a SAB torque an abnormal coupling with EF was generated (as shown in the upper plot of Fig. 2). In six subjects the abnormal torque coupling could be reversed by electrical stimulation (Fig. 3).

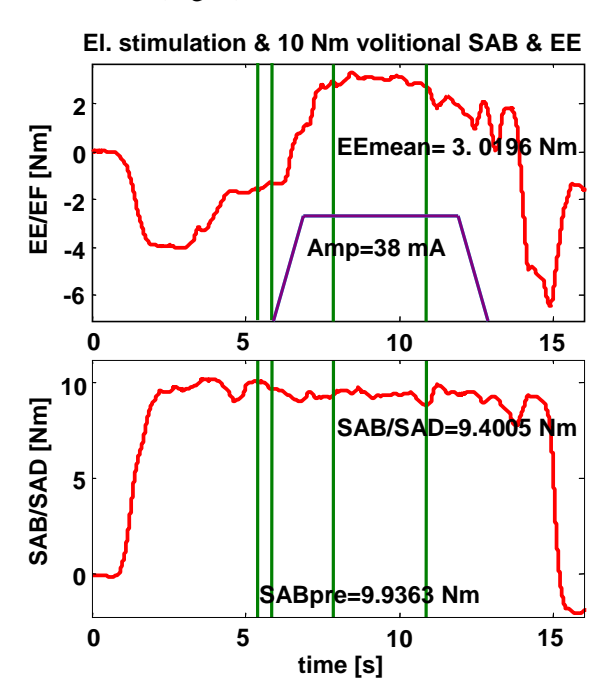


Fig. 4: In the third part of the experiment the subjects were asked to generate sub-maximal voluntary EE contraction during SAB. After EE was generated by the subject for about 2 s triceps stimulation was added to the voluntary contraction.

On average, while stimulating the triceps muscle subjects could achieve a SAB torque of

11.7 (± 7.2) Nm without generating concurrent EF torques. EF torque could be eliminated by generating FES-induced average EE torques of $6.7 (\pm 3.8)$ Nm. Four subjects could lift up their paretic arms against gravity (SAB torque of ~10 Nm) and have a net FES-induced EE torque at the same time. In two subjects the abnormal EF torque coupling could not be eliminated during SAB when electrically stimulating the triceps. When the subjects were instructed to volitionally assist triceps FES a SAB of 13.7 (± 7.0) Nm could be achieved while not generating abnormal EF torques (n=6, Figs 4 & 5). During stimulation of the triceps a net EE torque of 6.6 (\pm 4.2) Nm was generated. In the same two subjects no reversal from EF to EE was obtained during triceps stimulation, even if these subjects tried to volitionally extend their elbows during SAB. They were not able to lift up the arm against gravity and hold a constant torque level either.

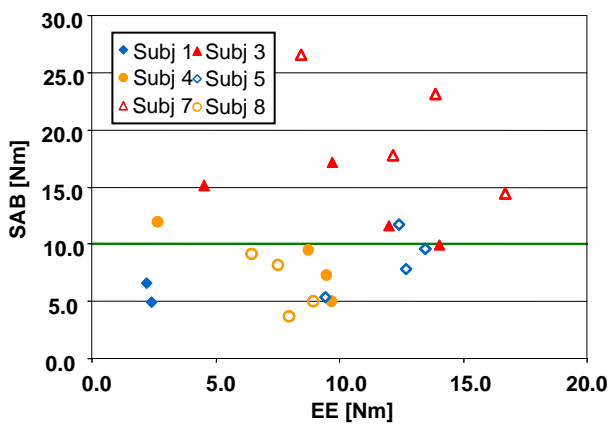


Fig 5: Six subjects could lift up the arm and produce together with triceps stimulation a net EE torque, which can be interpreted as a reaching out movement. Four subjects could perform SAB torques high enough to lift up the arm against gravity, while maintaining an EE net torque during stimulation.

Discussion

In the present study the possibility of using triceps stimulation to overcome abnormal torque patterns in chronic stroke subjects was investigated under isometric conditions. In six out of eight subjects the results showed that FES of the triceps muscle could generate enough torque to overcome abnormal EF coupling during SAB. In four subjects triceps stimulation could overcome abnormal EF torques when the subjects were generating SAB torques higher than 10 Nm. Such SAB torques are necessary to lift up the arm against gravity. The measured net EE torque during SAB that were higher than 10 Nm indicate that the subjects would be able to lift the arm and generate a net extension torque due to triceps stimulation. However, two subjects could not generate the SAB torques necessary to lift up the

arm against gravity. Furthermore, in these subjects triceps stimulation could not overcome their abnormal elbow/shoulder torque coupling.

The results showed that the torques generated by triceps stimulation added to the voluntarily generated EE torques and therefore may have beneficial effects during dynamic reaching [5,6]. The EE torque increase was possible, because the volitionally generated EE torques were submaximal. The subject at the same time had to generate EE torques and keep the SAB torque constant. Such dual tasks could only be performed with sub-maximal voluntary contractions and require training [12].

In the present study we only performed isometric measurements. Dynamic experiments that directly show an increase of the active workspace generated by triceps stimulation will be investigated in future experiments.

A future goal of our work will be to develop a suitable control strategy that enables FES-assisted arm movements and takes into account voluntary arm movement. A system that enables controlled FES-assisted arm movements may help subjects suffering from stroke to enlarge the active workspace. It could be used to train the subjects to overcome their abnormal torque synergies.

References

- [1] Brunnstrom S.: Movement therapy in hemiplegia. New York: Harper and Row, 1970, pp.192.
- [2] Dewald J.P., Pope P.S., Given J. D., Buchanan T.S., Rymer W.Z.: Abnormal muscle coactivation patterns during isometric torque generation at the elbow and shoulder in hemiparetic subjects. Brain, 118(2), 1995, 495-510.
- [3] Dewald J.P., Beer R.F.: Abnormal joint torque patterns in the paretic upper limb of subjects with hemiparesis. Muscle Nerve, 24(2), 2001, 273-283.
- [4] Beer R.F., Given J.D., Dewald J.P.: Task-dependent weakness at the elbow in patients with hemiparesis. Arch Phys Med Rehabil 80,1999, 766-772.
- [5] Dewald J.P., Sheshadri V., Dawson M.L., Beer R.F.: Upper-limb discoordination in hemiparetic stroke: implications for neurorehabilitation. Top Stroke Rehabil, 8, 2001, 1-12.

- [6] Beer R.F., Dewald J.P., Dawson M.L., Rymer W.Z.: Task-dependent effects of support condition on planar arm movements in chronic hemiparesis. Experimental Brain Research, 156, 2004, 458-470.
- [7] Peckham P.H., Keith M.W., Kilgore K.L., Grill J.H., Wuolle K.S., Thrope G.B., Gorman P., Hobby J., Mulcahey M.J., Carroll S., Hentz V.R., Wiegner A.: Efficacy of an implanted neuroprosthesis for restoring hand grasp in tetraplegia: a multicenter study. Arch Phys Med Rehabil, 82(10), 2001, 1380-1388.
- [8] Popovic M.R., Popovic D.B., Keller T.: Neuroprostheses for grasping. Neurol Res, 24(5), 2002, 443-452.
- [9] Crago P.E., Memberg W.D., Usey M.K., Keith M.W., Kirsch, R. F., Chapman G.J., Katorgi M.A., Perreault E.J.: An elbow extension neuroprosthesis for individuals with tetraplegia. IEEE Trans Rehabil Eng, 6(1), 1998, 1-6.
- [10] Popovic D., Popovic M.: Tuning of a non-analytical hierarchical control system for reaching with FES. IEEE Trans Biomed Eng, 45(2), 1998, 203-212.
- [11] Keller T., Popovic M.R., Pappas I.P., Muller P.Y.: Transcutaneous functional electrical stimulator "Compex Motion". Artif Organs, 26(3), 2002, 219-223.
- [12] Ellis M.D., Holubar B., Acosta A., Dewald J.P.: Reduced constraints in elbow/shoulder joint torque patterns in hemiparetic stroke using a multi-DOF isometric strengthening protocol. Society for Neuroscience, New Orleans, LA, November 2003.

Acknowledgements

This work was supported by the grant No. 823B-067648 from the Swiss National Science Foundation and the US National Institutes of Health (RO1 HD39343).

Author's Address

Dr. Thierry Keller Automatic Control Laboratory ETH Zentrum, ETL K 28 Physikstrasse 3 CH-8092 Zurich

e-mail: kellert@control.ee.ethz.ch home page: www.control.ethz.ch/~fes

ASSESSMENT OF MUSCLE LAYER THICKNESS OF QUADRICEPS MUSCLE IN INTENSIVE CARE UNIT PATIENTS DURING A PERIOD OF NMES TREATMENT USING ULTRASONOGRAPHY - PRELIMINARY DATA

Gruther W.*, Zöch C.*, Crevenna R.*, Paternostro-Sluga T.*, Spiss C.**, Kraincuk P.**, Kainberger F.***, Peceny R.****, Quittan M.****

- * Dept. of Physical Medicine and Rehabilitation, Vienna University Hospital, Austria
- ** Dept. of Anesthesiology and Intensive Care, Vienna University Hospital, Austria
- *** Dept. of Radiology, Division of Osteology, Vienna University Hospital, Austria
- **** Dept. of Physical Medicine and Rehabilitation, Kaiser Franz Josef Hospital, Austria

Abstract

Background: Intensive care unit patients (ICUP) show an enormous loss of muscle mass due to immobilization. Neuromuscular electrical stimulation (NMES) has been shown to be an effective method to enhance strength and endurance capacity of the skeletal muscles for patients who are not able to perform active exercise. This pilot study aimed to evaluate effects of NMES on mass of knee extensor muscles in ICUP.

Methods: Thirty-three ICUP (length of stay at ICU: at least 14 days) were enrolled in this randomized, controlled, double-blind pilot study. These patients were stratified into 2 groups based on their immobilization period on the ICU: acute patients (AP <7 days) and longtime patients (LP >14 days). Both cohorts were randomized in stimulation group (SG) and controls (CG) differing in terms of stimulation intensity (strong muscle contractions in SG, sensory input without muscle contractions in the CG). The electrical stimulation was applied via surface electrodes during a period of 4 weeks (session-time up to 60 min, 5 sessions/week). The NMES protocol consisted of biphasic rectangular impulses with a pulse width of 350 µs and a frequency of 50 Hz (on-/off= 8s/24s). Before and after the stimulation period, ultrasonography was performed to quantify muscle layer thickness of knee extensor muscles.

Results: In all AP a significant loss of muscle mass of > 36 % (p<0.01) could be observed. The stimulated LP showed a significant increase of muscle mass of 4.9 % (p<0.05) in contrast to the LP controls showing a slight decrease in muscle mass.

Conclusion: These findings indicate that NMES with a protocol as used in this small pilot study does not seem to be effective in preventing muscle atrophy in ICUP. Nevertheless NMES seems to enhance muscle mass in long time ICUP.

Introduction

Neuromuscular electrical stimulation (NMES) has been shown to be an effective method to enhance strength and endurance capacity of skeletal muscles for patients who are not able to perform active exercise [1, 2, 3].

Atrophy of skeletal muscles has been observed after space flight, bed rest and immobilization [4, 5]. Most intensive care unit patients (ICUP) show a prolonged catabolic state inducing loss of muscle mass. To our knowledge there are no comparable data about changes in muscle mass and morphology in intensive care patients during immobilization, yet.

To evaluate the physiological muscle morphology of human thigh and leg muscles, several equal imaging techniques as CT, MRI or ultrasound can be employed [6, 7].

This pilot study aimed to evaluate effects of NMES on knee extensor muscle mass (e.g. muscle layer thickness) using ultrasonography - and their time dependency - in ICUP.

Material and Methods

Study design

Prospective, randomized, controlled, double-blind, comparative pilot study of NMES or sham treatment.

Setting

This pilot study was conducted at the ICU as a cooperation of the Dept. of Physical Medicine and Rehabilitation with the Dept. of Anesthesiology and Intensive Care, and with the Dept. of Radiology / Osteology (all Vienna Medical University, General Hospital of Vienna). All procedures were approved by the University Ethics Committee, and informed consent was obtained from all patients.

Study population

Forty-six consecutive patients of an ICU (54±11 patients' male/female: 28/5. for vears. characteristics see table 1) were enrolled in this pilot study. Thirty-three patients completed the study. Exclusion criteria were a stay at the ICU shorter than 14 days, age less than 19 years, a muscle layer thickness = MLT total > 25 cm, implanted stimulation devices (PM, ICD), neuromuscular disorders or myopathy, epilepsy, allergic reactions to the electrodes, peripheral edemas, severe ischemia of the lower extremities, obesity/BMI>30, dermatological diseases at the stimulation sites.

Based on their immobilization period on the ICU, patients were stratified 1) in an acute patient group (AP - time between their arrival at the ICU and the beginning of the NMES therapy had to be less than one week), and 2) in a longtime patient group (LP - time between their arrival at the ICU and the beginning of the NMES therapy had to be longer than 2 weeks). After this stratification (AP, LP), a balanced randomization in stimulation group (SG) and control group (CG) was performed using the sealed envelope method (4 blocks, 4 patients each, see table 1).

Group	AP-	AP-	LP-	LP-
Group	SG	CG	SG	CG
Sex m/w	7/1	7/1	7/1	6/2
Age *	52	48	61	64
	(± 10)	(± 12)	(± 10)	(± 8)
Multiple trauma	3	4	2	1
Pneumonia	0	1	1	2
Tumor	1	1	2	2
Transplant	2	1	2	1
Cardiovascular disease	2	2	1	2
Incomplete (Death/Transfer):	1/2	2/1	3	3/1

Table 1: baseline characteristics of ICUP, *Mean \pm SD

Treatment

For the NMES stimulation Compex®-P-Sport devices (Medi-Konzept GmbH) were used. Details about the stimulation protocols are given in table 2.

NMES was applied via self-adhesive surface electrodes (2"x2" and 2"x4", Compex®, Medi-Konzept GmbH) on both quadriceps muscles. The electrodes were placed bilaterally on the ventral aspect of the thigh, medial and lateral, 3 cm proximal of the upper border of the patella and 5 cm distal of the inguinal fold.

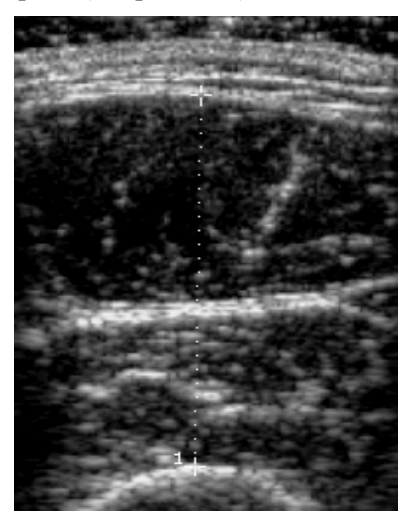
Duration of impulse	0.35 msec biphasic symmetric rectangular		
Frequency of repetitive stimulation	50 Hz		
Stimulus regime – on/off	8/24 sec		
Duration per day	beginning with 30 min. increasing up to 60 min.		
Intensity SG	strong tetanic contraction		
Intensity CG	above sensory threshold without any palpable or visible muscle contraction		

Table 2: Verum stimulation protocol NMES and sham stimulation protocol NoNMES

Patients received either verum treatment (resulting in a strong muscle contraction) or sham treatment (stimulation above sensory threshold, but without any palpable or visible muscle contraction) in identical manner. During a treatment period of 4 weeks, each patient received 5 NMES sessions a week.

Outcome measurement

To detect changes from baseline, muscle layer thickness of the quadriceps muscle was measured by high resolution real-time ultrasonography as described in other studies [4, 8]. All the ultrasound examinations were performed by a single operator with a portable ATL ultrasound system (HDI-1000), using a L7-4 transducer with a 5 cm linear array footprint (see picture 1).



Pic.1: transverse image from the anterior aspect of the thigh

Muscle layer thickness of quadriceps was assessed bilaterally 1) at the border between the lower and upper two thirds, and 2) in the middle of the distance between the anterior superior iliac spine and the upper pole of the patella, with the legs relaxed lying flat in extension. Muscle layer thickness mean (MLT) was calculated by mean of

the four measurements. The coefficient of variation for a single muscle layer thickness measurement is close to the obtained 3% by Bleakney [8]. MLT measurement used in the present study improves the coefficient to 0.25%.

Statistics

Data were analyzed using Statistical Package for Social Sciences (SPSS 12.0 for Windows). Descriptive statistics were calculated and Wilcoxon signed rank test was used to compare the distribution of two related variables. Group comparison was done with Mann-Whitney U-Test. Significant level was set at p<0.05.

Results

In AP MLT significantly decreased in SG (p=0.012) as well as in CG (p<0.008).

In LP MLT significantly increased with NMES (p=0.036) but remained unchanged in CG.

Group comparison between AP-SG and AP-CG did not show any statistical significance concerning MLT decrease. In contrast a significant difference in MLT (p=0.014) was detected comparing LP-SG and CG (see table 3 and figure1).

	Baseline	4 weeks	D%
MLT AP - SG	28.9	18.3	- 36.7 *
	(± 6.57)	(± 3.2)	
MLT AP - CG	32.9	20.1	- 38.9 **
METTI CO	(± 9.71)	(± 5.44)	20.5
MLT LP - SG	18.4	19.3	+ 4.9 *
METEL 50	(± 4.24)	(± 3.79)	1.5
MLT LP - CG	18.6	18	- 3.2
WIET ET	(± 5.87)	(± 5.76)	3.2
group comparison AP - SG/CG			1.4
group comparison LP - SG/CG			8.3 *

Table 3: MLT at baseline and after 4 weeks (mm, mean \pm SD); D% = difference in %; *p<0.05; **p<0.01;

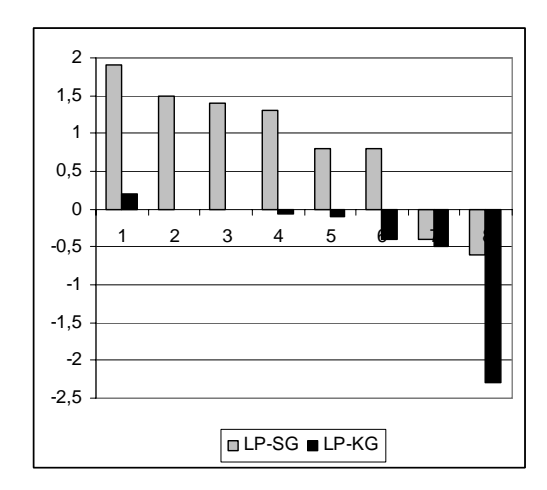


Figure 1. MLT (mm) difference diagram between baseline and 4 weeks in each patient of LP - SG/CG.

Discussion / Conclusion

Especially due to its easy practicability, it was decided to use high resolution real-time ultrasonography for this small pilot study in ICUP because it has been described to be a relatively simple and reproducible imaging [4,8].

Ultrasonography revealed a significant loss of muscle mass of >36% (p<0.01) in AP-SG and AP-CG. The LP-SG showed a significant increase of muscle mass of 4.9 % (p<0.05) in contrast to the LP-CG showing a slight decrease in muscle mass.

These findings indicate that NMES with a protocol as used in this small pilot study does not seem to be effective in preventing muscle atrophy in ICUP. Nevertheless NMES seems to enhances muscle mass in long time ICUP.

References

- [1] Vinge OD et all: Effect of transcutaneous electric muscle stimulation on postoperative muscle mass and protein synthesis. H:S Hvidovre Hospital, kirurgisk gastroentrologisk og rontgendiagnostisk afdeling. 1998 Jan 12;160(3):283-6
- [2] Quittan M, Sochor A, Wiesinger GF, Kollmitzer J, Sturm B, Pacher R, Mayr W. Strength improvement of knee extensor muscles in patients with chronic heart failure by neuromuscular electrical stimulation. Artif Organs 1999; 23:432-35 IF:0,919
- [3] Nuhr M, Pette D, Berger R, Quittan M, Crevenna R, Huelsman MF, Wiesinger G, Moser P, Fialka-Moser V, Pacher R. Beneficial effects of chronic low-frequency stimulation of thigh muscles in patients with advanced chronic heart failure. Eur Heart J. 2004 Jan; 25(2): 136-43.

- [4] Kawakami Y et all: Changes in muscle size and architecture following 20 days of bed rest. J Grav Physiol 2000; 7(3): 53-60
- [5] Gibson JNA, Smith K, Rennie MJ: Prevention of disuse muscle atrophy by means of electrical stimulation: maintenance of protein synthesis. Lancet 1988; 1:767-70
- [6] Dupont AC, Sauerbrei EE, Fenton PV, Shragge PC, Loeb GE, Richmond FJ: Real-time sonography to estimate muscle thickness: comparison with MRI and CT. J Clin Ultrasound. 2001 May;29(4):230-6.
- [7] Walton JM, Roberts N, Whitehouse GH. Measurement of the quadriceps femoris muscle using magnetic resonance and ultrasound imaging. Br J Sports Med. 1997 Mar;31(1):59-64
- [8] Bleakney R, Maffuli N: Ultrasound changes to intramuscular architecture of the quadriceps following intramedullary nailing. J Sports Med Phys Fitness 2002; 42:120-5

Acknowledgements

We thank Dr. Völker R. (Medi-Konzept GmbH) for supporting our study with COMPEX® Sport-P devices and electrodes.

Author's Address

Dr. Wolfgang Gruther Univ. Klinik für Phys. Med. und Rehab. Währingerstraße 18-20 A-1090 Wien

Email: wolf1978@gmx.at

Session 10

Technology: Implants and Electrodes

Chairpersons:

M. Sawan (Montreal, Canada) H. Lanmueller (Vienna, Austria)

AN ANALOG WAVELET PROCESSOR FOR A FULLY IMPLANTABLE CORTICAL SIGNALS RECORDING SYSTEM

V. Simard, B. Gosselin, M. Sawan

PolySTIM Neurotechnologies Laboratories

Dept. of Elec. Eng., École Polytechnique de Montréal, Qc, Canada

Abstract

We present in this paper the preprocessing unit of a wireless fully implantable multichannel cortical data acquisition system. The first part of the preprocessing unit is a low-power front-end module that removes low-frequency noise and offset voltage using Chopper stabilization technique. The second module is an analog wavelet processor which improves the efficiency of on-chip signal processing methods such as spike detection. This preprocessing unit has been designed using low-power log-domain techniques and its implementation area has been optimized. The preprocessing unit has been sent for fabrication in CMOS 0.18um technology. The front-end module has an input referred noise below 30nV/\day{Hz} and its power consumption is less than 20uW, while the analog wavelet processor consumes 20uW.

Introduction

Needs for researches in neurophysiology and recent advances in micromachining technologies carried out to the development of new dedicated sensing and stimulation tools. Powerful monitoring devices are implemented by combining integrated circuits to microprobes. These circuits integrate several channels on-chip to acquire extracellular potentials simultaneously from many neurons. These emergent systems are powered wirelessly and exchange data over a same radio frequency (RF) link. The numerous hardwire leads and percutaneous connectors which may induce infections and make currently used recording setup cumbersome are then avoided. A fully implantable acquisition system is depicted on fig. 1. These devices will eventually be integrated into a higher level system which will communicate through a wireless network, controlling each applications involved. Various kinds of prosthetic devices and user applications dedicated to patient suffering from specific central nervous system (CNS) dysfunctions could be included. All of these components could be activated on the decisions made by the host, represented by biopotentials collected directly on the cortex by the monitoring devices. To extend the capability and performances of acquisition, the implementation of a fully implantable device is undertaken by our team.

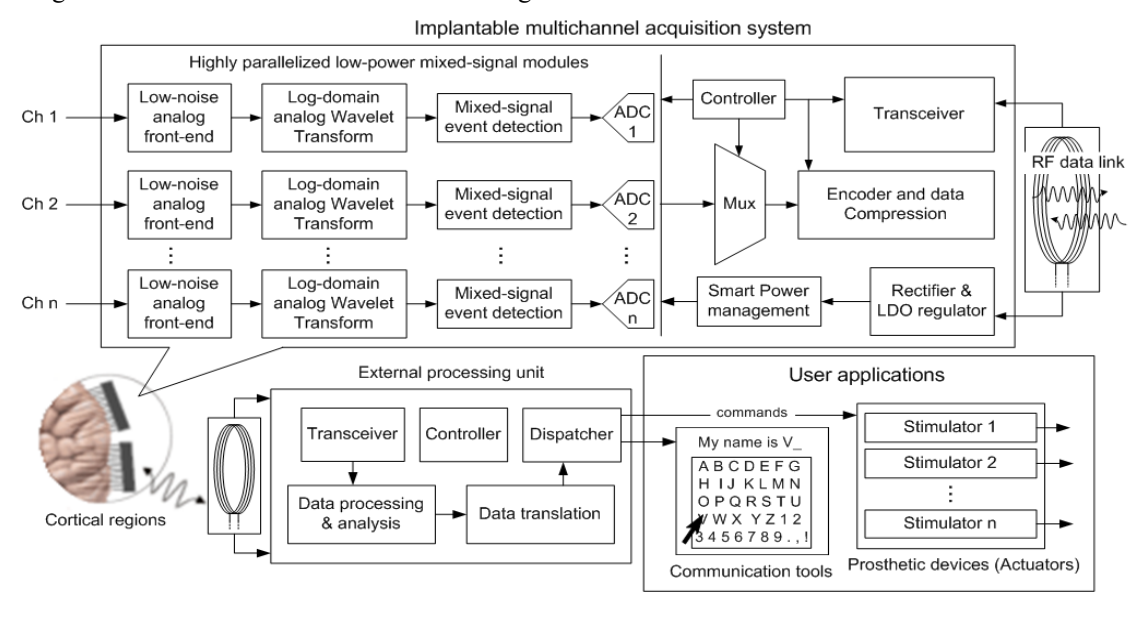


Fig 1. Block diagram of the multichannel cortical data acquisition system

However, several obstacles still need to be addressed prior to the advent of such systems. Extracellular cortical signal recording collects huge amount of data and one of the first limitation encountered is the RF data link bandwidth performances. The transfer rate reachable with Load Shift Keying (LSK) is unfortunately still insufficient to transmit the activity of the large number of cells needed to control sophisticated prosthesis with an adequate sampling rate.

We present in this work a preprocessing integrated module suitable for a fully implantable multichannel acquisition system. Moreover, a solution for increasing the number of channels of such systems is proposed.

Material and Methods

The front-end module

A block diagram of the analog front-end is shown on fig. 2. Usage of Chopper modulation for this module enables minimum area occupation and enhances noise performances as it has been reported in [1].

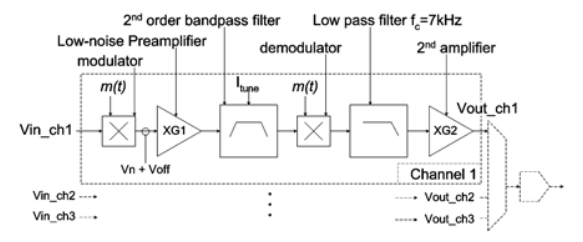


Fig 2. Block diagram of the analog front-end

Low-power consumption and small silicon area make this module parallelizable over all channels. These great advantages leave room for more embedded circuits such as the event detection module which will be detailed in next sections.

Event detection

Event detection has been used in past work. A simple buffered threshold detector has been implemented with several digital signal processors (DSPs) working in parallel [2]. The effective transfer rate reached with event detection has been found to be around 15% of the theoretical maximum rate. It is worthwhile to see that the capability of wireless monitoring systems could be extended based on this principle. By integrating an efficient event detection method, a monitoring system designed for 16 channels could be extended to more than 100 channels with the same transceivers and sampling rate specifications. Consequently, event detection is a well indicated solution to overcome the wireless data link bandwidth issue of such systems.

Wavelet Transform

Wavelet Transform (WT) is a tool known for its suitability for biomedical signals analysis [3]: some common usages are compression [4], denoising [5], spike detection and sorting [6]. Spike detection may be implemented quite easily by using an amplitude threshold, but this method results in a lot of detected false spikes and omitted real action potentials, especially in a noisy environment such as cortical extracellular background. Wavelet transform performs a multiresolution analysis in time and scale (related to frequency). The scale variations adapt the wavelet to low-frequency large structures as well as high-frequency transients of the signal, while the time translations track the exact moment of event occurrence. The preciseness of the resultant analysis makes the relevant signal usually well separated from the background noise [7].

The continuous WT (CWT) equation is

$$CWT(\tau, a) = \int f(t) \cdot \frac{1}{\sqrt{a}} \cdot \psi\left(\frac{t - \tau}{a}\right) dt \tag{1}$$

where a is the scale and τ the time translation, related to the subsequent sampling of CWT. This equation shows the convolution between the signal f(t) with the wavelet function $\psi(t)$; it corresponds to the filtering of f(t) by a filter of which impulse response is $\psi(t)$. By varying the scale a by a factor of 2^i , a filterbank of Q-constant filters, whose respective center frequencies f_{oi} are logarithmically spaced, is obtained and sampled at a frequency of $2f_{oi}$.

In order to perform a good analysis, a wavelet must have a compact effective support, that is, being negligible outside a certain section both in time and frequency. Analog filters cannot achieve a real compact support but can still sufficiently approach it. The 6th order transfer function

$$\frac{0.4786s^3}{s^6 + 2.058s^5 + 3.139s^4 + 2.537s^3 + 1.569s^2 + 0.5145s + 0.125}\tag{2}$$

is approximated from gaussian function; the filterbank is made up of 6 of these 6th order bandpass filters of which center frequencies have been chosen to provide a full coverage of action potentials frequency range (100 Hz to 6kHz): 0.156, 0.3125, 0.625, 1.25, 2.5, and 5kHz. Each filter is composed of three 2nd order filters in parallel. To reduce the implementation area, use of transitional filter techniques [8] with transfer function manipulations have permitted the sharing of a 2nd order filter between each 6th order filter neighbors. This leads to 13 2nd order filters for the whole wavelet processor as depicted on fig. 3.

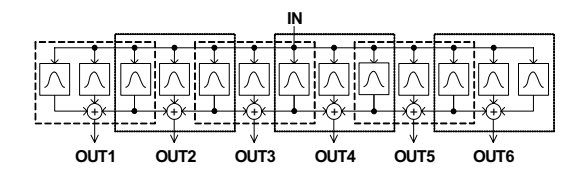


Fig. 3 Parallel implementation of the filterbank

Circuit implementation

CMOS log-domain techniques have been used to implement the filters. Usage of CMOS transistors biased in weak inversion allows to reach the very low power consumption needed for an implantable device. Log-domain filters logarithmically compress an input current into internal voltages that are processed before being expanded back; therefore they are well suited for low-voltage circuits. Straightforward implementation of the state-space model derived from the transfer function results in circuits often impossible to realize because of the wide range of bias current capacitance size. Several state-space transformations have been applied on the model to ensure good performances while minimizing area of implementation. The filter coefficients have been balanced to make sure that the biasing currents are equal or at least in the same range. This enables the sharing of biasing circuits between elements. Then a dummy input has been added to make the internal state variables having the same operating point [9]. Currents I_{BLAS} and I_F , respectively setting the signal range and the cut-off frequency, have been made independent so frequency tuning is possible while maintaining acceptable range for input signal, current level and capacitance size. The state-space implementation are illustrated on fig. 4.

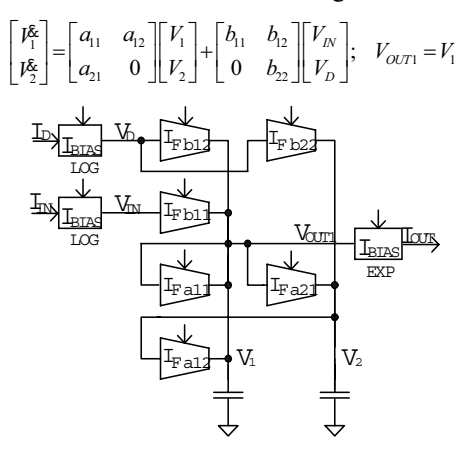


Fig. 4 Block diagram of state-space model realization

Results

The front-end achieves an input referred noise of 2.5uVrms for a power consumption of less than

20uW. The whole module occupies a chip area of 0.0705mm². Table 1 gives a summary of the main characteristics of the front-end.

Table 1. Frond-end performances summary		
Power consumption	<20uW	
Total input noise	30nV/√Hz	
1/f noise attenuation (1-20kHz)	70-20dB	
Bandwidth	DC - 7kHz	
Total gain	80 dB	
One channel integration area	0.0705mm ²	

Fig. 5 shows the ability of the Chopper modulated front-end to reduce a low-frequency input noise.

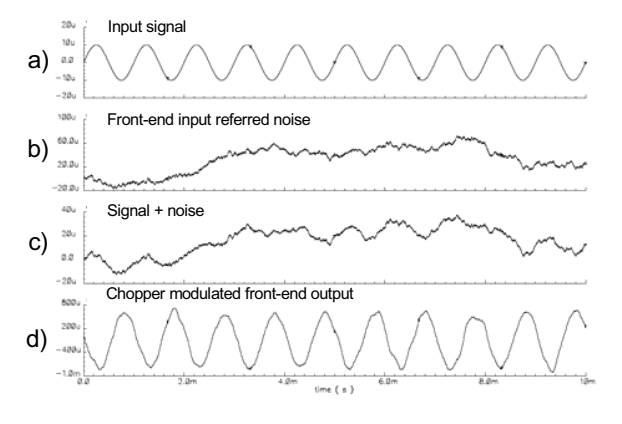


Fig. 5 Low amplitude signal retrieval with the Chopper modulation front-end

Fig. 6 shows the frequency and time responses of the wavelet analog processor.

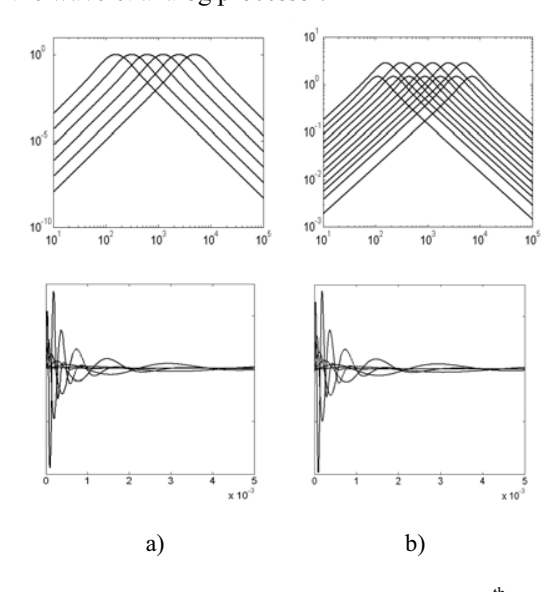


Fig. 6 Frequency and impulse responses of a) 6^{th} order filterbank b) 2^{nd} order parallel implementation (impulse response of each group of three 2^{nd} order filters are summed)

Table 2 presents some characteristics of the analog wavelet processor.

Table 2. Wavelet processor performances summary		
Power consumption	<20uW	
Bandwidth	100Hz - 6.8kHz	
Input dynamic range	>49dB	

Discussion

We have presented the first stages of a wireless fully implantable multichannel cortical signal acquisition system. The analog front-end and wavelet processor are needed as signal conditioning and preprocessing modules prior to on-chip event detection. By allowing to send only relevant data, spike detection is one solution to optimize the usage of RF link bandwidth, which is a bottleneck for wireless multichannel recording devices.

After neural signal decomposition by the wavelet transform, event detection is performed by applying a threshold, straightforward to implement using a simple comparator. After detection, the kept data is only a window that delimitates the signal from a short period of time before and after the event occurrence in order to enable further data processing steps such as spike sorting. This implies that a portion of the signal must be buffered. With a 30kHz sampling rate and 8 bits/sample, the required buffer size is 256 bytes per channel for a 8.5ms time window. However, implementing memory can be challenging for the chip area constraints. For a 32-channel recording system, the memory size can be as large as 2.6mm². This issue must be addressed in future work.

RF transceivers developed by our laboratory achieves a transmission rate up to 1.13Mbits/s [10]. Therefore, without any kind of data reduction, only 5 channels of raw data can be transmitted. As reported before, event detection can reduce the relevant part of signal to be sent up to 15% of the original data. Taking advantage of this means that the same RF link could accommodate more than 32 channels. Further data compression, which is also currently undertaken by our team, will enable to handle an even greater number of channels.

References

- [1] Gosselin B., Simard V., Sawan M.: Low-Power Implantable Microsystem Intended to Multichannel Cortical Recording, IEEE-ISCAS, Vancouver, May 2004
- [2] Guillory K. S., Normann R. A.: A 100-channel system for real time detection and storage of

- extracellular spike waveforms, Journal of Neuroscience Methods (91), 1999, 21–29
- [3] Unser M., Aldroubi A.: A Review of Wavelets in Biomedical Applications, Proc. of the IEEE, vol. 84, no. 4, April 1996, 626-638
- [4] Abo-Zahhad M., Rajoub B. A.: ECG Compression Algorithm Based on Coding and Energy Compaction of the Wavelet Coefficients, IEEE ICECS, vol. 1, 2001, 441-444
- [5] Folkers A., Mösch F., Malina T., Hofmann U. G.: Realtime Bioelectrical Data and Processing from 128 Channels Utilizing the Wavelet-Transformation, Neurocomputing 52-54, 2003, 247-254
- [6] Hulata E., Segev R., Ben-Jacob E.: A Method for Spike Sorting and Detection based on Wavelet Packets and Shannon's Mutual Information, Journal of Neuroscience Methods (117), 2002, 1-12
- [7] Samar V. J., Bopardikar A., Rao R., Schwartz K.: Wavelet Analysis of Neuroelectric Waveforms: A Conceptual Tutorial, Brain and Language 66, 1999, 7-60
- [8] Paarmann L. D.: Design and Analysis of Analog Filters: a Signal Processing Perspective, Kluwer, 2001
- [9] Serra-Graells F., Rueda A., Huertas J. L.: Low-Voltage CMOS Log Companding Analog Design, Kluwer, 2003
- [10]Coulombe J., Gervais J.-F., Sawan M.: A Cortical Stimulator with Monitoring Capabilities using a novel 1Mbps ASK Data Link, IEEE-ISCAS, vol. 5, 2003, 53-56

Acknowledgements

The authors would like to acknowledge the support from the National Sciences and Engineering Research Council of Canada (NSERC) and the Canadian Microelectronics Corporation (CMC).

Author's Address

Virginie Simard

École Polytechnique de Montréal Department of Electrical Engineering C. P. 6079, Succ. Centre-Ville, Montréal (Québec) Canada, H3C 3A7

e-mail: <u>Virginie.Simard@polymtl.ca</u> home page: www.polystim.polymtl.ca

PROGRAMMABLE STIMULATION-RECORDING CIRCUITRY FOR CUFF AND SIEVE ELECTRODES

J. Sacristán¹, N. Lago², X. Navarro² and T. Osés¹

¹Electronic Circuits & Systems Design, CNM-IMB (CSIC), Spain

² Department of Cell Biology, Physiology and Immunology, UAB, Spain

Abstract

In this paper, an ASIC Stim/Rec circuit to be used with different type of electrodes has been designed, implemented in a CMOS technology and tested in acute experiments with rats. The performances of this Stim/Rec are: fully programmability of waveform parameters, 4 stimulation and 1 recording channel extensible to 16 and 4 respectively, anodes and cathodes can be chosen independently allowing the current to go in a longitudinal or transversal way for cuff electrodes. A very low noise (5nV/\mathbf{O}Hz) amplifier has been got with digitally programmable bandwidth and gain.

Introduction

The use of functional electrical stimulation (FES) technique [1] is used not only restoring motor activity in SCI subjects but also for therapeutic or prosthesis control. Nowadays, there is not much work done on development of implantable systems with stimulation and recording capability into the same ASIC with the benefit of a reduction in the size of the resulting implantable device although it seems a new line on this direction is starting [2]. In this paper a stimulation/recording circuitry implemented in the same ASIC is presented. The system is designed without being tied to a specific application and allowing to operate in a closed loop system using the stimulator to provide information to the subject and the recording to sense a certain motor action as in the case of controlling a hand prosthesis or inversely for a motor action in SCI people. The parameters of the system are digitally programmable from the external control and once programmed the only requirement for an autonomous operation is the power supply. The hierarchical strategy allows modifying the number of channels in an easy way.

Material and Methods

1. System structure.

The system proposed consists in a four channels electrical stimulator, an external electrode selector, full channel ENG signal recording, two step/up voltage regulators providing the high voltage for the stimulator and a control digital block to program and control the above blocks. This system

corresponds with the internal unit (without telemetry) in an implantable stimulation-recording system like that shown in Fig. 1.

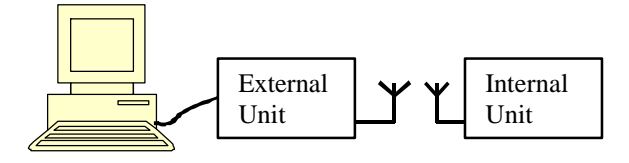


Fig. 1: Implantable system

A simplified blocks schema for the mentioned system is shown in Fig. 2. This system is designed to work with sieve and cuff electrodes then an electrode selection module for the sieve and independents anode-cathode pairs for cuff have been implemented. Moreover, all these blocks have been designed in an ASIC using a high voltage technology I2T CMOS 0.7 micron. This is a preliminary version of a multiple channel stimulator—recording circuitry provided with a bidirectional telemetric link for energy and data transmission that is being developed in the framework of Cyberhand project.

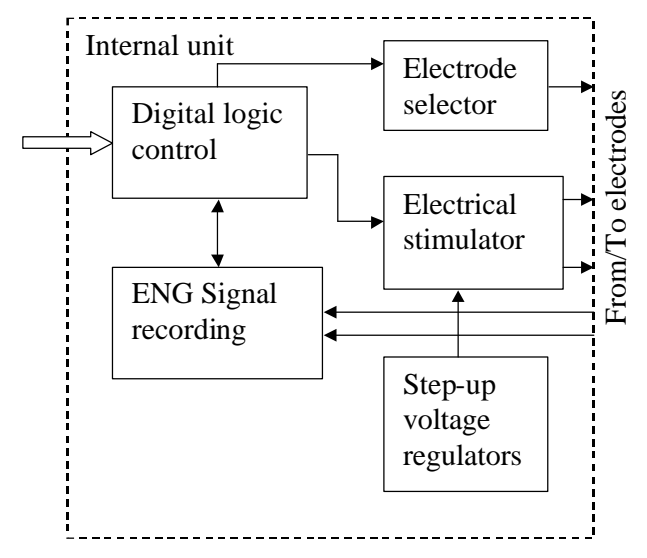


Fig. 2: Blocks schema for stimulation-recording circuitry

2. Digital logic control.

The structure for the digital logic control (**DLC**) is based on an internal memory that can be programmed according with the kind of electrode and the application to be implemented. The functionality associated to this block has been split in several simple blocks, as shown in Fig. 3, all of

them connected by an internal bus whose access will be managed by the main block named **MainCtrl**. Each block has its own internal address through which they can intercommunicate. The functionality associated to each module is briefly described in the following paragraphs.

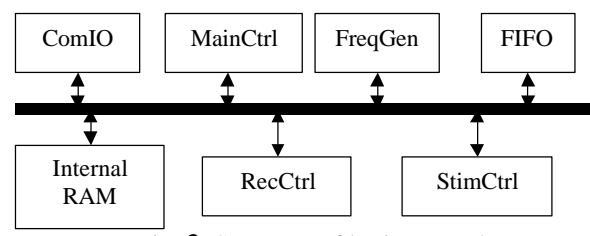


Fig. 3: Structure of logic control

ComIO: This block acts as interface between the DLC and the external controller or telemetry system. Frames are identified and processed activating the internal signals addressing the information to destination. FreqGen: This block is responsible for generating the frequencies of stimuli. Is based in a general counter of 19 bits, containing the period of the stimuli, with a clock of 4MHz, only the 12 most significant bits are needed for the frequency control in a range of 7 to 200 Hz with 1 Hz resolution. When more than one frequency is activated before generating the stimuli, a collision is produced and the pending stimulation waveform is sent to a FIFO for a later activation. Internal Ram: In this block all the stimulator parameters are stored. This is a RAM of 256 words of 12 bits that allows programming 16 frequencies for 16 different stimulation waveforms. The parameters for the programmed waveform will be stored in consecutive positions. A normal waveform consists in a prepulse followed by a stimulation pulse an interdelay and finally a recovery phase. An exponential charge recovery phase can be programmed to compensate the residual charge due to finite resolution in parameters definition. **FIFO 8x4:** This FIFO of 8 levels deep and 4 bits wide is used to solve the collisions problem. Then when a stimulation is activated from FregGen module, this is introduced in the FIFO and will be read after finishing the actual stimulation. MainCtrl: The task of this module is to control the access to the internal bus. Any module can need the bus at any time for accessing to any of the other blocks, then a request is sent and the MainCtrl block assigns the bus based in a priority table already established. The highest priority is assigned to the FreqGen module to avoid any frequency loss, second ComIO to assure the reception of data coming from outside, third StimCtrl and finally the RecCtrl. StimCtrl: This block implements the algorithm for stimuli generation reading parameters from memory and generating signals controlling the stimulator.

Single stimulus or bursts at the programmed frequency can be generated. The process for a stimulus generation follows the sequence below:

- 1. The module **FreqGen** finish the count for a frequency
- 2. Module **FreqGen** write in the **FIFO** the frequency identifier
- 3. If the **FIFO** is not empty, the **StimCtrl** reads from the **FIFO** the pointer to one of the 16 waveforms
- 4. **StimCtrl** reads the initial **RAM** address for this waveform
- 5. **StimCtrl** reads the parameter and execute the sequence for stimulus generation
- 6. The **RAM** address is increased to the next one
- 7. Step 5 and 6 are repeated as many times as the number of parameters in the waveform
- 8. When the contents of the **RAM** is equal 0 then the waveform is finished and next position of the **FIFO** is read.

Finally, the **RecCtrl**: It is the last module in the DLC generating the control signals required for amplifier activation, electrode selection, sampling of information and control signals for ADC conversion. Moreover, digital data from ADC will be stored in in specific registers for a posterior transmission to the exterior controlled by the ComIO module. Although only one channel has been implemented, the module has been designed to fulfil the final specifications concerning the number of recording channels.

3. Electrical stimulator.

The electrical stimulator is based in programmable current sources providing biphasic stimuli of constant current in the range of 2 to 126 μA with resolution $2\mu A$ or 20 to 1260 μA with resolution $20\,\mu A$.

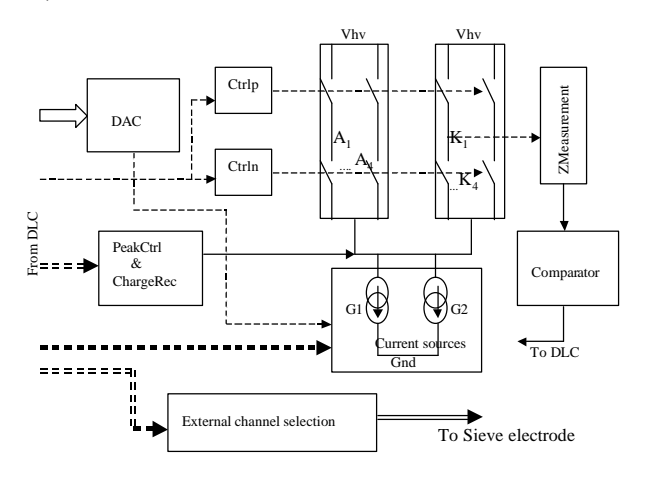


Fig. 4: Blocks structure of electrical stimulator

The H-structure used for the output stage assures the same current amplitude in the positive and negative phase because the same current source is used and only the current through the electrode is reversed. A blocks schema for the stimulator is shown in Fig. 4. The DLC will generate all the control signals for the stimulus shape, amplitude/duration of the stimulation and recovery phase, frequency and channel activation among other programmable features.

When using the stimulator with cuff electrodes, any anode can be associated to any cathode allowing not only longitudinal stimulation but also transversal. The sieve electrode has been housed with a multiplexer to reduce the number of wires to access any specific electrode contact then the external channel selector will generate the number of pulses to select an specific cathode in the sieve. Stimuli are applied between the selected cathode and a common anode.

Specific circuitry and channel activation sequence has been implemented to reduce initial spikes in stimuli generation and also an impedance measurement module with electrode testing purposes has been added to each cathode terminal.

4. One channel recording.

A full differential preamplifier followed by two signal amplifiers has been designed, fabricated and tested to have very good performances such as a low noise $(5nV/\sqrt{Hz})$, very low input $(1-200 \mu V)$, low frequency range (100-5000 Hz), high gain (70-100 dB) and high common mode rejection ratio (90 dB). A linear implementation with a CMOS technology has been used to assure the high CMRR because there are not components between the electrode and amplifier inputs. Specific design techniques have been used to obtain high time constants in a reduced silicon area to solve one of the most important problems appearing working with neural signals. The solution implemented has been proven to be very efficient to obtain a band pass amplifier for the above range of frequencies.

5. Method to use the Stim/Rec

The Stim/Rec circuit has been developed thinking that it can be used in different applications like a general-purpose stimulator or as a part of an implantable stimulator [Cyber]. If it is used in a local bus, for example with a microcontroller to control the stimulator, the system uses a 8 bits bus for Data, Rd/Wr and CS signals. On the other hand if the Stim/Rec is used in an implantable system a 3 wires serial bus for data and 2 for power supply will allow placing the system as near as possible to the electrodes and far from the telemetry. For programming the Stim/Rec a frame with the format (Ic-Number, Command, Parameters) is used. To implement all possibilities and make the design

simple each command is the internal bus address used in the Stim/Rec. In Table 1 can be shown 3 different actions and its frames.

Action	Command	Parameter
Program Frequency 1	0x100	Period
Enable Frequency 9 & 1	0x009	0x021
Force Stimulation Ch 2	0x010	0x002

Table 1: Example of frames for programming

The methodology used to implement the proposed stimulation-recording circuitry is that followed in a mixed (analogue/digital) circuit. The recording block and the analogue part of the stimulator is a full custom analogue CMOS design while for the digital logic block a semi-custom strategy is followed. Because the high voltage requirement of the analogue part of stimulator, a high voltage technology is needed then, I2T100 compatible with CMOS 0.7 micron has been used. A microphotograph of the developed circuit is shown in Fig. 5.

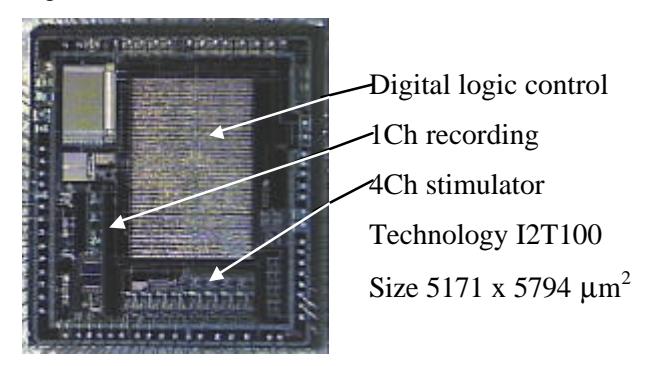


Fig. 5: Picture of recording-stimulation circuitry

Results

The full operation of stimulator and recording circuitry including the digital part for programming and controlling the two blocks have been tested at the laboratory and also the monolithic prototype developed with the test application has been used in experiments with animals. Results in Table 2 show the electrical characterization of stimulator.

The resolution in the amplitude is higher than specified resulting in a higher full range. Moreover, a higher stimulation frequency can be programmed with a lower resolution if necessary but this is not considered of interest in biomedical applications. Table 3 shows typical parameters defining the full amplifier operation, it is important to notice the perfect correspondence between the experimental and simulation results.

In this amplifier the gain in the band as well as the low cut-off frequency are digitally programmed for a better adaptation to input signal.

Parameter	Value
Amplitude	3 - 184 μA resolution 3 μA
	30 - 1840 μA resolution 30 μA
Pulse duration	
and Inter-delay	$4-1024 \mu s$ resolution 1 μs
	16 different waveforms
Standard	
waveform	
Charge recovery	Exponential programmable extra
	charge recovery
Stimulation	7 - 200 Hz resolution 1 H
frequency	200 - 300 Hz resolution 3 Hz
	16 different frequencies
Impedance	$500-22 \mathrm{k\Omega}$
measurement	

Table 2: Stimulator electrical characterization

When the higher low cut-off frequency is programmed a better noise performance is got and the rejection of muscular and electrode interface contamination is also higher. The decay of gain for the low and high corners is 60 and 40 dB respectively.

Parameter	Simulation	Experimental
Gain in the band (dB)	75, 83, 97, 103	76, 80, 96, 102
Noise (nV/√Hz)	4.9	5
CMRR (dB)	96	94
Low cut-off freq. (Hz)	97,116,206,385	106,119, 201,352
High cut-off freq. (Hz)	5.3 kHz	8 kHz

Table 3: Results for recording amplifier

The developed monolithic prototype optically isolated has been used in experiments with animals. It was used to test muscular activity produced with biphasic charge compensated stimuli applied at different frequencies and also spatial selectivity is accomplished using amplitude and pulse width modulation. In Fig. 6 results obtained with a Sprague-Dawley rat stimulating the tibial nerve and signal recording in plantar muscle using microneedle electrodes for the recruitment with amplitude modulation is shown.

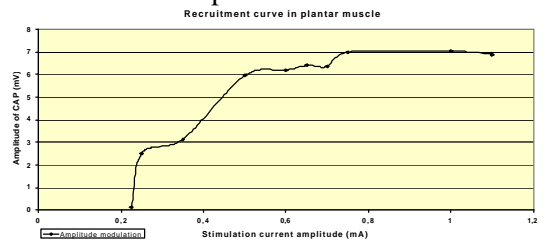


Fig. 6: Recruitment curve with amplitude modulation

Finally, in Fig. 7 the ENG signal recorded with a cuff electrode [3] in sciatic nerve in response to repeated pinpricks on hind limb skin is shown.

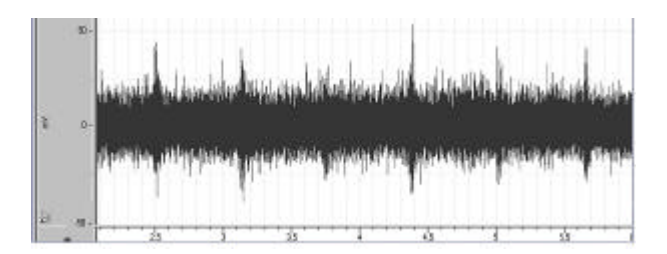


Fig. 7: Response to mechanical stimulation

Discussion

Actually functional electrical stimulation is being used in many applications and also in closed loop operation in order to improve restoring functions but there is not reported any system including natural sensors (stimulation and recording circuitry in the same ASIC) to implement the full system. Here we are presenting a general purpose stimulation-recording circuitry that can be used to fulfil these requirements in SCI subjects or in amputees. The system characterization obtained by electrical measurement at the laboratory and also the work carried out in acute experiments with rats has proven to work properly. Moreover, and because of its modular implementation, the system performances can be improved concerning the number of channels for the Stim/Rec device and also logical control flexibility allows to connect several devices with a few wires to the telemetric unit in implantable systems.

References

- [1]Popovic MR, Keller T, Pappas I, Dietz V, Morari M. Surface-stimulation technology for grasping and walking neuroprostheses. IEEE Eng. in Medicine and Biology. 2001 pp 82-93.
- [2]P.R. Troyk et al. Modular VLSI electronic design for implantable neural prosthesis. Proc. 2nd Joint EMBS/BMES Conference. 2002.
- [3]T. Stieglitz et al. Micromachined multichannel cuff electrodes for interfacing small nerves. Proc. 1st Joint EMBS/BMES Conference. 1999.

Acknowledgements

European Commission with the project CyberHand (IST-25394) and Spanish CICyT have founded this work. We would like to thank all partners in the project for discussions on system definition.

Author's Address

Eng. Jordi Sacristán

Electronic Circuits & Systems Design department Campus de la UAB, 08193 Bellaterra, Spain

e-mail: <u>Jordi.Sacristan@cnm.es</u>, home page: www.cnm.es

A POWER EFFICIENT ELECTRONIC IMPLANT FOR A VISUAL CORTICAL STIMULATOR

J. Coulombe, S. Carniguian, M. Sawan

PolySTIM Neurotechnologies Laboratory,
Dept. of Elec.Eng., Ecole Polytechnique de Montreal, Canada

Abstract

An integrated micro-stimulator designed for a cortical visual prosthesis is presented, along with a pixel reordering algorithm, together minimizing the peak total current and voltage required for stimulation of large number of electrodes at a high rate.

In order to maximize the available voltage for stimulation at a given supply voltage for generating biphasic pulses, the device uses monopolar stimulation, where the return electrode voltage is dynamically varied. Thus, voltage available for stimulation is maximized, as opposed to the conventional fixed return voltage monopolar approach, and impedance is significantly lower than what can be achieved using bipolar stimulation with micro-electrodes. This enables the use of a low voltage power supply, minimizing power consumption of the device.

An important constraint resulting from this stimulation strategy, however, is that current generation needs to be simultaneous and in-phase for all active parallel channels, imposing heavy stress on the wireless power recovery and regulation circuitry in large electrode count systems such as a visual prosthesis. An ordering algorithm to be implemented in the external controller of the prosthesis is then proposed. Based on the data for each frame of the video signal to be transmitted to the implant, the algorithm minimizes the total generated current standard deviation between time multiplexed stimulations determining the most appropriate combination of parallel stimulation channels to be activated simultaneously.

A stimulator prototype has been implemented in CMOS technology and successfully tested. Execution of the external controller reordering algorithm on an application specific hardware architecture has been verified using a System-On-Chip development platform. Near 75% decrease in the total stimulation current standard deviation was observed with a one-pass algorithm, whereas a recursive variation of the algorithm resulted in a greater than 95% decrease of the same variable.

Introduction

Integrated circuits are now used in several biomedical applications as implantable stimulators for rehabilitating physical disorders [1-3]. In many cases, these are controlled by an external processor and they get their supply energy from an inductive link. The available power for these implants is especially limited because the electromagnetic field through tissues is limited by standards for safety, and for avoiding excessive heating, maximum power efficiency is required. Therefore, both current and voltage shall be kept to a minimum.

The voltage required at the output stage of the implant is dictated by the combination of the current used for stimulation and the electrodetissue interface impedance. In most cases, to provide the stimulator with sufficient voltage compliance, designers have chosen to use relatively high voltage technologies, either aging or non standard [4-5]. However, for complexe systems, numerous digital operations need to be performed. If one wants to include flexibility in stimulation patterns with high pulse rates, despite a limited bandwidth imposed by the use of low frequency carrier for reduced absorption by tissues. data compaction shall be used. Also, safety features such as communication error detection and correction capability, as well as implant status monitoring, are highly desirable. Such tasks require significant processing capability. Added to the need for high power efficiency and low physical dimensions, low voltage state-of-the-art technologies are preferred. Unfortunately, the use of high voltages is then either impossible or not reliable for long term usage.

To limit stimulation voltage swing, one can usually still inject sufficient charge with low current, provided that extended pulse period are applied. However, when the total number of sites is very large and stimulation has to be performed at a high rate, as in the case of a visual prosthesis, this results in the need for very high parallelism. Hence, the total current supply need remains important.

We discuss in the next section the several options available for current based stimulation, and select an optimal approach with respect to the voltage compliance of the stimulator output stage. The intended scheme, however, although easily implemented on devices with few channels, brings regulation concerns and affects power efficiency. An algorithmic approach to solve this issue by minimizing the total peak current according to the data to be processed will then be introduced. Implementation results and a summary will follow.

Low-Voltage Biphasic Stimulation

For chronic stimulation, the preferred approach consists of applying constant current signals, most commonly pulse shaped [6]. To avoid degradation of the tissues, charge balanced biphasic pulses are mandatory. Fig. 1 shows a simplified model of an output stage capable of performing both bipolar and monopolar stimulation, with a simplified electrode-tissue impedance model, in which R_S is the series ohmic resistance, while C_D and R_D are the capacitive and resistive components of the double-charge layer at the electrode-electrolyte interface. Note that the off-chip return electrode is not intended for stimulation, therefore it can be large and its impedance can be neglected.

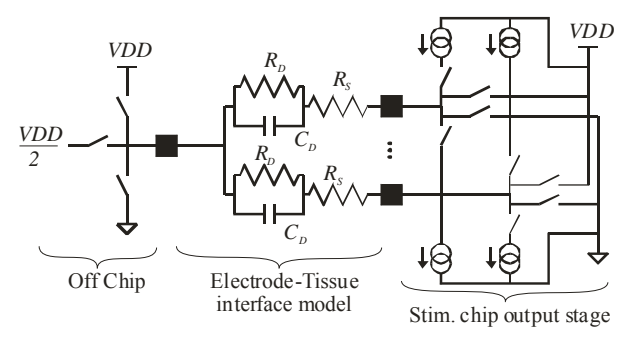


Fig. 1. Simplified schematic of the stimulator output stage for two electrodes on a single channel, with their associated electrode-tissue interface impedances.

Bipolar stimulation presents the advantage of allowing much larger voltage swing than monopolar stimulation at a given supply (VDD, vs VDD/2, neglecting current sources saturation voltages), while the latter approach has nearly half the total electrode-tissue impedance. When the stimulation pulse is shorter than what is required for the voltage to reach its theoretical maximum, which is the case in most applications, the higher ohmic resistance of the bipolar path reduces the charge that can be injected/withdrawn in/from the tissues (Q_2 vs Q_1 in Fig. 2).

In the same conditions, if the off-chip return current electrode is set dynamically such that its voltage is *VDD* (*VSS*) for cathodic (anodic)

stimulation, both highest voltage swing and lowest impedance are obtained. Note that because of the non-linear rise of the electrode voltage during stimulation, doubling the allowable voltage swing for a given electrode-tissue impedance allows for more than twice the maximum charge (Q_3) .

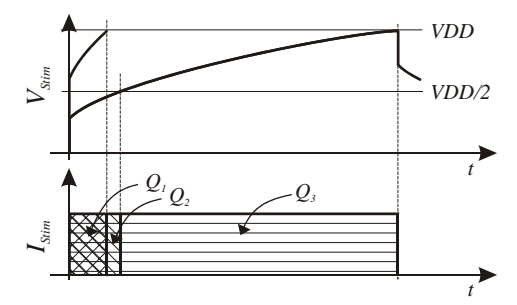


Fig. 2. Typical electrode voltage waveform (a) when applying a constant current pulse (b).

Stimulating in a monopolar configuration with a return electrode alternatively set to *VDD* or *VSS* has been used in the past [7]. However, serious concerns arise when this has to be applied to a stimulator with a large number of parallel channels. Since, at any time, either of the current sources or sinks is unusable, anodic and cathodic stimulation cannot be performed simultaneously on parallel channels. Therefore, a high instantaneous total current is required, putting heavy strain on the regulating circuitry.

Because of their low noise performance and small size, linear devices are generally the preferred components for voltage regulation. However, their power efficiency is very poor if their voltage drop from input to output is large.

In an effort to minimize the peak current and total current variance, hence reducing the drop-out voltage through the regulator, we propose an algorithm that adapts the scanning sequence depending on stimulation parameters.

Reordering

Consider a visual prosthesis driving an NxM electrode matrix, where N is the number of parallel channels, each driving M electrodes in M successive time periods for forming an NxM image. Let N=M=8 and the simple image in Fig. 3 a) be created by relative current intensities represented by integer values in Fig. 3 b).

Scanning parallel rows in a predefined left-to-right manner would result in the total current consumption pattern depicted in Fig. 4 a). A simple yet relatively efficient way of smoothing the total current deviation is to sort the *M* elements of odd and even numbered channels in increasing and decreasing order, respectively, prior to sending the stimulation data to the implant. Applying this

operation (Opposite Sort Sum - OSS algorithm) to the example of Fig. 3 leads to the total current consumption pattern of Fig. 4 b).

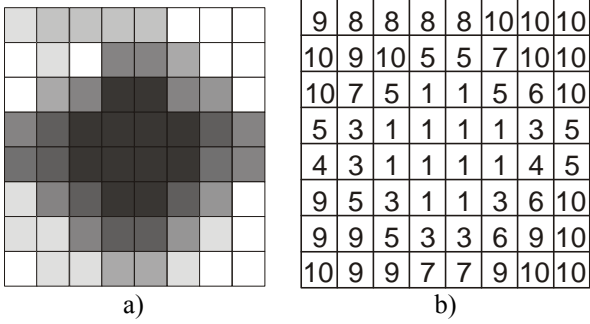


Fig. 3. Simple 8x8 image (a) with its associated current intensities (b).

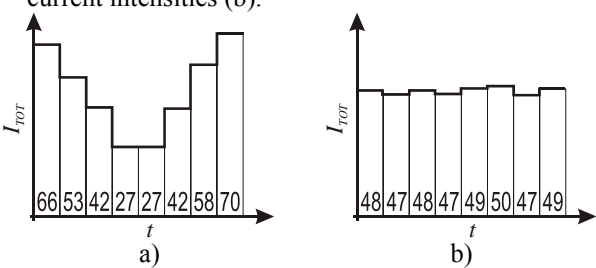


Fig. 4. Total stimulation current before (a) and after (b) OSS algorithm.

Although this technique significantly reduces the maximum instantaneous current consumption and the mean deviation of the total current in many cases, the algorithm is not very effective on inhomogeneous images because of evaluation of data limited to only pairs of lines. To make the algorithm more reliable for any input image, the algorithm can be applied recursively on growing sets of sorted parallel channels.

After a first iteration, identical to that described in the OSS case, pairs of channels are considered together and their M summed elements are sorted in either increasing or decreasing order. In this second iteration, N/2 sorts of M elements are performed, where N/4 of them are increasing and as many are decreasing. Subsequent iterations can be performed until single increasing and decreasing sorts are performed on the total currents

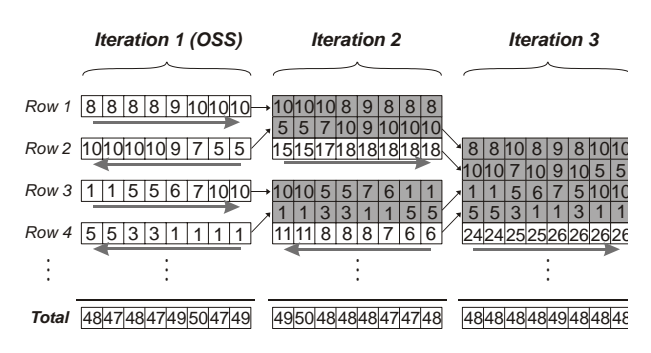


Fig. 5. Data flow of recursive algorithm applied to the upper half of the sample image in Fig. 3.

of two sets of N/2 channels. A near optimal smoothing can be reached after $Log_2(N)$ iterations. Fig. 5 depicts this processing, named Smoothing Of Set of Opposite Sort summation algorithm (SOSOS), applied on the example used above.

Implementation Results

Two independent test benches were created. First, an integrated stimulator prototype with 16 stimulation sites in 4 channels driving 4 electrodes each was fabricated in a CMOS 0.18 µm process, as described in [8]. The implant interface module controller was implemented using discrete components and a pattern generator for testing the various stimulation strategies via microelectrodes in a physiological solution.

Complementarily, a dedicated computation unit was implemented on a SOC rapid prototyping platform and tested on a stimulator prototype not intended for implantation. The latter comprises the same hardware structure as the integrated device, but is intended to drive a large matrix of LEDs in order to display images in real-time, enabling the testing of controller hardware and algorithms prior to the availability of a large electrode-count implantable device. The implemented test set-ups are presented in Fig. 6.

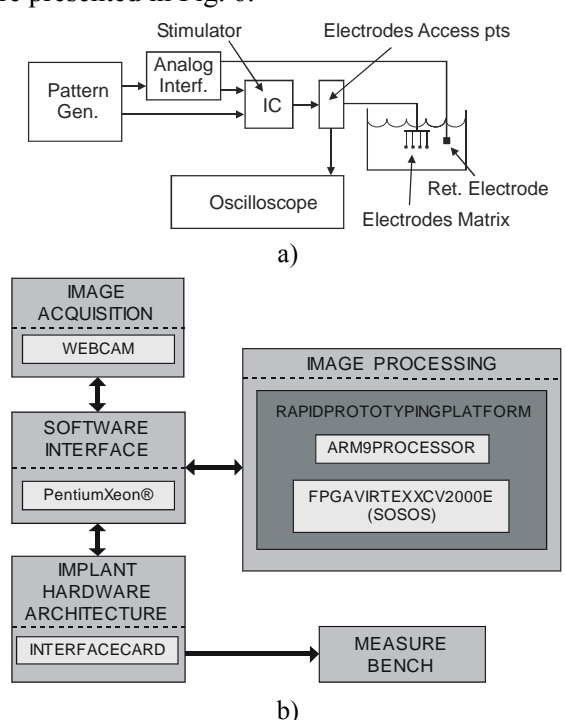


Fig. 6. Test set-ups.

Fig. 7 shows the clear advantage of using dynamic return electrode when the voltage swing is limited by a low supply. The maximum allowable current is more than doubled when current sources saturation voltages are taken into account. Also, maximum charge per phase when the phase duration determines the peak stimulation voltage is

also significantly increased, leading to effective stimulation being possible in greater number of situations.

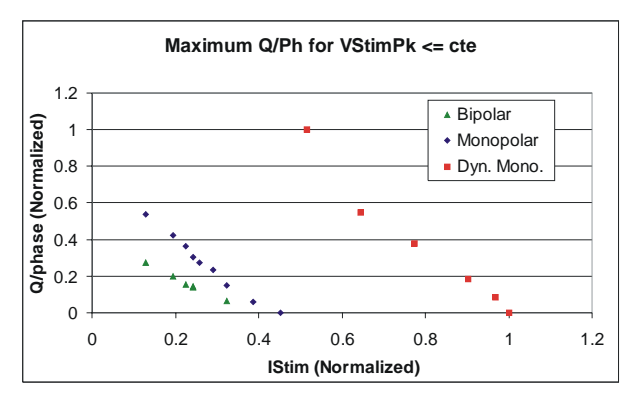


Fig. 7. Maximum charge per phase vs current applied with integrated stimulator (VDD = 3.3V) for monopolar, bipolar and dynamic return monopolar stimulations.

Fig. 8 depicts the results of applying the reordering algorithms to pseudo-random and real images prior to sending data to the implant. Both maximum instantaneous consumption and variations are reduced by applying the single step algorithm, and the recursive approach leads to near optimal preregulation. Reduction in the total current standard deviation reaches near 75% and more than 95% when applying the OSS and SOSOS algorithms, respectively.

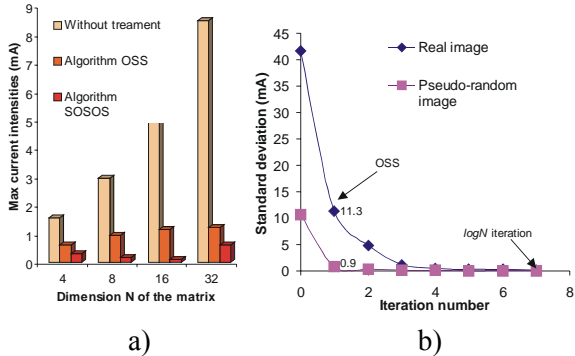


Fig. 8. Peak (a) and standard deviation (b) of total current for square images before and after OSS and SOSOS processing.

Summary

An effective stimulation strategy for applying constant current pulses has been presented, along with a data processing algorithm that enables smooth current consumption for large electrodecount implantable systems.

Combining these two concepts allows for maximum efficiency at a given supply voltage, and for minimum regulator drop-out, making the use of state-of-the-art technologies for implant fabrication notably efficient and reliable.

References

- [1] S. Boyer, et al.: Implantable Selective Stimulator to Improve Bladder Voiding: Design and Chronic Experiments in Dogs, IEEE Trans. Rehab. Eng., 8(4), Dec. 2000, 464-470.
- [2] Liu, W. et al.: A neuro-stimulus chip with telemetry unit for retinal prosthetic device, IEEE JSSC, vol. 35, Oct. 2000, 1487 –1497.
- [3] C.M. Zierhofer, I.J. Hochmair-Desoyer, E.S. Hochmair,: Electronic design of a cochlear implant for multichannel high-rate pulsatile stimulation strategies, IEEE Trans. Rehab. Eng., Vol 3, Mar 1995, 112 –116.
- [4] Ghovanloo M, Beach K, Najafi K,: A BiCMOS Wireless Interface Chip for Micromachined Stimulating Microprobes, IEEE-EMBS Special Topics Conference on Microtechnologies in Medicine and Biology, May 2002, 277-282.
- [5] DeMarco, et al.: An Arbitrary Waveform Stimulus Circuit for Visual Prostheses Using a Low Area Multibias DAC, IEEE J. Solid-State Circuits, V. 38, No. 10. Oct. 2003.
- [6] Agnew, W.F, McCreefy, D.B, Neural prostheses: fundamental studies. Prentice hall, Englewood Cliffs, NJ, 1990, 322 pp.
- [7] Gudnason, G, Bruun, E., Haugland, M.: An Implantable Mixed Analog/Digital Neural Stimulator Circuit, Proc. ISCAS, Orlando, 1999.
- [8] Coulombe, J., Buffoni L.-X., Sawan M.: A Mixed-Signal IC for Multiple Cortical Stimulation Strategies, Proc. 45th MWSCAS, Tulsa, August 2002.

Acknowledgements

Authors wish to thank the Canadian Microelectronics Corporation for fabrication and technical support, as well as NSERC for financial support.

Author's Address

Jonathan Coulombe
Department of Electrical Engineering
École Polytechnique de Montréal
2900 Edouard-Montpetit, Qc, Canada
e-mail: jonathan.coulombe@polymtl.ca
home page: www.polystim.polymtl.ca

IMPLANTABLE STIMULATOR FOR THE CONDITIONING OF DENERVATED MUSCLES IN RABBIT.

Hermann Lanmüller*, Ewald Unger*, Martin Reichel*, Zoe Ashley**, Winfried Mayr*, Andreas Tschakert*

* Department for Biomedical Engineering and Physics, Medical University of Vienna, Austria

** Muscle Research Group, Department of Human Anatomy & Cell Biology, University of Liverpool, UK

Abstract

The implantable stimulation device was developed for the conditioning of long-term denervated degenerated muscles. The goal of this still running project is the examination of the muscular regeneration by the use of different stimulation protocols in an animal experiment in rabbit. In comparison with the stimulation of an innervated skeletal muscle, a high current density and pulse duration is required to cause a contraction of a denervated muscle.

The stimulator is controlled by a microcontroller and powered by two Lithium Thionyl Chloride batteries. The pulse parameters and training parameters are programmable via a bidirectional telemetry circuit. The output stage provides a biphasic constant current pulse for muscle excitation. The final size of the stimulator is 46x38x17 mm; it weighs 45 g. The electrodes are manufactured of stainless-steel and embedded in silicone rubber. A thin sheet of 0.1mm is spot welded to the lead, one side isolated by silicon rubber and shaped like a pear to touch the whole muscle. The stimulation data are input using a notebook computer. Each modification is stored automatically and can be processed in conjunction with comments by the user to create an individual study protocol for each animal.

The design of the stimulator turned out as resistant and long-term stable. Up till now 41 units had been used in the study. No functional defects were discovered over an implantation duration of 2-24 weeks.

Introduction

The described implantable stimulation device was developed for an animal experiment in rabbit as a part of a research project of the European Union called "RISE". In this project a novel clinical rehabilitation method for patients suffering from long-term flaccid paraplegia (denervated degenerated muscles - DDM) with no chance of recovery of the nervous system, will be developed. It will restore their muscle fibres (and mass), muscle function (tetanic contractions, weight

bearing) and thus their ability to rise ('standing up') and maintain a standing posture ('standing'). Based on the results of animal experiments on rabbit and pig and initial clinical trials the associated technology will be developed. The method addresses the needs of about 20 new patients per million EU inhabitants per year. First results of this project had been published by Carraro U.[1], Kern H.[2], and Mayr W.[3].

The implatable stimulator is used for the conditioning of the denervated M. tibialis anterior in rabbit. Different stimulation patterns will be used and the change of the muscle fibres and function will be analysed.

In comparison to an implantable nerve stimulator [4], the architecture of a muscular stimulator is quite similar. Differences are given by the electrodes and the stimulation patterns. For the excitation of a denervated muscle the electrical field had to spread into the whole volume of the muscle. Therefore, the active area of the electrodes had to be enlarged and covers more or less the whole surface of the muscle. Additionally, an increased current density is required. Both effects are increasing the pulse charge, necessary for the contraction of a denervated muscle, by a factor between 100 to 500 compared to an innervated muscle.

The development of the device was aimed to fulfil the following principles. Basically, the device should be long term stable for an implantation duration of 12 weeks, with the opportunity to modify the stimulation patterns and the device itself in a easy and fast way. The device should be user friendly and safe against operating errors. At least, the device should support and simplify the realization and analysis of the animal experiment.

Material and Methods

The stimulation device is composed of a programmer with a transmitter unit, a programmable stimulator, and epimysial electrodes (Fig. 1). Implant programming is achieved by a notebook computer, supported by a graphical user interface.

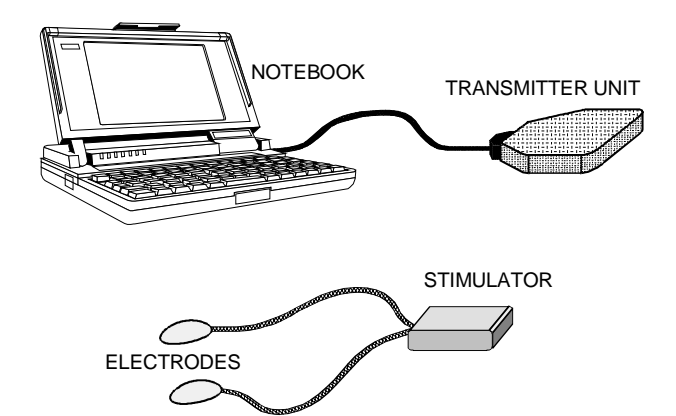


Fig.1. Schematic drawing of the stimulation device

Programmable stimulator

The stimulator includes an output stage, a transmitter unit, and a microcontroller (PIC16F874, Microchip Technology Inc., Arizona USA). Each training sequence had to be triggered by the programmer and is terminated automatically by the microcontroller.

The microcontroller activates the output stage for each burst. The pulse parameters (frequency, pulse width, pulse amplitude) and training parameters (burst duration, burst pause, period of training) are set by the controller. All parameters and functions are programmable via the bidirectional telemetry circuit. Data transfer in both directions is carried out using radio-frequency telemetry. The output stage provides a biphasic constant current pulse for muscle excitation. An additionally capacitor on the output is used to guarantee charge balance.

Stimulation Amplitude	max. 10 mA (40 μA)	
Pulse Width per Phase	0,5 - 40 ms (0.5 ms)	
Stimulation Frequency	1 - 64 Hz (1 Hz)	
Period of Training	10 - 180 min(10min)	
Burst Duration	0,1 - 10 s (0.1s)	
Pause Duration	0,1 - 10 s (0.1s)	
Maximum Electrode Impedance	500 Ω	

Table 1. Technical specifications for the stimulator () Resolution of this parameter $\$

The stimulator is powered by two Lithium Thionyl Chloride batteries (LPC-7PN, Eagle-Picher Industries, Missouri, USA) with an open circuit voltage of 3.67 V and a capacity of 750 mAh. The operating time is mainly influenced by the stimulation parameters. The power consumed by controlling (130 μ W during stimulation, 55 μ W in stand by) and data transmitting can almost be neglected.

The electronic circuitry of the stimulator is fabricated in surface mount technology (SMT). The hybrid is enclosed in a hermetically sealed (resistance seam welded) gold-plated flatpack (Olin Aegis, MA, USA). The flatpack still connected to the batteries, the receiver coil, the output capacitor for DC decoupling and the electrode connector are embedded in medical grade epoxy resin. The final size of the stimulator is 46x38x17 mm; it weighs 45 g.



Fig.2. Programmable stimulator embedded in epoxy resin, controlled by a microcontroller and powered by two batteries.

Electrodes

The electrodes are manufactured of stainless-steel and embedded in silicone rubber. A temporary pacing lead (Medtronic, Inc., Minneapolis, MN, USA) is used to connect the stimulator with a thin stainless-steel sheet of 0.1mm. The active electrode area is about 150 mm². The sheet is spot welded to the lead, one side isolated by silicon rubber and shaped like a pear to touch the whole muscle.

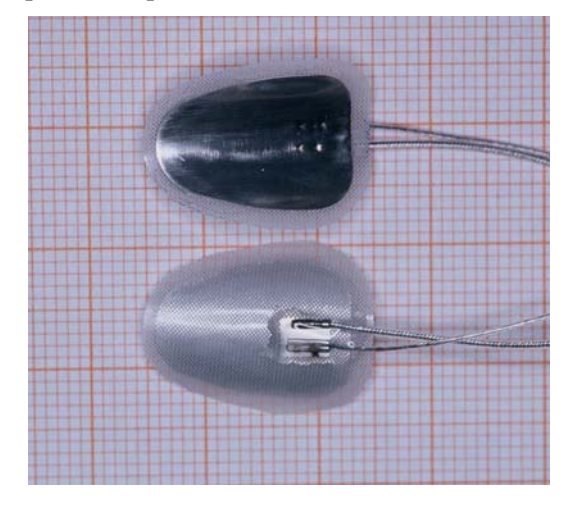


Fig.3. Epimysial electrodes manufactured of stainlesssteel and silicone rubber with an active area of 150 mm²

Programmer and transmitter unit

The stimulation data are input using a notebook computer (IBM-PC or compatible). A graphical user interface facilitates the setting and modification of parameters. Each modification is stored automatically and can be processed in conjunction with comments by the user to create an individual study protocol for each animal.

Data are transferred from the PC to the implanted device using a bidirectional radio-frequency transmitter unit linked to the serial port (RS-232) on the PC. Transmission to the implant is achieved by using Amplitude Shift Keying (ASK) and Load Shift Keying (LSK) for back transmission. The transmission link operates over a vertical displacement of up to 40 mm with a horizontal displacement of +/-30mm at a data rate of 1200 bit/s and a carrier frequency of 100 kHz. Transmission reliability is increased by the stimulator sending its serial number and each individual data word back to the programmer for checking. Furthermore, the modified stimulation data are only accepted after a check sum transmitted from the programmer has been verified by the implant.

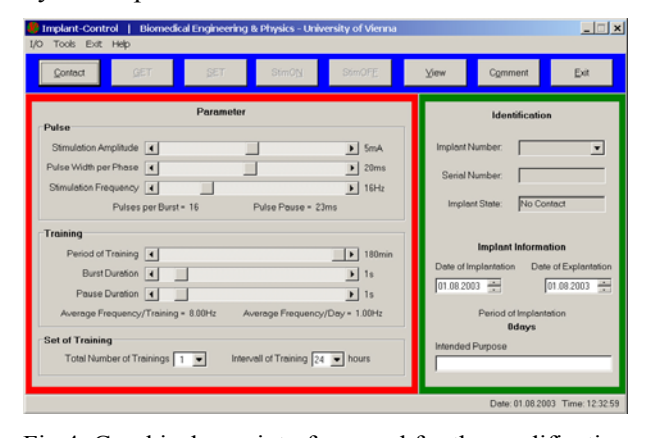


Fig.4. Graphical user interface used for the modification of stimulation patterns

Results

Up till now 41 units out of a serial of 54 units had been used in the animal study. No functional loss occurs over an implantation duration between 2-24 weeks.

During production 5 units had been lost by mechanic (2) or electrical (1) manufacturing faults and by the failure of single electronic components (2). The production of one unit takes the amount of approximately 20 man-hours.

Discussion

The design of the stimulator turned out as resistant and long-term stable. A failure rate during

production below 10% is acceptable. The long-term stability in vivo without any functional loos is very satisfactory.

The functionality of the device turned out as userfriendly and efficient. Additional features, for example a measurement module for the detection of the strength - duration curve, had been edit-in during the ongoing experiment.

An interesting technical problem could be recognized during the development. The frequency of the implant resonance circuit increases stepwise by tempering the implant at the end of production process. Mechanical stress between the ferrite core and the epoxy resin capsule could be detected as the cause of this phenomenon. Micro cracks in the ferrite core are obviously decreasing the conductance, which increases the resonance frequency. To solve this problem we are now coating the ferrite core by a thin elastic silicone layer before casting.

References

- [1] Carraro U.: Modulation of trophim and fiber type expression of denervated muscle by different patterns of electrical stimulation. BAM 2002;12(6):263-272
- [2] Kern H., et al.: Functional electrical stimulation (FES) of long-term denervated muscles in humans: Clinical observations and laboratory findings. BAM 2002;12(6):291-29
- [3] Mayr W., et al.: Functional electrical stimulation (FES) of long-term denervated muscles: existing and prospective technological solutions. BAM 2002;12(6):287-290
- [4] Lanmüller H., et al.: Multifunctional implantable nerve stimulator for cardiac assistance by skeletal muscle. Artif-Organs Apr 1999; 23 (4): 352-359

Acknowledgements

This work was supported by EU Commission Shared Cost Project RISE, Contract Nr. QLG5-CT-2001-02191.

Author's Address

Hermann Lanmüller Ph.D.
Department of Biomedical Engineering and
Physics, AKH 04L,
Währinger Gürtel 18-20, A1090 Vienna, Austria,
e-mail: hermann.lanmueller@univie.ac.at
home page: www.bmtp.akh-wien.ac.at

IMPEDANCE EFFECTS IN SPINAL CORD STIMULATION: CONTACT IMPEDANCE VARIABILITY

Paul Meadows ¹, Clayton Varga ², John Oakley ³, Elliot Krames ⁴, Kerry Bradley ¹

¹ Advanced Bionics Corporation, Valencia, CA USA

² Pasadena Rehabilitation Institute, Pasadena, CA USA

Abstract

In spinal cord stimulation (SCS), two types of pulse generators (PG) are used: single-channel and multi-channel. In any PG, the physiologic impedance (Z) of the tissue surrounding the stimulating contacts is important in determining the amount and distribution of the stimulating current to the spinal nerves. To evaluate these effects, in 35 patients, undergoing percutaneous trial of SCS for chronic pain, we measured the Z of common SCS leads (Medtronic Models 3487A and 3890) to characterize the difference in Z between contacts on the same lead and on dual-parallel leads in the same patient. We found a significant difference in the monopolar Z between contacts on the same lead (median: 35 Ω , 25%-75% quartiles: 18-76 Ω ; P < 0.05). We also found a significant difference between the bipolar Z on matched bipoles on dual-parallel leads implanted in the same patient (79 Ω , 28-132 Ω ; P < 0.05). These results have clinical implications for SCS, as the ability to provide "balanced" multiple pain site coverage is difficult with single-channel PG's. The use of multi-channel stimulators or stimulators with independently programmable current sources for each contact can mitigate these problems.

Introduction

Spinal cord stimulation (SCS) has been employed in the treatment of chronic, intractable neuropathic pain for over 30 years [1]. Technical advancements in SCS systems have improved the long-term efficacy of the therapy: these include an increase in the number of stimulating contacts on a lead [2] and the ability to deliver stimulation current from dual leads [3, 4].

A relatively underexplored factor of achieving consistent stimulation results in SCS is the contact impedance. Earlier reports have focused on the impedance of simple contact combinations (e.g., bipoles) and their variation over time. [5, 6, 7].

However, since the selectivity of the stimulation field (stimulating desired nerve fibers while avoiding the stimulation of undesired nerve fibers) is primarily determined by the distribution of the anodes and cathodes along the implanted contacts, achieving optimal paresthesia coverage for patients with complex pain often requires more complex contact combinations [3, 4, 8]. In such combinations, the impedance of each contact plays a role in the delivery of the stimulation current and thus can affect the resulting paresthesia. We investigated and analyzed the variability of the impedance of individual implanted contacts on a per-lead and across-lead basis.

Methods

Clinical

Patients were enrolled who were undergoing a percutaneous trial of SCS for a variety of chronic pain conditions. We limited our impedance study to patients implanted with two of the most common Medtronic lead models: the 3487A Pisces Quad and the 3890 Pisces Z Quad. These quadripolar leads with the following isodiametric 1.27mm diameter; characteristics: cylindrical contact shape of 3mm contact length, 6mm edge-to-edge intercontact spacing; platinum iridium alloy contact material [9, 10]. In order to impedance of these accurately study the percutaneous SCS contact arrays, we employed a ohmmeter system with custom greater measurement accuracy than the ~11% reported by Andersen for standard SCS programming systems [3]. For the period of the study, patients were disconnected from their commercially-available trial stimulator and connected to the ohmmeter The ohmmeter circuitry was batterypowered and communicated via an infrared link to a laptop/pen tablet PC, which ran custom software. The custom software was able to make pulsatile impedance measurements. The measurable range

³ Yellowstone Neurosurgical Associates, Billings, MT USA

⁴ Pacific Pain Treatment Center, San Francisco, CA USA

of impedance was $0 - 3024 \Omega$ with a resolution of 1Ω .

Impedance Measurement Technique: The impedance between any two contacts was defined as a 'vector.' The value of an impedance vector was determined as follows: a four-pulse burst of 1.0mA, 20µs pulses was delivered within a 500ms period. The voltage value at the middle of the 20µs pulse was sampled by the stimulator system. Each voltage value was then divided by 1.0mA and all four measurements were averaged to form one impedance value for a single vector. Multiple (3-6) impedance values were obtained for each impedance vector. The impedance for a number of vectors was obtained using 'blocks,' where each block was a randomized collection of impedance vectors. . All block files were run with the patient in the sitting position. The patient was instructed not to move during the measurements. Two types of impedance measurements were made: monopolar, where the impedance between each implanted contact was measured with respect to a 10cm self-adhering TENS patch; and bipolar, where the impedance was measured between adjacent contacts on the same lead.

Impedance Calibration, Correction, and Assessment of Error

Stimulator Calibration for Systematic Error: In order to get accurate estimates of the impedance, the stimulator system was calibrated to a known resistive load (1% accuracy) so that corrective factors could be estimated and used to adjust the measured impedance values. The impedance circuit was verified to be linear ($R^2 > 0.9999$), on resistive loads over a typical clinical range [5, 6, 7]: $200 - 1750 \Omega$, but to have a systematic error due to an offset at all points in the measurable range. A correction factor was estimated from resistive load measurements this factor was then added/subtracted from each measured value. The calibration process resulted in a reduction of the systematic error to < 3%.

Impedance Correction: Lead Wire Resistance: In order to determine the "physiological" aspect of the impedance values (the impedance due to the tissue surrounding the contacts), the resistive portion of the impedance due to the wire conductors within the lead was subtracted from the calibrated impedance values. Estimates of the wire impedance were made from several dry bench samples of each lead type. It was found that the 3487A lead had approximately 101 and 146 Ω of wire impedance per monopolar vector for the

33cm and 45cm models, respectively. The 3890 had approximately 3 and 5 Ω per bipolar vector for the 33cm and 45cm models, respectively. These values were subtracted from the measured values to provide the "physiological" impedance.

Random Measurement Error: The measurement variability for each impedance vector was calculated from the calibration measurements as well as from measurements on patients. The mean error of the impedance measurement due to measurement circuit variability on a known resistive load was no greater than \pm 6 $\Omega_{\rm s}$, independent of the scale of the impedance. The mean error of the impedance measurement due to measurement circuit variability in patients was slightly higher, but was no greater than \pm 9 $\Omega_{\rm s}$, independent of the scale of the impedance

Data Analysis Monopolar: Since the monopolar impedance measurements included the impedance of the TENS patch electrode, the difference between monopolar impedances measured on adjacent contacts on a lead was used to estimate the impedance variability along the lead. Three pairs of contacts on each lead were used to calculate these differences ($Z_{e1} - Z_{e2}$, Z_{e2} - Z_{e3} , Z_{e3} - Z_{e4} ; where e1 is the most rostral contact and e4 is the most caudal contact).

Bipolar: To characterize the variability between leads, the impedance between matched bipolar contact pairs was assessed (e.g., $Z_{\rm el-e2}$ on lead 1 was compared to $Z_{\rm el-e2}$ on the lead 2. Typical duallead stimulation combinations often have the same polarity (anodic or cathodic) on adjacent contacts on dual leads placed in perfect parallel (or slightly staggered) [3]; this is done to achieve superposition of the stimulation field into the dorsal columns [11]. Thus, using these matched pairs can give insight into how any differences in impedance might affect the clinical outcome.

Impedance measurements for all patients were transferred into a spreadsheet analysis program (*Microsoft Excel 9.0*; Microsoft Corp, Redmond, WA) for statistical description and analysis. For non-parametric analyses, a statistical add-in analysis package (*statistiXL ver 1.2*, statistiXL.com) was employed. Non-parametric analyses were performed as appropriate to the distribution of the data. Statistics are reported as 'median (25% - 75% quartiles). The level of statistical significance was set at P < 0.05.

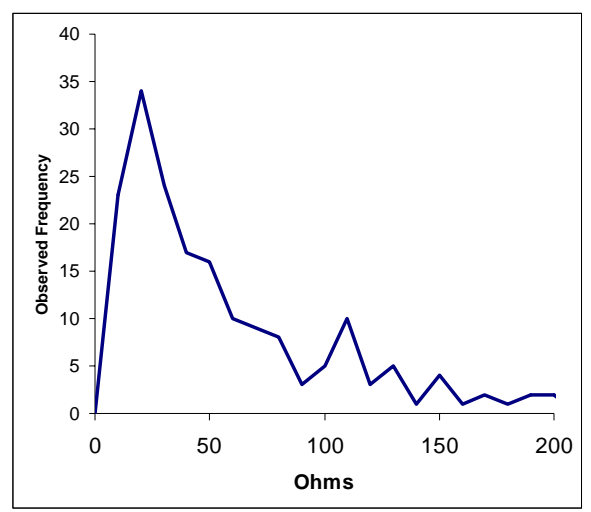
Results

Number of Patients		35
Gender		13M / 22F
Median Age		51.3y (35-80)
Mid-Cervical Leads		10
Mid- to Low-Thoracic Leads		53
Primary Pathology	FBSS (Low Back/Leg Pain)	23
	RSD/CRPS	3
	Neuropathy	3
	FNSS	3
	Post-Surgical Pain	2
	Other	1

 Table 1. Patient Demographics

Monopolar Impedance Variability: For the monopolar impedance analysis, 35 patients, implanted with 63 leads, were analyzed. Across all patients, we found that on any lead, there was a mean 45% likelihood that the monopolar impedance of the adjacent contact significantly different (P < 0.05). Overall, the monopolar impedance was found to vary by 35 (18-76) Ω from contact to contact on the same lead (see Fig 1). Other studies of epidural leads in SCS with similar lead geometries have shown that the acute physiological monopolar impedance is approximately 270Ω [12]. Thus, the impedance can vary approximately 13% from contact to contact on the same lead.

Figure 1. Variation in Physiologic Monopolar



Impedance from Contact-to-Contact on Same Dorsal Epidural Lead. Median (25% - 75% quartiles): 35 (18 - 76) Ω .

Bipolar Impedance Variability: In 16 patients implanted with dual parallel leads, we found that the bipolar physiologic impedance on all leads was $464 (228 - 1001) \Omega$. We also found that the crosslead impedance from matched bipolar pairs varied by 79 $(28 - 132) \Omega$. In 57/67 comparisons, a matched comparison revealed a significant

difference (P < 0.05) in the impedance of matched bipoles on adjacent leads.

Discussion

The variability of the impedance on a per-lead implications has for single-channel stimulator (where a 'channel' is defined to be a pulse generator with a single anode and single cathode termination, with controllable pulse amplitude, pulse rate, and pulse width). A channel can have a controlled voltage (CV), controlled current (CI), or continuous current distribution (CCD; where the current output from each contact is individually controlled) output architecture; all will yield different results in physiologic systems with varying contact impedance. In a simple monopolar stimulation condition, a CV system will have a variable current output, depending primarily upon the impedance of the cathodic contact. This can result in variability in measured stimulation thresholds. If a CI system is used, the stimulation current is consistent regardless of the variable contact impedances. This represents an improvement over CV systems.

However, stimulation combinations are rarely simple monopoles; complex stimulation combinations involving multiple contacts defined as anodes and cathodes are the clinical norm, especially in patients with complex pain conditions [3, 4, 8]. When single-channel CV or CI systems are connected in such complex combinations, the control of the stimulation current to individual contacts will be compromised by variable impedances among the contacts. Only a CCD system avoids these issues by controlling the current from each contact.

In our first analysis, we found that the impedance on adjacent contacts often varies and the median difference is about 13% from contact-to-contact. In our 2^{nd} analysis, we found that the impedance of matched bipoles measured on two leads placed in parallel in the spinal column differed by a median 79 Ω . This \sim 17% difference can have clinical implications.

For example, assume that the two leads are placed in perfect parallel, with perfect symmetry to the physiologic midline (Fig. 2). If bipoles are programmed on each lead, then, just due to the difference in impedance between the two leads, the stimulation current delivered to each bipole will differ by 17 %. This will result in an unbalanced stimulation current, likely resulting in paresthesia stronger to one side of the patient's body. This result is true for both CV and CI single-channel systems.

In order to correct for this imbalance, there are several options. First, the clinician may attempt to redistribute the anodes and cathodes to different contacts in order to re-balance the stimulation This is likely a time-consuming and unpredictable process. Second, the clinician may employ a dual-channel stimulator system, where one channel of stimulation is dedicated to each Then each channel can be individually lead. programmed to output the necessary voltage or current to compensate for the impedance difference. This is a viable solution, though it requires a more complex stimulator. A possible drawback is that, if a single channel of stimulation is required to achieve the necessary spatial superposition from the two leads for greater dorsal column activation [11], multi-channel devices that use time-interleaved pulsing will not suffice. To achieve balanced simultaneous bilateral currents from both leads, a CCD stimulator can be used.

Conclusion

We found that the impedance on single SCS percutaneous leads can vary significantly from contact-to-contact, typically by 13%. Also, we found that the impedance between matched bipoles on dual parallel SCS leads typically varied by 17%. These variations in impedance may have clinical ramifications for consistent stimulation results.

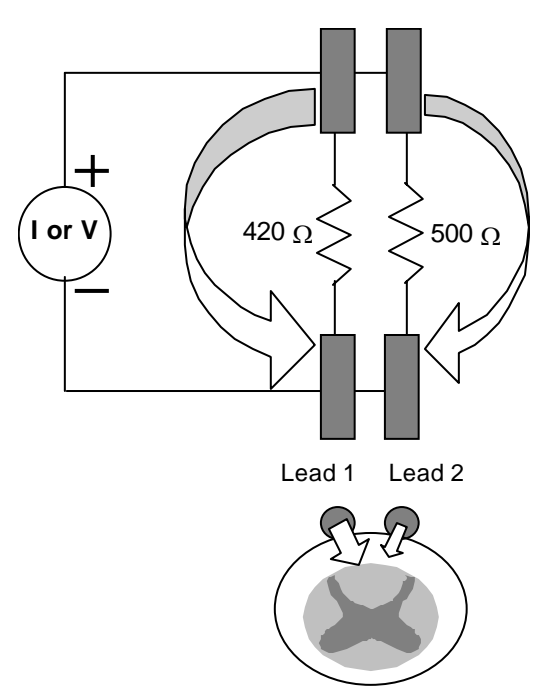


Figure 2. Unbalanced current flow from single-channel pulse generator connected to matched bipoles on dual-parallel leads. Even with perfect symmetrical placement with respect to physiological midline, difference in impedance between bipoles results in imbalanced current flow and may cause unbalanced paresthesia coverage and intensity.

References

- [1] Shealy CS, Taslitz N, Mortimer JT, *et al.* Electrical Inhibition of Pain: Experimental Evaluation. *Anesth Analg*, 46: 299-305, 1967.
- [2] North RB, Ewend MG, Lawton MT, *et al.* Spinal Cord Stimulation for Chronic, Intractable Pain: Superiority of "Multi-Channel" Devices. *Pain*, 44: 119-130, 1991.
- [3] Alo KM, Yland MJ, Kramer DL, *et al.* Computer Assisted and Patient Interactive Programming of Dual Octrode Spinal Cord Stimulation in the Treatment of Chronic Pain. *Neuromodulation*, 1(1): 30-45, 1998.
- [4] Alo KM. Spinal Cord Stimulation for Complex Pain: Initial Experience with a Dual Electrode, Programmable, Internal Pulse Generator. *Pain Practice*, 3(1): 31-38, 2003.
- [5] De Jongste MJL, Nagelkerke D, Hooyschuur CM et al. Stimulation Characteristics, Complications, and Efficacy of Spinal Cord Stimulation Systems in Patients with Refractory Angina: A Prospective Feasibility Study. PACE, 17(I): 1751-1760, 1994.
- [6] Andersen C. Time Dependent Variations of Stimulus Requirements in Spinal Cord Stimulation for Angina Pectoris. *PACE*, 20(I): 359-363, 1997.
- [7] Spangenberg P. Time-Dependent Variation of Stimulus Requirements of Single SCS (Spinal Cord Stimulation) Leads with Respect to Pain Relief. 54th Annual Meeting of the German Society of Neurosurgery, Saarbrucken, May 25-28, 2003
- [8] Sharan A, Cameron T, Barolat G. Evolving Patterns of Spinal Cord Stimulation in Patients Implanted for Intractable Low Back and Leg Pain. *Neuromodulation*, 5(3): 167-179, 2002.
- [9] Anonymous. Medtronic Pisces Quad^R Lead Kit for Spinal Cord Stimulation (SCS) Implant Manual Model 3487A Lead Kit. Minneapolis, MN: Medtronic, Inc., 1996.
- [10] Anonymous. Medtronic Pisces Z QuadTM 3890 Lead Kit for Spinal Cord Stimulation (SCS) Technical Manual. Minneapolis, MN: Medtronic, Inc., 2002.
- [11] Holsheimer J and Wesselink W. Effect of Anode-Cathode Configuration on Paresthesia Coverage in Spinal Cord Stimulation. *Neurosurgery*, 1997; 41(3): 654-660, 2002.
- [12] Oakley JC, Prager JP, Krames E, *et al*. Variability of Contact Impedance Over Time in Spinal Cord Stimulation. Submitted to ASSFN 2004: Neuromodulation Defining the Future, Cleveland, October 1-3, 2004.

Acknowledgements

Financial support provided by Advanced Bionics Corporation.

Author's Address

Kerry Bradley, MS 25129 Rye Canyon Loop Santa Clarita, CA 91355 USA Kerry.bradley@bionics.com

Excitability of the common peroneal nerve in rabbits, rats and mice

M Russold*, H Sutherland*, H Lanmüller**, M Bijak**, S Salmons*, JC Jarvis*

* Muscle Research Group, Department of Human Anatomy and Cell Biology,

University of Liverpool, Liverpool, L69 3GE, UK

** Department of Biomedical Engineering and Physics, AKH,

Medical University Vienna, A-1090 Vienna, Austria

Abstract

Motor nerve activation can be adjusted via the amplitude or duration of the stimulus pulse, but also depends on the properties of the nerve-electrode interface. Growth of connective tissue around implanted electrodes changes these properties over time. Recruitment characteristics are also influenced by the use of mono- or biphasic pulses, constant voltage or constant current stimulation and the nerve diameter.

The aim of this study was to establish the threshold of stimulation amplitude needed to activate motor axons in the common peroneal nerve of rabbits, rats and mice. Under general anaesthesia, loop electrodes were placed close to or under the nerve. Animals were reanaesthetised for a terminal experiment and electrodes were placed acutely in a similar position in the contralateral limb. The tibialis anterior or extensor digitorum longus muscle was carefully freed from the surrounding tissues and connected to the measurement system by its distal tendon. Measurements were performed at optimum length. Strength-duration curves were constructed from minimum stimulation amplitudes that generated a twitch force higher than 30% of that elicited by supramaximal stimulation.

The stimulator was designed specifically for these experiments. All parameters were controlled by a personal computer running custom software. A National Instruments data acquisition card was used to set muscle length and to measure muscle force.

The required stimulus amplitude was markedly higher for the implanted electrodes than for acutely placed electrodes. These results allow an objective choice of stimulation parameters for activating single nerves in small animals in which stimulus spread to adjacent nerves needs to be avoided. They also provide a reference dataset for applications that require stimulation of motor nerves in the 0.5-2mm range of diameters.

Introduction

The excitability of a nerve and its corresponding muscle is generally defined by its strength-duration curve (Fig. 1) [1]. For each pulse duration, the minimum stimulus amplitude that produces the defined response is plotted.

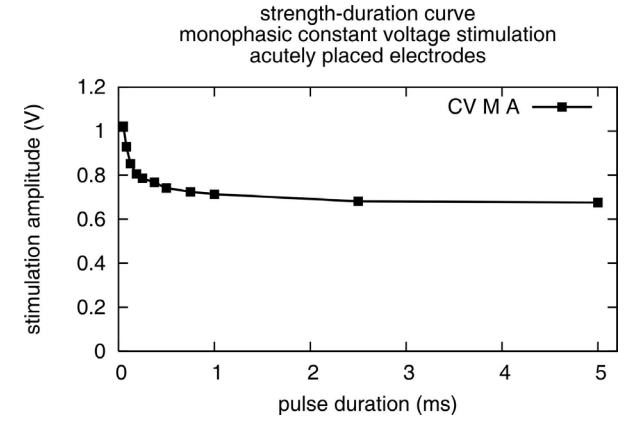


Fig. 1: Typical strength-duration curve, constructed from rat data (n=7).

Despite the widespread use of electrical stimulation of muscles in small mammals in research, little reference strength-duration data is available. Moreover no data seems to be available on strength-duration curves after chronic implantation of electrodes. Grill et al. stated that 'the resistivity of the encapsulation tissue is sufficient to alter shape and magnitude of the electric field generated by chronically implanted electrodes', but did not measure the effect these changes have on the stimulation amplitude required to elicit a muscle twitch [2].

Complete strength-duration data for rabbits, rats and mice allows objective design of the output stages of (implantable) stimulators. Use of the minimum effective stimulus amplitude can reduce stimulus spread and therefore the risk of discomfort associated with collateral stimulation of sensory structures.

Materials and Methods

Surgical procedures

All surgical procedures were carried out in accordance with the Animals (Scientific Procedures) Act 1986 that govers the use of experimental animals in the UK. All implant

procedures were performed under full aseptic conditions.

Five New Zealand White rabbits (2.5 - 3kg), 8 Wistar rats (250 - 300g) and 2 CD1-mice (25 -30g) were anaesthetised by means of inhalational anaesthesia (2% Isoflurane). In one species (rabbit) one loop electrode was placed under the common peroneal nerve and the second electrode was placed on the lateral head of the gastrocnemius muscle. In the two smaller species (rat and mouse) both loop electrodes were placed under the common peroneal nerve. Electrodes were made from stainless steel wire (Cooner Inc.) and had a small loop on one end, which was used to secure the electrodes in place. The free end of the electrode wire was left subcutaneously. Animals were allowed to recover anaesthesia and inspected on a daily basis.

In a second procedure under general anaesthesia – performed at least 14 days after the initial implantation – two loop electrodes and a flap electrode were implanted in the contralateral limb of one species (rabbit) and two loop electrodes were implanted in the two smaller species (rat and mouse). Electrodes were implanted in a position similar to that used in the initial implantation. The tibialis anterior (TA) muscle was exposed in one species (rabbit) and the extensor digitorum longus (EDL) muscle in the two other species (rat and mouse). All muscles were carefully freed from surrounding tissues. The free ends of the electrode wire were deinsulated and used to connect an external stimulator to the electrodes.

Measurements

The muscles of two species (rabbit and rat) were connected to a servomotor (Cambridge Technology, Inc., USA); the mouse EDL muscle was connected to a load cell (UL4 and microscale UL5, Statham Instruments, Inc., USA), which was connected to an amplifier (Fenlow Amplifier ZA2) and acted as one part of a Wheatstone bridge (Fig. 2).

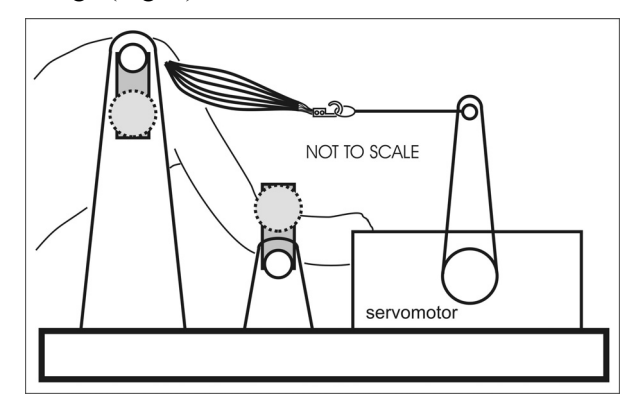


Fig. 2: Measurement setup for rabbit and rat. In mouse experiments a load cell was used.

Each muscle was connected via its distal tendon. Strength-duration curves were constructed from a series of twitch force measurements with pulse durations in the range from 100msec to 50µsec. Strength-duration measurements were performed at optimum length, which was determined prior to the experiments by a force-length test. A reference force was established before each test supramaximal stimulation. The stimulation amplitude resulting in a twitch force greater than 30% of that reference force was recorded. For each pulse duration two twitches separated by 5s - were measured and averaged. Stimulation was delivered by means of a stimulator designed specifically for experiments. The stimulator was capable of generating rectangular constant voltage and constant current pulses with pulse durations from 200ms to 50us and a maximum amplitude of 5mA or 5V. Measurements were performed using monophasic constant voltage (CV M), biphasic constant voltage (CV B), monophasic constant current (CC M) and biphasic constant current (CC B) stimulation (Fig. 3).

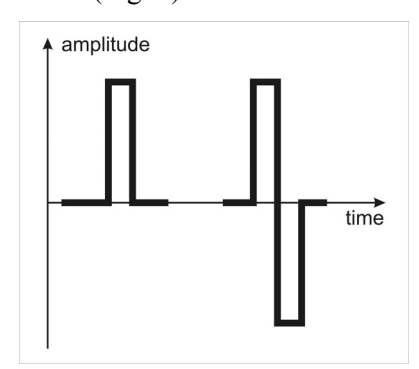


Fig. 3: left side: monophasic pulse; right side: biphasic pulse

Stimulator settings were controlled by a personal computer. Custom-made software was used to control the stimulator as well as the position of the servomotor. The same software was used to record the force in response to the stimulation. A National Instruments data acquisition card (PCI-6035E) was used to interface the measurement hardware with the personal computer. The percentage of the maximum twitch force was calculated during the experiments. When electrical noise could have influenced the results, a moving average over 4, 8 or 12 values was applied to the recorded force traces.

Data analysis

All data shown are expressed as mean \pm SEM. As the relevant changes in stimulation amplitude occurred at pulse durations lower than 1ms (Fig. 1), further analysis will concentrate on the 1ms - 50 μ s range. Such a range is relevant in the design

of implanted stimulators because pulse durations in the range from 1ms to 125µs can easily be generated using a PIC microcontroller and a watch quartz oscillator (32.768kHz).

Significance testing between implanted and acutely placed electrodes was performed by one-way ANOVA for each pulse duration. All analysis was performed using Minitab for Windows (Minitab Inc., USA). Statistical significance was accepted for p-values<0.05.

Results

Threshold stimulation amplitude

In general, threshold stimulation amplitudes were higher for chronically implanted electrodes than for acutely placed electrodes. They were also higher for monophasic stimulation pulses than for biphasic stimulation pulses (Fig. 4a, b). Whereas in rabbits there was some difference between the two electrode sets for biphasic stimulation, there was almost no difference between the two electrode sets in rats. As only the constant voltage data of two mice were available, no data on mice has been included here. The results of these two animals were however very similar to the results gained during the rabbit experiments.

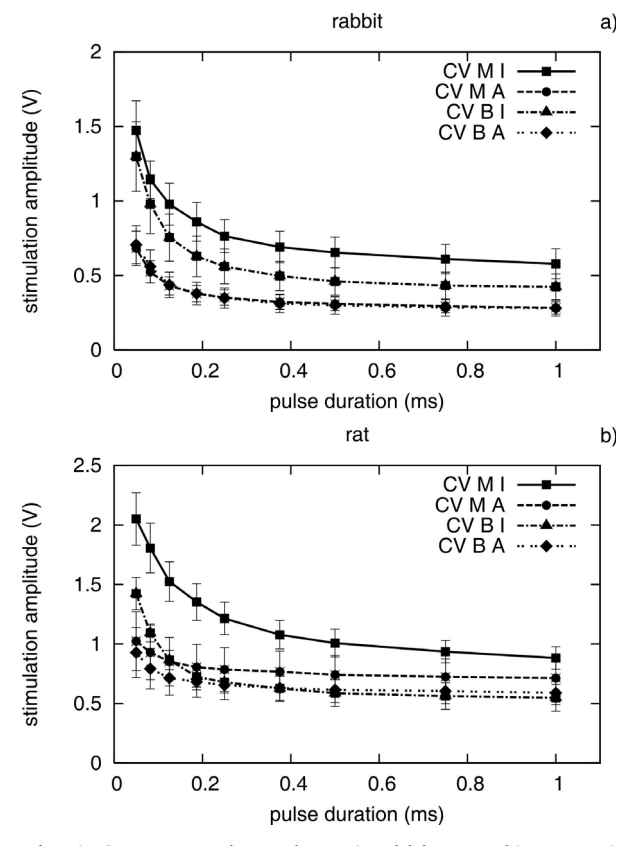


Fig. 4: Constant voltage data: a) rabbit, n=5, b) rat, n=4 for implanted electrodes (I), n=7 for acutely placed electrodes (A).

Data using constant current stimulation was similar to the data using constant voltage stimulation for each species (Fig. 5a, b).

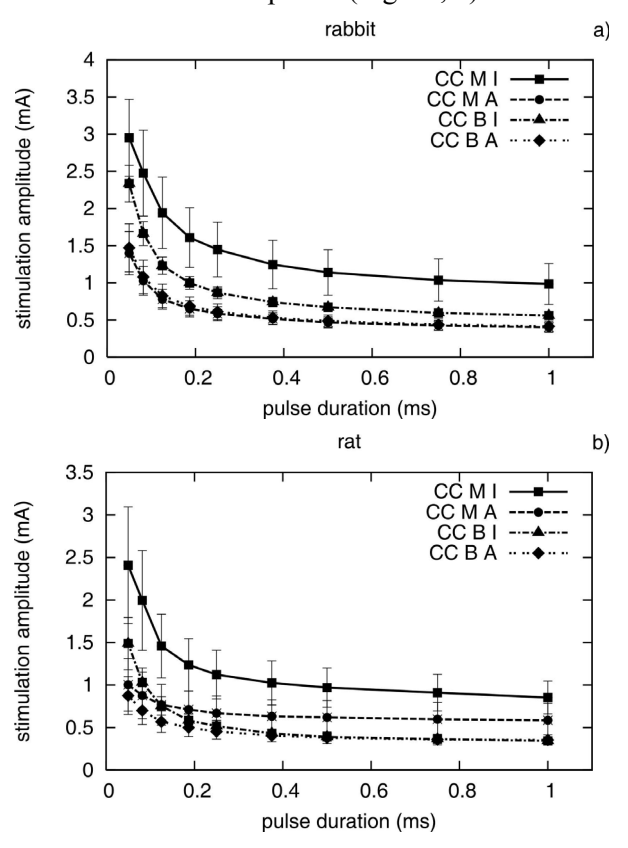


Figure 5: Constant current data: a) rabbit, n=5, b) rat, n=4 for implanted electrodes (I), n=7 for acutely placed electrodes (A).

Statistical significance

Although threshold stimulation amplitudes for implanted electrodes appeared to be greater in all experiments, only those for monophasic constant voltage stimulation at pulse durations shorter 1ms rabbits were statistically significant. Monophasic constant current stimulation in the same species at pulse durations shorter than 1ms was close to being statistically significant, with pvalues below 0.1. In rats and mice no statistically significant differences between the two electrode sets could be found. There were no statistically significant differences between implanted and acutely placed electrodes when biphasic stimulation was used. There were also no significant differences statistically between monophasic and biphasic stimulation in the same electrode set.

Discussion

Implantation time in rabbits was 17.4 ± 1.03 days (range 15-21 days), 47.5 ± 18.59 days (range 16-94 days) in rats and 16 ± 2 days (range 14-18 days) for the mice. Implantation interval was closely matched for rabbits and mice. In the rats,

two animals were implanted for 16 and 19 days ('short-term'); while two more animals were implanted for 61 and 94 days ('long-term'). No difference could be found between the 'short-term' implanted electrodes and the 'long-term' implanted electrodes, thus suggesting that any growth of connective tissue, which could influence the electrode-nerve interface, happens within the first two weeks after implantation.

Despite the lack, at this stage, of statistically significant data, our results indicate that, after a minimum of two weeks implantation, higher stimulation amplitudes are required to elicit a muscle twitch. The only statistically significant data were found in rabbits. This could either be caused by the differing electrode placement, whereas placing both electrodes under the nerve – as was done in rats and mice - resulted in a more stable electrode-nerve interface, or by species differences, such as the reaction of the rabbits to chronic implantation. It could be, for example, that the rabbit is more prone to the generation of connective tissue adjacent to an implanted electrode. Our data showed that thresholds for biphasic stimulation are less sensitive to than for implantation those monophasic stimulation. Constant current stimulation, as expected, reduces the influence of changes at the electrode-nerve interface. This has implications for the design if implantable stimulators. Where stimulator dimensions are of minor importance, a biphasic constant current output stage would be ideal. It may, however, be necessary to compromise when designing devices implantation into the smaller laboratory species.

The data sets allow the output voltages of future (implantable) stimulators to be adjusted to the values required. Unlike chronaxie and rheobase data alone, the complete curves presented allow us to take the pulse duration of the stimulus into consideration, thus aiding an objective choice of the required stimulation voltage. This will help to restrict stimulation to the intended target.

References

- [1] Geddes L.A., Bourland J.D.: The Strength-Duration Curve, IEEE Trans Biomed Eng, 32, 1985, 458-459
- [2] Grill M. Warren, Mortimer J. Thomas: Electrical Properties of Implant Encapsulation Tissue, Annals of Biomedical Engineering, 22, 1994, 23-33

Author's Address

Michael Russold Muscle Research Group Department of Human Anatomy and Cell Biology University of Liverpool, L69 3GE, UK e-mail: russmi29@liverpool.ac.uk

A PORTABLE FES SYSTEM INCORPORATING AN ELECTRODE ARRAY AND FEEDBACK SENSORS

A. Elsaify*, J. C. Fothergill*, W. Peasgood**

* Department of Engineering, University of Leicester, UK

** Clinical Physics and Bioengineering, Walsgrave Hospital, Coventry, UK

Abstract

In the UK and elsewhere, there is an increasing number of multiple sclerosis (MS), Stokes and Peripheral Nerve Disorders. These diseases affect the central nervous system and cause various nervous and muscular disabilities. Extremity muscle weakness is the most common difficulty that these diseases victims suffer such as foot drop, which affects the walking gait.

Surface electrode **Functional Electrical** Stimulation (FES) systems have been used for many years for the rehabilitation of lost movement extremities. Various surface stimulators have been designed for different applications and some of them are available commercially. Most of these surface stimulators do not completely satisfy the users. For example, patients find it difficult to place the electrodes correctly, and they experience fatigue, skin irritation and hot spots. Furthermore the stimulators are not self-tuning.

A completely new portable prototype surface electrode FES system been designed using the latest embedded systems technology. The new system uses sensors to monitor the movement and drives an array of surface electrodes for stimulation. Using feedback from the sensors, the optimum configuration of electrodes is chosen to produce correct stimulation and movement in real time. The system is also able to vary the chosen pattern of electrodes, the stimulation pulse parameters and shape during the stimulation process. This may enable some problems associated with fatigue and skin irritation to be reduced.

This system is being applied, in the laboratory, to solve the foot drop problem by placing the electrode array over the foot dorsiflexion and eversion muscles mainly to stimulate the deep and superficial branches of the common peroneal nerve. The exact foot movement can be controlled using the feedback sensors and the surface electrode array. The system will tune itself in terms of electrode selection and stimulation pulse parameters to overcome the physiological changes during the stimulation. This system will provide more choice for physiotherapy departments to expand the use of surface electrode FES.

Introduction

A common disability amongst MS patients is foot drop, impaired or absent voluntary dorsiflexion of the foot which prevents the toes from clearing the ground during the swing phase of gait. Several FES systems have been developed over the years for foot drop clinical use. Common problems and factors seem to limit the use of these devices, such as finding the optimum stimulation site for the electrodes [1], sensor location and achievement of optimum movement at the ankle. An intelligent, user friendly and low cost system has been developed at the University of Leicester to overcome these problems. The system is small, portable and is based on the latest embedded microprocessor technology. The stimulation system uses a surface adaptive electrode array for to allow automatic optimisation and adjustment without having to remove and replace the electrodes during set-up. The system incorporates a new sensor combination to detect the response of the functional movement.

The improved ease of electrode placement and the achievement of optimum ankle dorsiflexion are expected to achieve better gait normalisation, optimise comfort, and improve confidence and safety in use of FES. In addition, the new system offers the capability to vary stimulation pulse output such that a more normal degree of foot movement in each part of the gait cycle is achieved. This system has wider applicability: it may be used for many other functional electrical stimulation applications, such as the hand.

Material and Methods

An overall block diagram for the stimulation system is shown in figure 1.

System Specification

• The stimulator produces 12 different waveforms (different shape, charge balanced or biphasic), but any wave shape can be pre-programmed into the stimulator.

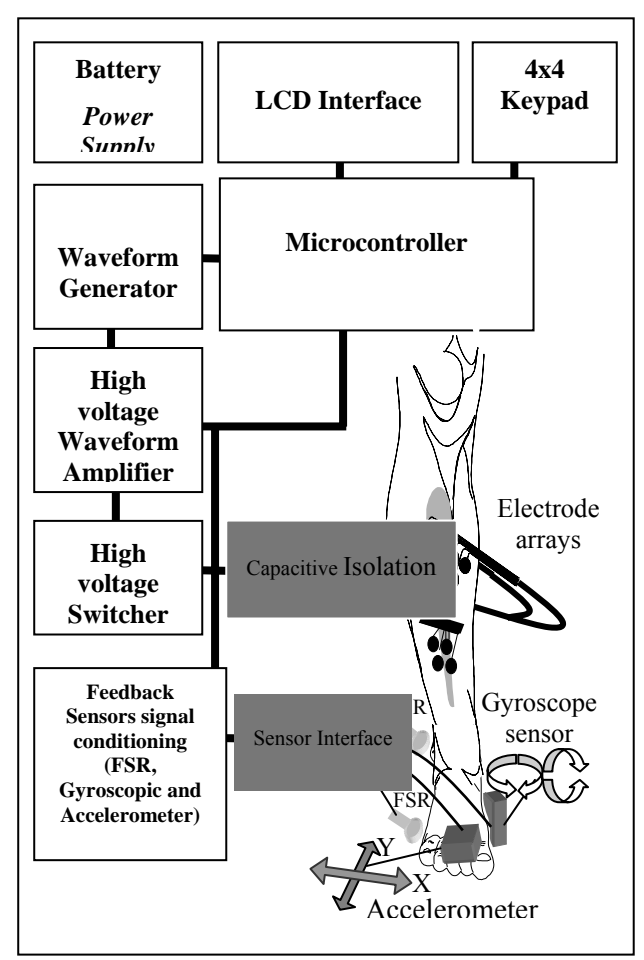


Figure 1: FES system block diagram

- The waveforms are split into 200 samples and stored in memory. The timing of the software interrupts are used to produce pulses of different pulse width
- Waveform pulse width range: 10μs -500μs in 10μs steps.
- Waveform repetition rate ranges: 1Hz to 100Hz in 5 Hz steps.
- Waveform amplitude: 0V 10V peak peak in 0.1V steps. These are amplified to 300V peak - peak using a transformer output.
- Capability to load user's set-up and control these parameters automatically using stimulation algorithms
- Switching of the stimulation waveform to 8 to 32 electrodes (electrode array) using a high voltage switching circuit.
- Multiple channel 10 bit on chip analogue to digital converter (A/D) to sample the feedback sensor data.
- Full display of all the stimulation parameters, output switches and the feed back using the liquid crystal display (LCD)

Battery power supply

The system is powered using 4AA rechargeable Nickel Metal Hydride batteries wired in series to give approximately 4.8V. Delivering full output (300V pk-pk) into a 1k ohm resistor (body load), approximately 100mA is drawn from the batteries. The circuit can therefore stay powered for up to 23 hours without the need to charge the batteries. The power supply circuits are based on step up DC–DC converters that generate regulated +5V and ±15V at 1A load current and 10W output power. Battery monitoring is used to detect battery charge, an LED on the front panel indicates when the batteries need charging.

Microcontroller

The microcontroller is the heart of this system; it allows real time control over the system. It is one of the latest Microchip PIC technology products. It is a low-power high-speed flash CMOS device, running at 40 MHz with operation up to 10 MIPs. It has a 10-bit 16-channel analogue-to-digital converter and in-circuit serial programming and debugging. A combination of assembly language and C language are used for programming this microcontroller.

Keypad and LCD

This system is controlled using a 4x4 keypad and 4-line x 20-character backlit LCD interface, which allows full interactive control over the system.

Waveform generator

Twelve waveforms are programmed into the microcontroller and some of these are shown in figure 2. These digital waveforms are converted using an 8-bit digital to analogue converter that provides very high speed performance to convert each stored digital waveform to a $\pm 500 \text{mV}$ peak-to-peak analogue signal.

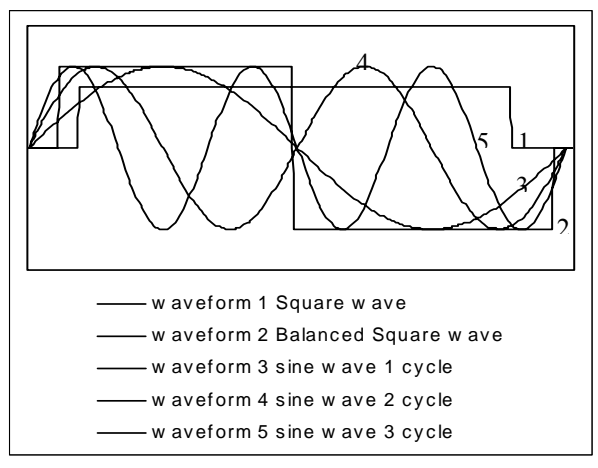


Figure 2: waveforms samples

This is then amplified to $\pm 5V$ using a high-speed operational amplifier with low input offset voltage and bias current, high input impedance, high slew rate and wide bandwidth.

High voltage Amplifier (output stage)

A power operational amplifier that can produce pulse currents up to 0.7A is used to drive a transformer to amplify the ±5V waveform to 300V peak to peak (suitable for use in surface electrode FES). The transformer is capacitively coupled using high voltage polystyrene capacitors, to the switcher circuit, which is then capacitively coupled to the electrodes. This double capacitive isolation is part of the safety features to prevent DC current being applied to the skin should an electronic fault occur. The circuit prevents any DC component in the stimulation waveform, which makes the stimulation very comfortable with no reddening of the skin under the electrodes during use.

High voltage switching circuit

The high voltage signal is switched between 8 to 32 channels using analogue MOSFET high voltage switcher circuits that are controlled digitally by the microcontroller.

The "switchers" have a very low quiescent power dissipation (10 μ A), 22 Ω output on-resistance and low parasitic capacitance. They can switch analogue signals up to a 10MHz with excellent noise immunity but require high voltage biasing up to $\pm 200 V$ to allow waveforms of up to $\pm 200 V$ to be passed. High voltage DC-DC converters are used for biasing the switching circuits, which convert +5V to ±200V high voltage DC. A protection circuit is used to monitor the input current to the dc-dc converters. Should a fault occur in the switcher circuit, DC current will flow out of the switcher. To control this fault condition, the short circuit current is limited to 2mA at the output of the DC-DC converter using a series resistor on each of the ±200V supply rails. An independent current monitoring circuit detects the rise in output current as a rise in the input current monitored at the 5V power supply, which energises a latching relay turning the 5V power off. Even if the stimulation unit is turned off and then on the latching relay will always remain in the off state until the short circuit fault is repaired.

Electrode array

The array consists of multiple small closely-spaced electrodes covering the muscle/nerve groups of interest and the stimulation is achieved by connecting one or more electrode to the stimulator

output stage. A typical example of electrode array is shown on figure 3.

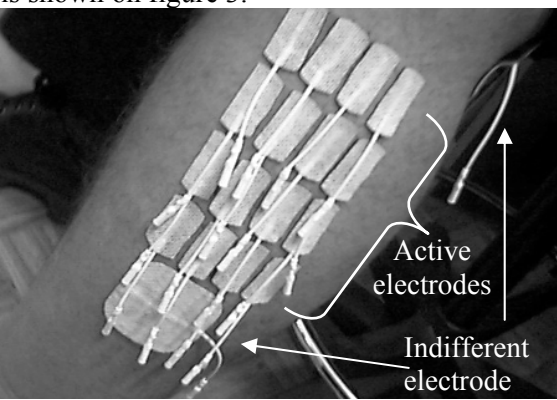


Figure 3: Electrode array

Feedback sensors

Artificial sensors have been a key element of FES systems. They provide the controller with real time feedback information about the movement to facilitate efficient and precise FES control. The main problem with most of the sensors used with FES is the size and mass such as accelerometers [4] and gyroscopes [5]. Recent technological advancements in micro-machined electro mechanical sensors have overcome these problems.

Accelerometer:

A two-axis MEMS miniature accelerometer is used and negative acceleration positive measurement to maximal level of ±2g with 12.5% per (g) sensitivity. This accelerometer can measure dynamic and static acceleration. It produces an analogue output (voltage proportional to acceleration) and duty cycle output (ratio of pulse width to period proportional to acceleration). It has a faster and more sensitive response than liquid tilt sensors. This accelerometer sensor is used to detect foot acceleration in the planes of dorsiflexion/plantarflexion and eversion/inversion.

Gyroscope:

Two miniature MEMS gyroscopes (angular rate sensors) are used to measure angular velocity <±150°/s. These produce positive output for clockwise rotation and negative output for anti clockwise. These gyroscope sensors are used to detect foot angular rotation in the planes of dorsiflexion/plantarflexion and eversion/inversion.

FSR (force sensitive resistor) sensor:

This is a tactile sensor, which responds to applied physical pressure by exhibiting decreasing resistance: the greater the force the lower the resistance. This sensor is used as foot switch to detect heel or toe lift/strike.

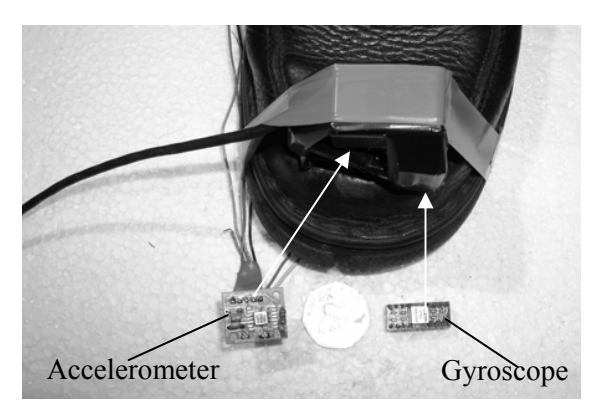


Figure 4: accelerometer & gyroscope sensors

Results and Discussion

The new FES system has undergone bench tests at University of Leicester to assess the reliability and validity of the System. One of these tests is to ensure that the sensors provide a clean signal during specific stimulation sequences. This signal is analysed using an algorithm programmed into the microcontroller to record the movements of the foot by stimulating different electrodes.

Other tests include stimulating an artificial body load of $1k\Omega$ resistor parallel with $0.1\mu F$ capacitor to ensure that the device conforms to BS EN 60601-2-10:2001. The design of the output stage facilitates comfortable near pain free stimulation and different waveform shapes allow user selection according to personal feeling. The software has been designed to allow different pulse rates of stimulation to be applied during the gait cycle with the aim to improve effectiveness of lifting the toes.

The electrode array is optimised by measuring the dorsiflexion/plantarflexion and eversion/inversion twitch response of each individual electrode, which have been shown to be indicative of the continuous response [3]. Combinations of electrodes give responses that are approximately the sums of the dorsiflexion/plantarflexion and eversion/inversion responses. The microcontroller can therefore calculate likely optimum electrode combinations from individual twitch responses.

Tests on 16 normal volunteers have produced encouraging results, which indicate good correlation between sensor outputs and observed movement. Field tests are being planned at the time of writing to assess the effectiveness of the stimulation system on multiple sclerosis and stroke patients with foot drop.

Conclusion

A stimulation system is described that has been designed to take into account easier electrode

placement for foot drop applications. The electrode array concept was originally developed during EU TIDE project number 1250, FESTIVAL (1993-1996) and the work presented here is a continuation of these concepts to bring the device closer to the users. With current state of the art microcontroller and sensor technology, the complexity of surface stimulation is becoming more affordable for use in everyday life.

References

- [1] Taylor PN, Burridge JH, Wood DE, Norton J, Dunkerley A, Singleton, C, Swain ID. Patient perceptions of the Odstock Drop Foot Stimulator. *Clinical Rehabilitation*, 13: 333-340, 1999.
- [2] Whitlock TL., Peasgood W. Fry ME, Bateman A, Jones R. Self-optimising electrode arrays. *Proc. of 5th IPEM Clinical Functional Electrical Stimulation Meeting*. Salisbury March 1997:767)
- [3] Elsaify A., Fothergill J. C., Peasgood W. Portable FES System optimises Electrode Array using Twitch Response. 9th Annual Conference of the IFESS, Bournemouth, UK, 2004
- [4] Willemsen ATHM, Bloemhof F, Boom HBK, Automatic Stance-Swing Phase Detection from Accelerometer Data for Peroneal Nerve Stimulation. *IEEE Trans Biomed Eng* 1990.
- [5] J. R. Henty and D. J. Ewins, "Applications of gyroscopic angular velocity sensors in FES systems" presented at 6th International Workshop on Functional Electrostimulation, Vienna, Austria, 1998.

Acknowledgements

Thanks are given to EPSRC grant number GR/N13029 for supporting this project.

Author's Addresses

Mr A. Elsaify
Department of Engineering,,
University of Leicester, Leicester, LE1 7RH, UK
e-mail: aaas2@le.ac.uk

Prof. J. C. Fothergill
Department of Engineering,,
University of Leicester, Leicester, LE1 7RH, UK
e-mail: jef@le.ac.uk

Dr W. Peasgood Clinical Physics and Bioengineering Walsgrave Hospital, Coventry, CV2 2DX, UK e-mail: william.peasgood@uhcw.nhs.uk

ELECTRICAL STIMULATION OF THE FINGER FLEXORS USING 'VIRTUAL ELECTODES'

Marc Lawrence*, Tünde Kirstein**, Thierry Keller*

* ETHZ Zürich, Automatic Control Laboratory, Physikstrasse 3, 8092 Zürich, Switzerland

** ETHZ Zürich, Wearable Computing Laboratory, Gloriastrasse 35, 8092 Zürich, Switzerland

Abstract

Transcutaneous Functional Electrical Stimulation normally uses self-adhesive electrodes to deliver the required stimulation pulses to the correct muscle groups in order to achieve a functional movement. Identifying the optimal electrode placement on individual patients is a time consuming process, and prone to misplacement when undertaken by users. Virtual Electrodes (VE's), the location of which can be electronically controlled in space and time, can overcome such problems and allow the potential for new applications for advanced functional movement.

VE's can be formed from a two dimensional array of small electrode elements, each of which can be switched between 'stimulation' and 'off' (high impedance) states. A novel 16 element Fabric Transcutaneous Electrode Array (FTEA) was manufactured from silver coated fibres, embroidered into square elements (10mm×10mm) arranged in a 4×4 pattern, with 2mm inter-element spacing.

The finger flexors (little, ring and index) of volunteers were stimulated using a Compex Motion Stimulator connected to a device that can multiplex stimulation currents between any of 16 channels. A self-adhesive anode electrode (Compex, 5cm×5cm) was placed at the inner wrist, and the FTEA above the finger flexor muscles (cathode). Force measurements from the middle tarsal of each finger were recorded for 1) maximum voluntary contractions (MVCs), 2) normal electrode stimulation and 3) a series of different VE's moved around the FTEA. The obtained results showed that FTEA's were well tolerated by the volunteers; and produced controllable forces comparable to normal electrical stimulation.

Introduction

Developing advanced neuroprostheses that provide useful functional movements to patients with paralysed limbs requires the ability to accurately control specific muscle groups. Implantable systems that stimulate muscle nerves close to the insertion point (e.g. Freehand [1]) have been

developed; however the technology is expensive and difficult to configure.

Neuroprostheses' that make use of transcutaneous electrodes tend to be cheaper and more acceptable for patients. Transcutaneous electrodes are relatively easy to reconfigure in order to optimise functional activation and accommodate changing patient conditions (e.g. functional recovery). However the daily reapplication of numerous sets of self-adhesive electrodes results in prolonged 'donning and doffing' sessions, which are prone to misplacement. Dynamically reconfigurable systems should enable selective muscle activation and faster donning and reconfiguration.

Studies using one dimensional transcutaneous electrode belts [2,3] have shown that hand and wrist muscles can be selectively stimulated; but only when precisely aligned. Livshitz et al [4] have shown that for a 2×2 array it is possible to influence the charge distribution within tissue, and that alignment with respect to motor points is also important.

We propose to use 'Virtual Electrodes', (VE's) which can be formed from an array of elements, each of which can be independently switched between 'stimulation' and 'off' states. The size and position of the VE's can then be electronically manipulated by switching stimulation pulses to different subsets of array elements.

A multiplexer has been developed [5] to switch stimulation pulses (e.g. from a modified Compex Motion stimulator [6]) between any of combination of 16 channels. The device was connected to a 16 element (4×4×1cm²) Fabric Transcutaneous Electrode Array (FTEA) manufactured from silver coated fibres embroidered into a fabric using a pseudorandom pattern [7]

The FTEA and multiplexer were used to stimulate the finger flexors of healthy volunteers in order to determine to what extent the electrode array could influence muscle selectivity and force generation.

Material and Methods

Subjects

Healthy volunteers with no known physiological deficit were recruited for the study (3 female, 9 male; age 22-35), with measurements and stimulation applied only to the dominant arm (3 left, 9 right). Data from left-handed volunteers was transcribed to allow comparison with right-handed results.

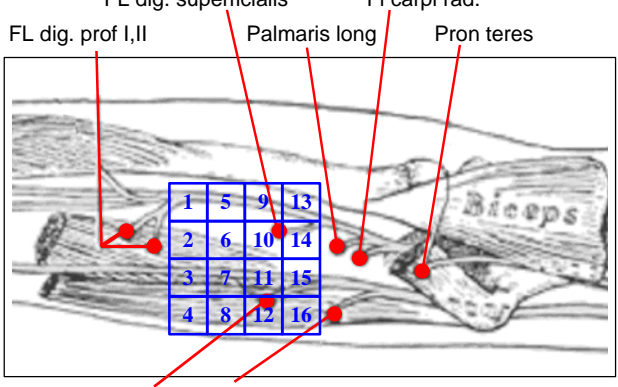
Equipment

The 'Dynamic Grasp Assessment System' (DGAS) [8] uses miniature load cells to record the axial force generated from the four fingers during grasp. The finger flexor forces were recorded from the middle tarsals, the insertion points of the extrinsic finger flexor muscles. The spacing and orientation of the device was adjusted to give volunteers a comfortable grasp whilst ensuring wrist fixation. The forces from the DGAS were recorded with a data acquisition card with a sampling frequency of 100 Hz.

One square self-adhesive electrode (~24cm², Compex) was used as the anode, and placed anterior arm proximal to the wrist. The depolarising cathode electrode (FTEA or Compex) was placed proximal to the anterior elbow (Fig 1). Bi-phasic monopolar [9] stimulation pulses of 250 µs were provided from a Compex Motion transcutaneous electrical stimulator, with a repetition frequency of 20 Hz. The current amplitude was increased to identify the maximum tolerable level for each volunteer (typically 11-15 mA). The location of the cathode was adjusted to produce optimal flexion of the little (digitorum profundus III, IV), ring (digitorum. superficialis) and middle fingers.

Experiment

In the first part of the experiment, the volunteers were asked to produce four maximum voluntary contractions (MVC) lasting 5 seconds with one-minute rest periods. In the second part of the experiment, normal Compex electrodes were used at the cathode and anode positions. Electrical FL dig. superficialis



FI dig. prof III, IV FI carpi ulnaris

Fig 1: Location and orientation of transcutaneous electrodes. Original image (c) 1993 Florence P Kendall.

stimulation was applied 5 seconds at the volunteer's maximum tolerable amplitude. The stimulation was repeated four times with rest intervals of 20 seconds.

The location of the self-adhesive cathode electrode was marked on volunteers arm, and replaced with the FTEA (Fig 1). Conductive gel (Compex) was used to ensure good contact between the conductive fibres and volunteer's skin.

A series of measurements were undertaken with the multiplexer configured to produce a range of different VE sizes and positions on the FTEA. These are summarised as:

- 1) All 16 elements active to compare with normal FES electrode stimulation
- 2) 9 (3×3) and 8 (2×4) active elements in four positions to determine effect of moving VE.
- 3) 1 active element randomly moved between all 16 positions to determine mapping of underlying motor points.

Stimulation with each type of virtual electrode lasted 5 seconds, and was repeated four times at 20-second intervals. Rest periods of 5 minutes were provided between different electrode configurations. The ordering of the virtual electrode configurations was randomised between all volunteers.

The average force value during three seconds of contraction was calculated one second after onset of stimulation in order to remove transient effects. The average baseline prior to contraction was calculated in a similar way, and subtracted from the measured recordings to determine the average contractile force for each finger.

Preliminary Results

The forces generated by electrical stimulation were approximately 25% the maximum voluntary contractions (see Fig 2). The FTEA with 16 active elements generally produces smaller forces than the normal electrode, which may be due different current densities per unit area. The increased forces seen in volunteer 6 may be due to misalignment of the FTEA with respect to the normal Compex electrode.

The maximum tolerable stimulation current amplitudes were therefore used for VE's on the FTEA.

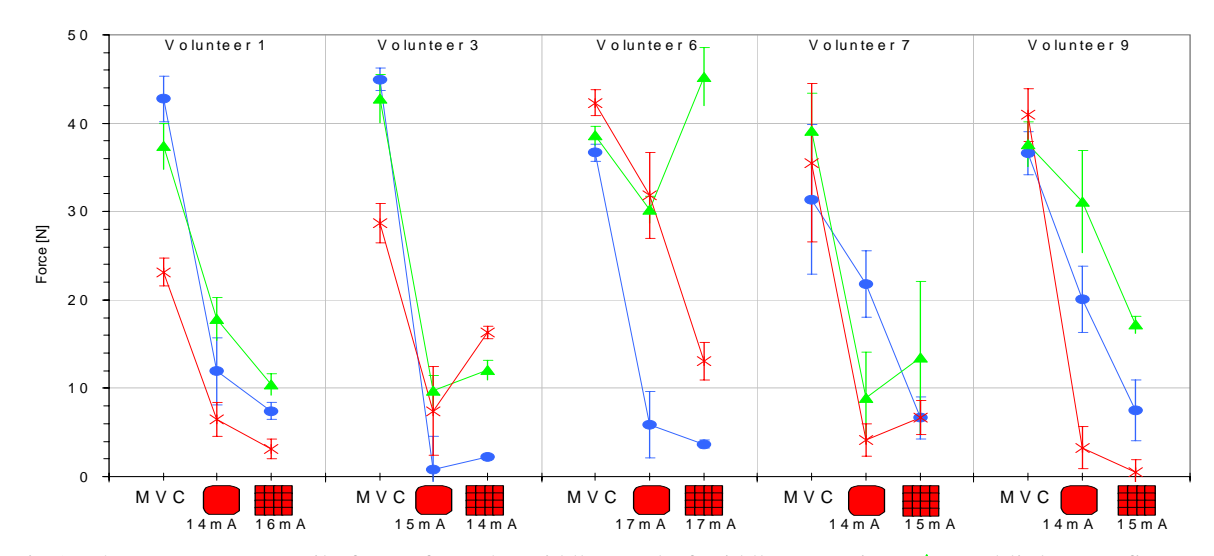


Fig 2: The average contractile forces from the middle tarsal of middle (→), ring (→) and little (★) fingers generated from MVC and electrical stimulation with a normal electrode ■ and 16 element virtual FTEA ■

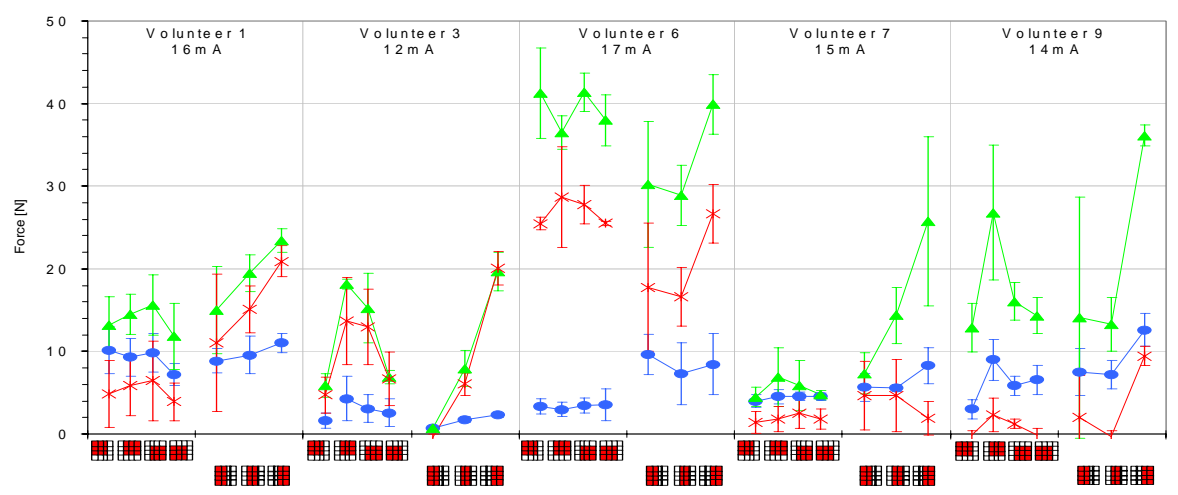


Fig 3: The average contractile forces for a 3×3 and 2×4 virtual electrode moved around the FTEA.

A series of 3×3 and 2×4 VE's were generated on the FTEA and moved between different locations (Fig 3). For some volunteers forces comparable to MVC were observed using both types of virtual electrodes. A 1 cm change in the VE position had an effect on the measured forces; however this was not statistically significant. Ring and little finger forces clearly increase as the virtual electrode is moved above their respective motor points.

Some volunteers were able to tolerate a 1cm² (1 element) virtual electrode at stimulation current amplitudes sufficient to get reliable force measurements (>12mA). An example of randomly moving the 1 element around the electrode pad is shown in Fig 4 for volunteer 1. Clearly as the virtual electrode approached the major motor points there was a significant increase in the measured finger forces. The high forces from activation of pad 13 may correspond to the flexor digitorum superficialis. Similar pad 16 may correspond to activation of flexor digitorum profundus III & IV whereas pads 14 and 15 are in-

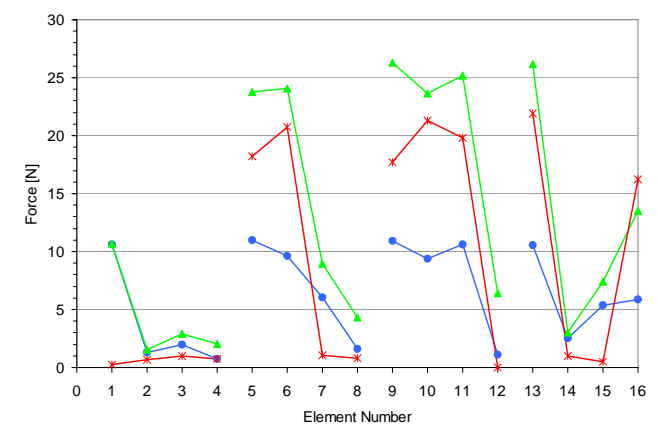


Fig 4. Contractile forces resulting from 1 active element moved around the FTEA (compare element numbers with Fig 1)

between and show low activation. Similar results were observed for five volunteers.

Discussion

A series of VE's were generated on a FTEA placed proximally to the anterior elbow. Force

measurements from the activated flexor muscles were recorded at the middle tarsals of each finger.

Different forces were observed for a variety VE configurations and placements on the FTEA. Large changes in force measurements were observed from step changes in the virtual electrode position. Small differences in the effective area of the virtual electrode $(3\times3, 2\times4)$ did not have a large effect.

Such results indicate that arrays with a high number of small elements are required to achieve precise placement of VE's. Consequently the position and size of VE's could be fine tuned to provide optimal stimulation of selected motor points required for a functional task.

We could not influence stimulation of the index finger and the little finger at the same time due to the restricted size of our FTEA. Therefore we decided to predominantly activate the motor points of the middle, little and ring fingers (dig prof III & IV).

Integrating electrodes into wearable textiles has the potential to allow high-density transcutaneous electrode arrays to be fabricated. We have shown that such fabric transcutaneous electrodes can be used to produce electrical stimulation with results comparable to normal electrodes.

Our results show that a single stimulating element (1cm×1cm) moved around the electrode array was able to illicit individual motor points (e.g. flexor digitorum). However, to be able to compare array electrode performance amongst subjects, .it is first necessary to identify motor points for each subject.

We are developing higher density FTEA's to be able to perform finer movements of VE's over larger areas in order to eliminate the restrictions we had with our current system.

References

- [1] Peckham P., Keith M. W., Kilgore K. L., Grill J. H., Wuolle K. S., Thrope G. B., Gorman P., Hobby J., Mulcahey M. J., Carroll S., Hentz V. R., Wiegner A.: Efficacy of an Implanted Neuroprosthesis for Restoring Hand Grasp in Tetraplegia: A Multicenter Study. Arch Phys Med Rehabil, vol 82. 2001, 1380-8
- [2] Nathan R. H, "Functional electrical stimulation of the upper limb: charting the forearm surface (joint moments)," Med Biol Eng Comp, vol. 17, 1979, 729-36
- [3] Nathan R. H., "The isometric action of the muscle drives of the wrist joint," ASME J Biomech Eng, vol. 114, 1992, p162

- [4] Livshitz, L.M., Mizrahi, J. and Einziger, P.D.: Interaction of array of finite electrodes with layered biological tissue: Effect of electrode size and configuration. IEEE Trans. on Neural Systems & Rehabilitation Engineering, 9(4) 2001, 355-361.
- [5] Pietz O., Peters S.: "Smart Electrodes" Diploma Thesis, Electronics Laboratory, Eidgenössische Technische Hochschule Zürich, February 2003
- [6] Keller T., Popovic M.R., Pappas I.P., Muller P.Y.: Transcutaneous functional electrical stimulator "Compex Motion". Artif Organs, 26(3), 2002, 219-223
- [7] Kirstein T., Lawrence M., Tröster G.: Functional Electrical Stimulation (FES) with Smart Textile Electrodes. New Generation of Wearable Systems for eHealth, International Workshop, Lucca Italy, Dec 11-14, 2003
- [8] Keller T., Popovic M. R., Ammann M., Andereggen C., Dumont C., "A System for Measuring Finger Forces During Grasping", Proceedings of International Functional Electrical Stimulation Society (IFESS 2000) Conference, Aalborg, Denmark, June 2000. 386-9
- [9] Keller T.: Surface Functional Electrical Stimulation (FES) Neuroprostheses for Grasping, Diss. ETH No. 14481, 2001

Acknowledgements

The authors would like to thank the work of O. Pietz, S Peters and T Zürbrugg without whom the collection of data would not have been possible.

Author's Address

M Lawrence

Instutit für Automatik Paralab

ETL K28 Uniklinik Balgrist
Physikstrasse 3 340 Forchstrasse
8092 Zürich 80008 Zürich
Email: Lawrence@control.ee.ethz.ch
Home page: www.control.ethz.ch/~fes

MULTI-FIELD SURFACE ELECTRODE FOR SELECTIVE ELECTRICAL STIMULATION

Ana Popović-Bijelić¹, Goran Bijelić², Nikola Jorgovanović³, Dubravka Bojanić³, Dejan B. Popović^{3,4}, Mirjana B. Popović^{4,5}

¹ Faculty of Physical Chemistry, University of Belgrade, SCG
 ² Institute of General and Physical Chemistry, Belgrade, SCG
 ³ Faculty of Engineering, University of Novi Sad, SCG
 ⁴ Center for Sensory Motor Interaction, Aalborg University, Denmark
 ⁵ Center for Multidisciplinary Studies, University of Belgrade, SCG

Abstract

We designed a 24-fields array and a control box that on-line selects the fields that conduct electrical charge. Final pattern and size of the electrode (combination of the conductive fields) are determined after testing various combinations of fields in vivo. The array was made from a conductive micro fiber textile, silver twocomponent adhesive, and the conductive ink imprint on the polycarbonate. The control box comprises 24 switches that correspond one-to-one to the conductive fields on the array. Each field can be made conductive of non-conductive manually by means of the push-button switches. We present here test representative results obtained from three tetraplegic patients during externally assisted grasping. Therapists could easily select the appropriate conductive fields for the best grasp pattern based on visual feedback. When stimulating over the forearm the array provided effective grasping with minimal wrist flexion, extension, and uncontrolled ulnar and radial deviations. The patterns formed by selected fields in most cases had a branched look. The main advantages of the electrodes were: 1) the selection of the stimulation site was achieved without moving of the electrode; and 2) the pattern (size and layout) was changed during the movement. The later quality is of special interest if the electrode relatively moves with respect to the motor points (e.g., grasping in parallel with pronation and supination).

Introduction

Electrical stimulation of nerves and muscles *via* surface electrodes is being used for various applications (e.g., pain reduction, muscle strengthening, activation of paralyzed muscles, and training of sensory-motor mechanisms). Common to all applications of surface electrodes for stimulation is that it requires a great deal of skill and patience of the user and/or the therapist to place the electrodes in the optimal position for the function to be performed. It is difficult to predict

precisely which anatomic structures will be activated for any given position and electrode configuration. Very often self-adhering electrodes are used, which must be taken off before they can be repositioned at a different location on the skin. This process is time-consuming, and it can also be painful and compromises the adhesion of the electrode to the skin. It is difficult to try many different electrode sizes. For all these reasons a non-optimal electrode position and electrode size are often chosen for stimulation sessions.

Here we describe the advantages of a new multiplecontact surface electrode combined with an easyto-use interface that allows the user to try many different electrode sizes and positions, without removing the electrode from the skin. This arrayelectrode was developed to replace in daily use a single-field electrode in applications where selective activation is required for regaining a functional movement.



Fig. 1: Actitrode®: The 24-field electrode array (right) and the control box for selecting of the conductive fields (left).

<u>Apparatus.</u> The system that was evaluated comprised: 1) the programmable stimulator (Actigrip CS®¹) [1,2], and 2) the selective electrode (Actitrode®, Fig. 1).

195

¹ Actigrip CS® is a four-channel programmable stimulator available from Neurodan A/S, Aalborg, DK (www.neurodan.dk).

The Actigrip CS® is a multi-channel programmable stimulator allowing control of stimulation parameters, and delivering programmed sequences of pulses following the trigger signals [3]. Other stimulators can also be used in conjunction with the Actitrode® in the current version as long as the stimulator output voltage is lower than 100 V.

The Actitrode® consists of the following: 1) an electrode-array comprising a substrate for application to the skin (Fig. 1, right), and 2) an user operable switch setting electrical connection between the selected elements of the array and the stimulator (Fig. 1, left).

The electrode-array comprises 24 conductive fields. The conductive fields are circular, and they are evenly spread over the flexible substrate with the size of 5cm x 8cm. The flexible substrate was made out of biocompatible polycarbonate. The electrode array uses the conductive ink imprint, a silver two-component adhesive, and a conductive biocompatible micro fiber textile that should be moisture when applied to the skin. The description of the electrodes, and testing of their properties are described elsewhere (available on request to the authors). The electrode resistance when all fields are turned on is about 750 Ω , and it increases with the decreased number of fields being turned on to the maximum of 1,9 k Ω .

The switching box has 24 push-button switches that control a matrix of transistor-based switches designed for operation beyond 100 Volts. The control logic was realized by using the microcontroller PIC16F877. The control box comprises the infrared communication link for wireless communication with a PC computer (not used in this study). Each of the switches has a light indicator; hence, the user is aware at all times about the fields that are conducting.

<u>Data acquisition system.</u> We used Penny and Giles flexible goniometers [4], and the laboratory acquisition system based on NI DAQ 6024 for PCMCIA and LabVIEW 6.1 custom designed software. The instrumentation allowed analysis of six joints: flexion and extension of the index and ring fingers (Proximal Inter Phalangeal – PIP, and Meta Carpo Phalangeal - MCP joints), ulnar and radial deviation, and wrist flexion/extension. The sampling rate was 100 samples per second. The resolution of the system was 2 degrees. The data was smoothed using the 4th order Bessel filters.

Procedure

The Actigrip CS® was programmed for application of four channels (Fig. 2). The common anode was positioned over the carpal tunnel. Two cathode-

arrays were positioned at the dorsal and volar sides of the forearm approximately in the middle between the elbow and wrist to control fingers and wrist movements. Each of the two cathodes was connected to one of the stimulation channels. The two remaining cathodes were positioned to control the thumb opening and closing.

We considered that the following muscles are of importance: finger flexors (Flexor Digitorum Profundus m. and Flexor Digitorum Superficialis m.), finger extensors (Extensor Digitorum Communis m., and Extensor Indicis m.), thumb extensor (Extensor Pollicis Longus m., and Extensor Pollicis Brevis m.), and the Thenar muscles (Abductor Pollicis Longus m., and Opponens Pollicis m.); yet, minimizing the activation of Extensor Carpi Radialis Longus m., Extensor Carpi Radialis Brevis m., Flexor Carpi Ulnaris m., and Flexor Carpi Radialis m.

During the grasp the attention was paid to avoid stimulation of the following muscle groups: Extensor Carpi Radialis Longus m., Supinator m., Pronator Teres m., and Pronator Quadratus m. in order to minimize pronation and supination.

Fig. 2 shows the stimulation sequences for the palmar grasp. We stimulated the fingers and thumb flexion and extension simultaneously because of the stimulator limitation to maximum of four channels. The levels of stimulation in Fig. 2 are shown with respect the maximum level of activation that was determined for each subject. The activation of agonist and antagonistic muscles are intentionally shown facing up and down to point to the opposing effects of their activity.

The stimulation parameters were set at 50 pulses per second. The stimulator delivers constant current compensated monophasic pulses with the duration that was at 250 μ s. All parameters were adjustable by using the bush-button controls on the Actigrip CS®. The pulse amplitude was changed on-line to accommodate the needs of each selected electrode-

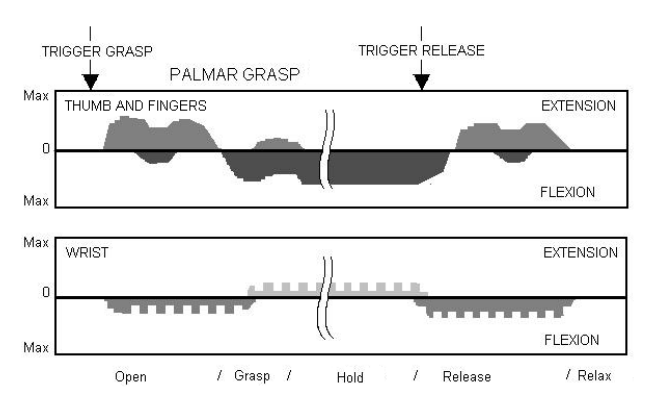


Fig. 2: The pattern of four-channel stimulation: 1) thumb and fingers extension, 2) thumb and fingers flexion, 3) wrist extension, and 4) wrist flexion for the palmar grasp applied with the Actigrip CS® stimulator and Actitrode® electrodes.

array, i.e., selected set of conductive fields. The pulse amplitude was varied between 5 mA and 40 mA.

The pilot experiments included three patients with an injury at C5/C6 level who had no voluntary movement of fingers, and very little wrist control against the gravity, but whose muscles responded to electrical stimulation. Patients signed the consent form that was approved by the local ethics committee following the Declaration of Helsinki.

The task in the experiments was to generate functional movement. The movement was considered functional if it provided fingers flexion leading to a strong grasp with the wrist deviating for less than 15 degrees, and fingers extension leading to the release of the object with the wrist deviating for less than 15 degrees. The deviation included palmar/dorsal flexion and radial/ulnar deviation.

The testing included systematic change of the conductive or non-conductive fields on the electrode-array. The initial position of the fields to be active followed the anatomic considerations of the muscles that normally contribute to movements; although, the muscles responded very differently in tetraplegic patients due to the disuse atrophy, and partial denervation.

Results

We here show only the results for the palmar grasp of a small glass bottle (diameter 9 cm, height 19 cm, mass 200 grams). Fig. 3 shows the variation of the wrist joint angles in parallel with the reproducible flexion of the fingers measured in one tetraplegic patient when the conductive fields were changed.

Four plots (Fig. 3) correspond to movements that were characterized with undesirable wrist flexion/extension, and/or ulnar/radial deviation. In all four cases it was possible to generate effective flexion at PIP and MCM joints for the desired palmar grasp, yet the movement of the hand with respect the forearm compromised the function.

Fig. 4 shows the joint angles in three tetraplegic patients in the case that the conductive fields were selected to form a preferred layout for the palmar grasp. The PIP and MCP joint rotations shown in Fig. 4 are comparable to the ones in Figs. 3; yet, the ulnar/radial deviation and wrist flexion/extension angles were limited to the preferred rotation of ± 15 degrees from the resting (neutral) position. The pronation and supination required the change of the pattern of the array [5].

There was a substantial difference between the locations of conductive fields among three patients

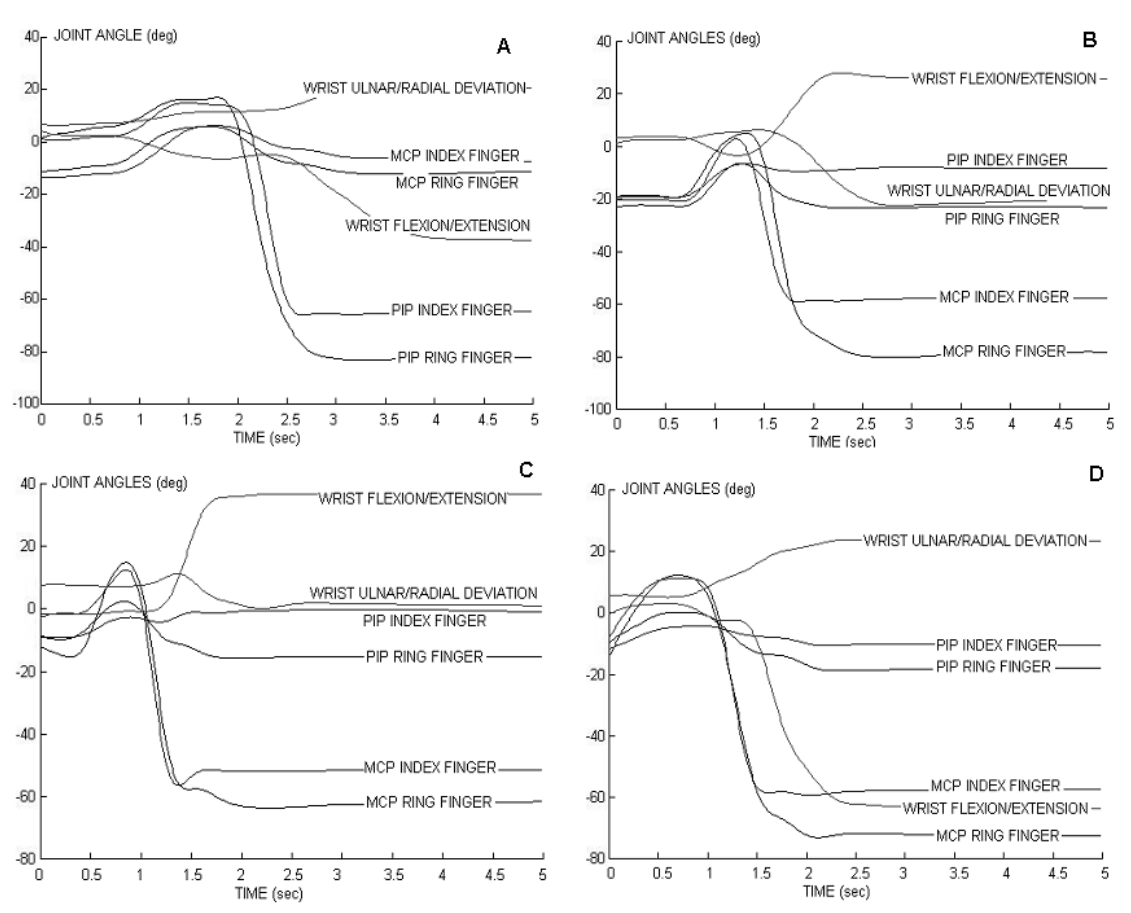


Fig. 3: Joint angles recorded in one tetraplegic subject. Each of the plots shows undesired wrist rotation: A) extensive wrist flexion, B) extensive radial deviation, C) extensive wrist extension, and D) extensive wrist ulnar deviation.

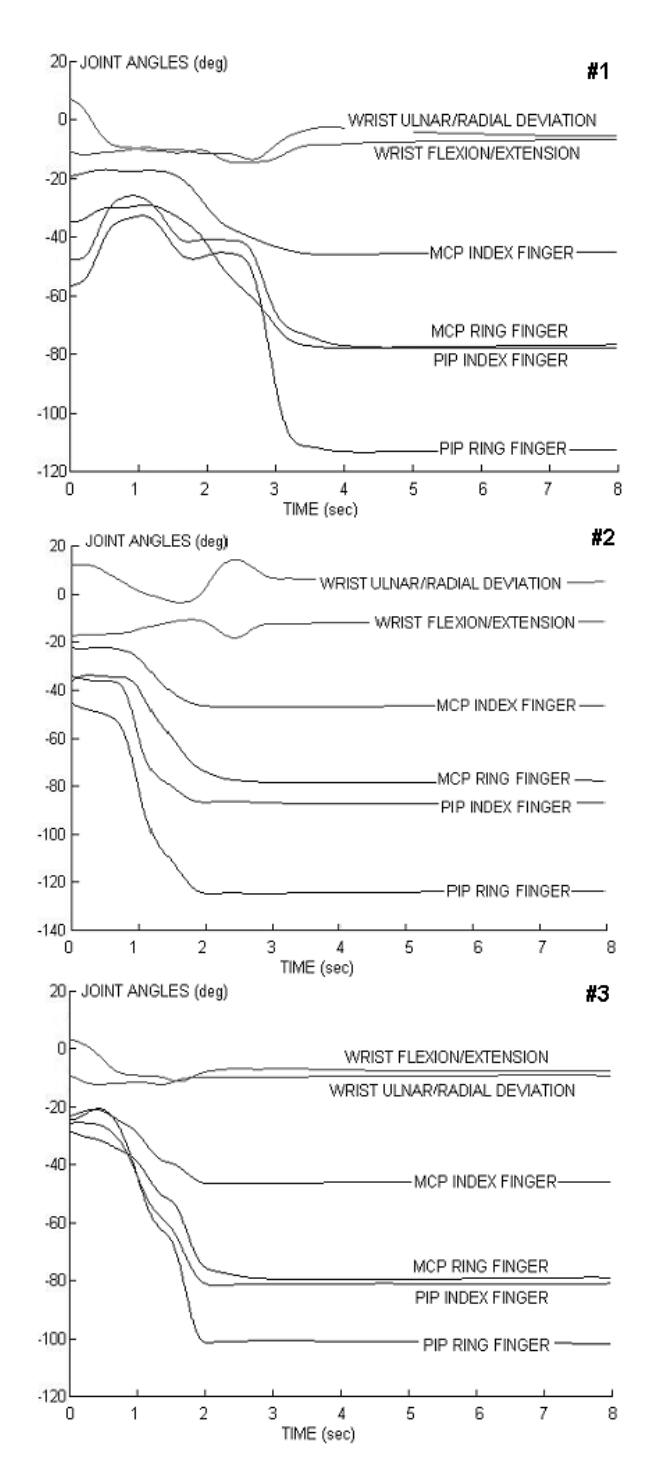


Fig. 4: Joint angles recorded in three tetraplegic patients (#1, #2, and #3) with the conductive fields selected in a preferred way that resulted with the adequate fingers flexion, and controlled wrist stiffness and movement.

(Fig. 5). An important finding was that increased level of stimulation for more than 20 percent from the one that resulted with functional movement lead to stronger fingers flexion or extension; yet, still limited wrist movement.

Conclusion

The new multi-field electrode-array is an effective tool for applying surface electrical stimulation. The selectivity is of special interest when the neural prosthesis is applied to produce functional

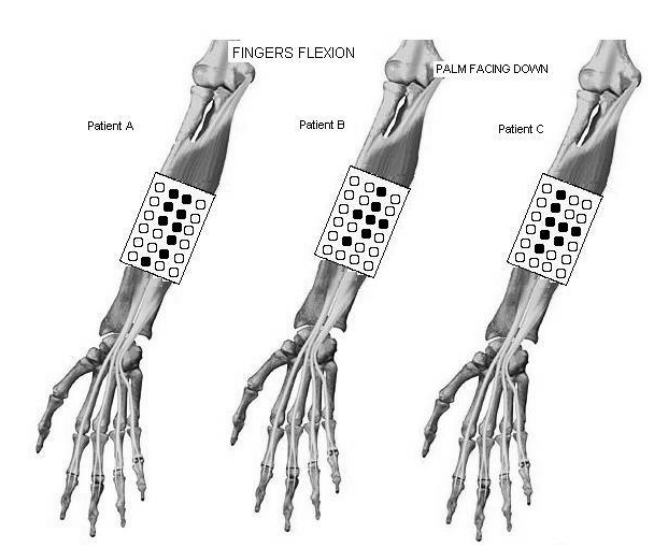


Fig. 5: Black dots show the conductive fields used for control of finger flexors that resulted with the movements in Fig. 4.

movement. The dynamic control of conductive fields is the next step in the development. This control could provide the needed adaptation for movements that include pronation and supination.

References

- [1] Popović M.B., Popović D.B., Sinkjær T., Stefanović A., Schwirtlich L: Clinical Evaluation of Functional Electrical Therapy in Acute Hemiplegic Subjects, J Rehab Res Develop, 40(5):443-454, 2003.
- [2] Popović M.B., Popović D.B., Schwirtlich L., Sinkjær T: Clinical Evaluation of Functional Electrical Therapy (FET) in chronic hemiplegic subjects. Neuromod 7(2):133-140, 2004.
- [3] Jorgovanović N: Control for Neural Prosthesis used in Neurorehabilitation contributing to Reaching and Grasping. Ph.D. Thesis, Faculty of Engineering, University of Novi Sad, 2003.
- [4] Biometrics, Gwent, U.K., Internet site: http://www.biometricsltd.com/
- [5] Bijelić G., Jorgovanović N., Bojanić D., Popović-Bijelić A., Popović D.B: ACTITRODE®: A new surface electrode-array for selective electrical stimulation, Proc 10th MEDICON, Ischia, Italy, July 30-Aug 2, 2004 (accepted).

Acknowledgments

Danish National Research Foundation, Denmark; Serbian Ministry for Science and Environmental Protection, Belgrade; and UNA Consulting, Belgrade, SCG supported the work on this project. We acknowledge the help of our clinical colleagues in trials with tetraplegic patients.

Author's Address:

Ana Popović-Bijelić

Faculty of Physical Chemistry, Belgrade University Studentski trg 12-16, Belgrade, SCG

E-mail: ana@ffh.bg.ac.yu

Session 11

FES from Head to Toe

Chairpersons:

- J. Rozman (Ljubljana, Slovenia)
- S. Sauermann (Vienna, Austria)

THREE TYPES OF EYE MOVEMENT PATTERNS ELICITED BY ELECTRICAL STIMULATION OF CATS SUPERIOR COLLICULUS AND OCCIPITAL CORTEX: PATTERN OF EYE MOVEMENTS AND RECEPTIVE FIELD PROPERTIES

G. Novikov, T. Moshonkina

Pavlov Institute of Physiology, Russian Acad. Sci., St. Petersburg, Russia

The eye movements (EMs) play a significant role in visual behavior. The superior colliculus (SC) and occipital cortex (OC) are known as a key structures for initiation of saccadic eye movements

The electrical stimulation of the mammalian SC and OC elicits saccadic EMs towards a region of the visual space where adjacent cells have their movement fields related retinotopically to the stimulus site. Amplitude and direction of EMs depend on the locus position in the SC and OC retinotopic map and the initial eye position. So the SC and OC neurons have receptive and movement fields simultaneously. Its the base for using these structures as a beautiful experimental model of the oculomotor interaction.

We compared the data of saccade EMs elicited by the local electromicrostimulation and the pattern of impulse activity of these neurons for the adequate visual stimulation (using the same sites in SC and OC).

The EMs were elicited by the local electrical stimulation with square impulses (pulse frequency 100-400 Hz, impulse duration 0.5-2.0 ms, the strength of current was depended on the SC layer and varied from 10 to 2 mA) using the same electrodes. The accuracy of the EMs recordings were 1-2 deg.

Probably data obtained throw a light upon to the functional interconnections between the directional properties of the single SC and OC neurons and the spatial characteristics of EMs elicited by local microstimulation of the same neurons.

We propose the principle schema of the transformation of the visual signals to the signals for initiation of the saccadic EMs on the SC or OC level. This schema reflects a possible mechanism of the visual information transmission about objects movement direction (angle of directional tuning) into the saccade parameters (amplitude and direction of EMs) in foveation process in vision.

Author's Address

Tatiana Moshonkina, Dr Pavlov Institute of Phisiology nab.Makarova, 6 199034 St.Petersburg, , Russia

e-mail: tm@pavlov.infran.ru

COMPARISON BETWEEN THE POWER OUTPUT OF A SKELETAL MUSCLE VENTRICLE AND THE LEFT VENTRICLE IN THE SAME CIRCULATION

I. Ramnarine*, M. Capoccia*, H. Sutherland*, Z. Ashley*, M. Russold*, F. Li*, N. Summerfield**,

S. Salmons*, J. C. Jarvis*

* Department Human Anatomy & Cell Biology

** Department of Clinical Veterinary Science & Animal Husbandry

University of Liverpool, Liverpool, UK

Abstract

Cardiomyoplasty makes sub-optimal use of the power available from a transposed skeletal muscle. A skeletal muscle ventricle (SMV) can be configured to work more efficiently. We compared the power produced by the SMV with that of the native left ventricle (LV) in the same circulation and assessed the ability of the SMV to produce effective counterpulsation.

In 8 pigs the left latissimus dorsi muscle (LDM) was conditioned by electrical stimulation and then configured as an SMV connected to the descending aorta. The SMV was activated during every third cardiac diastole. Haemodynamic parameters during SMV assisted beats and unassisted beats were compared.

SMV assist increased the mean aortic diastolic pressure from 46.8 ± 5.0 to 58.0 ± 6.5 mmHg (P = 0.0001) and the endocardial viability ratio from 0.85 ± 0.09 to 1.13 ± 0.11 (P = 0.0004).

The power produced during SMV and LV ejection was calculated from the intraluminal pressures and the flows produced during ejection. Mean power output during SMV ejection was 1.68 (range 0.39 - 5.39) W; mean power output during LV ejection was 2.59 (1.39 - 3.33) W. Thus SMV ejection produced 63 (21 - 184)% of the power output of LV ejection in the same pig. Mean stroke work of the SMV was 0.33 (0.07 - 1.08) J; that of the LV was 0.89 (0.42 - 1.35) J. Mean SMV stroke volume was 29.4 (10.1 - 58.3) ml; mean LV stroke volume of 80.6 ml (59.7 - 117.8) ml.

SMV power output and volume ejected therefore compared favourably with that of the native LV. The SMV produced effective counterpulsation. The grafts that performed best were those in which the contractile activity had been most effectively maintained during the operative procedure.

The SMV power in this acute operative setting demonstrates an impressive potential for cardiac assist.

Introduction

The number of heart transplants has declined with the decreased availability of suitable donor hearts. This has highlighted the need for suitable alternative therapies for the treatment of end-stage heart failure. Biological cardiac assist is potentially more attractive than transplantation because there is no need for immunosuppression. Cardiomyoplasty has been used in over 2000 cases worldwide [1], but the design resulted in suboptimal use of the power available from the transposed skeletal muscle.

A skeletal muscle ventricle (SMV) was configured to produce cardiac assist and connected to the circulation. We compared the pumping power of the SMV with that of the native left ventricle (LV) in the same circulation.

Material and Methods

All animals were cared for and operated on in strict accordance with the Animals (Scientific Procedures) Act of 1986, which governs experimental animal research in the United Kingdom.

Anaesthetic technique: implantation of stimulator

Eight female adult Large White pigs were premedicated with 2 mg/kg of intramuscular Stresnil (azaperone; Janssen Animal Health). General anaesthesia was induced with a 50:50 mixture of oxygen and nitrous oxide and 1-3% (Forene; Abbott, Isofluorane Wiesbaden, Germany). An intravenous injection of 2 mg/kg of propofol (Propofol-LipuroTM; Braun, Melsungen, Germany) was followed by intubation. Anaesthesia was maintained with a 50:50 mixture of oxygen nitrous oxide and 1-3% Isofluorane administered through a re-breathing anaesthetic circuit (Ohmeda, Essex, UK). Pain relief and respiratory depression was supplied via a continuous intravenous infusion of 3-5mg/hr Alfentanil (Rapifen; Janssen-Cilag; Bucks, UK).

The lateral border of the left latissimus dorsi muscle (LDM) was exposed via a flank incision. The LDM was carefully reflected medially to reveal the thoracodorsal neurovascular bundle. The single stimulating electrode consisted of a stainless steel wire with its terminal end de-insulated and placed on a silicone backing. This electrode was carefully placed across the thoracodorsal neurovascular bundle and connected to monopolar neuromuscular programmable stimulator (Itrel SP 7421, Medtronic, Minneapolis, MN) that was implanted subcutaneously in the flank.

Muscle training

The pigs were allowed to recover for one week after surgery, at which stage the stimulator was switched on. The left LDM was subjected to continuous electrical stimulation with amplitude of 1.5 to 2.5 volts and a frequency of 30 Hz for 0.19 sec on and 6 sec off. The voltage was adjusted to the minimum that produced palpable stimulation of the entire LDM. Conditioning lasted for 28 to 36 days. This pattern converts the muscle fibres from 2B to 2A phenotype, which is both fast-contracting and fatigue resistant.

Pulmonary artery and aortic homografts were obtained from fresh porcine cadavers. The pulmonary artery branches were ligated and the valve excised. The SMV lining was completed by anastomosing the pulmonary artery annulus to a conduit of descending aorta with a double layer of running 5/0 polypropylene suture.

Acute experiment

At the end of the conditioning period the pigs weighed between 56 and 95 kg. The animals were anaesthetised for a second operation with the same anaesthetic protocols, except that pain relief and respiratory depression was achieved with the use of 3-6 mg/hr Diamorphine (Evans Vaccines, UK). A median sternotomy was performed. Pressure catheters (Gaeltec, Scotland) were introduced to monitor the aortic and left ventricular pressures, ultrasound volume flowmeters (Transonic Systems Inc, Ithaca, NY) were used to monitor aortic root blood flow and flow in the SMV conduit; and a volume conductance catheter (CD Leycom, The Netherlands) was placed in the LV. CODAS software (Datag Instruments, Akron, OH) was used to acquire and to store the data.

The left LDM was mobilised, leaving the neurovascular bundle pedicle and attachment to the humeral head intact. An SMV was constructed by wrapping the LDM anti-clockwise around the preformed homograft lining. A double layer of 2/0

polypropylene suture was used to close the LDM around the lining. The third and fifth left ribs were removed. The SMV was introduced into the thorax through the upper rib space. The proximal descending aorta was dissected and a vascular clamp applied to occlude part of the cross-section of the descending aorta. A longitudinal incision was made in the side-clamped aorta and the SMV conduit was anastomosed to it with a single layer of running 5/0 polypropylene. The SMV was deaired and the vascular clamp released (Fig. 1). A flow probe was placed around the base of the SMV and pressure was recorded via a cannula within the SMV lumen (Gaeltec, Scotland).

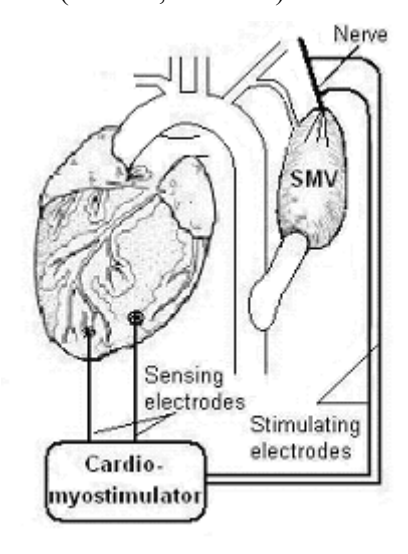


Fig. 1: Schematic diagram of SMV.

SMV stimulation was controlled by a bench-top Pulse Generator (Model DS2A, Digitimer Ltd, Hertfordshire, UK). Contraction was timed to occur in every third cardiac cycle starting at the end of systole (defined as the dicrotic notch on the aortic pressure trace) and continuing for 80% of diastole. The stimulating voltage was at three times the threshold, and delivered with a frequency of 50 Hz and a pulse width of 0.2 msec. Haemodynamic parameters were recorded during cardiac cycles in which the SMV was active. The haemodynamic parameters during the SMV-assisted beat (Assist) were compared with those during the preceding beat (Pre-assist).

Results

During LV ejection, the mean LV pressure was 70.4 ± 6.0 mm Hg and the mean aortic flow was 14.1 ± 0.9 l/min.

During SMV ejection the mean SMV pressure was 65.5 ± 10.0 mm Hg and the mean SMV flow was 9.4 ± 1.4 l/min (Fig. 2 &Fig. 3).

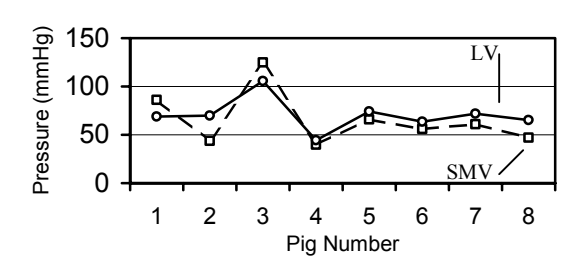


Fig. 2: Mean intraluminal pressure during ejection (LV vs SMV).

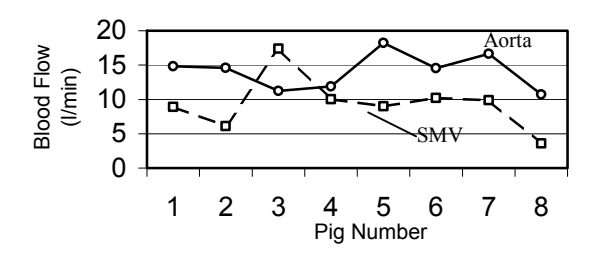


Fig. 3: Blood flow during ejection (Aorta vs SMV).

Mean power output of the SMV during ejection (Fig. 4) was 1.68 (range 0.39 - 5.39) W. As the mean power output of the LV during ejection was 2.59 (1.39 - 3.33) W, SMV ejection produced 63 (21 - 184) % of the power output of LV ejection in the same pig. Mean stroke work of the SMV was 0.33 (0.07 - 1.08) J; that of the LV was 0.89 (0.42 - 1.35) J.

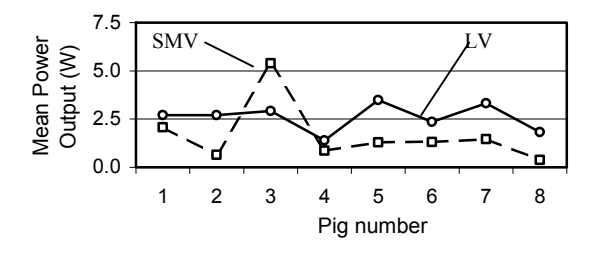


Fig. 4: Mean power output (LV vs SMV).

Maximum SMV power output was 3.6 (range 0.7 - 4.7) W compared to the maximum LV power output of 5.4 (range 2.9 - 6.9) W.

The mean SMV stroke volume (Fig. 5) was 29.4 (10.1 - 58.3) ml and the mean LV stroke volume was 80.6 ml (59.7 - 117.8) ml.

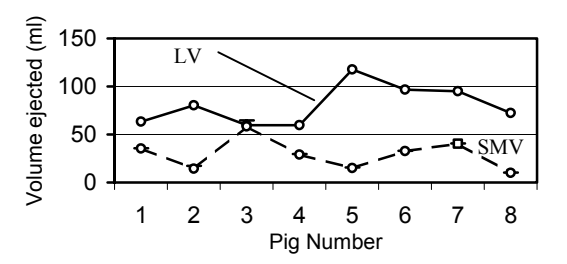


Fig. 5: Volume ejected (LV vs SMV).

When compared to Pre-assist values, SMV assist increased the mean aortic diastolic pressure from 46.8 ± 5.0 to 58.0 ± 6.5 mmHg (P = 0.0001) and the endocardial viability ratio from 0.85 ± 0.09 to 1.13 ± 0.11 (P = 0.0004).

Discussion

Transformed skeletal muscle possesses the power to provide cardiac assist [2]. However, in both aortomyoplasty and cardiomyoplasty, the geometry of the aorta and heart limited the efficient use of the available power from the muscle wrap. Despite the symptomatic benefits, clinical cardiomyoplasty consistently failed to provide demonstrable augmentation of cardiac contractile activity [3]. SMVs offer a more efficient configuration for harnessing muscle power [4].

The power generated from different canine LDM configurations was measured by Badhwar et al. [5]. LDM configured as a circular SMV produced approximately one-third of the peak power produced by linear LDM contraction and approximately twice as much peak power as when the LDM contracted against a chamber placed between itself and the chest wall.

Anderson et al. [6] used SMVs connected to a mock circulation device in dogs and calculated the power output from a chronically stimulated SMV pump at 0.021 W. They estimated that this represented 42% of the power output of the native canine right ventricle.

Both experiments used unconditioned LDM and testing against mock circulation devices. Mannion et al. [7] used conditioned LDM to construct SMVs in dogs and connected them to the circulation. SMV stroke work output was intermediate between that of the native right and left ventricles and SMV power output approximated that of the right ventricle.

Clinical protocols for cardiomyoplasty involved a single operation and a two-week recovery period before muscle conditioning was commenced. Unfortunately, some dynamic cardiomyoplasty patients died in the post-operative period before the benefits of cardiomyoplasty could be enjoyed. The use of the muscle-conditioning regime described here would allow cardiac support to be available immediately following SMV construction.

Considerable inter-animal variation between the SMVs was seen. One SMV (Number 3) produced approximately twice the power of the native LV, because of both the pressure it generated and the flow it produced. In other animals the LDM may have suffered some trauma during mobilisation. Chronic experiments may demonstrate improvement in SMV function as the animal and the muscle recuperate.

The intra-aortic balloon pump (IABP) is the clinical device most commonly used for the treatment of cardiac dysfunction. It produces cardiac assistance by increasing the diastolic blood pressure and by reducing the work of the heart. This effect is termed counterpulsation. The SMV also produced significant counterpulsation as was demonstrated by the increases in mean aortic diastolic pressure and endocardial viability ratio that resulted from SMV ejection. SMV volume ejected (mean 29 ml) is comparable to IABP volumes (34 and 40 ml) and the volumes ejected by the native LV (mean 80.9 ml).

The SMV power and level of cardiac assist provided in this acute operative setting demonstrated an impressive potential for cardiac assist.

References

- [1] Acker MA, Mannion JD, Brown WE, et al. Canine diaphragm muscle after 1 yr of continuous electrical stimulation: its potential as a myocardial substitute. J Appl Physiol 1987;62(3):1264-70.
- [2] Salmons S, Jarvis JC. Cardiac assistance from skeletal muscle: a critical appraisal of the various approaches. Br Heart J 1992;68(3):333-8
- [3] Jarvis JC, Mayne CN, Salmons S. Basic studies on skeletal muscle for cardiac assistance. J Card Surg 1991;6(1 Suppl):204-9.
- [4] Acker MA, Hammond RL, Mannion JD, Salmons S, Stephenson LW. Skeletal muscle as the potential power source for a cardiovascular

- pump: assessment in vivo. Science 1987;236(4799):324-7.
- [5] Badhwar V, Badhwar RK, Oh JH, Chiu RC. Power generation from four skeletal muscle configurations. Design implications for a muscle powered cardiac assist device. ASAIO J 1997;43(5):M651-7.
- [6] Anderson WA, Andersen JS, Bridges CR, et al. Skeletal muscle ventricles as a potential right heart assist or substitute. ASAIO Trans 1988;34(3):241-6.
- [7] Mannion JD, Acker MA, Hammond RL, et al. Power output of skeletal muscle ventricles in circulation: short-term studies. Circulation 1987;76(1):155-62.

Acknowledgements

Supported by A Programme Grant from the British Heart Foundation.

Author's Address

Mr Ian Ramnarine
Cardiac Surgical Research Fellow
Department of Human Anatomy & Cell Biology,
University of Liverpool,
Liverpool, L69 3GE,
United Kingdom
E-mail: iramn@liverpool.ac.uk

A FEEDBACK SYSTEM FOR AUTOMATIC ELECTRICAL STIMULATION OF ABDOMINAL MUSCLES TO ASSIST RESPIRATORY FUNCTION IN TETRAPLEGIA

H. Gollee¹, S. Coupaud¹, K.J. Hunt^{1,2}, D.B. Allan², M.H. Fraser², A.N. McLean²

¹Centre for Rehabilitation Engineering, University of Glasgow, UK

²Queen Elizabeth National Spinal Injuries Unit, Glasgow, UK

Abstract

People with tetraplegia have poor respiratory function leading to limited tidal volume (VT) and reduced cough peak flow (CPF). These problems may cause respiratory failure during both the initial admission and subsequent intercurrent illness. Electrical stimulation of abdominal muscles during expiration can improve respiratory function by increasing VT and CPF. We developed a feedback control system to automatically trigger muscle stimulation, synchronised with the subject's voluntary respiratory activity. The system was tested in a singlesubject proof-of-concept study. Significant increases in VT and CPF were observed suggesting that the technique may have potential use in both acute and established tetraplegia to increase minute ventilation and to improve cough clearance of secretions.

Introduction

People with tetraplegia have poor respiratory function due to: 1) intercostal paralysis causing reduced tidal volume (VT) and 2) abdominal paralysis reducing cough peak flow (CPF) [1]. These problems may cause respiratory failure during both the initial admission and subsequent intercurrent illness. It has been shown that electrical stimulation of abdominal muscles during expiration can improve respiratory function by increasing VT and CPF [2, 3]. While the increase in CPF is a direct result of the improved respiratory pressure due to the additional input from the abdominal muscles, the increase in VT can be attributed to the reduction of lung volume below the functional residual capacity and the subsequent passive recoil during inspiration.

Stimulation of the abdominal muscles is normally used in tetraplegic individuals with spontaneous breathing (although studies exist with individuals who are unable to breath spontaneously [4]). Stimulation therefore needs to be synchronised with their voluntary breathing activity. In previous stud-

ies manual intervention is typically needed to trigger the stimulation. This can be done either by the therapist [5] or by the individual, using for example a chin-controlled joystick [6].

Stanic et.al [7, 8] used a system to trigger the stimulation automatically depending on the individual's spontaneous breathing pattern. A measurement of the airflow at the mouth was used to determine the onset of expiration. The experiments reported are limited to quiet breathing.

This study is aimed at developing a feedback control system to automatically trigger muscle stimulation, synchronised with the subject's voluntary respiratory activity. The system works over a wide variety of breathing patterns, and it does not interfere with non-regular respiratory patterns (for example during speaking). It is designed to detect different situations such as quiet breathing and coughing which require adjustment of the stimulation pattern. While initially the flow at the mouth was used directly to generate the trigger signal, preliminary experiments suggest the suitability of other sensors such as a plethysmographic belt which are not located at the mouth and therefore do not interfere with other activities.

Methods

One subject (16-year-old, male, C4 complete, one year post injury) participated in the study. He breathes spontaneously but with reduced VT and CPF. The subject is in the normal sitting position in his wheelchair during the experiments.

We stimulated abdominal muscles bilaterally using self-adhesive surface electrodes (PALS, Axelgaard, 33mm×53mm rectangular and 50mm round). Four stimulation channels were used: two channels stimulated the mm. rectus abdominis, while the other two channels stimulated the lateral abdominal muscle group (mm. transversi and mm. obliqui ext. et int.) on both sides, cf. figure 1. The stimulation parameters were controlled from a laptop PC through a RS232 interface. A stimulation frequency of 50Hz

was used. Monophasic charge-balanced stimulation pulses were delivered with a constant current of 70mA and variable pulsewidths of 200-500µs. The pulsewidths were adjusted separetly for the mm. rectus abdominis and the lateral abdominal muscle group.

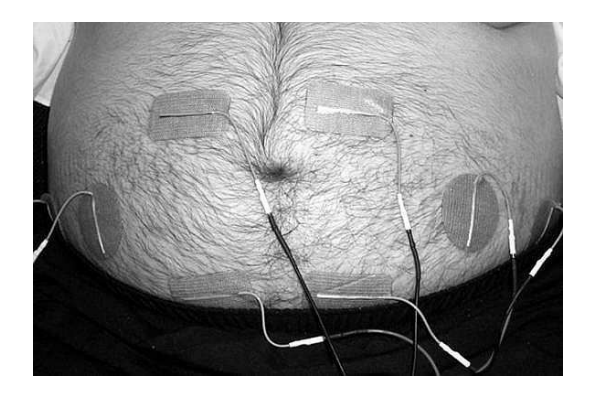


Figure 1: Placement of the electrodes.

A feedback control algorithm was used to automatically generate a trigger signal for stimulation which is synchronised with the voluntary respiratory activity. The respiratory activity was determined by direct measurement of air-flow at the mouth, using a spirometer (Microloop, Micromedical) with an RS232 interface. A plethysmographic belt (Protech) which measures changes in abdominal girth was used as an alternative way to observe the respiratory activity. It was connected to the PC using a custom-built signal amplifier and a data-acquisition card. Whereas measuring the air-flow directly at the mouth requires the subject to wear a face mask, the plethysmographic belt is simply worn around the abdomen.

Feedback control algorithms

The control algorithm uses a feedback signal of the respiratory activity (air-flow or abdominal girth) to generate a suitable stimulation signal which does not interfere with the voluntary breathing. The main task is to detect the end of inspiration or the beginning of expiration, and to synchronise the artificial stimulation signal accordingly.

Two approaches to generate the stimulation trigger signal from the measured respiratory activity were used: During quiet breathing, the onset of expiration was determined by observing the derivative of flow with respect to time. If this value exceeded a pre-set threshold, a zero-flow crossing from inspiration to expiration was detected. The stimulation was triggered at a specified time (usually 0.2s) af-

ter the onset of expiration. The maximal duration of one stimulation burst was limited to 1.5s. The stimulation burst would be terminated when inspiration was detected.

A modified algorithm was used for coughing, where stimulation was applied at the end of voluntary inspiration which was detected by observing the derivative of flow with respect to time, taking into account that the maximal inspired flow must exceed 1.0 l/s to be classified as an attempt to cough. The subject was instructed to hold his breath for a short time after inspiration to allow the abdominal muscles to contract and the pressure to build up before beginning of expiration. The length of the stimulation burst was set to 1.5s.

Results

The subject tolerated several minutes of stimulation without discomfort or other adverse effects. He could speak normally without inappropriate triggering of the stimulation.

Typical experimental results for quiet breathing, forced expiration and coughing are shown in figures 2-4, using the air-flow signal from the spirometer to generate the stimulation trigger.

Note that positive flow corresponds to expiration (volume increase), while a negative flow relates to inspiration (volume decrease). The bold horizontal lines indicate when stimulation was applied.

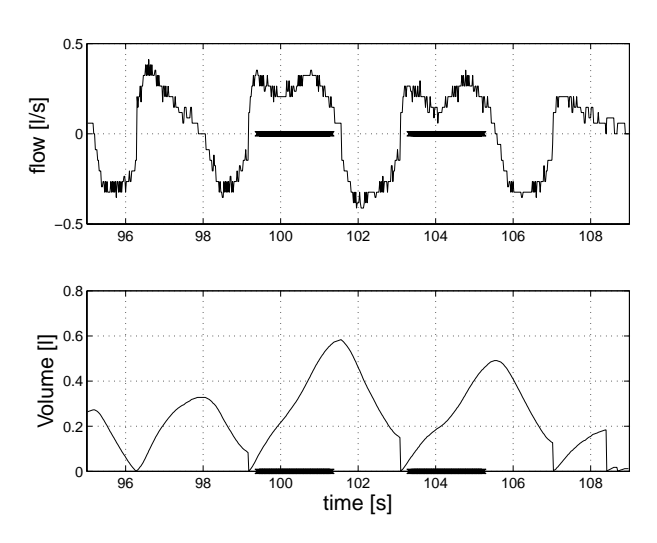


Figure 2: Quiet breathing. The bold lines indicate when stimulation is applied.

Figure 2 shows four quiet breaths, extracted from an experiment of approximately 3min duration. Stimulation is applied during the second and third breaths. The flow diagram shows a large additional expira-

tory flow as a result of the stimulation of the abdominal muscles. The tidal volume increases from approximately 0.31 without stimulation to over 0.551 with stimulation, cf. the bottom graph in figure 2.

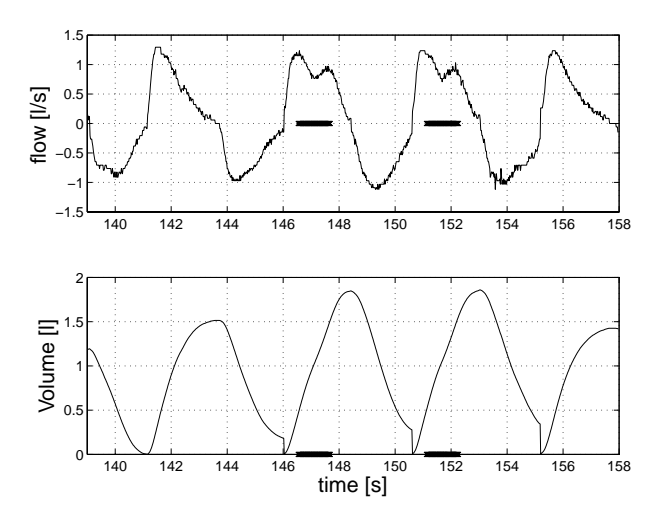


Figure 3: Forced expiration. The bold lines indicate when stimulation is applied.

The results shown in figure 3 were obtain when the subject was instructed to breath out forcefully. The four breaths shown here are extracted from an experiment of 3min duration. Stimulation is applied during the second and third breath. A larger expiratory flow can again be observed as a result of the stimulation. The maximal tidal volume increases from 1.51 without stimulation to 1.851 when stimulation is applied.

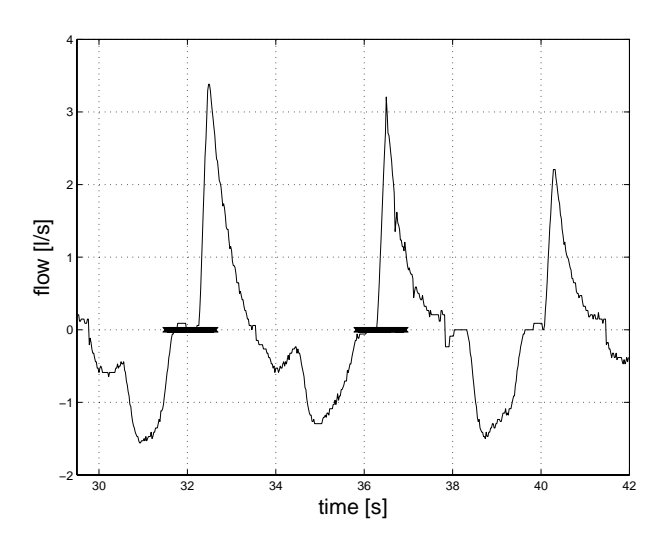


Figure 4: Coughing. The bold lines indicate when stimulation is applied.

A typical experimental result for coughing is shown in figure 4. The aim for assisted cough is to maximise the flow to allow better clearing of the airways. Tidal volume has therefore been omitted from the graph. Three coughs are shown: the first two coughs are with assistance from abdominal stimulation, while the final cough is unassisted. A clear increase in CPF can be observed when stimulation is applied. Note that the increase was consistently observed, independently of whether assisted cough preceded or followed unassisted coughs. We recorded an increase of CPF from 2.61/s to 3.41/s.

Plethysmographic Belt

Results of initial experiments with a plethysmographic belt to measure breathing activity are shown in figure 5. Stimulation is applied during the first two

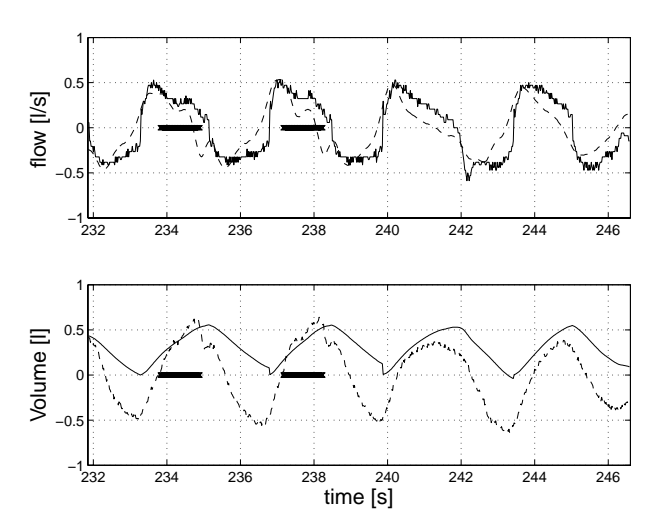


Figure 5: Quiet breathing, with plethysmographic belt measurements (dashed lines, no units). The bold lines indicate when stimulation is applied.

breaths shown, while the last two breaths are unassisted. In addition to the flow and volume traces, the figure also shows the measurements obtained from the belt. The dashed line in the bottom plot corresponds to the raw belt signal which is proportional to abdominal girth and therefore directly related to tidal volume. The dashed line in the top plot shows the differentiated belt signal which is a measurement of the rate of change of the abdominal girth and therefore related to the air-flow. In both plots it can be observed that the relevant belt signal relates well to the volume and flow signal. The feedback signal from the belt was used here to generate the stimulation signal.

Discussion

The results show that the closed loop system presented here can automatically ensure that abdominal stimulation is synchronised with the subject's own respiratory activity. Control algorithms for quiet breathing, forced expiration and for coughing have been implemented and experimentally evaluated. The results show a clear increase in VT (during quiet breathing and forced expiration) and CPF (during coughs). Direct observation of the air-flow at the mouth provides an accurate measure for the breathing activity and can be used as a feedback signal. Any measurement at the mouth interferes, however, with other activities and is therefore not suitable for a system which is to be used in everyday situations. We suggest that a plethysmographic belt which measures abdominal girth can be used to provide an accurate measure of the respiratory activity and can be used as a feedback signal to the stimulation control algorithm. Our initial results show the suitability of this approach.

This proof of concept technique may have potential use in both acute and established tetraplegia to increase minute ventilation and to improve cough clearance of secretions. Besides improving minute ventilation, continuous stimulation during quiet breathing can be used to strengthen the abdominal muscle, which could lead to further improvements in CPF.

References

- [1] A. Baydur, R. H. Adkins, and J. Milic-Emili. Lung mechanics in individuals with spinal cord injury: effects of injury level and posture. *J Appl Physiol*, 90(2):405–411, Feb 2001.
- [2] R. J. Jaeger, R. M. Turba, G. M. Yarkony, and E. J. Roth. Cough in spinal cord injured patients: comparison of three methods to produce cough. *Arch Phys Med Rehabil*, 74(12):1358– 1361, Dec 1993.
- [3] W. E. Langbein, C. Maloney, F. Kandare, U. Stanic, B. Nemchausky, and R. J. Jaeger. Pulmonary function testing in spinal cord injury: effects of abdominal muscle stimulation. *J Rehabil Res Dev*, 38(5):591–597, Sep-Oct 2001.
- [4] F. Kandare, G. Exner, J. Jeraj, A. Aliverti, R. Dellaca, U. Stanic, A. Pedotti, and R. Jaeger. Breathing induced by abdominal muscle stimulation in individuals without spontaneous ventilation. *Neuromodulation*, 5(3):180–185, Jul 2002.
- [5] A. Zupan, R. Savrin, T. Erjavec, A. Kralj,

- T. Karcnik, T. Skorjanc, H. Benko, and P. Obreza. Effects of respiratory muscle training and electrical stimulation of abdominal muscles on respiratory capabilities in tetraplegic patients. *Spinal Cord*, 35(8):540–545, Aug 1997.
- [6] P. N. Taylor, A. M. Tromans, K. R. Harris, and I. D. Swain. Electrical stimulation of abdominal muscles for control of blood pressure and augmentation of cough in a C3/4 level tetraplegic. *Spinal Cord*, 40(1):34–36, January 2002.
- [7] J. Sorli, F. Kandare, R. J. Jaeger, and U. Stanic. Ventilatory assistance using electrical stimulation of abdominal muscles. *IEEE Trans. Rehab. Eng.*, 4(1):1–6, Mar 1996.
- [8] U. Stanic, F. Kandare, R. Jaeger, and J. Sorli. Functional electrical stimulation of abdominal muscles to augment tidal volume in spinal cord injury. *IEEE Trans. Rehab. Eng.*, 8(1):30–34, Mar 2000.

Author's Address

Henrik Gollee
Centre for Rehabilitation Engineering
Department of Mechanical Engineering
University of Glasgow
Glasgow G12 8QQ, Scotland, UK
e-mail: h.gollee@mech.gla.ac.uk
home-page: http://fesnet.eng.gla.ac.uk/CRE

MODULATION OF PH IN THE STOMMACH OF A DOG BY SELECTIVE STIMULATION OF THE LEFT VAGUS NERVE

J. Rozman, M. Mihić, *M. Bunc, **T. Princi

ITIS d. o. o. Ljubljana, Center for Implantable Technology and Sensors, Lepi pot 11, *University of Ljubljana, Faculty of Medicine, Institute of Pathophysiology, Zaloška 4, 1000 Ljubljana, Republic of Slovenia, **University of Trieste, Piazzale Europa 1, Trieste, Italy

Abstract

The superficial region of the left vagus nerve of a dog, innervating the stommach, was selectively stimulated with implanted 39-electrode spiral cuff to modulate the pH. The cuff, having thirteen circumferential groups of three electrodes were chronically implanted on the left vagus nerve at the neck in two adult Beagle dogs. Corresponding superficial region, being in contact with certain group of three electrodes, was stimulated for 15 seconds with biphasic, rectangular and current pulses (2mA, 200 µs, 20Hz). The results showed that group of three electrodes No. 7 elicited the most acidic gastric juce within the stommach. Namely, it was shown that stimulation lasting 15 seconds lowered the pH from pH1.6 down to pH1.34. Results of this study clearly demonstrate that internal organs can be selectively stimulated via the selective stimulation of innervating superficial regions of the autonomic peripheral nerve.

Introduction

In the field of research considering the possibilities in the application of functional electrical stimulation (FES) of the autonomic nervous system, interest is relatively big. This is evident from the few, actually very good publications in literature [1, 3, 7]. The left vagus nerve is an important route of information into the CNS. One of its main functions is to monitor and control the activity of the internal organs and glands such as a heart, lung, stomach, bladder and pancreas. Accordingly, there is a revival of interest in the influence of the vagal nerve fibres on these organs [2].

The digestive system is innervated with nerve fibres of both the sympathetic and parasympathetic divisions, although the parasympathetic control dominates. The parasympathetic system increases digestive activity (secretion and motility), and the sympathetic system has a net inhibitory effect. The importance of the brain in regulation of upper gastrointestinal function is an exciting and growing

field within neuroscience (4). The research uses multiple and varied approaches providing a powerful tool for unraveling the complexity of brain-gut interactions. It was demonstrated that the key changes in metabolism that contribute to some eating disorders are largely controlled by the component of the autonomic nervous system carried by the vagus nerve to the digestive organs. The term 'Vagus Nerve Stimulation' (VNS) generally refers to several different techniques used to stimulate the vagus nerve. For practically all studies in humans, VNS refers to stimulation of the left cervical vagus nerve using various commercial devices. By using the method of selective stimulation of the corresponding superficial regions of the left vagus nerve, we could could externally control the gastrointestnal function.

The present study addressed the hypothesis that a certain superficial region of the peripheral autonomic nerve is composed mainly of fibres innervating a single internal organ or gland. Our study was aimed at the demonstration that the selective stimulation of the autonomic nerve with multi-electrode spiral cuff can be potentially used as a method for external modulation of function of the internal organs and glands. The main purpose of the study was therefore to investigate whether a 39-electrode spiral nerve cuff could be used to selectively stimulate the stommach of a dog via selective stimulation of the corresponding superficial regions of the left vagus nerve [6].

Material and Methods

A cuff was made by bonding two silicone sheets together. One sheet, stretched and fixed in that position, was covered by a layer of adhesive. A second unstretched one was placed on the adhesive and the composite was compressed. When released, the composite curled into a spiral tube as the stretched sheet contracted to its natural length.

Thirty-nine electrodes (0.6 X 1.5)mm were made of a 50μ m thick platinum ribbon and connected to lead wires that were mounted on a third silicone

sheet. They were arranged in three parallel groups each containing 13 electrodes. Then, thirteen groups of three electrodes (GTEs) in the same line in a longitudinal direction were formed. All electrodes of the central and two outer groups were connected to the corresponding lead wires. The silicone sheet with the arranged electrodes was then bonded on the inner side of the opened cuff. The cuff with the inner diameter of 2.5mm and the length of 18mm is shown in Fig. 1(1).

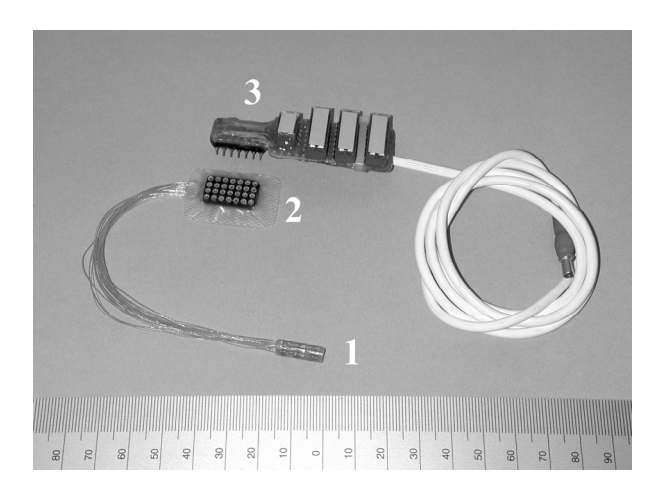


Fig. 1. The 33-electrode spiral cuff (1) with the subcutaneous common connector (2) and the switch module (3).

Lead wires were connected to a special connector to be implanted within the lateral subcutaneous tissue for the time between the experimental sessions. This connector, shown in Fig. 1(2), was designed to enable both mechanical and electrical connections to the switch module and to be also used during the stimulating sessions.

The experiment was performed on two Beagle dogs. All procedures were approved by the ethics committee at the Veterinary Administration of the Republic of Slovenia, Ministry of Agriculture, Forestry and Food.

The animals were premedicated with medetomidine 40µg/kg i.m. and methadone 0.2mg/kg s.c.. The induction was performed with propofol 1.0 to 2.0mg/kg i.v.. General anaesthesia was maintained with isoflurane 0.8 to 1.5 vol.% in 100% O₂. When necessary, during surgery analgesia was sustained with ketamine 0.5 to 2.0mg/kg i.v.. Antibiotics (cefazolin 20mg/kg i.v.) were administered perioperatively. According to our model the cuff was installed on the left vagus nerve at the neck. The leads of the cuff were routed and fixated to the connector under the skin.

Finally, the incision was closed and the animal awakened. Analgesia during the early recovery period was provided with methadone 0.3 to 0.5mg/kg s.c. TID. Tramadol 8.0mg/kg s.c. TID was administered for additional two days. To allow the animal to fully recover from anaesthesia and tissue healing, the first experiment was performed 30 days after the implantation.

After taking the implanted common connector out of the body, it was thoroughly cleaned and dried. The connector and the wound were then covered with self-adhesive surgical foil during the entire experiment. To connect the common connector to the outputs of the stimulator a special cable shown in Fig. 1(3), was developed. The connection itself was made simply by perforating the self-adhesive surgical foil with the pins of the switch module and inserting them into the common connector. The of the switching module switches were alternatively turned on so as to connect the electrodes in the certain GTE to the stimulator. The two outer electrodes of a certain GTE were shortcircuited and connected through an explanted connector and the switching module to one end of a electrical stimulator, while the corresponding central electrode was connected to the other end.

The relative position of GTE closest to the superficial region of the nerve innervating the stommach was determined experimentally by delivering stimuli to all 13 GTEs. Accordingly, all superficial regions, innervating different internal organs and glands, were selectively stimulated for 15 seconds with square-wave, biphasic, charge balanced, current pulses (100µs, 1.3 to 2mA, 20Hz). Each stimulation session was proceeded by a pause of 5 seconds during which the existing GTE was disconnected from the stimulator and the next one was connected. When the stimuli were delivered to the GTE No. 7, which was in contact with the superficial region of the left vagus nerve innervating the stommch, the pH within the stommach fell on the lowest value. This GTE was then indicated as relevant for the selective stimulation of the stommach.

To measure the changes of pH within the stommach a special Ion Selective Field Effect Transistor (ISFET) solid state pH Sensor Probe (IQ240, Scientific Instruments, Inc., San Diego, CA, USA.), was used [5]. The signal from the pH meter was then delivered to a DigiPack 1200 (Axon Instruments), high performance data acquisition system connected to a personal computer. At the conclusion of the last experimental protocol, the animals were euthanized using the veterinary drug T61 (Hoechst, Frankfurt, Germany).

Results

The results of the three year study, during which 8 experiments were conducted on two Beagle dogs, show almost the same degree of selectivity in stimulations of the stommach via the left vagus nerves. We present the results obtained in the last of four experiments conducted on the second implanted animal.

The five records of responses elicited in the heart, the lung and the stommach by the stimuli delivered for 15s on the GTE No. 7 which was closest to the region a innervating the stommach are presented in Fig. 2. The trace No. 1, represents the change in the pH within the stommach. As can be seen the decrease in pH starting from pH1.6 at the beginning of stimulation to pH1.34 at the end of stimulation. The trace No. 2, representing the breathing frequency does not show any disturbance in breathing during the stimulating period. The trace No. 3, representing ECG, does not show any disturbance in ECG during the stimulating period, and, therefore the heart rate remained unchanged. Similarly, left vagus nerve stimulation did not induce any disturbance in the arterial pressure as shown in the traces number 4.

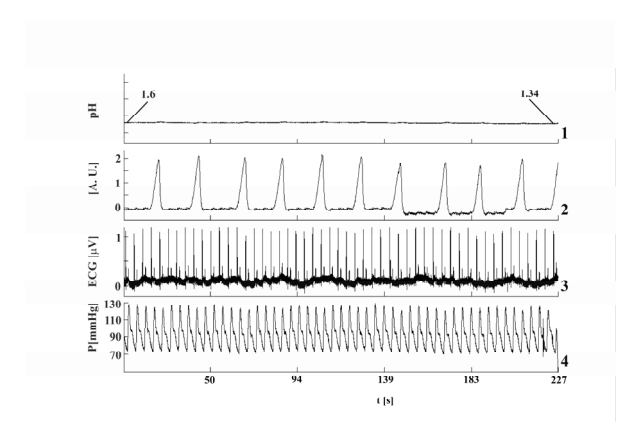


Fig. 2. Fig. 2. Physiological responses of the heart represented by the arterial blood pressure (trace No. 4) and ECG (trace No. 3), of the lung represented by the breathing frequency (trace No. 2), and of the stommach represented by the pH excursion (trace No. 1).

In Fig. 3, the response of the stommach on the consecutive selective stimulation of the superficial regions of the left vagus nerve using all thirteen GTEs is represented. The results of pH measurements showed that only GTE No. 7, which was close to the region innervating the stommach, caused a considerable fall of pH within the stommach.

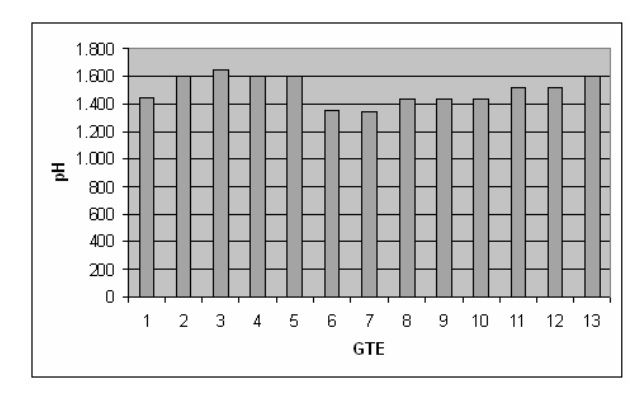


Fig. 3. Physiological response of the stommach represented by the changes in the pH, elicited by the stimulation with the GTE No. 7.

Discussion

Gastric secretory studies combined with selective vagal stimulation may be useful in patients with suspected gastric hypersecretion. Furthermore, gastroparesis is a condition in which the stomach does not empty at a normal rate. One among causes of chronic gastroparesis are neurologic disorders affecting the vagus nerve. Nevertheless, intact vagus nerve is considered necessary gastric appropriate emptying. Instead medications widely used to treat the illness, VNS coud be potentially used as alternative method. Therefore, it could be expected that the future research efforts will be oriented towards to identification of neural mechanisms coordinating motility and secretion. Very important challenge will be also identification the brain regions mediating peripheral autonomic responses to visceral stimuli arising in the gastrointestinal tract. The long-range goal of our research, however, will be to understand how the various branches of the utonomic nervous system regulate the function of the gastrointestinal organs and glands.

References

- [1] Berthoud H.R., Hennig G., Campbell M., Volaufova J., Costa M.: Video-based spatiotemporal maps for analysis of gastric motility in vitro: effects of vagal stimulation in guinea-pigs. Neurogastroenterol. Motil. 14, 2002, 677-88.
- [2] Berthoud H.R., Neuhuber W.L.: Functional and chemical anatomy of the afferent vagal system. Auton. Neurosci. 85, 2000, 1-17.
- [3] Berthoud H.R., Powley T.L.: Characteristics of gastric and pancreatic responses to vagal stimulation with varied frequencies: evidence for different fiber calibers? J. Auton. Nerv. Syst. 19, 1987, 77-84.

- [4] Hayashi N., Mizumoto A., Itoh Z.: [Inhibition of gastric acid secretion normalizes interdigestive motor activity in the stomach in dogs] [Article in Japanese] Nippon Shokakibyo Gakkai Zasshi. 88(5), 1991, 1168-76.
- [5] van Herwaarden M.A., Samsom M., Smout A.J.: 24-h recording of intragastric pH: technical aspects and clinical relevance. Scand J Gastroenterol Suppl. 230, 1999, 9-16.
- [6] Kholeif H., Larach J., Thomforde G.M., Dozois R.R., Malagelada J.R.: A canine model for the study of gastric secretion and emptying after a meal. Dig Dis Sci. 28(7), 1983, 633-40.
- [7] Tougas, G., D. Fitzpatrick, et al.: "Effects of chronic left vagal stimulation on visceral vagal function in man." Pacing Clin Electrophysiol 15(10 Pt 2), 1992, 1588-96.

Acknowledgements

This work was financed by Research Grant: J2-0542 from the Ministry of Education, Science and Sport, Ljubljana, Republic of Slovenia and supported in part by the European Community's Human Potential Programme under contract HPRN-CT-2000-00030, [NeuralPRO].

Author's Address

Dr. Janez Rozman, ITIS d. o. o. Ljubljana, Center for Implantable Technology and Sensors, Lepi pot 11, 1000 Ljubljana, Republic of Slovenia, e-mail: janez.rozman@guest.arnes.si

DIFFERENT PARAMETERS FOR CHRONIC PUDENDAL NERVE STIMULATION WITH PUDENDAL PERCUTANEOUS IMPLANT (PPI) RELATED ON NEUROGENIC SITUATION

M. Spinelli, S. Malaguti, M. Lazzeri, G. Giardiello, L. Zanollo, J. Tarantola

Ospedale Civile "G.Fornaroli", Magenta, Italy

There have been several attempts to stimulate the pudendal nerve in order to achieve a beneficial effect on multiple impaired pelvic functions such as urinary and/or fecal incontinence, retention or constipation. During the last few years, physicians have tried applying sacral neuromodulation to neurogenic patients and this was reported to have inconsistent degrees of success.

Our original method for chronic pudendal stimulation (PPI) uses the same system for minimally invasive sacral nerve stimulation (staged implant with tined lead), with the possibility to implant a lead, close to pudendal nerve, under neurophysiological guidance.

Methods

Fifteen neurogenic patients (8 male, 7 female – mean age 38, 21-66) complaining symptoms of urge incontinence due to neurogenic overactive bladder, underwent PPI which is performed using neurophysiological monitoring to implant a lead into the Alcock's canal close to the pudendal nerve.

All patients were neurogenic: 8 non traumatic (6 myelitis, 1 syringomelia, 1 cerebellum neoplasia), 7 had trauma (incomplete lesion at the cervical level in 3, at level D12-L1 in 2, complete dorsal lesion in 2).

All patients were submitted to complete neurophysiological and urodynamic evaluation at baseline and follow-up and were asked to fill out a bowel and voiding diary for 7 days.

After implant all patients were submitted to a weekly evaluation to set best parameters of stimulation.

Results

Eight patients became continent during the screening phase and 2 patients improved by more 88% (from 9 to 1 daily incontinence episodes), 2 patients reduce by 50% the number of incontinence episodes and 3 patients had no improvement.

Four out of the 7 patients with constipation increased weekly evacuations from 2.5 to 7. One patient with associated fecal incontinence became continent.

Urodynamic evaluation showed objective improvement in maximum cystometric capacity and in maximum pressure. Twelve patients implanted with permanent stimulator achieved continence at the last follow-up (average follow-up eight months) although one of these was explanted one month after IPG implant because of erosion of the skin at the site of the connection between lead and extension cable.

Actually seven patients with myelitis uses a stimulation on demand (5 Hz) at appearance of urge obtaining continence and increasing of time to go to the toilet (mean 45 minutes).

Three patients with cervical trauma obtain results with IPG on (15 Hz.) during the day and off during the night. They use nocturnal stimulation only to obtain bowel voiding.

Two patients, one siringomielia and one complete dorsal lesion uses a continuous stimulation (5 Hz.).

Comments

The method of pudendal percutaneous implant under neurophysiological guidance seems to be a new way in treatment of neurogenic overactive bladder, better than sacral nerve stimulation. The procedure is safe and reversible. From these preliminary data, a strategic issue is to find best parameters of stimulation and time of application of the therapy.

A continuous monitoring of results related on parameters is the way to achieve further informations. Parameters setting seems related on neurophysiological baseline situation. A multicentric protocol is going to start to obtain a larger experience.

Author's Address

Michele Spinelli, Dr. Ospedale Civile "G.Fornaroli" Via Donatori di sangue, 50 20013 Magenta (MI), , Italy e-mail: gins@ginsnet.org

SPASTIC BLADDER AND SPINAL CORD INJURY. 17 YEARS OF EXPERIENCE WITH SACRAL DEAFFERENTATION (SDAF) AND IMPLANTATION OF AN ANTERIOR ROOT STIMULATOR (SARS).

J. Kutzenberger, B. Domurath, D. Sauerwein

Clinic for Neuro-Urology, Werner-Wicker-Hospital, Bad Wildungen, Germany

Abstract

Introduction: Spinal cord injured patients with a suprasacral lesion usually develop a spastic bladder. The hyperreflexia of the detrusor and the external sphincter causes incontinence and threatens those patients with recurrent urinary tract infections (uti), renal failure and autonomic dysreflexia. All of these severe disturbances may be well managed by sacral deafferentation (SDAF) and implantation of an anterior root stimulator.

Material and Method: 464 paraplegic patients (220 female, 244 male) received a SDAF-SARS since Sept. 1986 to Dec. 2002. Almost exclusively the SDAF was done intradurally, which means with one operation field there can be done two steps (SDAF and SARS).

Results: 440 patients have a follow-up with 6.6 years (at least > 6 months-17 years). The complete deafferentation was successful in 94.1%. 420 paraplegics may use the SARS for voiding, (frequency 4.7 per day) and 401 use it for defecation (frequency 4.9 per week). Continence was achieved in 364 patients (83%). UTI declined from 6.3 per year preoperatively to 1.2 per year postoperatively. Kidney function presented stable. Early complications were 6 CSF leaks, 5 implant infections. Late complications with receiver or cable failures made us do surgical repairs in 34 paraplegics. A step by step program for trouble-shooting differentiates implant failure, myogenic or neurogenic failure.

Conclusion: SDAF is able to restore the reservoir function of urinary bladder and to achieve continence. Autonomic dysreflexia disappeared in most of the cases. By means of an accurate adjustment of stimulation parameters it is possible to accomplish low resistance micturition. The microsurgical technique requires an intensive education. One has to be able to manage late implant complications.

Introduction

After spinal cord injury with subsequently complete suprasacral lesion there almost obligatory

develops a hyperreflexia of the bladder and the external sphincter (detrusor-sphincter-dyssynergia parasympathetic DSD). The conal somatomotoric reflex-center has lost its controlling function by the pontine micturition and storing centers. The hyperreflexia impairs the reservoir function of the urinary bladder. The DSD causes a high resistance against micturition, which may only take place with either increased pressure. Those paraplegic patients suffer from reflex incontinence, recurrent urinary tract infections (UTI), autonomic dysreflexia and finally they are threatened by failure of kidney function. Conservative treatment not infrequently fails; such as the sphincterotomy, which is supposed to allow a reflex-voiding with low resistance, or such as the anticholinergic therapy or the botulinum-toxine injection into the detrusor-muscle and the intermittend (self)-catheterism. There had to get developed a long term therapy: the sacral deafferentation (SDAF) and the anterior root stimulation (SARS). The idea for the sacral deafferentation was the complete transsection (Sauerwein) of those afferent dorsal roots S2 to S5 Thus there was restored a normal reservoir-function and urinary continence by interrupting the relex activity. The second step with the implantation of the anterior root stimulator enables paraplegics to void voluntarily by means of an external transmitter. G.S.Brindley [4], [5] developed the implant and external device (1969-1978) (Fig.1)



Fig. 1: The intradural implant, the external transmitter and the charging device

Material and Methods

There was done the SDAF and the implantation of the SARS in 464 paraplegic patients, 220 females and 244 males, since September 1986 and December 2002. The procedure took place almost exclusively intradurally. That way it was possible to do both steps, the SDAF and the SARS as well within one operation field. The intradural deafferentation requires microsurgical techniques. An intraoperative urodynamic and arterial blood pressure registration allows to distinguish the dorsal and anterior roots by electro stimulation with 10V and 30Hz (Fig. 2). Electro stimulation of the anterior root provokes a detrusor contraction and a accompanying somatomotoric reaction (plantar flexion and contraction of the anal sphincter (S4), S3; contraction of m. gluteus medius), whereas the dorsal roots may only show an increase of blood pressure.

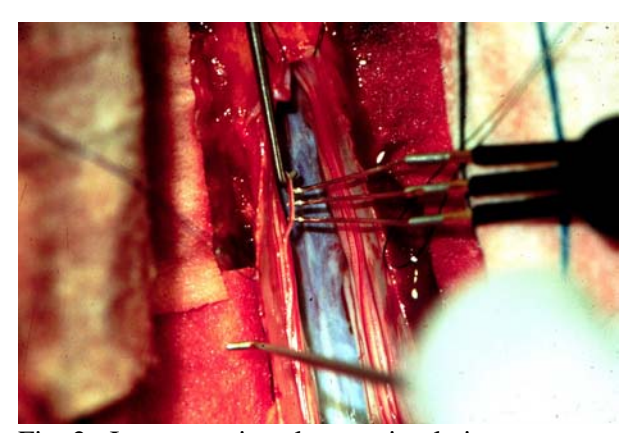


Fig. 2: Intraoperative electro stimulation

Within the first 7 day postoperatively there is done an urodynamic examination, which reveals the successful complete deafferentation and the program of the external transmitter can be set. Patients can now start to void and defecate by anterior root stimulation. The micturition by SARS is a post-stimulus voiding. Because of the quick relaxation of the striated muscles of the pelvic floor at the end of the stimulus, voiding takes place with low resistance (Fig. 3).

Stimulation of S2 may be used for the erection in men and lubrification of the vagina in women.

Results

Clinical und urodynamic findings Sept. 1986 – Sept. 2003

440 patients are still in a continuous follow-up for a mean time of 6.6 years (at least more than 6 months up to 17 years). SDAF was completely successful in 419 patients (94.1%) with a stable reservoir-function and a mean capacity of 470ml (173ml preoperatively). In 8 patients there had to be done a second deafferentation at the conus in order to achieve a complete interruption of hyperreflexia. Continence was achieved in 364 patients (83%), in 22 patients by means of the additional implantation of an artificial sphincter. 420 paraplegics are able to void voluntarily by SARS with a daily frequency of 4.7 and 401 paraplegics are able to use SARS for defecation with a frequency of 4.9 per week. UTI diminished from 6.3 per year preoperatively to 1.2 per year The kidney-function did not postoperatively. change, in deed it did not deteriorate. autonomic dysreflexia disappeared in all 187 cases but two.

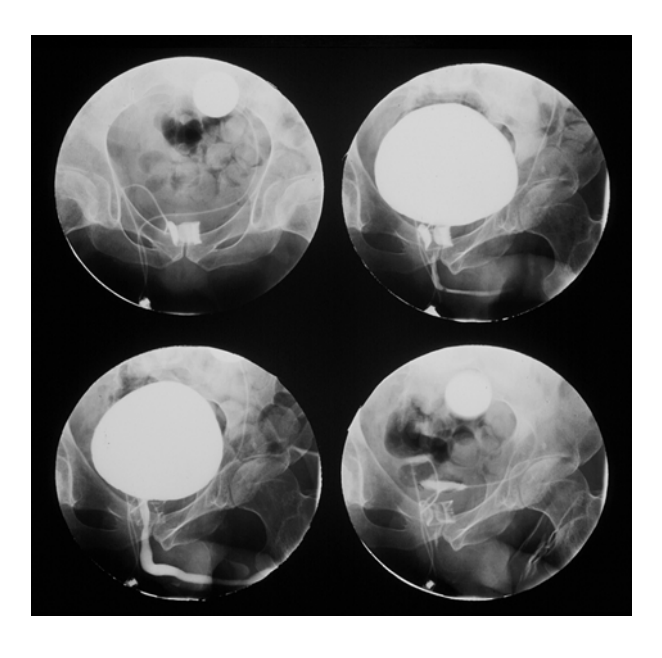


Fig. 3: Mictiogram: Low resistance micturition with additional artificial sphincter

Complications

Early

Six cerebrospinal fluid leakages required a surgical revision with no further complication. Five infections on the implant (1%) made us to do an explantation. In 3 cases it was possible to restore the function by reimplantation of an extradural device 6 months later. Two wound dehiscences

required a surgical revision and two haemorrhages did not need any further consequences.

Late

More often there happen late complications related to the implant. Failures of SARS may be caused by a defect of the external transmitter, a defect of the implant or by neurogenic or myogenic deterioration. Defects of the transmitter can be found by checking the function with a "flasher". All the other failures require an exact exploration of micturition history and a video-urodynamic, but in order to diagnose a neurogenic or myogenic damage a transrectal electro stimulation with simultaneous cystometry is necessary additionally. 70 defects of the implant (16%) were detected, although not all of them resulted in a loss of function. But in 34 cases implant repair surgery was necessary (exchange of the receiver 16, exchange of the receiver and cable-repair 5, cable repair 4, extradural implant 9). Myogenic damage because of over distension requires CIC for weeks or months; neurogenic failures do happen very seldom and require CIC for ever.

Conclusion

SDAF interrupts the spastic activity of the urinary bladder in paraplegics. By means of this surgical method a normal reservoir-function is restored. The organ is preserved. These paraplegic patients regain safe urinary continence in most of the cases. Micturition is voluntary by an implant and an external transmitter. High morbidity because of recurrent UTI, failure of kidney-function and autonomic dysreflexia disappears. An accurate adjustment of stimulation parameters allows a post-stimulus voiding with low resistance.

The microsurgical technique requires an intensive education. The intradural way offers a second Chance for the deafferentation in case of an incomplete deafferentation with re-entry of a hyperreflexia and there is a second chance for a new extradural implant in case of necessary repair. In order to take care of late implant complications a highly efficient trouble-shooting is mandatory. Implant failures can be repaired.

Implants with cable-plugs could make repair procedures easier. Development of microelectronic devices without cables could help to avoid implant complications.

Nevertheless the satisfaction of our paraplegic patients with the outcome after SDAF and SARS is very high and they improve in independence and in quality of life.

References

- [1] Sauerwein D.: Funktionelle Elektrostimulation der Harnblase: Erste Erfahrungen mit sakraler Deafferentation (SDAF) und Vorderwurzelstimulation (SARS) nach Brindley in Deutschland. Vb Dtsch Ges Urol 39: 1987, 595-597
- [2] Madersbacher H., Fischer J., Ebner A.: Anterior root stimulator (Brindley): Experiences especially in women with neurogenic urinary incontinence. Neurourol Urodyn 7: 1988, 593-601
- [3] Sauerwein D.: Die operative Behandlung der spastischen Blasenlähmung bei Querschnittlähmung. Urologe [A] 29: 1990, 196-203
- [4] Brindley G.S.: Emptying the bladder by stimulating ventral roots. J Physiol 237: 1972, 15-16
- [5] Brindley G.S., Polkey C.E., Rushton D.N.: Sacral anterior root stimulators for bladder control in paraplegia. Paraplegia 20: 1982, 365

Auther's Address

Dr. med. J. Kutzenberger Klinik für Neuro-Urologie Werner-Wicker-Klinik Im Kreuzfeld 4

D 34537 Bad Wildungen

e-mail: jkutzenberger@werner-wicker-klinik.de

ELECTRICAL STIMULATION TO INDUCE PROPULSIVE CONTRACTIONS IN THE DESCENDING COLON OF THE PIG

C. Sevcencu***, N. J. M. Rijkhoff*, H. Gregersen***, T. Sinkjær*

* Center for Sensory-Motor Interaction, Aalborg University, Denmark ** Center for Visceral Biomechanics and Pain, Aalborg Hospital

Abstract

Electrical stimulation of the colon can improve transit in slow transit constipation, or enable controlled emptying in colostomy patients. Preliminary studies showed that sequential stimulation of consecutive colon segments induced serial contractions resulting in colonic propulsion. This study was performed to optimize the stimulation parameters. The active sites of the electrodes were inserted under the serosa of the descending colon of pigs. Charge balanced rectangular pulses at 10 Hz were delivered in consecutive sessions. *Electrically* evoked (ECs)contractions were monitored using impedance planimetry and manometry. The luminal pressure and cross-sectional area (CSA), the latency and velocity of CSA decrease, and the wall tension were compared for ECs induced using 3 ms pulses of 9, 12, 15 and 30 mA. When using 15 mA, ECs induced by 0.03, 0.3 and 3 ms long pulses were compared. A current increase from 9 to 30 mA induced a significant increase of the pressure generated by contraction. The increase of pulse duration from 0.03 to 3 ms resulted in shorter latency, faster contraction, higher pressure and higher wall tension. It is concluded that, at a frequency of 10 Hz, the best combination of current and pulse duration to elicit propulsive contractions in the descending colon of pigs is 15 mA and 3 ms.

Introduction

After resection of the distal part of the colon due to various colonic diseases, a colostomy is common practice. Patients with a colostomy have no control over the evacuation of the colon content. Currently, they have to wear a colostomy bag, or to perform irrigation procedures in order to empty the colon. An alternative for emptying the colon could be the use of electrically induced colon contractions. In addition, electrical stimulation of the colon could accelerate transit in slow transit constipation (STC).

Several authors reported successful results with electrical stimulation of the gastrointestinal tract to improve gastric emptying [1] and to induce propulsive contractions in the small intestine [2].

Colon transit could also be improved in spinalized cats by stimulation of the colon wall [3], and semifluid content was propelled by sequential stimulation of the descending colon in dogs [4]. Our experiments in rats showed that sequential stimulation of consecutive colon segments induced displacement of a solid bolus over the length of the stimulated region [5], and preliminary studies indicated this was also possible in pigs [6]. Several authors have shown that electrical stimulation of the intestinal wall using amplitudes of 20 to 50 mA and pulse duration of 10 to 50 ms may result in thermal or electrolytic injuries of the tissue surrounding the electrodes [2]. In addition, high stimulation amplitudes and long pulse durations are power consuming, which may be a drawback if a fully implantable stimulation system is used. Therefore, the aim of the present work was to find the lowest values for the stimulation amplitude and pulse duration to induce propulsive contractions in the descending colon of the pig.

Material and Methods

Surgical procedures. Five female pigs, 40 - 50 kg weight, were used in accordance with an experimental protocol approved by the Danish Animal Welfare Committee. After anesthesia was induced, the colon was exposed and emptied by irrigation with warm saline.

Electrodes positioning and stimulation pattern. The electrodes were made of Teflon insulated multistranded stainless steel wires (0.4 mm diameter, AS634 Cooner Wire Inc. Chatsworth, CA). The deinsulated sites of 9 electrodes (e1-e9 in Fig. 1) were inserted under the serosa of the descending colon. The most distal electrode (e9) was located about 6 cm orally to the rectum, and the distance between 2 neighboring electrodes was of 2 cm. After a 30 min resting period, the colon was stimulated sequentially with charge balanced rectangular pulses generated by a NoxiTest stimulator (NoxiTest Biomedical A/S, Aalborg, Denmark). Several stimulation series were applied on each colon. A complete stimulation series consisted of 8 consecutive sessions (S1-S8 in Fig. 1). The first stimulation session S1 used electrodes e1 and e2, and elicited contraction in the colon segment delimited by the electrodes. After the

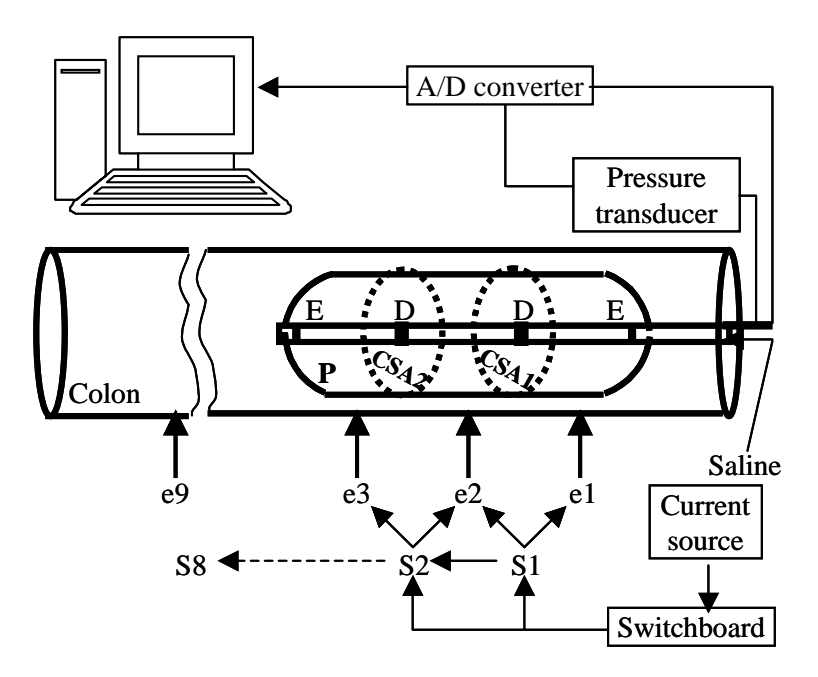


Fig. 1. Experimental setup (see text for explanations).

contractile response, stimulation session S2 followed, and contraction in the second stimulated segment was evoked. Based on visual control, stimulation continued in this way until all of the 8 segments had been stimulated. Each stimulation session lasted for about 10 s. To investigate the effects of current amplitude on the contraction characteristics, contractions induced using 9, 12, 15 and 30 mA, 3 ms, 10 Hz pulses were compared. In order to investigate the effects of pulse duration, contractions induced using 15 mA, 0.03, 0.3 and 3 ms, 10 Hz pulses were compared as well.

Data acquisition. The contractions evoked in the proximal part of the stimulated colon were monitored using impedance planimetry and pressure recording (Fig. 1). Through a small incision in the colon wall, a polyurethane balloon (7 cm long, 3 cm in diameter) was placed inside the colon lumen. The balloon was mounted on a probe with 2 excitation electrodes (E) and 2 pairs of detection electrodes (D). A volume of 30 ml saline was injected in the balloon through an infusion channel. The excitation electrodes were supplied with an AC current of 0.1 mA at 10 kHz. Cross-sectional areas CSA1 and CSA2 at the detection sites were estimated based on Ohms law. The detection sites were 2 cm apart, each at a distance of 2 cm from the neighboring excitation electrode. The probe was positioned so that the first detection site was located between e1 and e2. and the second detection site between e2 and e3 (see Fig. 1). The pressure (P) inside the balloon was also measured. Data acquisition processing was performed using the software package Openlab (GMC, Hornslet, Denmark).

Data analysis. To characterize the colon contractions, the following parameters were measured or calculated:

- the latency of contraction, defined as the time interval between stimulation offset and the start of the contraction;
- the CSA decrease;
- the mean velocity of CSA decrease;
- the luminal pressure change, as percent change relative to the baseline value (the pre-contraction pressure).
- the active tension (T_a) of the colon wall. The wall tension was calculated according to the law of Laplace for cylindrical structures as: T=Pr, where T is the wall tension, r is the balloon radius, and P is the pressure. The total tension (T_t) , was calculated considering the post-contraction radius and pressure. The passive tension (T_p) , was calculated considering the precontraction radius and pressure. The T_a , which expresses the contribution of the

smooth muscle contraction, was calculated as: $T_a = T_t - T_p$.

The values are expressed as means \pm SEM. They were statistically compared using 1 Way ANOVA.

Results

1. Electrically induced colon contractions

Electrical stimulation by 9 to 30 mA, 0.03 to 3 ms, 10 Hz pulses induced local contractions that started after the stimulation offset ("off" type contractions). Contractions developed between the electrodes, and were similar in all of the stimulated segments. Irrespective to the current amplitude or pulse duration, the CSA decreased by similar magnitude during the evoked contractions. When stimulation was applied in consecutive sessions S1-S8, serial contractions were induced and coordinated along the 16 cm long stimulated colon segment.

2. Effects of current amplitude

Latency (Fig. 2A): Contraction started 1.8 to 2.5 s after the stimulation offset. The latencies were similar for contractions induced by different current amplitudes.

Velocity of CSA decrease (Fig. 2A): The velocity of CSA decrease was 20.8 to 24.9 mm²/s. No significant difference was present between contractions induced by different current amplitudes.

Pressure increase (Fig. 2B): As compared to the pre-contraction value of 16.4 ± 1.2 cm H_2O , pressure increased by 15 ± 2 %, 27 ± 5 %, 40 ± 8 % and 39 ± 12 % in contractions induced by 9, 12, 15 and 30 mA pulses, respectively. Significant

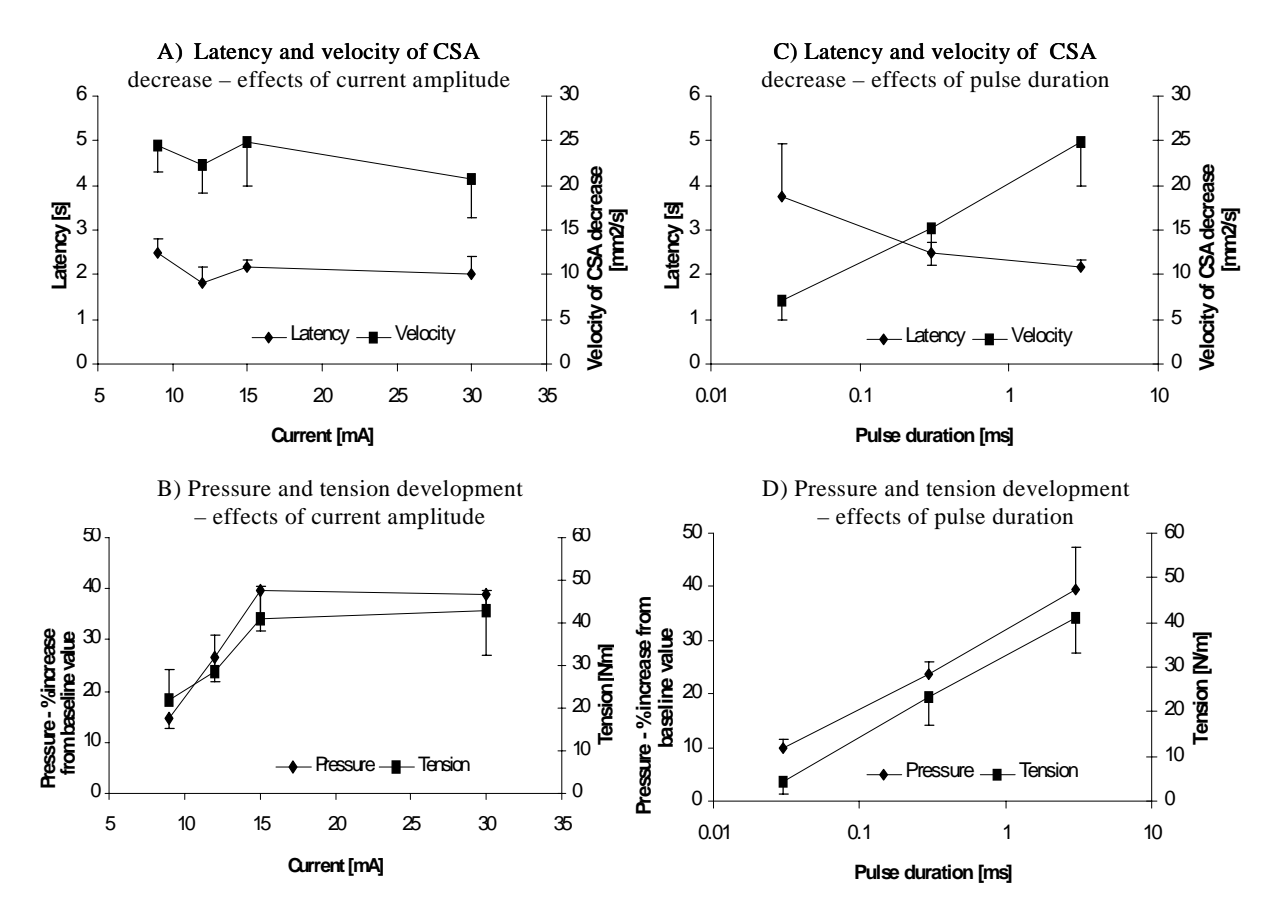


Fig. 2. Effects of current amplitude (A and B) and pulse duration (C and D) on the parameters of the electrically induced colon contractions.

differences were present between contraction induced by 9 mA pulses, and those induced by 15 and 30 mA pulses, respectively (p < 0.05 for both of the differences).

Active tension (Fig. 2B): The wall tension was between 22 to 43 N/m. No significant difference was present between contractions induced by different current amplitudes.

3. Effects of pulse duration

Latency (Fig. 2C): The latency of contraction induced by 0.03 ms long pulses was 3.7 ± 1.1 s. Shorter latencies preceded contractions induced by 0.3 (with 1.3 s, p < 0.05) and 3 ms long pulses (with 1.6 s, p < 0.05).

Velocity of CSA decrease (Fig. 2C): The velocity of CSA decrease in contractions induced by 0.03 ms long pulses was 2 and more than 3 times smaller as compared to that in contractions induced by 0.3 and 3 ms long pulses, respectively (p < 0.01). In contraction induced by 3 ms long pulses, the velocity of CSA decrease was by 9.7 mm²/s (p < 0.05) larger than that during contraction induced by 0.3 ms long pulses.

Pressure increase (Fig. 2D): The pressure increase in contraction induced by 0.03 ms long pulses was less than half of that generated by contraction induced by 0.3 ms long pulses (p < 0.05) and 4

times smaller than that generated by contraction induced using 3 ms long pulses (p < 0.001). The pressure increase in contraction induced by 3 ms long pulses was by 68 % larger than that in contraction induced by 0.3 ms long pulses (p < 0.05).

Active tension (Fig. 2D): Contractions induced by 0.3 and 3 ms long pulses generated 5 (p > 0.05) and 10 (p < 0.05) times larger wall tension than that generated by contraction induced by 0.03 ms long pulses.

Discussion

This study shows that electrical stimulation of the descending colon in pigs by 9 to 30 mA, 0.03 to 3 ms, 10 Hz charge balanced rectangular pulses evokes "off" type local contractions. By sequential stimulation of consecutive colon segments, the serially induced contractions could be coordinated to result in a peristaltic-like activity along the stimulated colon. Consistent with our results, "off" contractions of intestinal muscles were induced by others, either when electrical stimulation was applied on muscle strips [7], or when stimulation of the intestine wall was performed *in vivo* [2].

With respect to the monitored local contractions, a current increase from 9 to 15 mA resulted in 3-fold

increase of the generated luminal pressure. Since a 30 mA current did not further increase pressure, 15 mA is probably the optimum amplitude to generate maximum segmental pressure in the colon of pigs. When using 15 mA pulses, an increase of pulse duration from 0.03 to 3 ms reduced latency, and increased the velocity of CSA decrease, the luminal pressure and the wall tension generated by contraction. Most likely, the increase of current and pulse duration results in the activation of a larger number of circular muscle cells, possible due to recruitment of a larger number of enteric excitatory fibers innervating the muscles. This expands the contracting colon region, which results in larger pressure generated by contraction. As a result, wall tension increases as well. At the same time, the longer the pulse duration, the more cells are activated simultaneously, and this accelerates contraction. While larger luminal pressure and wall tension results in larger propulsive force, shorter latency and faster contraction results in faster propulsion.

In conclusion, for a frequency of 10 Hz and a stimulation duration of 10 s, the best combination of pulse amplitude and duration to induce fast contractions in the descending colon of pigs is 15 mA and 3 ms. By comparison, Bruninga et al. [3] improved colon transit in cats by stimulation the colon wall for 60 s with 25-35 mA, 40 Hz, 1 ms long pulses, and Hughes et al. [8] elicited emptying contractions in dogs by stimulation of the colon for 120 s with 30-35 mA, 10 Hz, 0.5 ms pulses. Lower values for the stimulation parameters were used in this study, and this is an advantage with respect to the power supply if a fully implantable system could be used for colon stimulation.

References

- [1] Abell, T., McCallum, R., Hocking, M., Koch, K., Abrahamsson, H., Leblanc, I., Lindberg, G., Konturek, J., Nowak, T., Quigley, E. M., Tougas, G., and Starkebaum, W.: Gastric electrical stimulation for medically refractory gastroparesis, Gastroenterology, 125(2), 2003, 421-428.
- [2] Moritz, A., Grundfest-Broniatowski, S., Ilyes, L., Kasick, J., Jacobs, G., and Nose, Y.: Contractile response to electrical stimulation of the small intestine in anesthetized and awake dogs, Artif.Organs, 13(6), 1989, 553-557.
- [3] Bruninga, K., Riedy, L., Keshavarzian, A., and Walter, J.: The effect of electrical stimulation

- on colonic transit following spinal cord injury in cats, Spinal Cord, 36(12), 1998, 847-853.
- [4] Amaris, M. A., Rashev, P. Z., Mintchev, M. P., and Bowes, K. L.: Microprocessor controlled movement of solid colonic content using sequential neural electrical stimulation, Gut, 50(4), 2002, 475-479.
- [5] Sevcencu, C., Rijkhoff, N. J. M., Laurberg, S., and Sinkjaer, T.: Method for inducing and monitoring propulsive activity in the rat descending colon. Proc. 7th Ann. Meeting IFESS, Ljubljana, Slovenia, 2002, 282-284.
- [6] Sevcencu, C., Rijkhoff, N. J. M., Gregersen, H., and Sinkjaer, T.: Propulsive contractions induced by electrical stimulation in the descending colon of the pig. Proc.8th Ann.Meeting IFESS, Maroochydore, Australia, 2003, 241-244.
- [7] Ng, W. W., Jing, J., Hyman, P. E., and Snape, W. J., Jr.: Effect of 5-hydroxytryptamine and its antagonists on colonic smooth muscle of the rabbit, Dig.Dis.Sci., 36(2), 1991, 168-173.
- [8] Hughes, S. F., Scott, S. M., Pilot, M. A., and Williams, N. S.: Electrically stimulated colonic reservoir for total anorectal reconstruction, Br.J.Surg., 82(10), 1995, 321-326.

Acknowledgements

Biomedical Laboratory, Aalborg Hospital. This work was supported by the Danish National Research Foundation and the Danish Research Council and Coloplast Company.

Author's Address

Cristian Sevcencu Center for Sensory-Motor Interaction, Aalborg University, Denmark e-mail: sevcr@smi.auc.dk

Posters

SIMULATION OF THE STS TRANSFER USING A MLP WITHOUT EMBEDDED INTERNAL FEEDBACK

Mehran Emadi, Fariba Bahrami, M. J. Yazdanpanah

Control and Intelligent Processing Center of Excellence (CIPCE), University of Tehran

Abstract

In FES-controllers developed based on a tracking approach, the desired movement in a specified space (e.g., trajectories of the joint angles) is used as the input of the controller. In answer to the question how the desired movement for each particular subject should be defined, a new method has been developed to generate the subject-dependent trajectories of the joint angles during the sit-to-stand (STS) movement.

Introduction

Many researchers have been worked on the prediction of the STS (e.g., [1]-[3]). In most of these works, the movement is predicted by applying different optimization algorithms with different object functions. Moreover, body-skeletal dynamics is described by applying movement equation for different links (depending on the degree of freedom used in the model). One of the important questions in these methods is to find a suitable trade-off between the exactness of the mathematical model and the complexity of the calculations. The un-modeled dynamics is another question to be answered in the model-based methods. Considering all of these questions, in this work an algorithm is proposed that is based on the nonlinear characteristics of the artificial neural networks (ANN). A Multi Layer Perceptron (MLP) with one hidden layer including 42 neurons was implemented. Using this method, reconstructed joint angle trajectories had errors of less than 4%. Moreover, in comparison with a model-based algorithm which uses a mathematical description of the body-skeletal dynamics, this method predicts the flexion of the upper body before leaving the seat more accurately.

Material and Methods

Model

To define the movement pattern, the body skeletal system was simplified to a rigid three-link model in the sagittal plane. The links represent the shanks, thighs and upper body. Thereby, ankle, knee and hip joint angles plus the length of each link describe uniquely the body-state at each moment in the sagittal plane.

The Neural Network

An MLP with one hidden layer including 42 neurons was implemented. Activation function of the hidden layer was sigmoid and activation function of output layer was linear. The input data for the MLP network are the limb lengths and the body height and weight, and given initial and final body states (initial sitting position and the final standing posture). These values are derived from recorded STS tasks performed by 6 subjects.

Outputs of the implemented MLP are the coefficients of the Fourier Half Amplitude Cosine Expansions (FHACE) of the joint angles. Trajectories of the joint angles are reconstructed with the help of these coefficients (see Fig. 1). During the learning process, the calculated error between the desired joint angles (obtained from recorded movements) and the reconstructed ones are fed back to the MLP (global feedback). In usual approaches, an internal feedback in the body of the MLP implements the dynamics of the modeled systems. Since the coefficients of the FHACE describe the inherent dynamics of the body-skeletal system, we could avoid the feedback in the body of the MLP. Back propagation (BP) method was used to get the optimized weights for the MLP.

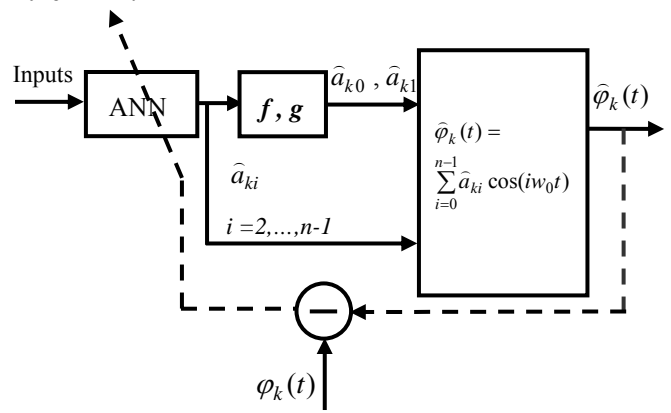


Fig. 1: Implemented MLP system with the global feedback used in the process of learning. Where, $\varphi_k(t)$ is the kth joint angle at time t and $\widehat{\varphi}_k(t)$ is the estimated kth joint angle; and k=1 for the ankle joint, k=2 for the knee, and k=3 for the hip; a_{ki} is the ith coefficient of FHACE of the measured kth joint angle and \widehat{a}_{ki} is the ith estimated coefficients.

Learning Data

The STS movement of six healthy subjects has been recorded. Each subject repeated the task 20 times. 16 out of 20 movements of each subject have been used for the learning process of the MLP. Input data was normalized between 0 and 1.

Results

After completing the learning process, the recorded movements, which have not been used during learning procedure, were applied as recall ones. Using this method, maximum error of the reconstructed trajectories was less than 4% (Table 1).

The implemented system has been used to predict the movement of a subject whose data were not used in the process of the learning. The resulted movement had a satisfactory similarity to the measured one. The maximum errors are depicted in Table 2.

Table 1: Percentage of the maximum error of the predicted trajectories. The values of the maximum errors are averaged over six subjects.

Marina	Training			Recall		
Maximum Error	Ankle	Knee	Hip	Ankle	Knee	Hip
	4.0	3.7	1.8	3.9	3.6	2

Table 2: Percentage of the maximum error of the predicted joint angle trajectories for a new subject.

Maximum Error	New Subject		
	Ankle	Knee	Hip
	5.6	10.2	5.1

Our results indicate that the prediction of the ankle and knee joint angles was accomplished with a higher rate of the error relative to the hip joint angle.

Stability of the predicted movement after leaving the seat (i.e., the position of the center of pressure, COP, under the two feet) was investigated. For all of the predicted movements COP was under the feet.

Discussion

One of the important features of this method is the application of the FHAC expansion. This helps us to be able to implement a global feedback during the learning process, which reduces the complexity of the system. It should be recalled that the internal feedback increases the dimension of weight matrix in a MLP network, which in turn means more complexity.

In comparison with a model-based algorithm, which used an explicit mathematical description of the body-skeletal dynamics (e.g., [1], [2], [5], and with a maximum error of the predicted hip angle of 10.5%), this method predicted the flexion of the upper body before leaving the seat more accurately.

References

- [1] Papa E., Stroppa R., Cappozzo A., Benvenuti F., and Mecacci R., Joint trajectory generation using ground reaction data: application to rising from a chair, Gait & Posture, Vol. 9, 1999, pp. 121-122.
- [2] Emadi M., Bahrami F., and Jabedar P., "Prediction of the movement pattern considering limited isometric muscle forces in the lower extremities," in Proceedings. of the ninth Iranian Conference on Biomedical Engineering, Tehran, Iran, May 1-4, 2000, pp. 419-423.
- [3] Pandy M. G., Garner B. A., and Anderson F. C., "Optimal control of non-ballistic muscular movements: a constraint performance criterion for rising from a chair", J. Biomech. Eng., Vol. 117, 1995, pp. 15-25.

Authors' Address

PhD Candidate Mehran Emadi,

Dr. Fariba Bahrami

Dr. Mohammad Javad Yazdanpanah

University of Tehran
Faculty of Engineering
Department of Electrical and Computer
Engineering,
P.O.Box 14395/515 Tehran, Iran

Email: fbahrami@ut.ac.ir

PRESENT STATUS OF HEARING ELECTRICAL ACTIVATION.

Chouard C

Paris VI University ENT, France

Since Graham Bell, deafness improvement depends on electrical activation, which successively provided external ear, then inner ear, and recently ossicular chain in the middle ear with sound frequency information, as a function of progress in electrical management and transducers miniaturization.

Presently 3 types of auditory prosthesis are available:

1- external (or conventional) hearing aids, which selectively amplify the sound different frequency bands of the auditory canal air column;

2-cochlear implants, which supply the different frequency parts of the cochlear keyboard with specific electrical stimulation, depending of each frequency bands of the sound;

3- middle ear implants, which directly mobilize the ossicular chain using an implanted miniaturized vibrator.

To-day the respective indications of these 3 prostheses clearly depend on the deafness parameters. The next future device will probably be the marriage of middle ear and cochlear implants.

This poster reflects the thirty years author's experience in surgical and electronic deafness management.

Author's Address

Claude-Henri Chouard, Prof. Paris-VI University 10 Boulevard Flandrin F-75116 Paris, France

email: recorlsa@club-internet.fr

MUSCLE FUEL SELECTION IN GOVERNING PREFERRED RATES OF MOVEMENT: A MOTOR CONTROL ISSUE

Herman R ^{1,2}, Willis W ².

Banner Good Samaritan Medical Center, Phoenix, AZ, USA (1) Department of Kinesiology, Arizona State University, Tempe, USA (2)

The time-honored concept regarding the coincidence between minimization of energy cost (e.g., O2 cost of transport) and preferred rates of walking is not generalizable to all forms of locomotion. The difference between the minimum aerobic demand at the preferred rates of movement and the aerobic demand at higher/lower rates may be as low as 10%. Can such a limited decrease in aerobic demand describe such a global influence on motor control? Is O2 enough to describe energy consumption, given that both O2 AND fuel consumption pathways are necessary components for aerobic metabolism?

In able-bodied humans, we observed O2 cost of transport and fuel consumption during treadmill and overground walking at various rates and walking conditions.

Under normal locomotion conditions, while O2 cost at 2 (53.6 m/min) and 4 (107.3 m/min) mph was always < 10 % higher than the nadir of O2 cost of transport at the preferred speed at 3 mph (80.5 m/min), the carbohydrate (CBO) oxidation rates were > 10 fold over this range of speeds. Minimizing effort correlated with minimizing CBO oxidation (i.e., to the level of gluconeogenesis) under all conditions. The inflection point of the exponential curve between CBO oxidation and speed was always at the level of preferred speed.

At higher rates of walking (>3 mph), when increasing sense of effort correlated robustly with increasing CBO oxidation and poorly with fat oxidation, CBO-induced fall in cellular energy in skeletal muscle may provide important inputs into the CNS during walking.

These signals ensure that the CNS selects a walking speed with minimal CBO demand, thus maximizing metabolic range of motor activity and sparing CBO fuel for emergency burst activity. Thus humans self-select ("prefer") a walking speed that can supported almost exclusively by fat combustion. Apparently, the motor control system attempts to control CBO oxidation to gain economical advantage.

Author's Address

Richard M Herman, Research Director Banner Good Samaritan Medical Center 1111 E. McDowell Rd 85006 Phoenix Arizona US

e-mail: richard.herman@bannerhealth.com

ANALYSIS OF CALCULATED ELECTRICAL ACTIVATION OF DENERVATED MUSCLE FIBRES IN THE HUMAN THIGH

J. Martinek*, M. Reichel*, F. Rattay**, W. Mayr*

* Department of Biomedical Engineering and Physics, Medical University of Vienna, Austria

** TU-Biomed, Vienna University of Technology, Austria

Abstract

Finite difference models of the human thigh are used to analyse the excitation process in the fibres of denervated skeletal muscles in conjunction with Functional Electrical Stimulation (FES) via surface electrodes. The Matlab Tool "FES-Analyze" was developed to simulate and analyse the super-threshold regions in a human thigh. Action potential is simulated with a muscle fibre model of the Hodgkin Huxley type and with a generalised form of the activating function.

Introduction

To achieve excitation of denervated muscles with Functional Electrical Stimulation (FES) it is necessary to use rectangular biphasic stimulation-impulses with, compared to nerve stimulation, longer pulse duration and higher amplitude. Numeric simulation could be one possibility to find the best stimulation parameters (pulse amplitude, pulse duration, shape and position of the electrode,...) for the treatment of paraplegics.

Material and Methods

Starting from a 3D model of the human thigh [2], it is possible to calculate the distribution of the electrical field during FES with the method of finite differences, which is based on computer tomography data [3]. To examine and optimise the influences of the electrode positions and the simulation parameters, the calculated electric field is analysed by means of the tool "FES-ANALYZE" [4], which was developed with MATLAB GUIDE (Fig.1).

The analysis is based on a model of a denervated muscle fibre, which is applied to every point of the musculature in the electrical field [5]. The effect of the distribution of the electrical potential is determined with two forms of the activating function [4,6,7]. On the one hand the end of the muscle fibre is considered, using the first order gradient for the evaluation of the potential distribution ("first order activating function" –

AF1). On the other hand the central part of the muscle fibre is considered, using the second order gradient and the gradients of its neighbours in the muscle fibre to calculate the activation ("second order activating function" – AF2).

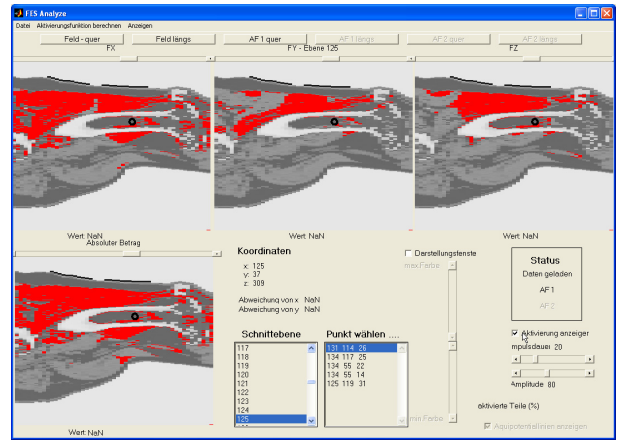


Fig.1: graphic user interface of FES ANALYZE; representation of the first order activating function in the length section;

With "FES-ANALYZE" it is possible to compare the stimulation at the end of the muscle fibre with the stimulation at the central part of the muscle fibre, both in cross and longitudinal section, as well as the observation of the effect of different impulse's intensities and lengths during FES. The results are displayed qualitatively in the cross and longitudinal sections, as well as quantitatively in the percentage of the muscle's total volume.

Results

Electrical Field

As an example, the electrical field during FES (Fig. 2) with a pulse duration of 20 ms and an amplitude of 80 V and both activating functions in a human thigh were calculated (Fig. 3). The rectangular (8x10 cm) electrodes were fixed in the centre of the human thigh. The edge to edge distance of the electrodes is 8 cm. The electrical field was produced with FES and is displayed by equipotential lines (distance 8V). In this simplified example the direction of the straight muscle fibres is assumed to be parallel to the length axis of the thigh.

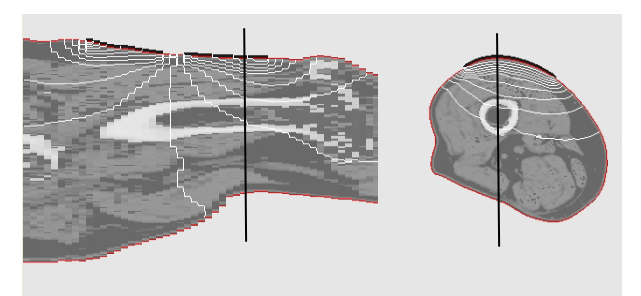


Fig. 2: Calculated electrical Field produced by FES in length section (left) and cross section (right); distance between equipotential lines approx. 8V;

For further visualisation of the results a central length section is used. The activated parts of the muscle are shown in the pictures as coloured area. Muscle fibres are assumed to be stimulated if they have at least one of their endings in the coloured regions. The percentage of the activated area is calculated for each muscle separately (e.g. 5 % of quadriceps means, that 5 % of the quadriceps are activated) (Fig. 3 - 7)

Activating Functions AF1 and AF2

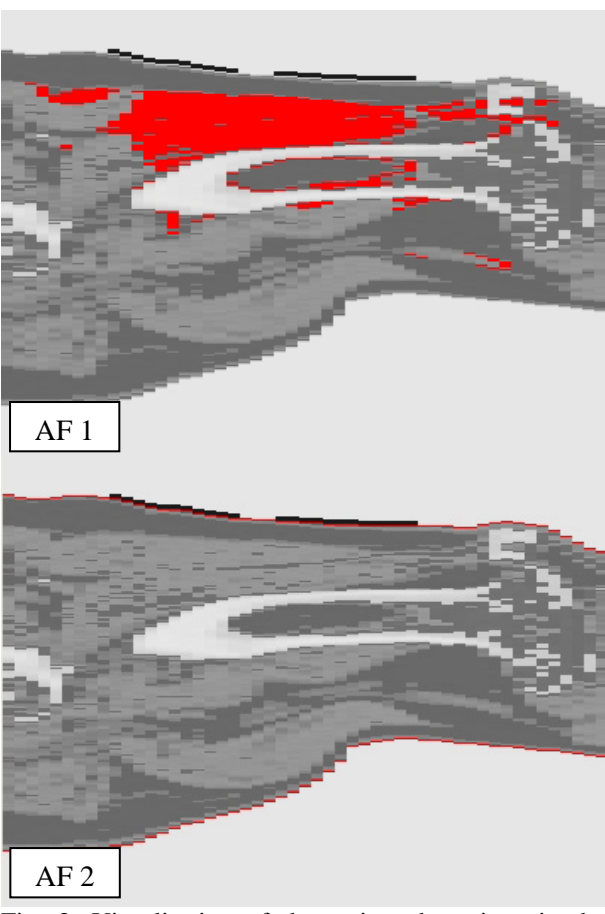


Fig. 3: Visualisation of the activated sections in the thigh using "Standard Values" of pulse duration (20 ms) and amplitude (80 V); AF1 – stimulation at the end of the muscle fibre; AF2 – stimulation at the central part of the muscle fibre;

Simulating with "standard values" of the pulse duration (20 ms) and the amplitude (80 V), one

discovers that the main part of the activation takes place at the end of the muscle fibre (AF1) (Fig. 3).

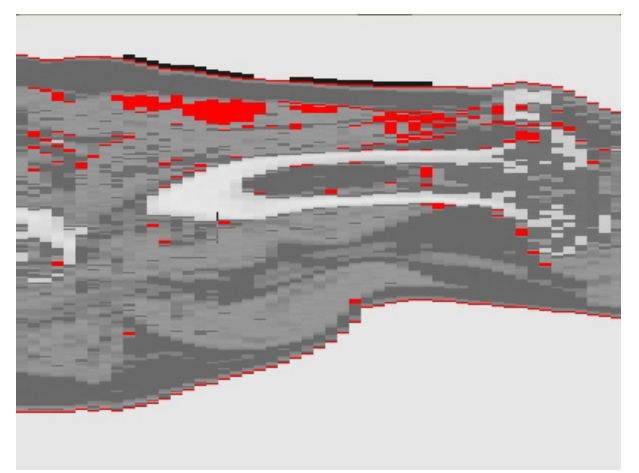


Fig. 4: Visualisation of the activated sections looking at the AF2 (central part of the muscle fibre) using a very long pulse duration (100 ms) and a very high amplitude (200 V);

To obtain activation at the central part of the muscle fibre higher amplitudes and longer pulse durations of the stimulation pulses are needed (Fig. 4).

AF1 - Varying pulse duration and amplitude

Because the main part of the activation takes place at the end of the muscle fibre, the influences of shorter / longer pulse duration or higher / lower amplitude will only be shown for the AF1.

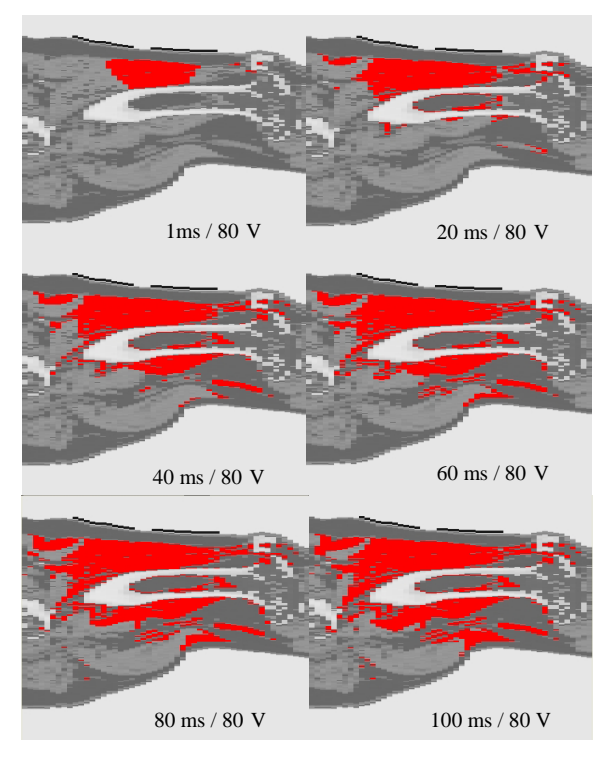


Fig. 5: AF 1; Visualisation of the activated sections in the thigh while varying the duration of the stimulation pulse;

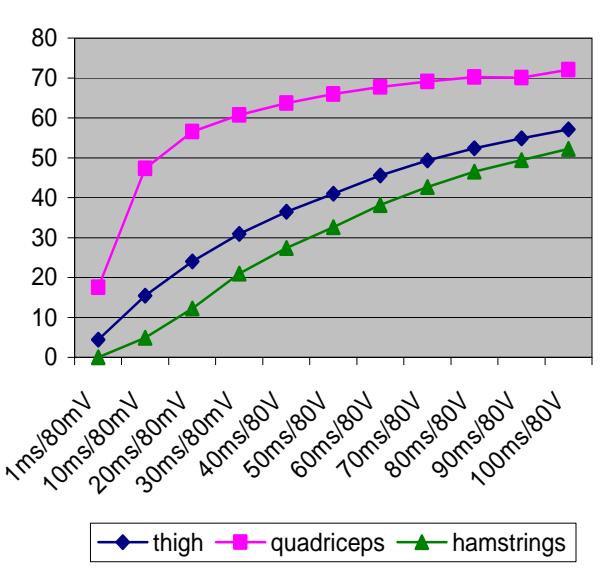


Fig. 6: Percentage of activated muscles in the thigh, quadriceps and hamstrings while varying the duration of the stimulation pulse;

Examining the activation at the end of the muscle fibre (AF1), one discovers that mainly the area between the electrodes is activated. With longer duration (Fig. 5 and Fig. 6) or higher amplitude (Fig. 7 and Fig. 8), the area below the electrodes is activated as well and the activated area reaches deeper into the thigh.

One of the aims of FES is to achieve an extension of the knee. Therefore it is necessary to activate the quadriceps, which leads to an activation of the muscle and to an extension of the knee. Activating the hamstrings - the antagonists of the quadriceps—would be contra-productive and therefore it is necessary to avoid activation of large amounts of the hamstrings.

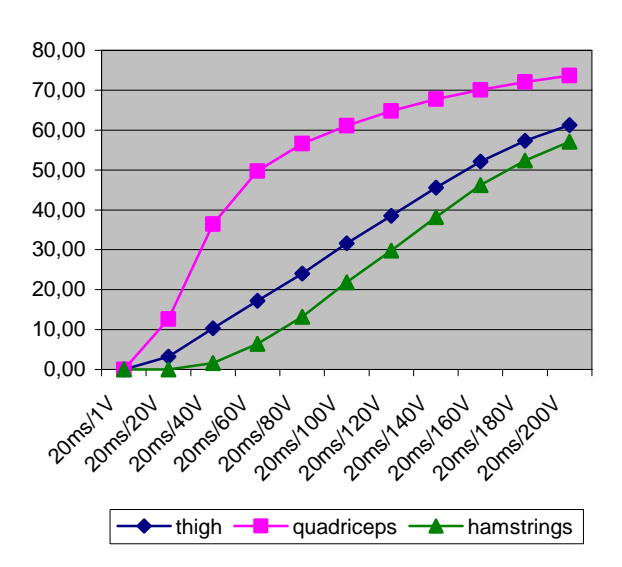


Fig. 7: Percentage of activated muscles in the thigh, quadriceps and hamstrings while varying the amplitude of the stimulation pulse;

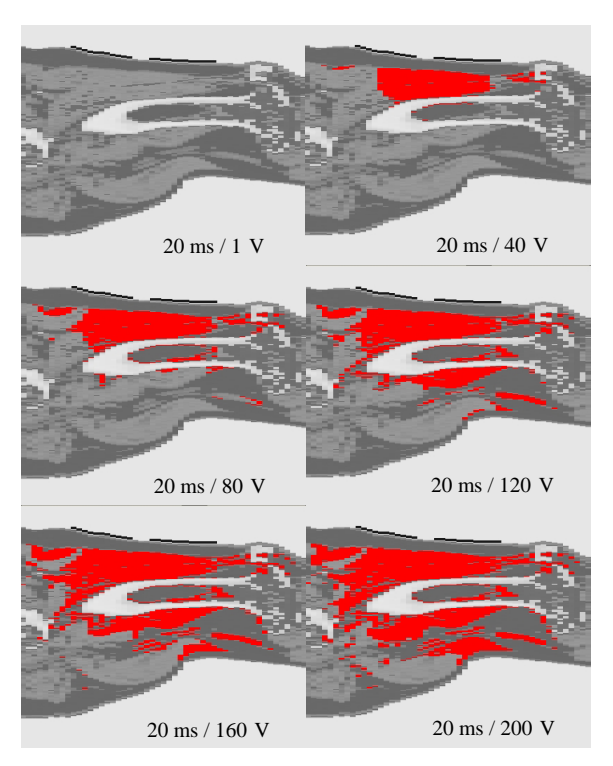


Fig. 8: AF 1; Visualisation of the activated sections in the thigh while varying the amplitude of the stimulation pulse;

AF1 - Varying the position of the electrodes

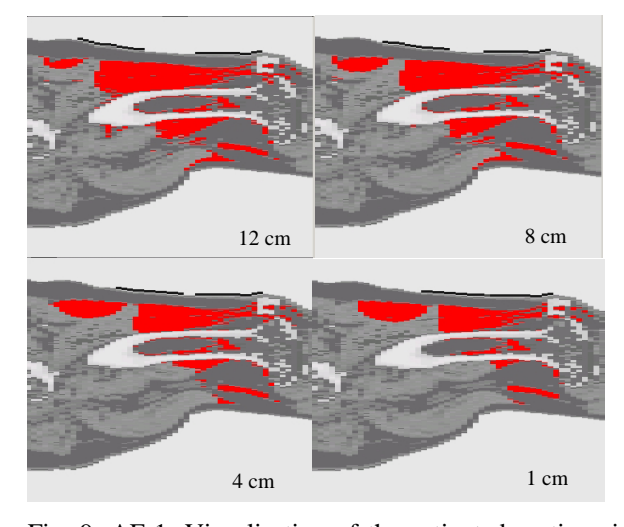


Fig. 9: AF 1; Visualisation of the activated sections in the thigh while varying the distance of the electrodes (20 ms / 80 mV);

The electrodes are rectangular (8x10 cm) and were fixed in the centre of the human thigh. The distal electrode is fixed near the knee and the proximal one in varying distances to the distal electrode (Fig. 9 and Fig. 10).

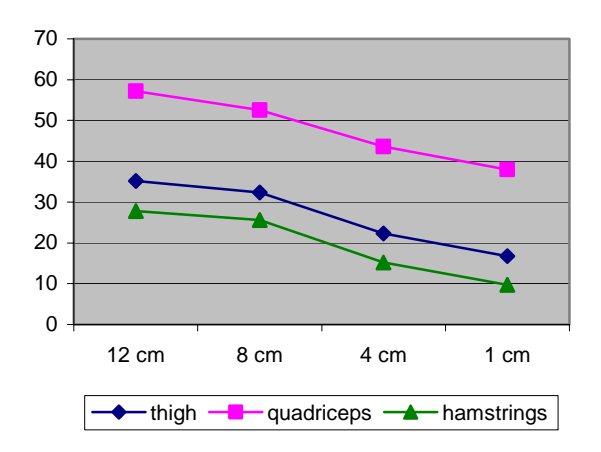


Fig. 10: Percentage of activated muscles in the thigh, quadriceps and hamstrings while varying the distance of the electrodes;

Discussion

The application FES ANALYZE was developed for an evaluation of the electrical field at FES in the human thigh of paraplegics. Based on the distribution of the electric potential in a muscle fibre it is possible to calculate the AF1 and the AF2. AF1 describes the conditions only in the first and the last segment of a muscle fibre and AF2 the conditions in the central part of the muscle fibre.

It is demonstrated that the main part of the activation is initiated at the end of the muscle fibre (AF1). For activation at the central part of the muscle fibre (AF2) much higher voltages and longer durations of the stimulation impulse are needed.

With the "standard values" of pulse duration (20 ms) and amplitude (80 V) the hamstrings are only activated in a small part. Therefore nearly no cocontractions are expected and the stimulation causes a contraction of the quadriceps and thus an extension of the leg.

Increasing the distance between the electrodes leads to a larger amount of activated muscles in the thigh, because mainly the muscles between the electrodes were activated.

References

- [1] Kern H. 1995: Funktionelle Elektrostimulation paraplegischer Patienten. (in German), Österr. Z. Phys. Med. Heft 1, Supplementum
- [2] Reichel M., Breyer T., Mayr W. and Rattay F.: Simulation of the three dimensional electric field in the course of functional electrical stimulation. Artificial Organs 26 (3), 2001, 252-255.
- [3] Grotz B.: Simulation der Funktionellen Elektrostimulation an denervierter Skelettmuskulatur im anisotropen 3-D Modell des menschlichen Oberschenkels. (in German), Master-Thesis, Vienna University of Technology, 2002
- [4] Martinek J.: Analyse der Aktivierung von denervierten Muskelfasern im menschlichen Oberschenkel bei Funktioneller Elektrostimulation. (in German), Master-Thesis, Vienna University of Technology, 2003
- [5] Reichel M.: Funktionelle Elektrostimulation denervierter Skelettmuskulatur – Modellbildung und Simulation (in German), Doctor-Thesis, Vienna University of Technology, 1999
- [6] Rattay F.: The basic mechanism for the electrical stimulation of the nervous system. Neuroscience 89, 1999, 335-346
- [7] Reichel M., Mayr W. and Rattay F.: Simulation of Exitation Effects at the Muscle-Tendon Junction in Denervated Muscle Fiber. Proc. of 7th Ann. Conf. International Functional Electrical Stimulation Soc. (IFESS), 2002, 152-154

Author's Address

DI Johannes Martinek Department of Biomedical Engineering and Physics, Medical University of Vienna Währinger Gürtel 18-20, A-1090 Vienna, Austria

e-mail: johannes.martinek@novellus.at

CALCULATION OF CURRENT DENSITY DISTRIBUTION IN BIOLOGICAL MATTER WITH THE FINITE ELEMENT METHOD

H. Eike, R. Koch, F. Feldhusen*, H. Seifert

Veterinarian Highschool of Hannover, Institute for General Radiology and Medical Physics

* Lower Saxony Federal State Office for Consumer Protection and Food Safety,

Veterinary State Institute for Fish and Fishery Products

Abstract

The current density through layers with different electrical features in the head of a pig during electric stunning was calculated and visualised with an FEM computer program. The anatomic model of the pig's head was transferred to the computer programme Ansys. Ansys offers the possibility of calculating the current density between electrodes in any position using the mathematical "Finite Element Method" (FEM) model. After calculation the current density distribution can be visualised in planes in any direction through the pig's head. The simulation confirmed the common practice of positioning the electrodes for electric stunning.

Introduction

German animal protection legislation demands that animals must be stunned before slaughtering. Electric stunning is the method most commonly used for slaughter pigs in Germany. During this procedure the animal is stunned by an sufficiently high current through the animal's brain which induces an epileptic attack causing unconsciousness. This is achieved by placing the electrodes in the eye to eye or eye to ear area. In everyday use displacement of the electrodes occurs [1]. As a consequence the animal is not stunned [2].

Material and Methods

At different placements of the electrodes at pigs head the current density distribution in the brain should be measured. Bones and the three dimensionality of the head inhibit a direct measurement of the current. Therefore the three dimensional current density distribution was calculated by the Finite Element Method [3].

The calculation is made by the following steps:

- Division of the complete structure into a finite number of elements (discretisation)
- Calculation of the attributes for each element
- Re-combination to form the complete structure
- Calculation of the attributes of the complete structure from the results of the elements.

The model of the pig's head was constructed by

deep-freezing a pig's head and then cutting 4cm slices perpendicular to the longitudinal axis of the carcass. From these slices, the outlines of brain, bones, muscle and fat were transferred into a coordinate system from which measurement points were defined and their co-ordinates translated into Ansys terms.

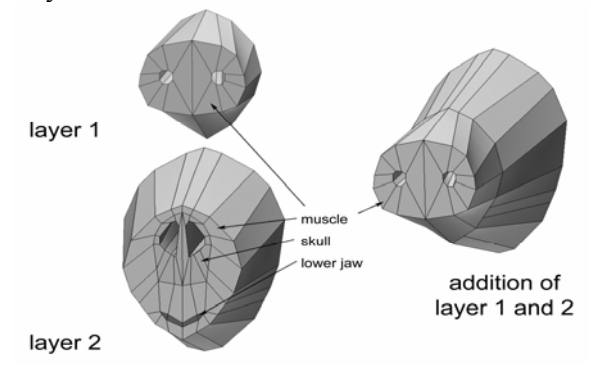


Fig. 1: Composition of the model from slices

Figure 1 demonstrates the composition of the head from single slices by the computer. The different anatomic structures are conserved. After meshing 20 slices the program can calculate the finite elements. This model can be viewed from any perspective, tissues can be extracted and displayed individually. Figure 2 shows brain and blood vessels.

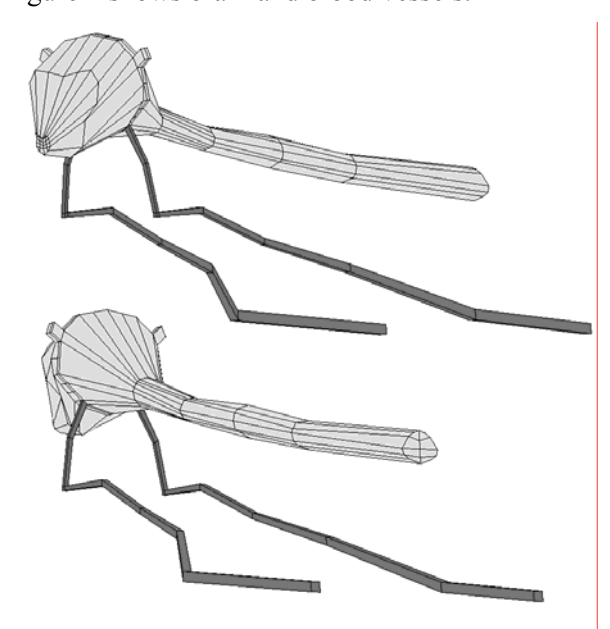


Fig. 2: ZNS and blood vessels

Fig. 3 shows a longitudinal section of the model across the median plane of the head.

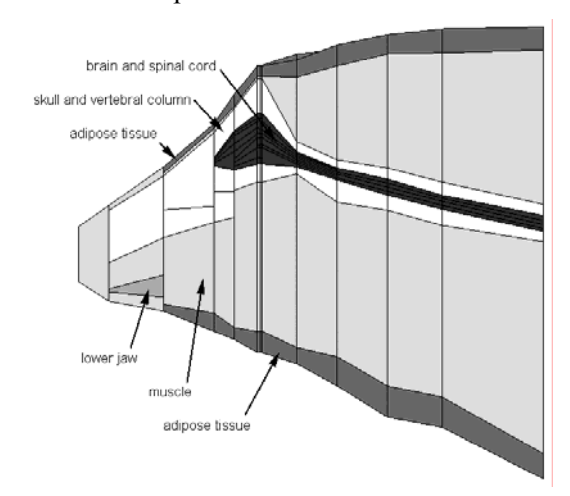


Fig. 3: Longitudinal section through pigs head

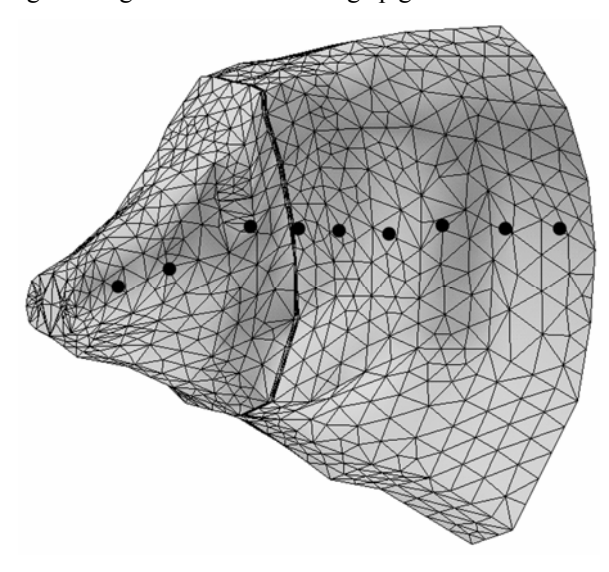


Fig. 4: Pigs head with positions of electrodes

In figure 4 the calculated grid at the surface of pigs head and the positions of electrodes are shown. These positions are symmetrically at both sides of the head. After input of the specific resistance [4] of each tissue the program calculates the current density distribution in the head in any plane and section you want and print out the results.

Results

In an preliminary experiment the potential distribution of a dipol in an electrolytic basin was measured and calculated. As expected a very good congruence could be seen.

Figure 5 shows the calculated result for a vertical cross section through the head. The electrode position is left and right.

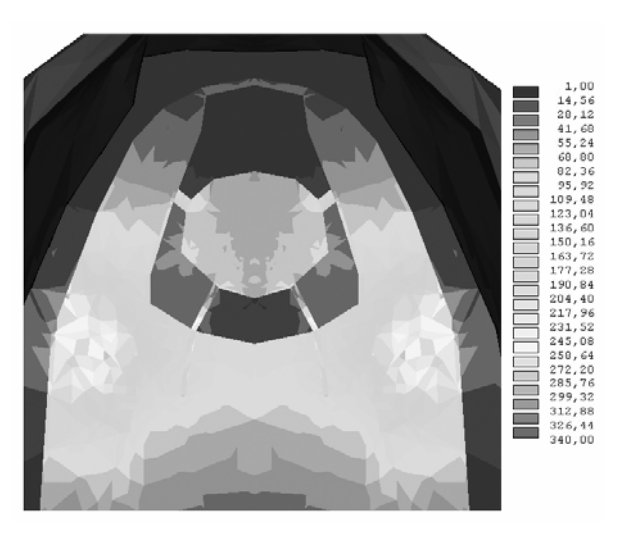


Fig. 5: Current density distribution in a vertical cross section (In the original the values are coloured)

Figure 6 shows the calculated current density at different points in the brain dependent from the electrode positions marked in figure 4.

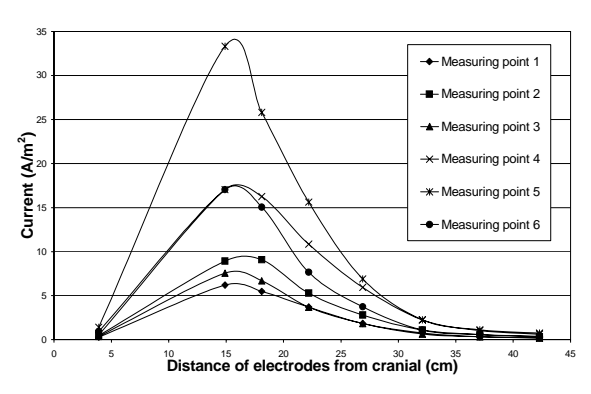


Fig. 6: Current density in the brain at different electrode positions

The analysis describes the optimal position in the area eye to eye. In this position the current density is maximal in the brain at every point of calculation.

Discussion

This FEM model of a pig's head made it possible to calculate and illustrate the current density distribution in a pig's head during electric stunning for the first time.

The current densities clearly follow the anatomic structures (see Fig. 5). Bone has a low conductibility and shows a lower current density than brain. Except at the point of contact between the electrode and the head, the highest densities occur in the nervus opticus and in the blood vessel. This shows that a large part of the current reaches the brain through these tissues (with high current density) because the resistance of these tissues is lower than that of bone.

It was shown, that even complex anatomic structures can be handled by a program for calculation with the FEM.

Our calculation was done for DC or low frequency AC. But if the values of conductibility are known, even higher frequency current density distribution may be calculated.

References

- [1] Tröger, K., Woltersdorf, W. Die Elektrobetäubung von Schlachtschweinen. Dtsch. tierärztl. Wochenschrift 96, pp 100 103, 1998
- [2] Warris, P. D.: Pig handling guidelines for the handling of pigs ante mortem, Meat Focus Int., dec 1996, 491 494, 1995
- [3] Zienkiewicz, O. C., u. R. L. Taylor, The finite element method. 5. Aufl. Volume 1 The basics, Verlag Butterworth-Heinemann, 2000
- [4] Brucher, Meyer-Warden, R., K. u. Rechnergestützte Ermittlung gefährlicher Gesamtströme im menschlichen Körper, Köln, Inst. Erforschung elektrischer Unfälle der Berufsgenossenschaft Feinmechanik der und Elektrotechnik, 1985

Acknowledgements

We thank the RRZN for providing support and calculation time.

Author's Address

Dr. Heinz Eike, Dr. Rainer Koch, Prof. Dr. Hermann Seifert

Veterinarian Highschool of Hannover, Institute for General Radiology and Medical Physics, Bischofsholer Damm 15, D - 30173 Hannover

Dr. Frerk Feldhusen

Lower Saxony Federal State Office for Consumer Protection and Food Safety, Veterinary State Institute for Fish and Fishery Products, Schleusenstr. 1, D-27472 Cuxhaven, Germany

e-mail: Rainer.Koch@tiho-hannover.de

STEPPING RESTORATION IN CHRONICALLY SPINALIZED RATS BY TREADMILL TRAINING

T. Moshonkina, G. Novikov, E. Gilerovich, E. Fedorova, Y. Gerasimenko (St.Petersburg, Russia)

The investigation is devoted to the ways of the locomotor rehabilitation after spinal cord trauma. Stepping restoration by treadmill training was investigated in spinalized rats by behavioral and histological methods.

Adult female Sprague-Dawley rats were treated with the complete spinal cord lesion at the Th 9-10 level. The rats were trained to realize stepping movement on the treadmill starting next day after the injury during 8 weeks. Control animals were not. Motor activity, restoration of the hindlimbs movements and weight bearing were tested weekly. Eight weeks after the injury the rats were euthanatized, spinal cord was fixed and prepared for the light microscopy investigation.

It was revealed that treadmill training increased the motor activity of the rats after the complete spinal cord lesion, induced the locomotor movements of the hindlimbs and preserved the available motoneurons in the distal part of the spinal cord. Weight bearing by the hindlimbs was occurred on the running treadmill ribbon after training to realize stepping cycle.

Its supposed that the ability of the distal isolated part of the spinal cord to realize locomotor movements was carried out by the central pattern generator (CPG) localized in the lumbar thickening of the spinal cord. Treadmill training can start the CPG through the afferent system.

Supported by RFBI 03-04-48307a.

Author's Address

Tatiana Moshonkina, Dr Pavlov Institute of Phisiology nab.Makarova, 6 199034 St.Petersburg, , Russia e-mail: tm@pavlov.infran.ru

IMMEDIATE EFFECT OF MANUALLY ASSISTED TREADMILL STEPPING ON THE MOTOR UNITS ACTIVITY OF LEG MUSCLES IN COMPLETE SPINAL CORD INJURED PATIENTS

- I. Persy ¹, S. Harkema ^{2,3}, J. Beres-Jones ³, M. Moedlin ¹, H. Kern ¹, K. Minassian ¹, M.R.Dimitrijevic ⁴
 - 1 Ludwig Boltzmann Institute of Electrical Stimulation and Physical Rehabilitation, Vienna, Austria
 - 2 Brain Research Institute, University of California, Los Angeles, CA, USA
 - 3 Department of Neurology, University of California, Los Angeles, CA, USA
- 4 Department of Physical Medicine and Rehabilitation, Baylor College of Medicine, Houston, TX, USA

Abstract

The aim of this paper was to study the direct effect of patterned sensory input to the lower spinal cord induced during the first steps of assisted stepping using body weight support on a treadmill (BWST) in complete spinal cord injured (SCI) patients. In particular, we sought to find out whether steppinglike EMG patterns can be generated by lumbar neuronal circuits under such conditions. Motor units activities of the ankle dorsiflexor (tibialis anterior, TA) and plantar flexor (soleus, SOL) muscles of four non-disabled and of eleven clinically complete SCI patients were recorded during manually assisted, load-bearing stepping stepping using BWST. Results can be divided into two groups of patients with characteristic EMG output patterns: Group 1 (n=6) demonstrated no motor output, while patients of Group 2 were showing low amplitude motor output and could be categorized into three subgroups: Group 2A (n=2)showed coactivity of TA and SOL, Group 2B (n=2)demonstrated activity of SOL and no activity in TA and Group 2C (n=1) showed no SOL, but slight TA output. These results demonstrate that the same externally controlled maneuver of passive loadbearing stepping can induce different motor output patterns in SCI individuals of similar clinically complete SCI classification. We hypothesize that different central states of excitability of the lumbar spinal processing network caused these different motor unit activity responses to the stereotyped afferent input produced by the manually assisted stepping movements. None of the leg muscle EMG patterns generated during passive stepping showed alteration between agonists and antagonists characterizing functional stepping-like movement. We conclude that afferent input associated with initial manually assisted stepping using BWST did not provide enough stimuli to fully establish a pattern generating set-up of lumbar neuronal networks in the absence of a significant amount of central state of excitability.

Introduction

It has been previously demonstrated that sustained, non-patterned (tonic) epidural stimulation of lumbar posterior roots at frequencies of 25-50 Hz can induce patterned, stepping-like EMG activity in the lower limb muscles in supine, motor complete SCI patients [1,2]. The stimulus-evoked EMG activity was characterized by alternating phases of burst-style activity in the recruited lower limb muscles, demonstrating reciprocal amplitude variations in antagonists. The pattern and strength of the induced muscle activity was appropriate to alternating flexion and extension movements. This effect could be achieved immediately when epidural stimulation with the appropriate stimulus parameters was delivered.

In the present paper we studied the capability of untrained lumbar neuronal circuits to process rhythmic sensory input induced by manually assisted stepping using BWST to generate rhythmic motor output. In particular, we were interested in the direct effect of patterned, sensory input to the lower spinal cord on the activation of the ankle plantar (soleus) and dorsiflexor (tibialis anterior) muscles. Furthermore, we sought to assess whether patients with clinically complete spinal cord injury can generate stepping-like EMG patterns of the leg muscles. We define "steppinglike" leg muscle activity as the timing and coordination of the motor output with activation of the soleus muscle during the stance phase and the tibialis anterior during the swing phase, as occurs during stepping in able-bodied individuals. Note, that all included patients had a motor complete, accidental SCI and never participated in a locomotor training program prior to the study.

Locomotor training with partial body weight support on a treadmill has emerged as a promising therapy for improving walking capabilities in individuals with incomplete spinal cord injury [3,4]. This technique is dependent upon the repetitive presentation of appropriate afferent input to the lower spinal cord through persistant step training. The mechanisms of this approach have been attributed to (i) activation of spinal neuronal circuits with the capacity to generate complex locomotor patterns and (ii) plastic changes in these spinal cord circuitries within the period of training ("learning").

The immediate effect of passive stepping using BWST on the activation of leg muscles in complete spinal cord injured individuals was not systematically described, yet. Dobkin et al. [5] demonstrated that bursts of rythmical EMG activity emerged from most of the sampled leg muscles of complete spinal cord injured patients during passive stepping on a moving treadmill belt. The EMG burst oscillations were consistantly timed to the gait cycle. Dobkin and collegues have further shown that muscles with the most prominent bursting patterns varied between patients and from one leg to another. Furthermore, the ankle dorsiflexor muscles tended to cocontract with the ankle plantar flexors during the stance phase [5]. Dietz and collegues presented data showing that low-amplitude, tonic gastrocnemius EMG activity and inappropiate tibialis anterior activation during stance phase was induced in complete SCI subjects during treadmill stepping [3]. In the present study we shall demonstrate that the same externally controlled maneuver of manually assisted stepping using BWST generates immediatly a variety of leg muscle activation patterns within a patient population of similar spinal cord injury profile (clinically complete).

Material and Methods

Patient population

Four able-bodied and eleven chronic SCI patients have been included in this study. Apart from their neurological deficit the SCI patients have been healthy with a closed, post-traumatic SCI and free of any medication for spasticity; In the SCI patients, complete absence of volitional or other suprasegmental activation of movements and sensory perception below the spinal cord lesion was demonstrated. According to the American Spinal Injury Association (ASIA) impairment scale [6] all were classified as ASIA A. The injury levels were between C2 to T9 and all patients were in a chronic condition (mean 5.6 years since injury).

Experimental procedure

Patients wore a harness connected to an overhead support that provided partial body weight support (Fig. 1). Trainers manually facilitated the patients' lower limbs through the step cycle. Each spinal cord injured patient stepped with manual assistance at a constant treadmill speed (range 1.0–3.5 m/s, mean 2.3 m/s). Body weight support (BWS) of SCI patients was at a level at which knee flexion during stance could be avoided using moderate assistance by the trainers (range 48–64% BWS, mean 56% BWS). SOL and TA EMG activity induced by the step-associated sensory input to the lower spinal cord was recorded. Furthermore, hip, knee and ankle angles were measured to ensure consistency of kinematics between all patients. We collected data bilaterally from eight consecutive steps.

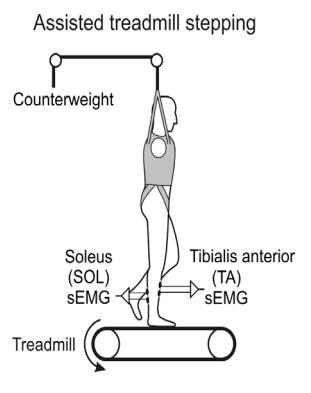


Fig. 1 Schematic drawing of a patient walking passively with the help of trainers on a treadmill wearing a harness to get partially body weight support. Motor units activity of soleus and tibialis anterior are recorded.

Data Acquisition

EMG was collected along with joint angle, footswitch and body weight support data at 1 kHz using a 24-channel hard-wired analog to digital board. EMG data were sampled and AC coupled amplifier into differential (Konigsberg Instruments, Pasedena, CA). Joint angles were electrogoniometers measured using placed bilaterally at the ankle, knee, and hip. Body weight support was recorded using a loadcell in series with the cable attached to the harness.

Data analysis

To find out if the induced EMG activities were temporally synchronized with the stepping cadence and to illustrate the amount of muscle activity in relation to the phases of the step cycle, the averaged EMG activity versus normalized time was calculated for each patient. Only the left leg was considered in the present study. The original raw EMG data was rectified. From these data 180 data points were calculated for each stance phase and 120 data points for each swing phase (ratio 60:40). This was done regardless of the duration of individual stance or swing phases. After this time normalization, the EMG activity of each stance phase and each swing phase consisted of the same

number of data points and allowed averaging the EMG activity of consecutive stance phases or swing phases. The EMG activity of 8 stance phases and 8 swing phases was averaged separately. For illustration, a ratio of 60:40 between stance and swing phase was chosen. Furthermore, the total amount of EMG activity (TotAct) was calculated for 10 intervals during each gait cycle (6 intervals per stance and 4 per swing phase). Corresponding values (mean EMG activity within a time interval of gait) were averaged for eight consecutive steps and were illustrated using bar diagrams. This allowed the comparison of the EMG patterns between different patients.

Results

Figure 2A shows the rectified EMG patterns of tibialis anterior (TA) and soleus (SOL) with respect to time normalized stance and swing phases during active stepping on a treadmill from able-bodied individuals (full weight bearing). Data was derived from four able-bodied patients and was averaged within this group. The main features of the EMG patterns were reciprocity of the leg muscle activities. SOL was active during the stance phase with its maximum at 45 % of the gait cycle. TA was active during swing phase, showing the main activity at the transition from swing to stance phase. These alternating SOL and TA bursting patterns will be referred to as stepping-like.

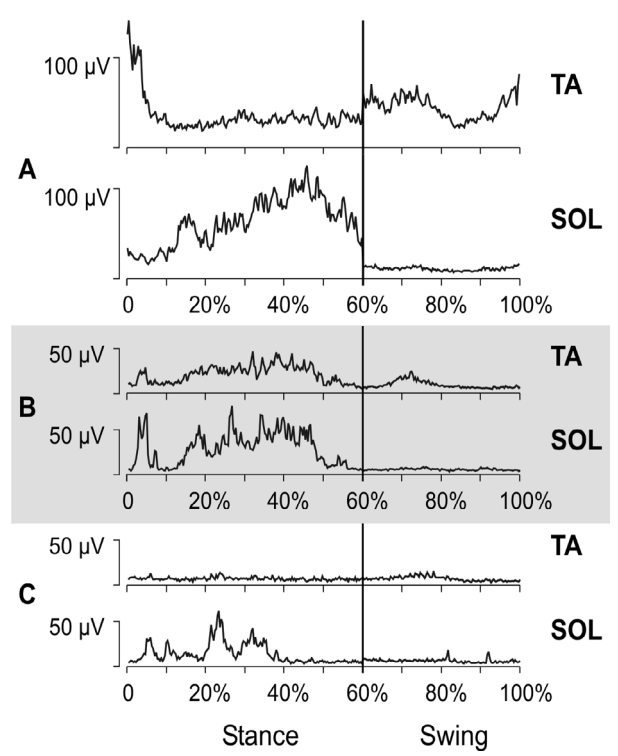


Fig. 2 EMG activity of tibialias anterior (upper trace) and soleus (lower trace) with respect to normalized gait cycle. A, averaged activity of four able bodied (reference), mean time of stance to swing is 0.70:0.42 s, B representative case of Group 2A (time of stance to swing is 0.96:0.81 s) and C single case representing Group 2B EMG pattern (0.75:0.73 s) of SCI patients.

The data analysis of SCI patients demonstrated a variety of EMG patterns induced by the same externally controlled maneuver of assisted stepping on a treadmill using BWST. Figure 2B shows an example of motor units output derived from a complete SCI patient. EMG bursts temporally synchronized to the gait cycle were induced in TA and SOL by the cyclic mechanical stimulation during passive stepping. Both muscles were active during the stance phase. Thus, the ankle plantar (SOL) and ankle dorsiflexor (TA) muscles demonstrated coactivation during stance. Also the case displayed in Fig. 2C shows an activation pattern, which is different from the stepping-like pattern observed in the able-bodied. In this patient the stepping movements imposed by the trainers induced no activity in the TA and low-amplitude activity in the SOL during stance phase.

The variety of the motor output patterns in the complete SCI patients induced by the same externally controlled maneuver of passive treadmill stepping imposed by trainers could be categorized in four characteristic groups according to the output of TA and SOL. Figure 3A illustrates Group 1 (n=6) characterized by no motor output (TotAct less than 10% of able bodied). Group 2 was showing low amplitude motor output (TotAct about 25 % of able bodied) and could be divided into three further subgroups: Figure 3B exemplifies Group 2A (n=2), where coactivation of TA and SOL during stance phase is demonstrated. Group 2B (n=2) showed activity in SOL during stance, whereas TA did not show consistent rhythmicity of EMG activity synchronized to any specific phase of the step cycle (Fig. 3C). Figure 3D depicts Group 2C (n=1), where SOL was inactive, and TA displayed low output. Figure 3E shows the results of the same analysis used for the SCI patients carried out for able-bodied (n=4). This stepping pattern including both, the TA as well as the SOL output, was compared with the above described patterns of SCI patients. None of the different groups of SCI patients demonstrated the timing and coordination in the TA and SOL muscles that corresponded to a stepping-like EMG pattern.

Discussion

In previous studies it has been demonstrated that sensory input associated with assisted, load-bearing stepping using BWST delivered repetitively to the lumbar cord over an extended period of time can activate spinal neuronal circuits with the capacity to generate complex locomotor patterns [3,4]. Is it possible to activate such a spinal pattern generating network in complete SCI patients by sensory feedback input induced during the first manually assisted steps on a moving

treadmill belt? Particularly in patients, who never underwent a regular locomotor training before? However, results in this study demonstrated that the same externally controlled maneuver of passive load-bearing stepping can induce different patterns of motor output in spinal cord injured individuals of similar ASIA A classification. Our hypothesis is that these differences in the expression of this activity may be due to differing degrees of preservation of suprasegmental brain influence on lumbar network activity below the lesion. Such

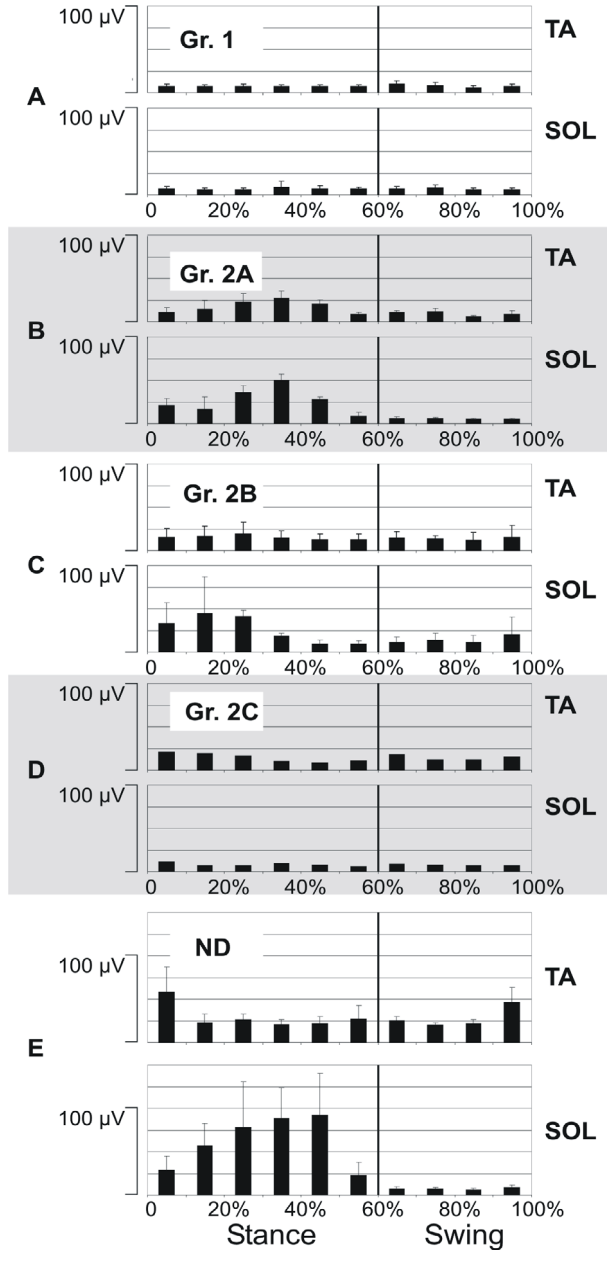


Fig. 3 Bar diagrams showing the total amount of EMG activity (TotAct) of tibialis anterior and soleus. Each diagram shows 10 % of the stance (10-60 %) and 10 % of the swing phase (70-100 %). Averaged values within 8 gait cycles of (A) 6 patients included in Group 1, (B) 2 patients included in Group 2A, (C) 2 patients included in Group 2B, (D) one patient characterized as Group 2C and (E) 4 able bodied patients are illustrated.

residual facilitatory brain influence on segmental structures has been previously demonstrated in patients with clinically complete SCI [7]. It should be noted that brain "influence" does not necessarily imply volitional brain "control". Furthermore it has to be considered that the BWS and treadmill speed used during stepping trials may also be factors that contribute to the differing neuromuscular patterns.

The main finding reported herein demonstrates that the patterned, sensory input to the lower spinal cord was not sufficient to generate stepping-like EMG patterns of the leg muscles in patients with clinically complete spinal cord injury during their initial stepping trial. However, the peripheral feedback helped to express some features of lumbar spinal networks involved in locomotor control, even when a pattern generating set-up was not fully established.

References

[1]Dimitrijevic M.R., Gerasimenko Y., Pinter M.M.: Evidence for a spinal central pattern generator in humans. Ann. N.Y. Acad. Sci., 860, 1998, 360-376

[2]Minassian K., Jilge B., Rattay F., Pinter M.M., Binder H., Gerstenbrand F., Dimitrijevic M.R.: Stepping-like movements in humans with complete spinal cord injury induced by epidural stimulation of the lumbar cord: Electromyographic study of compound muscle action potentials. Spinal Cord, 42(7), 2004 Jul, 401-416

[3]Dietz V., Colombo G., Jensen L., Baumgartner L.: Locomotor capacity of spinal cord in paraplegic patients. Ann. Neurol., 37, 1995, 574-582

[4]Dietz V., Harkema S.J.: Locomotor activity in spinal cord-injured persons. J. Appl. Physiol., 96, 2004, 1954-1960

[5]Dobkin B.H., Harkema S.J., Roy R.R., Edgerton V.R.: Modulation of locomor-like EMG activity in patients with complete and incomplete spinal cord injury. J. Neurol. Rehab., 9, 1995, 183-190

[6]Maynard F.M. et al.: International standards for neurological and functional classification of spinal cord injury. American Spinal Injury Association. Spinal Cord, 35, 1997, 266-274

[7]Sherwood A.M., Dimitrijevic M.R., McKay W.B.: Evidence of subclinical brain influence in clinically complete spinal cord injury: discomplete SCI. J. Neurol. Sci., 110(1-2), 1992 Jul, 90-98

Author's Address

Dipl. Ing. Ilse Persy Ludwig Boltzmann Institute for Electrical Stimulation and Physical Rehabilitation, Montleartstraße 37, 1160 Vienna, Austria e-mail: ilse.persy@wienkav.at

PRELIMINARY RESULTS WITH TWO IMPLANTABLE DIAPHRAGM PACING SYSTEMS

Cosendai G¹, de Balthasar C¹, Ignagni A², Onders R³, Bradley K⁴, Purnell K¹, Ripley A¹, Mortimer JT³, Davis R¹, Zilberman Y¹, Schulman J¹

Alfred Mann Foundation, Valencia, CA, USA
 Diaphragm Pacing Services, Cleveland, OH, USA
 Case Western Reserve University, Cleveland, OH, USA
 Advanced Bionics a Boston Scientific Company, Valencia, CA, USA

Diaphragm Pacing Stimulation (DPS) for ventilator-dependent patients provides several advantages over conventional techniques such as phrenic nerve pacing or mechanical ventilator support. It avoids potential phrenic nerve injury as well as high cost hospitalization. Synapse Biomedical (Cleveland, OH) is commercializing a device with intramuscular electrodes that are implanted laparoscopically into the diaphragm near the phrenic nerve motor points.

Currently, five patients have been implanted with this leaded system attached externally to a Pulse Generator (PG). Two patients maintain their full-time respiratory requirements with DPS only. Two patients are in the process of weaning from ventilator support and use the DPS System for several hours per day. One patient was unable to receive ventilatory support from the DPS System due to severe denervation atrophy of the diaphragm. However, for a widespread use of this technique it would be more appropriate to use a totally implantable version of this system, without the wires exiting the skin. We present here the results of a preliminary feasibility study of two different pulse generators that could be used for an implantable DPS. One radio frequency powered PG, one battery powered PG, and the current external PG was tested. Each was attached to the externalized part of the wires to the diaphragm and Tidal Volume (TV) was measured in one ventilator-dependent patient who has been using the perctuaneous device for 3 years. No significant differences were observed between the three PG systems when stimulating the electrodes as used in the patient's own chronically attached PG system. We found that TV increased with increases in charge and frequency as expected when stimulating the patient's electrodes individually and in combination with each PG system. These results are a significant step forward to developing a totally implantable DPS for the ventilator-dependent patients. Further clinical tests to demonstrate the safety and efficacy of a fully implanted DPS are warranted.

Author's Address

Gregoire Cosendai, PhD Acting Director - Program Manager - Principal Scientist Alfred E. Mann Foundation for Scientific Research 25134 Rye Canyon Loop, Suite 200, PO Box 905 Valencia, CA 91355, USA

e-mail: gregc@aemf.org

APPLICATION OF STEREOLITHGRAPHIE IN MONITORING MUSCLE GROWTH INDUCED BY ELECTRICAL STIMULATION OF DENERVATED DEGENERATED MUSCLES

T. Helgason*, P. Gargiulo*, F. Johannesdottir*, P. Ingvarsson**, S. Knutsdottir**, V. Gudmundsdottir**, S.Yngvason**

* Dep. for Research and Development, HTS, Landspitali-University Hospital, Reykjavik, Iceland ** Dep. for Rehabilitation Medicine, Landspitali-University Hospital, Reykjavik, Iceland

Abstract

Spiral CT is used to gather three-dimensional data of upper leg tissue. Data representing muscle tissue type is isolated for measurement purposes. This is done in order to monitor muscle growth induced by electrical stimulation treatment. This treatment of paraplegic patients with denervated degenerated muscles is done in the framework of the EU funded project RISE. Computer models and models made with rapid prototyping methods are made to display and demonstrate the muscle Results show that time and spatial growth. dependencies of muscles growth can be monitored and studied quantitatively and qualitatively with the aid of three-dimensional data set displayed on the computer screen or in form of plastic models.

Introduction

In the frame of the RISE project [1], [2] three paraplegic patients with fully denervated and to a great extent degenerated muscles in the lower extremities are treated with electrical stimulation. These long-term flaccid paraplegic patients have no hope of gaining their muscle function with traditional treatment. On the contrary they suffer from side effects of their lesion. This includes decubitus ulcer, reduced bone density and thus higher risk of breaking the bones, lower metabolism exc. The goal of the electrical stimulation is to restore muscle fibres, mass and function in order to make the patients able to stand up and maintain a standing posture with the aid of electrical stimulation. Body balance is maintained with the aid of bars or other external aids. The muscles force should be enable the legs to bear the Building up mass, force and patients weight. function of a denervated and degenerated muscle has been shown to be possible [1] with long-term electrical stimulation treatment. The muscles are stimulated one or two times a day, six days a week for two years. During that time the muscle is expected to gain considerable in mass and size and thus its ability to perform work. Throughout the treatment the patient's progress is monitored by several means. The monitoring methods are aiming at histology and cell biology, the muscles

function and at its mass and shape. For the shape, CT scans are taken, in the case of the m. quadriceps, with a regular 10 cm interval beginning at the trochanter and going down to the knee [1]. In total five scans are taken. comparison of two scans taken on two different times on the same height shows well the muscle growth in that specific place in the given time. Comparing five scans, taken with 10 cm interval, gives an estimation of the total muscle growth in the same time. However it does not show the growth of the whole muscle. Also the data from only 10 scans is not sufficient data to use as for of three-dimensional calculations distribution in the leg. They are done to estimate the necessary current intensity to depolarise the muscle cell above threshold and hence produce muscle contraction.

In this work we use a different approach witch will be discussed in the following.

Material and Methods

Spiral CT

With four months interval a spiral CT is taken of each of the three RISE patients in treatment in our institution. This has been done since beginning of treatment and will be done for the two years time of the RISE project. Giving in total a six scans of each patient. The scans are taken beginning at the trochanter and going down below the knee, with a pitch of 0,8 mm giving in total around 750 CT slices depending on patient's size. Each slice has 512 x 512 pixels. Each pixel has a grey value in the Houndsfield scale of 4096 grey scale values meaning that it is represented with a 12-bit value. A total dataset from a single scan is therefore 512 x $512 \times 750 \times 12 = 2.2$ GBit or 300 MB. This dataset gives a complete three-dimensional description of the tissue and hence the muscles in both upper legs.

Tissue differentiating

The dataset is loaded into a computer program used to extract the tissue of interest. This can

easily be done to separate bone from muscles or fat from muscles. It is partly done automatically with filters built in the programme and/or partly in an interactive way by the user. The user defines the grey scale values he wants to display, area of interest and some other properties the object has to fulfil that he wants to display. By these means we have however not been able to separate the different muscles or different muscles parts from each other, meaning that we can only show the muscles as one object.

Display

The tissue of interest can then be displayed as a three dimensional object on a computer screen. Thereby different tissue type can be put together on the same image. Figure 1 shows an example of this.

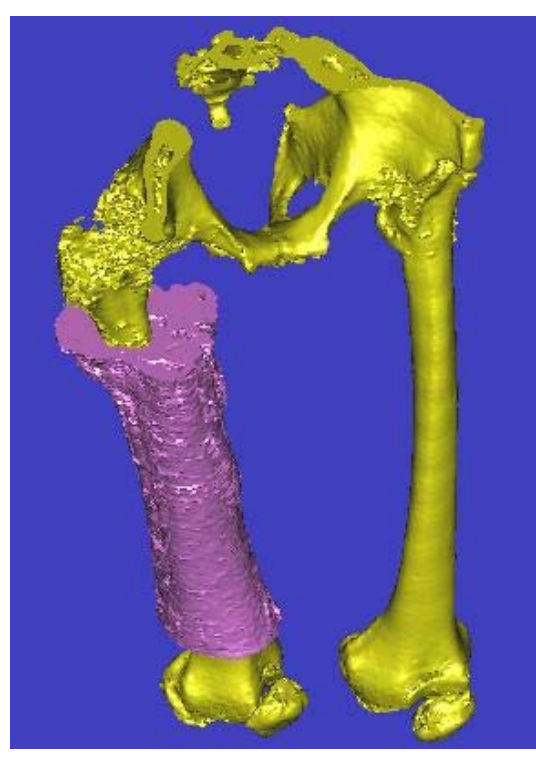


Fig. 1: The two femur bones and the pelvis of a car accident patient. The enervated and degenerated muscles on the right leg are partly shown. Note that the pelvis has suffered from the accident.

Measurements

To monitor the treatment measurements are made with the help of the data representing the isolated muscle tissue and its portion of total tissue in a single slice. Slice area, muscle volume, muscle mass, density are examples on parameters that can be measured or estimated. This will be done in due time to access muscle growth.

Stereolithographie models

Solid models of various materials are done of the muscles of the upper leg with the associated femur

bone. These models are done in colour so that bone tissue is clearly distinguished from muscle tissue. These models will be done for every measurement instance. The result is a row of models from every patient showing the patient's progress throughout the treatment. This will be used for demonstration purposes.

Results

Three dimensional computer models of denervated degenerated upper leg muscles of paraplegic patients have been made. These models are the first in a row to monitor the outcome of an electrical stimulation treatment. In due time they will show the muscle growth throughout the treatment period. Since the models are made with data taken periodically every four months they will show the muscle growth rate in every period. They will also show the spatial distribution of the muscle growth, which is believed to be unequal along the length of the muscle.

Discussion

In further work other data sampling modalities than CT will be used. MRI and ultrasound are among the candidates. This gives hope of solving the problem of isolating muscles from one another or separating muscle parts.

References

- [1] Kern, H.; Hofer, C.; Mödlin, M.; Forstner, C.; Mayr, W.; Richter, W.: "Functional Electrical Stimulation (FES) of Long-Term Denervated Muscles in Humans: Clinical Observations and Laboratory Findings." Basic Appl Myol, 12, (6): 291-299, 2002.
- [2] Mayr, W.; Hofer, C.; Bijak, M.; Rafolt, D.; Unger, E.; Reichel, M.; Sauermann, S.; Lanmueller, H.; Kern, H.: "Functional Electrical Stimulation (FES) of Denervated Muscles: Existing and Prospective Technological Solutions." Basic Appl Myol, 12, (6): 287-290, 2002.

Acknowledgements

This work has been supported by: Health Technology Venue (HTV, www.htv.is) and The Icelandic Student Innovation Fund.

Author's Address

Dr. Thordur Helgason Department of Research and Development Landspitali-University Hospital, Eiriksgata 5, 101 Reykjavik, Iceland.

e-mail: thordur@landspitali.is home page: www.landspitali.is

$oxed{A}$	\mathbf{D}	
Al-Khodairy Abdul 117 Allan David B. 205	Danieli D. Davis Ross	70 240
Andersen Ole K. 84	De Balthasar C.	240
Arendt-Nielsen Lars 84	De Kegel Alexandra	98
Ashley Zoe 52, 58, 176, 201	De Ruijter Sigried	98
	Dennis Robert G.	63
В	Dewald Jules P. A.	154
$oldsymbol{D}$	D'Hont Yves	98
D.1	Dimitrijevic Milan	2, 8, 12, 236
Bahrami Fariba 224	Dimitrijevic MM	2
Bajd Tadej 102, 129	Dobrowolny Gabriella	48
Barberi Laura 48 Beres-Jones J. 236	Domurath Burkhard	215 63
Beres-Jones J. 236 Bijak Manfred 24, 94, 122, 132, 183	Dow Douglas E.	03
Bijelić Goran 195		
Biral Donatella 67, 70	\mathbf{E}	
Bittner R. 39	_	
Bogacheva Irina 19, 21	Eike Heinz	232
Bojanić Dubravka 195	El Makssoud Hassan	113
Boncompagni Simona 36	Ellis Michael D.	154
Borau A. 125	Elsaify Ahmed	187
Bouri Mohamed 117	Emadi Mehran	224
Bradley Kerry 179, 240		
Briers Lucia 98	\mathbf{F}	
Brodard Roland 117		
Bunc Matjaž 209	P.11: 36	22 50 52
	Fabbian M.	32, 70, 73
\mathbf{C}	Faulkner John A.	63
	Fedorova Elena Feldhusen Frerk	235 232
Caccavale S. 32	Fend Martin	40
Cacho Enio 88	Forstner Claudia	2, 27, 32
Capoccia Massimo 201	Fothergill John	187
Carharts M. 16	Fournier Jacques	117
Carniguian Sylvain 172	Fraisse Philippe	113
Carraro Ugo 32, 36, 67, 70, 73	Fraser Matthew H.	205
Cerrel Bazo Humberto A. 92	Futami Ryoko	129
Chomontowska H. 67		
Chouard Claude-Henri 226	\mathbf{G}	
Cikajlo Imre 129	G	
Clavel Reymond 117		40, 100
Cliquet Jr. Alberto 88	Gallasch Eugen	40, 122
Cosendai Gregoire 240 Coulombe Jonathan 172	Gargiulo P.	241
Coupaud Sylvie 205	Gerasimenko Yuri Germinario E.	18, 19, 21, 235 70
Crevenna Richard 158	Giacinti Cristina	48
Cit tellia recitata 150	Giardiello Gainluca	213
	Gilerovich Elena	235
	Cite Cite Diving	230

INDEX OF AUTHORS

C' 1 XX			
Girsch Werner	62	Keller Thierry	154, 191
Goljar Nika	109	Kern Helmut 2,	8, 12, 27, 32, 36,
Gollee Henrik	205	40, 5	8, 70, 73, 94, 236
Gosselin Benoit	164	Kinz Gudrun	40
Graham Geoffrey	80	Kirstein Tünde	191
Gregersen Hans	218	Knauf U.	76, 77
Greshnova Irina	20	Knutsdottir Sigrun	241
Gruber Helmut	39	Koch Rainer	232
Gruther Wolfgang	158	Krafczyk S.	106
Gudmundsdottir Vilbor	g 241	Kraincuk P.	158
Guiraud David	113	Krames Elliot	179
		Krawczyk Kazimierz	67
		Kucher Valeriy	21
		Kurstjens G.A.M.	125
		Kutzenberger Johannes	215
Hanke Sten	135		
Harkema S.	236		
He J.	16	L	
Helgason Thordur	241		
Herman Richard	16, 227	Lago N.	168
Hofer Christian	8, 24, 32, 62,	_	, 58, 122, 76, 183
Tiorer Christian	70, 73, 94, 122	Lawrence Marc	191
Högemeier O.	76, 73, 71, 122	Lazzeri Massimo	213
Höllwarth U.	32	Li F.	52, 58, 201
Hoshimiya Nozomu	129, 138	Lisiński Przemysław	152
Huber Juliusz	152	Lishiski i izemiysiaw	132
Hunt Ken J.	205		
Trunt Ixon 5.	203	\mathbf{M}	
_			
		Magliano Mariano	153
		Malaguti Silvia	213
Ignagni A.	240	M / 1 T 1	44 220
Ilieva-Mitutsova Lidia		Martinek Johannes	44, 228
ilic va iviitatso va Liaia	18	Martinek Jonannes Masani Kei	44, 228 146
		Masani Kei	146
Ingvarsson Pall	18		146 102, 109, 129
	18	Masani Kei Matjačić Zlatko Mayr Winfried	146 102, 109, 129 4, 32, 36, 40, 58,
	18	Masani Kei Matjačić Zlatko Mayr Winfried 62, 70, 73,	146 102, 109, 129 4, 32, 36, 40, 58, 94, 122, 176, 228
	18	Masani Kei Matjačić Zlatko Mayr Winfried	146 102, 109, 129 4, 32, 36, 40, 58, 94, 122, 176, 228
	18	Masani Kei Matjačić Zlatko Mayr Winfried 62, 70, 73, Mazurkiewicz Przemysł	146 102, 109, 129 4, 32, 36, 40, 58, 94, 122, 176, 228 taw 152
Ingvarsson Pall	18 241	Masani Kei Matjačić Zlatko Mayr Winfried 62, 70, 73, Mazurkiewicz Przemysł McLean Alan N.	146 102, 109, 129 4, 32, 36, 40, 58, 94, 122, 176, 228 daw 152 205
Ingvarsson Pall J Jakubiec-Puka Anna	18 241 67	Masani Kei Matjačić Zlatko Mayr Winfried 62, 70, 73, Mazurkiewicz Przemysł McLean Alan N. Meadows Paul	146 102, 109, 129 4, 32, 36, 40, 58, 94, 122, 176, 228 taw 152 205 179
Jakubiec-Puka Anna Jarvis Jonathan	18 241 67 52, 58, 183, 201	Masani Kei Matjačić Zlatko Mayr Winfried 62, 70, 73, Mazurkiewicz Przemysł McLean Alan N. Meadows Paul Megighian A.	146 102, 109, 129 4, 32, 36, 40, 58, 94, 122, 176, 228 daw 152 205 179 70
Jakubiec-Puka Anna Jarvis Jonathan Jilge B.	18 241 67 52, 58, 183, 201 8	Masani Kei Matjačić Zlatko Mayr Winfried 62, 70, 73, Mazurkiewicz Przemysł McLean Alan N. Meadows Paul Megighian A. Métrailler Patrick	146 102, 109, 129 4, 32, 36, 40, 58, 94, 122, 176, 228 taw 152 205 179 70 117
Jakubiec-Puka Anna Jarvis Jonathan Jilge B. Johannesdottir F.	18 241 67 52, 58, 183, 201 8 241	Masani Kei Matjačić Zlatko Mayr Winfried 62, 70, 73, Mazurkiewicz Przemysł McLean Alan N. Meadows Paul Megighian A. Métrailler Patrick Mihic M.	146 102, 109, 129 4, 32, 36, 40, 58, 94, 122, 176, 228 taw 152 205 179 70 117 209
Jakubiec-Puka Anna Jarvis Jonathan Jilge B. Johannesdottir F. Jorgovanović Nikola	18 241 67 52, 58, 183, 201 8 241	Masani Kei Matjačić Zlatko Mayr Winfried 62, 70, 73, Mazurkiewicz Przemysł McLean Alan N. Meadows Paul Megighian A. Métrailler Patrick Mihic M. Mina Stefan	146 102, 109, 129 4, 32, 36, 40, 58, 94, 122, 176, 228 law 152 205 179 70 117 209 135
Jakubiec-Puka Anna Jarvis Jonathan Jilge B. Johannesdottir F.	18 241 67 52, 58, 183, 201 8 241	Masani Kei Matjačić Zlatko Mayr Winfried 62, 70, 73, Mazurkiewicz Przemysł McLean Alan N. Meadows Paul Megighian A. Métrailler Patrick Mihic M. Mina Stefan Minassian Karen	146 102, 109, 129 4, 32, 36, 40, 58, 94, 122, 176, 228 taw 152 205 179 70 117 209 135 8, 12, 236
Jakubiec-Puka Anna Jarvis Jonathan Jilge B. Johannesdottir F. Jorgovanović Nikola	18 241 67 52, 58, 183, 201 8 241	Masani Kei Matjačić Zlatko Mayr Winfried 62, 70, 73, Mazurkiewicz Przemysł McLean Alan N. Meadows Paul Megighian A. Métrailler Patrick Mihic M. Mina Stefan Minassian Karen Mödlin Michaela	146 102, 109, 129 4, 32, 36, 40, 58, 94, 122, 176, 228 taw 152 205 179 70 117 209 135 8, 12, 236 27, 70, 236
Jakubiec-Puka Anna Jarvis Jonathan Jilge B. Johannesdottir F. Jorgovanović Nikola	18 241 67 52, 58, 183, 201 8 241	Masani Kei Matjačić Zlatko Mayr Winfried 62, 70, 73, Mazurkiewicz Przemysł McLean Alan N. Meadows Paul Megighian A. Métrailler Patrick Mihic M. Mina Stefan Minassian Karen Mödlin Michaela Mohammed Samer	146 102, 109, 129 4, 32, 36, 40, 58, 94, 122, 176, 228 taw 152 205 179 70 117 209 135 8, 12, 236 27, 70, 236 113
Jakubiec-Puka Anna Jarvis Jonathan Jilge B. Johannesdottir F. Jorgovanović Nikola	18 241 67 52, 58, 183, 201 8 241 195	Masani Kei Matjačić Zlatko Mayr Winfried 62, 70, 73, Mazurkiewicz Przemysł McLean Alan N. Meadows Paul Megighian A. Métrailler Patrick Mihic M. Mina Stefan Minassian Karen Mödlin Michaela Mohammed Samer Molinaro Mario	146 102, 109, 129 4, 32, 36, 40, 58, 94, 122, 176, 228 taw 152 205 179 70 117 209 135 8, 12, 236 27, 70, 236 113 48
Jakubiec-Puka Anna Jarvis Jonathan Jilge B. Johannesdottir F. Jorgovanović Nikola K Kaczmarek Monika	18 241 67 52, 58, 183, 201 8 241 195	Masani Kei Matjačić Zlatko Mayr Winfried 62, 70, 73, Mazurkiewicz Przemysł McLean Alan N. Meadows Paul Megighian A. Métrailler Patrick Mihic M. Mina Stefan Minassian Karen Mödlin Michaela Mohammed Samer Molinaro Mario Mortimer J.	146 102, 109, 129 4, 32, 36, 40, 58, 94, 122, 176, 228 taw 152 205 179 70 117 209 135 8, 12, 236 27, 70, 236 113 48 240
J Jakubiec-Puka Anna Jarvis Jonathan Jilge B. Johannesdottir F. Jorgovanović Nikola K Kaczmarek Monika Kaczmarek Piotr	18 241 67 52, 58, 183, 201 8 241 195	Masani Kei Matjačić Zlatko Mayr Winfried 62, 70, 73, Mazurkiewicz Przemysł McLean Alan N. Meadows Paul Megighian A. Métrailler Patrick Mihic M. Mina Stefan Minassian Karen Mödlin Michaela Mohammed Samer Molinaro Mario Mortimer J. Moser-Thier K.	146 102, 109, 129 4, 32, 36, 40, 58, 94, 122, 176, 228 taw 152 205 179 70 117 209 135 8, 12, 236 27, 70, 236 113 48 240 39

INDEX OF AUTHORS

Musaro Antonio Musienko Pavel	48 19, 21	R
N		Rafolt Dietmar 24, 40, 62, 122, 132 Rakos Monika 94
Navarro X.	168	Ramn Arine Ian 201 Raschka Doris 94
Navario A. Nikitin Oleg	18	Rattay Frank 8, 12, 44, 228
Novikov Gennady	200, 235	Reichel Martin 24, 44, 122, 176, 228
	,	Rijkhoff Nico 125, 218
		Ripley A. 240
		Rodríguez A. 125
	170	Rosselli Diego Piero 153
Oakley John Okhocimski Dmitri	179 18	Rossini Katia 32, 73 Rossmanith W. 39, 62
Olenšek Andrej	102, 109	Rossmanith W. 39, 62 Rozman Janez 209
Onders R.	240	Rusjan Spela 109
Oses M. Teresa	168	Russold Michael F. 52, 183, 201
Otsuka Masayuki	138	
		S
P		D
		Sacristan Jordi 168
Partridge T.	77	Salmons Stanley 52, 58, 183, 201
Paternostro-Sluga Tatjana	158	Sauermann Stefan 24, 122, 132
Peasgood William	187	Sauerwein Dieter 215
Peceny Ronald	158	Sawan Mohamad 164, 172
Pelosi Laura	48	Schäfer R. 76, 77
Persy Ilse	2, 236	Scherbakova Natalia 21 Schmitt Carl 117
Platonov Aleksandr Poignet Philippe	18 113	Schmitt Carl 117 Schulman Joseph 240
Ponulak Filip	152	Seifert Hermann 232
Popovic Milos R.	80, 146	Sevcencu Cristian 218
Popović Dejan B.	142, 195	Simard Virginie 164
Popović Mirjana B.	142, 195	Sinkjær Thomas 125, 218
Popović-Bijelić Ana	195	Spaich Erika G. 84
Princi T. Protasi Feliciano	209 36	Spinelli Michele 213 Spiss Christian 158
Protz Peter	132	Stanonik Irena 109
Purnell K.	240	Straube Andreas 106
- 4		Strohhofer Maria 94
		Summerfield Nuala 201
Q		Sutherland Hazel 52, 58, 183, 201
Ovintara Isalasa	107	Szecsi Johann 106
Quintern Jochen Quittan Michael	106 158	
Quittaii iviiciiaci	130	\mathbf{T}
		Tarantola Jessica 213
		Thrasher Adam 80
		Tschakert Andreas 176

INDEX OF AUTHORS

U

Unger Ewald 24, 58, 62, 122, 132, 176

$\overline{\mathbf{V}}$

Van Vaerenbergh Jo	98
Vandenberghe Sara	98
Varga Clayton	179
Vette Albert H.	146
Vetter Karl	122
Vidal J.	125
Vindigni V.	70
Vogelauer M.	12, 32
Vrola Maurizio	153

W

Watanabe Takashi	138
Weigel Gerlinde	62
Wernig Anton	76, 77
Wernig G.	76
Wernig M.	76
Willis W.	16, 227
Wojtysiak Magda	152

Y

Yazdanpanah Mohammad-Javad	224
Yngvason S.	241
Yoshizawa Makoto	138

7

Zanin Maria Elena	32, 70, 73
Zanollo Lucia	213
Zilberman Y.	240
Zöch Carina	158
Zweyer M.	76, 77